Université de Toulouse

THÈSE

En vue de l'obtention du

DOCTORAT DE L'UNIVERSITÉ DE TOULOUSE

Délivré par :

Université Toulouse 3 Paul Sabatier (UT3 Paul Sabatier)

Présentée et soutenue par :
Agnese CRISTINI

Le Vendredi 13 Novembre

Titre :

DNA double-strand break formation and signalling in response to transcription-blocking topoisomerase I complexes

---

ED BSB : Biotechnologies, Cancérologie

Unité de recherche :

UMR 1037 - CRCT - Equipe 3 "Rho GTPase in tumor progression"

Directeur(s) de Thèse :

Dr. Olivier SORDET

Rapporteurs :

Dr. Laurent CORCOS, Dr. Philippe PASERO, Dr. Philippe POURQUIER

Autre(s) membre(s) du jury :

Dr. Patrick CALSOU (Examinateur)
Pr. Gilles FAVRE (Président du jury)

Ai miei genitori…

…Grazie

Merci aux Dr. Laurent Corcos, Dr. Philippe Pasero et Dr. Philippe Pourquier d'avoir accepté d'évaluer mon travail de thèse et d'avoir été présent pour ma soutenance. Merci aussi au Dr. Patrick Calsou d'avoir accepté d'être examinateur de ma soutenance et merci aussi pour la discussion précieuse, les conseils et le matériel que vous nous avez apporté pour ce projet.

Un grand merci à Olivier. Merci d'avoir accepté que je vienne travailler avec toi pour mon stage. Merci de m'avoir fait confiance et d'avoir su me faire participer activement aux discussions depuis le début. Pourtant mon début n'a pas été « brillant » avec les barrières de la langue, tu as toujours été patient et tu as cru en moi. Merci d'avoir été à l'écoute des mes idées, de mes critiques et des problématiques du travail en me laissant beaucoup de liberté. Merci surtout pour la discussion scientifique constante qu'on a pu avoir pendant ma thèse, ça m'a vraiment beaucoup apporté et je pense que c'est extrêmement formateur. Ça a été une « bonne guerre » de discuter chacun avec ses idées et son point de vue et j'ai trouvé très fructueux et stimulant le fait de ne pas être forcément d'accord. Merci aussi de m'avoir remotivé dans mes moments de pessimisme et de m'avoir calmé dans mes moments d'énervement facile. Merci aussi de m'avoir permis de participer à plusieurs projets du laboratoire.

Merci au Pr. Gilles Favre de m'avoir accueilli dans votre équipe. Merci aussi pour m'avoir permis de partir en congrès au Canada, cela a été pour moi une très belle expérience personnellement et scientifiquement, cela m'a permis de voir « la science » au delà de l'océan et de mettre les visages à beaucoup de noms que j'ai lu quotidiennement sur PubMed. J'ai eu beaucoup de chance de pouvoir faire cette expérience.

Merci à Giovanni pour m'avoir donné envie en premier de travailler sur les dommages à l'ADN et pour avoir accepté de m'encadrer lors de mon stage de M2R. Merci pour avoir cru en moi en premier et pour m'avoir « envoyer » chez Olivier quand j'ai demandé de faire une partie de mon stage à l'étranger et pourtant je n'étais pas vraiment enthousiaste de partir en France!! Merci aussi d'être venu deux fois à Toulouse pendant ma thèse pour suivre mon travail et nous donner de précieux conseils. J'espère qu'on pourra continuer à travailler ensemble. Merci aussi aux membres de son labo, en particulier Stefano, la Jessica et « le vieu » Davide.

Merci à Gaëlle, pour m'avoir accueilli dans son labo pour m'apprendre « sur le terrain » la ChIP !! Merci aussi pour avoir participé à mon comité de thèse et nous avoir aidé dans ce projet.

Merci à Joonette pour sa participation à ce travail. Tu es vraiment quelqu'un de très très gentil, j'ai passé des moment très drôles avec toi et j'ai découvert plein de trucs sur la culture asiatique ! Dommage que mes plans pour te faire avoir la nationalité française soient tombés à l'eau !! Merci pour tes macros « time saving ». Tu es vraiment un petit geek !!

Merci à tous les membres de l'équipe, les anciens, les nouveaux, ceux qui sont passés par là quelques temps, en ces 4 ans tous vous m'avez apporté quelque chose de différent, j'ai pu créer de très bons rapports et aussi de vrais amitiés. Le persone vanno e vengono ma ci sono quelli che restano.

Un grand merci à Jean-Charles même à la retraite tu es toujours là !! Quand je suis arrivée en stage et je ne comprenais rien du tout, tu as toujours été là pour me faire une blague, pour m'expliquer, pour m'aider, pour m'intégrer et surtout pour m'appeler pour manger à 11h30 !! Merci pour tes conseils toujours utiles du début jusqu'aux révisions du papier…

Merci à ma Kenzina, merci de m'avoir expliqué et appris plein de choses, clairement en français !! Je n'oublie pas que tu m'as toujours parlé en français pour MON bien !! Les fous rire, le BIEN ou BIENG ? Le travail pour la gloire ou pour RIENG ! Merci de m'avoir appris la différence entre être CHIIIEN et CHIANT avec l'accent, pour nos sorties et pour avoir été un peu la grande sœur protectrice (que tu sais bien faire) à mon état de lieu, pour mon concours de l'école doc, pour mes débuts au labo.

Merci à mes amies Margi et Magdu, mes deux petites conasses préférées. Margi, entre nous ça a été une histoire de coup de foudre, de voisinage du bureau et des regards qui ne trompent pas.. ahahah merci d'avoir été et d'être toujours là pour moi, pour m'écouter et me remonter le moral et me calmer quand j'ai « la veine qui pette » !! Merci pour tous les rires, les blagues et les conneries. Je sais que ce n'est pas fini, notre histoire tiendra la distance !! Je suis très contente pour ton nouveau travaille ! Merci à Magdu, merci d'être toujours prête à partir en guerre à mes côtés ! Merci pour les délires et pour mettre l'ambiance et aussi pour toutes les quiescences que tu as induites pour moi les dimanches !! Merci de m'avoir appris le polonais (gruba kurwa), ça me servira beaucoup dans ma vie future ! Merci de m'avoir autant fait rire avec tes conneries, tes gaffes trop drôles et pour avoir été toujours là pour m'aider et me remotiver en particulier pendant la rédaction.. Maintenant, c'est à toi, ne te démotives pas et ne te plains pas ok ? Boh je sais que tu ne comprends rien à la biblio mais ça ira (ahahah) ! Il ne te reste qu'à faire ton Nature letter avant la fin de décembre, tu as encore du

temps ne désespère pas !! Merci aussi à Jeremstar et Laurent, clairement… entre la neige et les courses, ils ont tous leur mérite !!

Merci à mon IoIo, merci de m'avoir toujours fait sentir en sécurité à côté de toi, tu as toujours chassé les monstres qui hantent le labo et les eaux de Tahiti !! En plus tu es un peu une muse inspiratrice pour moi mais aussi pour tout le monde, je trouve que depuis ton départ il y beaucoup moins d'imagination dans l'air et on a perdu notre souffre douleur. On a commencé ensemble et depuis le métro en panne, avec toi ça a été toujours très drôle (ahahah), ça a continué avec l'appendicite, les urgences pour la peur, les histoires de cannibalisme… bref tu me manques IoIo !! Merci pour tout et même si tu fais le dur à cuir tu es un gentil et tu m'as aidé plein de fois ! Maintenant bouges toi !!

Merci à Audrey (j'ai pris sur moi stronzina pour ne pas faire semblant de t'oublier), merci de m'avoir débloqué sur « mes problèmes western », de m'avoir fait compagnie souvent le weekend et d'avoir fait au moins 5 fêtes de départ. Merci à Oliver, le gros poussin, merci beaucoup pour ta gentillesse et pour tes nombreux conseils personnels et scientifiques toujours désintéressés, merci pour tes blagues et même si tu as 45 ans je trouve que tu restes très jeune dans ta tête. J'espère très sincèrement que tu auras ton concours car tu le mérites vraiment et tu as toutes les qualités pour être chercheur. Merci à Rémi, le chef Millicù et test Myco, merci de prendre soin de nous et de t'occuper si bien de tes responsabilités (!!), merci de ne jamais te vexer quand je te dis « petit con » ou « tête de cul », de toute façon c'est très mignon, merci de m'avoir appris plein des mots comme « gorette», je te promets de ne jamais l'oublier, merci aussi de nous en apprendre d'avantage sur ta culture gipsy et sur tes expériences à la Rocco ART Academy et merci aussi de continuer à me parler malgré l'énorme succès de Kenjoue, tu as gardé les pieds sur terre!!

Merci à Fatumata, de m'avoir appris comment une vrai demoiselle se porte à table (on ne peut pas compter sur Magda, c'est clair..), merci aussi de partager avec moi les histoires des Princes de l'amour et de m'avoir appris comment regarder avec « les yeux de l'amour », merci aussi pour nos discussions scientifiques (eh oui des fois on travaille !). Merci à Bernardo alias Laetitia, merci d'avoir fait un stage si long (tu es déjà là depuis plus qu'un an quand même).. Merci pour les bons moments, pour les blagues et pour les discussions dans le bus, je te laisse la relève dans le groupe « instabilité génomique » et à côté de Magdu comme petite conasse, vous êtes la nouvelle génération, je te souhaite bon courage avec Rnd1, la protéine invisible ! Merci à Christine, à Anne-Laure, à Julia avec ses confitures de figues, à Aurore ma coloc du CRCT et à Sarah pour m'avoir appris plein de choses sur les grenouilles et merci à Cathy pour sa folie et ses danses. Merci à Thèo, j'espère qu'on continuera à boire des rum e pera et à travailler ensemble, Adriano dal sangue latino, bella vita Guillaume, Pauline1 j'espère aussi qu'on continuera à se voir et discuter ensemble, ma

petite Morgane avec ses histoires « romantiques », Pauline2 et ma petite bisou bisou Marion et Charlène.
Merci à Claire et Patrick pour leur gentillesse et leur intérêt envers les gens, pour faciliter la vie de tout le monde en s'occupant et en gérant des tas de choses au labo. Merci aussi à Fafita, Stéphanie, Aurélien, Isa et Sylvie pour leurs conseils pendant ces 4 ans. Merci aussi à Jeanine et Marie-Ange pour leur aide précieuse.

Merci aux personnes des autres équipes de l'ICR et aussi aux nouveaux du CRCT : merci à Maud, on a commencé ensemble et on a fini ensemble à partir de soirées alcooliques de la première année jusqu'au stress partagé de la fin de thèse, Julie ma petite Julie Senseo je n'ai absolument pas oublié que je te dois une petite vengeance même si on peut dire que tu me nourris tous les jours avec ta carte, Pauline et Ada les deux belles découvertes de cette dernière année mais aussi Laure, Perrine, Aurèlie, Philippe, Nico, Judith, Mika, Renaud…
Merci aussi au vigil de l'ICR (Kader) pour ses blagues du dimanche sur les italiens, merci aux cuisiniers de la fin de l'ICR pour leurs blagues sur le foot !!

Merci à mes amis de Toulouse hors du labo : merci à Aurèlie d'avoir été toujours là avec ta folie, de m'avoir fait autant rire avec ton animation et tes plans improbables, avec ton arbre sur la colline, ta tournée des bars pourris, ton gîte dans les villages déserts, ta samba d'halloween, tes randonnées qui commencent à 16h de l'aprèm et je pourrais continuer longtemps, tu es vraiment une très bonne copine pour moi. Merci à Nicola pour ta surprise, pour ton hospitalité, pour ton exploit vodka-puffo et pour être toujours si calme et posé, merci à minchia mia Geremia pour ton trop beau couple avec Nicola dommage que tu habites si loin de Toulouse, alla mia mogliettina Sonia pour être toujours là, venir me voir à Toulouse, Bologna ou n'importe où, Alessandro et nos rencontres dans les aéroports, Roberto et tes très bons barbecues à Rue Bayard, Domenico et le groupe des italiens, Julie et nos soirées folles à la coloc, les déguisements et tes conseils, Vincenzo, Gianni, Anna et Nacho, Fabio, Alexis.
Merci à mes amis de toujours éparpillés un peu partout : la Marta, merci pour ton soutien même par Skype, pour me connaître si bien et malgré nos caractères et nos disputes pour rester toujours si liées, merci al Gabri mon ami de toujours, mon point de repère dès que je rentre, juste toi peux m'amener al Green en plein stress de thèse, merci à Bonini, Divano-Bonni avec son super appart da scapolo d'oro à Brisbane et tu me manques souvent toi avec tes blagues. Il Lori, l'ami de succès dont on peut se vanter devant tout le monde, Niccolin sola per fortuna che posso spiarlo a Bologna, Umbi, il Dani poeta sognatore e vicolini, la Claudina regina della moda, le petit macaron Valeghina,

mes amis de la fac, la Sarina, la Silvia, Claudiano, la Michi. Mes copines lamarine la Gio, la Silvia, la Eva, le Giulie, la Chiara, la Cri.

Merci à ma famille, sans laquelle je n'aurais jamais pu en arriver là. Grazie mamma, de m'avoir appris l'amour pour la culture mais surtout pour m'avoir toujours aidé en tout, pour être mon exemple et pour avoir tout sacrifié pour me permettre de faire l'Université, pour avoir toujours mis mes choix devant tes envies. Grazie babbo, c'est pour toi que j'ai voulu travailler dans la recherche et en particulier dans la cancérologie, merci pour tout ce que tu m'as appris, je sais que tu es quand même là. Grazie alla Lisa e all'Anna, j'aime bien quand on se dispute constamment pour des conneries, j'ai l'impression de ne jamais vieillir, merci d'être toujours con la mamma et merci d'être venues malgré la grand crainte de l'avion (merci à Alex aussi !!).

Merci à la famille de Nico, pour m'avoir accueilli si chaleureusement entre eux et pour être venue encore une fois sur Toulouse pour ma thèse, merci à son papa, à ses tantes, à Sabrina et à Pauline.

Et merci à toi Nico, pour être toujours là pour me soutenir, supporter, conseiller, consoler, aider, motiver et pour cuisiner (!!). Merci pour tes conseils au labo et hors du labo, pour m'avoir aidé avec ma thèse, je pense que tu dois connaître les topoisomerases par coeur !! Toi t'es trop organisé, tu sais tout le temps quoi faire et comment, j'espère que ça va se débloquer pour toi, tes papiers, tes projets car tu as bossé beaucoup et bien et tu le mérites.. Des fois je me suis demandée pourquoi j'avais choisi la recherche, pourquoi je suis venue en France ? Et après je me dis que ça devait être comme ça pour se trouver et là j'espère que ça sera de mieux en mieux..

Et enfin (par pour importance) merci à mon petit Pico !! Tu as toujours été à côté de moi pour la rédaction de ma thèse à me faire compagnie et plein de câlins (et aussi à bouffer mes papiers !!). Il faut absolument que tu aies la double nationalité !!

TABLE OF CONTENTS

ABBREVIATION TABLE

4OHT: 4-hydroxy tamoxifen
53BP1: tumor protein p53 binding protein 1
9-1-1: Rad9-Hus1-Rad1 complex
aa: amino acid
Abraxas/CCDC98: BRCA1-A complex subunit Abraxas
AID: activation-induced cytidine deaminase
Alt-NHEJ: alternative NHEJ
AP: apurinic-apirimidic
APE1: apurinic-apirimidic endonuclease
APH: aphidicolin
APLF: aprataxin-PNK-like factor
APOBEC: apolipoprotein B mRNA editing enzyme, catalytic polypeptide
AR: androgen receptor
ASF/SF2: serine/arginine-rich splicing factor 1
AT: ataxia telangiectasia
ATLD: AT-like disorder
ATM: ataxia telangiectasia mutated
ATMi: ATM inhibitor
ATMIN: ATM interacting protein
ATP: adenosine triphosphate
ATR: ataxia telangiectasia and Rad3-related protein
ATRIP: ATR-interacting protein
BARD1: BRCA1-associated ring domain protein 1
BCL10: B-cell CLL/lymphoma 10
BER: base excision repair
BLM: bloom syndrome, RecQ-helicase-like
BMI1 : murine leukemia viral (Bmi-1) oncogene homolog
bp: base pair
BRCA1: breast cancer 1
BRCA2: breast cancer 2
BRCC36: BRCA1/BRCA2-containing complex subunit 36
BRCC45: BRCA1/BRCA2-containing complex subunit 45
BRCT: breast cancer C-terminal domain
Bru: bromouride
BrUTP: 5-bromouridine triphosphate
CAND1: cullin-associated NEDD8-dissociated 1
CCT6A: chaperonin containing TCP1, subunit 6A
Cdk: cyclin-dependent kinases
CENPA: centromere protein A
CENPF: centromere protein F
CFTR: cystic fibrosis transmembrane conductance regulator
CHD3: chromodomain helicase DNA binding protein 3
CHFR: checkpoint with forkhead and ring finger domains
ChIP: chromatin immunoprecipitation
ChIP/DNA: chromatin/DNA immunoprecipitation
ChIP-Seq: ChIP-sequencing
Chk1: checkpoint kinase 1
Chk2: checkpoint kinase 2
CK2: caseine kinase 2
CPD: cyclobutane pyrimidine dimers
CPT: camptothecin
CS: cockayne syndrome
CSB: cockayne syndrome group B protein
CSN: COP9 signalosome
CSR: class switch recombination
CTD: carboxy-terminal domain
CtIP: carboxy-terminal binding protein-interacting protein
Cul: cullin
DDR: DNA damage response
DDRNA: DNA damage response RNAs
DHFR: dihydrofolate reductase
DNA-PK: DNA-dependent protein kinase
DNA-PKcs: DNA-dependent protein kinase catalytic subunit
DNA-PKi: DNA-PK inhibitor
DRB: 5,6-Dichloro-1-β-D-ribofuranosylbenzimidazole
DSB: double-strands break
dsDNA: double-strand DNA

DSEs: double-strands ends
DSS1: deleted in split hand/split foot protein 1
DUB: deubiquitylating enzyme
E1: ubiquitin-activating enzyme
E2: ubiquitin-conjugating enzyme
E3: ubiquitin ligase
ENL: myeloid/lymphoid translocated
ERCC1: excision repair cross-complementing group 1
eRNAs: enhancer RNA
Et743: ecteinascidin 743
FA: Fanconi anemia
FACT: facilitates chromatin transcription
FDA: US food and drug administration
FEN1: flap structure-specific endonuclease 1
FHA: forkhead-associated domain
FK2: ubiquitinylated proteins
FLV: flavopiridol
FRDA: Friedreich ataxia
FXN: frataxin
GFP: green fluorescent protein
GO: gene ontology
HDAC: histone deacetylase
HECT: homology to E6AP C-terminus
HERC2: HECT and RLD domain containing E3 ubiquitin protein ligase 2
HIF-1α: hypoxia-inducible factor 1-alpha
HIRA: histone regulator A
HMGN1: high mobility group nucleosome binding domain 1
hMOF: human ortholog of drosophila males absent on the first
HP1: heterochromatin-binding protein 1
HR: homologous recombination
ICC-FISH: immunocytochemistry staining followed by fluorescence in situ hybridization
IgH: immunoglobulin heavy chain
IKZF1: IKAROS family zinc finger 1
IR: ionizing radiation
IRIF: ionizing radiation induced foci
ISG15: interferon-stimulated gene 15
JMJD: jumonji domain containing protein
KAP1: KRAB-associated protein-1
KD: kinase dead
L3MBTL1: lethal(3) malignant brain tumour-like protein 1
LCR: locus control region
LEDGF: lens epithelium-derived growth factor
LET: linear energy transfer
Lig3: DNA ligase 3
Lig4: ligase 4
MCSZ: microcephaly with early-onset, intractable seizures and developmental delay
MDC1: mediator of DNA-damage checkpoint 1
MDM2*:* mouse double minute 2
MERIT40: mediator of RAP80 interactions and targeting subunit of 40 kDa
MIU: motifs interacting with ubiquitin domain
MR: mental retardation
Mre11: meiotic recombination protein 11
MRN: Mre11-Rad50-Nbs1 complex
mRNP: messanger ribonucleoprotein particles
mTOR: mammalian target of rapamycin
Mus81: Mus81 endonuclease homolog (yeast)
NAE1: NEDD8 activating enzyme
NBS: Nijmegen breakage syndrome
NBSLD: NBS-like disorder
ncRNA: non-coding RNA
NCS: neocarzinostatin
NEDD8: neural precursor cell expressed developmentally downregulated 8
NER: nucleotide-excision repair
NHEJ: non-homologous end-joining
nt: nucleotide
NuRD: nucleosome remodelling and deacetylase
OTUB1: OTU deubiquitinase, ubiquitin aldehyde binding 1
P-TEFb: positive transcriptional elongation factor b

p53: tumor protein p53
PA200: proteasome activator 200
PA28: proteasome activator 28
PARG: PAR-glycohydrolase
PARP: poly [ADP-ribose] polymerase
PARPi: PARP inhibitor
PAXX: paralog of XRCC4 and XLF
PCNA: proliferating cell nuclear antigen
PI3K: phosphoinositide 3-kinase
PIAS: protein inhibitor of activate STAT protein
PIKK: phosphatidylinositol-3-kinase-like kinase family
PLD: phospholipase D
PNKP: polynucleotide kinase phosphatase
POH1: 26S proteasome-associated PAD1 homolog 1
POMP: proteasome maturation protein
PP: protein phosphatase
PR-Set7: PR/SET domain-containing protein 07
PRC: Polycomb repressive complex
PROMPTs: promoter upstream transcripts
PSF: protein-associated splicing factor
PSMD4: proteasome 26S subunit, non-ATPase, 4
PTIP: PAX transcription activation domain interacting protein 1 like
PTM: post-translation modifications
Rad: radiation sensitivity abnormal
Rap80: receptor associated protein 80
RBM8A: RNA binding motif protein 8
RBR: ring between ring
RBX: ring box 1
rDNA: ribosomal DNA
REV7: REV7 homolog
RFC: replication factor C
RIDDLE: radiosensitivity, immunodeficiency, dysmorphic features, and learning difficulties
RIF1: rap1-interacting factor 1 homolog
RING: really interesting new gene
RNAP: RNA polymerase
RNF: ring finger protein
ROS: reactive oxygen species
RC-DSB: replication-coupled DSB
RPA: replication protein A
Rpb1: RNA polymerase II subunit B1
RS-SCID: radiosensitive T-B- severe combined immunodeficiency
SAE1: SUMO1 activating enzyme subunit 1
SCAN1: spinocerebellar ataxia with axonal neuropathy
SCC1: SCC1 homolog
SENP: SUMO-specific protease
Seq: sequencing
SET2: SET domain containing 2
SIM: SUMO-interacting motif
siRNA: small interfering RNA
SIRT: sirtuin
SLX: SLX structure-specific endonuclease subunit
SMARCA2: SWI/SNF related, matrix associated, actin dependent regulator of chromatin, subfamily A, member 2
SMG1: suppressor of mutagenesis in genitalia 1
Sp1: specificity protein 1
Spo11: sporulation protein 11
SR: serine arginine rich protein
SSA: single-strand annealing
SSB: single strand break
ssDNA: single strand DNA
SUMO1/2/3: small ubiquitin-related modifier-1, -2 or -3
suv39h1: suppressor of variegation 3-9 homolog 1
Suv4-20: suppressor of variegation 4-20 homolog 1
TALEs: transcription activator-like effectors
TBP: TATA box binding protein
tBRCT: tandem BRCT domains
TC-DSB: transcription-coupled DSB
TCR: transcription-coupled repair
Tdp1: tyrosyl-DNA phosphodiesterase 1
TERT: telomerase reverse transcriptase
TF: transcription factor

TIP: type 2A-interacting protein
Tip60: tat interacting protein, 60kDa
TOBP1: topoisomerase-binding protein 1
Top1: topoisomerase I
Top1cc: Top1 cleavage complexes
Top2: topoisomerase II
Topors: topoisomerase I-binding RS proteins
TRF1/2: telomere repeat factor 1 / 2
TRRAP: transformation/transcription domain-associated protein
TSS: transcription start site
TTF2: transcription termination factor, RNA polymerase II
tTudor: tandem Tudor domains
Ub: ubiquitin
UBA: ubiquitin-like modifier activating enzyme
Ubc: uquiquitin-containing enzyme
UBD: ubiquitin-binding domains
UBE: ubiquitin-conjugating enzyme
UBLs: ubiquitin-like proteins
UDR: ubiquitylation-dependent recruitment motif
UIM: motifs interacting with ubiquitin domain-related ubiquitin-binding domain
UNG: uracil-DNA glycosylase
UPS: ubiquitin-proteasome system
USP: ubiquitin-specific protease
UV: ultraviolet
VCP/p97: valosin containing protein
WIP1: wild-type P53-induced phosphatase 1
WRN: Werner syndrome, RecQ helicase-like
WSTF: Williams syndrome transcription factor
XLF: XRCC4-like factor
XPA/B/C/D/F/G: xeroderma pigmentosum group-A/B/C/D/F/G complementing protein
XRCC: X-ray repair cross-complementing protein
ZFNs: site-specific zink-finger
Zn1/2: zinc finger domain 1 / 2
γH2AX: H2AX phosphorylated

ILLUSTRATION TABLE

FIGURES

TABLES

INTRODUCTION

CHAPTER I: Inhibition of Topoisomerase I and transcription

I.1 DNA Topoisomerases

DNA topoisomerases are ubiquitous and highly conserved enzymes that relax DNA (Champoux, 2001; Schoeffler and Berger, 2008; Wang, 2002).

DNA topoisomerases are molecular machines that regulate the topological state of the DNA in the cell. The interest in DNA topoisomerases in recent years derives not only from the recognition of their crucial role in managing DNA topology, but also from the wide variety of topoisomerase-targeting drugs that have been identified. These topoisomerase poisons include both antimicrobials and anticancer chemotherapeutics, some of which are approved by US Food and Drug Administration (FDA) to treat human cancers or infectious diseases.

Human somatic cells encode six topoisomerases (**Table 1**). A seventh topoisomerase is Spo11 but its expression is restricted to germ cells (Bergerat et al., 1997). Bacteria tend to have a simpler organization, with only four topoisomerases in *Escherichia coli* (Pommier et al., 2010).

All topoisomerases cleave the DNA phosphodiester backbone by nucleophilic attack from a catalytic tyrosine residue that becomes transiently linked to the phosphate end (P-Y) of the DNA break. On the base of the number of strand cleaved (I, II) and the polarity of the cleavage, DNA topoisomerases are divided into different classes and subfamilies.

Table 1: Classification of human topoisomerases*

Type	Polarity	Mechanism	Genes	Proteins	Drugs
IA	5'-PY	Strand passage	TOP3A TOP3B	Top3α Top3β	none none
IB	3'-PY	Rotation	TOP1 TOP1MT	Top1 Top1mt	anticancer none
IIA	5'-PY	Strand passage ATPase	TOP2A TOP2B	Top2α Top2β	anticancer anticancer

*(Pommier, 2013)

Topoisomerases that cleave only one strand of the DNA are defined as type I. In particular, if the protein is attached to the 5’ phosphate of the DNA (5’ P-Y), it is a type IA subfamily member. If it is attached to the 3’ phosphate (3’ P-Y), the enzyme is a type IB subfamily member. Moreover, these enzymes also differ for their catalytic mechanisms. Type IA topoisomerases work by passing one strand through the single-strand break (SSB) generated by the enzymes (Viard and de la Tour, 2007) (**Figure 1**). These topoisomerases are able to relax highly negatively supercoiled substrates and to efficiently unknot and decatenate DNAs containing single-stranded regions or nicks (hemicatenanes and double-holiday junctions) (Wu and Hickson, 2003). Type IB topoisomerases

use a “controlled rotation” mechanism by letting the broken strand rotate around the intact one (see section *I.2.3*) (Champoux, 2001) (**Figure 1**). These enzymes catalyse the relaxation of both negatively and positively supercoiled DNAs (Koster et al., 2005).

In humans, topoisomerases 3α and 3β (Top3α, Top3β) belong to type IA subfamily whereas the nuclear topoisomerase I (Top1) and the mitochondrial topoisomerase I (Top1mt) are members of the type IB subfamily (**Table 1**).

Topoisomerases that cleave both strands to generate a double-strand break are grouped together in the type II family of topoisomerases. Type II topoisomerases are multi-subunit enzymes, and form double-strand breaks with enzyme subunits covalently linked to 5’ ends at the DNA cleavage site. The enzymes work by passing a second DNA duplex through the cleavage of the first DNA segment with a mechanism dependent on ATP and Mg^{2+} (Liu et al., 1983; Nitiss, 2009) (**Figure 1**). Those topoisomerases act as full decatenases, unlinking pre/catenanes, interlinked DNA products of replication (Nitiss, 2009). Type IIA topoisomerases are widespread in nature. Topoisomerase 2α and 2β (Top2α, Top2β) are the human type IIA topoisomerase (**Table 1**). Type IIB enzymes are confined to Archaea, plants, and some algae.

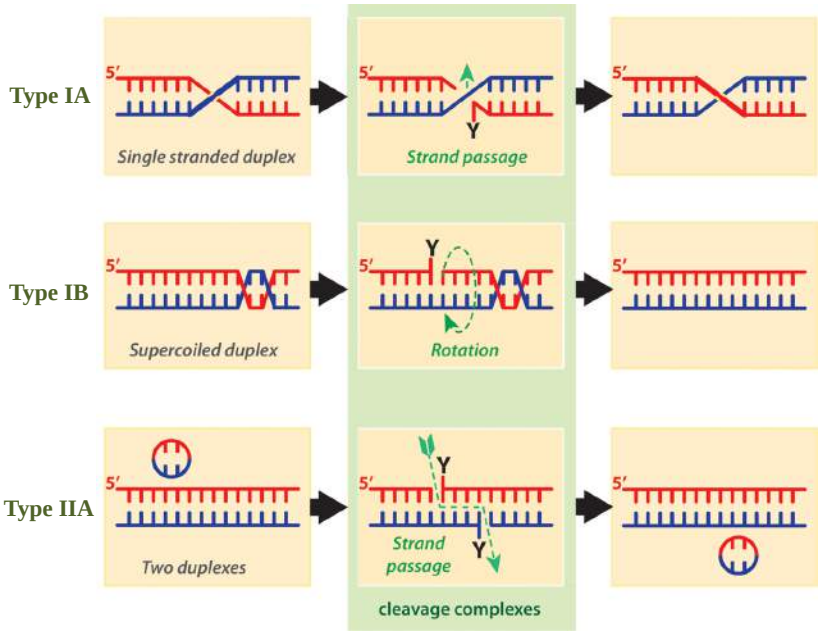

Figure 1: Different catalytic mechanisms of topoisomerases. Type IA and IIA enzymes act by strand passage with one single-strand break or one double-strand break, respectively. Type IB acts by controlled rotation. (Pommier, 2013)

I.2 Human DNA Topoisomerase I (Top1)

All eukaryotes harbor at least one type IB topoisomerase (Top1). Top1 is a nuclear enzyme, which is essential in vertebrates and in *Droshophila* (Lee et al., 1993) but not in yeast (Goto and Wang, 1985; Uemura and Yanagida, 1984), probably because it can be substituted by other topoisomerases. Top1-null mouse embryos fail to develop (Morham et al., 1996). Cell lines expressing low levels of Top1 exist, for example the murine cell line (p388/CPT45) selected for resistance to camptothecin (CPT) (Eng et al., 1990; Tuduri et al., 2009) or the human cancer cell lines stably expressing siRNA against Top1 (HCT116-siTop1 and MCF-7-siTop1) (Miao et al., 2007). Features of those cells are genomic instability, replication defects and altered gene expression (Miao et al., 2007; Tuduri et al., 2009).

Top1 expression is constitutive throughout the cell cycle, similar in cycling and non-cycling cells (Baker et al., 1995). Although it is expressed throughout the nucleus, it is enriched in the nucleolus where it supports high rate of ribosomal DNA (rDNA) transcription (Muller et al., 1985; Zhang et al., 1988).

I.2.1 Structural domains of Top1

The human TOP1 gene is located on chromosome 20q11.2-13.1 and encodes a 91 kDa protein that has been subdivided into four distinct domains (**Figure 2**) (Champoux, 1998; Pourquier and Pommier, 2001; Stewart et al., 1996):

- *N-terminal domain*: It is composed of 214 amino acids and it is the most variable region. This domain is dispensable for relaxation activity *in vitro*. It contains four putative nuclear localization signals, from which only two are functional (Mo et al., 2000). This domain also possesses sites for interaction with other cellular proteins such as nucleolin, SV40 T-antigen, certain transcription factors (TF), p53 and WRN (Werner syndrome, RecQ helicase-like).
- *Core domain*: Constituted by 421 amino acids, it is a conserved domain that is required for enzyme activity. It contains all the residues required for the catalytic activity of Top1 except the active site tyrosine. It can be divided into three subdomains (I, II, III).
- *Linker domain*: It is composed of 77 amino acids and it is dispensable for enzyme activity. It connects the core domain to the C-terminal domain.
- *C-terminal domain*: It possesses 53 amino acids. It is the most conserved domain and it contains the active site T723, which covalently binds to DNA end it is essential for relaxation activity of Top1.

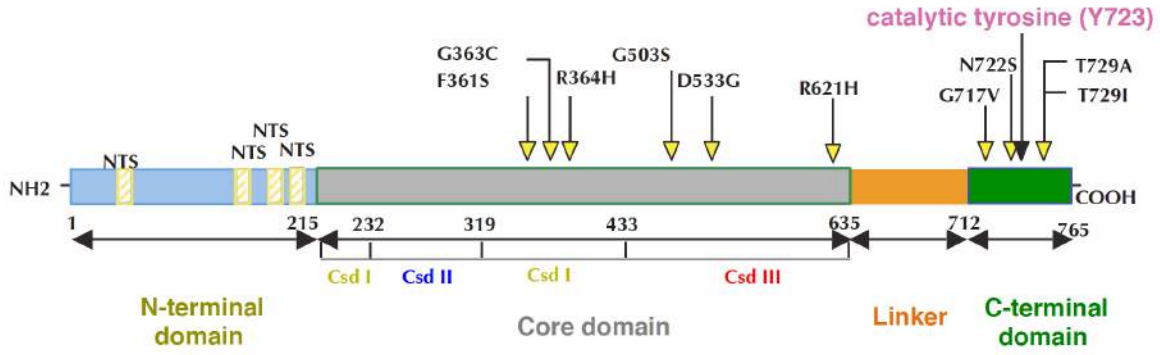

Figure 2: Schematic of Top1 domains. The four main domains of Top1 and catalytic tyrosine (pink) are illustrated. NTS indicates the nuclear translocation signals. Arrows correspond to Top1 mutations that are responsible for resistance to Top1 inhibitors (see section *I.4.1* for details). Adapted from (Pourquier and Lansiaux, 2011).

Several crystal structures of different fragments of the human Top1 covalently or not covalently bound to DNA are available (Lesher et al., 2002; Redinbo et al., 2000; Redinbo et al., 1998; Stewart et al., 1998). These structures show that Top1 is a bi-lobed protein that tightly encircles the DNA like a clamp (**Figure 3**). One of the lobes represents the "cap" of the protein and it comprises core subdomains I and II. Core subdomain III and the C-terminal domain constitute the second lobe that forms a base around the DNA. The two lobes are connected by a long α-helix ("connector"). The "lips" are pairs of opposing loops positioned on the opposite side to the connector: they allow non-covalent interactions of the cap with the base of the protein. The break of this interaction and lifting of the cap results in the opening and closing of the protein clamp during the catalytic cycle. Finally, the linker domain forms a coiled-coil structure protruding from the base of the protein (Champoux, 2001; Redinbo et al., 2000).

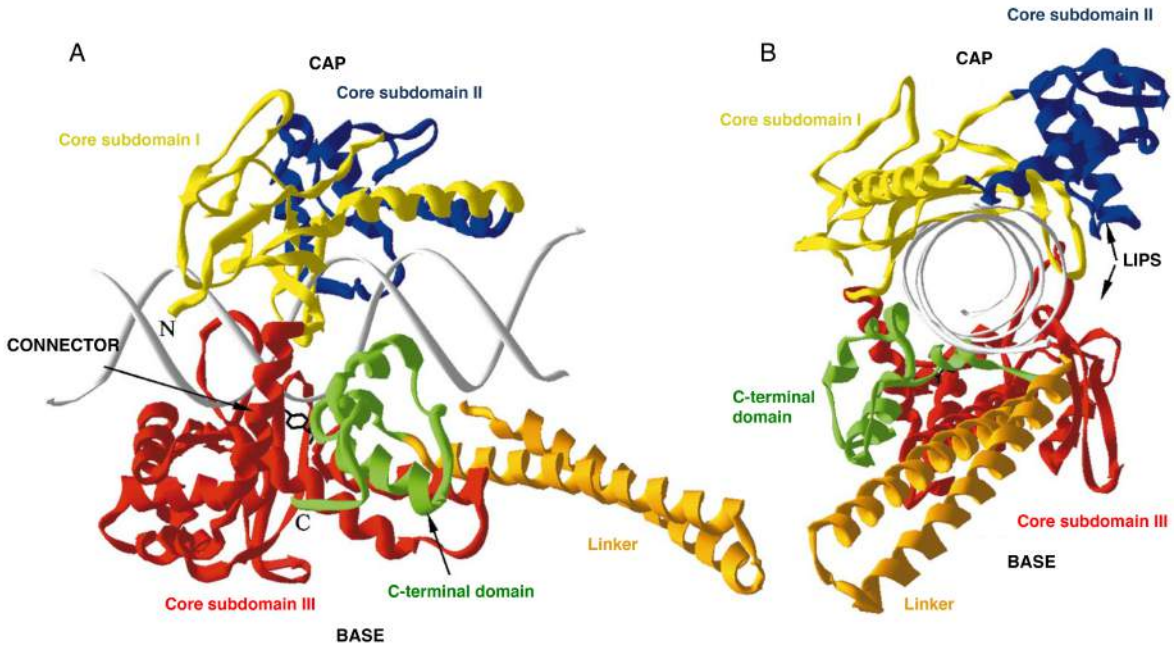

Figure 3: Two views of the structure of the human Top1 non-covalently complexed with DNA. The structure of the enzyme (PDB entry 1A36) is viewed from the (**A**) side with the DNA axis horizontally oriented and (**B**) looking down the axis of the DNA. The N-terminal domain is missing from the structure. The cap is composed of core subdomain I (yellow) and core subdomain II (blue). The base is composed of core subdomain III containing the long α-helix connector (red) and the C-terminal domain (green) containing the active site tyrosine represented in (A) in black and ball stick. The linker forms a coiled-coil structure protruding from the base (gold). Lips are indicated in (B) and they are the regions where the protein opens during DNA binding and unbinding. Adapted from (Champoux, 2001).

I.2.2 Substrate specificity

The substrate specificity of Top1 has been determined in relation to both DNA sequence and DNA structure. A preference was observed for nucleotides that extend from positions -4 to -1, 5'-(A/T)(G/C)(A/T)T-3' with the enzyme covalently attached to the -1 thymine residue (Been et al., 1984; Bonven et al., 1985; Tanizawa et al., 1993). Occasionally a cytosine residue is found at the -1 position.

Based on structural data, the only identified contact Top1-DNA is the interaction by hydrogen-bond between K532 of the Top1 and the oxygen in position 2 of the thymine base located at the -1 position (Redinbo et al., 1998). It appears that additional protein-DNA interactions play an important role in cleavage site selection (Champoux, 2001).

Several studies reveal that Top1 has a preference for binding to double-stranded DNA (Been and Champoux, 1984) and most efficiently supercoiled over relaxed DNA *in vitro* (Camilloni et al., 1988; Madden et al., 1995; Muller, 1985). Since the enzyme preferentially binds to positive and negative supercoiled DNA, it seems likely that the structural feature recognized by Top1 in the DNA is a bent DNA segment. Alternatively, the enzymes may recognize the node where two duplexes cross; this is the case of replication (Zechiedrich and Osheroff, 1990).

I.2.3 Catalytic cycle

The catalytic cycle of Top1 can be divided in four steps (Pommier et al., 1998; Pourquier and Pommier, 2001) (**Figure 4**):

1) *Non-covalent DNA binding.* Top1 non-covalently binds DNA at preferred sites (see section *I.2.2*). Before binding, the enzyme is in an open conformation, with the cap and the catalytic Y723 spreading apart. As Top1 binds to DNA, these domains adopt the clamp configuration around the duplex (Redinbo et al., 1998). The binding footprint is approximately 20 bp (base pair) with the cleavage site centrally located (Stevnsner et al., 1989).

2) Cleavage of one strand of the DNA duplex: DNA and Top1 are covalently linked by transesterification between the hydroxyl group of the catalytic tyrosine (Y723) and the phosphate of the DNA strand (Champoux, 1981). These DNA-Top1 covalent complexes are referred to as "Top1 cleavage complexes" (Top1cc).

3) *Controlled rotation*: Top1 relaxes supercoiled DNA changing its linking number, a parameter indicating the number of times the two helical strands are interwound, by step of one. To relax DNA, the enzyme allows the rotation of the broken strand around the intact one. A "controlled rotation" mechanism has been proposed on the base of biochemical and structural data indicating that the structural domains of the Top1 likely control over the rate of rotation (Stewart et al., 1998). In fact, rotation is slowed by contacts of DNA with the inner cavity of the enzyme and with the linker.

4) *Religation*: Top1 religates the single-strand break by reversing its covalent binding in the absence of energy cofactors. This transesterification reaction occurs between the free 5'-OH of the broken strand that mediates the nucleophile attack and the Top1-DNA bond. Religation requires the alignment of the 5' end of the cleaved strand with the tyrosine-DNA bond. Under normal conditions, Top1cc are transient as religation is favoured (Pourquier and Pommier, 2001).

The catalytic cycle of Top1 is very fast, up to 6000 cycles per minute (Seol et al., 2013).

Top1 can also religate exogenous DNA strands harbouring a 5'-OH free end (Christiansen et al., 1993; Christiansen and Westergaard, 1994; Pourquier et al., 1997a). Misalignment of the 5'-OH with the scissile-phosphodiester bond by drugs or by DNA modification results in stabilized Top1cc (see section *I.4*) and increases the probability of illegitimate recombination (Christiansen et al., 1993; Christiansen and Westergaard, 1994; Pourquier et al., 1997a).

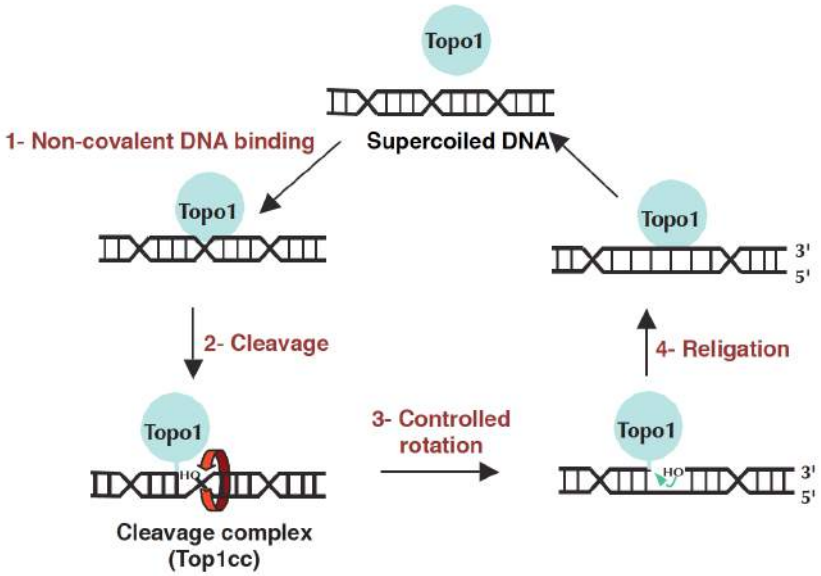

Figure 4: Topoisomerase I catalytic cycle. DNA relaxation by Top1 can be divided in four steps: 1) Non-covalent DNA binding, 2) Cleavage of one DNA strand, 3) Relaxation by controlled rotation and 4) Religation. See text for details. Figure adapted from (Pourquier and Lansiaux, 2011).

I.3 Biological functions of Top1

I.3.1 Relaxation of DNA supercoiling during transcription and replication

The main function of Top1 is to relax DNA supercoiling generated during transcription and replication (Champoux, 2001; Wang, 2002). In normal relaxed B-DNA, each strand crosses the other once every 10.4 bp with a right-handed turn, therefore DNA twisted in a right-handed fashion generates positive supercoiling (crossing < 10.4 bp) whereas DNA twisted in a left-handed fashion (crossing > 10.4 bp) generates negative supercoiling (Wang, 2002).
Top1 is efficient to relax both positively and negatively supercoiled DNA with a preference for positive supercoiling (Koster et al., 2007; McClendon and Osheroff, 2006; Wang, 2002).

Replication

As the replication fork advances during replication, the replication machinery forces the helical interwines of the DNA ahead of it and DNA becomes overwound; behind the advancing fork, the replicated bubble becomes progressively larger (Wang, 2002). If the replication machinery is allowed to rotate around the helical axis of the unreplicated DNA, positive supercoils ahead of the ongoing fork are redistributed into the region behind it, leading to the intertwining of the pair of duplicated double helix (Wang, 2002). However, because of the size of replication machinery, it is

plausible that this complex does not rotate freely around DNA helix consequently leading to positively supercoiled DNA upstream of the replication fork.

Not surprisingly, in the absence of Top1, replication forks are slower (0.7 kb/min in HCT116 shTop1 cells compared to 1.1 kb/min in HCT116 shControl cells) and pause or stall more frequently (Tuduri et al., 2009).

Transcription

Similarly to replication, during transcription elongation, the transcription complex cannot continuously rotate around the DNA helix, which forces the DNA strand to rotate around its own helix axis. As a result, positive supercoiling accumulates ahead of the advancing transcriptional complex, and negative supercoiling behind it. This is the "twin-supercoiled-domain" model proposed by *Liu* and *Wang* in 1987 (Liu and Wang, 1987) and further supported by several studies (Cook et al., 1992; Leng and McMacken, 2002; Lodge et al., 1989; Lynch and Wang, 1993). Left unresolved, this supercoiled DNA can impact transcription in different ways (Blot et al., 2006; Drolet, 2006; Gartenberg and Wang, 1992; Peter et al., 2004). For instance, high levels of positive supercoiling can inhibit transcription (Drolet, 2006; Gartenberg and Wang, 1992) whereas negative supercoils may enhance transcriptional initiation at promoters either by helping RNA Polymerase (RNAP) to form an open complex or by helping to recruit transcription factors (Hatfield and Benham, 2002; Ma and Wang, 2014; Mizutani et al., 1991a; Mizutani et al., 1991b). In addition, negative supercoiling favours the formation of R-loop (Drolet et al., 1994; Drolet et al., 2003; Higgins and Vologodskii, 2015) and non-B DNA structures such as Z-DNA (Nordheim et al., 1982), both affecting transcription (see section *I.5.2.5*).

By removing DNA supercoiling, Top1 is required for proper transcription. This may explain why Top1 has been found to bind and cleave preferentially transcribing genes (Gilmour et al., 1986; Khobta et al., 2006; Kroeger and Rowe, 1992; Stewart et al., 1990; Zhang et al., 1988). Despite its important role in transcription, works in yeast indicate that neither Top1 nor Top2 are essential for RNAPII transcription, while ribosomal RNA synthesis is highly reduced in the absence of both enzymes (Brill et al., 1987).

Another source of torsional stress is nucleosome remodelling in active transcribed regions and Top1 has been implicated in. It has been shown that either Top1 or Top2 is required for efficient transcription of a chromatin template, but not for *in vitro* transcription of naked DNA (Mondal and Parvin, 2001; Mondal et al., 2003). Interestingly, repression of transcription was detected without topoisomerases when RNA transcripts were above 200 bp (Mondal et al., 2003). Evidences in literature suggest that Top1 can affect gene expression through regulation of chromatin structure

and histone modifications. For example, a genome-wide analysis in *S. pombe* reveals that topoisomerase activity promotes transcription by modulating histone density. Indeed, absence of Top1 and Top2 leads to higher H3 occupancy in the promoter regions of highly transcribed genes correlating with reduced RNAPII occupancy and reduced expression profile (Durand-Dubief et al., 2010). Negative supercoiling left by transcribing RNAP favours nucleosome incorporation. Thus, authors suggested a function of Top1 (in concert with the chromatin remodeller Hrp1) in maintaining a low histone density at promoters to allow for efficient RNAPII recruitment. In addition, Top1-Top2 double mutants exhibit increased transcriptional levels in the 3' transcription terminator region of the genes compared to wild-type (Durand-Dubief et al., 2011). These findings indicate that Top1 activity also controls supercoiled DNA at 3' end of the genes thereby contributing to nucleosome disassembly and transcriptional termination. **Figure 5** illustrates the model proposed by the authors for the function of Top1 and Top2 in regulating DNA topological state and chromatin structure during transcription initiation, elongation and termination (Durand-Dubief et al., 2011). Oppositely to this report, another work shows that Top1 activity negatively regulates transcription at telomere-proximal regions in *S. cerevisiae* by favouring a repressed chromatin organization (Lotito et al., 2008).

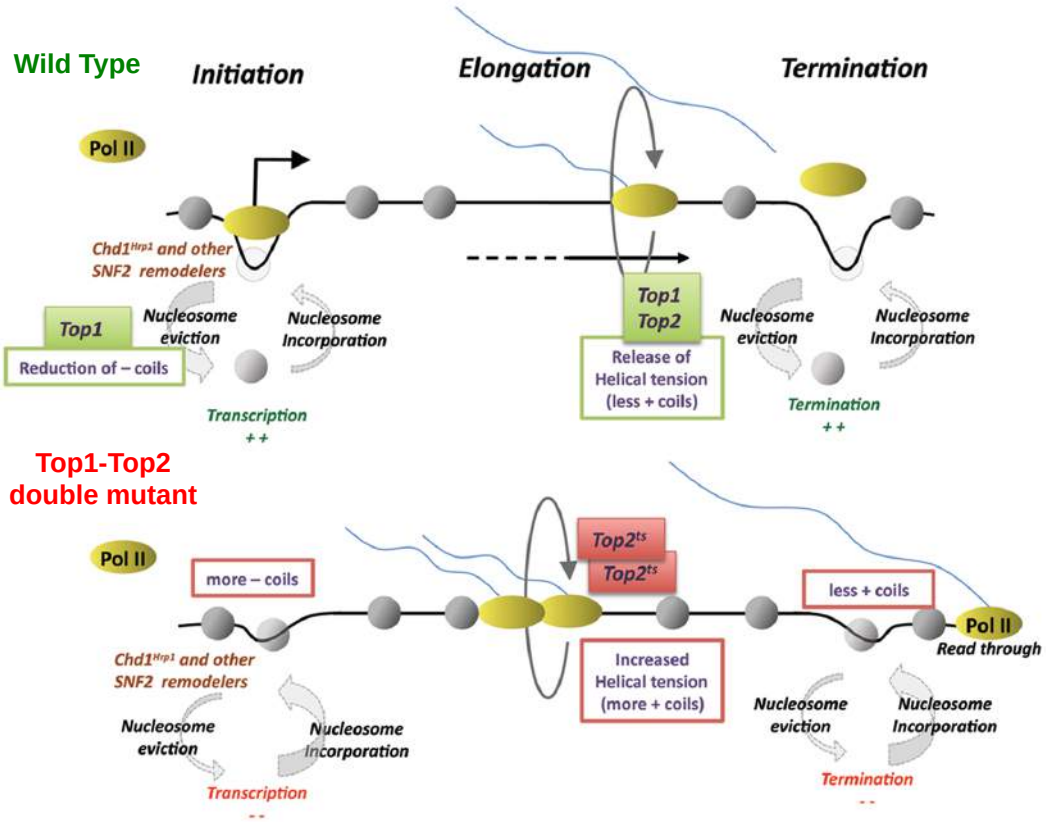

Figure 5: Model of transcriptional regulation in all steps by Top1 and Top2 activity. In the initiation phase and pre-initiation complex formation, Top1 removes negative supercoils facilitating nucleosome disassembly at promoter. In the elongation phase, Top1 and Top2 act in concert to resolve topological tension generated by ongoing RNAP as predicted by the "twin-supercoiled-domain" model. Then in transcription termination, topoisomerase activity is required for histone disassembly and transcription termination (Durand-Dubief et al., 2011).

Top1 regulates transcription also by acting at enhancer regions (Puc et al., 2015; Rosenberg et al., 2013). The main mechanism by which enhancers are thought to regulate transcription is through DNA looping that brings distant enhancers in contact with promoters (Lam et al., 2014). Enhancers are also transcription units that can generate noncoding RNA transcripts identified as eRNAs (enhancer RNAs) (De Santa et al., 2010). eRNAs appear to be functionally important for the proper formation of chromosomal looping between enhancers and transcription start site (TSS) of regulated genes (Lam et al., 2014). DNA looping and eRNA transcription are potential source of topological stress. First evidences of Top1 involvement on enhancers' regulation come from chromatin immunoprecipitation experiments (ChIP) showing an enrichment of Top1 at the β-globulin locus control region (LCR) (Rosenberg et al., 2013). Then, ChIP-Seq (ChIP-sequencing) analysis reveals that Top1 is rapidly recruited to several AR (androgen receptor)-regulated enhancers in prostate cancer cells (Puc et al., 2015). Top1-depleted cells or cells complemented with a catalytically inactive Top1 mutant exhibit reduced production of eRNAs and coding gene RNAs for most of these AR-regulated genes. Authors showed that Top1 recruitment to enhancers occurs at the same regions of AR in proximity of TSS and causes a SSB that is necessary for eRNA synthesis and enhancer activation. This study identifies a novel function of Top1 dependent on its catalytic activity in the control of the cell-specific transcriptional program by ligand-driven enhancer activation (Puc et al., 2015).

I.3.2 Transcriptional roles of Top1 independent of its nicking-closing activity

Top1 regulates transcription independently of its nicking-closing activity by acting in concert or by interacting with transcriptional activators and general transcription factors. Non-canonical Top1 functions include:

- *Activation/repression of transcription:*

In vitro studies show that Top1 is able to either repress basal transcription as well as to co-activate transcription (Kretzschmar et al., 1993; Merino et al., 1993; Shykind et al., 1997). Top1 seems to activate transcription by enhancing the formation of the TFIID-TFIIA-DNA complex at promoters (Shykind et al., 1997). This function of Top1 does not require its nicking-closing activity since a catalytically inactive Top1 mutant can stimulate transcription as the wild type.

- *Recruitment of RNAP:*

Top1 may also favour the recruitment of RNAPII at transcription sites either directly by its ability to bind the C-terminal region of Rpb1 (Carty and Greenleaf, 2002; Rose et al., 1988) or indirectly by interacting with Topors (topoisomerase I-binding RS proteins), small nuclear RING-finger

proteins harbouring E3 ubiquitin- and SUMO1 (small ubiquitin-related modifier-1)- ligase activities (Haluska et al., 1999). A similar model has been proposed for RNAPI recruitment at transcriptionally active ribosomal genes either by its direct interaction with Top1 (Rose et al., 1988) or nucleolin (Bharti et al., 1996).

- *RNA splicing:*

In higher eukaryotes, Top1 has a specific kinase activity and it can phosphorylate splicing factors such as SR proteins (serine/arginine-rich protein, like ASF/SF2) (Rossi et al., 1996), thus promoting the formation of messenger ribonucleoprotein particles (mRNPs) and the maturation of nascent RNA (Rossi et al., 1996; Soret et al., 2003). The interaction between Top1 and ASF/SF2 seems to inhibit Top1 relaxation activity (Andersen et al., 2002). Top1 has also been reported to interact with PSF (protein-associated splicing factor), a co-factor of RNA splicing, which in complex with the RNA-binding protein p54 stimulates Top1 relaxing activity (Straub et al., 1998). In *Drosophila*, Top1 associates with and phosphorylates the SR protein B52 (Juge et al., 2010). This interaction is important to target Top1 to RNAPII-active chromatin loci. Furthermore, a proteomic analysis of Top1-containing complexes reveals that 10 out of the 36 proteins identified as Top1 partners are involved in RNA splicing (Czubaty et al., 2005).

- *Suppression of transcription-associated replication stress:*

A function of Top1 in mammalian cells, which is dependent on both its nicking-closing activity and its kinase activity, is to suppress the transcription-associated replication stress in an ASF/SF2-dependent manner (Tuduri et al., 2009). Top1 and mRNPs biogenesis avoid interference between replication and transcription and the formation of R-loop-mediated genome instability in S-phase (Tuduri et al., 2009).

I.3.3 Roles of Top1 in DNA damage signalling/repair

As Top1 can be trapped by a number of DNA modifications (see section *I.4.2*), it has been speculated that Top1 could play a role in DNA damage signalling and/or repair in response to DNA lesions. For instance, ultraviolet (UV) -induced DNA damage stimulates Top1cc formation *in vivo* (Subramanian et al., 1998). The authors suggested that UV-induced Top1cc may result from (i) cyclobutane pyrimidine dimers (CPD) and photoproducts, which alter the DNA local conformation causing a misalignement of the 5' broken end impeding the religation step or (ii) active recruitment of Top1 at DNA lesions. Two hypothesis, mutually not exclusive, have been proposed for the possible roles of trapped Top1 at DNA lesions (reviewed in (Leppard and Champoux, 2005; Pourquier and Lansiaux, 2011)):

1) Targeting repair proteins to DNA damage:

Top1 may act as a "sensor" of DNA damage, which recruits repair proteins to damaged chromatin. Accordingly with this possibility, *Mao et al.* show Top1's involvement in nucleotide-excision repair (NER) (Mao et al., 2000a). Indeed, the repair of UV lesions and the recruitment of the NER factor PCNA (proliferating cell nuclear antigen) are reduced in Top1 depleted cells. Another evidence suggesting a role of Top1cc in DNA repair is its ability to interact with DNA damage response proteins (DDR) such as p53 (Albor et al., 1998; Mao et al., 2000a; Smith and Grosovsky, 1999) and PARP1 (Poly [ADP-ribose] polymerase 1) (Czubaty et al., 2005; Drew and Plummer, 2009). In particular, the interaction of Top1 with p53 stimulates Top1 catalytic activity and Top1 recruitment at UV-induced lesions (Mao et al., 2000a). Finally, a recent report shows that the recruitment of Top1 at AR-regulated enhancers is kinetically accompanied by the recruitment of the MRN complex (Mre11-Rad50-Nbs1 complex, see section *II.5.1.1*) and ATR (ataxia telangiectasia and Rad3-related protein, see section *II.3.2*), followed by additional components of the DDR (Puc et al., 2015).

2) Induction of apoptosis:

Top1 may promote apoptosis when DNA damage persists and cannot be repaired. Accordingly with this hypothesis, Top1 depletion reduces some apoptotic nuclear features and it has been suggested that Top1 might act as a nuclear effector of apoptosis (see section *I.4.3*). Furthermore, the association of Top1 trapped at UV-lesions with p53 might support a possible role for Top1 in the p53-dependent apoptosis in response to DNA damage (Mao et al., 2000a).

I.4 Trapping of Top1

Despite their frequency throughout the genome, in physiological conditions, Top1cc are extremely transient and almost undetectable. These complexes can be stabilized generally by 5'-OH DNA-end misalignment that prohibits religation. Top1cc can be stabilized by camptothecins and non-campthotecins Top1 inhibitors (Pommier, 2006; Pommier, 2013), by DNA alterations (Pommier et al., 2006), by ribonucleotide misincorporation (Kim et al., 2011) and during apoptosis (Sordet and Solier, 2012).

I.4.1 Trapping of Top1 by Top1 inhibitors

Camptothecin and Camptothecin-like Top1 inhibitors

Camptothecin (CPT) and CPT-like inhibitors block the religation step of the Top1 catalytical cycle.

More precisely, they inhibit the second transesterification reaction (Hsiang et al., 1985) (**Figure 6A**). CPT is an alkaloid compound isolated from the bark of the Chinese tree *Camptotheca acuminata* in 1966 (Wall, 1966). CPT was tested clinically in the 1970s, showing anticancer activity and SSB induction that rapidly disappear as the drug is removed (Gottlieb et al., 1970; Horwitz et al., 1971; Kessel, 1971; Kessel et al., 1972; Muggia et al., 1972; Spataro and Kessel, 1972). However, the severe side effects discouraged the clinical development. The discovery that Top1 is the cellular target of CPT came 10 years after (Eng et al., 1988; Hsiang et al., 1985; Nitiss and Wang, 1988) and led to the development of CPT derivatives.

A key feature of CPT is that Top1 is its only cellular target (Pommier, 2006; Pommier et al., 2010): (i) only the natural 20-S enantiomer is active (Hsiang et al., 1989b; Jaxel et al., 1989), (ii) yeasts deleted for TOP1 (Top1Δ) are completely resistant to CPT (Eng et al., 1988; Nitiss and Wang, 1988), (iii) cells selected for CPT resistance bear single point mutations in the TOP1 gene (Pommier et al., 1999), (iv) plants producing CPT harbour a point mutation in TOP1 gene (Sirikantaramas et al., 2008) that renders Top1 refractory to the drug (Fujimori et al., 1995). Chemically, CPT is a 5-ring heterocyclic containing a α-hydroxylactone within its E-ring (**Figure 6A**).

Mechanistically, CPT traps Top1cc by docking at the enzyme-DNA interface (**Figure 7A**). Hence, it represents a paradigm for "interfacial inhibitors" (Jaxel et al., 1991; Marchand et al., 2006). The formation of this ternary complex (DNA-CPT-Top1) was initially suggested by DNA-sequencing experiments (Capranico and Binaschi, 1998; Capranico et al., 1990; Jaxel et al., 1991; Pommier et al., 1991) and by the stereospecific nature of CPT activity. Then, it was confirmed by crystallographic data (Ioanoviciu et al., 2005; Staker et al., 2005; Staker et al., 2002). CPT binds simultaneously both to DNA by hydrophobic stacking interaction and to Top1 by three hydrogen bonds involving R364, D533 and N722 (Marchand et al., 2006). CPT traps only a subset of Top1cc, those with a thymine at the -1 position and a guanine at the +1 position (Jaxel et al., 1991). Another key feature of CPT is the reversible nature of its binding to Top1cc (Covey et al., 1989).

Some of the characteristics that render CPT a powerful pharmacological tool are also the causes of its clinical limitations (Pommier, 2006; Pommier, 2013; Tomicic and Kaina): (i) long infusions as Top1cc are rapidly reverted upon drug removal, (ii) chemical instability due to its inactivation at physiological pH by lactone E-ring opening (**Figure 6A**), (iii) relatively low potency and despite its selectivity, CPT has to be applied at µM concentration, (iv) dose-limiting side effects because of the destruction of bone narrow progenitors, (v) cross-resistance in cells expressing the drug efflux membrane ABC transporters.

Three water-soluble CPT derivatives are approved for clinical use: topotecan, irinotecan and

belotecan (in South Corea) (**Figure 6A**). Topotecan is approved for ovarian cancer and recurrent small cell lung cancer. Irinotecan, which is a prodrug converted to its active metabolite SN-38 by plasma and cellular carboxylesterases, is used in colon and rectal cancer. Both drugs are also used in glioblastomas, sarcomas and cancer of the cervix (Pommier, 2013).

Different modifications of CPT and water-soluble CPT derivatives have been produced to improve solubility, clinical tolerability and allow oral administration (such as gimatecan, lurtotecan and exatecan). Two approaches have been used to overcome the chemicals instability of CPTs: the addition of a methylene group as in homocamptothecins (Lavergne et al., 1998) or the substitution of the E-ring with a five-member ring as S39625 (Takagi et al., 2007).

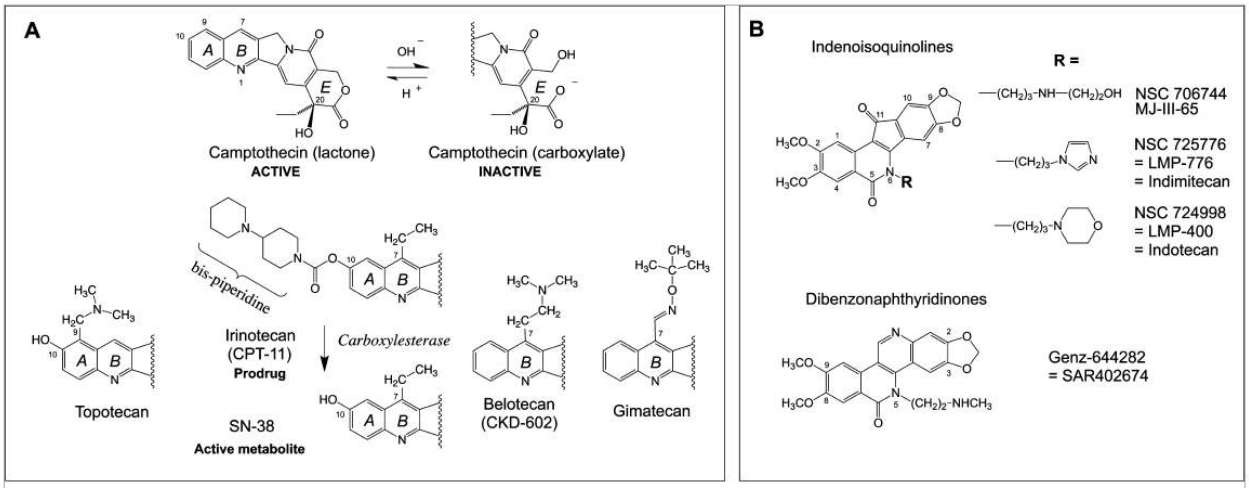

Figure 6: Structures of some Top1 inhibitors. (**A**) Camptothecins. (**B**) Non-camptothecin Top1 inhibitors in clinical trials. Adapted from (Pommier, 2013).

Non- Camptothecin Top1 inhibitors

After the discovery that Top1 is the selective target of CPT, the search for Top1 inhibitors not based on the structure of CPT began. Screening of chemical library and natural products led to the discovery of various compounds (Meng et al., 2003). There are three classes of non-CPT Top1 inhibitors (Teicher, 2008) (**Figure 6B**):

- Indolocarbazoles: Edotecarin reached Phase III clinical trials but like other indolocarbazoles, it has been found unselective (Urasaki et al., 2001)
- Phenanthridine derivatives: ARC-111 compound has been entered in Phase I clinical trials
- Indenoisoquinoline derivatives: they are selective for Top1, chemically stable, they trap Top1cc at different sites of CPT, they are not substrate of ABC transporters and they show the same antiproliferative activity of CPT (Antony et al., 2007a; Antony et al., 2003; Antony et al., 2005; Tanizawa et al., 1994). Indotecan (LMP400) and indimitecan (LMP776) are in Phase I clinical

trials.

Top1 catalytic inhibitors

Unlike Top1 poisons, catalytic inhibitors do not trap the Top1cc. They interact with free enzyme or with DNA impeding Top1 to bind or cleave DNA (for review see (Bailly, 2000)) (**Figure 7B**). Those inhibitors are generally unselective and they need to be used at elevated concentration (> 1 µM) (Pourquier and Lansiaux, 2011). Currently, there is no specific Top1 catalytic inhibitor known.

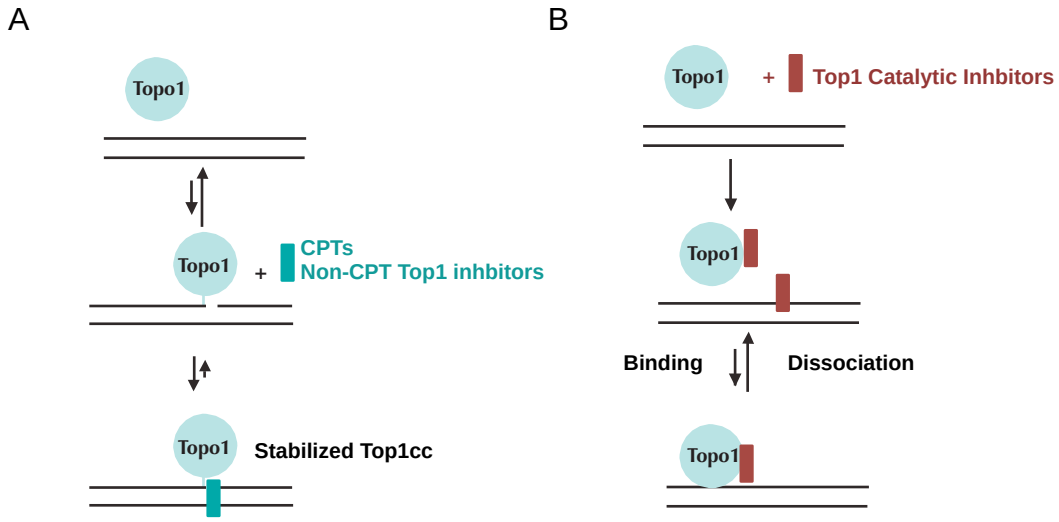

Figure 7: Mechanism of action of CPTs and non-CPT Top1 inhibitors and Top1 catalytic inhibitors. (**A**) CPTs and non-CPTs inhibitors trap Top1cc by blocking DNA religation. (**B**) Top1 catalytic inhibitors block the binding and/or the cleavage of DNA by Top1. Adapted from (Pourquier and Lansiaux, 2011).

I.4.2 Trapping of Top1 by DNA modifications

Top1 may encounter damage and alternative structures of DNA with high frequency by virtue of its abundant and ubiquitous nature. **Table 2** summarizes different lesions and DNA alterations from endogenous or exogenous sources that can trap Top1cc (reviewed in (Pommier et al., 2006; Pommier et al., 2014; Pourquier and Pommier, 2001)). Top1cc trapping is likely to be frequent and biologically important, in particular in neurons that are characterized by high oxidative metabolism and long transcripts (Huang et al., 2012; Powell et al., 2013). Spontaneous abasic sites have been estimated at a frequency of ≈ 10^4 per cell per day (Lindahl and Nyberg, 1972). The accumulation of Top1cc is generally associated to religation inhibition because of 5'-OH- end misalignment (see section *I.2.3*) but it can also be due to an enhancement of Top1 binding or of its cleavage reaction (Pommier et al., 2006). The localization of the DNA alteration is another parameter determining Top1 outcome (reviewed in (Pourquier and Pommier, 2001)). In general, single lesions at position

+1, +2 or +3 from the cleavage site lead to Top1cc accumulation whereas lesions at position -1, -2 and -3 (and to lesser extent abasic sites at -4, -5 and -6) suppress Top1-mediated DNA cleavage.

Moreover, DNA modifications can produce reversible or irreversible Top1cc. Irreversible Top1cc are constituted by a break on one or both strands in association with Top1 covalently bound to the 3' DNA-end. These complexes are termed "suicide complexes".

Recently, different works investigated a special form of abortive Top1cc related to the RNA nicking activity of Top1 (Kim et al., 2011; Sparks and Burgers, 2015; Williams et al., 2013). This endoribonuclease activity has been at first described *in vitro* (Sekiguchi and Shuman, 1997) and it consists in the conversion of a ribonucleotide embedded in cellular DNA into a 2'-3'-cyclic phosphate nick by Top1 (Kim et al., 2011; Sparks and Burgers, 2015). This activity of Top1 could represent an alternative repair pathway to RNaseH2 for misincorporated ribonucleotides during DNA replication. However, it can also promote genomic instability. The endoribonuclease activity of Top1 has been linked to Top1-mediated mutations in yeast by initiating short base deletions and by creating nicks or cyclic phosphate intermediates (Kim et al., 2011; Sparks and Burgers, 2015).

Table 2: Endogenous and exogenous factors able to produce Top1cc (Pommier et al., 2006)

Type of DNA modification	Mechanism[(a)]	Reversibility[(b)]	References
Endogenous factors			
Single base mismatches	T[(c)]	r[(f)]	(Pourquier and Pommier, 2001; Pourquier et al., 1997b)
Mismatched loops	T	ir[(g)]	(Pourquier et al., 1997b)
Abasic sites	T	Ir	(Pourquier et al., 1997b)
8-oxoguanosine	B[(d)]	R	(Lesher et al., 2002)
5-hydroxycytosine	?	R	(Lesher et al., 2002)
SSB	T	Ir	(Pourquier et al., 1997a; Wang et al., 1998)
Cytosine methylation	F[(e)]+T	R	(Leteurtre et al., 1994)
Triple helix formation	F+T	R	(Antony et al., 2004a)
Apoptotic chromatin fragmentation	B+T	Ir	(Sordet et al., 2003; Sordet et al., 2004a; Sordet et al., 2004b; Sordet et al., 2004c)
Exogenous factors			
UV lesions	?	?	(Lanza et al., 1996; Subramanian et al., 1998)
IR lesions	T	Ir	(Pourquier et al., 1997a)
O6-methylguanine	T	R	(Pourquier et al., 2001)
O6-dA-benzo[a]pyrene adducts	T	R	(Pommier et al., 2000b)
O6-dG-benzo[a]pyrene adducts	F	Ir	(Pommier et al., 2000a) (Pommier et al., 2002)
O6-dG-benzo[c]phenantrhrene adducts	T	R	(Pommier et al., 2002)
N6-Ethanoadenine	T	R	(Pourquier et al., 1998)
N2-dG-ethyl adducts	T	R	(Antony et al., 2004b)
N2-dG-crotonaldehyde adducts	T	Ir	(Dexheimer et al., 2008)

[(a)]Mechanism for Top1cc accumulation: [(c)]T, Inhibition of religation; [(d)]B, enhancement of binding; [(e)]F, enhancement of cleavage.
[(b)]Reversibility of Top1cc: [(f)]r, reversible; [(f)]ir, irreversible.

I.4.3 Trapping of Top1 during apoptosis

Top1cc are also stabilized in cells undergoing apoptosis. These complexes, referred to as "apoptotic Top1cc", have been described in different mammalian cell lines exposed to various apoptotic-inducing agents that do not have direct effect on Top1 (**Table 3**) (Ganguly et al., 2007; Rockstroh et al., 2007; Soe et al., 2004; Sordet et al., 2006; Sordet et al., 2008a; Sordet et al., 2004a; Sordet et al., 2004c). Apoptotic-Top1ccs are found on the genome with an average of approximately 1/100 kbp in early phases and 1/10 kbp in late phases of apoptosis (Rockstroh et al., 2007; Sordet et al., 2008a).

Table 3: Agents known to induce apoptotic Top1cc (Sordet and Solier, 2012)

Agents	Cellular target(s)	References
Etoposide **Doxorubicin** **m-AMSA**	Stabilization of Top2 cleavage complex	(Sordet et al., 2006)
Vinblatin **Taxol** **Colcemid**	Insertion at the interface of the tubulin heterodimer	(Sordet et al., 2006) (Rockstroh et al., 2007)
TRAIL	Activates the plasma memebran receptors DR4 DR5	(Rockstroh et al., 2007) (Sordet et al., 2008a)
Fas ligand	Activates the plasma membrane receptor Fas	
TNF-α	Activates the plasma membrane receptor TNFR1	
Antimycin **BH3I-2'**	BH3 mimetics that bind to and inhibit the antiapoptotic effect of Bcl-xL at the mitochondria	(Sordet et al., 2008a)
Arsenic trioxide	Induces the intracellular accumulation of ROS	(Sordet et al., 2004c)
Staurosporine	Inhibitor of protein kinases: Chk1, Chk2, PDK1, PKC	(Sordet et al., 2004a) (Ganguly et al., 2007; Sen et al., 2007)
UV radiation	Production of pyrimidine dimers, 4,6-photoproducts and oxidative DNA lesions	(Soe et al., 2004)

In the current model, the common mechanism to trap Top1cc during apoptosis is the ROS (reactive oxygen species)-dependent formation of oxidative DNA lesions (Sordet et al., 2006; Sordet et al., 2008a; Sordet et al., 2004a; Sordet et al., 2004b). Most apoptotic stimuli activate the apoptotic mitochondrial pathway and subsequently caspase-3, both responsible for ROS intracellular accumulation. Along with its contribution to ROS production, caspase-3 also cleaves Top1 generating an 80 kDa-truncated form that is still able to form Top1cc (Samejima et al., 1999) and rather it is the preferred form producing apoptotic-Top1cc (Sordet et al., 2008a).

Several studies, in particular experiments performed in cells depleted for Top1 (by siRNA or shRNA), show that Top1 participates in the execution of apoptosis by contributing to the apoptotic-associated nuclear modifications, such as nuclear fission, apoptotic body release and chromatin

condensation (Ganguly et al., 2007; Sordet et al., 2008a; Sordet et al., 2004a; Sordet et al., 2004c). Currently it is not clear if the role of Top1 in apoptosis is dependent or not on its catalytic activity.
Taken together these finding propose a role for Top1 in the apoptotic program. It remains to be elucidated if Top1 participates to apoptosis like an apoptotic endonuclease, if it functions amplifying the apoptotic process or if it contributes to the proper recognition and elimination of apoptotic cells (for review see (Sordet et al., 2003; Sordet et al., 2004b; Sordet and Solier, 2012)).

I.5 Cellular consequences of CPT-mediated trapping of Top1cc

The cellular consequences of CPT-mediated trapping of Top1 are related to (i) the induction of protein-linked DNA nicks (Covey et al., 1989) and (ii) the inhibition of Top1 activity and topological stress (Duann et al., 1999; Koster et al., 2007).
CPT-stabilized Top1cc are normally rapidly reversed, as CPT does not cause directly a misalignment of the 5'-OH DNA-end. Early experiments demonstrated that short exposures (less than 60 minutes in cell culture) to CPT are relatively non-cytotoxic (Holm et al., 1989; Horwitz et al., 1971; O'Connor et al., 1991). The cytotoxicity of CPT is not the direct consequence of Top1 inhibition, it is rather associated to the conversion of the reversible Top1cc into irreversible complexes and DNA damage after processing by replication and transcription machineries (Pommier, 2006). These observations are consistent with a time-dependent production of Top1-suicide complexes and cytotoxicity. The probability for forming irreversible Top1cc is enhanced by CPT treatment because Top1 religation activity is slowed down.
The relative contribution of DNA replication and transcription depends on CPT concentration, cell type and proliferation status. In highly proliferative cancer cells, replication-induced DNA damage (notably DNA double-strand breaks, DSBs, see section *I.5.1*) is the main responsible for cytotoxicity, which is achieved at low CPT doses (Holm et al., 1989). In contrast, transcription contributes to cytotoxicity at high doses of CPT in slowly and non-proliferating cells (Hsiang et al., 1989b; Huang et al., 2010). Exceptions are given by non-dividing neurons and lymphocytes that can be killed in a transcription-dependent manner at pharmacological concentrations (Morris and Geller, 1996; Stefanis et al., 1999).

I.5.1 Replicational consequences of CPT-mediated trapping of Top1cc

The two main replicational consequences of CPT-mediated stabilization of Top1cc are (i) inhibition of DNA synthesis and (ii) production of replication-coupled DSBs (RC-DSBs).

After CPT treatment, inhibition of DNA synthesis is intense (≥80%), rapid (within minutes) and persistent (up to 8h) after drug removal (Shao et al., 1999). The mechanisms leading to DNA duplication arrest may include: (i) collision between replication machinery and Top1cc that directly blocks fork progression (Snapka, 1986; Strumberg et al., 2000; Tsao et al., 1993), (ii) inhibition of thymidine kinase (Voeller et al., 2000) and (iii) S-phase checkpoint activation (Shao et al., 1999) (Seiler et al., 2007).

Top1cc can be converted in RC-DSBs by its collision with the ongoing replication forks (Pommier, 2006). Such RC-DSBs are the primary cytotoxic mechanism of Top1 inhibitors in proliferating cells. Indeed, cells tend to be immune to CPT when they are outside of S-phases or when replication is arrested by aphidicolin treatment (Borovitskaya and D'Arpa, 1998; Horwitz and Horwitz, 1973). At least two mechanisms have been described for the production of RC-DSBs by Top1cc: (i) the "replication run-off" (Hsiang et al., 1989a; Strumberg et al., 2000) and (ii) the Mus81-Eme1 cleavage (Regairaz et al., 2011) (**Figure 8**).

Analysis of the broken ends by ligation-mediated PCR in the ribosomal RNA gene cluster in mammalian cells shows the extension of the leading strand up to the last nucleotide at the 5' end of the Top1cc resulting in 5' phosphorylated blunt-ended DSBs (also called DNA double-strands ends, DSEs) by "replication run-off" (Strumberg et al., 2000) (**Figure 8A**). Since the 5'-OH terminus enables the reversibility of the Top1cc, the 5' phosphorylation should prevent religation by Top1 itself (Strumberg et al., 2000).

RC-DSBs can also be mediated by the 3' flap endonuclease Mus81-Eme1 (Regairaz et al., 2011). Mus81-deficient cells have a reduced level of CPT-induced DSBs. *Regairaz* and coworkers proposed that DSEs could be the result of the Mus81-Eme1-dependent cleavage of replication fork stalled by trapped Top1cc. Although Mus81-Eme1-cleaveage leads to DSBs production, the primary function of this pathway is to dissipate the excess of positive supercoils resulting from CPT-induced Top1 inhibition and to promote replication fork recovery and cell survival. Indeed, Mus81-deficient cells are hypersensitive to CPT (**Figure 8B**).

CPT-induced RC-DSBs initiate a pleiotropic DDR with checkpoint activation, DNA repair and apoptosis (reviewed in (Pommier et al., 2006; Sordet et al., 2003; Tomicic and Kaina)). This DDR includes the activation of the ATR-Chk1 (ataxia telangiectasia Rad3-related protein - checkpoint Kinase 1), ATM-Chk2-p53 (ataxia telangiectasia mutated - checkpoint kinase 2 - tumour protein

P53) pathways, the DNA-dependent protein kinase (DNA-PK) and the phosphorylation of H2AX (γH2AX) and RPA (replication protein A) (see *Chapter II*). Defects in these pathways sensitize cancer cells to Top1-mediated DNA damage (reviewed in (Pommier et al., 2006; Tomicic and Kaina)). Although both Chk1 and Chk2 are rapidly activated upon exposure to low doses of CPTs, it seems that the ATR-Chk1 axis is the predominant pathway in response to RC-DSBs (Furuta et al., 2003; Huang et al., 2010), which are the predominant lesions in replicating cells treated with pharmacological doses of CPT. ATR-Chk1 activation induces Cdc25A degradation and consequent S-phase delay and G2/M arrest (Xiao et al., 2003).

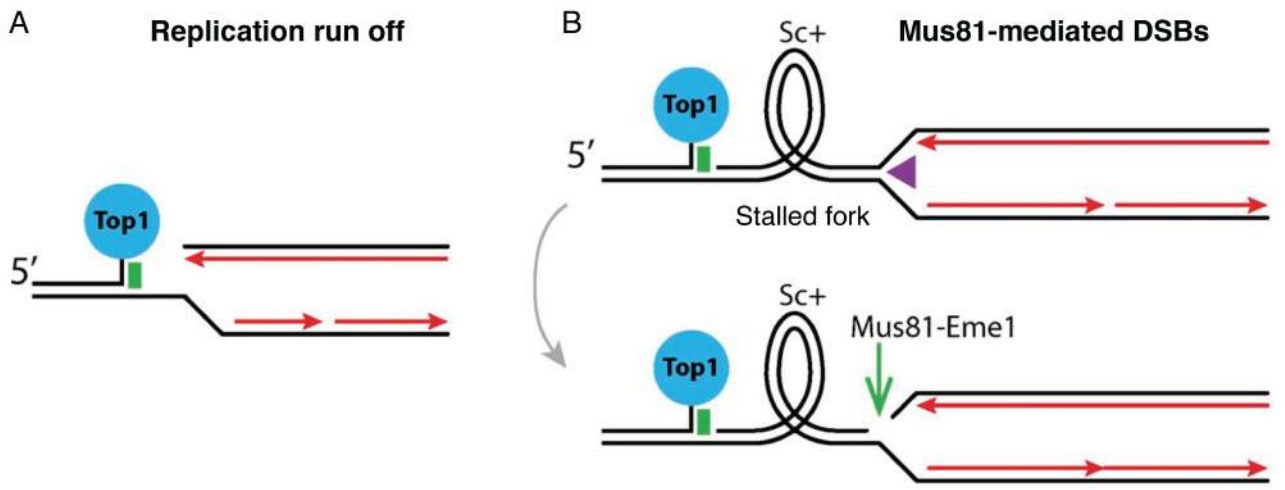

Figure 8: Mechanisms of production of replication coupled DSBs (RC-DSBs) by Top1cc. (**A**) Replication run off (Strumberg et al., 2000). (**B**) Mus81-Eme1 cleavage of the stalled replication fork (Regairaz et al., 2011). Adapted from (Regairaz et al., 2011).

I.5.2 Transcriptional consequences of CPT-mediated trapping of Top1cc

Since Top1 is enriched at transcribed regions (Gilmour et al., 1986; Khobta et al., 2006; Kroeger and Rowe, 1992; Stewart et al., 1990; Zhang et al., 1988) where it exerts several functions that are both dependent- and independent- of its catalytic activity (see section *I.3.1* and *I.3.2*), Top1 poisoning may occur primarily in actively transcribed regions and can uncouple transcriptional regulation processes leading to multiple cellular consequences.

I.5.2.1 General transcription downregulation and alteration of gene expression patterns

An immediate effect of CPT in cultured cells is the broad and general inhibition of both nucleoplasmic (mRNA) and nucleolar (rRNA) transcription elongation (Alagoz et al., 2013; Desai

et al., 2003; Horwitz et al., 1971; Kann and Kohn, 1972; Lin et al., 2013). *In vitro* studies suggested that this inhibition can result from the physical blockage of the RNAPII elongation complexes by Top1cc (Bendixen et al., 1990) and/or by the accumulation of DNA supercoils by ongoing transcription (Darzacq et al., 2007; Garg et al., 1987). ^{3}(H)uridine incorporation measurements show that transcription is reduced to 20%, within 10 minutes of CPT treatment (Desai et al., 2003; Horwitz et al., 1971).

Although the overall level of transcripts decreases quickly after CPT treatment, topoisomerase inhibition differently affects the gene expression. One of the first evidences of the alteration of gene expression patterns is given by the study of *Collins et al*. (Collins et al., 2001). The authors showed that CPT enhances the expression of C-FOS, downregulates C-MYC and does not impact the transcription of the HSP70 and GADPH genes. Later works have allowed the measurements of global changes in gene expression patterns induced by CPT-stabilized Top1cc by using microarray technology (Lotito et al., 2009; Solier et al., 2013; Zhou et al., 2002). *Zhou et al.* highlighted the different changes in gene expression profiles associated with high and low concentrations of CPT (Zhou et al., 2002). Low CPT concentrations are associated with the downregulation of cell cycle-related genes whereas high CPT concentrations induce up-regulation of p53-related stress genes (Zhou et al., 2002). *Lotito* and coworkers analysed the CPT-induced alteration of gene expression in yeast (Lotito et al., 2009). 73 genes, mainly related to Gene Ontology (GO) components such as vesicle-mediated transport, organelle and cell wall organisation and protein modifications, were downregulated by CPT. The authors also reported the up-regulation of 22 genes mainly related to cell cycle, mitosis and DNA replication which are regulated by the transcription factors Mbp1 and Swi4 (Lotito et al., 2009). In human cells, the genome-wide transcriptional response to CPT has been recently characterized by two independent groups employing different technologies. The group of *Pommier* performed the genome-wide analysis of CPT-treated cells at exon resolution by using the exon array platform (Solier et al., 2013). They found that in response to CPT, 20% of the analysed genes are downregulated while 5% are upregulated (by at least 2-fold). CPT-induced Top1cc preferentially downregulate genes highly expressed at basal level and upregulate lowly expressed genes. The probability for a gene to be downregulated increases with the increasing of both the gene length and the exons' number. Interestingly, downregulation of a large number of genes is mediated by the upregulation of at least one specific miRNA, miR-142-3p, in response to CPT. Among the most significant GO category for the downregulated genes, the authors found the ubiquitin- and RNA degradation-related pathways genes (Solier et al., 2013). The importance of gene length was confirmed by *Ljungman*'s group employing the Bru-Seq method, which consists in the metabolic labelling of RNA using bromouridine (Bru) followed by specific isolation of Bru-

labeled nascent RNA and genome-wide analysis (Veloso et al., 2013). The authors reported also that CPT affects transcriptional termination by stimulating transcriptional read-through past the 3' end of small genes and it enhances the expression of eRNA from certain enhancer elements. In addition, this work highlights the effect of CPT in shifting the balance of apoptosis-regulated genes by reducing the relative transcription rate of large anti-apoptotic genes and enhancing the expression of a set of smaller pro-apoptotic genes (Veloso et al., 2013).

Another recent RNA-Seq analysis has been performed to survey changes in gene expression in mice cortical neurons after a 3-day topotecan treatment (King et al., 2013). This study shows that, like in cancer cells (Solier et al., 2013; Veloso et al., 2013), topotecan reduces the transcription of long genes (>200 kb) in post mitotic neurons by impairing transcription elongation (King et al., 2013). Importantly, the topotecan-downregulated genes are related to GO components of synapses, cell adhesion and neurotransmission and a number of these genes are associated with autism (King et al., 2013). The transcriptional downregulation of these genes is accompanied by the depletion of multiple synaptic proteins and the suppression of the excitatory and inhibitory synaptic activity in topotecan-treated neurons (Mabb et al., 2014). These studies highlight the role of Top1 in post-mitotic neurons in maintaining proper synaptic function. For instance, a *de novo* Top1 mutation has been found in individuals with autism spectrum disorder (Iossifov et al., 2012; Neale et al., 2012).

By contrast to replication, transcription inhibition recovers rapidly. The transcriptional recovery starts after 15 min of CPT exposure and continues gradually during the next 4h (Desai et al., 2003). Following removal of CPT, the rate of RNA synthesis reaches the 90% of the control sample within minutes (Horwitz et al., 1971). Indeed, transcription spreads as a wave in a 5' to 3' direction with no recovery of transcription apparent from RNAPII stalled in the body of genes (Ljungman and Hanawalt, 1996; Veloso et al., 2013). The inability of cells to resume elongation from within the body of genes suggested that blocked RNAPII are discarded rather than recycled.

However, transcription recovers with a reduced elongation rate (around 1.1-1.3 kb/min after CPT removal compared to 2 kb/min in untreated cells). It is possible that this reduced elongation rate is due to a requirement for repair of Top1cc-associated DNA damage to take place before transcription can resume (see section *I.5.2.7*) (Veloso et al., 2013).

Importantly, the recovery of RNA synthesis depends on Top1 degradation (see section *I.5.2.4*) (Alagoz et al., 2013; Desai et al., 2003). The requirement of transcription-coupled nucleotide excision repair (TCR) for transcription resumption is controversial. Some studies have shown that Cockayne syndrome (CS) cells that are deficient in TCR (CSB factor) are hypersensitive to CPT and have defects in RNA synthesis recovery (Desai et al., 2003; Squires et al., 1993), while others studies have found no defects (Sakai et al., 2012; Veloso et al., 2013).

I.5.2.2 Effects on RNA Polymerase II

CPT-induced Top1cc have immediate and specific effects on RNAPII:

- *Hyperphosphorylation of RNAPII:*

Within few minutes, CPT triggers the hyperphosphorylation of the largest subunit (Rpb1) of RNAPII in both primary and transformed cancer cells (Amente et al., 2009; Desai et al., 2003; Dutertre et al., 2010; Khobta et al., 2006; Sordet et al., 2008b). Indeed, the conserved heptapeptide repeats of the carboxy-terminal domain (CTD) of Rpb1 (YSPTSPD) is phosphorylated/dephosphorylated during the transcription cycle and the hyperphosphorylated form of the RNAPII corresponds to the transcriptionally active polymerase (Sims et al., 2004). RNAPII phosphorylated at serine 5 (S5) peaks early in the transcription cycle and decreases towards the 3' end of the gene correlating with transcription initiation and early elongation (promoter clearance). By contrast, phosphorylation at serine 2 (S2) predominates in the body and toward the 3' end of the gene correlating with productive elongation (Sims et al., 2004).

CPT produces selectively hyperphosphorylation on the S5 that is mediated by Cdk7, a component of the transcription factor TFIIH (Sordet et al., 2008b). Although Cdk9 mainly induces S2 phosphorylation, the implication of Cdk9 in CPT-induced S5 hyperphosphorylation cannot be completely excluded. Indeed, Cdk9 can phosphorylate RNAPII at S5 (Ramanathan et al., 2001) and CPT triggers the activation of the P-TEFb complex containing the Cdk9 kinase activity (Amente et al., 2009). The hyperphosphorylation of Rpb1 on S5 is consistent with others studies proposing that CPT-induced Top1cc block elongation and stimulate RNAPII transcription initiation (Khobta et al., 2006; Ljungman and Hanawalt, 1996). However, the study of *Dutertre et al.* reports that 1 h of CPT induces also hyperphosphorylation of RNAPII on S2 and that this form of hyperphosphorylated RNAPII is slightly enriched at the 3' end of the MDM2 (mouse double minute 2) gene (Dutertre et al., 2010).

- *Redistribution of chromatin-bound RNAPII:*

A second immediate effect of CPT on RNAPII is the redistribution of chromatin-bound RNAPII along transcribed genes in human cells in a manner dependent on Cdk activity (Baranello et al., 2010; Khobta et al., 2006). The *Capranico*'s group reported that RNAPII levels are reduced at promoter pause site and are transiently increased at internal exons in response to CPT (Capranico et al., 2007; Khobta et al., 2006). The authors provided evidences that CPT-induced Top1cc trigger the escape of RNAPII from promoter-proximal pause site of the HIF-1α (hypoxia-inducible factor 1α) gene and suggested a new role for Top1 in regulating RNAPII pausing (Baranello et al., 2010; Capranico et al., 2010). Before starting the productive elongation, RNAPII synthesizes a short RNA

and pauses partially at 20-50 bases from TSS. This pausing step functions as checkpoint for elongation and assures the recruitment of the capping and splicing factors to promote RNA processing (Sims et al., 2004). The proposed model is that Top1 facilitates the polymerase pausing thus; Top1 inhibition by CPT activates PTEF-b, which in turns phosphorylates the CTD of RNAPII favouring pausing escape (Baranello et al., 2010; Capranico et al., 2010). Others studies are consistent with this model. ^{3}(H)uridine pulse labelling and nuclear run-on measurements of the transcription rate in the rodent DHFR (dihydrofolate reductase) gene and genome-wide Bru-Seq data in human cells show that CPT enhances transcription signal from the 5' ends of the genes while reduces transcription signal at promoter-distal sequences (Ljungman and Hanawalt, 1996; Veloso et al., 2013). A kinetic analysis of RNAPII transcription at a gene-array locus reveals that RNAPII often pauses during elongation. CPT increases the efficiency of intragenic pausing without affecting the pausing time that results in a reduction of the elongation rate (to ¼ of the normal rate) but not in a complete inhibition of elongation (Darzacq et al., 2007). The authors explained the effect of CPT by the slower DNA unwinding related to the inhibition of Top1 activity rather than to the physical block of RNAPII by Top1cc (the collision model).

- *RNAPII degradation:*

Another effect of CPT on RNAPII that has been described by *Desai et al.* is the proteasomal degradation of Rpb1 (Desai et al., 2003). UV light, cisplatin, ecteinascidin 743 (Et743) and hydrogen peroxide also induce RNAPII degradation (Aune et al., 2008; Inukai et al., 2004; Jung and Lippard, 2006; Somesh et al., 2005) suggesting that, in a similar manner, Top1cc-induced stalled RNAPII complexes are targeted to degradation. However, CPT induces hyperphosphorylation of CTD at S5 (Sordet et al., 2008b) and this phosphorylation, but not phosphorylation on S2, has been described to protect RNAPII from ubiquitylation in response to UV (Somesh et al., 2005). Furthermore, compared to RNAPII degradation-induced by UV, Et743 or hydrogen peroxide that is a rapid and massive event, CPT-induced RNAPII degradation is a relatively late (6h) and modest event. Stalled RNAPII may be recognized and ubiquitinated differentially depending on the types of DNA lesions. Hence, further studies are needed to characterize mechanistically the fate of RNAPII stalled by transcription-blocking Top1cc.

I.5.2.3 Alteration of mRNA splicing

Several studies have involved Top1 in splicing because of its catalytic activity and its ability to interact with and phosphorylate splicing factors (see section *I.3.2*). Thus, it is not surprising that CPT profoundly affects splicing events. CPT blocks the SR-kinase activity of Top1 (Rossi et al.,

1996). However, two different studies suggest that the splicing effects of CPT are unrelated to defects of Top1 relaxation and/or kinase activity (Dutertre et al., 2010; Solier et al., 2010).

Different studies have reported that CPT alters the splicing of single genes resulting in alternative splicing (Baranello et al., 2010; Dujardin et al., 2014; Dutertre et al., 2010; Eisenreich et al., 2009; Listerman et al., 2006; Shkreta et al., 2008; Solier et al., 2010; Solier et al., 2008; Solier et al., 2004). Alternative splicing is the regulation of splice-site selection and it seems to occur in 50%-70% of human genes resulting in the transcriptome diversity produced by a limited number of genes (Stamm et al., 2005).

Listerman et al. studied the impact of CPT in the *Fos* pre-mRNA (Listerman et al., 2006). CPT enhances splicing factors accumulation on the FOS gene but not on intronless genes and this accumulation correlates with higher levels of cotranscriptional splicing. The authors suggested that CPT, by slowing down RNAPII elongation, allows more time for the splicing factors to bind to the nascent RNA. The decrease in RNAPII elongation rate by CPT has also been described to promote the skipping of exon 9 (E9) of the CFTR (cystic fibrosis transmembrane conductance regulator) gene by opening a time window to the negative splicing factor ETR-3 to be recruited (Dujardin et al., 2014). Interestingly, this study shows that the changes in the E9 splicing induced by CPT are not caused by an alteration of the abundance or phosphorylation of the SR proteins, likely excluding an effect dependent on the kinase activity of Top1 (Dujardin et al., 2014). Another example of alternative splicing driven by CPT is given by MDM2 (Dutertre et al., 2010). In unstressed cells, MDM2 expression is positively regulated by p53 and then, MDM2 negatively regulates p53 by suppressing p53-transcriptional activity (Oliner et al., 1993) or by targeting p53 for proteasomal degradation (Haupt et al., 1997). CPT induces cotranscriptional skipping of several MDM2 exons leading to numerous alternative transcripts that do not give rise to stable protein isoforms. However, CPT removal suppresses alternatively spliced variants of MDM2 and the protein is expressed again. In response to CPT, p53 is activated (Ljungman and Lane, 2004; Ljungman et al., 2001). Hence, the CPT-induced MDM2 exon skipping may be a mechanism to prevent the accumulation of the MDM2 protein thus avoiding p53 degradation (Dutertre et al., 2010).

In addition to the study of the effects of CPT in the alternative splicing of some specific genes, two reports analyse the consequences of CPT on splicing at global genome level in human cells (Dutertre et al., 2010; Solier et al., 2010). Both studies agree that CPT is able to induce both exon skipping and exon inclusion. *Solier et al.* describe a time-dependent effect of splicing in response to CPT (Solier et al., 2010). While the appearance of novel exons is an early (1 h, 2 h and 4 h) and a late event (15 h and 20 h), the exons skipping is mostly a late event. Splice events occur all along the transcripts and tend to augment with the length of the transcript (Solier et al., 2010). Genes that

are downregulated in response to CPT have a higher probability to be spliced compared to unchanged and upregulated genes (Solier et al., 2013). Three genes categories are more affected by the CPT-induced alternative splicing: genes encoding splicing factors, genes related to mitosis and genes related to methylation (Solier et al., 2010). These data open the possibility that the splicing alterations of several genes in response to Top1cc could be due to the effect of CPT on genes encoding splicing factors. *Solier et al.* proposed that CPT-induced RNAPII hyperphosphorylation could trigger alternative splicing by affecting RNAPII pausing and splicing site selection and/or modulating the interaction with splicing factors. Accordingly to this hypothesis, DRB (5,6-dichloro-1-β-D-ribofuranosylbenzimidazole), which inhibits Cdk9 and RNAPII phosphorylation, prevented CPT-mediated alternative splicing of RBM8A (RNA binding motif protein 8) and caspase-2 genes (Solier et al., 2010). By contrast, *Dutertre et al.* found that DRB does not suppress CPT-induced alternative MDM2 transcripts indicating that RNAPII phosphorylation-independent mechanisms also exist in response to CPT (Dutertre et al., 2010). The authors suggested that exon skipping induced by CPT could be caused by the de-coupling of transcription and splicing. In particular, they showed that CPT disrupts the interaction between the transcriptional coregulator EWS and the spliceosome-associated factor YB-1. The depletion of those factors reproduces the exons skipping induced by CPT in eight genes, including MDM2 (Dutertre et al., 2010).

In addition to these two mechanisms, a recent paper shows that CPT treatment causes selective chromatin displacement of late-stage spliceosomes in non-replicating cells (Tresini et al., 2015). This spliceosome displacement may be another mechanism by which CPT promotes alternative splicing.

I.5.2.4 Top1 downregulation

Top1 downregulation corresponds to the reduction of Top1 cellular content during prolonged CPT treatment and it has been described for the first time by *Beidler* and *Cheng* in 1995 (Beidler and Cheng, 1995). The protein level of Top1 is strongly reduced in a time-dependent manner in less than 6 h of CPT treatment (Desai et al., 2003) with Top1 half-life dropping from 10-16 h down to 1-2 h (Desai et al., 1997). CPT-induced Top1 downregulation correlates with Top1cc formation (Beidler and Cheng, 1995; Desai et al., 2003) suggesting that Top1 trapping triggers Top1 downregulation (Desai et al., 2003).

Top1 downregulation is part of the transcriptional response to CPT since it is selectively dependent on transcription and independent on replication. Indeed, it is suppressed by the transcription inhibitors DRB and α-amanitin but not by the replication inhibitor aphidicolin (Beidler and Cheng,

1995; Desai et al., 1997; Desai et al., 2003; Huang et al., 2010; Lin et al., 2008; Sakasai et al., 2010a; Sordet et al., 2008b). Similarly, cycloheximide, that inhibits protein synthesis, does not prevent CPT-induced Top1 downregulation excluding the involvement of a reduced *de novo* synthesis (Desai et al., 1997). Top1 downregulation appears to be specific of CPT-induced Top1cc, since UV-trapped Top1 is not downregulated (Subramanian et al., 1998).

The *Liu*'s laboratory has shown that CPT-induced transcriptional Top1 downregulation is the result of Top1 K48-polyubiquitylation and degradation by the 26S proteasome (Ban et al., 2013; Desai et al., 2001; Desai et al., 1997; Desai et al., 2003; Lin et al., 2008). Several evidences support this conclusion:

1- Proteasome inhibitors (MG132, lactacystin) prevent Top1 downregulation and Top1cc decreasing after prolonged CPT exposure (Desai et al., 2001; Desai et al., 1997; Desai et al., 2003; Huang et al., 2010; Lin et al., 2008; Sordet et al., 2008b).

2- siRNA against POMP (proteasome maturation protein), a factor which promotes the 20S proteasome assembly (Fricke et al., 2007), abolish Top1 downregulation (Ban et al., 2013; Lin et al., 2009).

3- siRNA against ATPases and non ATPases 19S components hinder Top1 degradation (Ban et al., 2013).

4- CPT induces the formation of Top1-ubiquitin conjugates (Ban et al., 2013; Desai et al., 2001; Katyal et al., 2014; Kerzendorfer et al., 2010; Lin et al., 2008; Lin et al., 2009; Zhang et al., 2004) in a transcription-dependent manner (Lin et al., 2008).

5- The ubiquitin isopeptidase inhibitor G5, which depletes the free ubiquitin pool (Aleo et al., 2006), blocks Top1 downregulation (Lin et al., 2008).

6- Top1 downregulation is inhibited in the temperature-sensitive E1 activating enzyme mutant cell line ts85 (Finley et al., 1984) at the restrictive temperature that triggers UBA1 (ubiquitin-like modifier activating enzyme 1) degradation (Ban et al., 2013; Desai et al., 1997).

7- Transfection of cells with the dominant-negative mutant, K48R-Ub (K48 is mutated to R on HA-Ub) but neither K29R-Ub nor K63R-Ub, suppresses Top1 downregulation (Ban et al., 2013; Lin et al., 2008).

More recently, the same laboratory has reported a new ubiquitin-independent mechanism for the degradation of etoposide-induced Top2β-DNA cleavage complexes colliding with elongating RNAPII (Ban et al., 2013). Degradation of Top2β roadblocks requires only 19S ATPases and 20S proteasome (Ban et al., 2013). Based on the new findings on Top2β and on previous studies demonstrating that 19S ATPases are associated with elongating RNAPII (Ferdous et al., 2001; Ferdous et al., 2002; Gillette et al., 2004; Gonzalez et al., 2002; Muratani and Tansey, 2003), the

authors speculated about a possible new model for Top1 degradation depending on Top1cc polarity (Ban et al., 2013) (**Figure 9**): (i) Top1cc in the non-template strand could be unfolded by 19S ATPases leading elongating RNAPII to read-through Top1cc and Top1 to be ubiquitinated or (ii) Top1cc in the template strand could arrest elongating RNAPII leading to Top1 degradation by the same ubiquitin-independent pathway as for Top2β. Even if authors suggested that ubiquitin-dependency may simply reflect a higher rate of ubiquitin-dependent degradation of Top1; currently there is no evidence supporting a possible ubiquitin-independent degradation pathway for Top1cc.

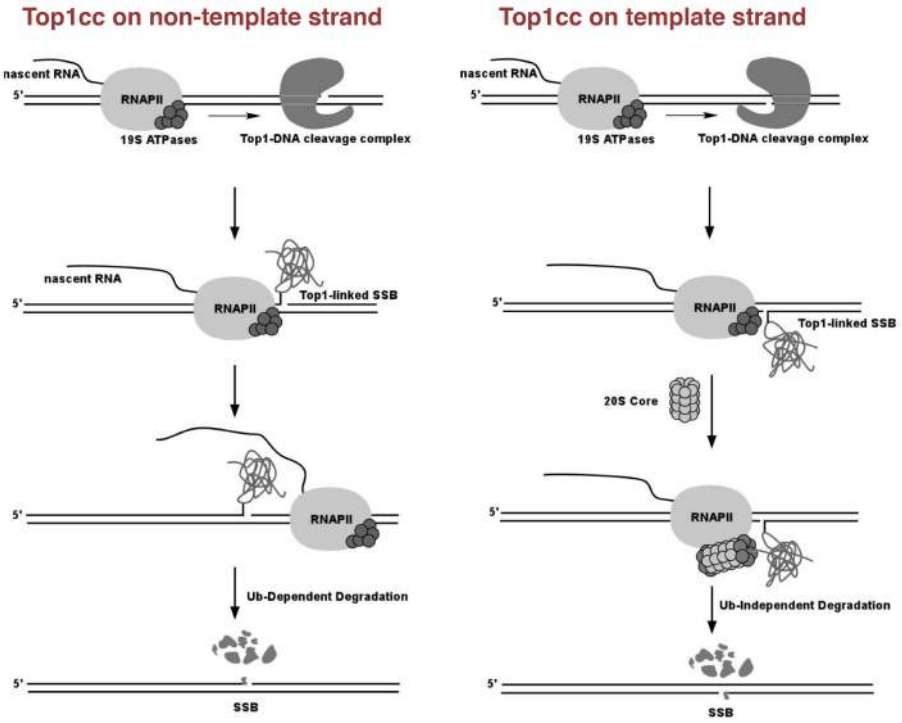

Figure 9: Proposed model for CPT-induced Top1 degradation based on Top1cc polarity. Top1cc on the non-template strand are proposed to be degraded by an ubiquitin-dependent mechanism whereas Top1cc on the template strand could be degraded by an ubiquitin-independent mechanism similarly to Top2β degradation in response to etoposide (Ban et al., 2013).

Top1 ubiquitination

The ubiquitination cascade is carried out by the sequential action of three enzymes: E1 (ubiquitin-activating enzyme), E2 ubiquitin-conjugating enzyme and E3 ubiquitin-ligase (see section *II.5.3.4* and **Figure 29**). Defects in Top1 downregulation in ts85 cells treated with CPT (Ban et al., 2013; Desai et al., 1997) suggest that the E1 enzyme responsible for Top1 ubiquitylation is UBA1 as in these cells, UBA1 is rapidly degraded at restrictive temperature (Baugh et al., 2009). Four E3 ligases have been described as potential E3 candidates for Top1 ubiquitylation: Cullin 3 (Cul3) (Lin et al., 2009; Zhang et al., 2004), BRCA1 (breast cancer 1) (Sordet et al., 2008b), Cullin 4A (Cul4A) and Cullin 4B (Cul4B) (Kerzendorfer et al., 2010). Depletion of one of these E3's activity is able to prevent, at least partially, Top1 downregulation in response to CPT. Modulating the protein level of

Cul3, Cul4A or Cul4B by overexpression or depletion is able to reduce or enhance Top1cc and Top1 ubiquitin-conjugates, respectively (Kerzendorfer et al., 2010; Zhang et al., 2004). Interestingly, Cul4B is one of the most commonly mutated genes in X-linked mental retardation (MR) patients (Tarpey et al., 2007). Those patients present some clinical features similar to SCAN1 (spinocerebellar ataxia with axonal neuropathy) patients and MR-derived cells show increased level of CPT-induced SSBs similar to that of SCAN1 cells (Kerzendorfer et al., 2010). Although published data suggest that all four E3 ligases can act on Top1 ubiquitylation, additional studies are needed to show whether those E3 ligases can directly ubiquitylate Top1 *in vitro* and *in vivo* and on which residues.

Top1-ubiquitin conjugates are discernible after DNAse treatment of cell lysates following Top1 immunoprecipitation, suggesting that Top1cc are ubiquitylated on the DNA (Desai et al., 2003). However, it is not known whether ubiquitylated Top1 is degraded on DNA and/or it is released from chromatin and then degraded away. The first possibility is supported by the action of Tdp1 (tyrosyl-DNA phosphodiesterase 1), which removes Top1 from DNA more efficiently when it is proteolysed (Debethune et al., 2002) and by recent finding showing that etoposide treatment induces the accumulation of 19S factors into chromatin in a transcription-dependent manner (Ban et al., 2013).

Impact of ubiquitin-like modifications of Top1 on Top1 downregulation

In addition to ubiquitin, two others ubiquitin-like proteins (UBLs), SUMO1/2/3 (see section *II.5.3.6*) and ISG15 (interferon-stimulated gene 15), has been proposed to influence Top1 downregulation (Desai et al., 2008; Kanagasabai et al., 2009; Mao et al., 2000b). UBLs are post-translational modifications of target protein substrates and have been described on the base of their structural similarity and sequence homology to ubiquitin (for review see (Streich and Lima, 2014)). UBLs are conjugated to target proteins in a way similar to ubiquitin but using distinct E1, E2 and E3 enzymes (Streich and Lima, 2014).

The SUMO-conjugates of Top1, have been originally visualized, but erroneously interpreted as ubiquitin-conjugates, by *Desai et al.* (Desai et al., 1997) and later characterized by *Mao et al.* (Mao et al., 2000b). Similarly to ubiquitylation, Top1 is SUMOylated in response to CPT and it has been proposed that the Top1cc, rather than Top1 undergoes SUMO-conjugation (Desai et al., 2003; Mao et al., 2000b). Unlike Top1 ubiquitination, Top1 SUMOylation is transcription- and replication-independent (Mao et al., 2000b). Top1 can be conjugated to SUMO1 (Desai et al., 2001; Desai et al., 2003; Horie et al., 2002; Katyal et al., 2014; Mao et al., 2000b) or to SUMO2/3 (Kanagasabai et al., 2009). *Horie et al.* proposed that SUMO1 conjugation to Top1 amplifies the formation of Top1cc in

response to CPT (Horie et al., 2002). SUMO1 conjugation to substrates has been suggested to antagonizes their ubiquitination and to prevent their proteolysis by the 26S proteasome (Muller et al., 2001). Thereby, it is possible that SUMO1 may serve to prevent Top1 ubiquitination. Another group showed that purified CPT-induced Top1cc are enriched in SUMO2/3 chains and ubiquitin (Kanagasabai et al., 2009). Since SUMO2/3 polychains serve as a signal for polyubiquitylation and proteasome-dependent proteolysis (Weisshaar et al., 2008) and since SUMOylation and ubiquitylation coexist in Top1cc, SUMOylation with SUMO2/3 has been proposed to target Top1cc for ubiquitylation and proteolysis (Kanagasabai et al., 2009). However, further studies are needed to clearly show the role of SUMOylation in Top1 downregulation.

Desai et al. showed that ISGylation is elevated in many tumours and interferes with the ubiquitin/26S proteasome pathway, leading to altered degradation of many cellular targets likely by hampering ubiquitylation through substrate competition at the E2/E3 level (Desai et al., 2006). Accordingly to these finding, depletion of ISG15 or UbcH8 (retinoic acid-induced gene B protein, the major E2 for ISG15) in breast cancer ZR-75-1 cells results in increased rate of Top1 downregulation without affecting the level of CPT-induced Top1cc (Desai et al., 2008).

Impact of DDR/Repair proteins on Top1 downregulation

In addition to BRCA1, other DDR and repair proteins have been described to promote Top1 downregulation in response to CPT (Alagoz et al., 2013; Christmann et al., 2008; Katyal et al., 2014; Tomicic et al., 2005). Failure of Top1 degradation in response to topotecan was observed in cells deficient for WRN (Tomicic et al., 2005) or for p53 (Christmann et al., 2008). Both WRN (Laine et al., 2003) and p53 (Mao et al., 2000a) can directly interact with Top1. However, the physical interaction Top1-p53 is unlikely the regulator of Top1 downregulation because inhibition of p53 transcriptional activity by pifithrin-α also blocks Top1 degradation suggesting that p53 may control the transcription of a factor, which mediates Top1 degradation (Tomicic et al., 2005). Recently, the DDR kinase ATM (see section *II.3.1*) has also been implicated in Top1 downregulation (Alagoz et al., 2013; Katyal et al., 2014). Human and mouse cells knockout for ATM accumulate CPT-induced Top1cc, are defective for Top1 downregulation and fail to recover transcription after CPT removal (Alagoz et al., 2013; Katyal et al., 2014). ATM deficiency leads to a marked reduction of Top1-ubiquitin and -SUMO1 conjugates induced by CPT (Katyal et al., 2014). How ATM deficiency impairs Top1 ubiquitylation and SUMOylation in response to CPT remains to be established. However, AT (ataxia telangiectasia) cells, that are deficient for ATM, also display elevated expression of the ISG15 conjugation pathway that correlate with impaired proteasome-mediated protein degradation (Wood et al., 2011).

Cellular function of Top1 downregulation

The functional meaning of Top1 downregulation has been linked to: (i) repair of Top1cc and then recovery of RNA synthesis by exposing the Top1-DNA binding to be processed by Tdp1 (see section *I.6.2*) (Debethune et al., 2002; Desai et al., 2003; Lin et al., 2008); (ii) decrease of the total cellular pool of Top1 consequently limiting further trapping of Top1 and Top1cc-induced DNA damage (see section *I.5.2.7*) (Beidler and Cheng, 1995; Desai et al., 2001).

In agreement with these possibilities, CPT-induced downregulation of Top1 appears to be a mechanism of cellular resistance to avoid accumulation of Top1cc and DNA damage. Indeed, cell lines selected for CPT resistance have reduced amount of Top1 (Chang et al., 1992) and the extent of CPT-induced Top1 downregulation correlates with CPT resistance in some cancer cells (Desai et al., 2001). Moreover, modulating factors that influence Top1 downregulation (**Figure 10**) results in altered CPT sensitivity:

- Proteasome inhibition, which blocks Top1 degradation, increases tumour cell sensitivity to CPT (Desai et al., 2001), particularly in S-phase (Zhang et al., 2004).
- Overexpression of Cul3, which increases Top1 downregulation, confers resistance to CPT (Zhang et al., 2004).
- BRCA1-deficient cells are defective for Top1 degradation and hypersensitive to CPT (Fedier et al., 2003; Sordet et al., 2008b).
- Cell lines from patients with CUL4B mutations exhibit reduced Top1 ubiquitylation and increased CPT sensitivity (Kerzendorfer et al., 2010).
- siRNA depletion of Cul4A decreases Top1 downregulation and enhances CPT sensitivity (Kerzendorfer et al., 2010)
- Cell lines selected for CPT resistance downregulate ISG15 expression and siRNA depletion of ISG15 or UbcH8 increases Top1 downregulation and decreases CPT sensitivity (Desai et al., 2008).

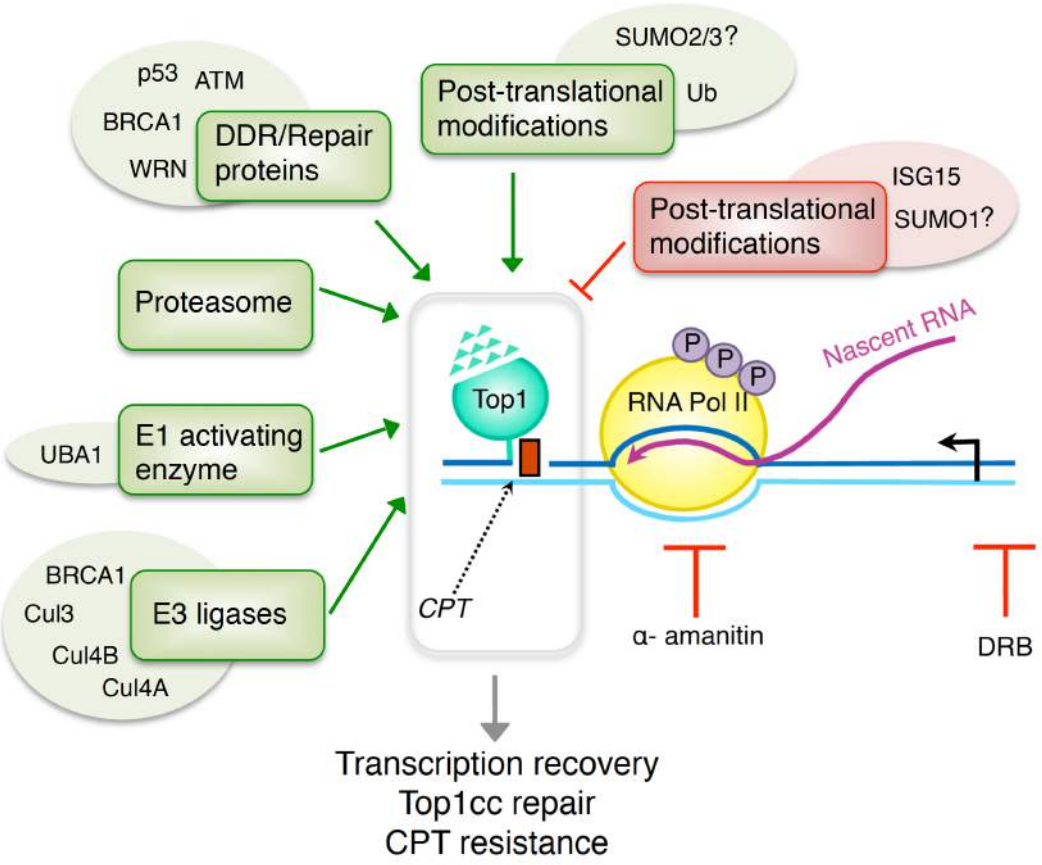

Figure 10: Model of Top1cc degradation. The diagram depicts factors described to promote (green arrows) or to inhibit (red arrows) Top1 degradation and cellular consequences of Top1 downregulation. Adapted from (Sordet et al., 2008b).

CPT-induced Top1 downregulation occurs in normal cells but it is defective in many tumour cells (Desai et al., 2001). Cancer cells with impaired Top1 downregulation are hypersensitive to CPT (Desai et al., 2001). Similarly, in a nude mouse model, topotecan treatment causes Top1 downregulation in many normal tissues (as blood, brain, kidney, liver, and skin) but not in xenografted MDA-MB-435 breast cancer cells (Desai et al., 2003). Furthermore, patients receiving topotecan therapy also display reduced Top1 levels in normal peripheral blood cells but not in leukemic cells (Hochster et al., 1997; Rubin et al., 1995). Most tumour cells are defective in CPT-induced Top1 downregulation, which could explain in part the increased sensitivity of tumour cells to CPT (Desai et al., 2001). The molecular basis for the defective degradation of Top1 in many cancer cells is not clear. It could be related to BRCA1 inactivating mutations that occur frequently during tumorigenesis (Silver and Livingston, 2012) or to mutations in cullins and cofactors proteins (Carlucci and D'Angiolella, 2015).

I.5.2.5 Topological stress and R-loops

According to the "twin-supercoiled-domain" model (see section *I.3.1*), RNAP would generate approximately seven supercoils per second depending on the rate of transcription, the length of the transcribed unit and the arrangement of promoters (for example, divergent transcription) (Darzacq et al., 2007). These supercoils are resolved by DNA topoisomerases, and if not dissipated, they create a torsional stress (Kouzine et al., 2013). Several studies in bacteria, yeast and human cells have shown that deletion of Top1 increases supercoiling in front of the elongating RNAP and leads to melting of the DNA and the formation of R-loops behind the RNAP (Drolet, 2006; Drolet et al., 1994; El Hage et al., 2010; Masse and Drolet, 1999a; Tuduri et al., 2009). Less works have investigated the topological stress induced specifically by CPTs. *Koster* and colleagues measured the real-time uncoiling rate of human Top1 in the presence of topotecan in the context of a single-molecule (Koster et al., 2007). They reported both *in vitro* and *in cellulo* (yeast) that topotecan significantly hinders Top1-dependent DNA uncoiling, with a more important impact on the removal of positive versus negative supercoils thus showing that topotecan induces an accumulation of positive supercoils (Koster et al., 2007). More recently, the *Levens*'s lab mapped transcription-dependent dynamic supercoiling in human cells by using psoralen photobinding and they clearly demonstrated that both Top1 and Top2 prevent the build-up of negative supercoiling in promoter regions *in cellulo* (Kouzine et al., 2013). Five min of CPT treatment strongly increases negative supercoils at the TSS and upstream of all genes, indicating a broad requirement for Top1 activity at promoters, but the effect of CPT is stronger in moderately expressed genes than in highly expressed genes. Effectively, moderately expressed genes depend only on Top1 whereas highly expressed genes recruit Top2 additionally to Top1 (Kouzine et al., 2013). Interestingly, Bru-Seq in response to CPT reveals a strong enrichment in PROMPTs (promoter upstream transcripts) (Veloso et al., 2013), that are a product of divergent transcription (Kapusta and Feschotte, 2014). The activity of divergent promoters may be mechanically coupled through dynamic supercoiling thus, a possible scenario is that the negative supercoiling induced by CPT at promoter could facilitate DNA melting, open complex formation and divergent transcription (Kouzine et al., 2013).

The accumulation of negative supercoiling can promote the formation of non-B DNA structures such as Z-DNA, cruciforms and most likely R-loops that can affect gene expression (Drolet, 2006). R-loops are three-stranded structures formed by an RNA-DNA hybrid plus a displaced single strand DNA (ssDNA), identical to the RNA molecule (Aguilera and Garcia-Muse, 2012) (**Figure 11**).

The first R-loops were characterized *in vitro* in 1976 (Thomas et al., 1976), *in cellulo* in bacteria in 1994 (Drolet et al., 1994) and then showed in different organisms (reviewed in (Aguilera and

Garcia-Muse, 2012; Groh and Gromak, 2014; Hamperl and Cimprich, 2014; Skourti-Stathaki and Proudfoot, 2014)). In living cells, R-loops can form *in cis* during transcription (co-transcriptional R-loop). The first model for R-loop formation envisages that R-loops are a direct extension of the RNA-DNA hybrid within the transcription bubble ("extended RNA-DNA hybrid" model) but this scenario is not consistent with the crystallographic structure of RNAPII (Westover et al., 2004). The most accepted mechanism is the "thread back" model, in which the nascent RNA transcript passes through the exit pore of the RNA polymerase before threading back to anneal with the template DNA (Roy et al., 2008). However, recently the *Konsland*'s laboratory has shown that R-loops can be formed *in trans* (away from the initial transcription point) since RNA transcribed at one locus can invade an homologous DNA at another locus and this mechanism is dependent on Rad51 (Wahba et al., 2013).

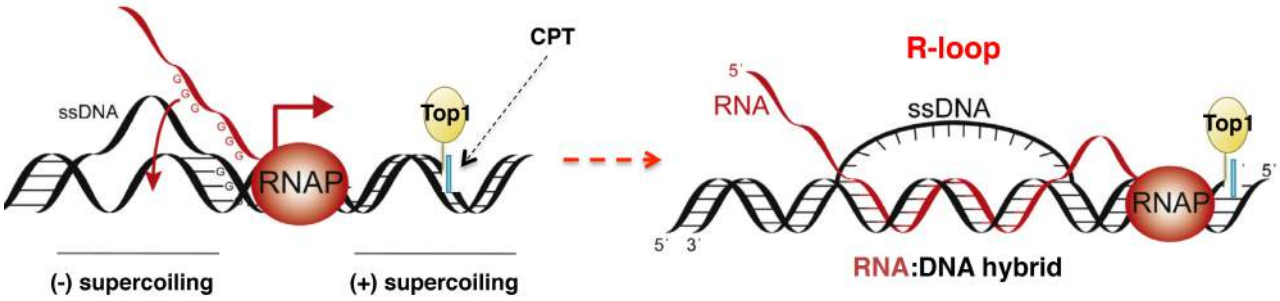

Figure 11: Inhibition of Top1 activity by CPT promotes R-loop formation. Trapping of Top1 by CPT results in SSB formation and accumulation of positive supercoils ahead of transcribing RNAPII and negative supercoils behind it. Negative supercoiling triggers partial unwinding of the DNA double helix, thereby facilitating the intrusion and the annealing of the nascent RNA with the complementary DNA strand (Adapted from (Hamperl and Cimprich, 2014)).

Transcription-dependent topological state and DNA sequence are important features controlling R-loop generation. The initial formation of an R-loop is facilitated *in vitro* by G clusters and DNA nicks downstream of the promoter on the non-template DNA strand, whereas negative supercoils and high G density promote the stabilisation and the elongation of the RNA-DNA hybrid (Roy et al., 2010). Once formed, R-loops are particularly stable since RNA-DNA hybrids are thermodynamically more stable than double-strand DNA (dsDNA) (Roberts and Crothers, 1992).

R-loops can be both beneficial and deleterious to cells. The programmed formation of R-loops is implicated in important biological processes, such as immunoglobulin class switch recombination (CSR) (Yu et al., 2003), regulation of gene expression (Tous and Aguilera, 2007), transcription termination (Skourti-Stathaki et al., 2011) and epigenetic mechanisms (Ginno et al., 2012). However, unscheduled R-loops can be a dangerous source of DNA damage because of the exposure of the ssDNA resulting from the RNA-DNA hybridization. ssDNA is chemically more unstable and

vulnerable to DNA-damaging agents than duplex DNA, thereby R-loops can promote genome instability or change the transcriptional landscape (for review (Aguilera and Garcia-Muse, 2012; Hamperl and Cimprich, 2014; Sollier and Cimprich, 2015)). Topoisomerases and RNA processing factors (such mRNA biogenesis factors) prevent R-loop formation while the RNaseH enzymes and RNA-DNA helicases act to remove R-loops (Hamperl and Cimprich, 2014; Skourti-Stathaki and Proudfoot, 2014).

The role of Top1 in preventing R-loop has been initially investigated in *E. coli* (Drolet, 2006; Drolet et al., 1994; Drolet et al., 1995; Masse and Drolet, 1999a; Masse and Drolet, 1999b). In *E. coli* the topology of its circular DNA is regulated by the concerted action of DNA gyrase that introduces negative supercoils and Topoisomerase 1 (TopA) that relaxes them. Transcription-dependent supercoils accumulate in TopA mutants and are responsible for defects in full-length RNA synthesis, metabolism and growth (Drolet et al., 1995). The phenotype of *E. coli* TopA mutants is reversed by RNAseH1 overexpression (Drolet et al., 1995). In yeast, the role of Top1 has been analysed in the highly transcribed ribosomal DNA cluster (El Hage et al., 2010). Yeast Top1 mainly resolves negative supercoils behind RNAPI, whereas Top2 resolves positive supercoils in front of it. Chromatin/DNA immunoprecipitation (ChIP/DNA) experiments by using the monoclonal antibody S9.6 directed against RNA-DNA hybrids reveal that R-loops form in the wild type yeast, in particular over the 18S 5' region. Those R-loops are significantly increased in yeast mutants lacking Top1 and/or Top2. The sites where R-loops accumulate correlate with truncated fragments of pre-rRNA and with piled up RNAPI in Top1 mutants (El Hage et al., 2010). Finally, human and murine cells expressing low to undetectable levels of Top1 display replication impairment at gene-rich regions. RNaseH overexpression suppresses this phenotype indicating that Top1 avoids R-loops accumulation coordinating supercoils relaxation and splicing thus preventing interference between replication and transcription (Tuduri et al., 2009).

CPT, by inhibiting the activity of Top1 and by triggering the accumulation of negative supercoiling, may have the same effect as Top1 downregulation in R-loop formation. RNaseH1 overexpression decreases the induction of γH2AX following CPT treatment in post-mitotic primary rat neurons and in replication-blocked and replicating HeLa cells (Sollier et al., 2014; Sordet et al., 2009). The direct impact of CPT treatment in accumulating and stabilizing R-loops *in cellulo* has also been shown by recent studies (Groh et al., 2014; Marinello et al., 2013; Powell et al., 2013; Stuckey et al., 2015). In response to CPT, R-loops, visualized by immunofluorescence with the S9.6 antibody, are rapidly stabilized at nucleoli and mitochondria in human cells with a kinetic that closely correlates with Top1cc formation (Marinello et al., 2013). By using ChIP/DNA *Powell et al.* show that topotecan increases R-loop levels over the *Snord116* paternal locus (Powell et al., 2013) (**Figure**

12). This R-loop accumulation causes chromatin decondensation and inhibition of RNAPII elongation resulting in the inhibited expression of the non-coding RNA (ncRNA) *Ube3a-ATS* and the expression of the paternal *Ube3a* gene, which is normally silenced by *Ube3a-ATS*. This study holds promise for using topotecan to treat Angelman syndrome, a neurodevelopmental disorder characterized by the loss of function of the expressed maternal *Ube3a* (Powell et al., 2013). CPT also enhances R-loop formation over expanded GAA in frataxin (FXN) gene in cells from Friedreich ataxia (FRDA), another neurodegenerative disorder (Groh et al., 2014). These R-loops are responsible for FXN transcriptional repression and promote formation of repressive H3K9me2 marks suggesting a molecular mechanism of the FRDA pathology (Groh et al., 2014).

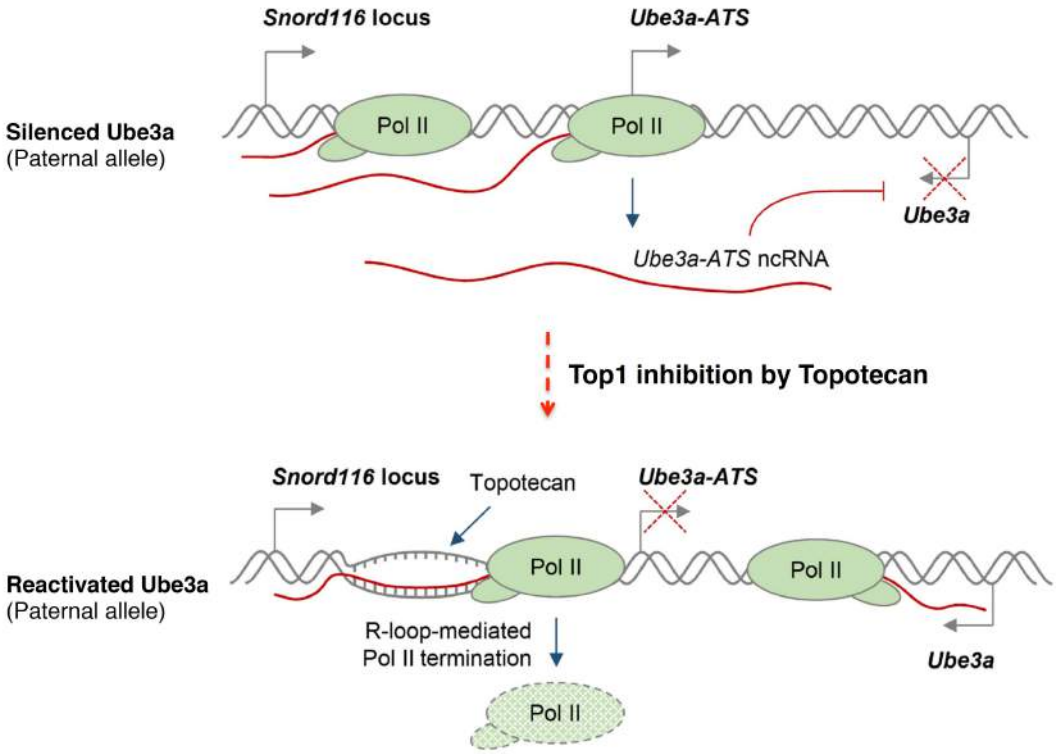

Figure 12: Topotecan-dependent reactivation of paternal Ube3a allele. ncRNA *Ube3a-ATS* expression represses paternal *Ube3a* in *cis*. Topotecan inhibits Top1 catalytic activity leading to R-loops accumulation over the *Snord116* locus that results in chromatin decondensation, inhibition of *Ube3a-ATS* transcription and reactivation of paternal *Ube3a* expression (Groh and Gromak, 2014; Powell et al., 2013).

I.5.2.6 Induction of antisense transcripts

A number of works from *Capranico*'s laboratory have described a transcriptional response to prolonged CPT treatment (4 h) likely linked to sustained CPT interference with RNAPII regulation (for review see (Capranico et al., 2010)). This response involves a more accessible chromatin conformation and the induction of low-abundance antisense transcripts (Baranello et al., 2010;

Bertozzi et al., 2011; Marinello et al., 2013). CPT triggers an increase of antisense transcripts at the 5' and 3' ends of the human HIF1α gene. These antisense transcripts overlap with the primary sense transcript of HIF1α gene and their expression correlates with a reduction of the mRNA (Baranello et al., 2010). The 5' antisense HIF1α localizes mainly at the nuclear membrane close to the nuclear pore protein Nup62 suggesting a role in the nucleus-cytoplasm transporting machinery (Bertozzi et al., 2011). Although antisense transcripts have been suggested to trigger silent chromatin assembly (Grewal and Moazed, 2003), the increasing level of HIF1α antisense transcripts is not associated with H3K9me2 repressive chromatin mark, but to a more accessible chromatin structure (Baranello et al., 2010). Those observations have suggested that CPT induces an imbalance of sense/antisense transcripts.

More recently, RNA-sequencing analysis in response to CPT (4 h) has revealed that Top1cc specifically enhance antisense transcripts at CpG island promoters of intermediate activity in different human cell types (Marinello et al., 2013). Those promoter-associated antisense transcripts have features of divergent promoters: symmetrical chromatin architecture with two peaks of paused RNAPII, and two domains of the active H3K4me3 and H3K27ac marks. CPT-induced antisense transcripts are Cdk9-dependent and replication-independent. Since bidirectional promoters have a higher rate of transcription-generated negative supercoils, it is possible that the accumulation of R-loops and/or torsional stress at CpG island promoters of moderately expressed genes may lead to antisense transcript accumulation. However, the torsional stress generated by the inhibition of Top1 activity is not sufficient to explain the induction of antisense transcripts by CPT because depletion of Top1 by siRNA or shRNA decreases the levels of antisense transcripts indicating that their induction is dependent on Top1cc (Baranello et al., 2010; Marinello et al., 2013). Indeed, K+SDS immunoprecipitation to map Top1cc at TSS-proximal regions of active divergent promoters shows a rapid burst of Top1cc that correlate with a transient RNAPII block at promoter (Marinello et al., 2013).

I.5.2.7 Induction of DNA damage and DDR activation

Similarly to replication, Top1cc stabilized by CPT can be converted into irreversible Top1cc upon collision with the transcriptional machinery, which determines DNA end misalignement and precludes end religation (Pommier, 2006; Wu and Liu, 1997). This collision results in the production of (i) Top1-linked SSBs (Hsiang et al., 1985) (**Figure 13A**), for review see (Ashour et al., 2015) and (ii) DSBs (Sordet et al., 2010; Sordet et al., 2009) (**Figure 13B**).

The *Liu*'s laboratory initially demonstrated the involvement of transcription in CPT-induced DNA damage (Wu and Liu, 1997). They showed that the conversion of reversible Top1cc into irreversible Top1cc by transcription occurs primarily on the template strand within the transcribed region with a maximal frequency near the promoter (Wu and Liu, 1997). This is in agreement with a gradual decrease in transcriptional activity at sites distal from the promoter (Bendixen et al., 1990; Khobta et al., 2006) (see section *I.5.2.2*). However, the authors also reported the generation of a number of transcription-dependent irreversible Top1cc in the non-template strand located upstream of the promoter (Wu and Liu, 1997).

In non-proliferative cells, CPT induces SSBs that can be visualized by alkaline comet assay in a replication-independent but transcription-dependent manner (Huang et al., 2010; Katyal et al., 2014; Lin et al., 2008). Those CPT-induced SSBs can be enhanced by inhibition of PARylation (Lin et al., 2008).

The other type of transcription-dependent lesions produced by CPT-stabilized Top1cc are transcription-coupled DSBs (TC-DSBs) (see *Chapter II* for description of DSBs). The production of TC-DSBs was first reported by *Sordet et al.* in post-mitotic primary neurons and lymphocytes and in EdU-negative cycling cells (cells outside of S-phase) (Sordet et al., 2010; Sordet et al., 2009) and then confirmed by several studies in different cellular models (Das et al., 2009; Huang et al., 2010; Katyal et al., 2014; Regairaz et al., 2011; Sakai et al., 2012; Sakasai et al., 2010a; Tian et al., 2009; Zhang et al., 2011). The nature of transcription-mediated DNA damage and downstream cellular responses is less well characterized than that of replication-induced damage.

The presence of DSBs can be monitored by the induction of comet tail moment in neutral condition and by the activation of DDR. In post-mitotic primary neurons and lymphocytes, CPT produces DSBs and activates DDR leading to the formation of large nuclear DDR foci containing activated ATM, γH2AX, activated Chk2, MDC1 (mediator of DNA-damage checkpoint 1) and 53BP1 (tumor protein p53 binding protein 1) (Sordet et al., 2009). Those replication-independent DSBs are dependent on RNAPII transcription as inhibition of transcription by DRB, flavopiridol (FLV) or α-amanitin suppresses DSB induction and the activation of the ATM-DDR pathway (Sordet et al., 2009). In addition, those TC-DSBs are located inside transcription factories since they colocalize with the euchromatin marker H3K9ac and S5-phosphorylated RNAPII (Sordet et al., 2009).

CPT-induced TC-DSBs form foci that have specific characteristics that make them different from replicational foci. In asynchronously growing cancer cells, *Sakasai et al.* distinguish 53BP1 foci associated to TC-DSBs from 53BP1 foci associated with RC-DSBs (Sakai et al., 2012; Sakasai et al., 2010a). The transcriptional 53BP1 foci are large foci compared to the smaller replicational foci characteristic of S-phase, they are completely dependent on ATM, they do not colocalize with RPA

and they appear only at CPT concentration > 1 µM. In addition, these foci are formed with a slower kinetic compared to replicational foci but are repaired more rapidly (Sakai et al., 2012).

The other key feature of CPT-induced TC-DSBs is the strong activation of ATM and the ATM-dependent DDR pathway (Huang et al., 2010; Katyal et al., 2014; Lin et al., 2008; Sakai et al., 2012; Sakasai et al., 2010a; Sordet et al., 2010; Sordet et al., 2009; Tian et al., 2009). In non-replicating cells, CPT-induced ATM activation is dependent on transcription (Huang et al., 2010; Katyal et al., 2014; Lin et al., 2008; Sakasai et al., 2010a; Sordet et al., 2009) and on proteasome activity (Huang et al., 2010; Katyal et al., 2014; Lin et al., 2008) and independent of replication. The DDR response to TC-DSBs is also dependent on ATM: γH2AX (Katyal et al., 2014; Sordet et al., 2009), 53BP1 (Sakasai et al., 2010a; Sordet et al., 2009), p53 (Tian et al., 2009) and Chk2-T68 (Sordet et al., 2009). This CPT-induced ATM-dependent DDR pathway can be enhanced by inhibition of PARylation (Lin et al., 2008; Sakai et al., 2012; Zhang et al., 2011) or depletion of Tdp1 (Das et al., 2009; Katyal et al., 2014).

In CPT-treated post mitotic cells, the induction of γH2AX foci has been described to be completely dependent of ATM (Katyal et al., 2014; Sordet et al., 2009) but independent of Nbs1 (Katyal et al., 2014), a component of the MRN complex, which acts as ATM cofactor (see *Table 6* and section *II.5.1.1*). In those cells, the kinase DNA-PK (see section *II.3.3*) is also activated in an ATM-dependent manner (Sordet et al., 2009) but the role of this activation is not known yet. DNA-PK inhibition does not impact CPT-induced γH2AX foci in post mitotic neurons (Katyal et al., 2014; Sordet et al., 2009). However, the maintaining of γH2AX foci after CPT removal is dependent on DNA-PK activity indicating a role for DNA-PK in the response to TC-DSBs that remain to characterize (Katyal et al., 2014). By contrast, the ATR kinase (see section *II.3.2*) is likely not implicated in the response to TC-DSBs since it is not or only weakly expressed in post mitotic cells (Jones et al., 2004; Sordet et al., 2009).

Mechanistically, the production of TC-DSBs involves R-loops (see section *I.5.2.5*) as RNaseH1 overexpression reduces the CPT-induced γH2AX foci in both post mitotic neurons treated with CPT as well as in HeLa cells in which replication was blocked before treatment with CPT (Sordet et al., 2009).

As discussed above, R-loops may form as negative supercoiling accumulates behind the transcription complexes arrested by Top1cc (Drolet et al., 1994) or by a possible interference with splicing regulated by the SR-kinase activity of Top1, which is also known to promote R-loops (Li and Manley, 2005; Soret et al., 2003). How DSBs arise from a transcription-blocked Top1cc and an R-loop remains to be established. Recently, it has been reported that R-loops can be converted in DNA damage by the TCR through the activity of the endonucleases XPF and XPG (xeroderma

pigmentosum group-F/G complementing protein) and the participation of the NER factors XPA, XPB, XPD and CSB (Sollier et al., 2014). Indeed, XPG depletion reduces γH2AX foci in replicating cells treated with CPT (Sollier et al., 2014). Further studies will be necessary to elucidate the mechanism of production of TC-DSBs and the role of R-loops and R-loop processing factors in TC-DSB production.

The R-loop-dependent nature of CPT-induced TC-DSBs raises the question whether TC-DSBs occur at specific genomic sites with features that promote R-loop formation. The co-staining of γH2AX foci and IgH locus by ICC-FISH experiments (immunocytochemistry staining followed by fluorescence *in situ* hybridization) shows an enrichment of γH2AX at those sites in unstimulated splenocytes treated by CPT (Sordet et al., 2010). IgH corresponds to immunoglobulin heavy chain locus where CSR occurs (Petersen et al., 2001). CSR is a process enabling mature B cells to change antibody isotypes and it involves transcription, R-loops and DSB production (Chaudhuri and Alt, 2004). Therefore, authors suggested that CPT-induced TC-DSBs may form at specific genomic sites (Sordet et al., 2010).

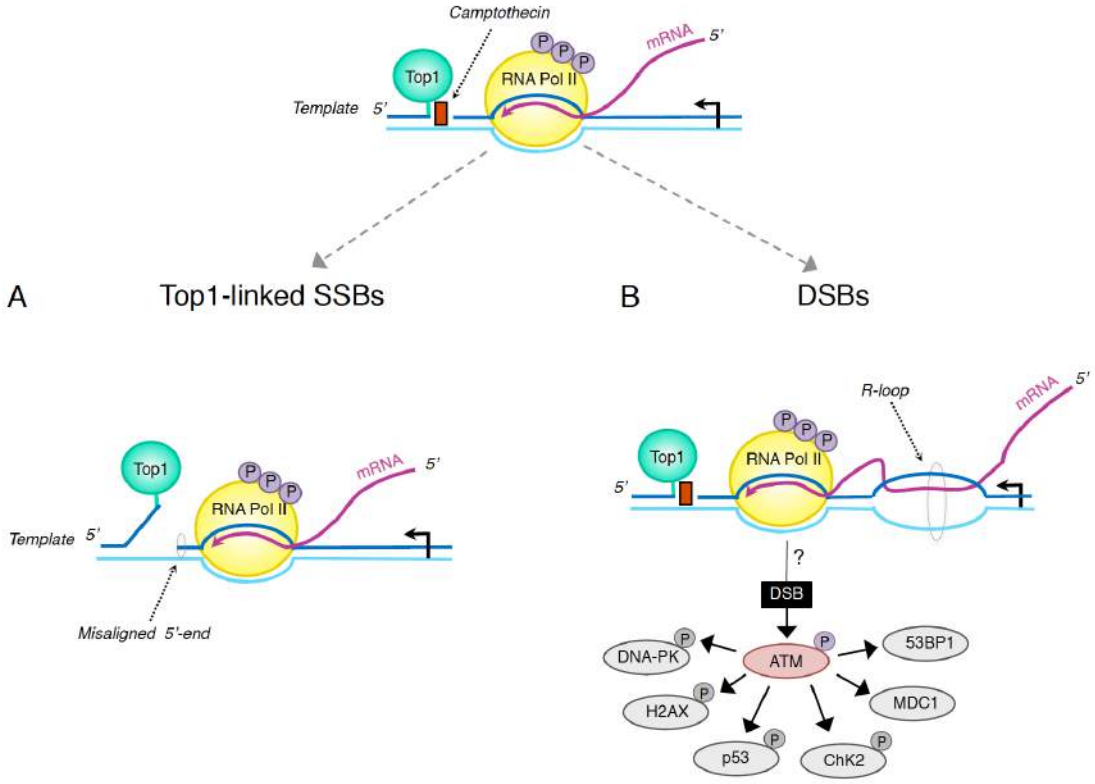

Figure 13: Schematic representation of the conversion of CPT-stabilized Top1cc in DNA damage by transcription. Top1cc trapped by CPT in the template strand collides with transcribing RNAPII. The collision converts reversible Top1cc into irreversible Top1cc resulting in the production of (**A**) Top1-linked SSBs or (**B**) DSBs by an R-loop dependent mechanism and activation of the ATM-DDR pathway (Adapted from (Sordet et al., 2009)).

In addition to replication-associated cytotoxicity, transcription-induced DNA damage can participate to CPT cytotoxicity (Katyal et al., 2014; Morris and Geller, 1996; Morris et al., 2001; Sakasai et al., 2010a; Stefanis et al., 1999). In cancer cells, CPT cytotoxicity becomes not only dependent on replication at high (>1 µM) concentrations (Holm et al., 1989; O'Connor et al., 1991). However, CPT induces cell-death in post-mitotic cells by inducing apoptosis in a transcription-dependent manner (Morris and Geller, 1996; Morris et al., 2001; Stefanis et al., 1999). In neurons, CPT-induced cell death is mediated by the activation of a Cdk5-ATM-p53 pathway, which triggers cell-cycle re-entry and expression of the p53 target genes related to death such as Puma and Bax (Tian et al., 2009). Although the ATM-dependent pathway controls cell fate, the ATM-mediated response appears to be different in post mitotic and cycling cells treated with CPT. Indeed, ATM promotes cellular survival in G1-phase cells exposed to CPT by activating the G1/S and S-phase checkpoint and by protecting cells from DNA-PK-induced cell killing (Sakasai et al., 2010a). The authors suggested two possible explanations for their observations: (i) the ATM-dependent checkpoint activation in G1 limits the number of DSBs by avoiding the entering of damaged cells in S-phase and the replication-dependent conversion of SSBs in DSBs that massively activate DNA-PK in S-phase or (ii) a complex cross-regulation between the two kinases exists (Sakasai et al., 2010a). In any case, transcription-dependent processing of the Top1cc may lead to the generation of an intermediate that is lethal to cells but the nature of this intermediate is not known.

It appears clearly that ATM signalling coordinates the response to DNA damage induced by transcription-dependent Top1cc by controlling Top1 degradation (Alagoz et al., 2013; Katyal et al., 2014), by promoting the activity of Tdp1 (Das et al., 2009), by regulating the level of ROS (Guo et al., 2010; Ito et al., 2004; Okuno et al., 2012) that can further trap Top1 (Daroui et al., 2004; Pourquier and Pommier, 2001), by regulating transcription in presence of damaged DNA (Alagoz et al., 2013; Shanbhag et al., 2010), by activating DDR response to transcriptional DSBs (Sordet et al., 2009) and by controlling cell's fate (Sakasai et al., 2010a; Tian et al., 2009).

I.6 Repair of irreversible Top1cc

As mentioned above, a trapped Top1cc creates a SSB associated with a covalently-linked Top1 molecule at the 3' end of the break and a free 5' end generally associated with a complementary strand. In the case of transcription-mediated Top1cc, the resulting double-strand termini are DNA-RNA hybrids, whereas in the case of replication-mediated Top1cc, the DNA-DSEs are composed of the DNA template and the newly synthesized leading strand. In the case of Top1cc formed by an SSB or by a neighbouring Top1cc on the opposing strand from the Top1 scissile strand, a staggered

DSB is formed. Those DNA termini are not suitable for repair as the proper substrate for DNA ligases are a 3'-hydroxyl and a 5'-phosphate.

Thus, the "cleaning" of DNA ends by removing Top1 covalent complexes is the requirement to repair the DNA damage associated with irreversible Top1cc and to allow transcription and replication restart. Deciphering the biochemical pathways involved in the repair of Top1 suicide complex started in yeast. The human orthologs of many of the yeast genes identified for Top1 repair are mutated in hereditary diseases predisposing to cancer and sensitize cells to CPT (for gene list, see (Pommier, 2006; Pommier et al., 2006)). The three main pathways (reviewed in (Ashour et al., 2015; Pommier et al., 2006; Pommier et al., 2003; Xu, 2015)) for irreversible Top1cc repair are: (i) the helicase pathway, (ii) Top1 excision by Tdp1, (iii) Top1 excision by nucleases. The apparent redundancy of the Top1 repair pathways is consistent with the formation of irreversible Top1cc under physiological conditions (Pourquier and Pommier, 2001). It seems that each pathway is preferentially used for a particular Top1cc (for example transcription mediated-Top1cc or replication-mediated Top1cc), and in a specific cellular context (for example replicating or post-mitotic cells). The choice of the pathway is at least in part determined by the nature of the DNA lesion. Further studies are necessary to clarify this point but the working model is: the preferential repair of transcriptional-Top1cc by the Tdp1 excision pathway and the preferential repair of replicational-Top1cc by the helicases or the endonucleases pathway.

I.6.1 Helicase pathway

This pathway is not possible for Top1cc produced by lesions affecting the 5' end of the broken DNA, since it relays on the efficacy of Top1 in religating a 5'-OH to the Top1cc. Top1 religation becomes possible in the case of replication- or transcription- dependent Top1cc following regression of the replication or transcription complexes (Pommier et al., 2006).

Replication fork regression leads to the formation of a "chicken foot" DNA structure by newly synthesized strands, which is topologically equivalent to a Holiday junction. These structures can be resolved by RecQ helicases, such as BLM (bloom syndrome, RecQ-helicase-like) and WRN, and Top3α (for review see (Pommier et al., 2006; Pommier et al., 2003)). WRN deficient cells are hypersensitive to Top1 inhibitors, show enhanced DNA replication block and S-phase arrest and accumulate DSBs suggesting a role of WRN in the resolution of stalled replication forks induced by trapped Top1 (Christmann et al., 2008). Recently, it has been shown that CPT-induced fork slowing and reversal is promoted by PARP1 activity, which inhibits the helicase RECQ1 locally, thereby restraining the restart of reversed forks until Top1cc repair is complete (Berti et al., 2013; Ray

Chaudhuri et al., 2012) (**Figure 16A**).

A similar mechanism may be also hypothesized for transcription following RNAP backtracking.

Top1 can also religate a non-homologous DNA strand bearing a 5'-hydroxyl end, which results in non-homologous recombination (Pommier et al., 1995).

I.6.2 Excision by Tdp1 pathway

I.6.2.1 Structure and function of the Tdp1 enzyme

Tdp1 was discovered in 1996 by *Nash* and coworkers in *Saccharomyces cerevisiae* as the enzyme capable of hydrolysing the covalent bond between the Top1 catalytic tyrosine and the 3' end of the DNA (Pouliot et al., 1999; Yang et al., 1996). This activity was named tyrosyl-DNA phosphodiesterase 1. Tdp1 generates a 3'-phosphate, which is further processed by a 3'-phosphatase, such as PNKP (polynucleotide kinase phosphatase) (Whitehouse et al., 2001).

Tdp1 is highly conserved in eukaryotes and belongs to the phospholipase D (PLD) superfamily (Interthal et al., 2001), which comprises a heterogeneous group of enzymes that catalyse phosphoryl transfer reaction. Human Tdp1 is a 68-kDa polypeptide ubiquitously expressed. Human Tdp1 has an analogous 3'-phosphotyrosyl processing activity to its yeast counterpart (Interthal et al., 2001), while having only about 15% sequence identity (Cheng et al., 2002). Human Tdp1 is constituted by 608 amino acids organised in two domains (Interthal et al., 2001; Pommier et al., 2014) (**Figure 14A**):

- *N-terminal domain* (1-148 aa): It is the poorly conserved domain or absent in lower eukaryotes. It is dispensable for enzymatic activity, yet it regulates Tdp1 recruitment and protein stability by receiving post-translational modifications (see section *I.6.2.3*).
- *C-terminal domain*: It is the catalytic domain belonging to the PLD family as it contains two catalytic HKN motifs (amino acids 262-289 the first HKN and 492-522 the second HKN), the most conserved regions among the Tdp1 orthologs, separated from each other by 210 amino acid residues. Differently from the other PLD family members, the aspartates in the HKD motifs are replaced by asparagines (HKN motifs) in Tdp1. Mutations of histidine (H263A) or lysine (K265S) in the first HKN motif results in complete loss of Tdp1 activity, whereas analogous mutations (H493A/R/N or K495S) in the second HKN motif lead to a strong decrease in Tdp1 activity (Interthal et al., 2001; Raymond et al., 2004).

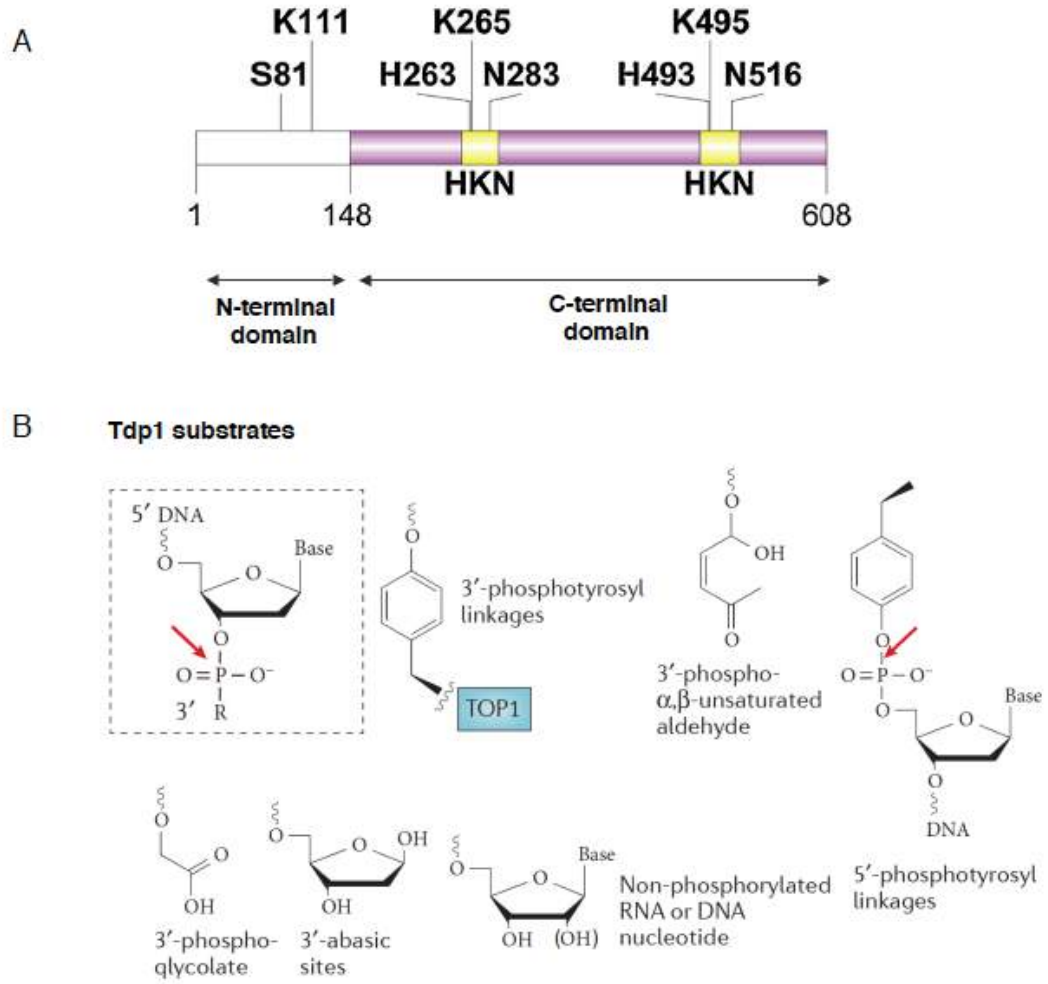

Figure 14: Schematic of Tdp1 and Tdp1 physiological substrates. (**A**) Representation of N-Terminal (white) and C-terminal (pink) domains of Tdp1. HKN motifs and the sites of phosphorylation (S81) and SUMOylation (K111) are indicated. Adapted from (Pommier et al., 2014). (**B**) Some DNA adducts that can be processed by Tdp1 are represented. Adapted from (Ashour et al., 2015).

Crystal structures demonstrate that Tdp1 acts as a monomer with the two HKN motifs in close proximity to form the catalytic site located inside an asymmetric substrate-binding channel (Davies et al., 2002a; Davies et al., 2002b; Davies et al., 2003). This “binding channel” is relatively narrow and positively charged to bind the single-stranded DNA substrate. The DNA substrate is stabilized by hydrophobic or polar interactions thereby the binding of Tdp1 to DNA is not restricted to particular base sequences. This is consistent with the ubiquitous nature of Top1cc on the genome and with the requirement of Tdp1 action irrespective of the DNA sequence environment. In addition, the characteristics of Tdp1 “binding channel” make Tdp1 able to resolve a broad spectrum of 3’-blocking termini (**Figure 14B**):

- *3’-phosphotyrosine/phosphotyrosyl peptide*: Tdp1 hydrolyses 3’-tyrosine in a variety of DNA structures, including dsDNA with 3’-tyrosine at a nick or a gap and 3’-tyrosine at blunt, frayed or tailed ends but with a preference for ssDNA (Raymond et al., 2004; Yang et al., 1996). Tdp1 can process 3’-peptides ranging from one to more than 100 aa and DNA fragments consisting

of at least 4 nucleotides with a major efficiency for longer oligonucleotides and shorter peptides (Debethune et al., 2002; Interthal and Champoux, 2011; Interthal et al., 2005a). The ability of Tdp1 to hydrolyse 3'-phosphotyrosyl linkage is consistent with a role for the enzyme in protecting cells against cytotoxic Top1-associated DNA damage. To be a good substrate for Tdp1, Top1 covalently linked to DNA has to be prior denatured or proteolyzed (see section *I.5.2.4*) (Debethune et al., 2002; Interthal et al., 2005a). Yeast Tdp1 has been reported to resolve 5'-phosphotyrosyl linkage (Nitiss et al., 2006) and recently a similar action has also been characterized *in vitro* for human Tdp1 (Murai et al., 2012) indicating a possible back-up role for Tdp1 in Top2cc repair.

- *3'-phosphoglycolate*: Tdp1 can process 3'-phosphoglycolate ends that are commonly produced by oxidative DNA damage or by radiotherapy (El-Khamisy et al., 2007; Inamdar et al., 2002).

- *3'-deoxyribose phosphate*: The nucleosidase activity of Tdp1 can remove a single nucleoside from the 3' end of DNA or RNA molecules where they are not 3'-phosphorylated (Interthal et al., 2005a). This action of Tdp1 results in the generation of one nucleotide shorter polymer bearing a 3'-phosphate group. Tdp1 can remove the abasic mimic tetrahydrofuran moiety (Interthal et al., 2005a) and the anti-viral and anti-cancer chain-terminating nucleoside analogues such as acyclovir, zidovudine and cytarabine (Huang et al., 2013). Tdp1 also processes 3'-deoxyribose lesions generated by alkylating agents after the apurinic or apyrimidinic lyase processing such in the case of methylmethanesulfonate and temozolomide (Alagoz et al., 2014; Lebedeva et al., 2011; Murai et al., 2012).

- *3'-synthetic DNA adducts*: Tdp1 can resolve a wide range of 3'-synthetic DNA adducts such as biotin and a variety of fluorophores. This Tdp1 property has been used for screening Tdp1 inhibitors and for mechanistic studies (Antony et al., 2007b; Dexheimer et al., 2010; Rideout et al., 2004).

To process its substrates, Tdp1 proceeds via a two step-reaction without nucleotide cofactor or metal (Interthal et al., 2001; Pommier et al., 2014) (**Figure 15**). The first step consists in a nucleophilic attack of the Top1-DNA phosphotyrosyl bond by H263 of the first HKN motif resulting in the liberation of Top1 and in the formation of a Tdp1-DNA covalent intermediate. This intermediate is resolved by a hydrolytic reaction driven by H493 of the second HKN motif leading to the liberation of Tdp1 and to a 3'-phosphate terminus.

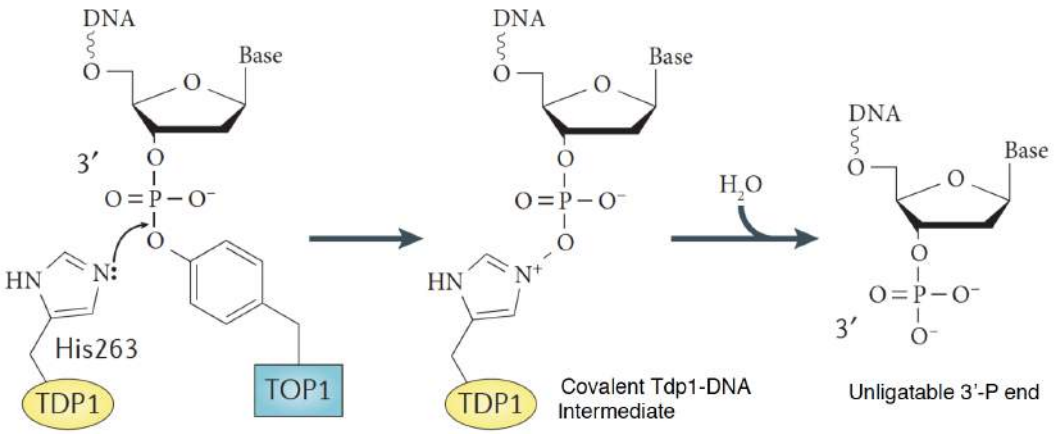

Figure 15: Tdp1 catalytic cycle. The nucleophilic attack of the phosphodiester bond Top1-DNA by H263 of Tdp1 results in the release of Top1 and the formation of a covalent Tdp1-DNA intermediate. Then, a second nucleophilic attack via an activated H_2O molecule by H493 of Tdp1 allows the release of Tdp1 and the generation of an unligatable 3'-phosphate (3'-P) end. Adapted from (Ashour et al., 2015).

I.6.2.2 Physiological consequences of Tdp1 mutations: SCAN1

Tdp1 is physiologically important since a mutation in the enzyme is responsible for an autosomal recessive called spinocerebellar ataxia with axonal neuropathy (SCAN1) (Takashima et al., 2002). To date, SCAN1 is restricted to nine patients from a single Saudi Arabian family. Clinically, affected individuals suffer from early onset ataxia (≈ 15 years), cerebellum atrophy and peripheral neuropathy but without involving cognitive decline (Takashima et al., 2002; Walton et al., 2010). SCAN1 patients lack extra-neurological symptoms like chromosomal instability and cancer predisposition that are found in individuals affected by other DNA repair-related disorders such as ataxia telangiectasia (Rass et al., 2007).

To date, the only mutation known to be associated with SCAN1 is a homozygous mutation resulting in the substitution of histidine by arginine (H493R) within the second HKN motif of the Tdp1 active site (Takashima et al., 2002). Recombinant mutated Tdp1 is ≈ 25-fold less active of wild-type (Interthal et al., 2001) and SCAN1 cell extracts display a Tdp1 activity reduced of ≈ 100 fold (Interthal et al., 2005b). The greater defect in SCAN1 extracts is likely to reflect the 2-3- fold reduction in Tdp1 protein level likely linked to instability of the mutant protein. The H493R mutation affects primarily the second step of Tdp1 catalytic reaction (**Figure 15**) thus leading to the liberation of Top1 adducts and the accumulation of Tdp1-DNA covalent intermediates (Interthal et al., 2005b). Wild-type Tdp1 can hydrolyse Tdp1-DNA covalent complex, which explains why heterozygote carriers for H493R mutation do not display SCAN1 symptoms (Interthal et al., 2005a). However, the relative proportion of unprocessed (and therefore Top1-associated) versus partially processed (and therefore Tdp1-associated) termini that accumulate in SCAN1 cells is unclear.

Consequently, the relative contribution of these covalent complexes to the SCAN1 phenotype is unknown.

Consistently, features of SCAN1 cells are hypersensitivity to CPT and defective repair of CPT-induced Top1cc associated with accumulation of SSBs, Top1-DNA and Tdp1-DNA covalent complexes (Barthelmes et al., 2004; El-Khamisy et al., 2005; Interthal et al., 2005b; Miao et al., 2006). The deficiencies in the repair of Top1cc have been proposed to be responsible for the neurodegenerative phenotype of SCAN1 patients but further studies are necessary to understand the molecular mechanism leading to neurodegeneration.

I.6.2.3 Post-translational modification of Tdp1

The action of Tdp1 is tightly regulated by post-translational modifications on its N-terminal domain:

- *Phosphorylation*: ATM and DNA-PK are able to phosphorylate Tdp1 on S81 (Chiang et al., 2010; Das et al., 2009). S81 phosphorylation is not required for Tdp1 enzymatic activity (Antony et al., 2007b; Chiang et al., 2010) but it promotes Tdp1 stability and controls its subcellular distribution (Chiang et al., 2010; Das et al., 2009). In response to CPT and IR, phosphorylated S81-Tdp1 forms foci that colocalize with γH2AX and with X-ray repair cross-complementing protein 1 (XRCC1) foci (Das et al., 2009). Indeed, S81 phosphorylation enhances the interaction with DNA ligase 3α (Lig3α) and XRCC1 (Chiang et al., 2010; Das et al., 2009) thereby promoting the formation of stable Tdp1 complex at Top1-linked damage sites that facilitate Top1cc repair and cell survival in response to CPT- and IR-induced DNA damage. The formation of S81-Tdp1 foci induced by CPT is prevented by both aphidicolin (APH) and DRB indicating that they are dependent on RC-DSBs and TC-DSBs (Das et al., 2009). Yet, it is still unclear whether S81 phosphorylation impacts both SSB and DSB repair, since the phosphorylation appears to be driven by DSB formation.
- *SUMOylation*: Tdp1 is SUMOylated at K111 in a DNA damage-independent manner (Hudson et al., 2012). K111R mutants do not display defects in Tdp1 catalytic activity and in Lig3α interaction but they show accumulation of SSBs and decreasing Tdp1 concentration at sites of DNA damage in response to CPT (Das et al., 2014; Hudson et al., 2012). In addition, upon transcription inhibition by DRB, the higher level of SSBs in Tdp1 K111R mutants treated with CPT, are decreased to a level comparable to wild-type Tdp1 cells (Hudson et al., 2012). These results indicate that the function of Tdp1 K111-SUMOylation is to promote Tdp1 accumulation at transcription-dependent Top1cc sites, which is consistent with the role of Tdp1 in protecting post-

mitotic neurons against Top1cc-induced damage.

- *PARylation*: PARP1 directly binds the N-terminal domain of Tdp1, and PARylates Tdp1 without affecting its catalytic activity (Das et al., 2014). The functional role of PARylation is to stabilize Tdp1 in response to Top1cc-induced DNA damage and to promote the recruitment of both Tdp1 and XRCC1 at Top1cc-induced DNA damage sites (Das et al., 2014). Tdp1 and PARP1 form complexes independently of DNA damage. PARP1 activation by Top1cc drives Tdp1 at damage sites acting as a molecular switch that channels Top1-DNA covalent complexes to the Tdp1 pathway, and it might protect DNA from non-specific endonucleolytic cleavage. This role of PARP explains the hypersensitization of PARP1 KO and PARP inhibitor-treated cells to CPTs (Bowman et al., 2001; Chatterjee et al., 1989; Patel et al., 2012; Zhang et al., 2011) and the absence of additional sensitization by Tdp1 depletion (Alagoz et al., 2014; Das et al., 2014).

I.6.2.4 Stepwise repair by Tdp1 pathway

The Tdp1 excision pathway is a sub-pathway of SSBR (SSB Repair) (for review see (Caldecott, 2008)), in which Tdp1 works with BER factors to carry out the detection, the excision of the 3'-phosphotyrosyl linkage Top1-DNA and the repair of the damage (**Figure 16B**).

Based on recent findings, a working model is that Tdp1 detects Top1-mediated DNA damage through PARP1, as Tdp1 and PARP1 form complexes in physiological conditions (Das et al., 2014). Once activated by Top1cc-associated SSBs (Bowman et al., 2001; Chatterjee et al., 1989; Das et al., 2014; Patel et al., 2012; Zhang et al., 2011), PARP1 catalyses PARylation at DNA lesions favouring the recruitment of repair complexes (such as XRCC1) and the release of PARP1 from DNA to facilitate DNA repair (Das et al., 2014). XRCC1 functions as a loading dock, which stabilizes, stimulates and facilitates the accumulation of SSB repair factors. XRCC1 is able to bind Tdp1 (Das et al., 2014; El-Khamisy et al., 2005; Plo et al., 2003), PARP1 (Das et al., 2014), PNKP, Polymerase β and Lig3α (Caldecott, 2008; El-Khamisy et al., 2005; Whitehouse et al., 2001).

Tdp1 accumulates at sites of Top1cc-associated damages (Das et al., 2009) and hydrolyses the phosphodiester bond Top1-DNA that is exposed after the proteasome-mediated degradation of Top1 (Desai et al., 1997; Desai et al., 2003). Tdp1 generates 3'-phosphate ends that cannot be directly religated to the 5'-OH. PNKP converts 3'-phosphate to 3'-OH and also 5'-OH to 5'-phosphate, making ends compatible for extension by a polymerase or directly for religation with no base loss (Yang et al., 1996). The rejoining of the 3'-OH and the 5'-phosphate ends is mainly mediated by Lig3α.

The requirement of end-processing by PNKP after Top1 excision explains why PNKP-defective

human cells and SCAN1 cells accrue similar levels of CPT-induced DNA damage (El-Khamisy et al., 2005). Multiple mutations in the PNKP gene have been recently identified by genome-wide linkage analysis to be tied to the hereditary disease, MCSZ, microcephaly with early-onset, intractable seizures and developmental delay (Shen et al., 2010). MCSZ is primarily a neurodevelopment disease, highlighting a key role for the DNA processing activity of PNKP in non-replicating cells (Reynolds et al., 2012).

The Tdp1 excision pathway is thought to repair preferentially transcription-mediated Top1cc (El-Khamisy et al., 2005; Hudson et al., 2012; Miao et al., 2006). First, Tdp1 action requires prior proteolysis of Top1 (Debethune et al., 2002) and Top1 proteasomal degradation is dependent on transcription and independent on replication (Desai et al., 2003; Sordet et al., 2008b). Second, the defective repair of CPT-induced Top1cc in SCAN1 cells is independent on replication whereas DRB pre-treatment reduces CPT-induced SSBs in these cells (El-Khamisy et al., 2005; Miao et al., 2006). These observations suggest that Top1cc accumulated in CPT-treated SCAN1 cells are likely to be transcription-associated lesions predominantly (Miao et al., 2006). Finally, Tdp1 exists in equilibrium between unmodified (the majority) and a SUMOylated version (a tiny proportion) (see section *I.6.2.3*). This SUMOylated Tdp1 has been shown to be, at least in part, engaged in resolving Top1-dependent transcription-blocking lesions (Hudson et al., 2012).

Tdp1 is an attractive target for cancer therapy. SCAN1 cells (Das et al., 2009; El-Khamisy et al., 2005; Interthal et al., 2005b; Miao et al., 2006), cancer cells treated with siTdp1 (Das et al., 2009) and Tdp1 knockout mice (Hirano et al., 2007; Katyal et al., 2007) are hypersensitive to CPT. In addition, the broad spectrum of Tdp1 substrates open the possibility that inactivation of Tdp1 might enhance the anticancer effect of IR or chemotherapy. Another reason that makes Tdp1 a good target is that Tdp1 knockout mice are viable and they present a mild phenotype suggesting that the pharmacological inhibition of Tdp1 may be well tolerated. However, to date any Tdp1 inhibitors have progressed to clinical trials because of their poor physiochemical properties (Huang et al., 2011).

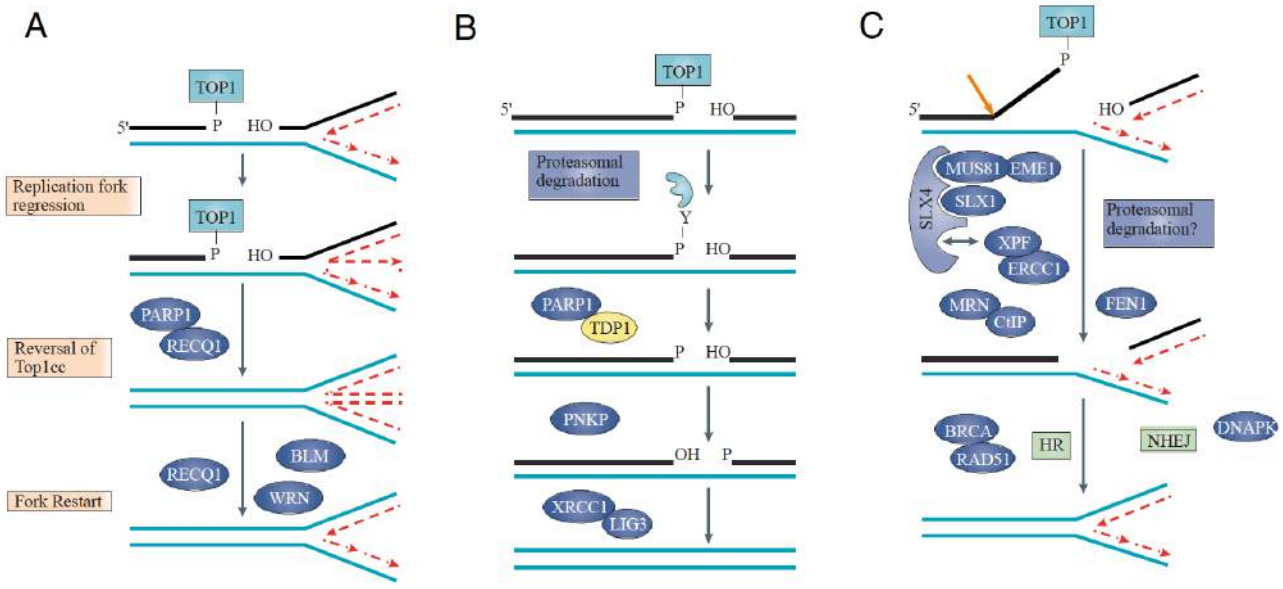

Figure 16: Schematic representation of the three main pathways for Top1cc repair. (**A**) Helicase pathway. Top1cc are reversed by 5' end religation after regression of the replication fork. Fork regression and restart requires helicase activity. (**B**) Tdp1 excision pathway. Top1 is degraded by the proteasome and the phosphodiester bond is cleaved by Tdp1. Tdp1 generates 3'-P ends that are processed by PNKP and religated by Lig3α. Tdp1, PNKP and Lig3α are part of the XRCC1 complex. (**C**) Endonuclease pathway. Top1cc are processed by non-specific nucleolitic cleavage of DNA, releasing Top1 and a fragment of DNA. Several endonucleases have been implicated. The resulting DNA lesions are likely processed by HR or by NHEJ. Adapted from (Ashour et al., 2015).

I.6.3 Excision by the endonuclease pathway

In addition to Tdp1, Top1-DNA lesions can be excised by 3'-flap endonuclease complexes (**Figure 16C**). It is not clear how the pathway choice is determined, but recent evidences highlight a possible role of PARP1 in channelling Top1cc repair to the Tdp1 excision pathway (Alagoz et al., 2014; Das et al., 2014). It is also not clear whether Top1 degradation has a role in the endonucleases pathway and in the pathway choice. The activity of the endonucleases is highly dependent on the structure of the Top1-associated DNA lesion and usually multiple nucleases are required to excise the DNA on the scissile strand to release Top1 and a fragment of DNA.

The endonuclease pathway has initially emerged from studies using genetically altered yeast strains to identify genes that function in CPT repair in the absence of Tdp1 (Deng et al., 2005; Pommier et al., 2006; Vance and Wilson, 2002). The budding yeast Tdp1 KO is viable and relatively insensitive to CPT (Pouliot et al., 1999) and it acquires CPT sensitivity only in the presence of additional mutations in other DNA repair/checkpoint genes or specific endonucleases. Some endonucleases identified for the repair of Top1cc in yeast and/or in vertebrates are:

- *XPF/ERCC1* (ortholog of yeast Rad1/Rad10) (Vance and Wilson, 2002): XPF forms a heterodimer with its non-catalytic partner ERCC1 (excision repair cross-complementing group 1) to generate a structure-specific endonuclease, which cleaves the duplex DNA segment immediately 5'

from the damaged region where the two DNA strands are separated (3'-flap, splayed arm or bubble) corresponding at about 3-4 nucleotides away from the 3' end (Ciccia et al., 2008). XPF/ERCC1 works in the NER pathway. Inactivation of the XPF/ERCC1 pathway increases the cytotoxicity of PARP inhibitors in CPT-treated mammalian cells (Zhang et al., 2011). In addition, siRNA downregulation of XPF reduces transcription- and replication-dependent γH2AX foci in response to CPT (Zhang et al., 2011).

- *Mus81/Eme1* (ortholog of yeast Mus81-Mms4) (Liu et al., 2002; Vance and Wilson, 2002): The heterodimer Mus81/Eme1 cleaves flap or branched DNA intermediates, but typically cleaves 3-6 base pairs 5' of the 3' single strand/duplex transition and requires the presence of a 5' end of DNA at the flap junction (Ciccia et al., 2008). Thereby it preferentially cleaves substrates mimicking stalled replication forks and nicked Holliday junctions. Recently it has been shown that Mus81/Eme1 is not involved in the direct excision of Top1cc in mammalian cells but rather participates in the repair and recovery of Top1cc-induced stalled replication forks (Zhang et al., 2011).

- *MRN complex* (ortholog of yeast MRX complex) (Deng et al., 2005; Liu et al., 2002): The nuclease of the MRN complex is Mre11 (see section *II.5.1.1*) and it preferentially cleaves 3'-single strand branched structures and requires a single-strand gap between the 3' end to be processed and the 5' end of the DNA (D'Amours and Jackson, 2002). The yeast MRX complex has a well-established role in the nucleolytic removal of Spo11 (Hartsuiker et al., 2009) and it has also been implicated in the removal of both trapped Top1 and Top2 from DNA independently of its function in DSB repair and meiosis (Hamilton and Maizels, 2010; Hartsuiker et al., 2009).

- *SLX4-SLX1* (ortholog of yeast Slx4-Slx1): The dimeric complex has a strong endonuclease activity in 3' flap and other substrates (Fricke and Brill, 2003). They have been identified in yeast as an alternative pathway to the Tdp1 excision pathway for protection against CPT (Deng Brown 2005). In addition, SLX4 (SLX4 structure-specific endonuclease subunit) is involved in the repair of CPT-induced Top1cc in mammalian cells working as a scaffold protein for SLX1 (SLX1 structure-specific endonuclease subunit), Mus81-Eme1 and XPF (Kim et al., 2013).

- *CtIP* (ortholog of yeast Sae2): CtIP (carboxy-terminal binding protein-interacting protein) is a 5' flap endonuclease that recognizes and cleaves branched DNA structures (Makharashvili et al., 2014). CtIP functions at the 5' DNA resection during homologous recombination (HR) (Sartori et al., 2007) and in the removal of Spo11 with the MRN complex (Hartsuiker et al., 2009). In yeast, Sae2 and MRX collaborate to remove Top2cc from DNA (Hartsuiker et al., 2009). In vertebrate, the BRCA1-CtIP interaction, which is dispensable for HR, plays a role in the nuclease mediated elimination of oligonucleotides covalently bound to polypeptides from DSBs, thus facilitating DSB

repair in response to Top1 and Top2 inhibitors (Nakamura et al., 2010). Consistently, CtIP S322A mutant DT40 cells deficient for BRCA1 interaction are hypersensitive to CPT (Nakamura et al., 2010) and CtIP S322A-Tdp1 KO DT40 double mutants have greater than additive sensitivity to CPT (Das et al., 2014).

- *FEN1* (the ortholog of yeast Rad27): FEN1 (flap structure-specific endonuclease 1) is a 5' flap endonuclease (Hiraoka et al., 1995). Deletion of yeast Rad27 causes mild sensitivity to CPT (Deng et al., 2005; Zheng et al., 2005) and this phenotype is rescued by human FEN1 (Zheng et al., 2005). The implication of FEN1 in Top1cc removal could be related to FEN1 ability to directly cleave stalled replication forks in complex with WRN (Zheng et al., 2005).

CHAPTER II: DNA Double-Strand Break and DNA Damage Response

II.1 Sources of DSBs

DNA is constantly assaulted by endogenous and environmental agents responsible for many thousands of DNA damages per cell every day (Lindahl and Barnes, 2000). The most severe form of DNA lesions are the double-strand breaks because they do not leave an intact complementary strand to be used as a template for DNA repair. A DSB is formed when both strands of the DNA duplex are severed by a break in the phosphodiester backbone at opposite sites within 10 bp. If left unrepaired, DSBs can lead to mutagenesis, chromosome breakage and rearrangement ultimately resulting in developmental defects, neurodegeneration, immunodeficiency, radiosensitivity, sterility, and cancer predisposition (Jackson and Bartek, 2009).
DSBs can be very different from each other since they can have multiple origins.

Endogenous DSBs

In various specialized contexts, DSBs are programmed by the cell. During meiosis, the Top2-related enzyme, Spo11 generates DSBs to promote exchange of genetic information between parental chromosomes by HR (Neale and Keeney, 2006). During immune system development, DSB-induced rearrangements at immunoglobulin genes, in the context of V(D)J recombination and CSR, occur in lymphoid cells to generate immunoglobulin and T-cell receptor diversity and for antigen-stimulated B-cell differentiation (Bassing and Alt, 2004; Chaudhuri and Alt, 2004). Telomeres also possess DNA ends that are sequestrated in the Shelterin complex to prevent them from being recognized as DNA damage and from fusions (de Lange, 2005). In addition, spontaneous DSBs can arise as a consequence of endogenous processes, such as DNA oxidation, generation of ROS, nitrogen species, reactive carbonyl species, oestrogen and cholesterol metabolites (Hoeijmakers, 2009). ROS are formed continuously in the cell as products of metabolic activities (Bonner et al., 2008; De Bont and van Larebeke, 2004). ROS are estimated to be responsible for about $5x10^3$ SSBs per cell per day, about 1% of which may lead to DSBs by the close proximity of two SSBs or by replication (Tanaka et al., 2006). The encounter of DNA replication fork with unrepaired DNA lesions is the major source of endogenous DSBs. The slowing or the stalling of the replication fork progression is defined as replication stress and in cell there are several sources of replication stress (reviewed in (Magdalou et al., 2014; Zeman and Cimprich, 2014)), including obstacles to fork progression (nicks, gaps, AP sites, DNA secondary structures, protein-DNA complexes…) (Lambert and Carr, 2013), interferences between replication and transcription (R-loops, early replicating fragile sites, topological stress,…) (Lin and Pasero, 2012), depletion of nucleotides or replication machinery components (Bester et al., 2011),

ribonucleotides misincorporation (Dalgaard, 2012), inappropriate firing of replication origins (common fragile sites) (Debatisse et al., 2012) or DNA accessibility (Zeman and Cimprich, 2014). The frequency of replication-associated DSBs is so high that the synthesis of both leading- and lagging-strand *in vivo* is considered to be discontinuous (Lehmann and Fuchs, 2006).

Exogenous DSBs

Exogenous DSBs can be produced directly by physical or chemical agents or as a secondary lesion upon collision with replication and transcription or as a by-product of repair. UV light from sun is an example of physical source of DNA damage. A single day of sun exposure can induce up to 10^5 UV photoproducts per cell to which inflammation-induced ROS damage can be sum up (Hoeijmakers, 2009). Another example of physical genotoxics that produce DSBs is ionizing radiation (IR) that can result from radioactive decay of naturally radioactive compounds or from medical treatment employing X-ray or radiotherapy. Chemical agents used in cancer chemotherapy can also produce DSBs. Among them, Top2 inhibitors (etoposide, doxorubicin...) that can produce DSBs directly or alkylating agent (methyl methanesulfonate, temozolomide…) and crosslinking agents that can produce DSBs indirectly. Today, one of the most prevalent environmental chemical than can induce a variety of adducts and ROS-dependent damages is cigarette smoking, on average ≈ 45-1000 aromatic DNA adducts per cell per day in the lung of smokers (Ciccia and Elledge, 2010).

Table 4 and **Figure 17** summarize the mechanisms of action and the amount of DSBs produced by some exogenous agents.

Table 4: Examples of DNA DSB inducing agents, mechanisms and amount of DSB induction

Agents		Characteristics and mechanism of DSB induction	Amount of DSBs	References
IR	γ-Irradiation	DNA damage by IR is formed by both direct energy deposition on DNA (especially particulate IR) and by indirect action in the surrounding environment, in particular, reactions with diffusible water radicals (especially for γ- and x-ray). The biological effects of IR arise from the production of DSBs and clustered DNA damage (lesions within 10 bp separation) randomly on the genome. IR generate a mixture of DNA lesions, ≈ 4-5% of them are DSBs.	1 Gy: 1 DSB/0.2x10^2 bp (≈ 30-60 DSBs/cell)[a]	(Cedervall et al., 1995; Ruiz de Almodóvar et al., 1994)
	α-particles, heavy ions		1 Gy: 41-73 DSBs/cell using α-particles with LET of 110 KeV/µM[b] or nitrogen ions with LET 80-225 KeV/µM[b]	(Claesson et al., 2007; Löbrich et al., 1996; Radulescu et al., 2004)
	X-ray		1 Gy: 0.8 DSB/0.2x10^2 bp (≈ 25 DSB/cell)	(Elmroth et al., 2003b)
UV	UVA	Photons of UV light are in the energy range of chemical bond and then alter the molecules that absorb energy. UVC (240-290 nm), UVB (290-230 nm) and UVA (320-400 nm) predominantly induce pyrimidine dimers. UVA and UVB produce SSBs and DSBs indirectly by reaction with oxygen molecules (generally replication-dependent DSBs).	1 DSB/0.95x10^6 bp with laser 364nm + Hoechst33342; 90-180 DSBs/stripe (equals to 3 Gy γ-Irradiation) with laser 337nm + BrdU. Laser generates a high number of breaks in a small nuclear volume	(Bekker-Jensen et al., 2006) (Kruhlak et al., 2006)
	UVB		—	(Peak and Peak, 1990)
	UVC		UVC through filters 0.0156: 6-4photoproducts + 0.05 cyclobutane pyrimidine dimers/10Kb/J/m2. Number of DSBs not determined.	(van Hoffen et al., 1995)
Drugs	Radiomimetics	DNA damage is directly induced by free radical attack on deoxyribose moieties in both DNA strands. They produce replication-independent DSBs, SSBs and base damage. Examples of radiomimetics are bleomycin, neocarzinostatin (NCS), calichemicin, C-1027, kedarcidin	Bleomycin: 10% of the induced lesions are DSBs; NCS: 20% of the induced lesions are DSBs; calicheamicin: 30% of the induced lesions are DSBs	(Elmroth et al., 2003a; Povirk, 1996)
	Bifunctional alkylators	Bifunctional alkylators have two reactive sites and they crosslink DNA with proteins or two DNA bases within the same DNA strand (intra-strand crosslinks) or on opposite DNA strands (inter-strand crosslinks). Examples are nitrogen mustard, mitomycin C and cisplatin. They can produce DSBs, DNA cross-links, replicative lesions and bulky adducts.	—	(Helleday et al., 2008) (Woods and Turchi, 2013)
	Replication inhibitors	These inhibitors target DNA synthesis. Aphidicolin directly inhibits DNA polymerase activity. Hydroxyurea inhibits ribonucleotide reductase. They can generate DSBs and replicative lesions.	—	(Saintigny et al., 2001)
	Topoisomerase inhibitors	These inhibitors trap topoisomerases in complex with DNA producing DSBs. They produce also SSBs and replicative lesions.	—	(Muslimović et al., 2009)

[a]Assuming 6x10^9 bp x diploid cell

[b]LET (Linear Energy Transfer) is defined as the average energy that an ionizing particle deposits per unit length of track (KeV/µm) as it traverses matter

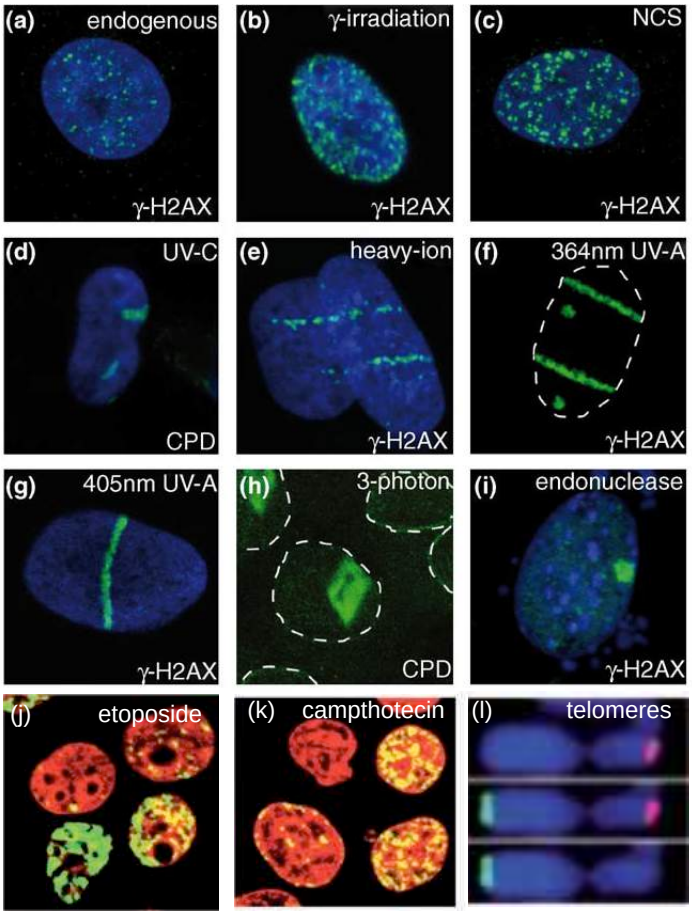

Figure 17: DNA damage in endogenous conditions or induced by genotoxic agents. DSBs are detected by γH2AX staining and cyclobutane pyrimidine dimers (CPD) are detected by antibody against CPD. (**A**) Non-treated HeLa cells. (**B**) U2OS cells 1 h after treatment with 10 Gy γ-Irradiation. (**C**) HeLa cells treated with 25 ng/ml NCS. (**D**) Human fibroblasts irradiated with UVC through a 3 µM pore-filter. (**E**) Human fibroblasts 15 min after carbon ion irradiation. (**F**) PA-GFP-H2AX in MEFs H2AX KO irradiated with 344 nm laser followed by Hoechst sensitization. (**G**) U2OS cells irradiated with 405 nm laser followed by BrdU (bromodeoxyuridine) sensitization. (**H**) Cells irradiated by a 3-photon NIR laser. (**I**) HeLa cells expressing I-SceI endonuclease. (**J**) Leukemic cells treated with etoposide. (**K**) Colon cancer cells treated with CPT. (**L**) Eroded telomeres in ageing cells. Telomeric DNA (red) and γH2AX (green) staining. Eroded telomeres display γH2AX foci but are too short to bind telomeric probe. DNA is blue for images (**A-I** and **L**) and red for images (**J**, **K**). γH2AX is green for all images. Adapted from (Nagy and Soutoglou, 2009) and (Bonner et al., 2008).

II.2 DDR: sensing DSB and signalling

The DNA damage response (DDR) is the global signalling network set up by cells to maintain genome integrity. DDR senses different types of DNA damages to mount a coordinated and multifaceted response.

DDR is most vigorously activated by DSBs. DDR proteins are classically divided in four categories according to their role: sensors, mediators, transducers and effectors. However, DDR proteins have a broad activity and this classification is for convenience and can vary from author to author. DNA damage is detected by sensors proteins. The signals are transmitted to transducers that, aided by the

mediators, amplify the signal and transmit it to the effectors in numerous downstream pathways (Niida and Nakanishi, 2006) (**Table 5**). These pathways slow down or stop the cell cycle progression at critical stages before (G1/S checkpoint) or during (intra-S checkpoint) DNA duplication and before cell division (G2/M checkpoint) giving time to the cell for DSB repair before replication and mitosis, respectively. In parallel, DDR stimulates the re-localization and the transcriptional and post-transcriptional regulation of DNA repair proteins enhancing repair (Harper and Elledge, 2007).

If DNA is efficiently repaired, DDR is inactivated and normal cell functioning can be restored. Alternatively, maintained DDR signalling activates apoptosis or senescence, both of which have potential antitumor functions (**Figure 18**).

Table 5: Main factors involved in DNA damage signalling

Functions	Class	Proteins
Sensors	RFC-like	Rad17, RFC2
	PCNA-like	Rad9-Rad1-Hus1 (9-1-1 complex)
	DSB recognition/repair	Mre11-Rad50-Nbs1 (MRN complex), RPA
Mediators	BRCT-containing (ATM signalling)	BRCA1, 53BP1, MDC1, MCPH1, PTIP
	BRCT-containing (ATR signalling)	Top1BP1
	Non-BRCT-containing (ATR signalling)	Claspin
Transducers	PI3K kinase-like protein	ATM, ATR, DNA-PK
	PIKK binding protein kinase	ATRIP, Chk1, Chk2
Effectors	Transcription factor	p53, p21
	Phosphatase	Cdc25A,B,C
	Protein kinase	Cdks, Cdc7

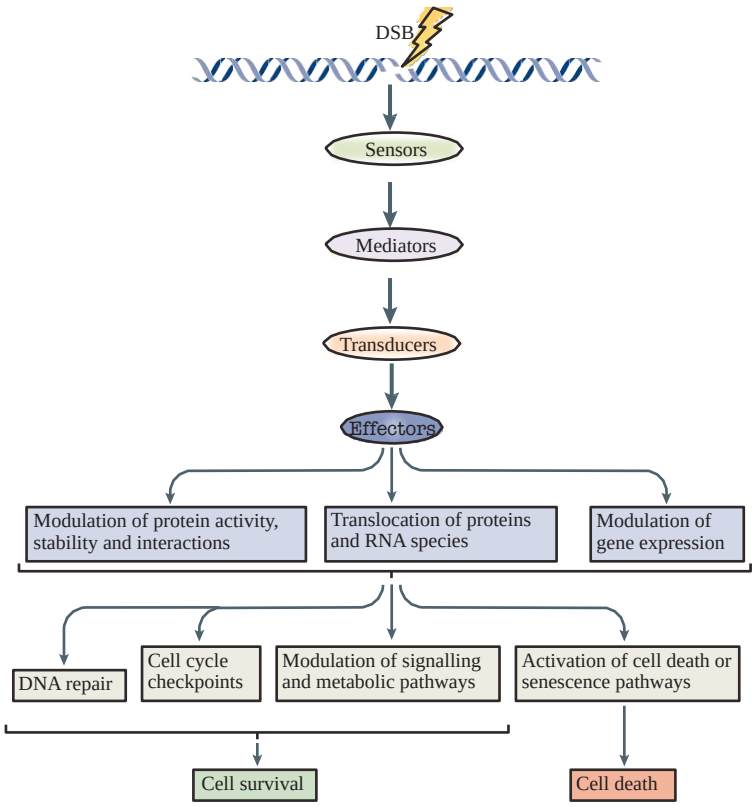

Figure 18: The DDR cascade. Schematic representation of the signal transduction of checkpoint responses and activation of cell survival or cell death pathways ensued. Figure adapted from (Shiloh and Ziv, 2013).

II.3 ATM, ATR and DNA-PKcs: three PI3-Kinases of the DDR

In mammalian cells, the ATM, ATR and DNA-PKcs are the most apical DDR kinases. These proteins are members of the phosphatidylinositol-3-kinase-like kinase family (PIKKs). Other members of this group are SMG1 (suppressor of mutagenesis in genitalia 1), mTOR (mammalian TOR) and TRRAP (transformation/transcription domain-associated protein).

The PIKKs are large proteins (between 2547 and 4128 amino acids) that share a similar domain organization. From the N-terminus to the C-terminus (Lempiäinen and Halazonetis, 2009; Lovejoy and Cortez, 2009) (**Figure 19**):

- *FAT domain:* the FRAP-ATR-TRAAP domain consisting of α-helical HEAT repeats (helix-turn-helix motifs).
- *PI3K-like domain*: the serine/threonine kinase domain, preferential phosphorylation of S/T-Q motifs.
- *PRD domain:* the PIKK-regulatory domain, its C-terminal half appears to be a site of post-translational modifications or protein–protein interactions that enhance PIKK kinase activity.
- *FATC domain:* the small (32 amino acids) and highly conserved FAT C-terminus domain that is required for PIKK kinase activity.

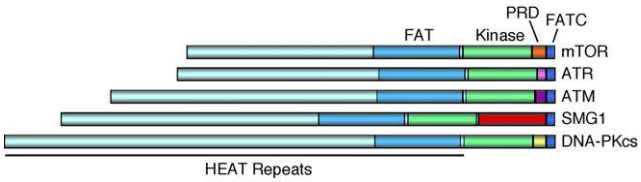

Figure 19: Schematic representation of the functional PIKK domains showing the locations of the kinase, PRD, FAT, and FATC domains (Lovejoy and Cortez, 2009).

The large N-terminal region of PIKKs is composed of numerous HEAT repeats with little sequence similarity between the kinases and may serve as a protein–protein interaction surface.

The precise functions of these PIKK domains remain unclear. This is related to the lack of structural data because of PIKK's size that challenges crystallization. However, the crystal structure of DNA-PKcs was obtained (6.6 Å resolution) (Sibanda et al., 2010). The domain structure of the others PIKKs comes principally from electron microscopy studies (Llorca et al., 2003; Unsal-Kaçmaz et al., 2002) and superposition of PIKK domains on PI3K three-dimensional structure.

II.3.1 ATM

The gene coding for the ATM kinase is localized to chromosome 11q22-23 and Shiloh and colleagues have discovered it in 1995 (Savitsky et al., 1995). ATM gene is mutated in Ataxia-Telangiectasia (AT), a rare autosomal recessive disorder. AT patients display progressive neurodegeneration, telangiectasia, immunodeficiency, extensive problems related to fertility and metabolism and increased risk of cancer (for review see (Lavin, 2008)).

AT cells show increased chromosome instability, premature senescence of cultured primary fibroblasts, high sensitivity to DSBs and defective signalling response such as cell cycle checkpoint and apoptosis that clearly contribute to cancer predisposition.

Not surprisingly, ATM is a key player in DDR and it has long been known that its activity is enhanced by DSBs (Banin et al., 1998; Canman et al., 1998). However, evidences have accumulated showing that ATM is part of many other signalling networks, including cell metabolism and growth, oxidative stress, and chromatin remodelling (reviewed in (Cremona and Behrens, 2014; Shiloh, 2014; Shiloh and Ziv, 2013; Stracker et al., 2013)).

The three main elements that drive ATM in response to DSBs are: re-localization, activation and chromatin retention.

Activation: In undamaged cells, ATM is present in a dimeric or multimeric configuration that, after damage, releases highly active ATM monomers (Bakkenist and Kastan, 2003). During this process, ATM undergoes autophosphorylation on at least four sites (S367, S1893, S1981 and S2996)

(Kozlov et al., 2006) (**Figure 20**). Autophosphorylation after DNA damage is required for monomerization (Bakkenist and Kastan, 2003) and mutations of the autophosphorylation sites to alanine result in defects in ATM-dependent phosphorylation and increased radiosensitivity (Kozlov et al., 2006). ATM autophosphorylation at S1981 is widely used as a read-out of ATM activation. ATM phosphorylation is regulated by different phosphatases (see **Table 6**). In particular, inactive dimeric ATM associates with protein phosphatase 2A (PP2A). This phosphatase seems to constitutively dephosphorylate ATM under physiological conditions (Goodarzi et al., 2004). Upon DSB induction, ATM-PP2A interaction is abolished and *trans*-phosphorylation of ATM ensues.
Phosphorylation is not the only post-translational modification that modulates ATM activity. *Sun et al.* showed that DSBs induce Tip60 (tat interacting protein, 60kDa) -mediated acetylation of ATM at K3016 (near the FATC domain) of ATM (Sun et al., 2005; Sun et al., 2007) (**Figure 20**). SiRNA depletion of Tip60 causes defects in ATM autophosphorylation and mutations on K3016 inhibit monomerization of inactive ATM, prevent the upregulation of ATM activity by DNA damage and the ATM-dependent p53 and Chk2 phosphorylation.

Re-localization: Upon DSB induction, the total amount of ATM does not change, but a portion of nuclear ATM is rapidly recruited to DSB sites, whereas another portion remains nucleoplasmic. Using live cell imaging of fluorescently-tagged ATM, *Davis* and colleagues showed that in response to laser-generated DSBs, ATM localizes at chromatin after 60 seconds reaching its maximal level in 10 minutes (Davis et al., 2010). ATM autophosphorylation is required for its association to chromatin (Berkovich et al., 2007) but at the same time, ATM recruitment to chromatin is an important part of its activation process. *Kitagawa et al.* showed that Nbs1 (a part of the MRN complex) and BRCA1 migrate to the sites of DSBs independently of ATM activation, but their presence is required to recruit activated ATM to chromatin (Kitagawa et al., 2004). *Berkovich et al.* showed that Nbs1 is required for ATM autophosphorylation as well as for the association of active ATM with chromatin after the induction of endonuclease-generated DSBs (Berkovich et al., 2007). The MRN complex has been shown by several groups in *in vitro* and *in cellulo* studies to be absolutely required for the ATM signalling pathway in response to DSBs (**Table 6**) (Lee and Paull, 2007).

Retention: The retention of ATM and other DDR proteins on chromatin is a crucial part of DDR signalling. Stable binding of single factors of the DDR machinery to chromatin is sufficient to induce the DNA damage response in the absence of DSBs (Soutoglou and Misteli, 2008).

YFP-tagged ATM is retained for a long-time at the site of laser-generated DSBs. Two hours after irradiation, the fluorescence intensity of ATM is still at 60% of its maximal level (Davis et al., 2010). In this work, the authors suggested that ATM is retained at chromatin to assist in processes of chromatin remodelling and to participate to DSB repair. Data showing that ATM is required for DSB repair in the heterochromatin by phosphorylating KAP1 (KRAB-associated protein-1) (see section *II.8*) support this hypothesis (Goodarzi et al., 2008). In addition, ATM autophosphorylation is shown to be required for sustained retention of ATM to DSBs. In particular, autophosphorylation at S1981 promotes ATM retention by allowing its interaction with the mediator protein MDC1.

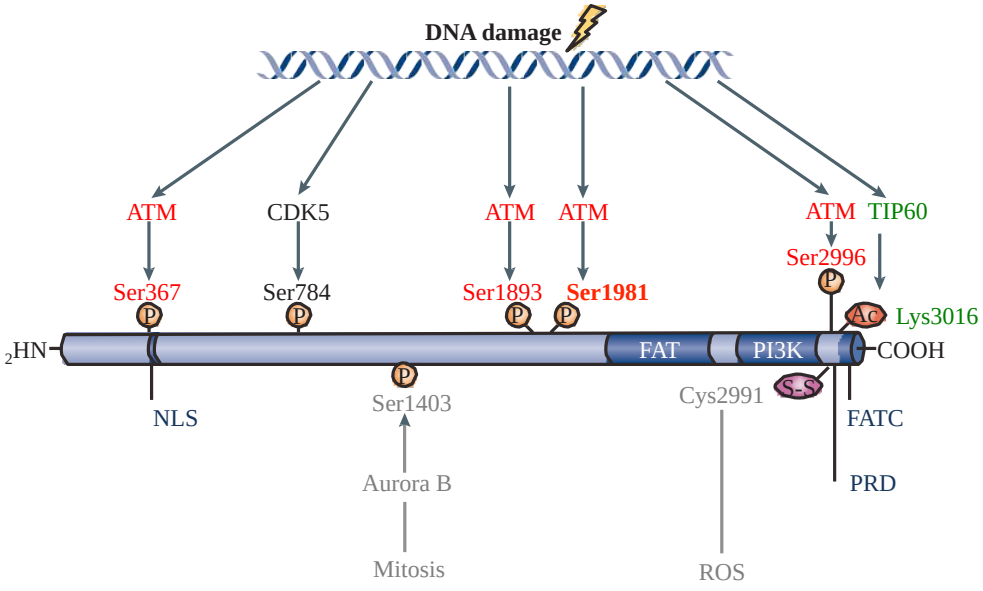

Figure 20: Schematic representation of ATM. The major domains, the sites of PTMs (post-translational modifications) and the proteins responsible for these modifications are represented. Figure is adapted from (Shiloh and Ziv, 2013)

Several questions remain opened about the mechanism of ATM activation: the nature of the initial signal that activates ATM and promotes its monomerization, the role of ATM recruitment to chromatin and the role of different PTMs. A huge amount of literature discusses and debates these open questions and sometime experimental results are contradictory depending on models, experimental conditions and the nature of the stimulus (reviewed in (Cremona and Behrens, 2014; Lavin, 2008; Shiloh, 2006; Shiloh and Ziv, 2013)).

There is growing agreement that the initial stimulus for ATM activation is a chromatin conformational change but the mechanism of action is still unclear. The importance of chromatin status is supported by the activation of ATM in response to chromatin changes in the absence of DNA damage (Bakkenist and Kastan, 2003). Chloroquine, histone deacetylase inhibitors or

hypotonic buffer activate ATM and induce p53 phosphorylation. However, activated ATM by these factors does not form nuclear foci and fails to phosphorylate its substrates bound to chromatin.

The importance of autophosphorylation in the ATM activation process in human cells is also a shared issue. On the other hand, studies in other organisms and *in vitro* have shown that autophosphorylation is dispensable for ATM monomerization and activation. For example, the expression of a non-phosphorylatable mutant S1987A (the mouse equivalent for S1981A) in ATM KO mice yields normal ATM-dependent phosphorylation of substrates and localization and retention at DSB sites (Pellegrini et al., 2006). Another report showed that autophosphorylation is accessory for the initial recruitment of ATM to DSB sites in *Xenopus egg* extracts (Dupré et al., 2006). Furthermore, *in vitro* studies using purified human components show that activation of ATM does not need its autophosphorylation (Lee and Paull, 2005). Despite these differences, it is likely that in human cells there are cellular factors that render autophosphorylation essential. **Table 6** summarizes several proteins described to regulate ATM activation.

Table 6: Some human cellular factors known to regulate ATM

Proteins		Characteristics	ATM regulation	Type of DSB	References
Activators	MRN complex	Mre11-Rad50-Nbs1 DSB sensor complex	MRN interacts with ATM in response to DSBs. Nbs1 is required for activation and recruitment of ATM to chromatin	Endonuclease-generated DSBs, IR, NCS	(Berkovich et al., 2007; Girard et al., 2002; Kitagawa et al., 2004; Uziel et al., 2003)
	Tip60	Histone acetyltransferase	Tip60 interacts constitutively with ATM. Tip60 activated by DSBs acetylates ATM (K3016) at chromatin in an MRN-dependent manner. Role in ATM activation	IR, Bleomycin	(Sun et al., 2005; Sun et al., 2007)
	MDC1	DDR mediator protein	Interaction with phospho-S1981-ATM. Role in ATM activation and retention at chromatin	IR, laser-irradiation, γ-irradiation	(Mochan et al., 2003; So et al., 2009)
	53BP1	DDR mediator protein	SiRNA against 53BP1 decrease ATM kinase activity, the phenotype is more pronounced in cells lacking Nbs1	IR	(DiTullio et al., 2002; Mochan et al., 2003; Wang et al., 2002)
	BRCA1	DDR mediator protein, E3 Ubiquitin ligase	It is required for ATM localization at chromatin and facilitates ATM-mediated phosphorylation of some ATM substrates	IR, UV	(Foray et al., 2003; Kitagawa et al., 2004)
	HMGN1	Nucleosome-binding protein	It regulates ATM activity by modulating histone H3 acetylation	IR	(Kim et al., 2009)
	RNF8 and CHFR	E3 Ubiquitin ligase	Regulators of ATM activity by synergic modulation of histone H4 acetylation	IR	(Wu et al., 2011)
	RNF2 and BMI1	Ubiquitin E3 ligase complex	It promotes the localization of activated ATM at chromatin by ubiquitinating H2A(X)	IR	(Facchino et al., 2010; Pan et al., 2011)
	hMOF	Histone acetyltransferase	Acetylation of H4. SiRNA against hMOF decreases ATM kinase activity	IR	(Gupta et al., 2005)
	PARP1	NAD+ ADP-ribosyltransferase	PARP1 rybosylates ATM in response to IR. ATM rybosylation seems required for ATM localization at chromatin but not for its autophosphorylation at S1981	IR, γ-irradiation	(Aguilar-Quesada et al., 2007; Haince et al., 2007)
	TIP	Negative regulator of PP2A	TIP positively regulates ATM autophosphorylation by interaction and inhibition of PP2A phosphatase	No DSBs: physiological conditions	(McConnell et al., 2007)
	PP5	Phosphatase	PP5 interacts with ATM in a DNA damage-inducible manner and stimulates its autophosphorylation	NCS, IR	(Ali et al., 2004)
Inactivators	PP2A	Phosphatase	It prevents ATM autophosphorylation by interacting with ATM under physiological conditions. It dissociates upon DSBs	No DSBs: Okadaic Acid, IR	(Goodarzi et al., 2004)
	Wip1	Phosphatase	ATM activity regulator. Wip1 dephosphorylates ATM S1981 in response to DSBs	IR	(Shreeram et al., 2006)
Cofactors	ATMIN	ATM cofactor	ATM activity regulator in the absence of DSBs. It interacts with ATM in response to chromatin conformational changes in Nbs1-independent manner	No DSBs: Cloroquine, hypotonic conditions	(Kanu and Behrens, 2007)

II.3.2 ATR

ATR has been discovered in 1996 in the human genome database as a gene with sequence homology to ATM and SpRad3, hence the name ATR (Cimprich et al., 1996).

ATR deficiency in mice results in early embryonic lethality (Brown and Baltimore, 2000). Individuals with hypomorphic mutations of ATR, causing a partial loss of its activity, develop the rare Seckel syndrome, which is characterized by microcephaly and growth retardation.

The primary signal for ATR activation is ssDNA coated with the ssDNA-binding protein RPA. ssDNA occurs predominantly at stalled or collapsed replication forks but ssDNA can be produced also by the processing of certain DNA lesions, such as pyrimidine dimers or nuclease-mediated resection of DSBs. In physiological conditions, the sources of replication stress are abundant. For example, in mammals, the rate of sister chromatid exchange suggests that ≈ 10 DSBs form at replication forks per cell division (Haber, 1999). The frequency of fork stalling is much higher because of the numerous sources of replication stress (see section *II.1*). This is the reason why, unlike ATM, ATR is essential. ATR is probably activated during every S-phase to regulate the firing of replication origins, the repair of damaged replication forks and to prevent premature entry into mitosis.

Once RPA-coated ssDNA appears, a canonical ATR signalling pathway is organised in four steps (Nam and Cortez, 2011) (**Figure 21**):

1) *Recruitment of ATR via ATR-interacting protein (ATRIP) to RPA-coated ssDNA*: ATRIP binds directly RPA to allow ATR recruitment at chromatin.

2) *ATR-independent recruitment of Rad9-Hus1-Rad1 proteins (9-1-1 complex) and topoisomerase-binding protein 1 (TOBP1)*: the junction of ssDNA/dsDNA is recognized by Rad17-replication factor C (RFC2) clamp loader that in turn, loads the 9-1-1 clamp at the 5’ primer junction. This loading brings the ATR activator, TOBP1 to the damage site through the interaction with the phosphorylated Rad9.

3) *TOBP1-mediated activation of ATR*: TOBP1 binds and activates ATR in an ATRIP-dependent manner. The mechanism of ATR activation by TOBP1 is unknown. A proposed model envisages that TOPB1 binding to ATR induces a conformational change of ATR that increases its kinase activity and/or its affinity for substrates (Mordes and Cortez, 2008).

4) *Phosphorylation of ATR substrates*: Chk1 and other ATR effectors are phosphorylated by active ATR. Currently, the most common measure of ATR activation is the phosphorylation of Chk1 on S317 and S345. ATR is phosphorylated at S428, S435, and T1989 and possibly at S436 and S437 (Daub et al., 2008; Dephoure et al., 2008; Liu et al., 2011; Nam et al., 2011). However, at

present only the phosphorylation at T1989 has been linked to ATR activation (Liu et al., 2011).

An important feature of the regulation of ATR signalling pathway is the independent recruitment of ATR-ATRIP and TOBP1. This characteristic represents a molecular version of the “two-man rule” for ATR activation (Cimprich and Cortez, 2008): by requiring multiple complexes to sense the problem, inappropriate launching of the checkpoint might be prevented.

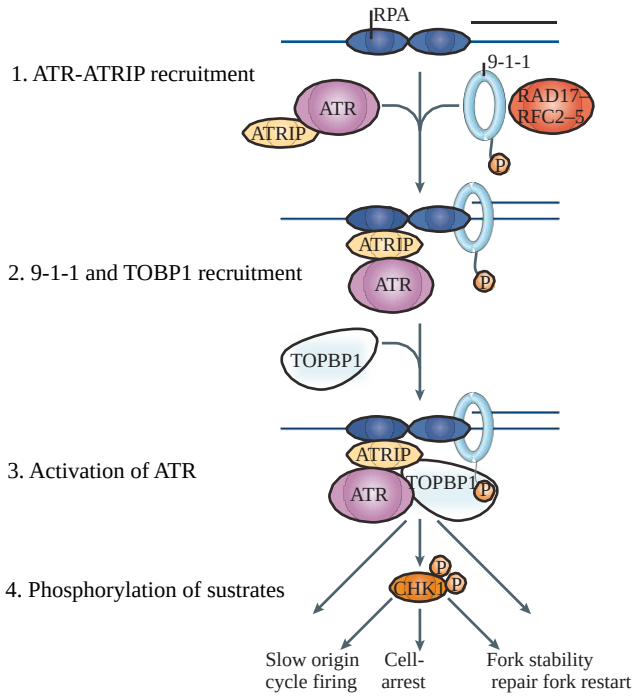

Figure 21: Canonical ATR signalling pathway. ssDNA coated by RPA induces the independent recruitment of ATR-ATRIP and TOBP1. TOBP1 activates ATR kinase, which in turn phosphorylates numerous substrates including Chk1 to regulate cellular responses to DNA damage and replication stress. Figure adapted from (Cimprich and Cortez, 2008).

Although a good model for ATR activation has emerged from the current body of work, much is still unclear. The recruitment of ATR to DNA damage sites and its mechanism of activation are poorly understood. In addition, a number of mechanisms of ATR regulation that do not fit into the canonical ATR signalling pathways are emerging. For example, DNA alkylating agents seem to activate ATR in an RPA-independent and mismatch repair-dependent mode (Yoshioka et al., 2006). Similarly, DSBs can induce ATM-dependent ATR activation in S and G2 phases of the cell cycle via the ATM and Mre11-mediated DSB-end resection (Jazayeri et al., 2006; Myers and Cortez, 2006). In addition, *Derheimer et al.* showed that the ATR pathway is also activated in response to transcriptional stress (Derheimer et al., 2007). Stalled elongating RNAPII complexes induce RPA-dependent ATR activation and accumulation of phosphorylated p53 (S15). The authors hypothesized that a region of ssDNA is formed after the blockage of transcription elongation that becomes coated with RPA, leading to the recruitment of ATR.

II.3.3 DNA-PK

The first clue that cells contain a DNA-activated protein kinase came from the work of *Andersons* and colleagues (Walker et al., 1985) and then DNA-PK was discovered in 1990 as part of the transcriptional complex Sp1 (specificity protein 1) (Jackson et al., 1990). Today, the best characterized function of DNA-PK is in the response to DSBs and in particular in the non-homologous end-joining (NHEJ) pathway for DSB repair. However, new cellular roles of DNA-PK are emerging in mitosis, transcription, viral infection and telomere maintenance (for review see (Goodwin and Knudsen, 2014; Jette and Lees-Miller, 2015)). DNA-PK is a holoenzyme composed of a large catalytic subunit (DNA-PKcs) and the DNA-end binding heterodimer Ku.

Ku

The heterodimer Ku was initially discovered as an auto-antigen, consisting of two subunits of 70 (Ku70) and 83 (Ku80) kDa (Mimori et al., 1986). Mice deficient for Ku display severe immunodeficiency, growth retardation and a hypersensitivity to IR (Manis et al., 1998; Nussenzweig et al., 1997). Ku heterodimer is extremely abundant in cells ($\approx 4x10^6$ molecules per cell) (Woodgett, 1993) and its stability depends on the presence of the two components: the depletion of Ku70 leads to Ku80 depletion (Gu et al., 1997) and vice versa (Boubnov et al., 1995). Ku shows high affinity for dsDNA ends (Kd $\approx 2.4x10^{-9} – 5x10^{-10}$ M) (Blier et al., 1993) and binds DNA in a sequence-independent manner. Ku has a ring structure that encircles DNA for approximately two turns of helix (Walker et al., 2001).

The main function of Ku is to detect DNA free ends and to target DNA-PKcs to them. In addition, Ku has a 5'-deoxyribose-5-phosphate/AP lyase activity (excision of 5'-terminal abasic sites) (Roberts et al., 2010). This activity is maximal at DSB ends suggesting that Ku may process DSB ends for ligation (Strande et al., 2012).

DNA-PKcs

The cDNA of DNA-PK has been isolated in 1995 by Jackson and colleagues (Hartley et al., 1995). The only germline missense mutation of the gene encoding DNA-PK has been described in a RS-SCID (radiosensitive T-B- severe combined immunodeficiency) patient (van der Burg et al., 2009). Like Ku, DNA-PKcs is extremely abundant in human cells ($\approx 5x10^6$ molecules per cell) (Woods and Turchi, 2013).

The X-ray structure of DNA-PKcs displays that the protein is composed of a "head" and an "arms/palm" domain organized in a pincer-shaped structure surrounding an open, central channel

proposed to bind dsDNA (Sibanda et al., 2010) (**Figure 22A**). Some characteristics of the "arms" domain suggest that it may be able to open and close around the central DNA binding channel and the phosphorylation of DNA-PKcs may modulate this process.

In physiological conditions, the activation of the kinase activity of DNA-PKcs requires its association with both the Ku heterodimer and a DNA terminus. Once activated, DNA-PKcs can phosphorylate different substrates including factors of NHEJ, histone H2AX and DNA-PKcs itself (reviewed in (Jette and Lees-Miller, 2015)).

In vitro, autophosphorylation of DNA-PKcs results in the inactivation of its kinase activity and the dissociation of DNA-PKcs from the Ku-DNA complex (Chan and Lees-Miller, 1996). DNA-PKcs can be phosphorylated at more than 40 sites *in vitro* and at 37 sites *in vivo* (Dobbs et al., 2010) (**Figure 22B**). The most studied DNA-PKcs phosphorylation sites are located in its N-terminal domain and have been termed the ABCDE (**T2609**, S2612, T2620, S2624, T2638, T2647) and PQR (S2023, S2029, S2041, S2053, **S2056**) clusters. These clusters have been studied by generating non-phosphorylatable mutants at each site. Ablation of only 1 or 2 sites in either cluster has little or no functional effect. However, complete ablation of ABCDE phosphorylation leads to a severe radiosensitive phenotype (Ding et al., 2003). In contrast, ablation of PQR phosphorylation imparts only a modestly radiosensitive phenotype (Cui et al., 2005). In the two cases, the complete mutation of those clusters does not impact the kinase activity but deregulates the end processing. Functionally, the two clusters seem to work in an opposite direction: phosphorylation of ABCDE promotes end access for NHEJ while phosphorylation of PQR inhibits it (Cui et al., 2005). In addition, mutation of the T2609 and S2056 residues leads to the increased stabilization of DNA-PKcs into DNA that interferes with NHEJ (Uematsu et al., 2007). Together these data support a model in which DNA-PKcs phosphorylation facilitates NHEJ by destabilizing the interaction of DNA-PKcs with DNA ends and is required for release of DNA-PKcs from damaged DNA *in vivo* (Dobbs et al., 2010) . ABCDE cluster can be also phosphorylated at T2609 and T2647 by ATM *in vivo* (Chen et al., 2007; Jiang et al., 2015).

Other phosphorylation sites that have functional importance include the JK (T976/S1104) and the N (S51/S72) clusters. In addition, phosphorylation of T3950, which is located in the catalytic domain, likely modulates the kinase activity (Douglas et al., 2007).

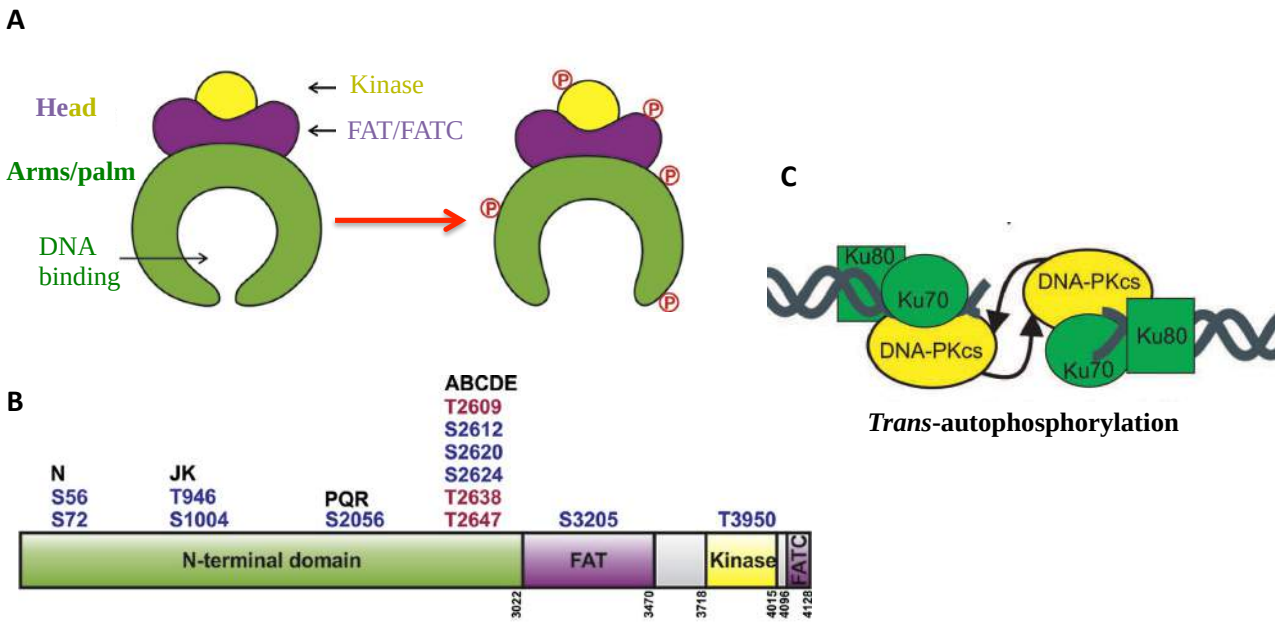

Figure 22: Model for structure, domains and *trans*-activation of DNA-PKcs. (**A**) Model of DNA-PKcs' structure: the "head" (yellow and purple) and arms/palm (green) with the DNA binding cavity in the center of the molecule before and after autophosphorylation. (**B**) Schematic representation of DNA-PKcs showing the main phosphorylation sites *in vivo*. A and B are adapted from (Wang and Lees-Miller, 2013) (**C**) Cartoon model of the *trans*-activation of DNA-PK (Woods and Turchi, 2013).

Activation of DNA-PK

In response to laser microirradiation fluorescent-tagged DNA-PKcs rapidly localizes to DSBs reaching its maximal level in ≈ 10 minutes (Davis et al., 2010). Precisely, how DNA-PKcs is recruited to Ku and how this recruitment leads to kinase activation remains unclear, but the binding of DNA-PKcs to Ku, enables Ku to translocate inward into the dsDNA allowing DNA-PKcs to bind the terminus of a DNA end (Frit et al., 2000).

A current model of DNA-PK's activation envisages the following steps (for review see (Meek et al., 2008)):

1) Ku recognizes and binds the two ends of a DSB.

2) DNA-PKcs is recruited at each end via Ku. DNA binding induces a conformational change in DNA-PKcs that results in closer association of the head and the palm domains.

3) Two DNA-PK molecules on adjacent sides of the DSB end can interact and form a synaptic complex (**Figure 22C**). These structures likely maintain broken ends in proximity and provide a platform for NHEJ factors, blocking access to nucleolytic activities.

4) Synapses favour the autophosphorylation of DNA-PKcs. It has been shown that autophosphorylation within the two major clusters occurs in *trans* (Meek et al., 2007) but the mechanism of all phosphorylation's events *in vivo* is still unclear (in *trans*, in *cis* or even on both

sides of the synapsis). ABCDE autophosphorylation in *trans* promotes access of DNA ends to end modifying factors (including the nuclease Artemis).

5) End alignment is "sensed" by DNA-PK resulting in PQR autophosphorylation that "locks" the two ends in aligned position favouring NHEJ.

6) Additional autophosphorylation occurs at undefined sites to facilitate the final step in NHEJ and to release DNA-PKcs.

7) After dissociation, DNA-PKcs is dephosphorylated and can be recycled. The question of how Ku is removed from the DNA remained unclear. Ku is ubiquitylated in response to DSBs (Brown et al., 2015). Hence, it has been suggested that Ku may be ubiquitylated and then degraded and/or released from chromatin and degraded (Brown et al., 2015; Feng and Chen, 2012).

II.3.4 Interplay of PIKKs

Although ATM, ATR and DNA-PK have distinct DNA damage specificities, convincing evidences are accumulating about their cross talk (Cimprich and Cortez, 2008; Shrivastav et al., 2009; Woods and Turchi, 2013).

PIKKs can regulate each other directly:

- Decreased expression of DNA-PK is associated with downregulation of ATM protein levels in various cellular models (Chan et al., 1998; Gately et al., 1998; Peng et al., 2005).
- DNA-PK can phosphorylate ATM on S1981 in apoptotic cells (Solier et al., 2009).
- ATM can phosphorylate DNA-PK on T2609 in response to IR (Chen et al., 2007) and during apoptosis (Solier et al., 2009). ATM-mediated DNA-PK phosphorylation is critical for the DSB repair activity of DNA-PK and radioresistance (Chen et al., 2007). In particular, it regulates end-processing at the step of Artemis recruitment (Jiang et al., 2015).
- ATR can phosphorylate DNA-PK on T2609 and T2647 in S-phase cells in response to UV (Chen et al., 2007; Yajima et al., 2006). However, the impact of these phosphorylations on DNA repair has not been evaluated.

In addition to the direct mechanisms of regulation, PIKKs can regulate each other indirectly by activating signalling pathways that in turn activate other PIKKs. For example, DNA-PK contributes to sustain ATR signalling in the presence of limited amount of ssDNA (Vidal-Eychenie et al., 2013). ATM can also promote the activation of ATR by phosphorylating TOPBP1 (Yoo et al., 2009) and by favouring the processing of DSBs to generate RPA-coated ssDNA (Jazayeri et al., 2006). Other important evidence of PIKKs's crosstalk is the overlap in substrates specificity. Most substrates are shared by PIKKs, the best example is given by H2AX (see section *II.5.3.2.1*).

II.4 Spatiotemporal dynamics of DDR proteins at DNA break

One important aspect that determines the effectiveness of DDR signalling in mammals is the tight spatiotemporal coordination of DDR factors at DSBs: they have to relocate to the right place at the right time. Unlike bacteria that activate a global transcriptional program to increase the availability of DDR proteins, eukaryotes primarily respond with a local up-concentration of DDR components already present in the cell. This local and sequential accumulation of DDR factors at DSBs usually leads to the formation of microscopically detectable foci, also referred as IRIF (ionizing radiation induced foci), that are widely used as marker of DSB presence and location (**Figure 23A**) (Lukas et al., 2011b).

The “spatial map” of IRIFs reveals two distinct compartments: the DSB-flanking chromatin and the ssDNA micro-compartment (Bekker-Jensen et al., 2006; Bekker-Jensen and Mailand). The proteins associated with DSB flanking chromatin, such as γH2AX (for details see **Figure 23B**), are able to spread out for megabases from the initial DSB and they can assemble throughout most of the cell cycle. The second compartment is much smaller and cytologically visible like “microfoci”. It localizes at RPA-coated ssDNA that forms after resection of the DSB. Accumulation of DDR proteins in this compartment is restricted to S- and G2-phases (**Figure 23C**). There is another group of proteins that is able to interact with DNA but the transient nature of this interaction (for example, Chk1 and Chk2) or the low concentration at DSBs (DNA-PK, NHEJ factors) technically challenges microscopy detection. Recently, *Britton* and colleagues developed a method, based on combined ribonuclease treatment, detergent pre-extraction and high-resolution microscopy, to visualize Ku and others NHEJ factors at DSBs (Britton et al., 2013). Interestingly, ATM, ATR and DNA-PK are located in distinct compartments: ATM in DSB-flanking chromatin, ATR in ssDNA micro-compartment and DNA-PK at unprocessed DSB ends.

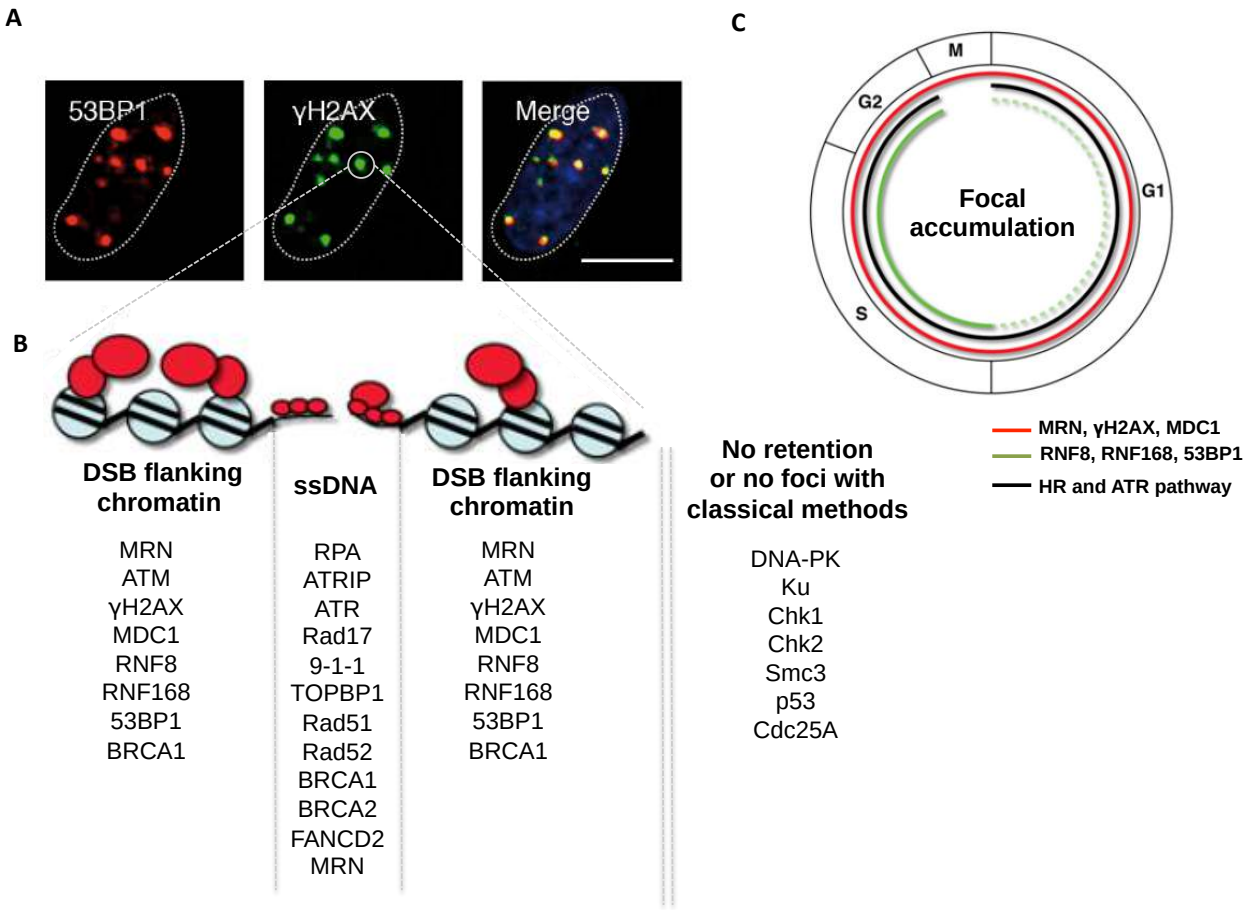

Figure 23: Spatiotemporal properties of DDR. (**A**) Example of the DDR proteins' foci organization after DSB induction: 53BP1 (red), γH2AX (green), DNA (blue) and merge (yellow). Each focus represents at least a DSB. (**B**) "Spatial map" of DDR proteins around DSBs. (**C**) Cell cycle regulation of DDR foci formation. Efficient foci formation is represented with solid lines and weak/undetectable foci are represented by a dashed line. Figure B and C are adapted from (Bekker-Jensen et al., 2006; Polo and Jackson, 2011).

II.5 Molecular mechanisms of DDR proteins assembly at DNA break

The mechanisms driving the highly coordinated spatiotemporal recruitment of DDR proteins at DSB sites are based on (1) direct recognition of DNA-breaks, (2) protein-protein interaction and (3) post-translation modifications.

II.5.1 Direct recognition of DNA-breaks

DDR factors that act as DSB sensors are the first proteins recruited to DSBs. Such proteins are able to directly recognize and bind broken DNA in a sequence-independent manner. The Ku heterodimer (see section *II.3.3*), the MRN complex, RPA (see section *II.3.2*) and the proteins PARP1 and PARP2 belong to this category.

II.5.1.1 The MRN complex

The MRN complex (Mre11/Rad50/Nbs1) consists of dimers of each subunit and structurally it can be divided into distinct “head”, “coil”, “hook” and “flexible adapters” domains (**Figure 24**) (Williams et al., 2010). The “head” is the DNA-binding and processing core of MRN, containing two Mre11 molecules and two ATPase domains of Rad50. Mre11 can bind DNA with the specific ability to synapse DSB ends and it has endonuclease and 3’→5’ exonuclease activities (the opposite polarity from what is required for HR *in vivo*). Rad50 provides ATPase and adenylate-kinase activities and can also bind/unwind DNA. Rad50 also forms an anti-parallel coiled-coil (“coil”) that terminates with a zinc hook motif (“hook”) (Hopfner et al., 2002). The “coil” is a flexible structure projected away from the DNA that can mediate long-range tethering of two DNA molecules by oligomerization via its zinc hook. Nbs1 constitutes the “flexible adapter” domain of MRN providing a regulatory and protein-protein interaction module. Nbs1 does not possess a known enzymatic activity itself. However, it is essential for the nuclear localization of the MRN complex (Desai-Mehta et al., 2001) and stimulates its DNA-binding and its nuclease activities (Paull and Gellert, 1999).

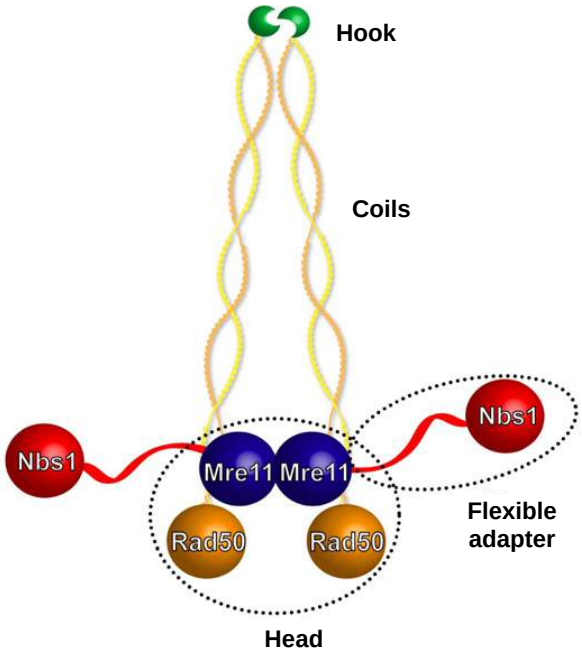

Figure 24: Scheme of MRN structure and domains. MRN can assemble as a heterohexamer with head, coils, hook and flexible adapter domains.

The MRN complex plays a role in both signalling and repair of DSBs (reviewed in (Lamarche et al., 2010; Riches et al., 2008)), in particular it participates to:

- Very early DSB detection and recruitment of ATM at chromatin
- Retention of ATM to DSB to achieve signal propagation
- Activation of ATR by contributing to the early step of end resection at breaks
- DNA tethering to bridge the ends of broken chromosomes

These multiple roles in DDR are reflected by human disorders associated with MRN mutations. Hypomorphic mutations in the NBS1 gene result in Nijmegen breakage syndrome (NBS), an autosomal recessive disorder characterized by microcephaly, immunodeficiency and cancer predisposition (Lavin, 2008). Mutations in MRE11 lead to AT-like disorder (ATLD) that resembles to the phenotypes of ATM deficiency (Lavin, 2008). Recently, a patient with hypomorphic mutation in RAD50 has been described to have a phenotype similar to NBS (NBSLD, NBS-like disorder) (Waltes et al., 2009). Cells from NBS, ATLD and NBSLD patients show increased radiosensitivity and checkpoint's defects.

II.5.1.2 PARP

PARP1, PARP2 and PARP3 are the members of the PARP family found to be induced in response to DNA damage. PARPs catalyse the polymerization of ADP-ribose units from donor NAD+ molecules on Glutamate, Lysine or Aspartate residues of target proteins, resulting in the attachment of linear or branched polymers. PARP1 can be activated by different types of damage such as SSBs, DSBs, DNA crosslinks and stalled replication forks while currently, PARP2 seems able to detect gaps and flap structures and PARP3 DSBs (Beck et al., 2014). Structurally and mechanistically the best characterized PARP member is PARP1. PARP1 can act like a DNA damage sensor by virtue of its DNA-binding domain, composed of two zinc finger domains (Zn1 and Zn2). A substantial body of data suggests a model for PARP recognition of DNA damage and activation (Ali et al., 2012). PARP1 is constitutively associated with chromatin likely via the weak interaction of Zn1 with the sugar-phosphate backbone and it has a very low basal activity. A discontinuity in the DNA backbone allows the binding of Zn2 and the formation of a functional break-recognition module via dimerization with a second PARP1 molecule thereby facilitating activation by trans-modification. The absence or the inhibition of PARP1 sensitizes cells to chemical drug-inducing DSBs and delays their repair (Boulton et al., 1999; Smith et al., 2005). This is in agreement with different key roles of PARP1 in DDR:

- PARylation targets DDR proteins to DNA breaks for DSB signalling

- PARP1 responds to collapsed replication fork facilitating HR repair (Bryant et al., 2009)
- PARP1 operates in the alternative-NHEJ repair pathway (Wang et al., 2006).

PARylation is negatively regulated by PARG (PAR-glycohydrolase) that hydrolyses the glycosidic linkage between the ADP-ribose units producing free ADP-ribose (Kim et al., 2005).

II.5.2 Protein-protein interactions

Downstream from DSB sensors, other DDR factors assemble to damage sites in a highly coordinated manner by protein-protein interactions. An example is given by MDC1, which constitutes a molecular binding platform for DDR components at DSB sites (see section *II.5.3.2.2*). Similarly, the apical DDR kinases, ATM, ATR and DNA-PK, are recruited to sites of DNA damage through analogous mechanisms involving a conserved C-terminal region present in Nbs1, ATRIP and Ku80, respectively (Falck et al., 2005).

II.5.3 Post-translational modifications

Along with protein-protein interaction the sequential protein assembly at DNA breaks is achieved by post-translational modifications. PTMs regulate recruitment, dissociation and/or retention of DDR proteins and drive the DNA damage-induced chromatin responses.

II.5.3.1 Poly(ADP-ribosyl)ation

PARylation (see section *II.5.1.2*) is one of the earliest modifications detectable at sites of DSBs and PAR chains are quickly removed by PARG providing a transient response lasting minutes (Ciccia and Elledge, 2010; Schreiber et al., 2006) (**Figure 25**). In response to DSBs, PARP1 PARylates target proteins, including histone H1 and H2B and PARP1 itself. PAR structures act as platforms to recruit factors that locally remodel chromatin at DNA damage sites to promote DSB signalling and/or repair. For instance, PAR-dependent recruitment of the NuRD (nucleosome remodelling and deacetylase) complex, the Polycomb histone-modifying complex and the histone variant macroH2A (via APLF, aprataxin-PNK-like factor), promotes transcriptional silencing and chromatin compaction around DNA lesions thereby minimizing the probability of encounter between transcriptional and repair machineries (Lukas et al., 2011b). In addition, PARylation plays a variety of different roles in DSB signalling such as the regulation of the exchange of histone variant H2AX with conventional H2A by inhibiting the exchange regulator FACT (facilitates chromatin

transcription) (Heo et al., 2008) and the ATM activation in response to IR (Aguilar-Quesada et al., 2007). Recently, a new mechanism by which PARylated proteins at DNA damage sites coordinate the spatiotemporal recruitment of DDR factors has been described (Altmeyer et al., 2015; Hyman et al., 2014; Patel et al., 2015). PARylated proteins at damaged sites trigger the rapid accumulation of intrinsically disordered proteins that results in the phase separation into liquid droplets (referred to as liquid demixing) and in the creation of a liquid-like compartment. This PAR-seeded compartment filters the access of DDR proteins to chromatin regulating the early phase of DDR, for example MDC1 can penetrate while 53BP1 is excluded.

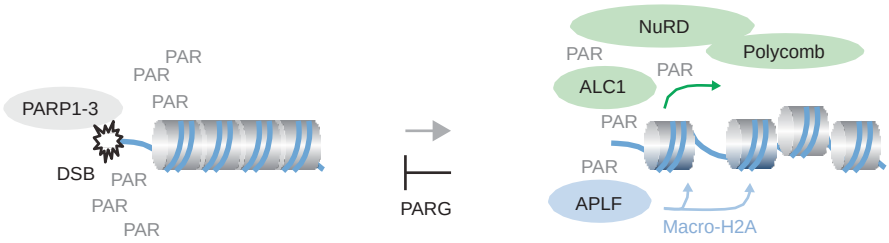

Figure 25: Poly(ADP-ribosyl)ation in response to DSBs. Proteins depicted in green determine alteration of chromatin status. See text for details. Figure from (Lukas et al., 2011b).

II.5.3.2 Phosphorylation

The importance of phosphorylation and dephosphorylation events in DDR is displayed by the large number of phosphorylation sites (more than 900 over 700 proteins) identified by mass spectrometry-based screens (Bennetzen et al., 2010; Matsuoka et al., 2007). The roles of this PTM are to:

- Directly regulate the activity or the structure of the target proteins
- Regulate the sequential recruitment of DDR factors having phospho-binding domains such as BRCT (breast cancer C-terminal) or FHA (forkhead-associated) domains

Phosphorylation can also promote the dissociation of proteins from the DSB sites. Examples are given by (i) DNA-PKcs autophosphorylation (as discussed before in section *II.3.3*), which triggers its dissociation from Ku (Chan and Lees-Miller, 1996), (ii) KAP1 that is released from heterochromatin upon ATM phosphorylation (Goodarzi et al., 2008) (see section *II.8*) or (iii) Chk1 and Chk2 that, after ATR or ATM phosphorylation, are able to migrate from chromatin to nucleoplasm to phosphorylate their substrates (Lukas et al., 2003; Smits et al., 2006).

The key role of phosphorylation in DDR is primarily exemplified by H2AX phosphorylation.

II.5.3.2.1 Phosphorylation of the histone H2AX: γH2AX

H2AX is a member of the histone H2A family. In mammalian cells, it comprises 2-25% of the H2A pool, depending on organism and cell types (Bonner et al., 2008; Rogakou et al., 1998). It exists as a component of the nucleosome core structure, constituted of eight histone proteins, two from each of the H2A, H2B, H3 and H4 families, and it is present in every fifth nucleosome on average.

H2AX consists of 143 amino acids and structurally, it is similar to other H2A species and in general to all histone core proteins. It is composed of a central globular highly conserved "histone fold" domain containing three α-helices connected by two loops and flanked by terminal "tails" that have very little secondary or tertiary structure. The "histone fold" domain is the site of interaction for H2A/H2B dimer formation and it provides stability to the nucleosome while, the "tails" protrude from the core and possess sites for a variety of post-translational modifications. Respect to the bulk H2A species, H2AX has an extended C-terminal tail with an SQEY phosphorylatable motif (Fernandez-Capetillo et al., 2004; Li et al., 2005).

The phosphorylation of the serine 139 (S139) of this motif is an early and key event in the response to DSBs. The phosphorylated form of H2AX, referred as γH2AX, appears within minutes after DSB induction (Rogakou et al., 1999) and leads to the formation of large foci detectable by immunofluorescence. The first studies of the *Bonner* laboratory (Rogakou et al., 1999; Rogakou et al., 1998) and recent studies using chromatin immunoprecipitation of γH2AX around sequence-specific DSBs (Iacovoni et al., 2010; Savic et al., 2009), provide a quite complete landscape of γH2AX distribution around a DSB. H2AX phosphorylation occurs over large domain from 0.5 to 2 Mb surrounding the DSB and the percentage of H2AX phosphorylated around the break is constant, ≈ 0.03% in yeast and mammals. Mapping of the γH2AX domains reveals also characteristically locus-specific, bidirectional, discontinuous and asymmetric distributions of γH2AX flanking DSB sites with a marked depletion in the ≈ 1 Kb proximal to the DSB (Berkovich et al., 2007; Iacovoni et al., 2010) (**Figure 26**). γH2AX propagation is spatially confined by domain boundaries but what defines these boundaries is still not completely understood.

In response to DSBs, ATM, ATR or DNA-PK can phosphorylate H2AX. A rough generalization is that H2AX phosphorylation is carried out by ATM and DNA-PK in a partially redundant way (Stiff et al., 2004) and by ATR in response to UV radiations or replicative stress (Ward and Chen, 2001). The real scenario is likely more complex. In normal cells, H2AX is primarily phosphorylated by ATM while in the absence of ATM, DNA-PK appears to be the primary H2AX kinase (Stiff et al., 2004). Another aspect to consider is the different mechanism of ATM and DNA-PK activation. Upon DSB induction, ATM is activated and distributed between soluble and chromatin-bound pools (Andegeko et al., 2001). This dynamism might make ATM able to phosphorylate H2AX within

large domains. DNA-PKcs, on the other hand, becomes active through its interaction with Ku and DNA ends and probably it has a reduced phosphorylation range requiring longer times for H2AX phosphorylation at longer distances (Kinner et al., 2008; Savic et al., 2009).

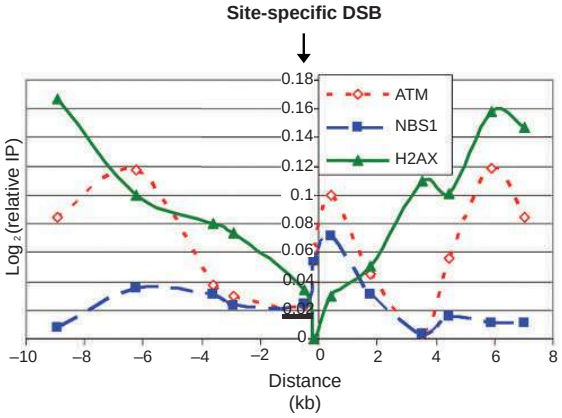

Figure 26: Distribution of the DDR proteins around a DSB. Distribution of γH2AX, ATM and Nbs1 around a I-Ppo-induced DSB assessed by ChIP. Nbs1 localizes at the DSB site, whereas γH2AX is depleted at DSB site and accumulates in adjacent regions. ATM distribution follows both γH2AX and Nbs1 distributions. From (Berkovich et al., 2007).

γH2AX must be removed to allow the repair and the restoration of pre-lesion chromatin status (Chowdhury et al., 2005). Currently, two non-exclusive mechanisms are proposed for γH2AX removal: γH2AX dephosphorylation or γH2AX replacement by histone exchange (Heo et al., 2008). Dephosphorylation seems to be the predominant mechanism in mammals. γH2AX dephosphorylation can take place in chromatin (Chowdhury et al., 2005) and several γH2AX phosphatases have been identified, such as PP2A (Chowdhury et al., 2005), PP1 (Nazarov et al., 2003), PP4 (Chowdhury et al., 2008), PP6 (Douglas et al., 2010) and Wip1 (Moon et al., 2010).

Another residue is phosphorylated in the C-terminal tail of H2AX, the tyrosine 142 (Y142) (Cook et al., 2009). This phosphorylation is deposited by the chromatin-remodelling factor WSTF (williams syndrome transcription factor) (Xiao et al., 2009) under basal conditions and it is removed by EYA phosphatase (EYA1 and EYA3) in response to DNA damage when the S139 site becomes phosphorylated (Cook et al., 2009). Persistent phosphorylation of Y142 promotes an apoptotic response over repair.

The H2AX gene is not essential. H2AX knockout mice survive well in unstressed conditions but they have defects in DSB repair, are radiosensitive and present increased chromosomal abnormalities (Bassing et al., 2002; Celeste et al., 2002). Similarly, studies in H2AX knockout cells show that the key function of γH2AX is to maintain and accumulate DDR components at DSBs (such as Nbs1, BRCA1 and 53BP1) while it is dispensable for their initial recruitment (Celeste et al., 2003).

Currently, γH2AX is the most popular DSB marker suitable for measuring induction and repair of DSBs in cells exposed to various genotoxic agents. It is accepted that a γH2AX foci represents at least a DSB. However, other cellular processes or genotoxic stresses can induce H2AX phosphorylation even if usually they do not form a focal pattern. Examples are given by UVC radiations that induce a γH2AX pan-nuclear staining in non-S-phase cells (Marti et al., 2006) or by apoptosis that can be marked by a γH2AX ring in early phases, followed by a nuclear pan staining and apoptotic bodies in late phases (Solier et al., 2009).

II.5.3.2.2 MDC1

The mediator protein MDC1 is a large protein principally constituted by three distinct interaction-domains: an N-terminal FHA domain, a central Proline/Serine/Threonine repeat domain (PST repeat) and a C-terminal tandem BRCT domain (tBRCT) (Coster and Goldberg, 2010) (**Figure 27A**).

MDC1 can bind several DDR proteins, including γH2AX (Stucki et al., 2005), the MRN complex (Chapman and Jackson, 2008), ATM (So et al., 2009), 53BP1 (Eliezer et al., 2009), RNF8 (Huen et al., 2007) and DNA-PK (Lou et al., 2004).

Upon DSB induction, γH2AX acts as a docking site for the tBRCT of MDC1 and this interaction protects γH2AX from dephosphorylation and mediates the γH2AX-dependent DDR signal. Since MDC1-deficient mice recapitulate many phenotypes of H2AX deficiency (Lou et al., 2003), it is proposed that the major role of MDC1 is to promote the γH2AX-dependent chromatin retention of DDR factors. In particular, MDC1 is required for the recruitment and the chromatin retention of ATM (Lou et al., 2006) and it drives the ATM-mediated spreading of γH2AX. Indeed, MDC1 can recruit ATM both directly by binding ATM phosphorylated on S1981 (So et al., 2009) or indirectly via Nbs1 (Chapman and Jackson, 2008). MDC1 constitutively interacts with Nbs1 through CK2-mediated phosphorylation of MDC1 (Chapman and Jackson, 2008). Thus, MDC1-Nbs1 interaction brings the recruitment of Nbs1-ATM dimers in regions flanking DSBs thereby triggering H2AX phosphorylation in distal regions (**Figure 27B**).

In the case of replication stresses, MDC1 promotes also the ATR-dependent spreading of γH2AX by recruiting TOBP1 (Wang et al., 2011).

Moreover, ATM-mediated phosphorylation of MDC1 in TQXF motifs, allows the interaction between MDC1 and the ubiquitin E3 ligase RNF8 (Huen et al., 2007), which drives the ubiquitin-dependent DDR signalling (see section *II.5.3.4*).

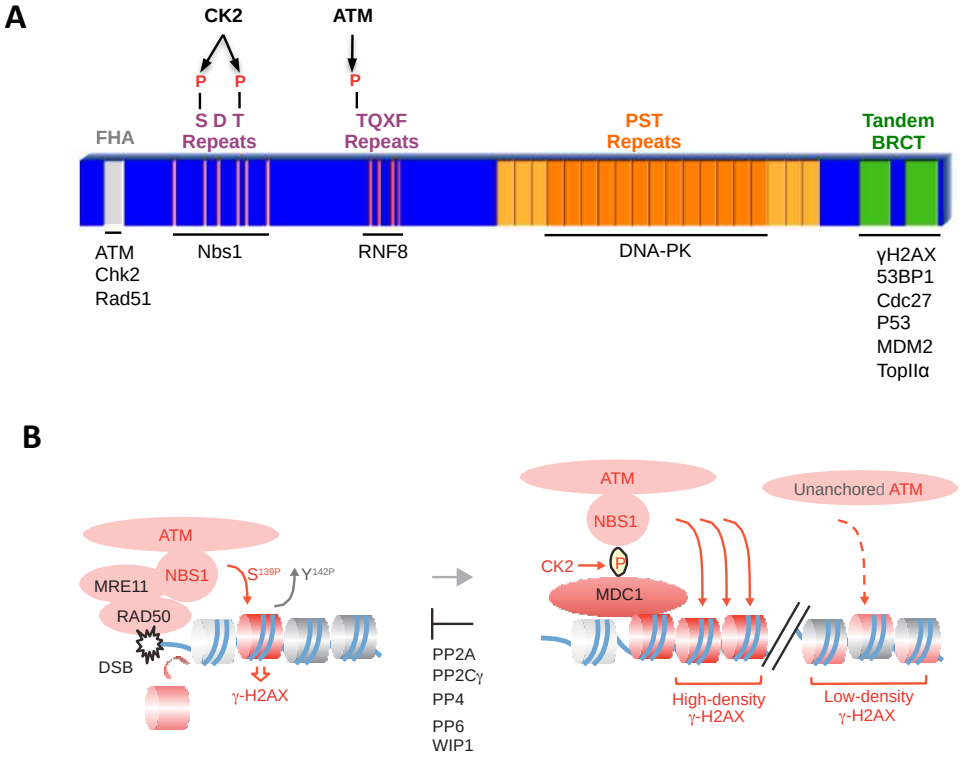

Figure 27: Schematic representation of MDC1 and model of MDC1-mediated γH2AX signalling. (**A**) Organization of MDC1's main domains showing the *in vivo* phosphorylation sites and MDC1 major partners. Adapted from (Coster and Goldberg, 2010) (**B**) Model of γH2AX recruitment of MDC1 and MDC1-mediated γH2AX spreading (Lukas et al., 2011b).

II.5.3.3 Acetylation

Histone acetylation regulates local chromatin structure on domains contiguous to DSBs, directly by modulating chromatin compaction or indirectly by recruiting chromatin-remodelling factors. Lysine acetylation facilitates the formation of open chromatin by neutralizing the negative charge on lysines and therefore decreasing both histone-DNA and histone-histone interactions within the nucleosomes. The formation of localized relaxed chromatin at the break sites may increase the accessibility of DNA for signalling and repair (reviewed in (Xu and Price, 2011)).

Tip60 has been identified has one of the first acetyltrasferases involved in DDR and DSB repair (**Figure 28**). Tip60 is recruited to DSBs via its interaction with the constitutively methylated K9 of histone H3 (H3K9me3) (Sun et al., 2009). H3K9me3 is "unmasked" by the transient release of HP1 (heterochromatin-binding protein 1) following DNA damage (Sun et al., 2009). Once activated, two main functions of Tip60 are to (i) acetylate ATM thus promoting its activation (Sun et al., 2005; Sun et al., 2007) and (ii) acetylate histones H2A and H4 at DSBs thus promoting chromatin relaxation and HR (Bird et al., 2002; Downs et al., 2004; Murr et al., 2006). Chromatin remodelling

frequently combines histone acetylation with the use of large motor ATPases to modify the chromatin architecture. An example is given by the SWI/SNF DNA-dependent ATPase p400. p400 is recruited to DSBs where it is required (i) for RNF8-dependent ubiquitination of histones and for the subsequent recruitment of 53BP1 and BRCA1 (see section *II.5.3.4.2*) (Xu et al., 2010) and (ii) for HR (Courilleau et al., 2012).

Histone deacetylases, like HDAC1, HDAC2 (histone deacetylase 1 and 2), SIRT1 and SIRT6 (sirtuin 1 and 6), also accumulate at chromatin in response to DSBs. HDAC1 and HDAC2 regulate deacetylation of histones H3 and H4 stimulating NHEJ (Miller et al., 2010), while SIRT1 and SIRT6 stimulate Rad51 foci formation promoting DSB repair by HR (Kaidi et al., 2010; Oberdoerffer et al., 2008).

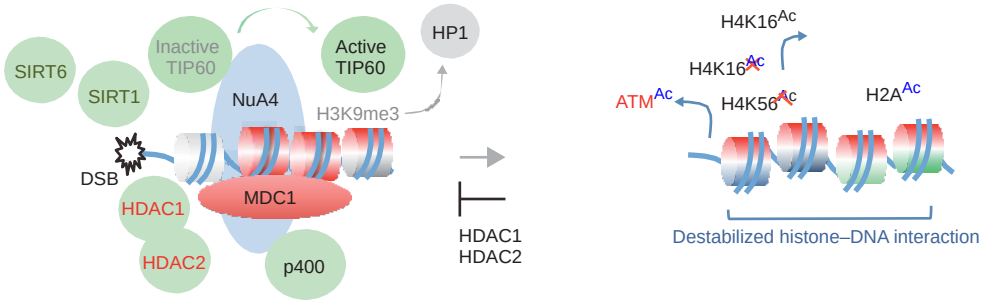

Figure 28: Acetylation in response to DSBs. Proteins depicted in green determine alteration of chromatin status. See text for details. Figure from (Lukas et al., 2011b).

II.5.3.4 Ubiquitylation

Ubiquitylation is the covalent attack of ubiquitin, a highly conserved 76 amino acid polypeptide, to a lysine residue on a target protein. It is a three-step process involving an ubiquitin-activating enzyme (E1), an ubiquitin-conjugating enzyme (E2) and an ubiquitin ligase (E3) (**Figure 29**). In humans, there are eight known E1s, two of which (UBA1 and UBA6) are specific for ubiquitin (Schulman and Harper, 2009), 35 active E2s (van Wijk and Timmers, 2010) and more than 1000 E3s divided in three major families, RING (really interesting new gene), HECT (homology to E6AP C-terminus) and RBR (ring between ring) (Berndsen and Wolberger, 2014). The biological outcomes of ubiquitin ligation to a protein are dictated by the fashion in which the ubiquitin chains are assembled and attached to the substrate: single ubiquitin monomer (monoubiquitylation), multiple ubiquitin monomer (multi-monoubiquitylation) or ubiquitin polymers (polyubiquitylation) linked via one of the seven lysines of ubiquitin (K6, K11, K27, K29, K33, K48, K63). The linkage specificity is largely determined by the pairing of specific E2s and E3s.

In response to DSBs, various protein-ubiquitin conjugates have been detected at DSBs sites (reviewed in (Brown and Jackson, 2015; Pinder et al., 2013)). The functions of this modification are:

- Target proteins for proteasomal degradation (usually at least four ubiquitin moiety linked by K48 or K11)
- Create docking sites to recruit DDR proteins (usually monoubiquitylation or K63-chains) containing ubiquitin-binding domains (UBDs), like MIU (motifs interacting with ubiquitin domain) and UIM (MIU-related ubiquitin-binding domain) domains.

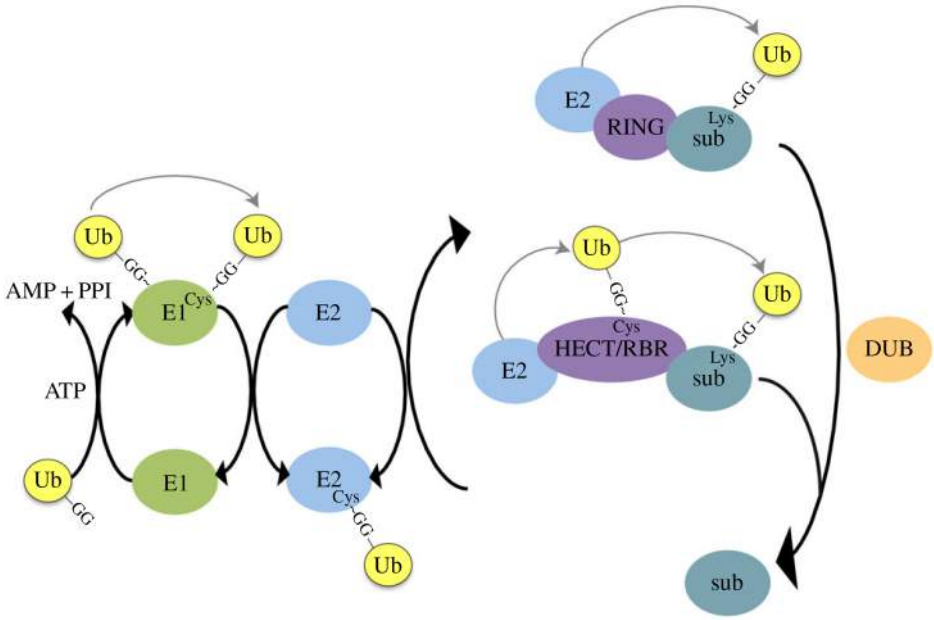

Figure 29: Schematic representation of ubiquitylation cascade. In an ATP dependent reaction, the E1 enzyme binds the GG-motif of ubiquitin (Ub) via its catalytic cysteine forming an E1-Ub intermediate. In the case of UBA1 a second Ub molecule is loaded on the E1. An E2 conjugating enzyme recognizes the ubiquitin-charged E1 and Ub is transferred to the catalytic cysteine of the E2. Then, the Ub is conjugated to the lysine of the substrate by the concerted action of E2 and E3 enzymes. Ring E3 ligases catalyse the Ub transfer from the E2 to the substrate by positioning the Ub moiety for conjugation. In the case of HECT and RBR E3 ligases, Ub is transferred from the E2 to the active cysteine of the E3 and then to the substrate. Ubiquitylation can be reversed by deubiquitylating enzymes (DUBs). Image from (Brown and Jackson, 2015).

II.5.3.4.1 RNF8/RNF168 ubiquitination cascade

The major players in ubiquitination cascade are the two E3 ligases RNF8 and RNF168. RNF8 consists of a N-terminal FHA domain and a C-terminal RING finger motif, while RNF168 possesses a N-terminal RING finger domain and two ubiquitin-binding domains (MIU1 and MIU2). Homozygous or biallelic heterozygous nonsense mutations in RNF168 gene have been identified as responsible for the RIDDLE (radiosensitivity, immunodeficiency, dysmorphic features, and learning difficulties) syndrome, which is a novel “AT-mimicking syndrome” (Devgan et al., 2011; Stewart et al., 2007). Cells from RIDDLE patients display an impaired accumulation of 53BP1 and BRCA1 at DSBs.

RNF8 binds ATM-phosphorylated MDC1 via RNF8-FHA domain (Huen et al., 2007; Kolas et al., 2007; Mailand et al., 2007), which allows the recruitment of RNF168 though RNF168-MIU domains (Doil et al., 2009; Stewart et al., 2009). The two E3 ligases act in concert to catalyse K63-ubiquitylation of H2A(X) on K13 and K15 (Gatti et al., 2012; Mattiroli et al., 2012). This polyubiquitination is required for focal accumulation of downstream DDR factors such as BRCA1 and 53BP1 but it does not impact on the formation of γH2AX, MDC1 and Nbs1 foci (Doil et al., 2009; Huen et al., 2007; Mattiroli et al., 2012). After the discovery of RNF8 and RNF168, the first model envisaged that RNF8 initiates the H2A(X) ubiquitylation on chromatin around the break and then RNF168 binds and amplifies the ubiquitin conjugates initiated by RNF8 (Bekker-Jensen and Mailand; Ciccia and Elledge, 2010; Lukas et al., 2011b; Polo and Jackson, 2011). The work of *Mattiroli* and colleagues challenges this hierarchy (Mattiroli et al., 2012). They show that, although the recruitment of RNF168 is dependent on its MIU domains and on RNF8 catalytic activity (Doil et al., 2009; Stewart et al., 2009), RNF168 is the priming ubiquitin ligase for histones. Therefore RNF8 may allow the ubiquitin-mediated recruitment of RNF168 by ubiquitinating another non-histone substrate. Even if this protein has not yet been identified, RNF8 is able to ubiquitylate other DDR proteins at DSB sites including Nbs1 (Lu et al., 2012), JMJD2A (jumonjii-domain containing protein 2A) (Mallette et al., 2012) and BCL10 (B-cell CLL/lymphoma 10) (Zhao et al., 2014). Once RNF168 recruited, it initiates H2A(X) ubiquitination on K13 and K15, which leads to K63-polyubiquitination on these lysines by RNF168 and/or RNF8 (Mattiroli et al., 2012) (**Figure 30**).
The others members of the RNF8/RNF168 ubiquitin cascade have also been identified:

- E1 enzyme: UBA1 (Moudry et al., 2012)
- E2 enzyme: Ubc13 (ubiquitin-containing enzyme E2N) (Huen et al., 2007; Kolas et al., 2007; Stewart et al., 2009), which is the only E2 ligase known to exclusively catalyse K63-linked ubiquitin chains
- E3 enzyme: HERC2 (HECT and RLD domain containing E3 ubiquitin protein ligase 2) (in addition to RNF8 and RNF168) (Bekker-Jensen et al., 2010). HERC2 is phosphorylated by ATM in response to DSBs. Phosphorylated HERC2 interacts with RNF8 and stabilizes RNF8-Ubc13 association providing specificity to E2-E3 interaction and promoting K63-linked ubiquitin chain formation. In addition, HERC2 stabilizes RNF168 protein level.

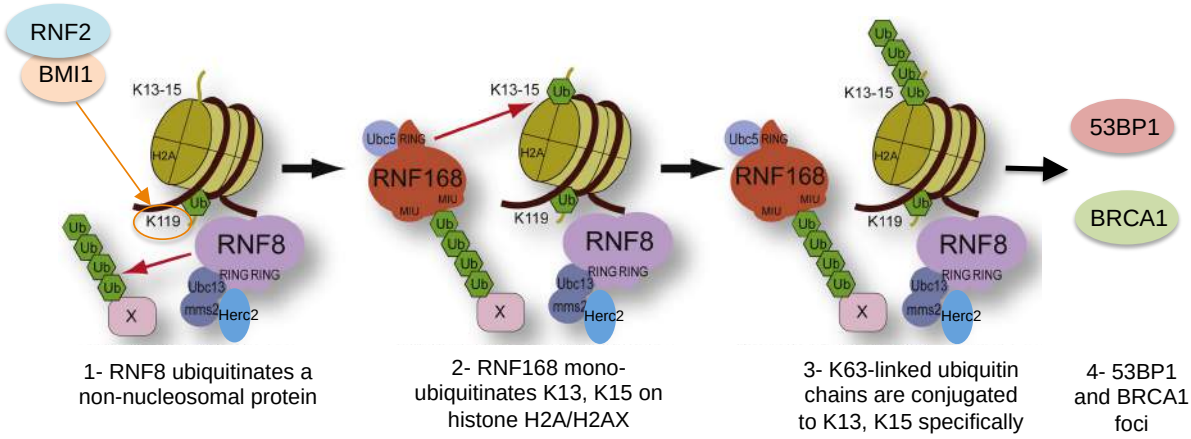

Figure 30: RNF8/RNF168-dependent signalling at DSBs. (**A**) Proposed model for RNF8/RNF168 ubiquitination cascade at DSBs. RNF168 is recruited to DSBs by the activity of RNF8 toward a non-nucleosomal substrate. RNF168 mono-ubiquitinates H2A-type histones on K13, K15 and this leads to K63-polyubiquitination on these lysines. Independently, RNF2-BMI1 monoubiquitinates H2A/H2AX on K119, K120. Adapted from (Mattiroli et al., 2012).

II.5.3.4.2 Recruitment of BRCA1 and 53BP1

BRCA1: K63-linked ubiquitin chains on histones surrounding DSBs constitute the specific signal for BRCA1 recruitment. BRCA1 is a tumour suppressor protein playing a central role in the maintenance of genome integrity (reviewed in (Silver and Livingston, 2012)). BRCA1 is a large protein (1863 amino acids) containing a C-terminal tandem BRCT (tBRCT) domain and a N-terminal RING-finger domain. Mutations in both domains of BRCA1 predispose to cancer (Rostagno et al., 2003).

The cellular levels of BRCA1 fluctuate in a cell cycle-dependent manner. BRCA1 is abundant in S- and G2-phase cells while it reaches a low steady-state level in G0/G1 cells. This process is regulated by both transcriptional mechanisms and ubiquitin proteasome-dependent degradation (Chen et al., 1996; Choudhury et al., 2004).

BRCA1 forms a stable heterodimer with BARD1 (BRCA1-associated ring domain protein 1) via its RING motif. BRCA1-BARD1 heterodimer is a functional ubiquitin E3 ligase, which catalyses the formation of K6-ubiquitin chains in complex with E2 UBCH5C (ubiquitin-conjugating enzyme E2D 3) (Nishikawa et al., 2004; Wu-Baer et al., 2003). BRCA1 is present in distinct biochemical complexes and it localizes at DSBs as member of the BRCA1-A complex (Rap80, Abraxas/CCDC98, BRCC36, BRCC45, MERIT40) (Feng et al., 2009; Kim et al., 2007; Wang et al., 2007). Abraxas interacts specifically with the BRCT domain of BRCA1 bridging it with Rap80. Rap80 recognizes and binds K63-ubiquitinated histones via two UIM motifs (Sobhian et al., 2007; Wang et al., 2007). Rap80 also binds SUMO at DNA damage sites via SIM motif (SUMO-interacting motif) (Guzzo et al., 2012) (see paragraph *II.5.3.6*). Interestingly, BRCC36

(BRCA1/BRCA2-containing complex subunit 36) possesses a deubiquitylating activity raising the possibility of a dynamic regulation of BRCA1 functions at DSBs (Sobhian et al., 2007).

53BP1: 53BP1 is a large protein (1972 amino acids) with not apparent enzymatic activity. 53BP1 functions in maintaining genomic integrity. Mice lacking 53BP1 show similar defects to ATM null mice and 53BP1 knockout cells have defects in checkpoint activation (Ward et al., 2003).

Structurally, 53BP1 contains a C-terminal tBRCT domain, an ubiquitylation-dependent recruitment motif (UDR), a tandem Tudor domains (tTudor) and a N-terminal S/T-Q site, which can be phosphorylated by ATM (or ATR) (Jowsey et al., 2007). In response to DSBs, 53BP1 accumulates at DNA lesions and forms foci (Anderson et al., 2001). γH2AX is dispensable for the initial recruitment of 53BP1 but γH2AX-dependent RNF8-RNF168 ubiquitination cascade is necessary for its retention (Celeste et al., 2003; Stewart et al., 2009). How 53BP1 is recruited to DSB has been a longstanding question. Several studies have provided new insights revealing a mechanism based in a specific combination of histone marks at damaged chromatin:

- Recognition of H4K20: 53BP1 binds H4K20me1 (monomethylated) and H4K20me2 (dimethylated) via its Tudor domains and this interaction is essential for 53BP1 foci formation (Huyen et al., 2004). In undamaged chromatin, H4K20me2 is masked by the Polycomb protein L3MBTL1 (lethal(3) malignant brain tumour-like protein 1) and by the demethylase JMJD2A (Lee et al., 2008; Min et al., 2007). Upon DSB induction, RNF8/RNF168 are required for 53BP1 recruitment at chromatin. Ubiquitylation of H2AK15 helps to expose the H4K20me2 mark, ubiquitylation of L3MBTL1 allows its eviction from chromatin by p97/VCP (valosin containing protein) and ubiquitylation of JMJD2A targets it to proteasome for degradation (Mallette et al., 2012; Meerang et al., 2011). Increased acetylation of H4K16 decreases the binding of 53BP1 to chromatin (Tang et al., 2013). Therefore, 53BP1 recruitment at DSBs is regulated by the antagonistic activities of Tip60 and HDAC1/HDAC2 (Hsiao and Mizzen, 2013).
- Recognition of H2AK15ub: The binding of 53BP1 to H4K20me2 is necessary but not sufficient for 53BP1 foci formation. 53BP1 needs to interact with H2AK15ub via its UDR motif (Fradet-Turcotte et al., 2013).

53BP1 only binds nucleosomes that have both H2AK20me2 and H2AK15ub marks.

It is emerging that 53BP1 and BRCA1 have an antagonistic relationship during DSB repair pathway choice. 53BP1 promotes NHEJ-mediated DSB repair protecting DSB ends from end-resection during G1 phase while BRCA1 favours HR during S and G2 phases probably by evicting 53BP1 and NHEJ factors (Chapman et al., 2013; Escribano-Diaz et al., 2013) (see also section *II.8*).

II.5.3.4.3 RNF2-BMI1 ubiquitination cascade

Another E3 ligase participates to DSB response, RNF2 with its co-activator BMI1 (Facchino et al., 2010; Ismail et al., 2010; Pan et al., 2011). RNF2 and BMI1, together with another E3 ligase, RNF1, form the RING domain-containing proteins of the Polycomb repressive complex 1 (PRC1) (Ginjala et al., 2011; Ismail et al., 2010). PRC1 ubiquitinates H2A and silences transcription (Wang et al., 2004).

The involvement of E3 ligases other than RNF8/RNF168 in H2A(X) ubiquitylation was initially suggested by the fact that depletion of RNF8 abrogates γH2AX polyubiquitylation without preventing the IR-induced γH2AX monoubiquitylation (Huen et al., 2007). This monoubiquitylation of H2AX at K119 and K120 (K118 and K119 in H2A) in response to DSBs is catalysed by RNF2–BMI1 (Facchino et al., 2010; Ismail et al., 2010; Pan et al., 2011). RNF2–BMI1 complex is recruited early (within minutes) at chromatin, forms foci that colocalize with DDR proteins and co-immunoprecipitates with DDR factors including H2AX, ATM, Nbs1, MDC1 and DNA-PK (Facchino et al., 2010; Ismail et al., 2010; Pan et al., 2011). Blocking the monoubiquitination of H2AX by downregulation of one component of RNF2-BMI1 complex or by using H2AX K119R/K120R mutants does not affect ATM activation (Pan et al., 2011) but impairs the recruitment of activated ATM at DSB sites (Facchino et al., 2010; Pan et al., 2011) and the subsequent foci formation of γH2AX and MDC1 (Facchino et al., 2010; Pan et al., 2011) and the downstream DDR response (FK2, 53BP1, BRCA1, pChk2) (Ismail et al., 2010).

Interestingly, BRCA1-BARD1 heterodimer is able to monoubiquitylate H2A *in vitro* (Xia et al., 2003). *Zhu* and co-workers demonstrated that BRCA1 E3 ligase activity is necessary for the maintenance of the monoubiquitinated H2A (Ub-H2A) within constitutive heterochromatic regions in mouse and human cells (Zhu et al., 2011). To date, it is not known if BRCA1-dependent monoubiquitylation of H2A could have a role in the response to DNA damage. However, cells lacking BRCA1 E3 ligase activity do not exhibit defects in HR (Reid et al., 2008) but expression of constitutive Ub-H2A in BRCA1 null cells is able to rescue about 50% of HR defects measured with the HR GFP reporter system after I-SceI expression (Zhu et al., 2011).

II.5.3.4.4 Negative regulation of ubiquitination

Ubiquitination process in DSB response is also negatively regulated. This opposite activity seems to be important in the context of DSB repair and repair pathway choice. Three mechanisms have been described to antagonize ubiquitin-dependent signalling at DSBs:

1) *Deubiquitylation*: Several deubiquitylating enzymes (DUBs) have been implicated in the clearing of DDR signal (for review see (Jacq et al., 2013)), including USP3 (ubiquitin-specific

protease 3) which deubiquitylates H2A and H2B (Nicassio et al., 2007), BRCC36 (Shao et al., 2009) and POH1 (26S proteasome-associated PAD1 homolog 1) that both antagonize RNF8 by removing ubiquitin residues induced by RNF8 (Butler et al., 2012). Interestingly, OTUB1 (OTU deubiquitinase, ubiquitin aldehyde binding 1), another DUB, opposes DSB-induced ubiquitylation by suppressing the activity of RNF168 through interaction and inhibition of Ubc13 rather than by using its catalytic activity (Nakada et al., 2010).

2) *Ejection of ubiquitinated proteins*: Ubiquitinated proteins can be ejected from chromatin by ubiquitin-directed segregases, such as p97/VCP (Meerang et al., 2011) (for review see (Ramadan, 2012; Vaz et al., 2013)).

3) *Competition*: RNF169, a RNF168 paralog, competes with UBD-binding proteins (53BP1 and Rap80) at DSB sites, thus inhibiting RNF8/RNF168-dependent signalling (Chen et al., 2012; Panier et al., 2012; Poulsen et al., 2012).

II.5.3.4.5 Role of proteasome in DDR

Ubiquitylation is a key component of DDR signalling but polyubiquitin chains (in particular K48 and K11), when associated with an unfolded protein region, also constitute a signal (also known as degron) for proteasomal degradation (for review see (Bhattacharyya et al., 2014)).

The 26S proteasome comprises a catalytic core particle (20S) containing the proteolytic active sites capped by one or two regulatory particle (19S). The 20S forms a compact cylinder composed of four stacked rings enclosing the catalytic sites that can be reached only by unfolded proteins through a very narrow pore. This pore is generally close in the 20S free particle and can be opened after docking of activators to the core particle (Groll et al., 2000). The 19S is a 20S activator complex composed by a “lid” working in the poly-Ub substrate recognition, binding and deubiquitylation and a “base” harbouring the ATPase function. The large 26S proteasome is localized in both the cytoplasm and the nucleus of all eukaryotic cells (Bhattacharyya et al., 2014). In addition to 19S cap, others proteasome activators have been identified and can form a complex with the 20S core: (i) the 11S cap, also known as PA28 (proteasome activator 28) (Dubiel et al., 1992), (ii) PA200 (proteasome activator 200) (Ustrell et al., 2002) and (iii) p97/VCP (Barthelme and Sauer, 2012; Barthelme and Sauer, 2013).

The proteasome is involved at different levels in the DSB response. First, the proteasome is required indirectly for ubiquitin signalling. Indeed, inhibition of the 20S catalytic activities (such as by MG132 or bortezomib) induces the accumulation of poly-Ub proteins, thus preventing the recycling of ubiquitin (Dantuma et al., 2006). Accumulation of ubiquitylated substrates coincides with the reduction of the nuclear free ubiquitin pool and of the histone-conjugated ubiquitin

(Dantuma et al., 2006). Thereby, in the presence of DSBs, the inhibition of the proteasome results in persistence of MDC1 foci, impairment of phospho-ATM, FK2, 53BP1 and BRCA1 foci formation and inhibition of both HR and NHEJ repair pathways (Butler et al., 2012; Cron et al., 2013; Galanty et al., 2012; Gudmundsdottir et al., 2007; Jacquemont and Taniguchi, 2007; Mailand et al., 2007; Meerang et al., 2011; Murakawa et al., 2007; Takeshita et al., 2009). Consistently, introduction of exogenous ubiquitin upon proteasome inhibition is able to rescue the production of 53BP1 foci in presence of DSBs (Butler et al., 2012).

The proteasome may also be implicated more directly in DDR, since several studies have revealed that 20S and 19S proteasome subunits, PA200, PA28 and p97/VCP accumulate at DSBs created by different sources (Ban et al., 2013; Blickwedehl et al., 2008; Blickwedehl et al., 2007; Butler et al., 2012; Galanty et al., 2012; Levy-Barda et al., 2011; Livingstone et al., 2005; Meerang et al., 2011; Ustrell et al., 2002) and can interact with DDR proteins (Brown et al., 2015; Butler et al., 2012; Galanty et al., 2012). In addition, some proteasome components are regulated by DDR proteins following DNA damage induction: 19S subunit PSMD4 (proteasome 26S subunit, non-ATPase, 4) is phosphorylated by the DDR protein kinases ATM and/or ATR (Matsuoka et al., 2007), PA28 is a target of ATM (Levy-Barda et al., 2011), DNA-PK activity drives the PA200-associated proteasome recruitment at chromatin (Blickwedehl et al., 2008) and p97/VCP can be phosphorylated by ATM and/or DNA-PK (Livingstone et al., 2005). The role of proteasome at DSBs is not clearly understood but different possibilities are emerging (reviewed in (Stone and Morris, 2014)):

- *Degradation of DDR proteins*: Degradation of DDR proteins can be part of the DDR cascade and DSB repair. For instance, MDC1 turnover is controlled by the proteasome (Luo et al., 2012), JMJD2 degradation is necessary for 53BP1 recruitment (Mallette et al., 2012) and BRCA1 is also degraded by the proteasome (Choudhury et al., 2004). If the proteasome degrades ubiquitylated proteins *in situ* or after their eviction from chromatin by p97/VCP, remains to be established.

- *Restriction of K63-Ub conjugates at DSBs*: The 19S deubiquitylating enzyme POH1 processes K63-Ub conjugates to restrain 53BP1 assembly at DSBs (Butler et al., 2012).

- *Participation in DSB repair*: The proteasome could be directly implicated in DSB repair. For example, DSS1 (deleted in split hand/split foot protein 1) is a component of the 19S proteasome (Wei et al., 2008) and a co-factor of BRCA2 (Marston et al., 1999). DSS1 is recruited to DSBs in a POH1-dependent manner (Butler et al., 2012) and the depletion of DSS1 impairs HR (Kristensen et al., 2010).

II.5.3.5 NEDDylation

NEDD8 (neural precursor cell expressed developmentally downregulated 8) is a member of the UBL family. Among the UBLs, NEDD8 is the most highly related to the ubiquitin at sequence and secondary structure level (reviewed in (Enchev et al., 2015)). NEDD8 is conjugated to a lysine using E1, E2 and E3 enzymes distinct to ubiquitin. The well-described conjugation pathway for NEDD8 involves the NAE1 (NEDD8 activating enzyme) as E1 enzyme, UBE2M or UBE2F (ubiquitin-conjugating enzyme E2M or E2F) as E2 enzyme and RBX1 or RBX2 (ring box 1 or 2) as E3 (Enchev et al., 2015). NEDD8 and neddylation-pathway components rapidly accumulate at DSB sites and colocalize with γH2AX (Brown et al., 2015; Ma et al., 2013). The role of neddylation in DDR is tightly connected to ubiquitylation. The predominant substrates of NEDD8 are the E3 ubiquitin ligase cullins. Neddylation of the cullins results in the activation of their ubiquitin transfer activity. A recent report from the *Jackson*'s laboratory shows that neddylation is required for ubiquitylation of Ku, probably mediated by cullins, and for the removal of Ku and NHEJ factors from DSBs (Brown et al., 2015) (**Figure 31**). The persistence of NHEJ factors at chromatin after completion of DSB repair could be the cause of the hypersensitivity to IR of cells deficient for neddylation processes (Brown and Jackson, 2015; Brown et al., 2015). In the last years, several non-cullin substrates of neddylation have also been reported including proteins involved in DDR such as p53 (Xirodimas et al., 2004), RNF168 (Li et al., 2014) and histone H4 (Ma et al., 2013) and H2A (Li et al., 2014). However, the presence of non-cullin substrates *in vivo* is debated, because of the redundancy between neddylation and ubiquitylation that makes the ubiquitin machinery able to catalyse neddylation in some experimental conditions (Brown and Jackson, 2015; Enchev et al., 2015).

Neddylation is negatively regulated by deneddylase enzymes, among them CSN (COP9 signalosome) is the predominant (Enchev et al., 2012). In the case of cullins, CAND1 (cullin-associated NEDD8-dissociated 1) acts also as a negative regulator since it binds deneddylated cullins and promotes their dissociation from the substrate (Zheng et al., 2002).

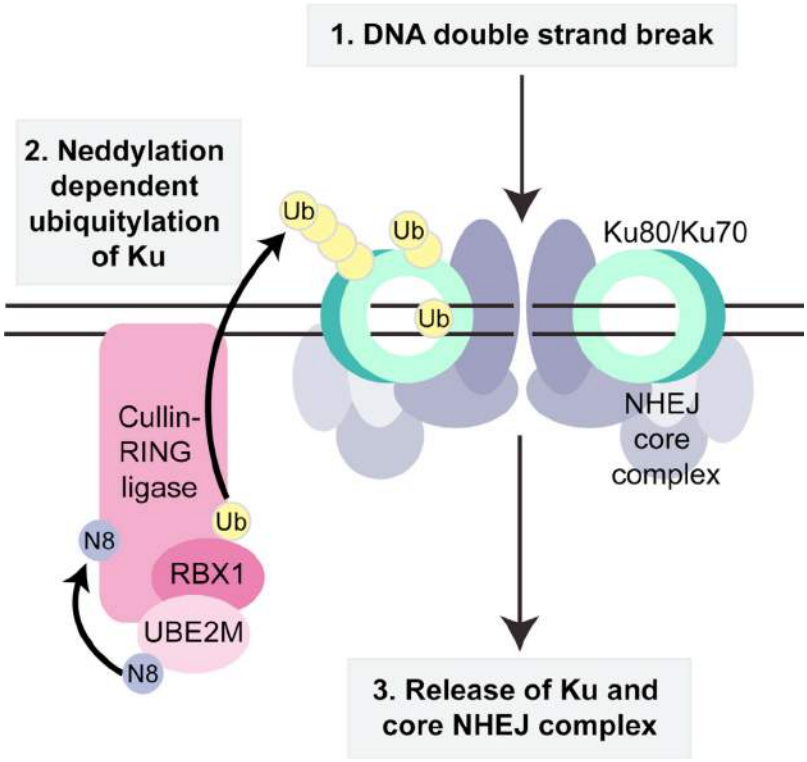

Figure 31: Model for neddylation-dependent ubiquitylation and release of Ku from chromatin. After DSB repair by NHEJ, cullin proteins are neddylated and ubiquitylate Ku favouring the release of Ku and NHEJ factors from chromatin. Figure from (Brown et al., 2015).

II.5.3.6 SUMOylation

SUMOylation reaction consists in the covalent attachment of a SUMO group to a lysine of a target protein. Similarly to ubiquitylation, SUMOylation involves a SUMO-activating enzyme (E1), a SUMO-conjugating enzyme (E2) and a SUMO-ligase (E3), which is not always required. In humans, the only known SUMO E1 and E2 are the heterodimer SAE1-UBA2 (SUMO1 activating enzyme subunit 1- ubiquitin-like modifier activating enzyme 2) and Ubc9 (ubiquitin-conjugating enzyme E2I), respectively whereas several SUMO E3 ligases exist (Desterro et al., 1999). Unlike ubiquitin, at least four SUMO isoforms have been described: SUMO1 is mostly associated with mono-SUMOylation, SUMO2/3 (so called because of their sequence similarities) can form poly-SUMO chains and SUMO4 appears to function in the cytoplasm with tissue-specificities. SUMO-modified proteins can be recognized by and interact with partners having SIMs motifs. Moreover, SUMOylation can be reversed by SUMO-specific proteases (SENPs).

SUMO1 and SUMO2/3 conjugates accumulate at DSB sites, form foci that colocalize with 53BP1 and persist at breaks for several hours after damage (Galanty et al., 2009; Morris et al., 2009). Similarly, SAE1, Ubc9 and the SUMO E3 ligases PIAS1 and PIAS4 (protein inhibitor of activate STAT protein 1 or 4) are also recruited at damaged chromatin and are required for SUMOylation at

DSBs. PIAS4 is necessary for 53BP1 SUMOylation and recruitment at DSBs while both PIAS1 and PIAS4 SUMOylate BRCA1 and favour BRCA1 focal accumulation (Galanty et al., 2009; Morris et al., 2009). The function of 53BP1 SUMOylation remains to be determined while SUMOylation of BRCA1 stimulates its E3 ligase activity *in vitro* (Morris et al., 2009).

In addition, several evidences suggest that SUMOylation may promote DSB-induced ubiquitylation:

- PIAS4 is needed for effective RNF168-mediated formation of ubiquitin-adducts at site of DNA damage (Galanty et al., 2009).
- HERC2 and RNF168 are DNA damage-dependent SUMOylation targets. SUMOylation of HERC2 is required to interact with RNF8 and to stabilize the RNF8-Ubc13 complex (Danielsen et al., 2012).
- RNF4 is an E3 ubiquitin ligase, harbouring SIMs motifs that enable its specific interaction with SUMOylated proteins at DSB sites where it functions to ubiquitylate and target proteins for removal by proteasome and/or by p97/VCP (Galanty et al., 2012). RNF4 localizes at DSBs sites and it is required for proper recruitment of Rap80, BRCA1 and Rad51 and for DSB repair (Galanty et al., 2012; Guzzo et al., 2012; Luo et al., 2012; Vyas et al., 2013). RNF4 is also important in controlling the turnover of MDC1 (Luo et al., 2012). Indeed, RNF4 ubiquitinates SUMOylated-MDC1 targeting it for proteasomal degradation, a process that promotes HR (Luo et al., 2012) (see also section *II.5.3.7* and **Figure 32**).

II.5.3.7 Methylation

Protein methylation consists in the addition of a methyl group to a lysine (up to three methyl groups) or to an arginine (up to two methyl groups) on a target protein. Methylation of a protein can promote its recognition by partners having Tudors domains, PDH finger domains or chromodomains, or it can modulate its biological activity. In the context of DDR, methylation can interest histone and non-histone proteins and it is catalysed by methyltransferases.

53BP1 and Tip60 give two intriguing examples displaying the importance of methylation in the DDR.

The requirement of H4K20me2 for 53BP1 recruitment has already been described in section *II.5.3.4.2*. H4K20 is constitutively methylated but different methyltrasferases can regulate this "mark" in response to DSBs. For instance, MMSET methyltrasferase is phosphorylated by ATM and recruited in an MDC1-dependent manner to chromatin where it increases the local H4K20 methylation and favours 53BP1 recruitment (Pei et al., 2011). Recently, the concerted activities of

two others methyltransferases PR-Set7 (PR/SET domain-containing protein 07) and Suv4-20 (suppressor of variegation 4-20 homolog 1) in catalysing H4K20me2 at DSBs have been identified as determinant for 53BP1 focal accumulation and proficient NHEJ repair (Tuzon et al., 2014).

Tip60 is activated by binding to H3K9me3 when HP1 dissociates from damaged sites (Sun et al., 2009). A recent work of *Ayrapetov et al.* shows that Tip60 can be activated upon DSB-induction in regions of euchromatin with low H3K9me3 density by a transient increase in H3K9me3 (Ayrapetov et al., 2014). They demonstrate that the methyltrasferase suv39h1 (suppressor of variegation 3-9 homolog 1) in complex with KAP1 and HP1 is rapidly loaded onto chromatin flanking DSBs where it catalyses tri-methylation of H3K9. The nascent H3K9me3 in turn recruits additional KAP1/HP1/suv39h1 complexes determining the spreading of H3K9me3 around the break. These H3K9me3 domains are transient, since they rapidly activate Tip60 and consequently ATM, which promote the release of KAP1/HP1/suv39h1 complex by phosphorylating KAP1 (see section *II.8*).

The methylation of H3K36 is also emerging as an important histone mark regulating DSB repair. The H3K36 di-methylation operated by the methyltransferase Metnase seems facilitate the DSB repair by NHEJ (Fnu et al., 2011) while the SET2 (SET domain containing 2)-dependent tri-methylation may promote DSB resection and HR (Aymard et al., 2014; Pfister et al., 2014).

Methylation is negatively regulated by demethylases (Mosammaparast and Shi, 2010). An example of demethylase functioning in DDR is JMJD1C (jumonji domain containing 1C), which participates to MDC1 regulation in response to DNA damage (Lu and Matunis, 2013; Watanabe et al., 2013). JMJD1C selectively promotes the recruitment of BRCA1 shuttling DSB repair toward HR pathway (Watanabe et al., 2013). Indeed, mechanistically, JMJD1C demethylates MDC1 at K45 thereby promoting MDC1-RNF8 interaction. This interaction favours the RNF8-mediated ubiquitylation of MDC1 and the recruitment of BRCA1 to the polyubiquitylated MDC1 (**Figure 32**).

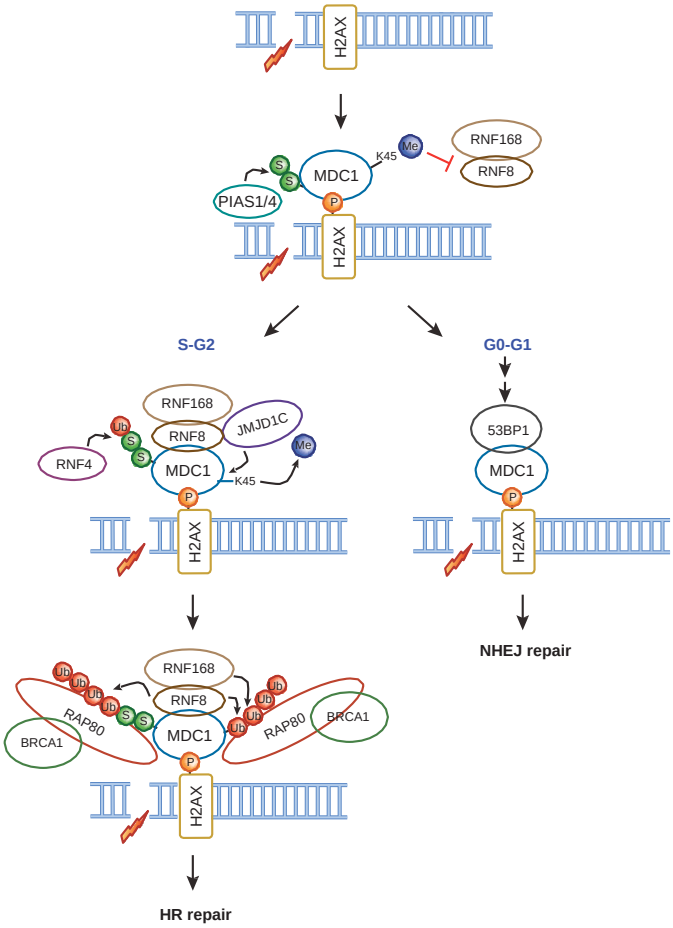

Figure 32: Methylation, SUMOylation and ubiquitylation regulate MDC1 and DSB repair pathway choice. Recruitment of PIAS1/4 at sites of DSBs leads to MDC1 SUMOylation and recruitment of JMJD1C results in demethylation of MDC1 at K45. MDC1 demethylation promotes RNF8-mediated ubiquitylation of MDC1. In addition to RNF8, RNF4 can also ubiquitinate SUMO-modified MDC1. The RAP80–BRCA1 complex is subsequently recruited through interactions with K63-linked polyubiquitin chains attached to MDC1. Alternatively, 53BP1 recruitment to MDC1 leads to NHEJ repair. Figure from (Lu and Matunis, 2013).

II.6 Importance of DDR foci for genome integrity maintenance

Despite the considerable advances in elucidating mechanistic and spatiotemporal regulation of DDR foci assembly, the understanding of the functional importance of these structures remains still limited. Kinetic modelling suggests that it is unlikely that all the molecules of a given factor immobilized near DNA lesions are directly involved in repair (Dinant et al., 2009). However, the evolutionary conservation of many proteins and motifs triggering focal assembly and the various pathologies associated with defects in DDR proteins (Jackson and Bartek, 2009) suggest a clear importance for DDR foci in the maintenance of genome stability. Notably, emerging and proposed roles for DDR foci include:

- *Amplify the DNA damage signalling*. In support of this idea, local chromatin immobilization of DDR factors was shown to be sufficient to trigger, amplify and maintain robust DDR activation in a damage-independent fashion (Soutoglou and Misteli, 2008). Amplification of DNA damage

signalling may have a particular importance in physiological conditions to efficient checkpoint activation at low levels of DSBs.

- *Promote DSB repair in regions where DNA repair is difficult to achieve like heterochromatin* (Goodarzi et al., 2011; Goodarzi et al., 2008) (see section *II.8*).

- *Stabilize broken ends and protect them from decay and/or illegitimate resection and repair processes.* For example, 53BP1 collaborating with Rif1 (rap1-interacting factor 1 homolog) and PTIP (PAX transcription activation domain interacting protein 1 like) prevents DSB resection in G1 (Chapman et al., 2013; Zimmermann et al., 2013). Similarly, the BRCA1-Rap80 complex restricts Mre11-CtIP-dependent end resection preventing excessive and deleterious end processing in S/G2 (Coleman and Greenberg, 2011).

- *DSB storage.* A clear example is given by 53BP1 nuclear bodies in G1-phase cells. They represent DSBs produced during mitosis by unresolved replication intermediates, particularly common at fragile sites that are chromosomal regions prone to breakage upon replication stress. Large chromatin domains enriched in 53BP1 sequestrate these DSBs transmitted to daughter cells and protect them from nucleases until repair mechanisms become available (Harrigan et al., 2011; Lukas et al., 2011a).

- *Coordination of DSB repair with other DNA metabolic activities such as transcription and replication.* Spreading of histone modifications, such H2A(X) monoubiquitination (Pan et al., 2011) and γH2AX (Iacovoni et al., 2010), along the chromatin around the site of break may indirectly affect repair by suppressing accidental ‘intrusions’ of advancing RNAPII into the sites of active repair. Indeed, transcription is negatively regulated when DSBs occur in expressed genes (see section *II.9*) (Shanbhag et al., 2010).

II.7 Targeting DDR proteins in cancer

Due to the important roles of DDR in maintaining genome stability, it is not surprising that defects in this pathway are associated with tumorigenesis. Loss of certain DDR components appears to be selected in early stages of tumorigenesis.

The connection between defects of DDR and tumours is the cornerstone of many anticancer-therapies. Other than surgery, the most prevalent cancer therapies are radiotherapy and chemotherapies that function by generating DNA damage. This implies that tumours with defects in DDR may be more vulnerable to genotoxic agents and it opens up the possibility of exploiting “synthetic lethality” in oncology. Because different repair pathways can overlap in function, the inhibition of the remaining pathway(s) in cancer cells should, in some cases, induces a greater

toxicity on the cancer cells compared to normal cells that can still rely on “back-up” pathways (**Figure 33**).

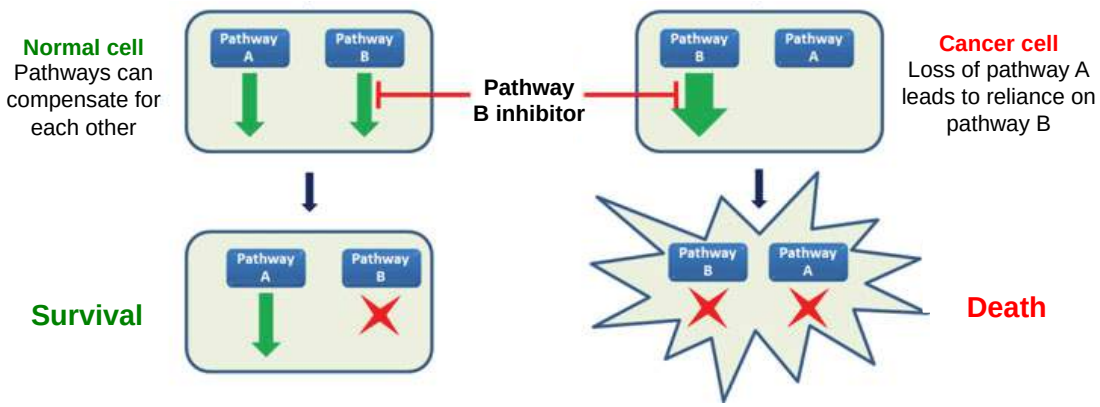

Figure 33: Synthetic lethality relationship. Normal cells have two DDR pathways, A and B. The elimination of pathway B results in genomic instability and eventually in cancer. Inhibition of the pathway B triggers cancer cells to death while normal cells, that still retain an active pathway A, survive (Jacq et al., 2013).

A paradigm of synthetic lethality is provided by PARP inhibitors that cause selective killing of tumours deficient in BRCA1 or BRCA2 with relatively low toxicity in normal cells (Bryant et al., 2009; Farmer et al., 2005). Inhibitors of PARP activity block SSB repair and also cause PARP to become trapped on DNA repair intermediates, resulting in DNA replication-associated DSBs that cannot be repaired correctly by HR in BRCA1/2 defective cells (Helleday, 2011). Similarly, inhibiting ATM seems a promising strategy to induce synthetic lethality in cancer having deficiencies in the Fanconi Anemia pathway (FA) (Kennedy et al., 2007; Landais et al., 2009). Despite these results, specific ATM inhibitors have currently not reached any clinical trials.

Table 7 illustrates some selected DDR inhibitors undergoing clinical trials (clinical trials information come from www.clinicaltrials.gov).

These therapies based on DDR deficiencies display the importance of understanding the stepwise cellular responses to DNA damage and the genotype of a specific tumour (Basu et al., 2012; Biss and Xiao, 2012; Jackson and Bartek, 2009; Jacq et al., 2013).

Table 7: Examples of DDR inhibitors undergoing or entered in clinical trials (www.clinicaltrials.gov)

Target	Inhibitors	Phase	Indications
DNA-PK/mTOR	CC-115	I	Solid tumours and hematologic malignancies
DNA-PK	CC-122	I/II	Solid tumours, non-Hodgkin lymphoma, multiple myeloma
	MSC2490484A	I	Solid tumours and hematologic malignancies
ATR	AZD6738	I/II	Solid tumours, leukaemia, lymphoma and ATM deficient adenocarcinoma
	VX-970	I/II	Solid tumours
Chk1/Chk2	LY2606368	I/II	Solid tumours, ovarian and breast cancer with BRCA1/2 mutations
Chk1	SCH900776	I/II	Leukaemia, lymphoma, solid tumours
PARP	Olaparib (AZD2281)	I/II/III and FDA/EMA Approved	Approved for advanced ovarian cancers with BRCA1/2 mutations. Clinical trials for solid tumours
	Veliparib (ABT-888)	I/II/III	Solid tumours, leukaemia, lymphoma. In particular in association with germline or sporadic BRCA1/2 mutations
	Rucaparib (AG-014699)	I/II/III	Advanced solid tumours, breast cancer, ovarian cancer. In particular in association with germline or sporadic BRCA1/2 mutations
	Niraparib	I/II/III	Ovarian cancer, prostate cancer, Ewing sarcoma, breast cancer BRCA1/2 mutated, Ewing sarcoma

II.8 DSBs repair and influence of DDR signalling on repair

Eukaryotic cells have evolved two main pathways to repair DSBs and thereby suppress genomic instability: the NHEJ and the HR. NHEJ promotes direct ligation of broken ends. It primarily involves the DNA-PK complex to recognize and tether broken ends and Artemis and other end-processing factors to prepare ends for ligation by XRCC4-XLF-Lig4 (X-ray repair cross-complementing protein 4 - XRCC4-like factor - ligase 4) complex and a new NHEJ component, PAXX (paralog of XRCC4 and XLF) (Ochi et al., 2015). NHEJ represents the major DSB repair pathway in mammalian cells. It is active throughout the cell cycle but it is of particular importance during G0/G1-phase (reviewed in (Grabarz et al., 2012; Hartlerode and Scully, 2009; Wyman and Kanaar, 2006)).

HR pathway uses a homologous undamaged sequence, such as a sister chromatid, as template. This process is normally accurate but requires an available sister chromatid generated by duplication and therefore it is generally restricted to cells in S- and G2-phases. HR starts with the resection of DNA ends by the concerted action of the helicase BLM and several nucleases (including CtIP, MRN complex, Exo1, Dna2) to yield 3'-ssDNA overhangs coated by RPA. The other key steps in HR consist in Rad51-mediated displacement of RPA with the help of mediator proteins (including BRCA1 and BRCA2), search for homology, DNA pairing and strand exchange (reviewed in (Grabarz et al., 2012; Hartlerode and Scully, 2009; Wyman and Kanaar, 2006)).

Along with these pathways, other "error-prone" processes have been described. Alt-NHEJ (alternative NHEJ) derives from NHEJ and is highly mutagenic and frequently uses micro-homologies distant from the break (Weinstock et al., 2007). Similarly, a derivative of HR pathway is the SSA (single-strand annealing). It always starts with resection but this step is not followed by strand invasion. In some cases it can lead to translocations (Richardson and Jasin, 2000).

An intense objet of current studies is the choice of DSB repair pathway and the molecular mechanism regulating this choice (reviewed in (Chapman et al., 2012b)). The major factor determining pathway's choice is the resection, such that long 3'-ssDNA ends become destined for HR. The primary mechanism regulating resection is the cell cycle. In particular, a phospho-dependent switch seems to turn on resection at G1/S transition. For instance, specific cyclin-dependent kinases (Cdks) are responsible for the phosphorylation and the activation of CtIP (Liu and Lee, 2006) and for the recruitment of Dna2 (Chen et al., 2011). CtIP is also degraded by the proteasome in G1 (Germani et al., 2003). However, HR and NHEJ coexist in S- and G2-phases indicating that other factors participate to the pathway's choice in addition to cell cycle. For example, DSBs' chromatin context drives the choice of DSB repair pathway, thereby transcriptionally active genes rich in H3K36me3 are repaired by HR (Aymard et al., 2014).

DDR signalling and repair are strictly connected each-other and some examples of DDR signalling components also implicated in DSBs repair are discussed below:

ATM is required for DSB repair in heterochromatin regions

Heterochromatin is a barrier to DSB repair and ATM is necessary to facilitate the repair in these regions. Indeed, loss of ATM activity results in persistent DSBs localized at the periphery of heterochromatin (Goodarzi et al., 2008). Mechanistically, ATM triggers localized heterochromatin relaxation to promote DSB repair by phosphorylating KAP1, a transcriptional co-repressor associated with the maintenance of heterochromatin structure. KAP1 is a SUMO E3 ligase, which undergoes auto-SUMOylation (Ivanov et al., 2007) and by virtue of this modification, it interacts with the SIM domain of CHD3 (chromodomain helicase DNA binding protein 3), a subunit of the NuRD complex, promoting ATP-dependent chromatin compaction. Upon DSB induction, ATM is activated and phosphorylates KAP1 at S824 (Goodarzi et al., 2011). This phosphorylation event interferes with the SUMOylated KAP1-CHD3 interaction and causes the release of CHD3 leading to the relaxation of the chromatin surrounding the DSB sites. Formation of phospho-KAP1 foci coincides with localized chromatin relaxation (Goodarzi et al., 2011; Noon et al., 2010) (**Figure 34**).

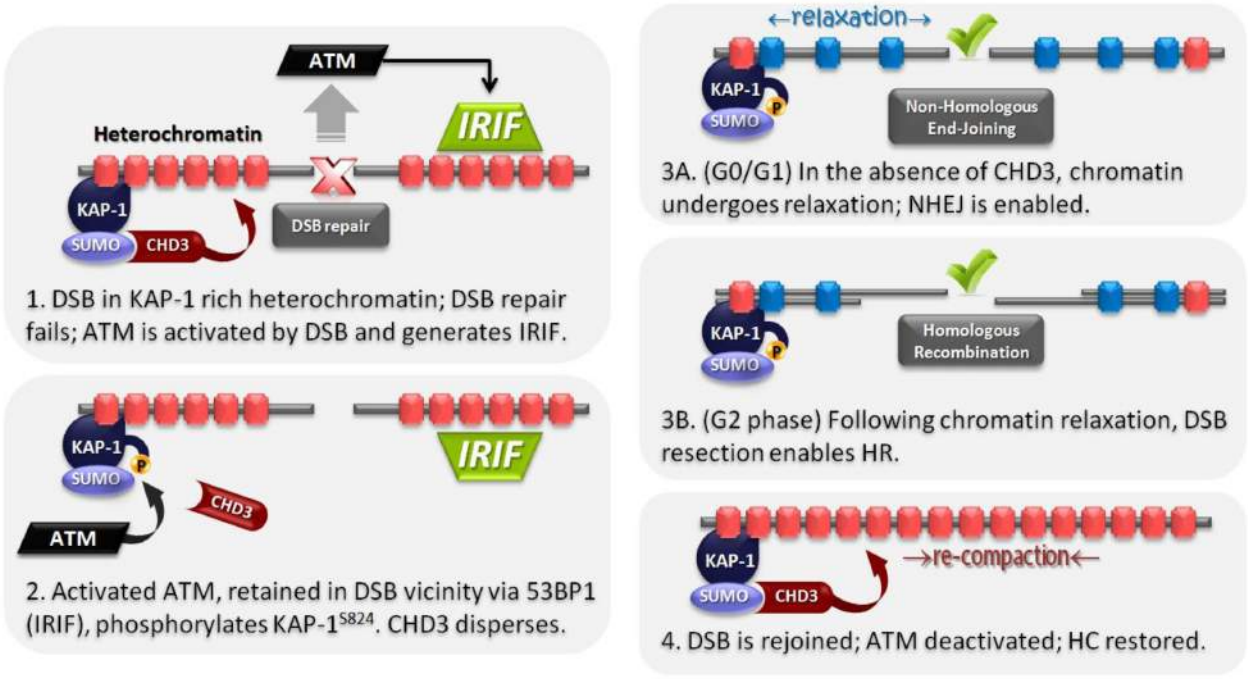

Figure 34: Model of ATM-dependent repair of DSBs in heterochromatin. A DSB in heterochromatin activates ATM. Activated ATM phosphorylates KAP1 and determines its dissociation from CHD3. In the absence of CHD3, the chromatin surrounding the DSB site relaxes allowing DSB repair by NHEJ or HR (Goodarzi and Jeggo, 2012).

53BP1 and BRCA1 oppositely regulate resection

53BP1 negatively regulates resection in G1 (Bothmer et al., 2010), while BRCA1 promotes 53BP1 removal and resection in S/G2 (Bunting et al., 2010). Deletion of 53BP1 restores HR and Rad51 foci in BRCA1 deficient cells (Bouwman et al., 2010; Bunting et al., 2010) demonstrating that 53BP1 and BRCA1 oppositely regulate HR. 53BP1 promotes NHEJ with the help of cofactors, RIF1 (Chapman et al., 2013; Zimmermann et al., 2013), PTIP (Callen et al., 2013) and the newly identified REV7 (REV7 homolog) (Boersma et al., 2015; Xu et al., 2015). The mechanisms by which 53BP1 blocks resection have not been elucidated. Super resolution microscopy gives architectural information about the antagonistic relationship between 53BP1 and BRCA1 at DSB foci (Chapman et al., 2012a). In G1 phase, 53BP1 occupies the core of IRIF probably correlating with NHEJ repair, while in S/G2-phase, 53BP1 is pushed to the periphery of the focus and the core is filled by BRCA1. The mechanism by which BRCA1 displaces 53BP1 is not known but it is likely that phosphorylated CtIP is the key mediator of this processes. BRCA1 can form a complex with CtIP and MRN (BRCA1-C complex) and one possibility is that this complex mediates the removal of 53BP1 (Daley and Sung, 2014).

Ku and DNA-PKcs

The binding of Ku heterodimer to broken ends represents the first engagement for NHEJ. Binding of Ku occurs during all phases of the cell cycle and Ku removal is necessary for resection (Shao et al., 2012). DNA-PKcs is also a strong inhibitor of resection since knockdown of DNA-PKcs leads to increased ssDNA formation at DSBs sites (Zhou et al., 2014).

II.9 Transcriptional DSBs

Transcriptional DSBs can be defined as DSBs produced in actively transcribed genes and/or by a transcription-dependent process. Compared to replication-dependent DSBs, transcriptional DSBs, both endogenous and exogenous, are a minority and their contributions to the cytotoxicity of DNA damage-inducing agents generally have not been characterized. In addition, the tumour selectivity and the cytotoxicity of the majority of chemotherapeutics are associated with replication. Despite this apparent minor role, DSBs in transcriptional units that remain unrepaired, or repaired by error-prone pathways, can have catastrophic consequences for the cell functioning, such as deleterious mutations in coding region, aberrant transcripts or prolonged transcription inhibition. For all these reasons, the study of the interplay between transcription and DSBs has recently emerged as a central topic of interest.

Knowledge on transcriptional lesions comes primarily from studies focused on UV-induced photoproducts and bulky adducts that have led to the identification of the TCR pathway. TCR is a sub-pathway of NER that targets DNA alterations interfering with the translocation of RNAP through expressed genes (Hanawalt and Spivak, 2008). A number of outcomes are possible following RNAPII arrest (Hanawalt and Spivak, 2008): (i) RNAPII can bypass the lesion possibly resulting in transcriptional mutagenesis, (ii) RNAPII can be displaced from the lesion (RNAPII backtracking), (iii) RNAPII can be ubiquitinated and degraded by the proteasome or (iv) prolonged RNAPII arrest can activate cell cycle checkpoints possibly leading to apoptosis.

However, different mechanisms of transcriptional regulation may exist at bulky adducts and DSBs. For instance, IR does not result in RNAPII ubiquitylation, unlike UV-induced damage (Bregman et al., 1996). UV damage or bulky adducts directly block RNAPII while the arrest at DSBs sites is controlled by DDR proteins, including ATM (Kakarougkas et al., 2014; Kruhlak et al., 2007; Shanbhag et al., 2010; Ui et al., 2015), DNA-PK (Pankotai et al., 2012), ATR (Jiang and Sancar, 2006), and PARP (Chou et al., 2010) and by chromatin modifications (Adam and Polo, 2014; Oliveira et al., 2014). Different studies often propose different models of response to transcriptional DSBs which might be related to the complexity of lesions, the localization of lesions (promoter or

body of the gene), the length of the gene, the transcription rate and the pre-existing transcriptional state of chromatin in which the break occurs. In general, transcriptional DSBs result in transient transcriptional inhibition in damaged chromatin that may be important to prevent interference between transcription and repair (Svejstrup, 2010). However, recent studies show that this inhibition does not concern all the transcripts. Indeed small non-coding RNAs are produced at DSB sites and regulate DSB signalling and repair; these RNAs are called DDRNA (DNA damage response RNAs) (Francia et al., 2012; Wei et al., 2012).

Some DDR proteins associate with the transcription apparatus, such as DNA-PK and BRCA1. In the case of DNA-PK, it has been shown that (i) the Ku heterodimer interacts with the elongating RNAPII (Mo and Dynan, 2002) (ii) DNA-PKcs has been initially identified in complex with the transcriptional factor Sp1 (Jackson et al., 1990) and (iii) DNA-PKcs efficiently phosphorylates RNAPII and the transcription factors TBP (TATA box binding protein) and TFIIB *in vitro* stimulating basal transcription (Chibazakura et al., 1997; Dvir et al., 1992; Maldonado et al., 1996).

In response to UV exposure, the heterodimer BRCA1-BARD1 ubiquitinates Rpb1 thus, initiating the proteasome-dependent RNAPII degradation (Kleiman et al., 2005; Starita et al., 2005). Hence, it is tempting to speculate that the association of DDR proteins with the transcriptional machinery may help to promote genome stability. When a DSB occurs, the signalling and repair machineries are immediately present and alerted to promote transcription arrest and repair.

II.9.1 Induction of transcriptional DSBs

In vivo transcriptional DSBs are produced by generation of site-specific DSBs or by drugs targeting transcription:

Site-specific DSBs

Site-specific nucleases generate DSBs at different and known genomic loci and thus, also in transcription units. This field was pioneered with yeast mating-type switch (HO) endonuclease (Rudin and Haber, 1988) and translated into mammalian cells by using I-SceI (Jasin, 1996) and I-PpoI (Berkovich et al., 2007) endonucleases. More recently, *Legube*'s laboratory has developed a mammalian system stably expressing the bacterial *AsiSI* restriction enzyme that recognizes a 8 bp sequence and generates approximately 150 sequence-specific DSBs distributed across the genome (Iacovoni et al., 2010). Site-specific DSBs can also be produced by the artificial engineering of site-specific zinc-finger (ZFNs) or TALEs (transcription activator-like effectors) DNA binding domain fused to the non-specific cleavage domain of Fok1 (Shanbhag et al., 2010).

Characteristics of these systems are, (i) the exclusive generation of DSBs, (ii) the generation of DSBs of the same complexity and (iii) the possibility to create inducible systems. For instance, the *AsiSI* restriction enzyme is fused to a modified oestrogen receptor hormone-binding domain that responds to the synthetic analog 4-hydroxy tamoxifen (4OHT). Treatment with 4OHT induces nuclear localization of *Asi*SI-ER enzyme and generate DSBs. Site-specific DSBs can be studied by using ChIP, which enables the detection of proteins strictly recruited to DSB ends and not forming foci and also enables the study of DDR spreading around a break. A major limit of these systems is that they must be turned off to study DSB repair (Aymard et al., 2014).

Drugs targeting transcription

Transcriptional DSBs can also be produced by drugs through mechanisms implicating transcription or through direct targeting of transcriptional machinery components. Drug-induced lesions that can be converted in DSBs by transcription usually can be also converted by replication thus, generating a mixture of TC- and RC-DSBs in cycling cells. Unlike to site-specific DSBs, drug-induced transcriptional DSBs are often not compatible with ChIP analysis, as their genomic localisation is not known. Usually the removal of drugs allows the study of DSB repair kinetics.

Table 8 shows the drugs currently known to produce transcriptional DSBs.

Table 8: Examples of drugs producing transcriptional-DSBs

Drug	Type of DSBs	DDR	Remarks	References
Ecteinascidin 743 (Et743)	TC- and RC-DSBs	TC- DSBs induce γH2AX, 53BP1, Mre11, pATM foci and activation of DNA-PK and Chk2. γH2AX phosphorylation by DNA-PK is required for full ATM activation.	TC-DSBs are dependent on TCR and MRN. Et743 induces RNAPII degradation. Et743 is an FDA approved drug for treatment of soft tissue sarcoma.	(Aune et al., 2008; Erba et al., 2001; Guirouilh-Barbat et al., 2008)
Pyridostatin	TC- and RC-DSBs	DSBs induce γH2AX foci, and phosphorylation of KAP1, Chk1, RPA and DNA-PK.	Pyridostatin stabilizes G-quadruplex structures at specific genomic loci. Telomeres loci are targeted at high concentration and non-telomere at low concentration. Functionally, pyridostatin leads to cell-cycle arrest and transcription downregulation of several genes.	(Rodriguez et al., 2012)
Camptothecin (CPT)	TC- and RC-DSBs	TC-DSBs induce γH2AX, 53BP1, MDC1, pATM foci and activation of Chk2 and DNA-PK.	See details in *Chapter I*. Campthotecin's derivatives are FDA-approved drugs.	(Huang et al., 2010; Sakasai et al., 2010a; Sordet et al., 2009)
Etoposide (VP16)	TC- and RC-DSBs	DSBs induce γH2AX, pATM, MDC1 and RPA foci and activation of DNA-PK.	Etoposide is an FDA-approved drug.	(Soubeyrand et al., 2010; Tammaro et al.; Zhang et al., 2006)

II.9.2 γH2AX in active transcribed genes

High-resolution mapping of γH2AX in chromatin surrounding DBSs induced by the restriction enzyme *Asi*SI displays a discontinuous signal, consisting of a series of "peaks" and "holes" (Iacovoni et al., 2010). Holes correspond to active genes rich in RNAPII in which transcription remains unchanged, indicating that undamaged active coding regions are refractory to γH2AX (**Figure 35A**). These observations agree with immunofluorescence data showing that transcription, monitored by *in vivo* incorporation of 5-bromouridine triphosphate (BrUTP), does not colocalize with IR-induced γH2AX foci (Solovjeva et al., 2007). The *Legube*'s laboratory has also shown that cohesin plays an antagonist role to γH2AX spreading (Caron et al., 2012). Cohesin is a multisubunit complex that participates in DSB repair and in transcriptional control by connecting the enhancers to the promoters of active genes (Kagey et al., 2010). Cohesin may play a role in isolating actively transcribed genes from the γH2AX response in the chromatin surrounding-DSBs and a tempting model is that cohesin may loop active genes outside of γH2AX foci. Indeed, depletion of the cohesin component SCC1 (SCC1 homolog) triggers an accumulation of γH2AX at cohesin-bound genes and a reduction of their transcriptional activity (**Figure 35B**). This protective effect is not induced by DSBs but rather the binding of cohesin to active genes seems to be constitutive (Caron et al., 2012).

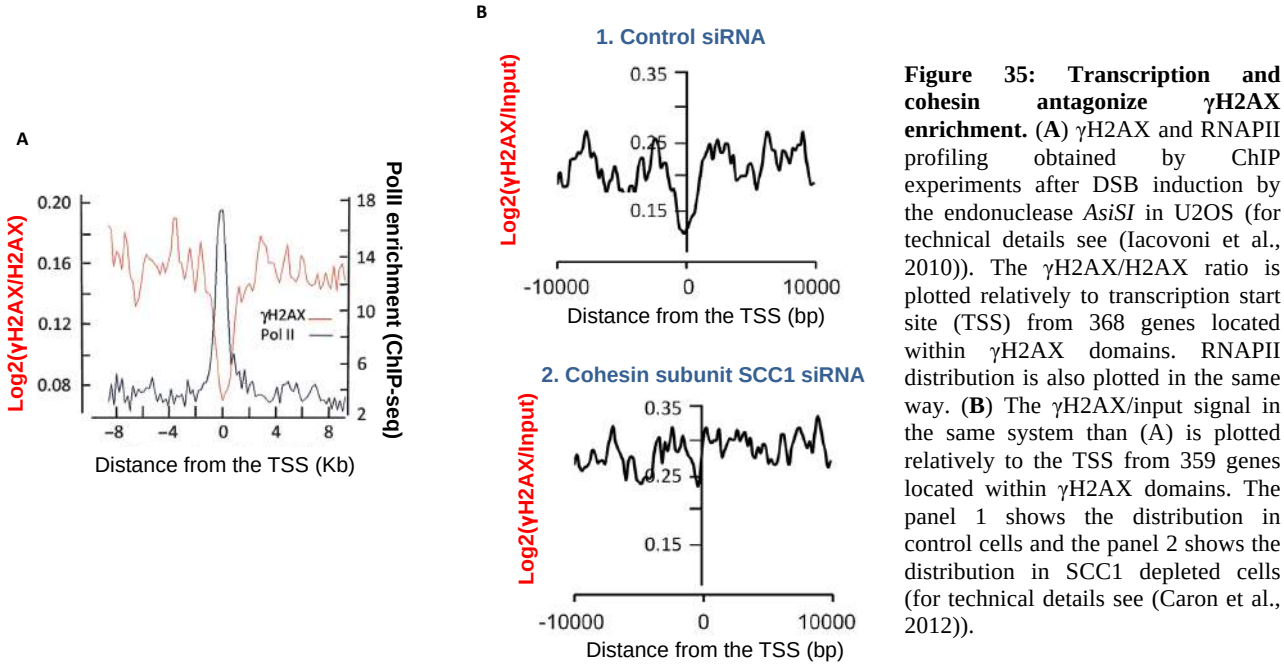

Figure 35: Transcription and cohesin antagonize γH2AX enrichment. (**A**) γH2AX and RNAPII profiling obtained by ChIP experiments after DSB induction by the endonuclease *AsiSI* in U2OS (for technical details see (Iacovoni et al., 2010)). The γH2AX/H2AX ratio is plotted relatively to transcription start site (TSS) from 368 genes located within γH2AX domains. RNAPII distribution is also plotted in the same way. (**B**) The γH2AX/input signal in the same system than (A) is plotted relatively to the TSS from 359 genes located within γH2AX domains. The panel 1 shows the distribution in control cells and the panel 2 shows the distribution in SCC1 depleted cells (for technical details see (Caron et al., 2012)).

II.9.3 Role of PARP

Chou et al described a role of PARP in setting up a repressive chromatin structure to block transcription at sites adjacent to DNA breaks in response to UV laser microirradiation (Chou et al., 2010). Transcriptional silencing is mediated by PARP-dependent recruitment at damaged chromatin of Polycomb group and NuRD complexes, which negatively regulate transcription. Indeed, by using an anti-7-methylguanosine antibody recognizing the cap structure of nascent RNA, the authors displayed the rapid loss of nascent transcripts at sites of γH2AX and this loss was further enhanced following PARG inhibition. In addition, elongating RNAPII is also lost at laser microirradiation-induced "stripe" as consequence of PARG inhibition.

II.9.4 Role of ATM

ATM plays a key role in repressing transcription in response to DSBs (Shanbhag et al., 2010). ATM-dependent inhibition of transcription in response to DSBs seems to favour recruitment of DSB repair factors and consequent DSB repair (Ui et al., 2015).

The *Greenberg*'s laboratory showed that the ATM-dependent transcription silencing spreads for kilobases of chromatin *in cis* to euchromatic DSBs (Shanbhag et al., 2010). They used a single-cell assay based in a transcriptional reporter system, which allows the simultaneous visualization of DDR and nascent transcription on a contiguous stretch of chromatin. By generating a DSB (induced by FokI nuclease) distal to the reporter gene promoter (4-13 kb), the authors found that ATM activity is responsible for the spreading of H2A monoubiquitinated at K119 (H2AK119ub) that mechanistically leads to the removal of the elongating RNAPII from the transcribed region. The reversal of silencing relies on the H2AK119ub deubiquitylating enzyme USP16. DSB induced-H2A monoubiquitination at K119 and the consequent transcription silencing are mediated by the Polycomb complexes (PRC1 and PRC2) (Kakarougkas et al., 2014; Mattiroli et al., 2012; Ui et al., 2015) (**Figure 36**). It is still unclear how ATM promotes Polycomb-mediated H2AK119ub. However, two ATM substrates have been recently involved in the ATM-mediated transcriptional repression by promoting H2AK119ub: (i) the SWI/SNF chromatin remodelling complex, PBAF (Kakarougkas et al., 2014) and (ii) the transcriptional elongation factor ENL (myeloid/lymphoid translocated) (Ui et al., 2015). ATM can phosphorylate PBAF (Matsuoka et al., 2007) and ENL (Ui et al., 2015) in response to DNA damage. It seems that the ATM-mediated phosphorylation of PBAF is responsible for the role of PBAF in transcriptional silencing (Kakarougkas et al., 2014). The ATM-dependent phosphorylation of ENL increases the interaction between ENL and PCR1 in

response to DSB, favouring the recruitment of PCR1 at transcriptional DSBs and the ubiquitination of H2A (Ui et al., 2015).

H2B monoubiquitination on K120 (H2BK120ub) is another histone mark associated with transcription elongation in unstressed cells and dependent on ATM in response to DSBs (Moyal et al., 2011). Monoubiquitination of H2B relies on the ATM-dependent phosphorylation of the E3 ligase RNF20-RNF140 heterodimer and its recruitment to DSB sites (Moyal et al., 2011). However, the primary role of H2BK120ub appears to be in DSB repair (Chernikova et al., 2010; Moyal et al., 2011; Nakamura et al., 2011) and this process seems to be uncoupled with transcription (Chernikova et al., 2010; Moyal et al., 2011; Nakamura et al., 2011; Shiloh et al., 2011).

Finally, along with the role of ATM in regulating RNAPII, ATM has been also described in controlling RNAPI transcription in presence of persistent DSBs within the rDNA (Harding et al., 2015; Kruhlak et al., 2007). IR- and etoposide-induced DNA damages result in ATM-dependent transient inhibition of both the assembly of RNAPI initiation complex and the elongation in the nucleolus (Kruhlak et al., 2007). This ATM-dependent transcriptional silencing induces nucleolar reorganization and the recognition of rDNA DSBs at the nucleolar periphery by the DDR factors (Harding et al., 2015).

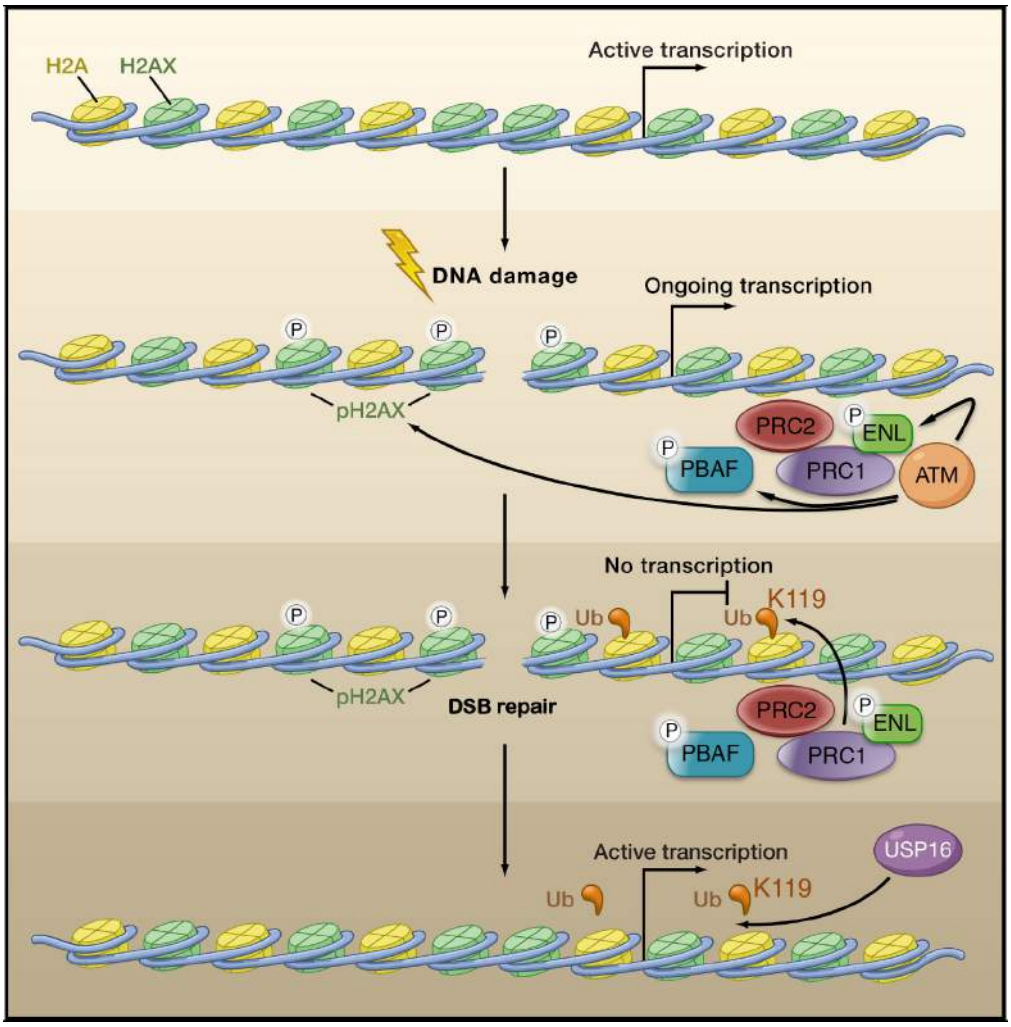

Figure 36: ATM-dependent DSB-induced silencing *in cis*. Working model representing how ATM regulates gene silencing: when a DSB is introduced at an actively transcribed region, ATM is activated and phosphorylates H2AX. ATM promotes H2A/H2AX monoubiquitination in K119 by phosphorylating the remodelling complex PBAF and the transcriptional elongation factor ENL. ENL interacts with PCR1 and triggers its recruitment at DSBs. PCR1 and PCR2 Polycomb repressive complexes ubiquitinate H2A. After DSB repair or recovery from DNA-damage signal, USP16 deubiquitinates H2A. Adapted from (Huen and Chen, 2010).

II.9.5 Role of DNA-PK

Pankotai et al reported a role for DNA-PK in transcriptional DSBs (Pankotai et al., 2012; Pankotai and Soutoglou, 2013). They analysed the impact of a single DSB encountered during RNAPII transcriptional elongation. Introduction of a single site-specific DSB in a transcribed gene by the meganuclease I-PpoI results in transient transcription arrest followed by re-initiation. In presence of a DNA-PK inhibitor, RNAPII remains associated with the promoter and the body of the transcribed gene and the same results are obtained by depletion of Ku heterodimer or DNA-PKcs. These data demonstrate that in the absence of DNA-PK, RNAPII can bypass the break and continues to elongate. Moreover, DNA-PK-dependent RNAPII removal requires the proteasome as proteasome inhibition or depletion of PSMD4 (19S subunit), rescues the transcriptional defect similarly to

DNA-PK inhibition. The authors speculated that a-yet unidentified protein might undergo DNA-PK-dependent phosphorylation and proteosomal degradation to remove RNAPII from the DSB site thus, preventing the synthesis of a mutant transcript (Pankotai et al., 2012; Pankotai and Soutoglou, 2013).

II.9.6 Role of histone mobilization

Recently, transcription chaperones, that mobilize histones in and out of chromatin, have been shown as key elements in transcription re-initiation after UV damage in human cells. In particular, the histone chaperones HIRA (histone regulator A) and FACT have been involved in transcription resumption and they are also recruited at DSB sites (Adam et al., 2013; Dinant et al., 2013; Yang et al., 2013). HIRA deposits newly synthetized H3.3 histones at sites of UV lesions and HIRA downregulation significantly inhibits transcription recovery. Mechanistically, the process is not completely understood but H3.3 histones generally carry posttranslational modifications that render chromatin permissive to transcription at sites of DNA damage (Adam et al., 2013). At endonuclease-induced DSB sites, HIRA is also known to depose H3.3 histones, which in turn promotes HR. However, the role of HIRA in transcription restart has not been addressed (Yang et al., 2013).
Similarly to HIRA, FACT is an H2A-H2B chaperone, which accelerates the exchange of H2A and H2B and favours transcription restart after DNA repair of the lesions blocking transcription (Dinant et al., 2013). In addition, FACT promotes HR-mediated repair of DSBs by localizing RNF20 at damaged chromatin (Oliveira et al., 2014) suggesting that FACT may be important for transcription resumption also at DSBs. Finally, FACT has an important function in the resolution of R-loop-mediated transcription-replication conflicts thus protecting cells against transcription-induced DNA damage (Herrera-Moyano et al., 2014).

II.9.7 Repair

Different works point up transcribed loci as regions particularly prone to chromosomal rearrangements (Gunn et al., 2011; Mathas and Misteli, 2009). Some critical factors that could favour chromosomal rearrangements are the incorrect end use during NHEJ repair of multiple DSBs, R-loops and exchange between chromosomal loci located in close spatial proximity at the time of DSB production (Nikiforova et al., 2000). By using a reporter system for NHEJ repair of multiple

DSBs located downstream from an inducible promoter, the *Stark*'s laboratory showed a higher frequency of incorrect end use during end-joining in active transcription units (Gunn et al., 2011).

Aymard and colleagues demonstrated that DSBs in actively transcribed human genes are preferentially repaired by HR. Active transcribed regions are marked by the transcription elongation-associated histone modification H3K36me3 that is probably recognized by LEDGF (lens epithelium-derived growth factor), which interacts with CtIP and initiates end-resection (Aymard et al., 2014). In parallel, two other groups, working on yeast models, have shown the importance of H3K36me3 histone mark and the methyltransferase Set2 (SETD2 in humans), responsible for this modification, in driving repair pathway choice (Jha and Strahl, 2014; Pai et al., 2014). Interestingly, in agreement with literature, *Aymard et al.* identified about 15% of the DSBs as HR-repaired in G2. They also found that XRCC4 depletion does not impair DSB repair at transcribed genes in G1 suggesting that these transcriptional-DSBs are not processed by NHEJ (Aymard et al., 2014). One possibility could be that these DSBs are repaired by HR as cells progress to S-phase. Furthermore, a recent work shows that in G0/G1 cells, homologous chromosomes frequently contact each other at the sites of DSBs produced by the restriction enzyme I-PpoI in coding regions, but not in intergenic regions (Gandhi et al., 2013; Gandhi et al., 2012). The authors suggested that this contact might have a role in DSB repair, since it requires ATM kinase activity. They also speculated the possibility that it could be a specialized DSB repair pathway operating in active genes that uses a homologous chromosome as a repair template and that could involve sequence-specific RNA molecules in homology searching.

In addition, in yeast a novel Rad52-dependent mechanism of DNA repair and HR has been characterised, in which endogenous transcript RNA is used as a template for DSB repair (Keskin et al., 2014). Human Rad52 can also promote RNA-DNA annealing *in vitro* raising the possibility that transcript-RNA-templated DNA repair could occur in human cells at highly transcribed loci and/or in non-dividing cells (Keskin et al., 2014).

OBJECTIVES

Top1 removes DNA supercoiling generated during transcription and replication by producing Top1-DNA cleavage complexes (Top1cc). These transient Top1cc can be stabilized by common DNA alterations and by CPT, from which anticancer drugs are derived.

One of the best-characterized consequences of Top1cc stabilization is the production of DSBs during replication. However, stabilized Top1cc are also potent transcription-blocking lesions and our understanding regarding the molecular processes resulting from the stalling of transcription complexes by Top1cc is currently limited. The laboratory has shown that stabilized Top1cc can lead to the production of transcriptional DSBs with activation of the ATM-dependent DDR pathway in post-mitotic cells (Sordet et al., 2009).

Hence, the main objective of my PhD was to characterize those transcriptional DSBs produced as a result of Top1cc stabilization. I used primarily serum-starved quiescent cells treated with CPT as a model to induce specifically transcription-blocking Top1cc and to determine:

1 – *The mechanism of DSB production*: The first objective of my PhD has been to decipher how stabilized Top1cc lead to DSB production by a transcription-dependent mechanism.

2 – *The DSB signalling*: The second objective has been to characterize the DDR signalling pathway that is activated by transcriptional DSBs and its role in Top1cc repair and cell survival.

3 – *The cellular relevance of transcriptional DSBs*: The third objective has been to investigate if transcriptional DSBs are cytotoxic to gain insights into their relevance in the context of (i) stabilized Top1cc that accumulate spontaneously in the case of deficiencies in Top1cc repair or DSB signalling such as in the neurodegenerative syndromes SCAN1 (Tdp1 deficiency) and AT (ATM deficiency) or (ii) Top1cc stabilized by CPT derivatives during chemotherapy.

4 – *The genomic distribution of transcriptional DSBs*: Finally, the last objective has been to test whether CPT-induced transcriptional DSBs were preferentially produced at specific genomic regions or at specific genes across the genome. This work has been initiated in collaboration with the groups of William Bonner (NIH, USA) and Giovanni Capranico (University of Bologna, Italy).

RESULTS

Article

Ubiquitination triggers DNA double-strand break formation and signalling in response to transcription-blocking topoisomerase-I lesions

Agnese Cristini, Joon-Hyung Park, Giovanni Capranico, Gaëlle Legube, Gilles Favre, Olivier Sordet

Previous work by *Sordet* and coworkers (Sordet et al., 2009) has shown that stabilized Top1cc produce transcription-dependent DSBs that activate the ATM-DDR pathway.
In this report, we characterize these DSBs by investigating the mechanisms of DSB production and signalling. To induce specifically transcription-blocking Top1cc, we used serum-starved quiescent cells treated with CPT and we showed that:

1- CPT-induced transcriptional DSBs are generated as a result of defective repair of Top1 associated SSBs: after Top1 proteolysis and before the action of Tdp1 and PARP.
2- CPT-induced transcriptional DSBs activate the ATM signalling pathway leading to the phosphorylation of ATM substrates such as H2AX and 53BP1.
3- ATM also activates DNA-PK, which promotes ubiquitination of H2A and H2AX that may in turn favour the proper assembly of activated ATM in nuclear foci. DNA-PK also promotes Top1cc degradation suggesting that DSB signalling further enhances Top1cc repair.
4- CPT-induced transcriptional DSBs can kill non-replicating cells and inhibition of DDR signalling hypersensitizes these cells to CPT.

Our study reveals a new mechanism of DSB production in response to stabilized Top1cc as well as a new function of DNA-PK in promoting ubiquitin signalling. These findings should prime further investigations on the cellular relevance of those transcriptional DSBs as we show that Tdp1, whose deficiency leads to the neurodegenerative syndrome SCAN1 with phenotypic similarities to AT, protects non-replicating cells against DSB formation.

Ubiquitination triggers DNA double-strand break formation and signaling in response to transcription-blocking topoisomerase-1 lesions

Agnese Cristini[1], Joon-Hyung Park[1], Giovanni Capranico[2], Gaëlle Legube[3], Gilles Favre[1], Olivier Sordet[1,*]

[1] Cancer Research Center of Toulouse, INSERM UMR1037, Toulouse, 31037, France
[2] Department of Pharmacy and Biotechnology, University of Bologna, Bologna, 40126 Italy
[3] LBCMCP, Université de Toulouse, Toulouse, 40126, France

* To whom correspondence should be addressed. Tel: +33 5 82 74 16 11; Fax: +33 5 82 74 16 85;
Email: olivier.sordet@inserm.fr

ABSTRACT

Although defective repair of DNA double-strand breaks (DSBs) leads to neurodegenerative diseases, the processes underlying their production and signaling in non-replicating cells are largely unknown. Stabilized topoisomerase-1 cleavage complexes (Top1cc) by natural compounds or common DNA alterations are transcription-blocking lesions whose repair depends primarily on Top1 proteolysis and excision by tyrosyl-DNA phosphodiesterase-1 (TDP1). We previously reported that stabilized Top1cc produce transcription-dependent DSBs that activate ATM in neurons. Here we use camptothecin (CPT)-treated quiescent cells to induce transcription-blocking Top1cc and show that those DSBs are generated during Top1cc repair from Top1 peptide-linked DNA single-strand breaks generated after Top1 proteolysis and before excision by TDP1. Following DSB induction, ATM activates DNA-PK whose inhibition suppresses H2AX and H2A ubiquitination and the later assembly of activated ATM into nuclear foci. Inhibition of DNA-PK also reduces Top1 proteolysis suggesting that DSB signaling further enhances Top1cc repair. Finally, we show that co-transcriptional DSBs kill quiescent cells. Together, these new findings reveal that DSB production and signaling by transcription-blocking Top1 lesions impact on non-replicating cell fate and provide insights on the molecular pathogenesis of neurodegenerative diseases such as SCAN1 and AT syndromes, which are caused by TDP1 and ATM deficiency, respectively.

INTRODUCTION

Topoisomerase I (Top1) is required to remove DNA supercoiling generated during transcription. It relaxes DNA by producing transient Top1 cleavage complexes (Top1cc), which are Top1-linked DNA single-strand breaks (SSB) (1). After DNA relaxation, Top1cc reverse rapidly, and Top1 is released as the DNA religates. The rapid resealing of Top1cc is inhibited by common DNA base alterations, carcinogenic adducts, DNA nicks and ribonucleotides misincorporated into DNA (2-4). Top1cc can also be trapped selectively by camptothecin (CPT) and its derivatives used to treat cancers, which bind at the Top1-DNA interface (1). Stabilized Top1cc are potent transcription-blocking DNA lesions (5,6) and their repair (removal) depends primarily on the tyrosyl-DNA phosphodiesterase I (TDP1) excision pathway. Top1cc excision by TDP1 requires prior proteolysis of Top1 by the

ubiquitin/proteasome system (7-14). Defective repair of Top1cc by inactivating mutation of TDP1 leads to the hereditary spinocerebellar ataxia with axonal neuropathy-1 (SCAN1) syndrome (15,16), indicating the importance of removing transcription-blocking Top1cc in non-replicating cells. A consequence of transcription-blocking Top1cc is the production of DSBs. These co-transcriptional DSBs have been detected in post-mitotic neurons and lymphocytes as well as in replicating cells out of the S-phase (17-19). Their production involves the formation of R-loops, a three-strand nucleic acid structure consisting of an RNA:DNA hybrid and displaced single-stranded DNA (20,21). Whether the Top1cc repair process is involved in the production of co-transcriptional DSBs is an unresolved question.

DNA double-strand breaks (DSBs) are among the most severe genomic lesions, and their repair requires the recruitment of DNA damage response (DDR) proteins in the vicinity of damaged chromatin, where they form discrete nuclear foci (22). The serine/threonine kinase ATM is critical for DDR (23) and its deficiency leads to the hereditary ataxia telangiectasia (AT) syndrome, which is primarily a neurodegenerative disease (15,24). ATM is readily activated by DSBs and phosphorylates various DDR proteins at damaged sites such as histone H2AX and MDC1. Phosphorylated H2AX (known as γH2AX) binds MDC1, which amplifies the damage signal around the break by recruiting additional ATM molecules (23). Accumulating studies indicate that histone ubiquitination regulates DDR both upstream and downstream of ATM. Ubiquitination of H2AX by the E3 ligase activity of RNF2-BMI1 complex triggers recruitment of activated ATM to DSBs allowing ATM to phosphorylates its targets at damaged sites (25,26). Then, ATM-mediated phosphorylation of MDC1 provides a binding site for the E3 ligase RNF8, which permits the recruitment of the E3 ligase RNF168. The concerted action of RNF8 and RNF168 allows ubiquitination of H2AX and H2A leading to the further recruitment of repair proteins such as 53BP1 and the BRCA1 complex (27-32). DNA-PK is also rapidly recruited at DSBs where it mediates repair by non-homologous end-joining (NHEJ) (33). Although DNA-PK can phosphorylate H2AX in response to DSBs (34), it is not clear whether it participates to DDR signaling asides from its role in DSB repair.

Here, we use serum-starved quiescent cells treated with CPT as a model to induce specifically transcription-blocking Top1cc and get molecular insights into the processes underlying both the production and signaling of DSBs. We found that those DSBs are produced during Top1cc repair from Top1 peptide-linked DNA single-strand breaks generated after Top1 proteolysis and before excision by TDP1. These data provide the first demonstration that TDP1, whose deficiency leads to neurodegeneration, protects non-cycling cells against the formation of DSBs. Analysis of DSBs signaling further reveals a novel function of DNA-PK in promoting protein ubiquitination leading to enhancement of Top1 proteolysis in a feedback look as well as to full ATM activity at DSB sites. Lastly, we found that those co-transcriptional DSBs kill quiescent cells indicating that the cellular response to transcription-blocking Top1 lesions impact on non-proliferative cell fate. Together, these findings provide new insights on the molecular pathogenesis of neurodegenerative diseases.

MATERIAL AND METHODS

Drugs and chemical reagents

BrdU, CPT, FLV, MG132 and Pyr-41 (35) were obtained from Sigma-Aldrich; lactacystin, G5 (36), KU55933 (37) and VE-821 (38) from Millipore; bortezomib, veliparib and olaparib from Selleckchem; and NU7441 (39) from Tocris.

Cell lines, culture and treatments

Primary human lung embryonic WI38 fibroblasts immortalized with hTERT were obtained from Estelle Nicolas (LBCMCP, Toulouse, France) and Carl Mann (CEA, Gif-sur-Yvette, France) (40). Cells were cultured in modified Eagle's medium (MEM) supplemented with 10% (v/v) fetal bovine serum, 1 mM sodium pyruvate, 2 mM glutamine and 0.1 mM non-essential amino acids. NHDF cells were isolated from healthy patients, as described previously (41), and human primary lung IMR90 fibroblasts were from ATCC. NHDF and IMR90 cells were cultured in Dulbecco's modified Eagle's medium (DMEM) supplemented with 10% (v/v) fetal bovine serum. To induce quiescence, cells were washed twice with serum-free medium and cultured for 72 in medium supplemented as described above but with 0.2% (v/v) serum instead of 10%. U2OS EV28 cells, stably expressing *Asi*SI-ER-HA enzyme (Iacovoni et al. 2010) were grown in DMEM supplemented with 10% (v/v) fetal bovine serum and 1 µg/ml puromycine. To induce DSBs, U2OS EV28 cells were treated with 300 nM 4-hydroxitamoxifen (Sigma-Aldrich) for 4 h. In Figure 3A and B, cells were gamma-irradiated with Gamma-cell Exactor 40 at 0.8 Gy. In all the experiments, untreated cells correspond to cells treated with the vehicle only.

Immunofluorescence microscopy, foci quantification and graphical representation

Cells were seeded in poly-L-lysine-coated Lab-Tek^{TM} RS chamber slides (NalgeNunc). After treatment, cells were washed twice with PBS and immunofluorescence was carried out as described previously (17). Where indicated, cells were pre-extracted with CSK buffer (10 mM Pipes (pH 6.8), 100 mM NaCl, 300 mM sucrose, 3 mM $MgCl_2$, 0.5% (v/v) Triton X-100) for 3 min at room temperature. Following two washes in PBS, cells were fixed with 2% (v/v) formaldehyde for 12 min at room temperature and washed three times. Cells were incubated with the primary antibody in PBS with 5% (v/v) fetal bovine serum for 1 h. Anti-ubiquityl-H2A antibody was incubated overnight at 4°C. Cells were washed twice and incubated with the appropriate secondary antibody coupled to Alexa Fluor 488, 594 or 568 (Life Technologies). After three washes, slides were mounted using Mowiol® 4-88 (Millipore) containing 4',6'-diamino-2-phenylindole (DAPI). Slides were visualized at room temperature by using a fluorescence microscope (Eclipse 90i, Nikon) or an inverted confocal microscope (LSM 710 or LSM 780; Carl Zeiss). Pictures were analyzed with Photoshop CS3 (Adobe) or ImageJ (version 1.48v). Primary antibodies used for microscopy were rabbit anti-53BP1 (NB100-305; Novus), rabbit anti-53BP1-pS1778 (2675; Cell Signaling), mouse anti-ATM-pS1981 (4526; Cell Signaling), mouse anti-BrdU (clone B44; BD Biosciences), mouse anti-γH2AX (05-636; Millipore), rabbit anti-γH2AX (NB100-384; Novus), mouse anti-DNA-PK-pT2609 (ab18356; Abcam), rabbit anti-MDC1 (ab11169; Abcam), mouse anti-ubiquityl-H2A (Ub-H2A; 05-678; Millipore), and mouse anti-ubiquitinated proteins (Ub-proteins; clone FK2, 04-263; Millipore).

Nuclear foci were counted manually and for nucleus with more than 20 foci, we set a default value of 25 foci. For Figure 4, nuclear foci were counted with imageJ software (version 1.48v). For graphical representation of foci distribution, we used box-and-whisker plots using GraphPad Prism 6 software with the following settings: boxes: 25-75 percentile range; whiskers: 10-90 percentile range; horizontal bars: median number of γH2AX foci. Each dot indicates an individual nucleus that is not in the 10-90 percentile range.

Cell extracts and Immunoblotting

Whole-cell extracts were obtained by lysing cells in 1% SDS and 10 mM Tris-HCl (pH 7.4) supplemented with protease (Sigma-Aldrich) and phosphatase (Halt phosphatase inhibitor cocktail; Thermo Scientific) inhibitors. Viscosity of the samples was reduced by brief sonication. For detection of ATM, ATM-pS1981, DNA-PK and DNA-PK-pS2056, cells were lysed for 15 min in buffer containing 50 mM Tris-HCl (pH 8.0), 300 mM NaCl, 0.4% NP-40, 10 mM MgCl2 and 5 mM DTT, supplemented with protease (Sigma-Aldrich) and phosphatase (Halt phosphatase inhibitor cocktail; Thermo Scientific) inhibitors. After centrifugation (10,000 x g, 20 min), supernatants were diluted (v/v) in 50 mM Tris-HCl (pH 8.0), 0.4% NP-40 and 5 mM DTT. Proteins were separated by SDS-PAGE and immunoblotted with the following antibodies: anti-actin (MAB1501; Millipore), anti-ATM (sc-23921; Santa-Cruz), anti-ATM-pS1981 (ab81292; Abcam), anti-ATR (ab2905; Abcam), anti-caspase-3 (9662; Cell Signaling), anti-cleaved caspase-3 (9661; Cell Signaling), anti-Chk2 (2662; Cell Signaling), anti-Chk2-pT68 (2661; Cell Signaling), anti-cullin 3 (ab108407; Abcam), anti-cullin 4B (A303-863A; Bethyl), anti-DNA-PK (NA57; Millipore, or ab18192; Abcam), anti-DNA-PK-pS2056 (ab18192; Abcam), anti-γH2AX (NB100-384; Novus), anti-H2AX (ab11175; Abcam), anti-histone H3 (ab1791; Abcam), anti-KAP1 (A300-274A; Bethyl), anti-KAP1-pS824 (A300-767A, Bethyl), anti-PARP (9542; Cell Signaling), anti-PSMA6 (2459; Cell Signaling), anti-p53 (DO-7, DakoCytomation), anti-p53-pS15 (9284; Cell Signaling), anti-topoisomerase I (ab109374; Abcam), anti-αTubulin (T5168; Sigma-Aldrich), anti-UBA1 (4890; Cell Signaling), anti-XLF (2854; Cell Signaling) and anti-XRCC4 (from Patrick Calsou, IPBS, Toulouse, France). Immunoblotting was revealed by chemiluminescence using autoradiography or a ChemiDoc MP System (Bio-Rad). Quantification of protein levels was done by using ImageJ (version 1.48v) in Figure 5E and with Image Lab software (version 4.1) in the other figures.

Cellular fractionation

Chromatin-bound proteins were isolated as described previously (42). Briefly, cells were extracted twice by lysis in extraction buffer (50 mM Hepes (pH 7.5), 150 mM NaCl, 1 mM EDTA) containing 0.1% (v/v) Triton X-100 supplemented with protease (Sigma-Aldrich) and phosphatase (Halt phosphatase inhibitor cocktail; Thermo Scientific) inhibitors for 15 min at 4°C followed by centrifugation at 14,000 x g for 3 min to separate soluble proteins. The collected supernatant was the fraction S1. The pellet was further resuspended in extraction buffer without Triton X-100 supplemented with 200 µg/ml RNAse A (Roche) for 30 min at 25°C under agitation. The fraction S2 was collected after centrifugation at 14,000 x g for 3 min. The remaining pellet was resuspended in

buffer containing 1% SDS and 10 mM Tris-HCl (pH 7.4) supplemented with protease (Sigma-Aldrich) and phosphatase inhibitors (Halt phosphatase inhibitor cocktail; Thermo Scientific) and sonicated.

Comet assays

Neutral Comet assays were performed according to the manufacturer's instructions (Trevigen), except that electrophoresis was performed at 4°C. Comet tail moments were measured with ImageJ software (version 1.48v) using a macro provided by Robert Bagnell (https://www.med.unc.edu/microscopy/resources/imagej-plugins-and-macros/comet-assay) or with the plugin OpenComet (http://opencomet.org/).

Detection of Top1-DNA cleavage complexes

Cellular Top1-DNA cleavage complexes (Top1cc) were detected as previously described (43), except that immunoblotting was revealed with a rabbit monoclonal anti-Top1 antibody from Abcam (ab109374) and with a ChemiDoc MP System (Bio-Rad).

Cell viability assays

Cell survival in Figure 8A was determined at times and conditions indicated in the text by counting adherent cells with Z1 Coulter Counter® (Beckman Coulter).

Chromatin immunoprecipitation (ChIP)

Chromatin immunoprecipitation was performed as described previously (Iacovoni et al. 2010) using a rabbit polyclonal anti-γH2AX antibody (ab81299) or a rabbit nonimmune antibody (control IgG) (catalogue number 02-6102, Life Technologies). ChIP were analyzed by real-time QPCR using primers proximal to two sites for the restriction enzyme *Asi*SI located inside genes (chr20:42089225-42089433: Gene 1-FW: AAAAGTCGCTCCCGGTAAAT, Gene 1-RV: CCGATCAGACTTGGGCTTAG; chr17:61847852-61848028: Gene 2-FW: TGCAAGGCATTCGACAATAA, Gene 2-RV: ATGGAAGCCATAATGCAAGC) or primers distal to *Asi*SI sites (chr21:25081874-25082075: Control-FW: TGGCTGGAACTGCTTTCTTT, Control-RV: GGTGAGTGAATGAGCTGCAA). All samples were analyzed in triplicates and data normalized to the maximal recovery in each experiment, which was set equal to 1.

Proteasome activity assay

P2 fractions were isolated as described above (Cellular fractionation). At each step of fractionation, the extraction buffer was supplemented with 10% (v/v) glycerol and 50 mM ATP without the addition of protease and phosphatases inhibitors. P2 fractions were solubilized in extraction buffer and briefly sonicated. Following centrifugation at 14,000 x g for 3 min, 30 µg of the collected supernatant were used to perform proteasome activity assay by using the Proteasome Activity Assay Kit (ab107921) according to the manufacturer's protocol. The chymotrypsin-like activity of proteasome was measured by the cleavage of a synthetic proteasome substrate linked to methyl coumarin amid (MCA). Cleavage of MCA in the presence or absence of the proteasome inhibitor MG132 was detected by

fluorescence emission using a Synergy™2 Multi-Mode Microplate Reader (Bio-Tek). Proteasome activity (U/ml) was calculated by subtracting for each sample, the background fluorescence given by the presence of the proteasome inhibitor MG132 (except in Supplementary Figure S5H) and by using an MCA standard curve.

siRNA transfection

Cells were transfected with siRNA duplexes using Dharmafect 4 transfection reagent (GE Healthcare) for 24 h before inducing quiescence for 72 h. siRNAs used are directed against cullin 3 (Silencer® Pre-designed siRNA CUL3, ID#217187, Ambion), cullin 4B (Silencer® Pre-designed siRNA CUL4B, ID#13299, Ambion), DNA-PK (M-005030-01, GE Healthcare), TDP1 (M-016112-01, GE Healthcare), XLF (5'-CGCUGAUUCGAGAUCGAUUGAdTdT-3'; Eurogentec), XRCC4 (5'-AUAUGUUGGUGAACUGAGAdTdT-3'; Qiagen) or a nontargeting sequence (SR-CL000-005; Eurogentec).

Statistics

Unless indicated otherwise, experimental differences were tested for significance using one-way ANOVA Tukey's multiple comparisons test with GraphPad Prism 6 software.

RESULTS

Top1cc stabilization induces transcription-dependent DSBs in quiescent cells

To investigate the production and signaling of transcription-dependent DSBs, we used primary human WI38 fibroblasts immortalized with hTERT (40). Non transformed cells normally have low genomic instability (44) and can be induced in quiescence following serum deprivation (45,46), thus allowing the analysis of replication-independent damage produced by stabilized Top1cc.

Microscopy analysis of bromodeoxyuridine (BrdU) incorporation showed that the percentage of WI38 hTERT cells in S-phase decreased from 26% to approximately 3% after a 3-day serum deprivation (0.2% serum) (Figure 1A and B), indicating that they efficiently entered quiescence. To determine whether CPT can induce replication-independent DSBs in those cells, we examined the phosphorylated histone H2AX on S139 (known as γH2AX) and its accumulation in nuclear foci. A single γH2AX focus reflects hundreds to thousands of γH2AX proteins that are concentrated around at least one DSB (47). We found that CPT induced γH2AX foci within 1 h, with an average of 2 to 10 foci per nucleus at CPT concentrations ranging from 1 to 25 µM, respectively (Figure 1C-E). Almost all cells formed at least 2 γH2AX foci at concentrations ≥ at 10 µM (Figure 1C and D). Similar results were obtained in serum-starved quiescent human IMR90 primary lung fibroblasts (Supplementary Figure S1A-D) and in serum-starved quiescent normal human dermal fibroblasts (NHDF) (Supplementary Figure S1E-H). These γH2AX foci colocalized with 53BP1, another DDR protein (Figure 1F), and a neutral Comet assay provided direct evidence for the presence of DSBs (Figure 1H and I). These results indicate that CPT induces replication-independent DSBs in quiescent cells.

To determine whether these breaks depend on transcription, we used the transcription inhibitor flavopiridol (FLV). Figure 1F and G show that FLV suppressed γH2AX and 53BP1 foci in CPT-treated

quiescent WI38 hTERT cells. To test whether FLV prevented DSBs or prevented DDR signaling by some other mechanisms, we performed neutral Comet assays. The significant decrease in Comet tail moment we observed in quiescent cells co-treated with FLV and CPT provides direct evidence for DSB suppression (Figure 1H and I). Together these results indicate that CPT induces transcription-dependent DSBs in quiescent cells, providing a robust model to further study their production and their signaling.

The formation of co-transcriptional DSBs requires Top1 proteolysis

Top1cc-mediated transcription block triggers Top1 degradation by the ubiquitin/proteasome system (12,13,48). Hence, we examined whether Top1 degradation would contribute to the formation of transcription-dependent DSBs. As expected, inhibition of transcription (FLV), ubiquitin (isopeptidase inhibitor G5) or proteasome (MG132) prevented Top1 degradation in CPT-treated quiescent WI38 hTERT cells (Supplementary Figure S2A-C). Then, we assessed whether inhibiting the ubiquitin/proteasome system would prevent DDR signaling. We found that the proteasome inhibitors MG132, lactacystin and bortezomib (also called PS-341) (Figure 2A and B) as well as the ubiquitin inhibitors G5 and Pyr41 (Figure 2D and E) prevented the induction of γH2AX and 53BP1 foci. Western blot analysis confirmed the suppressive effect of MG132 and G5 on γH2AX (Figure 2C and F). Importantly, DSB formation was also reduced by MG132, as indicated by a neutral Comet assay (Figure 2G and H). These results indicate that the ubiquitin/proteasome system is required for the formation of DSBs in CPT-treated quiescent cells.

Top1 is degraded selectively in response to CPT (1). To evaluate whether defective Top1 degradation accounts for the lack of DSBs following inhibition of the ubiquitin/proteasome system, we inhibited cullin 3 and cullin 4B, which targets Top1 for proteosomal degradation in CPT-treated cells (49,50). We observed that siRNA-mediated depletion of cullin 3 and cullin 4B in quiescent WI38 hTERT cells (Figure 3A) reduced CPT-induced Top1 degradation (Figure 3B) and γH2AX foci (Figure 3C). To further assess the role of Top1 degradation, we induced DSBs with ionizing radiation (IR) and the restriction enzyme *Asi*SI (51), which do not trigger Top1 degradation (Supplementary Figure S2D and E). We found that MG132 did not suppress γH2AX foci induced by IR in quiescent WI38 hTERT cells (Figure 3D and E) and by *Asi*SI in cycling U2OS cells (Figure 3F) indicating that genotoxics that do not promote Top1 degradation produce proteasome-independent DSBs. As expected, MG132, which causes depletion of free nuclear ubiquitin (52), prevented the ubiquitin-dependent focal accumulation of 53BP1 at DSB sites (31) in response to IR (Figure 3D) and *Asi*SI (Figure 3F). IR and *Asi*SI produce DSBs in both transcribed and non-transcribed regions whereas CPT likely produces co-transcriptional DSBs solely in transcribed regions. To assess whether proteasome activity is required simply because DSBs are located at transcribed regions, we analyzed γH2AX by chromatin immunoprecipitation (ChIP) at *Asi*SI sites located in genes. We found that MG132 did not suppress the induction of γH2AX in the two genes analyzed (Figure 3G). These results suggest that the requirement of proteasome activity for CPT-induced co-transcriptional DSBs is not only because these breaks are produced at transcribed regions but also because Top1cc are stabilized on chromatin. Altogether, these findings strongly suggest that the ubiquitin/proteasome-dependent

degradation of Top1 is required for the production of transcription-dependent DSBs following CPT treatment.

Co-transcriptional DSBs arise from SSB intermediates generated after Top1 proteolysis and before TDP1 action

Top1 degradation primes the repair of transcription-blocking Top1cc by TDP1. Top1cc excision by TDP1 requires prior proteolysis of Top1 to expose the covalent bond between the Top1 catalytic tyrosine and the 3'-end of the DNA to be attacked. TDP1 generates a 3'-phosphate, which is hydrolyzed by the polynucleotide kinase 3'-phosphatase (PNKP) before religation by ligase III (see Supplementary Figure S2F) (8-11,14). Because TDP1 deficient cells accumulate Top1 peptide-linked SSBs and causes hypersensitivity to CPTs (9,53,54), we examined whether transcription-dependent DSBs would arise from these SSB intermediates generated before TDP1 action.

We found that depletion of TDP1 with siRNA markedly increased the number of γH2AX and 53BP1 foci in CPT-treated quiescent WI38 hTERT cells (Figure 4A and B and Supplementary Figure S2G). Previous work showed that Top1cc excision by TDP1 requires PARP1 (10,55). PARP1 binds to and PARylates TDP1 leading to TDP1 stabilization and its recruitment at Top1cc-induced DNA damage sites. We therefore assessed whether inhibition of PARP1 would also increase DSBs in CPT-treated quiescent cells. We found that the PARP inhibitors veliparib (also called ABT-888) and olaparib (also called AZD-2281), both increased the number of γH2AX and 53BP1 foci (Figure 4C and D and Supplementary Figure S2H and I). DSB formation was also increased by veliparib, as indicated by a neutral Comet assay (Figure 4E). Inhibition of transcription (FLV) or proteasome (MG132), which prevented CPT-induced Top1 degradation (Supplementary Figure S2A and C), also prevented CPT-induced accumulation of γH2AX and 53BP1 foci following TDP1 depletion (Figure 4A and B) and PARP inhibition (Figure 4C and D), indicating that those breaks depend on Top1 degradation. To determine whether TDP1 and PARP1 are in the same pathway to prevent DSBs, we compared the number of γH2AX foci following co-treatment with CPT and PARP inhibitors when TDP1 is expressed or not. Figure 4F shows that TDP1 suppression with siRNA did not further increase the number of γH2AX foci in quiescent WI38 hTERT cells exposed to CPT and veliparib or CPT and olaparib, indicating that TDP1 and PARP1 are in the same pathway. Together, these results indicate that co-transcriptional DSBs produced in CPT-treated quiescent cells arise from SSB intermediates generated after Top1 proteolysis and before TDP1 action.

Activation of ATM and DNA-PK by co-transcriptional DSBs

Next, we studied the signaling of these co-transcriptional DSBs to gain insight into their functional relevance. To that end, we examined which kinases phosphorylate H2AX. ATM, ATR and DNA-PK are the main kinases for H2AX in response to DNA damage (47). To identify which of them induces γH2AX, we assessed whether γH2AX foci formation is prevented by specific chemical inhibitors of these kinases in CPT-treated quiescent WI38 hTERT cells; the ATM inhibitor (ATMi) KU55933, the DNA-PK inhibitor (DNA-PKi) NU7441 and the ATR inhibitor (ATRi) VE-821. We found that ATMi completely suppressed γH2AX foci and that DNA-PKi markedly reduced their number and size (Figure

5A and B and Supplementary Figure S3A and B). Analysis of DSBs by neutral Comet assays showed that ATMi and DNA-PKi did not decrease the Comet tail moment induced by CPT (Figure 5C), which exclude the possibility that fewer DSBs account for the reduced γH2AX levels. Similar results were obtained in quiescent IMR90 cells (Supplementary Figure S1A-D) and in quiescent NHDF cells (Supplementary Figure S1E-H). By contrast, ATRi did not reduce the number of γH2AX foci induced by CPT in quiescent WI38 hTERT cells (Figure 5A) under conditions where it prevented phosphorylation of the ATR substrate Chk1 in replicating cells (Supplementary Figure S3C). This is consistent with ATR being primarily activated by replication stress (56) and that it is expressed at low levels in non-cycling cells (Supplementary Figure S3D) (17,57). These data suggest that ATM and DNA-PK but not ATR are implicated in the induction of γH2AX in CPT-treated quiescent cells.

We therefore assessed whether ATM and DNA-PK are activated under conditions where γH2AX is induced. ATM autophosphorylation on S1981 (ATM-pS1981) marks activated ATM (58). In quiescent WI38 hTERT cells, we found that CPT induced ATM-pS1981 that colocalized with γH2AX foci (Figure 5D and Supplementary Figure S3E). We also observed phosphorylation of the ATM targets KAP1, Chk2 and p53 (Supplementary Figure S3E) (23). Similar to ATM, DNA-PK phosphorylation status regulates its activity. DNA-PK autophosphorylation on both S2056 and T2609 is required for the repair of DSBs by NHEJ (59,60). We found that CPT induced DNA-PK phosphorylation on both residues in quiescent WI38 hTERT cells (Figure 5D and E). Immunofluorescence microscopy further revealed that DNA-PK phosphorylated on T2609 formed discreet nuclear foci that colocalized with γH2AX (Figure 5D), indicating that similar to ATM, DNA-PK is activated at DSB sites. Previous work showed that ATM can phosphorylate DNA-PK on T2609 following IR (61). We found that inhibition of ATM prevented CPT-induced DNA-PK phosphorylation on T2609 and also on S2056 in quiescent WI38 hTERT cells (Figure 5D and E). Together these data suggest that in CPT-treated quiescent cells, transcription-dependent DSBs activate ATM, which in turn activates DNA-PK.

DNA-PK promotes the assembly of activated ATM in nuclear foci

Next, we considered whether cross talk between ATM and DNA-PK is mutual or limited to one direction in which ATM activates DNA-PK. To test this, we asked whether inhibiting DNA-PK would prevent MDC1 and 53BP1 foci, which depends, at least in part, on ATM (23). Supplementary Figure S3F shows that DNA-PKi suppressed CPT-induced MDC1 and 53BP1 foci in quiescent WI38 hTERT cells. To test more directly the role of DNA-PK on ATM, we analyzed the impact of DNA-PK inhibition on the induction of ATM-pS1981 and on its accumulation in nuclear foci. We found that DNA-PKi only slightly reduced CPT-induced ATM-pS1981 levels (Figure 5E), indicating that DNA-PK does not markedly contribute to ATM activation. Microscopy analysis confirmed that DNA-PKi did not suppress ATM-pS1981 following CPT treatment (Figure 5F, top panels). However, it revealed a pan staining for ATM-pS1981 rather than well-defined foci (Figure 5F, top panels), suggesting that activated ATM is not localized at damaged sites. Previous work showed that ATM associated with sites of DSBs was resistant to detergent extraction while unbound ATM was removed (62). Thus, we treated cells with a detergent-based extraction buffer known as cytosqueleton (CSK) buffer (63) before immunofluorescence staining for ATM-pS1981. We found that CSK buffer suppressed the pan-

staining signal for ATM-pS1981 in cells co-treated with DNA-PKi and CPT under conditions where it did not affect ATM-pS1981 foci in cells treated with CPT alone (Figure 5F bottom panels and G). Together, these data suggest that DNA-PK promotes the assembly of activated ATM into nuclear foci in CPT-treated quiescent cells.

To assess whether the role of DNA-PK on ATM foci formation is related to its function in DSB repair, we inhibited XLF and XRCC4, which mediate DNA-PK-dependent NHEJ (33). We found that contrary to DNA-PK inhibition, depletion of XLF or XRCC4 with siRNAs did not prevent CPT-induced ATM-pS1981 foci in quiescent WI38 hTERT cells (Supplementary Figure S4). These results suggest that the role of DNA-PK on ATM foci formation is independent of its function in DSB repair.

DNA-PK promotes ubiquitination of H2AX and H2A at DSB sites

H2AX and H2A are ubiquitinated in response to DSBs (27-32). Previous work showed that defective monoubiquitination of H2AX at K119/K120 in IR-exposed cells impaired the recruitment of ATM-pS1981 to DSBs and thereby reduced γH2AX and MDC1 foci formation (25,26), effects similar to those observed following DNA-PK inhibition in CPT-treated quiescent cells (Figure 5 and Supplementary Figure S3F). We therefore tested whether DNA-PK inhibition would prevent CPT-induced H2AX monoubiquitination in quiescent cells.

Western blot analysis using an antibody against H2AX showed that CPT did not significantly increase global H2AX monoubiquitination in quiescent WI38 hTERT cells (Supplementary Figure S5A). We though it might be because H2AX is monoubiquitinated only at damaged sites in response to DSBs (26), and CPT induced only few γH2AX foci in quiescent cells (Figure 1). Consistent with this hypothesis, detection of H2AX monoubiquitination by Western blot was previously reported at high doses of IR, typically 4 to 10 Gy (26,64). To examine specifically H2AX monoubiquitination at DSB sites, we analyzed γH2AX monoubiquitination. We found that CPT induced γH2AX monoubiquitination in quiescent WI38 hTERT cells, which was prevented by DNA-PKi (Figure 6A). To analyze more directly histone monoubiquitination at DSB sites, we performed immunofluorescence microscopy with an antibody against H2A monoubiquitinated at K119 (Ub-H2A). We found that CPT induced Ub-H2A foci that colocalized with the p53BP1 foci, and that those Ub-H2A foci were completely prevented by DNA-PKi (Figure 6B and C). Consistent with these results, CPT also induced DNA-PK-dependent FK2 foci (Figure 6D and E), which mark ubiquitinated proteins at DNA damage sites (65). siRNA-mediated depletion of DNA-PK confirmed the suppressive effect of DNA-PKi on FK2 foci formation (Supplementary Figure S5B and C). Altogether, these results indicate that DNA-PK promotes monoubiquitination of H2AX and H2A at site of co-transcriptional DSBs in CPT-treated quiescent cells. This in turn may favor the recruitment of activated ATM and phosphorylation of its downstream substrates.

DNA-PK promotes ubiquitin/proteasome-dependent Top1cc removal

Based on our results that DNA-PK promotes ubiquitination processes (Figure 6) and the fact that transcription-blocking Top1cc are removed following ubiquitination and proteosomal degradation of Top1 (Supplementary Figure S2A-C) (12,13,48), we examined the possibility that DNA-PK could

promote Top1 degradation. Figure 7A shows that DNA-PKi markedly decreased CPT-induced Top1 degradation in quiescent WI38 hTERT cells. Similar results were obtained in quiescent IMR90 and NHDF cells (Supplementary Figure S5D). Analysis of endogenous Top1cc confirmed that defective Top1 degradation following DNA-PK inhibition reflected defective Top1cc removal (Figure 7B). The role of DNA-PK in promoting Top1 degradation is unlikely related to its function in NHEJ repair as depletion of XRCC4 or XPF with siRNAs did not affect CPT-induced Top1 degradation in quiescent WI38 hTERT cells (Supplementary Figure S5E). Because we found that ATM activates DNA-PK (Figure 5), we examined whether ATM inhibition would also prevent Top1 degradation. Supplementary Figure S5F shows that ATMi also decreased CPT-induced Top1 degradation in quiescent WI38 hTERT cells.

Consistent with the ubiquitin/proteasome-dependent removal of Top1cc, we found that the E1 ubiquitin ligase UBA1 and the 20S-proteasome subunit PSMA6, which are both involved in DDR (66,67), tended to accumulate in chromatin-bound fraction (P2 fraction, see Supplementary Figure S5G) in CPT-treated quiescent WI38 hTERT cells (Figure 7C). Under these conditions, the global expression of PSMA6 remained unchanged while that of UBA1 slightly increased (Figure 7D). Accumulation of UBA1 and PSMA6 in P2 fraction was further associated with an increased activity of proteasome (Figure 7E). DNA-PKi suppressed the CPT-induced UBA1 and PSMA6 accumulation and proteasome activity in P2 fraction (Figure 7C-E). As a control, we showed that DNA-PKi is not a direct proteasome inhibitor (Supplementary Figure S5H). Altogether, these results suggest that DNA-PK promotes ubiquitin/proteasome-dependent removal of Top1cc in CPT-treated quiescent cells.

Transcription- and proteasome-dependent apoptosis of quiescent cells by stabilized Top1cc

To assess whether transcription-dependent DSBs can kill non-replicative cells, we analyzed the percentage of quiescent cells that remained attached to the culture flask following CPT treatment. Typically, cells detach as they undergo apoptosis. We found that CPT decreased the number of quiescent WI38 hTERT cells attached to the culture flask by approximately 70 % after 24 h (Figure 8A). This was associated with the appearance of biochemical markers of apoptosis such as the cleavage of caspase-3 and PARP, and the massive induction of γH2AX, which was reported in cells undergoing apoptosis (68) (Figure 8B). All these apoptotic marks were suppressed by the transcription inhibitor FLV (Figure 8A and B), suggesting that transcription-dependent DSBs are the initiating events for apoptosis induction. Consistent with this hypothesis, inhibition of CPT-induced DSBs with lactacystin (Figure 2A and B) also prevented caspase-3 and PARP cleavage and γH2AX induction (Figure 8C). By contrast, increased CPT-induced DSBs with veliparib or olaparib (Figure 4C-F and Supplementary Figure S2H and I) also increased PARP cleavage (Figure 8D).

To analyze the impact of DDR signaling on CPT-induced apoptosis of quiescent cells, we inhibited ATM and DNA-PK. Figure 8E and F shows that ATMi and DNA-PKi, both increased CPT-induced caspase-3 and PARP cleavage, indicating that the predominant role of ATM- and DNA-PK-dependent signaling is likely to promote cell survival after CPT-induced transcription-dependent DSBs.

DISCUSSION

Although defective repair of DSBs can lead to neurodegenerative diseases, the molecular processes of their production and signaling in non-replicating cells are largely unknown. Here we analyzed the transcription-dependent DSBs that form in non-replicating cells as a consequence of Top1cc stabilization (17). Our data support a model depicted in Figure 9 in which Top1cc stabilization blocks transcription elongation, which triggers partial Top1 proteolysis and the generation of a Top1 peptide-linked SSB, which is a substrate for TDP1. Defective repair of this SSB intermediate by TDP1 can give rise to a DSB, which leads to ATM activation and phosphorylation of its substrates such as H2AX and 53BP1. ATM also activates DNA-PK, which promotes H2AX and H2A monoubiquitination and the assembly of activated ATM into nuclear foci. ATM and DNA-PK also increase Top1 proteolysis suggesting that this pathway further enhances Top1cc repair after DSB induction. This is consistent with recent work showing that ATM deficiency increases Top1cc levels in CPT-treated quiescent astrocytes (69,70). Because we found that Top1 proteolysis primes DSB formation, DNA-PK could therefore increases DSB production in a feedback loop. This might be however compensated as DNA-PK can also phosphorylate TDP1, which increases its repair activity towards Top1cc (71). Nevertheless, we did not find that DNA-PK inhibition reduced the amount of DSBs in CPT-treated quiescent cells measured by a neutral Comet assay. DSBs event tend to accumulate, which might be related to the function of DNA-PK that we report here in promoting ATM signaling but also on its function in NHEJ repair (33).

Transcription-blocking Top1cc seem primarily repaired by the TDP1 excision pathway. Indeed, our study and previous reports indicate that Top1 degradation is transcription dependent following CPT exposure (12,13,48) and that TDP1 primarily repairs transcription-blocking Top1cc as compared to replication-blocking Top1cc (8,9). Consistent with the involvement of the TDP1 pathway in the repair of transcription-blocking Top1cc, Top1 degradation has been suggested to promote resumption of RNA synthesis (12). Our findings that DSBs produced in CPT-treated quiescent cells depend both on transcription and on Top1 degradation suggest that they arise during the repair of Top1cc. A further support to this is that inhibition of TDP1 or PARP1 (which is required for TDP1 activity (10,55)), increases transcription-dependent DSBs following Top1cc stabilization. Because TDP1 deficient cells accumulate Top1 peptide-linked SSB intermediates (9,53,54), our results suggest that transcription-dependent DSBs arise from these intermediates if TDP1 fails to repair them. How a Top1 peptide-linked SSB can give rise to a DSB is still an unresolved question. A DSB may result from two nearby SSBs on opposing DNA strands. It is also possible that the second SSB is caused by R-loop processing. Indeed, reduced Top1 activity causes R-loop formation (72) and we showed that CPT-induced R-loops are involved in the formation of transcription-dependent DSBs in post-mitotic cells (17). Also, a recent work showed that R-loops formed in response to CPT are cleaved by the endonuclease XPG (21).

It is now well documented that DNA-PK functions in cellular processes other than NHEJ such as gene regulation (73,74) and mitosis (75-77). Here we report a novel function of DNA-PK in the regulation of protein ubiquitination. Previous work suggested connection between DNA-PK and the proteasome. In the presence of DSBs, DNA-PK was reported to induce transcription arrest by a mechanism that depends on proteasome activity (78). Also, DNA-PK inhibition prevents the

accumulation of the proteasome activator PA200 on chromatin in response to IR (79). Phosphorylation is known to regulate protein ubiquitination in two main ways (80). First, substrate phosphorylation can create a recognition signal for binding of an E3 ligase. Second, phosphorylation of an E3 ligase can stimulate its ubiquitin transfer activity. Hence, it is possible that DNA-PK phosphorylates H2AX, H2A and Top1 and/or their respective E3 ligases following CPT treatment. The first possibility is plausible as the N-terminal domain of Top1 binds to DNA-PK (81) and possesses a potential phosphorylation site for DNA-PK (SQ motif on S10). DNA-PK can also phosphorylate H2AX on S139 (γH2AX) (34) but it is unlikely that this is what primes H2AX for ubiquitination because H2A lacks S139 but is also ubiquitinated in response to DSBs. Several E3 ubiquitin ligases have been reported for H2AX and H2A (RNF2, RNF8, RNF168) (25-31) and for Top1 (Cullin3, Cullin4A, Cullin4B, BRCA1) (13,49,50) but it is not known whether they can be phosphorylated by DNA-PK. It is also possible that DNA-PK favors the recruitment of the E1 ligase UBA1 at damaged sites as we found that DNA-PK inhibition prevented CPT-induced UBA1 accumulation on chromatin.

Lastly, our analysis demonstrates that co-transcriptional DSBs can kill non-replicating cells following CPT treatment. Co-transcriptional DSBs might occur spontaneously in cells as Top1cc are stabilized by common alterations of DNA (2-4) and therefore they may have a marked impact on non-replicating cell fate. Neurodegenerative diseases can arise from defective repair of Top1cc (SCAN1 caused by TDP1 deficiency) (16) as well as from defective response to DSBs (AT caused by ATM deficiency) (24). Neurons might be particularly prone to produce co-transcriptional DSBs as a result of high rates of oxygen consumption, which produces reactive oxygen species that can stabilize Top1cc (1,3,82). Hence, our findings raise the possibility that accumulation of co-transcriptional DSBs and the defective response to those breaks might contribute to the neurodegenerative phenotype of SCAN1 and AT patients, respectively.

ACKNOWLEDGEMENT

We thank P. Calsou for XRCC4 antibody and for helpful discussions, Y. Pommier for discussions and advices; E. Nicolas for WI38 hTERT and IMR90 cells and for reading the manuscript, K. Mamouni, N. Bery and A. Olichon for experimental advices and discussions; J. Cherier for NHDF cells; S. Monferran for cell irradiation; and L. Ligat, A. Canivet and S. Allart for assistance at the Microscopy and Cell Imaging Platform. We also thanks for S. Cabantous for reading the manuscript.

SUPPLEMENTARY DATA

Supplementary Data are available at NAR Online

FUNDING

This work was supported by the Association pour la Recherche Contre le Cancer; the Institut National de la Santé et de la Recherche Médicale; the Ministère de l'Enseignement Supérieur et de la Recherche [doctoral fellowship to A.C.]; and the Fondation pour la Recherche Médicale [FDT20140931166; doctoral fellowship to A.C.]. Funding for open access charge: Institut National de la Santé et de la Recherche Médicale.

Conflict of interest statement. None declared

REFERENCES

1. Pommier, Y. (2006) Topoisomerase I inhibitors: camptothecins and beyond. *Nat Rev Cancer*, **6**, 789-802.
2. Sparks, J.L. and Burgers, P.M. (2015) Error-free and mutagenic processing of topoisomerase 1-provoked damage at genomic ribonucleotides. *The EMBO journal*.
3. Pourquier, P. and Pommier, Y. (2001) Topoisomerase I-mediated DNA damage. *Adv Cancer Res*, **80**, 189-216.
4. Kim, N., Huang, S.Y., Williams, J.S., Li, Y.C., Clark, A.B., Cho, J.E., Kunkel, T.A., Pommier, Y. and Jinks-Robertson, S. (2011) Mutagenic processing of ribonucleotides in DNA by yeast topoisomerase I. *Science (New York, N.Y*, **332**, 1561-1564.
5. Capranico, G., Ferri, F., Fogli, M.V., Russo, A., Lotito, L. and Baranello, L. (2007) The effects of camptothecin on RNA polymerase II transcription: roles of DNA topoisomerase I. *Biochimie*, **89**, 482-489.
6. Ljungman, M. and Lane, D.P. (2004) Transcription - guarding the genome by sensing DNA damage. *Nat Rev Cancer*, **4**, 727-737.
7. Pouliot, J.J., Yao, K.C., Robertson, C.A. and Nash, H.A. (1999) Yeast gene for a Tyr-DNA phosphodiesterase that repairs topoisomerase I complexes. *Science (New York, N.Y*, **286**, 552-555.
8. El-Khamisy, S.F., Saifi, G.M., Weinfeld, M., Johansson, F., Helleday, T., Lupski, J.R. and Caldecott, K.W. (2005) Defective DNA single-strand break repair in spinocerebellar ataxia with axonal neuropathy-1. *Nature*, **434**, 108-113.
9. Miao, Z.H., Agama, K., Sordet, O., Povirk, L., Kohn, K.W. and Pommier, Y. (2006) Hereditary ataxia SCAN1 cells are defective for the repair of transcription-dependent topoisomerase I cleavage complexes. *DNA repair*.
10. Pommier, Y., Barcelo, J.M., Rao, V.A., Sordet, O., Jobson, A.G., Thibaut, L., Miao, Z.H., Seiler, J.A., Zhang, H., Marchand, C. *et al.* (2006) Repair of topoisomerase I-mediated DNA damage. *Prog Nucleic Acid Res Mol Biol*, **81**, 179-229.
11. Pommier, Y., Huang, S.Y., Gao, R., Das, B.B., Murai, J. and Marchand, C. (2014) Tyrosyl-DNA-phosphodiesterases (TDP1 and TDP2). *DNA repair*, **19**, 114-129.
12. Desai, S.D., Zhang, H., Rodriguez-Bauman, A., Yang, J.M., Wu, X., Gounder, M.K., Rubin, E.H. and Liu, L.F. (2003) Transcription-dependent degradation of topoisomerase I-DNA covalent complexes. *Mol Cell Biol*, **23**, 2341-2350.
13. Sordet, O., Larochelle, S., Nicolas, E., Stevens, E.V., Zhang, C., Shokat, K.M., Fisher, R.P. and Pommier, Y. (2008) Hyperphosphorylation of RNA polymerase II in response to topoisomerase I cleavage complexes and its association with transcription- and BRCA1-dependent degradation of topoisomerase I. *J Mol Biol*, **381**, 540-549.
14. Ashour, M.E., Atteya, R. and El-Khamisy, S.F. (2015) Topoisomerase-mediated chromosomal break repair: an emerging player in many games. *Nat Rev Cancer*, **15**, 137-151.
15. Rass, U., Ahel, I. and West, S.C. (2007) Defective DNA repair and neurodegenerative disease. *Cell*, **130**, 991-1004.
16. Takashima, H., Boerkoel, C.F., John, J., Saifi, G.M., Salih, M.A., Armstrong, D., Mao, Y., Quiocho, F.A., Roa, B.B., Nakagawa, M. *et al.* (2002) Mutation of TDP1, encoding a topoisomerase I-dependent DNA damage repair enzyme, in spinocerebellar ataxia with axonal neuropathy. *Nature genetics*, **32**, 267-272.
17. Sordet, O., Redon, C.E., Guirouilh-Barbat, J., Smith, S., Solier, S., Douarre, C., Conti, C., Nakamura, A.J., Das, B.B., Nicolas, E. *et al.* (2009) Ataxia telangiectasia mutated activation by transcription- and topoisomerase I-induced DNA double-strand breaks. *EMBO Rep*, **10**, 887-893.

18. Sordet, O., Nakamura, A.J., Redon, C.E. and Pommier, Y. (2010) DNA double-strand breaks and ATM activation by transcription-blocking DNA lesions. *Cell cycle (Georgetown, Tex*, **9**, 274-278.
19. Zhang, Y.W., Regairaz, M., Seiler, J.A., Agama, K.K., Doroshow, J.H. and Pommier, Y. (2011) Poly(ADP-ribose) polymerase and XPF-ERCC1 participate in distinct pathways for the repair of topoisomerase I-induced DNA damage in mammalian cells. *Nucleic Acids Res*, **39**, 3607-3620.
20. Aguilera, A. and Garcia-Muse, T. (2012) R loops: from transcription byproducts to threats to genome stability. *Molecular cell*, **46**, 115-124.
21. Sollier, J., Stork, C.T., Garcia-Rubio, M.L., Paulsen, R.D., Aguilera, A. and Cimprich, K.A. (2014) Transcription-coupled nucleotide excision repair factors promote R-loop-induced genome instability. *Molecular cell*, **56**, 777-785.
22. Lukas, J., Lukas, C. and Bartek, J. (2011) More than just a focus: The chromatin response to DNA damage and its role in genome integrity maintenance. *Nat Cell Biol*, **13**, 1161-1169.
23. Shiloh, Y. and Ziv, Y. (2013) The ATM protein kinase: regulating the cellular response to genotoxic stress, and more. *Nature reviews*, **14**, 197-210.
24. Savitsky, K., Bar-Shira, A., Gilad, S., Rotman, G., Ziv, Y., Vanagaite, L., Tagle, D.A., Smith, S., Uziel, T., Sfez, S. *et al.* (1995) A single ataxia telangiectasia gene with a product similar to PI-3 kinase. *Science (New York, N.Y*, **268**, 1749-1753.
25. Facchino, S., Abdouh, M., Chatoo, W. and Bernier, G. (2010) BMI1 confers radioresistance to normal and cancerous neural stem cells through recruitment of the DNA damage response machinery. *J Neurosci*, **30**, 10096-10111.
26. Pan, M.R., Peng, G., Hung, W.C. and Lin, S.Y. (2011) Monoubiquitination of H2AX protein regulates DNA damage response signaling. *J Biol Chem*, **286**, 28599-28607.
27. Doil, C., Mailand, N., Bekker-Jensen, S., Menard, P., Larsen, D.H., Pepperkok, R., Ellenberg, J., Panier, S., Durocher, D., Bartek, J. *et al.* (2009) RNF168 binds and amplifies ubiquitin conjugates on damaged chromosomes to allow accumulation of repair proteins. *Cell*, **136**, 435-446.
28. Stewart, G.S., Panier, S., Townsend, K., Al-Hakim, A.K., Kolas, N.K., Miller, E.S., Nakada, S., Ylanko, J., Olivarius, S., Mendez, M. *et al.* (2009) The RIDDLE syndrome protein mediates a ubiquitin-dependent signaling cascade at sites of DNA damage. *Cell*, **136**, 420-434.
29. Huen, M.S., Grant, R., Manke, I., Minn, K., Yu, X., Yaffe, M.B. and Chen, J. (2007) RNF8 transduces the DNA-damage signal via histone ubiquitylation and checkpoint protein assembly. *Cell*, **131**, 901-914.
30. Kolas, N.K., Chapman, J.R., Nakada, S., Ylanko, J., Chahwan, R., Sweeney, F.D., Panier, S., Mendez, M., Wildenhain, J., Thomson, T.M. *et al.* (2007) Orchestration of the DNA-damage response by the RNF8 ubiquitin ligase. *Science (New York, N.Y*, **318**, 1637-1640.
31. Mailand, N., Bekker-Jensen, S., Faustrup, H., Melander, F., Bartek, J., Lukas, C. and Lukas, J. (2007) RNF8 ubiquitylates histones at DNA double-strand breaks and promotes assembly of repair proteins. *Cell*, **131**, 887-900.
32. Mattiroli, F., Vissers, J.H., van Dijk, W.J., Ikpa, P., Citterio, E., Vermeulen, W., Marteijn, J.A. and Sixma, T.K. (2012) RNF168 ubiquitinates K13-15 on H2A/H2AX to drive DNA damage signaling. *Cell*, **150**, 1182-1195.
33. Davis, A.J., Chen, B.P. and Chen, D.J. (2014) DNA-PK: a dynamic enzyme in a versatile DSB repair pathway. *DNA repair*, **17**, 21-29.
34. Stiff, T., O'Driscoll, M., Rief, N., Iwabuchi, K., Lobrich, M. and Jeggo, P.A. (2004) ATM and DNA-PK function redundantly to phosphorylate H2AX after exposure to ionizing radiation. *Cancer research*, **64**, 2390-2396.
35. Yang, Y., Kitagaki, J., Dai, R.M., Tsai, Y.C., Lorick, K.L., Ludwig, R.L., Pierre, S.A., Jensen, J.P., Davydov, I.V., Oberoi, P. *et al.* (2007) Inhibitors of ubiquitin-activating enzyme (E1), a new class of potential cancer therapeutics. *Cancer research*, **67**, 9472-9481.
36. Aleo, E., Henderson, C.J., Fontanini, A., Solazzo, B. and Brancolini, C. (2006) Identification of new compounds that trigger apoptosome-independent caspase activation and apoptosis. *Cancer research*, **66**, 9235-9244.

37. Hickson, I., Zhao, Y., Richardson, C.J., Green, S.J., Martin, N.M., Orr, A.I., Reaper, P.M., Jackson, S.P., Curtin, N.J. and Smith, G.C. (2004) Identification and characterization of a novel and specific inhibitor of the ataxia-telangiectasia mutated kinase ATM. *Cancer research*, **64**, 9152-9159.
38. Reaper, P.M., Griffiths, M.R., Long, J.M., Charrier, J.D., Maccormick, S., Charlton, P.A., Golec, J.M. and Pollard, J.R. (2011) Selective killing of ATM- or p53-deficient cancer cells through inhibition of ATR. *Nat Chem Biol*, **7**, 428-430.
39. Leahy, J.J., Golding, B.T., Griffin, R.J., Hardcastle, I.R., Richardson, C., Rigoreau, L. and Smith, G.C. (2004) Identification of a highly potent and selective DNA-dependent protein kinase (DNA-PK) inhibitor (NU7441) by screening of chromenone libraries. *Bioorg Med Chem Lett*, **14**, 6083-6087.
40. Jeanblanc, M., Ragu, S., Gey, C., Contrepois, K., Courbeyrette, R., Thuret, J.Y. and Mann, C. (2012) Parallel pathways in RAF-induced senescence and conditions for its reversion. *Oncogene*, **31**, 3072-3085.
41. Aasen, T. and Izpisua Belmonte, J.C. (2010) Isolation and cultivation of human keratinocytes from skin or plucked hair for the generation of induced pluripotent stem cells. *Nat Protoc*, **5**, 371-382.
42. Drouet, J., Delteil, C., Lefrancois, J., Concannon, P., Salles, B. and Calsou, P. (2005) DNA-dependent protein kinase and XRCC4-DNA ligase IV mobilization in the cell in response to DNA double strand breaks. *J Biol Chem*, **280**, 7060-7069.
43. Regairaz, M., Zhang, Y.W., Fu, H., Agama, K.K., Tata, N., Agrawal, S., Aladjem, M.I. and Pommier, Y. (2011) Mus81-mediated DNA cleavage resolves replication forks stalled by topoisomerase I-DNA complexes. *J Cell Biol*, **195**, 739-749.
44. Lobrich, M., Shibata, A., Beucher, A., Fisher, A., Ensminger, M., Goodarzi, A.A., Barton, O. and Jeggo, P.A. (2010) gammaH2AX foci analysis for monitoring DNA double-strand break repair: strengths, limitations and optimization. *Cell cycle (Georgetown, Tex*, **9**, 662-669.
45. Dimri, G.P., Hara, E. and Campisi, J. (1994) Regulation of two E2F-related genes in presenescent and senescent human fibroblasts. *J Biol Chem*, **269**, 16180-16186.
46. Coller, H.A., Sang, L. and Roberts, J.M. (2006) A new description of cellular quiescence. *PLoS Biol*, **4**, e83.
47. Bonner, W.M., Redon, C.E., Dickey, J.S., Nakamura, A.J., Sedelnikova, O.A., Solier, S. and Pommier, Y. (2008) gammaH2AX and cancer. *Nat Rev Cancer*, **8**, 957-967.
48. Desai, S.D., Li, T.K., Rodriguez-Bauman, A., Rubin, E.H. and Liu, L.F. (2001) Ubiquitin/26S proteasome-mediated degradation of topoisomerase I as a resistance mechanism to camptothecin in tumor cells. *Cancer research*, **61**, 5926-5932.
49. Zhang, H.F., Tomida, A., Koshimizu, R., Ogiso, Y., Lei, S. and Tsuruo, T. (2004) Cullin 3 promotes proteasomal degradation of the topoisomerase I-DNA covalent complex. *Cancer research*, **64**, 1114-1121.
50. Kerzendorfer, C., Whibley, A., Carpenter, G., Outwin, E., Chiang, S.C., Turner, G., Schwartz, C., El-Khamisy, S., Raymond, F.L. and O'Driscoll, M. (2010) Mutations in Cullin 4B result in a human syndrome associated with increased camptothecin-induced topoisomerase I-dependent DNA breaks. *Hum Mol Genet*, **19**, 1324-1334.
51. Iacovoni, J.S., Caron, P., Lassadi, I., Nicolas, E., Massip, L., Trouche, D. and Legube, G. (2010) High-resolution profiling of gammaH2AX around DNA double strand breaks in the mammalian genome. *The EMBO journal*, **29**, 1446-1457.
52. Dantuma, N.P., Groothuis, T.A., Salomons, F.A. and Neefjes, J. (2006) A dynamic ubiquitin equilibrium couples proteasomal activity to chromatin remodeling. *J Cell Biol*, **173**, 19-26.
53. Katyal, S., el-Khamisy, S.F., Russell, H.R., Li, Y., Ju, L., Caldecott, K.W. and McKinnon, P.J. (2007) TDP1 facilitates chromosomal single-strand break repair in neurons and is neuroprotective in vivo. *The EMBO journal*, **26**, 4720-4731.

54. Interthal, H., Chen, H.J., Kehl-Fie, T.E., Zotzmann, J., Leppard, J.B. and Champoux, J.J. (2005) SCAN1 mutant Tdp1 accumulates the enzyme--DNA intermediate and causes camptothecin hypersensitivity. *The EMBO journal*, **24**, 2224-2233.
55. Das, B.B., Huang, S.Y., Murai, J., Rehman, I., Ame, J.C., Sengupta, S., Das, S.K., Majumdar, P., Zhang, H., Biard, D. *et al.* (2014) PARP1-TDP1 coupling for the repair of topoisomerase I-induced DNA damage. *Nucleic Acids Res*, **42**, 4435-4449.
56. Zeman, M.K. and Cimprich, K.A. (2014) Causes and consequences of replication stress. *Nat Cell Biol*, **16**, 2-9.
57. Jones, G.G., Reaper, P.M., Pettitt, A.R. and Sherrington, P.D. (2004) The ATR-p53 pathway is suppressed in noncycling normal and malignant lymphocytes. *Oncogene*, **23**, 1911-1921.
58. Bakkenist, C.J. and Kastan, M.B. (2003) DNA damage activates ATM through intermolecular autophosphorylation and dimer dissociation. *Nature*, **421**, 499-506.
59. Chan, D.W., Chen, B.P., Prithivirajsingh, S., Kurimasa, A., Story, M.D., Qin, J. and Chen, D.J. (2002) Autophosphorylation of the DNA-dependent protein kinase catalytic subunit is required for rejoining of DNA double-strand breaks. *Genes Dev*, **16**, 2333-2338.
60. Chen, B.P., Chan, D.W., Kobayashi, J., Burma, S., Asaithamby, A., Morotomi-Yano, K., Botvinick, E., Qin, J. and Chen, D.J. (2005) Cell cycle dependence of DNA-dependent protein kinase phosphorylation in response to DNA double strand breaks. *J Biol Chem*, **280**, 14709-14715.
61. Chen, B.P., Uematsu, N., Kobayashi, J., Lerenthal, Y., Krempler, A., Yajima, H., Lobrich, M., Shiloh, Y. and Chen, D.J. (2007) Ataxia telangiectasia mutated (ATM) is essential for DNA-PKcs phosphorylations at the Thr-2609 cluster upon DNA double strand break. *J Biol Chem*, **282**, 6582-6587.
62. Andegeko, Y., Moyal, L., Mittelman, L., Tsarfaty, I., Shiloh, Y. and Rotman, G. (2001) Nuclear retention of ATM at sites of DNA double strand breaks. *J Biol Chem*, **276**, 38224-38230.
63. Rodriguez, R., Miller, K.M., Forment, J.V., Bradshaw, C.R., Nikan, M., Britton, S., Oelschlaegel, T., Xhemalce, B., Balasubramanian, S. and Jackson, S.P. (2012) Small-molecule-induced DNA damage identifies alternative DNA structures in human genes. *Nat Chem Biol*, **8**, 301-310.
64. Mosammaparast, N., Kim, H., Laurent, B., Zhao, Y., Lim, H.J., Majid, M.C., Dango, S., Luo, Y., Hempel, K., Sowa, M.E. *et al.* (2013) The histone demethylase LSD1/KDM1A promotes the DNA damage response. *J Cell Biol*, **203**, 457-470.
65. Morris, J.R. and Solomon, E. (2004) BRCA1 : BARD1 induces the formation of conjugated ubiquitin structures, dependent on K6 of ubiquitin, in cells during DNA replication and repair. *Hum Mol Genet*, **13**, 807-817.
66. Moudry, P., Lukas, C., Macurek, L., Hanzlikova, H., Hodny, Z., Lukas, J. and Bartek, J. (2012) Ubiquitin-activating enzyme UBA1 is required for cellular response to DNA damage. *Cell cycle (Georgetown, Tex*, **11**, 1573-1582.
67. Levy-Barda, A., Lerenthal, Y., Davis, A.J., Chung, Y.M., Essers, J., Shao, Z., van Vliet, N., Chen, D.J., Hu, M.C., Kanaar, R. *et al.* (2011) Involvement of the nuclear proteasome activator PA28gamma in the cellular response to DNA double-strand breaks. *Cell cycle (Georgetown, Tex*, **10**, 4300-4310.
68. Solier, S., Sordet, O., Kohn, K.W. and Pommier, Y. (2009) Death receptor-induced activation of the Chk2- and histone H2AX-associated DNA damage response pathways. *Mol Cell Biol*, **29**, 68-82.
69. Alagoz, M., Chiang, S.C., Sharma, A. and El-Khamisy, S.F. (2013) ATM deficiency results in accumulation of DNA-topoisomerase I covalent intermediates in neural cells. *PLoS One*, **8**, e58239.
70. Katyal, S., Lee, Y., Nitiss, K.C., Downing, S.M., Li, Y., Shimada, M., Zhao, J., Russell, H.R., Petrini, J.H., Nitiss, J.L. *et al.* (2014) Aberrant topoisomerase-1 DNA lesions are pathogenic in neurodegenerative genome instability syndromes. *Nat Neurosci*, **17**, 813-821.

71. Das, B.B., Antony, S., Gupta, S., Dexheimer, T.S., Redon, C.E., Garfield, S., Shiloh, Y. and Pommier, Y. (2009) Optimal function of the DNA repair enzyme TDP1 requires its phosphorylation by ATM and/or DNA-PK. *The EMBO journal*, **28**, 3667-3680.
72. Tuduri, S., Crabbe, L., Conti, C., Tourriere, H., Holtgreve-Grez, H., Jauch, A., Pantesco, V., De Vos, J., Thomas, A., Theillet, C. *et al.* (2009) Topoisomerase I suppresses genomic instability by preventing interference between replication and transcription. *Nat Cell Biol*, **11**, 1315-1324.
73. Ju, B.G., Lunyak, V.V., Perissi, V., Garcia-Bassets, I., Rose, D.W., Glass, C.K. and Rosenfeld, M.G. (2006) A topoisomerase IIbeta-mediated dsDNA break required for regulated transcription. *Science (New York, N.Y*, **312**, 1798-1802.
74. Wong, R.H., Chang, I., Hudak, C.S., Hyun, S., Kwan, H.Y. and Sul, H.S. (2009) A role of DNA-PK for the metabolic gene regulation in response to insulin. *Cell*, **136**, 1056-1072.
75. Lee, K.J., Lin, Y.F., Chou, H.Y., Yajima, H., Fattah, K.R., Lee, S.C. and Chen, B.P. (2011) Involvement of DNA-dependent protein kinase in normal cell cycle progression through mitosis. *J Biol Chem*, **286**, 12796-12802.
76. Shang, Z.F., Huang, B., Xu, Q.Z., Zhang, S.M., Fan, R., Liu, X.D., Wang, Y. and Zhou, P.K. (2010) Inactivation of DNA-dependent protein kinase leads to spindle disruption and mitotic catastrophe with attenuated checkpoint protein 2 Phosphorylation in response to DNA damage. *Cancer research*, **70**, 3657-3666.
77. Wang, C.Y., Kao, Y.H., Lai, P.Y., Chen, W.Y. and Chung, B.C. (2013) Steroidogenic factor 1 (NR5A1) maintains centrosome homeostasis in steroidogenic cells by restricting centrosomal DNA-dependent protein kinase activation. *Mol Cell Biol*, **33**, 476-484.
78. Pankotai, T., Bonhomme, C., Chen, D. and Soutoglou, E. (2012) DNAPKcs-dependent arrest of RNA polymerase II transcription in the presence of DNA breaks. *Nat Struct Mol Biol*.
79. Blickwedehl, J., Agarwal, M., Seong, C., Pandita, R.K., Melendy, T., Sung, P., Pandita, T.K. and Bangia, N. (2008) Role for proteasome activator PA200 and postglutamyl proteasome activity in genomic stability. *Proceedings of the National Academy of Sciences of the United States of America*, **105**, 16165-16170.
80. Hunter, T. (2007) The age of crosstalk: phosphorylation, ubiquitination, and beyond. *Molecular cell*, **28**, 730-738.
81. Czubaty, A., Girstun, A., Kowalska-Loth, B., Trzcinska, A.M., Purta, E., Winczura, A., Grajkowski, W. and Staron, K. (2005) Proteomic analysis of complexes formed by human topoisomerase I. *Biochim Biophys Acta*, **1749**, 133-141.
82. Daroui, P., Desai, S.D., Li, T.K., Liu, A.A. and Liu, L.F. (2004) Hydrogen peroxide induces topoisomerase I-mediated DNA damage and cell death. *J Biol Chem*, **279**, 14587-14594.
83. Fang, J., Chen, T., Chadwick, B., Li, E. and Zhang, Y. (2004) Ring1b-mediated H2A ubiquitination associates with inactive X chromosomes and is involved in initiation of X inactivation. *J Biol Chem*, **279**, 52812-52815.

FIGURE LEGENDS

Figure 1. Induction of transcription-dependent DSBs in quiescent WI38 hTERT cells in response to CPT. **(A,B)** Cells were cultured in 10% serum or in 0.2% serum for 3 days to induce quiescence. Cells were then exposed to 100 µM BrdU for 30 min before staining for BrdU (green). DNA was counterstained with DAPI (blue). **(A)** Representative images. Bars: 50 µm. **(B)** Percentages of BrdU-positive cells from one representative experiment (> 300 cells were analyzed for each treatment) out of two. **(C-E)** Serum-starved cells were treated with the indicated CPT concentrations for 1 h before staining for γH2AX (green). DNA was counterstained with DAPI (blue). **(C)** Representative images. Numbers are the percentage of nuclei with at least 2 γH2AX foci (bottom) and the average foci per nucleus (top). Bars: 10 µm. **(D)** Number of γH2AX foci per nucleus. ****, $P < 0.0001$. **(E)** Quantification

of γH2AX fluorescence intensity per nucleus. Quantifications in panels C to E are from two independent experiments (209-246 nuclei were analyzed for each treatment). **(F,G)** Serum-starved cells were treated with FLV (1 µM) for 1 h before the addition of CPT (25 µM) for 1 h and then co-stained for γH2AX (green) and 53BP1 (red). **(F)** Representative pictures. Images were merged to determine colocalization (yellow). Nuclear contours, identified by DAPI staining (not shown), are indicated by dashed lines. Bars: 10 µm. **(G)** Number of γH2AX foci per nucleus from one representative experiment (99-133 nuclei were analyzed for each treatment) out of four. ****, $P < 0.0001$. **(H,I)** Detection of DSBs by neutral Comet assays in serum-starved cells treated with FLV (1 µM) for 1 h before the addition of CPT (7.5 µM) for 1 h. **(H)** Representative pictures of nuclei. **(I)** Quantification of neutral Comet tail moments from one representative experiment (101-106 nuclei were analyzed for each treatment) out of three. ****, $P < 0.0001$.

Figure 2. Induction of ubiquitin/proteasome-dependent DSBs in CPT-treated quiescent WI38 hTERT cells. **(A-F)** Serum-starved cells were treated with MG132 (50 µM, 1 h), lactacystin (10 µM, 1 h), bortezomib (1 µM, 4 h), G5 (1.5 µM, 0.5 h) or Pyr-41 (9 µM, 0.5 h) before the addition of CPT (25 µM) for 1 h and then co-stained for γH2AX (green) and 53BP1 (red) or analyzed by Western blot. **(A,D)** Representative pictures. Nuclear contours, identified by DAPI staining (not shown), are indicated by dashed lines. Bars: 10 µm. **(B,E)** Number of γH2AX foci per nucleus from two independent experiments (147-153 nuclei were analyzed for each treatment). ****, $P < 0.0001$. **(C,F)** Western blot of γH2AX. αTubulin: loading control. Dashed lines indicate that intervening wells have been spliced out. The top panels show quantification of γH2AX expression normalized to αTubulin (means ± SEM, n = 4 in panel C, n=3 in panel F). ***, $P < 0.001$; **, $P < 0.01$. **(G,H)** Detection of DSBs by neutral Comet assays in serum-starved cells treated with MG132 (25 µM) for 1 h before the addition of CPT for 1 h (7.5 µM for experiments (Exp) I and II; 5 and 7.5 µM for Exp III). **(G)** Representative pictures of nuclei from Exp I. **(H)** Quantification of neutral Comet tail moments for three independent experiments (95-133 nuclei were analyzed for each treatment in each experiment). ***, $P < 0.001$; ****, $P < 0.0001$. The untreated and CPT data from Exp I are from the same experiment as that of Figure 1I.

Figure 3. The production of DSBs depends on Top1 degradation in CPT-treated quiescent cells. **(A-C)** Serum-starved WI38 hTERT cells were co-transfected with siRNAs against cullin 3 and cullin 4B or against a control sequence and then treated with CPT (25 µM) for 1 h. **(A,B)** Western blotting of the indicated proteins. αTubulin: loading control. **(C)** Number of γH2AX foci per nucleus from one representative experiment (246-348 nuclei were analyzed for each treatment) out of three. ***, $P < 0.001$. **(D,E)** Serum-starved WI38 hTERT cells were treated with MG132 (50 µM) for 1 h before exposure to 0.8 Gy IR. One hour post-irradiation, cells were co-stained for γH2AX (green) and 53BP1 (red). **(D)** Representative pictures. **(E)** Number of γH2AX foci per nucleus from one representative experiment (162-180 nuclei were analyzed for each treatment) out of three. Ns: not significant. **(F,G)** U2OS EV28 cells were treated with MG132 (10 µM) for 1 h before the addition of 300 nM 4-hydroxitamoxifen (4OHT) for 4 h to express *Asi*SI in the nucleus (51). **(F)** Representative pictures of cells co-stained for γH2AX (green) and 53BP1 (red). **(G)** ChIP analysis using an anti-γH2AX antibody

(black) or a non-immune antibody (IgG, grey). Enrichment was assessed by QPCR amplification using primers proximal to two *Asi*SI sites located inside two genes (Gene I: SFRS6, Gene II: CCD47) and primers distal to an *Asi*SI site (Control). Enrichment was normalized to the maximum recovery for each experiment (means ± SEM, n = 3). Ns: not significant; *, P < 0.05. In the microscopic images, nuclear contours, identified by DAPI staining (not shown), are indicated by dashed lines. Bars: 10 µm.

Figure 4. Inhibition of TDP1 or PARP increases CPT-induced DSBs in quiescent WI38 hTERT cells. **(A,B)** Serum-starved cells were transfected with TDP1-targeting or nontargeting (Control) siRNAs and then treated with MG312 (25 µM) or FLV (1 µM) for 1 h before the addition of CPT (25 µM) for 1 h. Cells were then co-stained for γH2AX (green) and 53BP1 (red). **(A)** Representative pictures. **(B)** Number of γH2AX foci per nucleus from one representative experiment (152-233 nuclei were analyzed for each treatment) out of two to four. ****, P < 0.0001. **(C,D)** Serum-starved cells were treated for 1 h with veliparib (5 µM), either alone or in combination with MG132 (25 µM) or FLV (1 µM), before the addition of CPT (25 µM) for 1 h. Cells were then co-stained for γH2AX (green) and 53BP1 (red). **(C)** Representative pictures. **(D)** Number of γH2AX foci per nucleus from one representative experiment (120-223 nuclei were analyzed for each treatment) out of two. ****, P < 0.0001. (**E**) Detection of DSBs by neutral Comet assays in serum-starved cells treated with veliparib (5 µM) before the addition of CPT (7.5 µM). Data show the quantification of one representative experiment (226-249 nuclei were analyzed for each treatment) out of three. ****, P < 0.0001. **(F)** Serum-starved cells were transfected with TDP1-targeting or nontargeting (Control) siRNAs and then treated for 1 h with veliparib (5 µM) or olaparib (10 µM) before the addition of CPT (25 µM) for 1 h. Cells were then stained for γH2AX. The number of γH2AX foci per nucleus from one representative experiment (105-215 nuclei were analyzed for each treatment) out of two is shown. ****, P < 0.0001; ns, not significant. In the microscopic images, nuclear contours, identified by DAPI staining (not shown), are indicated by dashed lines. Bars: 10 µm.

Figure 5. Inhibition of DNA-PK prevents the formation of ATM-pS1981 foci in CPT-treated quiescent WI38 hTERT cells. **(A,B)** Serum-starved cells were treated with ATMi (10 µM), DNA-PKi (10 µM) or ATRi (10 µM) for 1 h before the addition of CPT (25 µM) for 1 h. Cells were then stained for γH2AX (green) and DNA was counterstained with DAPI (blue). **(A)** Representative pictures. Numbers are the percentage of nuclei with at least 2 γH2AX foci (bottom) and the average number of foci per nuclei (top). **(B)** Number of γH2AX foci per nucleus. Quantifications in panels A and B are from one representative experiment (159-306 nuclei were analyzed for each treatment) out of three. ****, P < 0.0001. **(C)** Detection of DSBs by neutral Comet assays in serum-starved cells treated with ATMi (10 µM) or DNA-PKi (10 µM) for 1 h before the addition of CPT (7.5 µM) for 1 h. Data show the quantification of one representative experiment out of two for ATMi (226-428 nuclei were analyzed for each treatment) and out of four for DNA-PKi (102-120 nuclei were analyzed for each treatment). ****, P < 0.0001; *, P < 0.05. The untreated and CPT data from the experiment with ATMi are from the same experiment as that of Figure 4E. **(D)** Right panels: colocalization of ATM-pS1981 foci (red) with γH2AX foci (green) in serum-starved cells treated with CPT (25 µM) for 1 h before staining. Similar

data were obtained in > 10 independent experiments. Left panels: serum-starved cells were treated with DNA-PKi (10 µM) or ATMi (10 µM) for 1 h before the addition of CPT (25 µM) for 1 h and then co-stained for DNA-PK-pT2609 (red) and γH2AX (green). Similar data were obtained in two independent experiments. Images were merged to determine colocalization (yellow). **(E)** Western blot of ATM-pS1981 and DNA-PK-pS2056 in serum-starved cells treated as described for panel D. The top panel shows quantification of ATM-pS1981 expression (means ± SD, n = 3). **, P < 0.01; ****, P < 0.0001. **(F)** Serum-starved cells were treated with DNA-PKi (10 µM) for 1 h before the addition of CPT (25 µM) for 1. Nucleosoluble proteins were then removed (lower panels) or not (top panels) with CSK buffer before co-staining for ATM-pS1981 (red) and γH2AX (green). Representative images are shown. The zoomed images are x4 magnifications of the main images. The yellow boxes indicate areas of magnification. **(G)** Quantification of ATM-pS1981 fluorescence intensity per nucleus shown in lower panel F (means ± SD, n= 3, 70-100 nuclei were analyzed for each treatment in each experiment). ****, P < 0.0001. In the microscopic images, nuclear contours, identified by DAPI staining (not shown), are indicated by dashed lines. Bars: 10 µm.

Figure 6. Inhibition of DNA-PK prevents monoubiquitination of H2AX and H2A in CPT-treated quiescent WI38 hTERT cells. **(A-E)** Serum-starved cells were treated with DNA-PKi (10 µM) for 1 h before the addition of CPT (25 µM) for 1 h. **(A)** Western blot of γH2AX. +Ub1 indicates γH2AX monoubiquitinated. The top panel shows quantification of Ub1-γH2AX expression normalized to αTubulin (means ± SEM, n = 4). **, P < 0.01. **(B,C)** Cells were pre-extracted with CSK buffer before co-staining for Ub-H2A (red) and 53BP1 phosphorylated on S1778 (p53BP1) (green). **(B)** Representative pictures. Images were merged to determine colocalization (yellow). The large Ub-H2AX focus at the periphery of the nuclei of untreated and CPT-treated cells may marks the inactive X chromosome as reported (83). **(C)** Percentages of nuclei with at least 5 Ub-H2A foci (means ± SEM, n = 3, 100 nuclei were analyzed for each treatment in each experiment). ***, P < 0.001. **(D,E)** Cells were co-stained for ubiquitinated proteins (FK2, red) and γH2AX (green). **(D)** Representative pictures. Images were merged to determine colocalization (yellow). **(E)** Number of FK2 foci per nucleus from one representative experiment (76-111 nuclei were analyzed for each treatment) out of three. ****, P < 0.0001. In the microscopic images, nuclear contours, identified by DAPI staining (blue in the merge images at bottom), are indicated by dashed lines. Bars: 10 µm.

Figure 7. Inhibition of DNA-PK prevents Top1 degradation and proteasome activity in CPT-treated quiescent WI38 hTERT cells. **(A-E)** Serum-starved cells were treated with DNA-PKi (10 µM) for 1 h before the addition of CPT (25 µM) for the indicated times. **(A)** Western blot of Top1. The top panel shows quantification of Top1 expression normalized to αTubulin (means ± SEM, n = 4). **, P < 0.01. **(B)** Detection of Top1-DNA cleavage complexes (Top1cc). Three concentrations of genomic DNA (5, 2.5, and 1.25 µg) were probed with an anti-Top1 antibody. Dashed lines indicate where panels have been reorganized to facilitate reading. **(C)** Western blot of UBA1, PSMA6 and Top1 in the P2 fraction (see Supplementary Figure S5G). Dashed lines in the UBA1 blot indicate that intervening wells have been spliced out. The top panel shows quantification of UBA1, PSMA6 and Top1 expression in the P2

fraction normalized to histone H3 (mean ± SEM; n = 4 for PSMA6 and Top1, n = 3 for UBA1). **(D)** Western blot of UBA1 (top) and PSMA6 (bottom) in whole cell extracts (WCE). **(E)** Chymotrypsin-like activity assessment in the P2 fraction (means ± SD of triplicates; each time point is representative of at least two independent experiments). αTubulin and histone H3 were the loading controls for Western blot experiments.

Figure 8. CPT induces transcription- and proteasome-dependent apoptosis in quiescent WI38 hTERT cells. **(A)** Serum-starved cells were treated with FLV (1 µM) for 1 h before the addition of CPT (25 µM) for 16 and 24 h. Cell survivals are percentages of cells that remained attached to culture flasks (means ± SD of quadruplicates). **(B-F)** Western blot of the indicated proteins in serum-starved cells treated for 1 h with FLV (1 µM) **(B)**, lactacystin (10 µM) **(C)**, veliparib (5 µM) or olaparib (10 µM) **(D)**, ATMi (10 µM) **(E)** or DNA-PKi (10 µM) **(F)** before the addition of CPT (25 µM) for the indicated times. Data shown are representatives from two to three experiments. $PARP^{CL}$: cleaved PARP. H2AX and αTubulin were the loading controls

Figure 9. Proposed molecular pathways for the production and signaling of DSBs by transcription-blocking Top1 lesions. "Y" is the catalytic tyrosine of Top1 covalently bound to the 3'-end of the broken DNA. Asterisks indicate proteins whose deficiency induces neurodegenerative diseases (TDP1 deficiency: SCAN1 syndrome; ATM deficiency: AT syndrome).

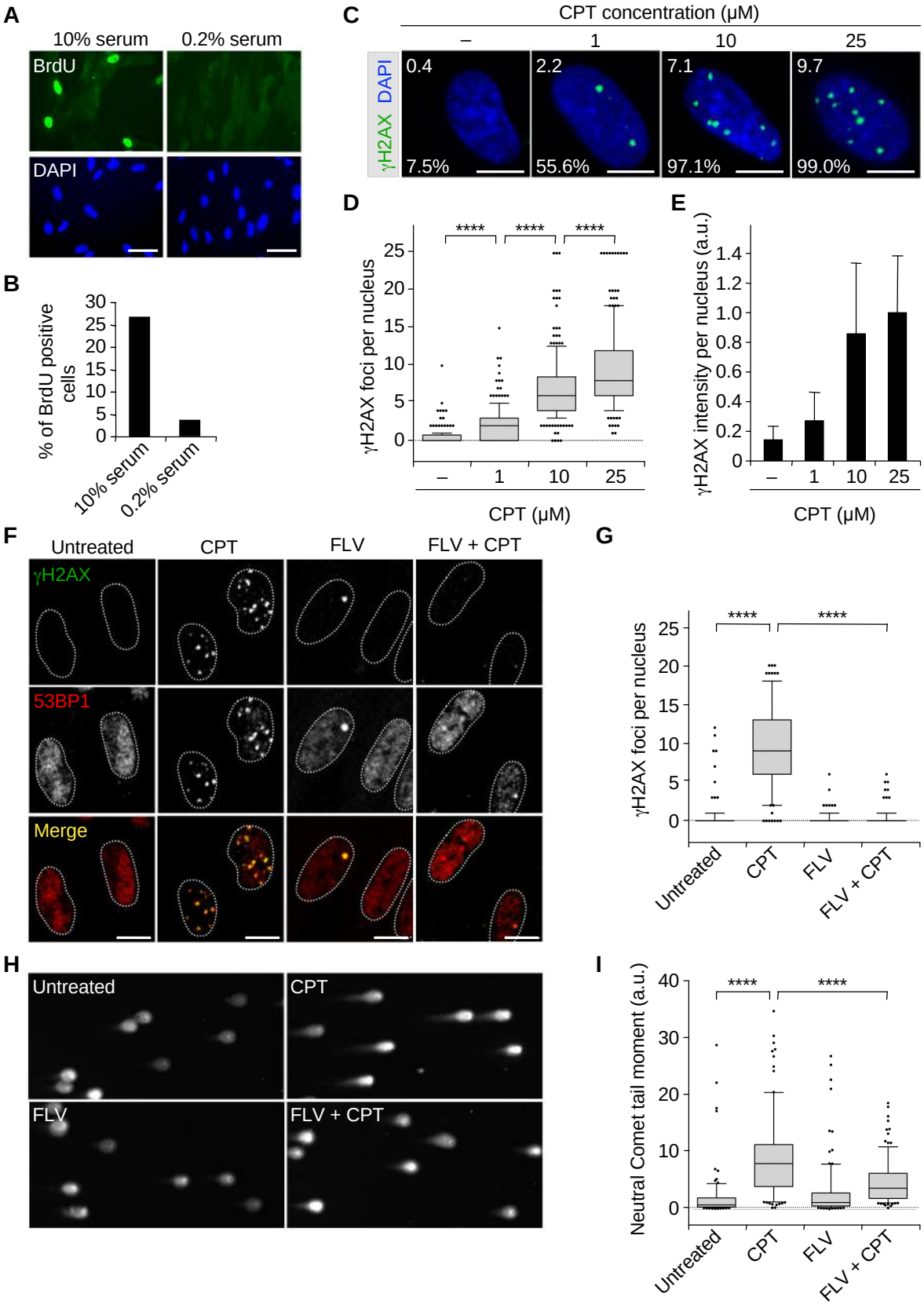
A
10% serum
0.2% serum
BrdU
DAPI
B
% of BrdU positive cells
10% serum
0.2% serum
C
CPT concentration (μM)
–
1
10
25
γH2AX DAPI
0.4
7.5%
2.2
55.6%
7.1
97.1%
9.7
99.0%
D
γH2AX foci per nucleus
****
CPT (μM)
E
γH2AX intensity per nucleus (a.u.)
CPT (μM)
F
Untreated
CPT
FLV
FLV + CPT
γH2AX
53BP1
Merge
G
γH2AX foci per nucleus
Untreated
CPT
FLV
FLV + CPT
H
Untreated
CPT
FLV
FLV + CPT
I
Neutral Comet tail moment (a.u.)

Figure 1

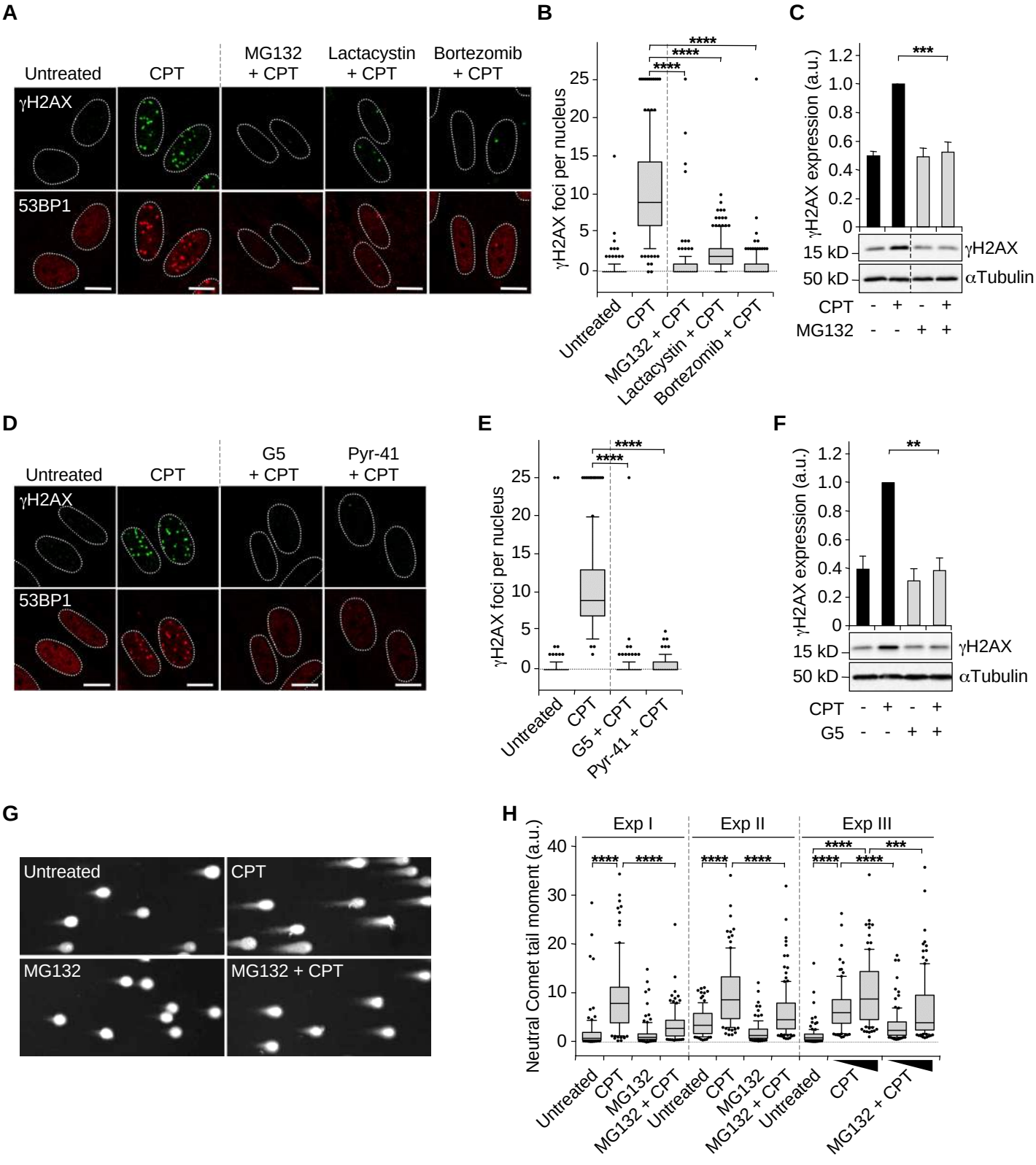
A
Untreated
CPT
MG132 + CPT
Lactacystin + CPT
Bortezomib + CPT
γH2AX
53BP1
B
γH2AX foci per nucleus
Untreated
CPT
MG132 + CPT
Lactacystin + CPT
Bortezomib + CPT
C
γH2AX expression (a.u.)
15 kD
50 kD
γH2AX
αTubulin
CPT
MG132
D
G5 + CPT
Pyr-41 + CPT
E
Pyr-41 + CPT
F
G5
G
H
Exp I
Exp II
Exp III
Neutral Comet tail moment (a.u.)

Figure 2

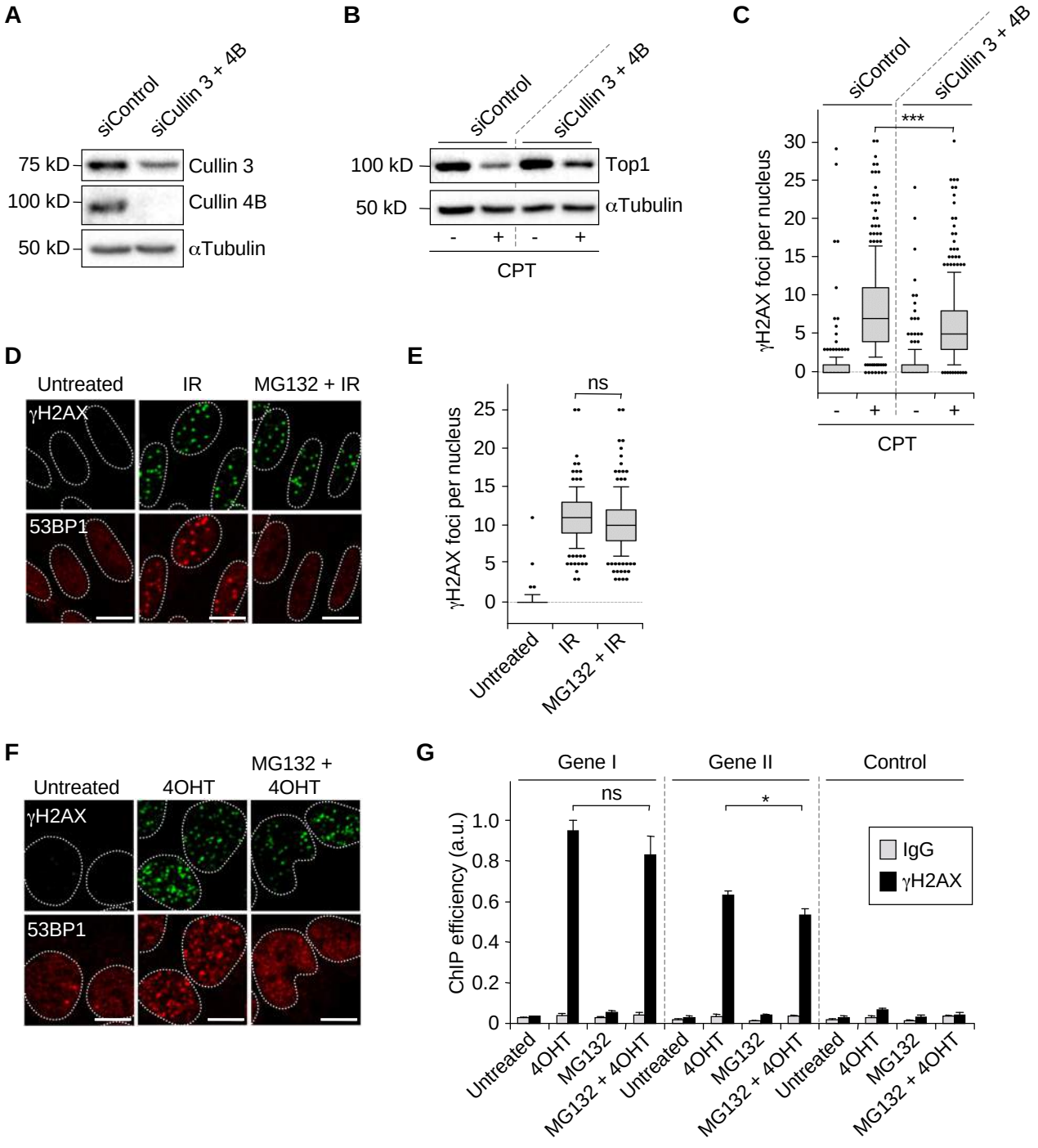
A
siControl
siCullin 3 + 4B
75 kD
Cullin 3
100 kD
Cullin 4B
50 kD
αTubulin
B
siControl
siCullin 3 + 4B
100 kD
Top1
50 kD
αTubulin
- + - +
CPT
C
siControl
siCullin 3 + 4B
***
γH2AX foci per nucleus
30
25
20
15
10
5
0
- + - +
CPT
D
Untreated
IR
MG132 + IR
γH2AX
53BP1
E
ns
γH2AX foci per nucleus
25
20
15
10
5
0
Untreated
IR
MG132 + IR
F
Untreated
4OHT
MG132 + 4OHT
γH2AX
53BP1
G
Gene I
Gene II
Control
ns
*
ChIP efficiency (a.u.)
1.0
0.8
0.6
0.4
0.2
0
IgG
γH2AX
Untreated
4OHT
MG132
MG132 + 4OHT

Figure 3

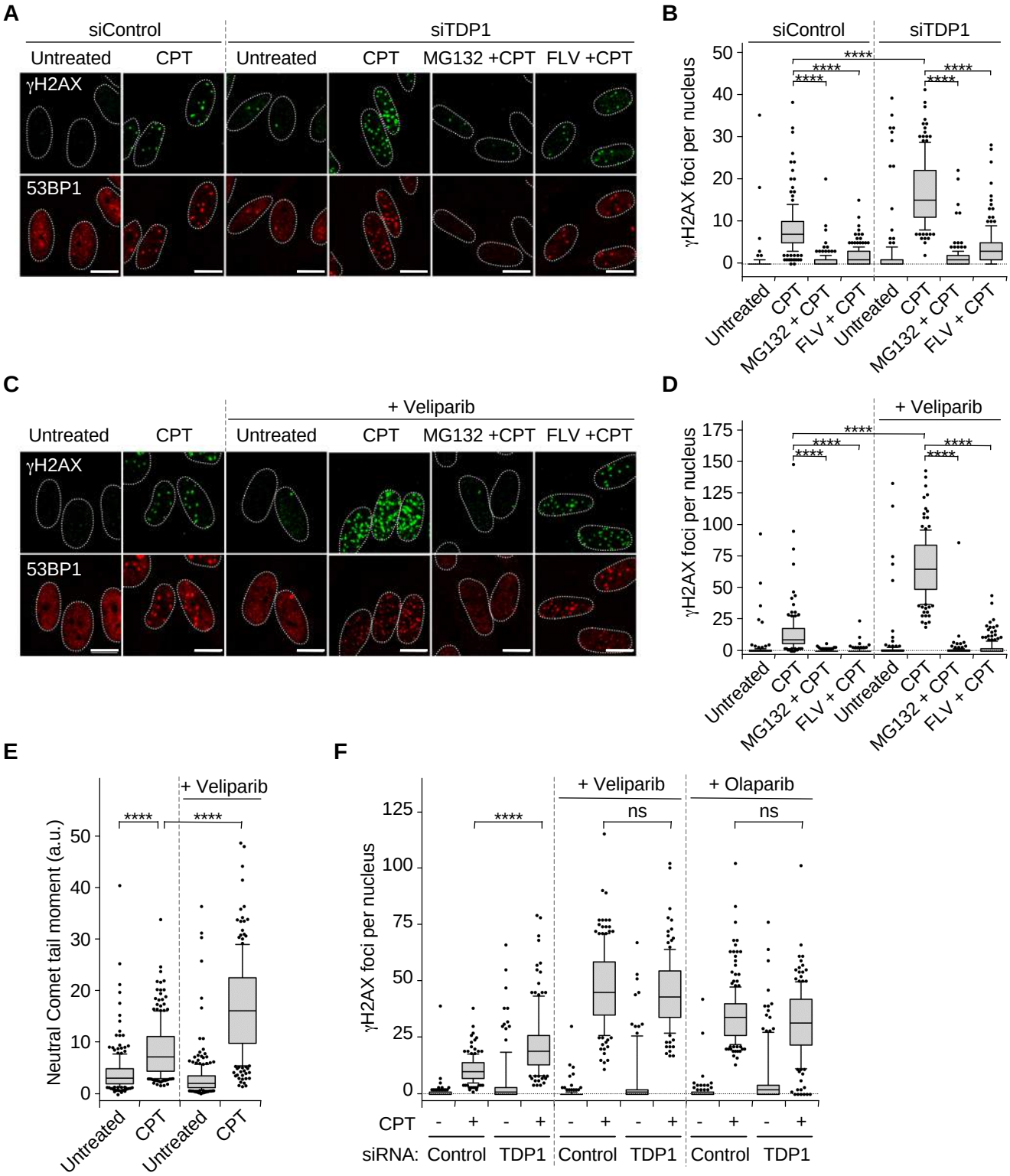
A
siControl
siTDP1
Untreated
CPT
Untreated
CPT
MG132 +CPT
FLV +CPT
γH2AX
53BP1
B
siControl
siTDP1
γH2AX foci per nucleus
Untreated
CPT
MG132 + CPT
FLV + CPT
C
+ Veliparib
D
E
Neutral Comet tail moment (a.u.)
F
+ Olaparib
ns
CPT
siRNA:
Control
TDP1

Figure 4

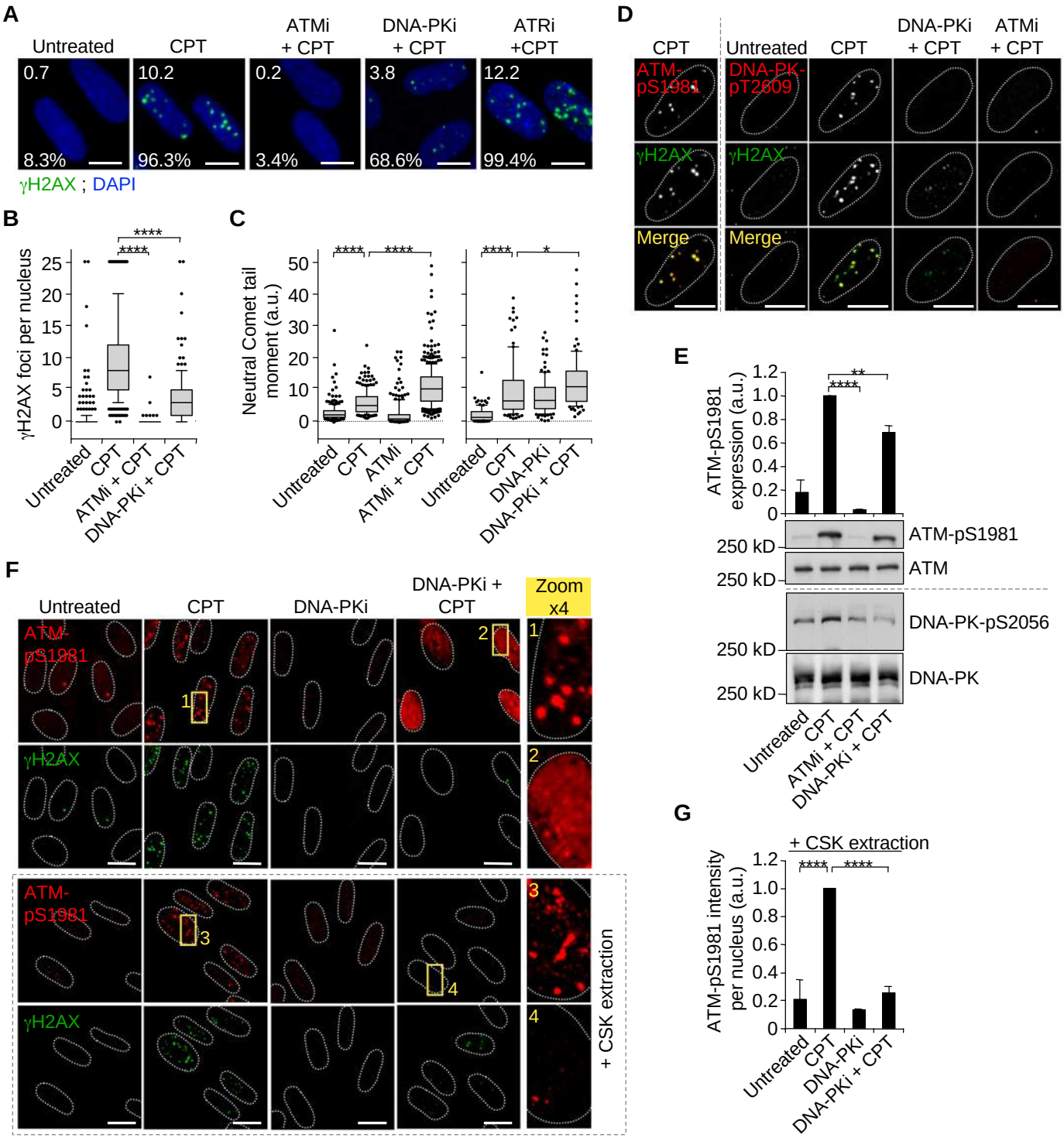
A
Untreated
CPT
ATMi + CPT
DNA-PKi + CPT
ATRi +CPT
0.7
8.3%
10.2
96.3%
0.2
3.4%
3.8
68.6%
12.2
99.4%
γH2AX ; DAPI
B
γH2AX foci per nucleus
Untreated
CPT
ATMi + CPT
DNA-PKi + CPT
C
Neutral Comet tail moment (a.u.)
Untreated
CPT
ATMi
ATMi + CPT
DNA-PKi
DNA-PKi + CPT
D
CPT
Untreated
CPT
DNA-PKi + CPT
ATMi + CPT
ATM-pS1981
DNA-PK-pT2609
γH2AX
Merge
E
ATM-pS1981 expression (a.u.)
ATM-pS1981
ATM
DNA-PK-pS2056
DNA-PK
250 kD
Untreated
CPT
ATMi + CPT
DNA-PKi + CPT
F
Untreated
CPT
DNA-PKi
DNA-PKi + CPT
Zoom x4
ATM-pS1981
γH2AX
+ CSK extraction
G
+ CSK extraction
ATM-pS1981 intensity per nucleus (a.u.)
Untreated
CPT
DNA-PKi
DNA-PKi + CPT

Figure 5

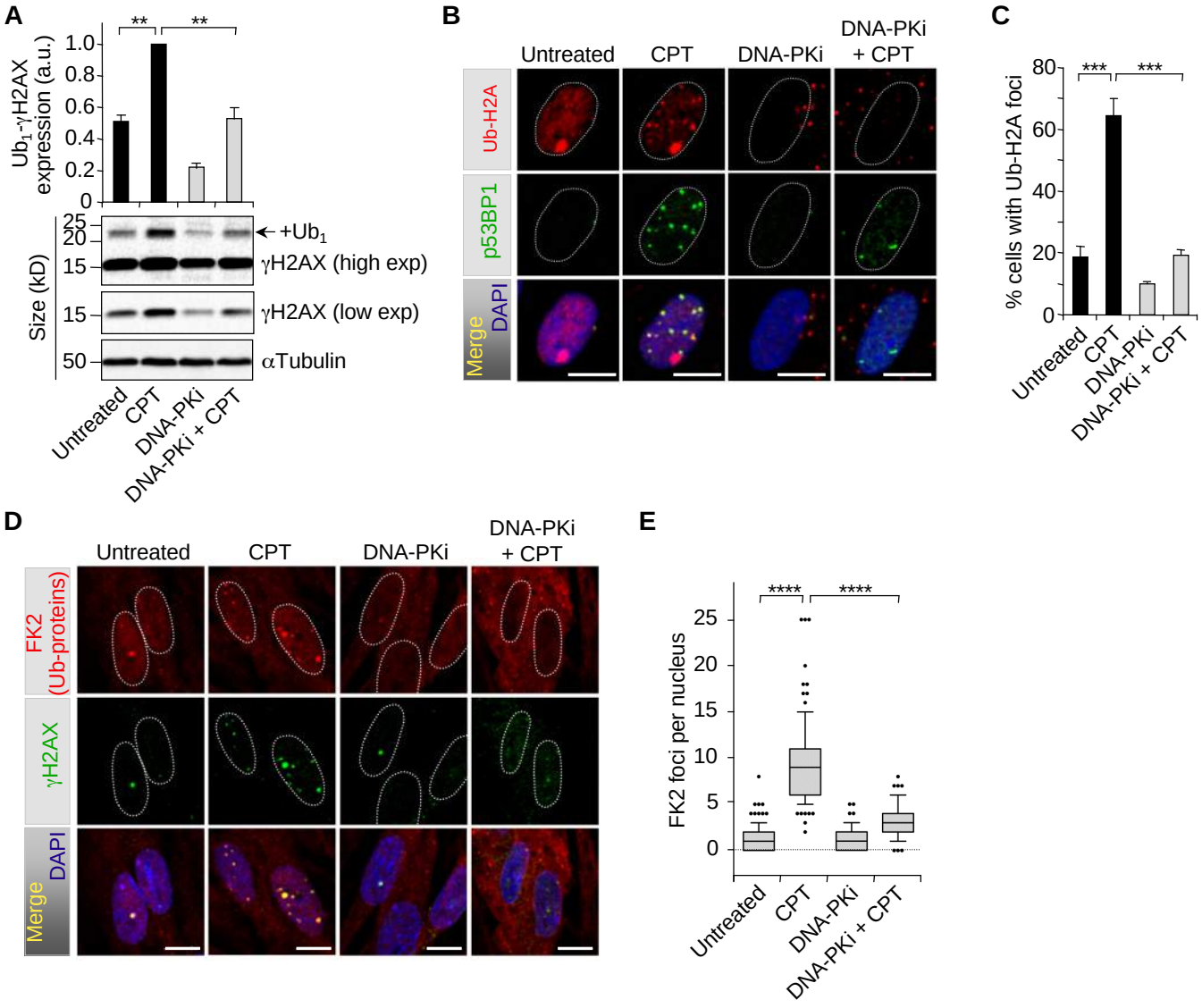
A
B
C
D
E
Untreated
CPT
DNA-PKi
DNA-PKi + CPT
Ub-H2A
p53BP1
Merge
DAPI
FK2 (Ub-proteins)
γH2AX
% cells with Ub-H2A foci
FK2 foci per nucleus
Size (kD)
+Ub1
γH2AX (high exp)
γH2AX (low exp)
αTubulin

Figure 6

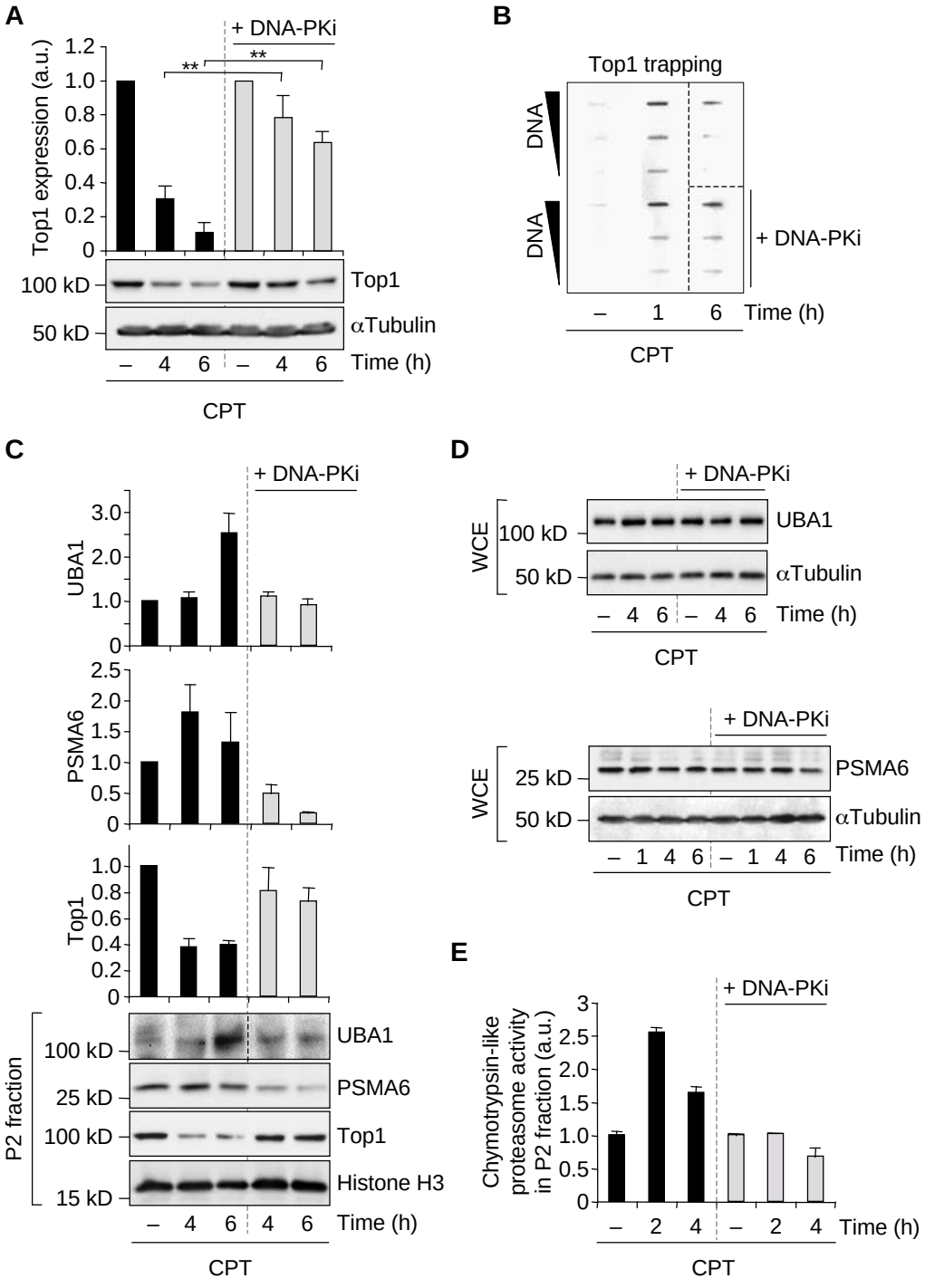
A
+ DNA-PKi
Top1 expression (a.u.)
1.2
1.0
0.8
0.6
0.4
0.2
0
**
**
100 kD
Top1
50 kD
αTubulin
– 4 6 – 4 6
Time (h)
CPT
B
Top1 trapping
DNA
DNA
+ DNA-PKi
– 1 6 Time (h)
CPT
C
+ DNA-PKi
UBA1
3.0
2.0
1.0
0
PSMA6
2.5
2.0
1.5
1.0
0.5
0
Top1
1.0
0.8
0.6
0.4
0.2
0
P2 fraction
100 kD
UBA1
25 kD
PSMA6
100 kD
Top1
15 kD
Histone H3
– 4 6 4 6
Time (h)
CPT
D
+ DNA-PKi
WCE
100 kD
UBA1
50 kD
αTubulin
– 4 6 – 4 6
Time (h)
CPT
+ DNA-PKi
WCE
25 kD
PSMA6
50 kD
αTubulin
– 1 4 6 – 1 4 6
Time (h)
CPT
E
+ DNA-PKi
Chymotrypsin-like proteasome activity in P2 fraction (a.u.)
3
2.5
2.0
1.5
1.0
0.5
0
– 2 4 – 2 4
Time (h)
CPT

Figure 7

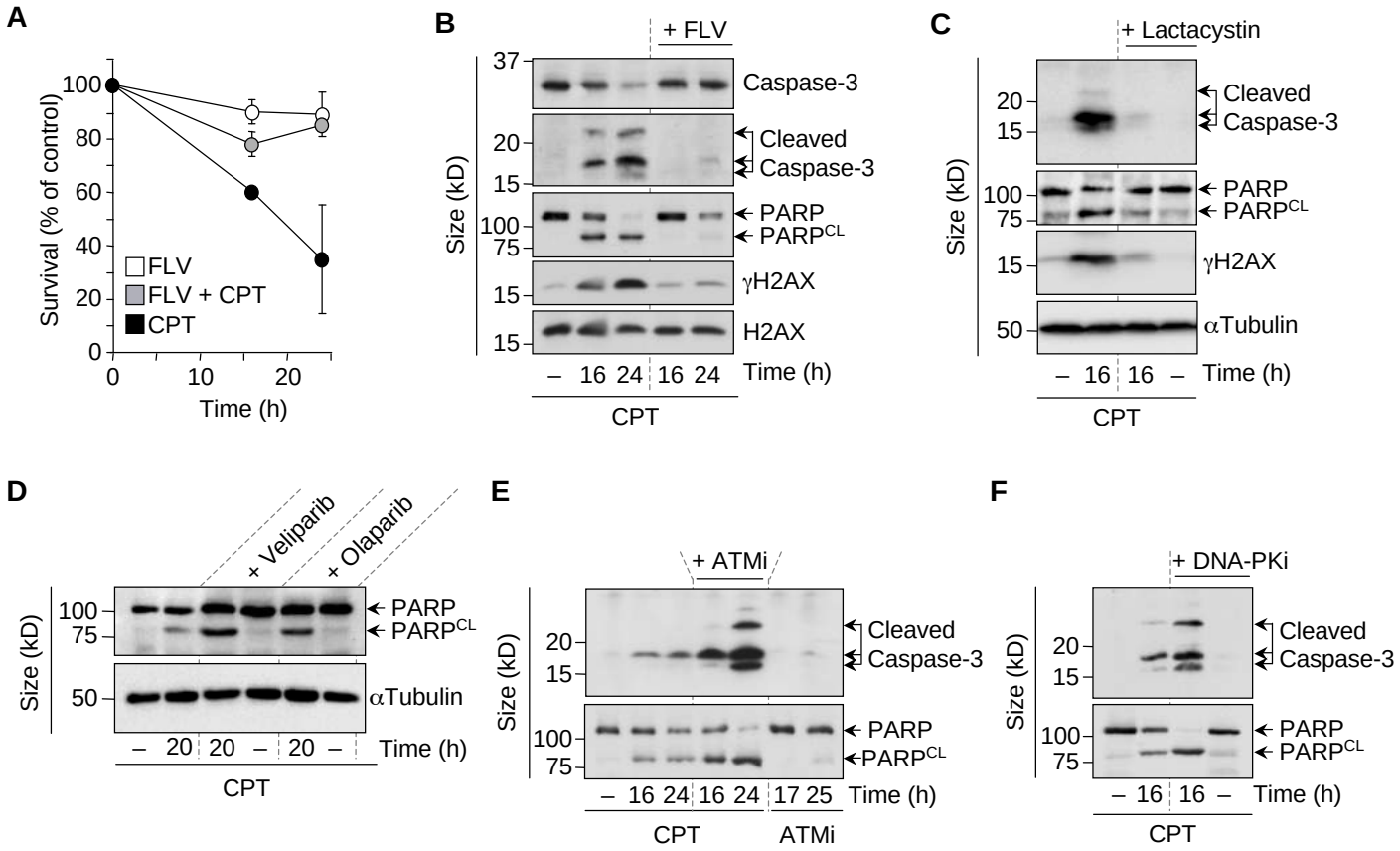
A
Survival (% of control)
100
80
60
40
20
0
0
10
20
Time (h)
FLV
FLV + CPT
CPT
B
+ FLV
Size (kD)
37
20
15
100
75
15
15
Caspase-3
Cleaved
Caspase-3
PARP
PARP^CL
γH2AX
H2AX
– 16 24 16 24
Time (h)
CPT
C
+ Lactacystin
Size (kD)
20
15
100
75
15
50
Cleaved
Caspase-3
PARP
PARP^CL
γH2AX
αTubulin
– 16 16 –
Time (h)
CPT
D
+ Veliparib
+ Olaparib
Size (kD)
100
75
50
PARP
PARP^CL
αTubulin
– 20 20 – 20 –
Time (h)
CPT
E
+ ATMi
Size (kD)
20
15
100
75
Cleaved
Caspase-3
PARP
PARP^CL
– 16 24 16 24 17 25
Time (h)
CPT
ATMi
F
+ DNA-PKi
Size (kD)
20
15
100
75
Cleaved
Caspase-3
PARP
PARP^CL
– 16 16 –
Time (h)
CPT

Figure 8

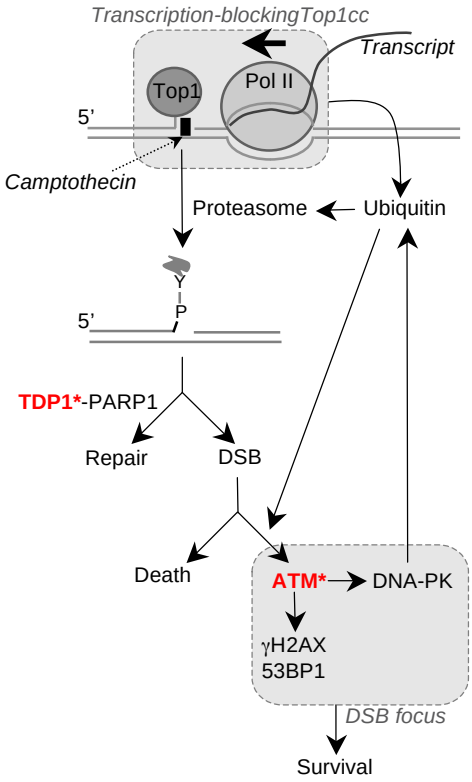
Transcription-blockingTop1cc
Transcript
Top1
Pol II
5'
Camptothecin
Proteasome
Ubiquitin
Y
P
5'
TDP1*-PARP1
Repair
DSB
Death
ATM*
DNA-PK
γH2AX
53BP1
DSB focus
Survival

Figure 9

Supplementary Data

Ubiquitination triggers DNA double-strand break formation and signaling in response to transcription-blocking topoisomerase-1 lesions

Agnese Cristini, Joon-Hyung Park, Giovanni Capranico, Gaëlle Legube, Gilles Favre, Olivier Sordet

---

SUPPLEMENTARY FIGURE LEGENDS

Figure S1. ATM- and DNA-PK-dependent induction of γH2AX in quiescent IMR90 and NHDF cells in response to CPT. Data in IMR90 cells are shown in panels A-D and data in NHFD cells are shown in panels E-H. **(A,E)** Cells cultured in 10% or 0.2% serum for 3 days were exposed to 100 µM BrdU for 30 min before staining for BrdU. Percentage of BrdU positive cells (> 300 cells were analyzed for each treatment). **(B-D, F-H)** Serum-starved cells were treated with ATMi (10 µM) or DNA-PKi (10 µM) for 1 h before the addition of CPT (25 µM) for 1 h. Cells were then stained for γH2AX (green) and DNA was counterstained with DAPI (blue). **(B,F)** Representative pictures. Numbers indicate the average number of foci per nucleus. Bars: 10 µM. **(C,G)** Number of γH2AX foci per nucleus (122-167 nuclei were analyzed for each treatment in panel C and 111-169 in panel G); ****, $P < 0.0001$. **(D,H)** Quantification of γH2AX fluorescence intensity per nucleus (means ± SD, 182-209 cells were examined per condition in panel D and 208-267 in panel H).

Figure S2. Top1 is degraded in response to CPT but not IR or *Asi*SI, and PARP inhibition increases γH2AX/53BP1 foci in CPT-treated quiescent cells. (A-C) Western blot of Top1 in serum-starved WI38 hTERT cells treated with FLV (1 µM, 1 h), G5 (1.5 µM, 0.5 h) or MG132 (10 µM, 1 h) before the addition of CPT (25 µM) for the indicated times in panels A and C or for 4 h in panel B. **(D)** Western blot of Top1 in serum-starved WI38 hTERT cells 4 and 6 h post-irradiation with 0.8 Gy IR. **(E)** Western blot of Top1 in U2OS EV28 cells treated with 300 nM 4OHT for the indicated times. **(F)** Schematic representation of the repair of a Top1cc. Top1 is partially proteolyzed by the ubiquitin/proteasome system to expose the covalent bond between the Top1 catalytic tyrosine and the 3'-end of the DNA to be attacked by TDP1. Top1cc excision by TDP1 requires PARP1. TDP1 generates a 3'-phosphate, which is hydrolyzed by PNKP before religation by ligase III. **(G)** Western blot of TDP1 in serum-starved WI38 hTERT cells transfected with TDP1-targeting or nontargeting (Control) siRNAs. αTubulin: loading control. (**H,I**) Serum-starved WI38 hTERT cells were treated for 1 h with olaparib (10 µM) before the addition of CPT (25 µM) for 1 h. Cells were then co-stained for γH2AX (green) and 53BP1 (red). **(H)** Representative pictures. Nuclear contours, identified by DAPI staining (not shown), are indicated by dashed lines. Bars: 10 µm. **(I)** Number of γH2AX foci per nucleus from one representative experiment (131-151 nuclei were analyzed for each treatment) out of two; ****, $P < 0.0001$.

Figure S3. Activation of ATM signaling and its prevention following DNA-PK inhibition in CPT-treated quiescent WI38 hTERT cells. (A,B) Serum-starved WI38 hTERT cells were treated with ATMi (10 µM) or DNA-PKi (10 µM) for 1 h before the addition of CPT (25 µM) for 1 h and stained for γH2AX (green). Representative pictures are shown in Figure 5A. **(A)** Quantification of γH2AX fluorescence intensity per nucleus (means ± SD, 172-307 nuclei were examined for each treatment). **(B)** Size of γH2AX foci (means ± SD, n = 3, > 320 foci from 50-70 cells were analyzed for each treatment in each experiment).**, $P < 0.01$; *t*-test. **(C)** Western blot of Chk1 phosphorylated on S345 (Chk1-pS345) and total Chk1 in replicating WI38 hTERT cells treated with ATRi (10 µM) for 1 h before the addition of CPT (25 µM) for the indicated times. **(D)** Western blot of ATM, DNA-PK and ATR in WI38 hTERT cells cultured in 10% serum or in 0.2 % serum for 3 days. **(E)** Phosphorylation of ATM on S1981 (ATM-pS1981), KAP1 on S824 (KAP1-pS824), Chk2 on T68 (Chk2-pT68) and p53 on S15 (p53-pS15) was determined by Western blot in serum-starved WI38 hTERT cells treated with the indicated concentrations of CPT for 1 h. Total ATM, KAP1, Chk2 and p53 were examined in parallel. **(F)** Serum-starved WI38 hTERT cells were treated with DNA-PKi (10 µM) for 1 h before the addition of CPT (25 µM) for 1 h and stained for 53BP1, 53BP1 phosphorylated on S1778 (p53BP1) or MDC1. Representative pictures from one experiment out of two. Nuclear contours, identified by DAPI staining (not shown), are indicated by dashed lines. Bars: 10 µm.

Figure S4. Inhibition of XLF or XRCC4 does not prevent the formation of ATM-pS1981 and γH2AX foci in CPT-treated quiescent WI38 hTERT cells. **(A,B)** Serum-starved WI38 hTERT cells were transfected with XLF-targeting or nontargeting (Control) siRNAs. **(A)** Western blot showing the efficiency of XLF silencing. Actin: loading control. **(B)** siRNA-transfected cells were treated with CPT (25 μM) for 1 h and pre-extracted with CSK buffer before co-staining for ATM-pS1981 (red) and γH2AX (green). Representative pictures. Nuclear contours, identified by DAPI staining (not shown), are indicated by dashed lines. Bars: 10 μm. **(C,D)** Similar experiments were performed following siRNA-mediated depletion of XRCC4.

Figure S5. Inhibition of DNA-PK or ATM but not XLF or XRCC4 prevents CPT-induced Top1 degradation in quiescent cells. (A) Western blot of H2AX in serum-starved WI38 hTERT cells treated with CPT (25 μM) for 1 h. +Ub1 indicates monoubiquitinated H2AX. **(B,C)** Serum-starved WI38 hTERT cells were transfected with DNA-PK-targeting or nontargeting (Control) siRNAs. **(B)** Western blot showing DNA-PK silencing. αTubulin: loading control. **(C)** siRNA-transfected cells were treated with CPT (25 μM) for 1 h before staining for ubiquitinated proteins (FK2). Number of FK2 foci per nucleus from two experiments (156-171 nuclei were analyzed for each treatment). ****, $P < 0.0001$, *t*-test. **(D)** Western blot of Top1 in serum-starved IMR90 cells (top) and serum-starved NHDF cells (bottom) treated with DNA-PKi (10 μM) for 1 h before the addition of CPT (25 μM) for the indicated times. αTubulin: loading control. **(E)** Western blot of Top1, XLF and XRCC4 in serum-starved WI38 hTERT cells transfected with siRNAs against XLF, XRCC4 or a nontargeting sequence (Control) before treatment with CPT (25 μM) for 6 h. Actin: loading control. **(F)** Western blot of Top1 in serum-starved WI38 hTERT cells treated with ATMi (10 μM) for 1 h before the addition of CPT (25 μM) for the indicated times. αTubulin: loading control. **(G)** Serum-starved WI38 hTERT cells were subjected to fractionation and proteins from whole cell extracts (WCE), 150 mM NaCl/0.1% Triton X-100 supernatant (S1), 150 mM NaCl/RNAse A supernatant (S2) and pellets (P2) were analyzed by Western blot. αTubulin and histone H3 control the S1 and P2 fractions, respectively. **(H)** DNA-PKi (10 μM) or MG132 (10 μM) were incubated with the P2 fraction of serum-starved WI38 hTERT cells and proteasome chymotrypsin-like activity was measured (means ± SEM, n = 3).

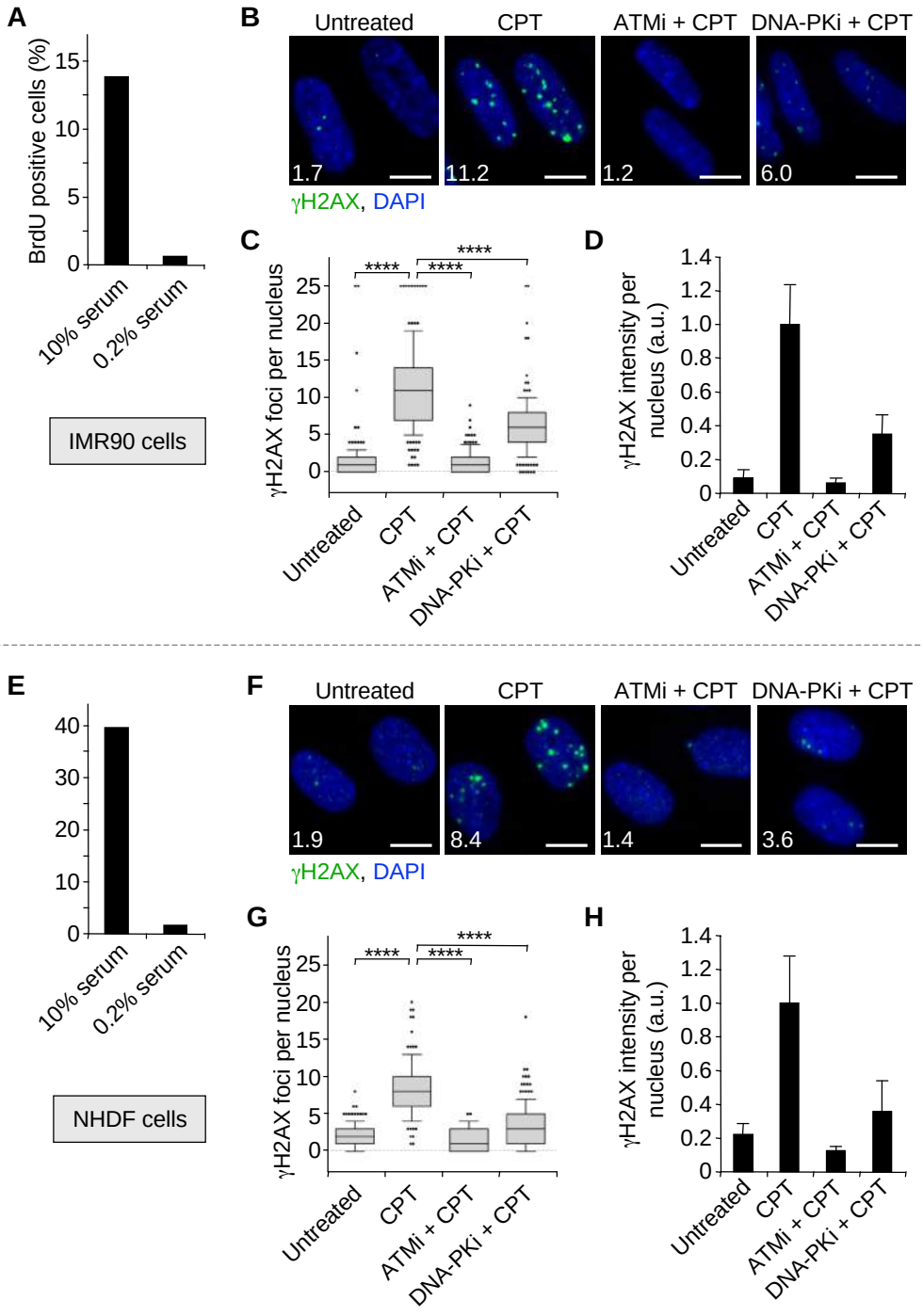
A
BrdU positive cells (%)
15
10
5
0
10% serum
0.2% serum
IMR90 cells
B
Untreated
CPT
ATMi + CPT
DNA-PKi + CPT
1.7
11.2
1.2
6.0
γH2AX, DAPI
C
γH2AX foci per nucleus
25
20
15
10
5
0
****
****
****
Untreated
CPT
ATMi + CPT
DNA-PKi + CPT
D
γH2AX intensity per nucleus (a.u.)
1.4
1.2
1.0
0.8
0.6
0.4
0.2
0
Untreated
CPT
ATMi + CPT
DNA-PKi + CPT
E
40
30
20
10
0
10% serum
0.2% serum
NHDF cells
F
Untreated
CPT
ATMi + CPT
DNA-PKi + CPT
1.9
8.4
1.4
3.6
γH2AX, DAPI
G
γH2AX foci per nucleus
25
20
15
10
5
0
****
****
****
Untreated
CPT
ATMi + CPT
DNA-PKi + CPT
H
γH2AX intensity per nucleus (a.u.)
1.4
1.2
1.0
0.8
0.6
0.4
0.2
0
Untreated
CPT
ATMi + CPT
DNA-PKi + CPT

Figure S1

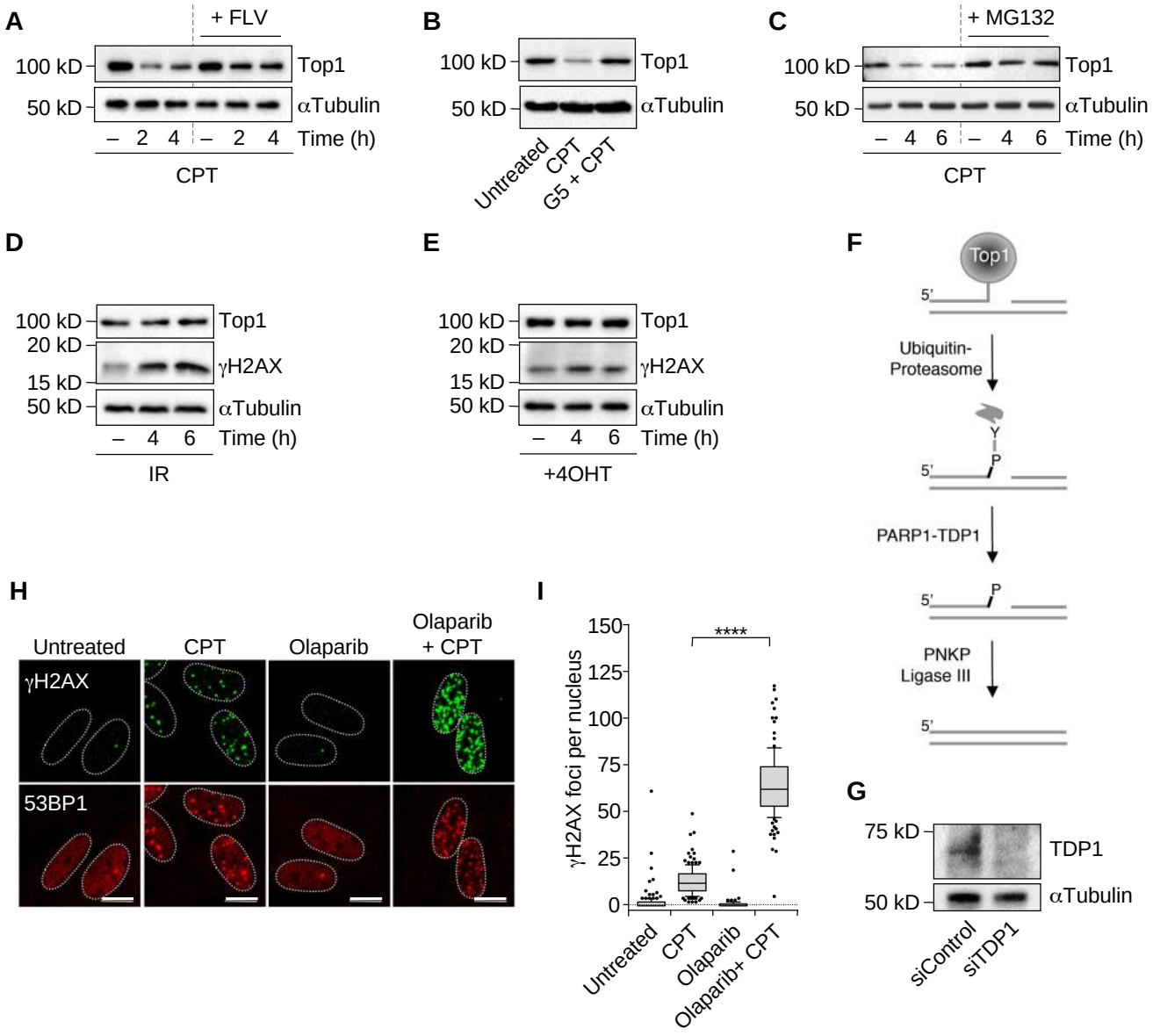
A
+ FLV
100 kD
50 kD
Top1
αTubulin
– 2 4 – 2 4 Time (h)
CPT
B
100 kD
50 kD
Top1
αTubulin
Untreated
CPT
G5 + CPT
C
+ MG132
100 kD
50 kD
Top1
αTubulin
– 4 6 – 4 6 Time (h)
CPT
D
100 kD
20 kD
15 kD
50 kD
Top1
γH2AX
αTubulin
– 4 6 Time (h)
IR
E
100 kD
20 kD
15 kD
50 kD
Top1
γH2AX
αTubulin
– 4 6 Time (h)
+4OHT
F
Top1
5'
Ubiquitin-
Proteasome
Y
P
5'
PARP1-TDP1
5'
P
PNKP
Ligase III
5'
G
75 kD
50 kD
TDP1
αTubulin
siControl
siTDP1
H
Untreated
CPT
Olaparib
Olaparib
+ CPT
γH2AX
53BP1
I
γH2AX foci per nucleus
150
125
100
75
50
25
0
****
Untreated
CPT
Olaparib
Olaparib+ CPT

Figure S2

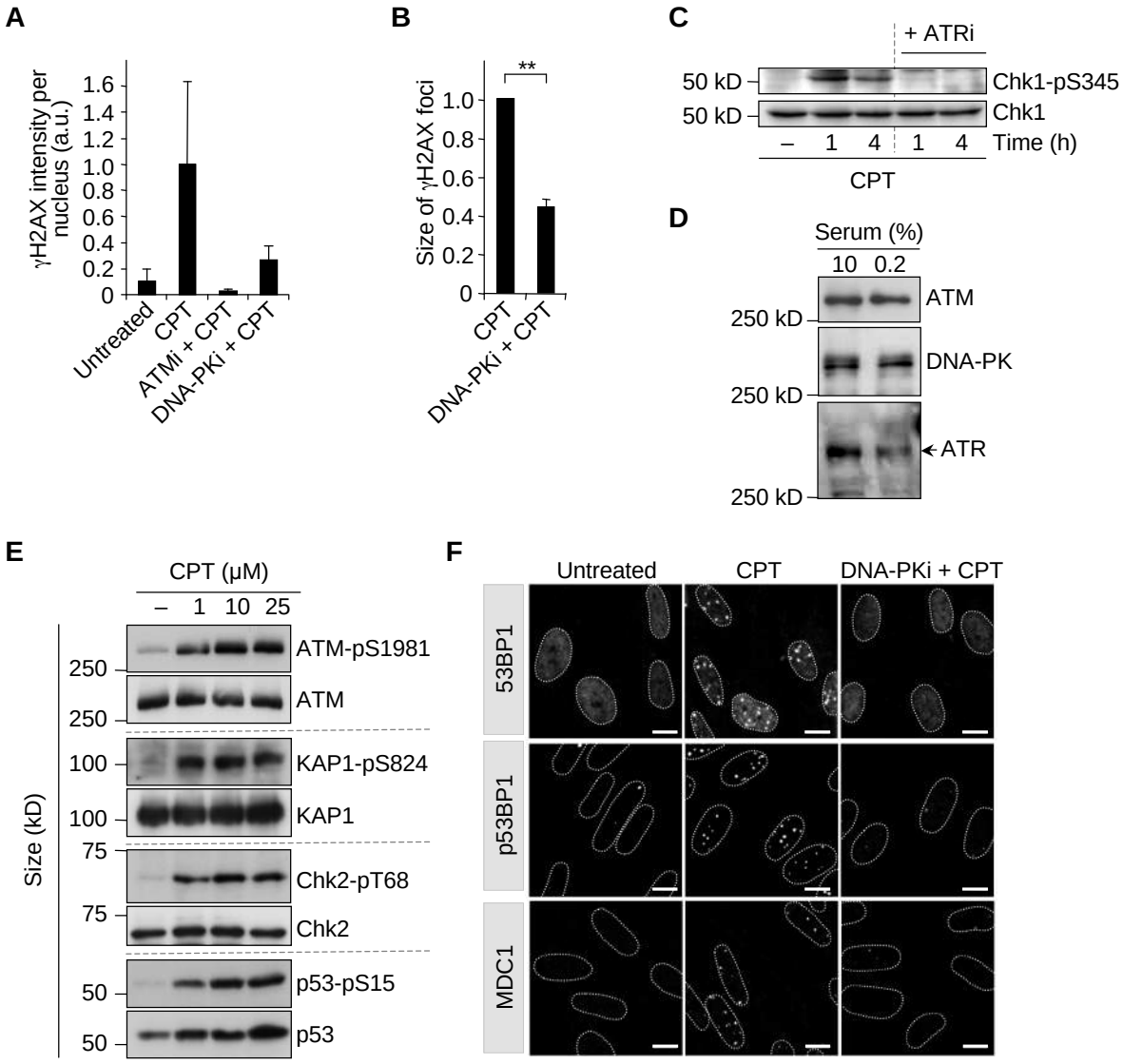
A
γH2AX intensity per nucleus (a.u.)
1.6
1.4
1.2
1.0
0.8
0.6
0.4
0.2
0
Untreated
CPT
ATMi + CPT
DNA-PKi + CPT
B
Size of γH2AX foci
**
1.0
0.8
0.6
0.4
0.2
0
CPT
DNA-PKi + CPT
C
+ ATRi
50 kD
Chk1-pS345
50 kD
Chk1
– 1 4 1 4 Time (h)
CPT
D
Serum (%)
10 0.2
250 kD
ATM
DNA-PK
250 kD
ATR
250 kD
E
CPT (μM)
– 1 10 25
Size (kD)
250
ATM-pS1981
250
ATM
100
KAP1-pS824
100
KAP1
75
Chk2-pT68
75
Chk2
50
p53-pS15
50
p53
F
Untreated
CPT
DNA-PKi + CPT
53BP1
p53BP1
MDC1

Figure S3

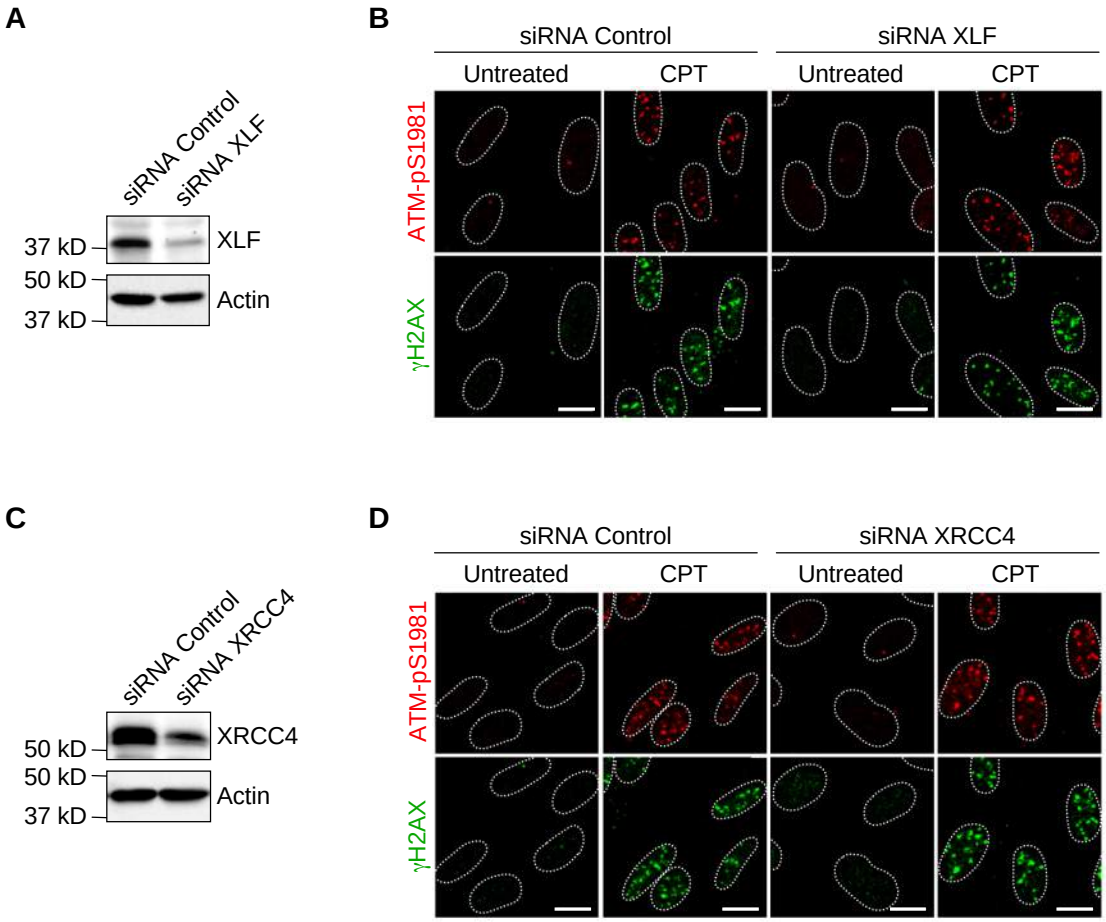
A
siRNA Control
siRNA XLF
37 kD
XLF
50 kD
37 kD
Actin
B
siRNA Control
siRNA XLF
Untreated
CPT
Untreated
CPT
ATM-pS1981
γH2AX
C
siRNA Control
siRNA XRCC4
50 kD
XRCC4
50 kD
37 kD
Actin
D
siRNA Control
siRNA XRCC4
Untreated
CPT
Untreated
CPT
ATM-pS1981
γH2AX

Figure S4

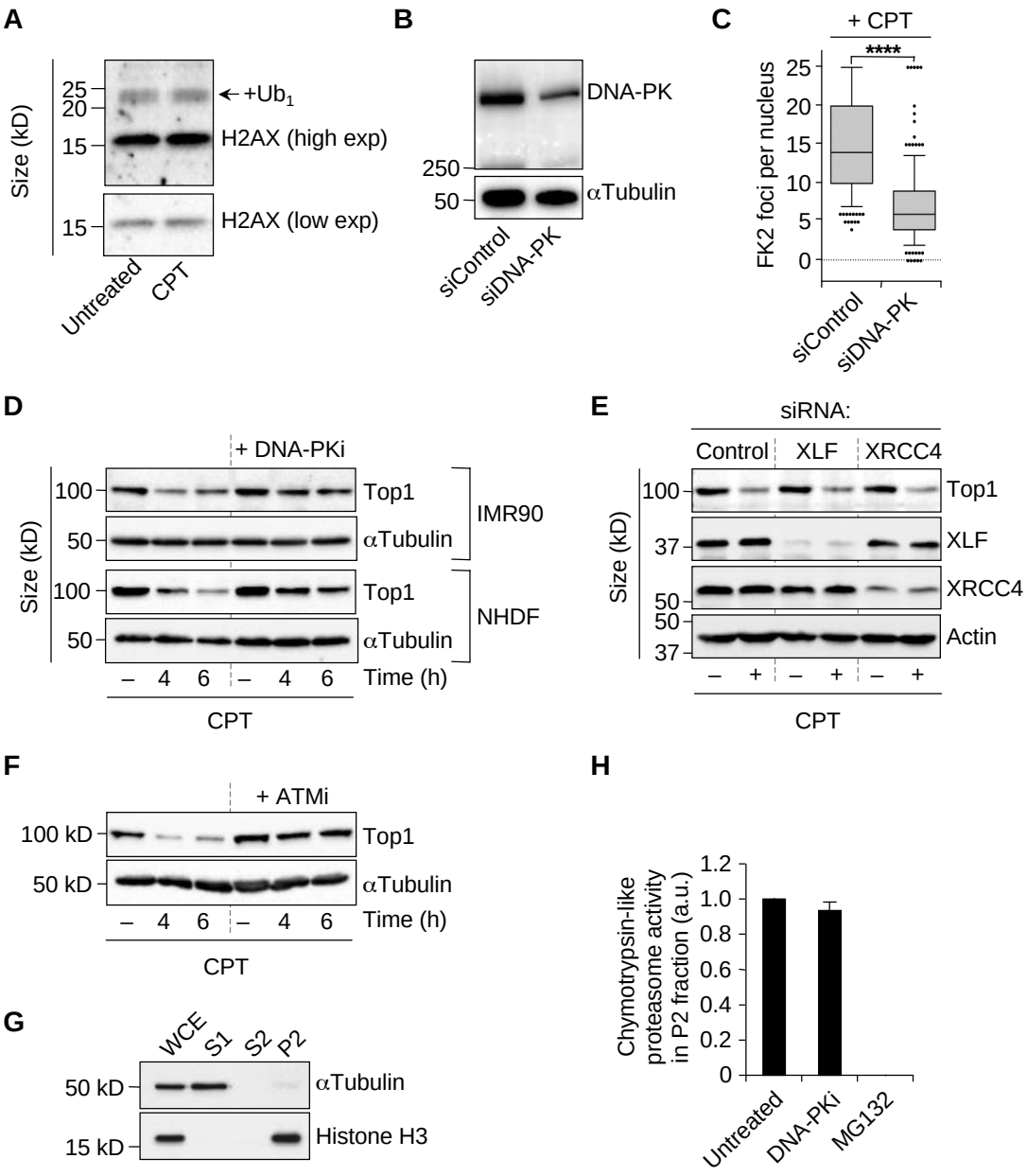
A
Size (kD)
25
20
15
+Ub1
H2AX (high exp)
15
H2AX (low exp)
Untreated
CPT
B
DNA-PK
250
50
αTubulin
siControl
siDNA-PK
C
+ CPT
****
FK2 foci per nucleus
25
20
15
10
5
0
siControl
siDNA-PK
D
+ DNA-PKi
Size (kD)
100
Top1
50
αTubulin
IMR90
100
Top1
50
αTubulin
NHDF
– 4 6 – 4 6
Time (h)
CPT
E
siRNA:
Control
XLF
XRCC4
Size (kD)
100
Top1
37
XLF
50
XRCC4
50
Actin
37
– + – + – +
CPT
F
+ ATMi
100 kD
Top1
50 kD
αTubulin
– 4 6 – 4 6
Time (h)
CPT
G
WCE
S1
S2
P2
50 kD
αTubulin
15 kD
Histone H3
H
Chymotrypsin-like proteasome activity in P2 fraction (a.u.)
1.2
1.0
0.8
0.6
0.4
0.2
0
Untreated
DNA-PKi
MG132

Figure S5

Supplementary Results

We have previously shown that transcriptional DSBs can arise during the repair of Top1 trapped into chromatin by CPT in serum-starved quiescent cells. We have proposed that Top1cc stabilization by CPT blocks transcription elongation, which triggers partial Top1 proteolysis and the generation of a Top1 peptide-linked SSB which is a substrate for Tdp1. Defective repair of this SSB intermediate by Tdp1 can give rise to a DSB (see **Figure 9, paper**). The unresolved question is how this SSB can be converted into a DSB in the absence of replication. To address this question, we are currently investigating the following points:

- Determine whether transcriptional DSBs that are produced during the repair of Top1cc arise specifically from Top1 peptide-linked SSBs or also by the other SSBs generated downstream of Tdp1 action (see the Top1cc repair pathway in **Figure S2F, paper**).
- Determine whether the second SSB is created by an endonuclease.
- Determine whether transcriptional DSBs are produced at hot-spot regions across the genome to gain insight into the mechanism of their production and signalling.
- Determine whether the mechanism of DSB production that we identified in serum-starved quiescent cells can be extended to replicating cells outside of S-phase. If so, that will allow the use of genetically modified cell lines that cannot be induced in quiescence for further studies.

Transcriptional DSBs arise from SSB intermediates generated during Top1cc repair by the Tdp1 excision pathway

To gain mechanistic insights in the production of transcriptional DSBs, we asked whether the nature of the SSB intermediate is important for DSB production. Indeed, DSBs may arise specifically from the Top1 peptide-linked SSBs or also from the other SSBs generated downstream from Tdp1. Following Tdp1 action, the Top1 peptide-linked SSB is converted into a 3'-phosphate SSB, which is hydrolysed by PNKP to generate a 3'-hydroxyl SSB, which is a substrate for LIG3 (**Figure S2F, paper**). To answer this point, we measured γH2AX foci upon inhibition of PNKP and LIG3, which increases the amount of 3'-phosphate- and 3'-hydroxyl-SSB intermediates, respectively, in CPT-treated cells. We found that depletion of PNKP or LIG3 with siRNAs increased the number of γH2AX foci in CPT-treated quiescent WI38 hTERT cells (**Figure IC and D**), under conditions where they also increased the amount of SSBs measured by alkaline comet assay (**Figure IE and F**). These results indicate that co-transcriptional DSBs produced in CPT-treated quiescent cells arise from SSB intermediates generated during Top1cc repair, independently of the nature of the SSB.

The production of transcriptional DSBs requires the endonuclease XPF

It has been previously reported that transcriptional DSBs are produced by a mechanism dependent on R-loops in post-mitotic cells treated by CPT (Sordet et al., 2009). More recently, it has been reported that R-loops can be cleaved by the TCR endonucleases XPF and XPG (Sollier et al., 2014). We therefore tested the possibility that XPF-dependent cleavage of R-loops could be implicated in the generation of the second SSB on the opposite strand to the first SSB produced by Top1cc repair then, leading to the production of a DSB.

We found that depletion of XPF with siRNA significantly decreased the number of γH2AX and 53BP1 foci in CPT-treated quiescent WI38 hTERT cells (**Figure IIA-C**). To get additional evidence of the role of XPF in the production of transcription-dependent DSBs, we assessed whether its depletion also reduced CPT-induced DSBs under conditions where Tdp1 or PARP are inhibited. **Figure IIB-E** show that XPF depletion with siRNA reduced the number of γH2AX and 53BP1 foci induced by CPT in quiescent WI38 hTERT cells where Tdp1 was depleted with siRNA or PARP was inhibited with olaparib. Together, these results indicate that XPF contributes to the production of transcription-dependent DSBs in CPT-treated cells and further raise the possibility that it could mediate a SSB in the R-loop at the proximity of a SSB generated during Top1cc repair on the opposing DNA strand.

Transcriptional DSBs are preferentially formed at subtelomeric regions

To get insights into the mechanism of production of CPT-induced transcriptional DSBs, we wondered if it would be possible to identify some loci or regions where transcription-dependent DSBs are preferentially produced. To map the genomic localization of CPT-induced transcriptional DSBs, we analysed the distribution of γH2AX in post-mitotic human lymphocytes and serum-starved WI38 hTERT fibroblasts treated with CPT. As subtelomeric regions are highly rich in transcribed genes and have G-rich sequences that may be prone to R-loop formation (Duquette et al., 2004), we tested the hypothesis that the production of transcriptional DSBs could be favoured at subtelomeres. By using immunocytochemistry staining followed by DNA fluorescence *in situ* hybridization (ICC/DNA-FISH) to simultaneously visualize γH2AX and telomeres, in collaboration with William Bonner's group (NIH, USA), we found that approximately 70% of γH2AX foci were localized in proximity of telomeres in post-mitotic human lymphocytes treated with CPT (**Figure IIIA and B**). In the same conditions, only 25% of γH2AX foci localized near telomeres in lymphocytes exposed to IR at a dose that induced approximately 2 γH2AX foci per cell (as 25 µM of CPT in those cells). As a control, we showed that γH2AX foci did not localize near centromeres in lymphocytes treated with CPT. Then, we confirmed these observations by assessing γH2AX enrichment by ChIP in CPT-treated lymphocytes. We found that γH2AX was enriched at

subtelomeres (Actin β, SMARCA2, Telomere I), while it was not enriched at centromeres (TTF2, CCT6A, IKZF1) (**Figure IIIC**). In addition, γH2AX enrichment at subtelomeric regions was dependent on transcription since it was completely suppressed by the transcription inhibitor flavopiridol (**Figure IIIC**).

Then, we investigated whether the CPT-induced transcriptional DSBs were preferentially formed at subtelomeres also in serum-starved quiescent fibroblasts. By co-staining γH2AX foci with the telomeric markers TRF1 or TRF2 (telomeric-binding protein 1 or 2) as described (Rodriguez et al., 2012) or with the centromeric marker CENPA, we found that approximately 60-70% of γH2AX foci formed in proximity of telomeres (**Figure IIIF and G**). The specificity of the immunostaining and the percentage of foci that colocalized by chance were evaluated by co-staining CENPA with TRF2 and TRF1 with TRF2 (**Figure IIID and E**). Taken together, these results suggest that transcriptional-DSBs induced by CPT are not randomly distributed across the genome and give a rational to determine more precisely where they are formed for example by using ChIP-sequencing analyses of γH2AX.

The production of transcriptional DSBs in G1- and G2-phase cells requires Top1 proteolysis

It has been reported that CPT-induced transcriptional DSBs are also produced in EdU-negative replicating cells (Regairaz et al., 2011; Sordet et al., 2009; Zhang et al., 2011). We wondered whether transcriptional DSBs are produced by the same mechanism in replicating cells outside of S-phase than in serum-starved quiescent cells. To answer this point, at first, we analysed the production of transcriptional DSBs in G1- and G2- phase cells treated with CPT. We showed the production of DSBs by analysing the induction of γH2AX and p53BP1 foci in response to CPT in asynchronously growing WI38 hTERT cells (**Figure IVA and B**). In response to CPT, G1- and G2-phase cells can be distinguished from S-phase cells by a dotted instead of a pan-nuclear γH2AX staining as described (Bonner et al., 2008). Then, G2 cells can be distinguished from G1 cells because they are positive for CENP-F staining and they have a high DAPI signal compared to G1 cells as described (Beucher et al., 2009). To determine if DSBs are produced by the same mechanism in replicating cells outside of S-phase than in quiescent cells, we checked whether inhibiting Top1 proteolysis by the inhibition of the ubiquitin/proteasome system would prevent DDR signalling. We found that the proteasome inhibitor MG132, prevented the induction of γH2AX foci in G1- and G2- cells and decreased γH2AX signal in S-phase cells (**Figure IVC**). Inhibition of ubiquitination by G5 also decreased CPT-induced γH2AX signal analysed by western blot (**Figure IVE**), under conditions where it prevented Top1 degradation (**Figure IVD**). These results indicate that the ubiquitin/proteasome system is required for the formation of DSBs in CPT-

treated cells outside of S-phase and strongly suggest that CPT-induced transcriptional DSBs are produced by a general mechanism that is not limited to serum-starved quiescent cells. These findings also give the rational for the use of genetically modified cell lines that cannot be induced in quiescence by serum-starvation for further mechanistic studies.

FIGURE LEGENDS

Figure I. Inhibition of PNKP or LIG3 increases CPT-induced DSBs in quiescent WI38 hTERT cells. (**A-F**) Serum-starved cells were transfected with PNKP- or LIG3-targeting or nontargeting (Ctrl) siRNAs and then treated with CPT (25 μM) for 1 h. (**A,B**) Western blotting of the indicated proteins. αTubulin or KAP1: loading control. (**C,D**) Detection of SSBs by alkaline comet assays. (**C**) Representative pictures of nuclei. (**D**) Quantification of alkaline comet tail moments from one representative experiment (60-249 nuclei were analysed for each treatment) out of three. ***, $P < 0.001$; ****, $P < 0.0001$. (**E,F**) Co-staining of γH2AX (green) and 53BP1 (red). (**E**) Representative pictures. (**F**) Number of γH2AX foci per nucleus from one representative experiment (152-233 nuclei were analysed for each treatment) out of three. ****, $P < 0.0001$. In the microscopic images, nuclear contours, identified by DAPI staining (not shown), are indicated by dashed lines. Bars: 10 μm.

Figure II. Inhibition of XPF decreases CPT-induced DSBs in quiescent WI38 hTERT cells. (**A**) Serum-starved cells were transfected with XPF-targeting or nontargeting (Ctrl) siRNAs. Western blotting of XPF. αTubulin: loading control. (**B,C**) Serum-starved cells were transfected with XPF- and/or Tdp1- targeting or nontargeting (Ctrl) siRNAs, treated with CPT (25 μM) for 1 h and then co-stained for γH2AX (green) and 53BP1 (red). (**B**) Representative pictures. (**C**) Number of γH2AX foci per nucleus from one experiment (113-300 nuclei were analysed for each treatment) out of one to four. ****, $P < 0.0001$. (**D,E**) Serum-starved cells were transfected with XPF-targeting or nontargeting (Ctrl) siRNAs and treated for 1 h with olaparib (10 μM) before the addition of CPT (25 μM) for 1 h. Cells were then co-stained for γH2AX (green) and 53BP1 (red). (**D**) Representative pictures. (**E**) Number of γH2AX foci per nucleus from one experiment (116-439 nuclei were analysed for each treatment). ****, $P < 0.0001$. In the microscopic images, nuclear contours, identified by DAPI staining (not shown), are indicated by dashed lines. Bars: 10 μm.

Figure III. Preferential formation of γH2AX foci at subtelomeric regions after CPT treatment in post-mitotic human lymphocytes and serum-starved quiescent human cells. (**A**) Left and middle panels: representative confocal microscopy images of immunostaining of γH2AX (green) and fluorescence *in situ* hybridization of telomeres (red) in lymphocytes after treatment with CPT (25 μM, 1 h) or after ionizing radiation (IR: 0.2 Gy, 30 min). DNA was counterstained with DAPI (blue). Both treatments induce the production of approximately 2 γH2AX foci per nucleus. Images show the preferential localization of γH2AX foci at the proximity of telomeres in response to CPT but not in response to IR. Right panel: co-staining of CPT-treated lymphocytes (25 μM, 1 h) for γH2AX (green) and CENPA (red, centromeric marker) show that γH2AX foci do not form at the proximity of centromeric regions. (**B**) Percentages of γH2AX foci that form at the proximity

(proximal, black bars) or at distance (distal, grey bars) of telomeres (Telomeric-FISH) or centromeres (CENPA). The data show the average of two independent experiments ± SD, 30-40 cells were counted for each experiment. (**C**) Lymphocytes treated or not with flavopiridol (FLV, 1 μM) for 1 h before the addition of CPT (25 μM, 1 h) were sonicated to generate long chromatin fragments (> 1 Kb with high variability) and then immunoprecipitated by using an anti-γH2AX antibody. γH2AX enrichment was assessed by qPCR amplification using primers localized in subtelomeric (Actβ, SMARCA2, Telomere I) or pericentromeric (TTF2, CCT6A, IKZF1) regions. DNA recovery is calculated by setting untreated samples to 1. Data show the average ± SD of triplicates. ChIP analysis was performed in parallel by using a non-immune antibody (IgG) as negative control and an anti-H3 antibody as positive control (data not shown). For qPCR amplification, primers recognizing α-satellite regions at centromere were also used as negative control (data not shown). (**D-G**) Serum-starved WI38 hTERT cells were treated with CPT (10 μM, 1 h) before staining for the indicated proteins. DNA was counterstained with DAPI (blue). Bars: 10 μm. (**D**) Representative confocal microscopy images of immunostaining of CENPA (green, centromeric marker, left panel) or TRF1 (green, telomeric marker, right panel) with TRF2 (red, telomeric marker). Images show the specificity of antibody staining, CENPA and TRF2 do not colocalize while TRF1 and TRF2 perfectly merged (yellow). (**E**) Percentages of TRF2 foci that form at the proximity (proximal, black bars) or at distance (distal, grey bars) of centromeres (CENPA) or telomeres (TRF1). The percentage of TRF2 foci proximal to CENPA gives a measure of colocalization by chance. Data show the average of TRF2 foci per cell ± s.e.m. , 181-265 TRF2 foci were counted per condition. (**F**) Representative confocal microscopy images of immunostaining of γH2AX (green) whit TRF1 (red, left panel) or TRF2 (red, middle panel) or CENPA (red, right panel). Images show that γH2AX foci form preferentially at the proximity of telomeric regions. (**G**) Percentages of γH2AX foci that form at the proximity (proximal, black bars) or at distance (distal, grey bars) of centromeres (CENPA) or telomeres (TRF1 and TRF2). Data show the average of γH2AX foci per cell ± s.e.m. , 201-365 γH2AX foci were counted per condition.

Figure IV. The production of CPT-induced DSBs is dependent on proteasome activity in replicating WI38 hTERT cells in G1 and G2 phases. (**A**) Identification of the cell cycle phases in WI38 cells treated with CPT (25 μM) for 1 h and then co-stained for γH2AX (green) and CENP-F (red). DNA is counter-stained with DAPI (blue). S-phase cells are CENP-F positive and exhibited a pan-nuclear staining of γH2AX. G1- and G2-phase cells were distinguished from S-phase cells by their dotted γH2AX staining. G1 cells are negative for CENP-F and have a low DAPI content. G2 cells are positive for CENP-F and have high DAPI content. (**B**) Representative pictures of co-staining with γH2AX (green) and 53BP1 phosphorylated on S1778 (p53BP1) (red). DNA is counter-stained with DAPI (blue). Images were merged to determine colocalization (yellow). (**C**) Representative pictures of replicating WI38 cells treated with MG132 (50 μM, 1 h) before the addition of CPT (25 μM) for 1 h and then co-stained with γH2AX (green) and CENP-F (red). DNA is counter-stained with DAPI (blue). (**D**) Replicating WI38 cells were treated with G5 (1.5 μM, 0.5 h) before the addition of CPT (25 μM) for 1 h and then analysed by western blotting for the indicated proteins. αTubulin: loading control. In the microscopic images, nuclear contours, identified by DAPI staining are indicated by dashed lines. Bars: 10 μm.

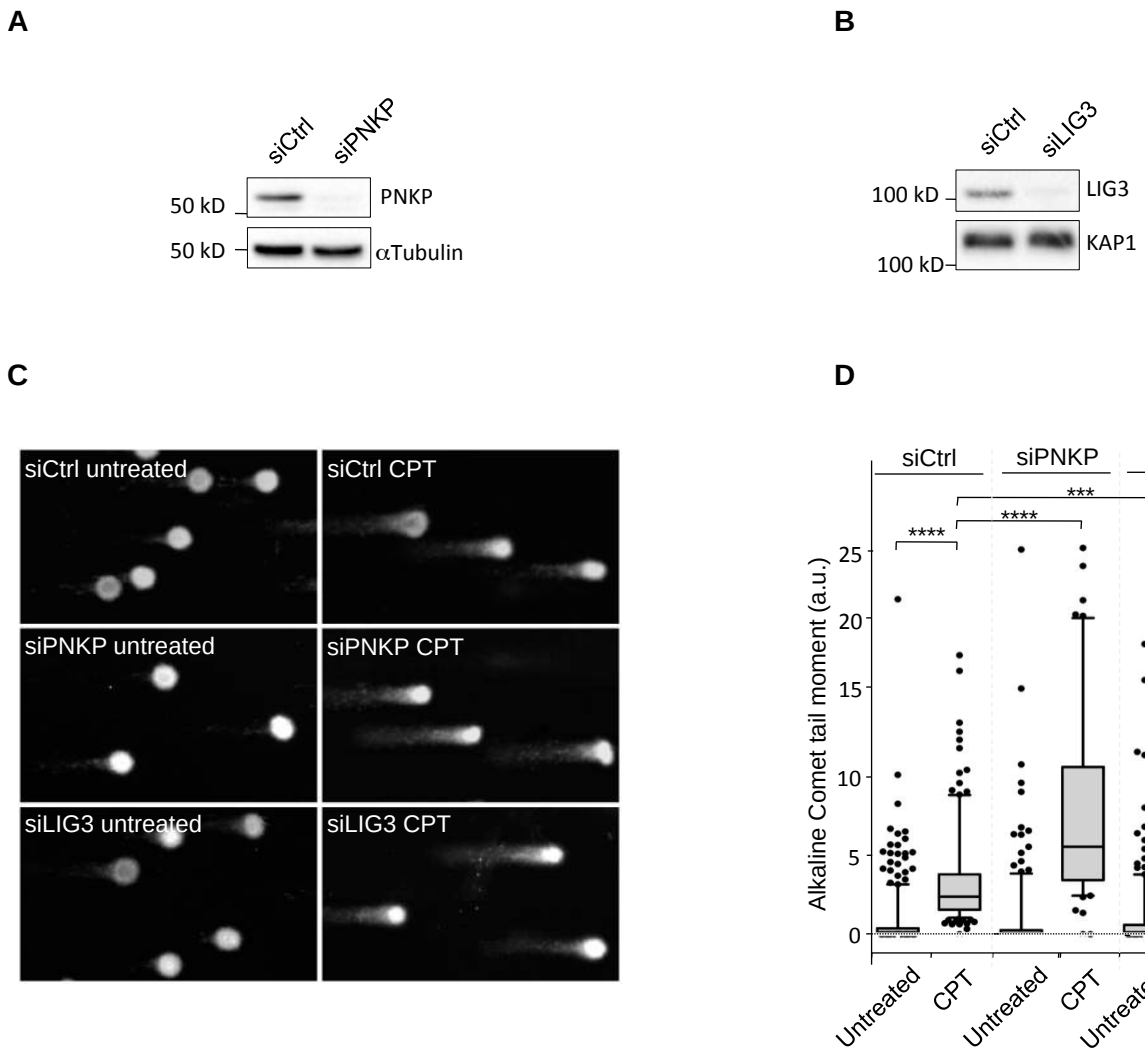
A
siCtrl
siPNKP
50 kD
PNKP
50 kD
αTubulin
B
siCtrl
siLIG3
100 kD
LIG3
100 kD
KAP1
C
siCtrl untreated
siCtrl CPT
siPNKP untreated
siPNKP CPT
siLIG3 untreated
siLIG3 CPT
D
siCtrl
siPNKP
siLIG3
****
****
***
Alkaline Comet tail moment (a.u.)
0
5
10
15
20
25
Untreated
CPT
Untreated
CPT
Untreated
CPT
E
siCtrl
siPNKP
siLIG3
Untreated
CPT
Untreated
CPT
Untreated
CPT
γH2AX
53BP1
F
siCtrl
siPNKP
siLIG3
****
****
****
γH2AX foci per nucleus
0
10
20
30
40
50
60
70
Untreated
CPT
Untreated
CPT
Untreated
CPT

Figure I

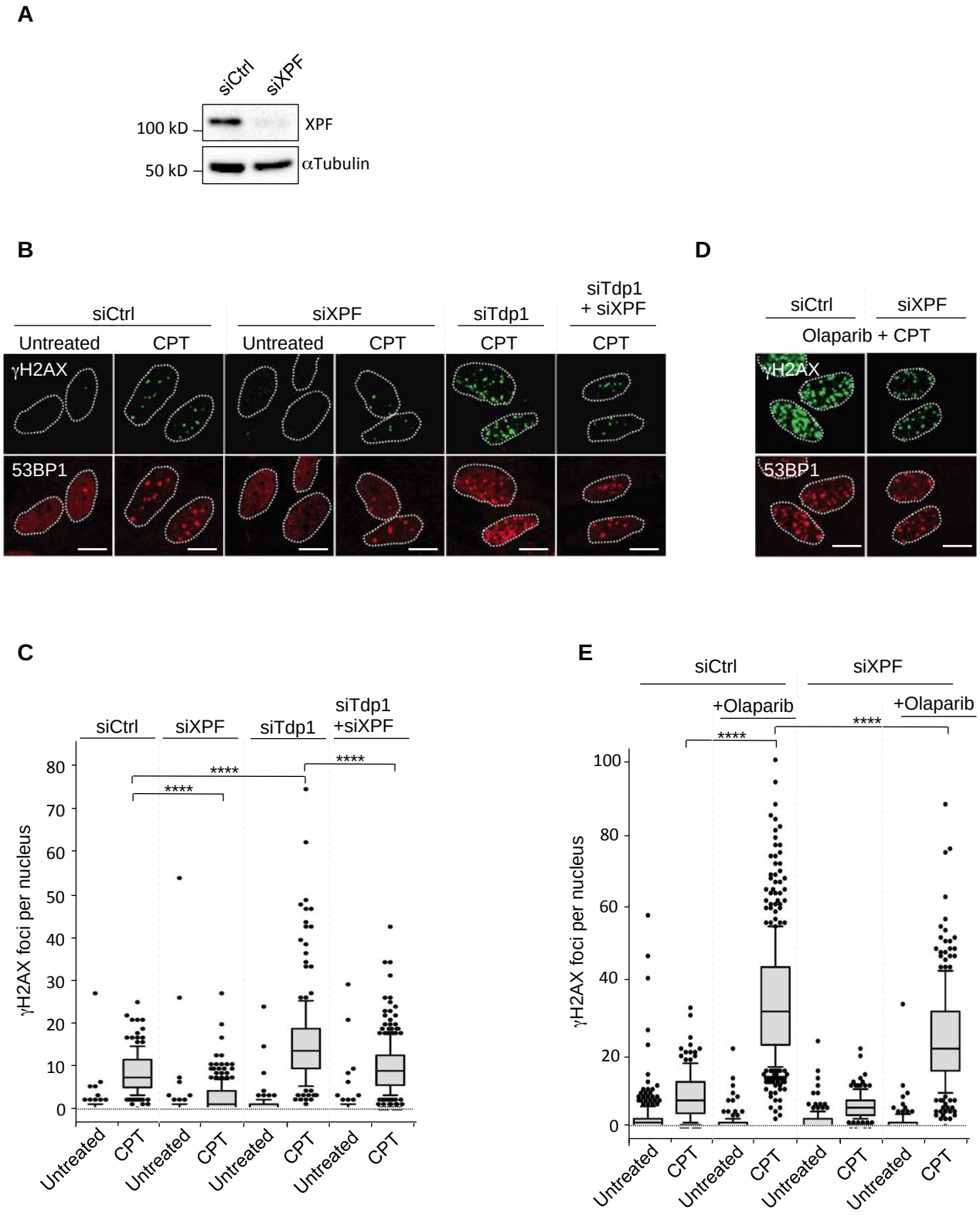
A
siCtrl
siXPF
100 kD
XPF
50 kD
αTubulin
B
siCtrl
siXPF
siTdp1
siTdp1 + siXPF
Untreated
CPT
Untreated
CPT
CPT
CPT
γH2AX
53BP1
D
siCtrl
siXPF
Olaparib + CPT
γH2AX
53BP1
C
siCtrl
siXPF
siTdp1
siTdp1 +siXPF
γH2AX foci per nucleus
****
****
****
Untreated
CPT
Untreated
CPT
Untreated
CPT
Untreated
CPT
E
siCtrl
siXPF
+Olaparib
+Olaparib
****
****
γH2AX foci per nucleus
Untreated
CPT
Untreated
CPT
Untreated
CPT
Untreated
CPT

Figure II

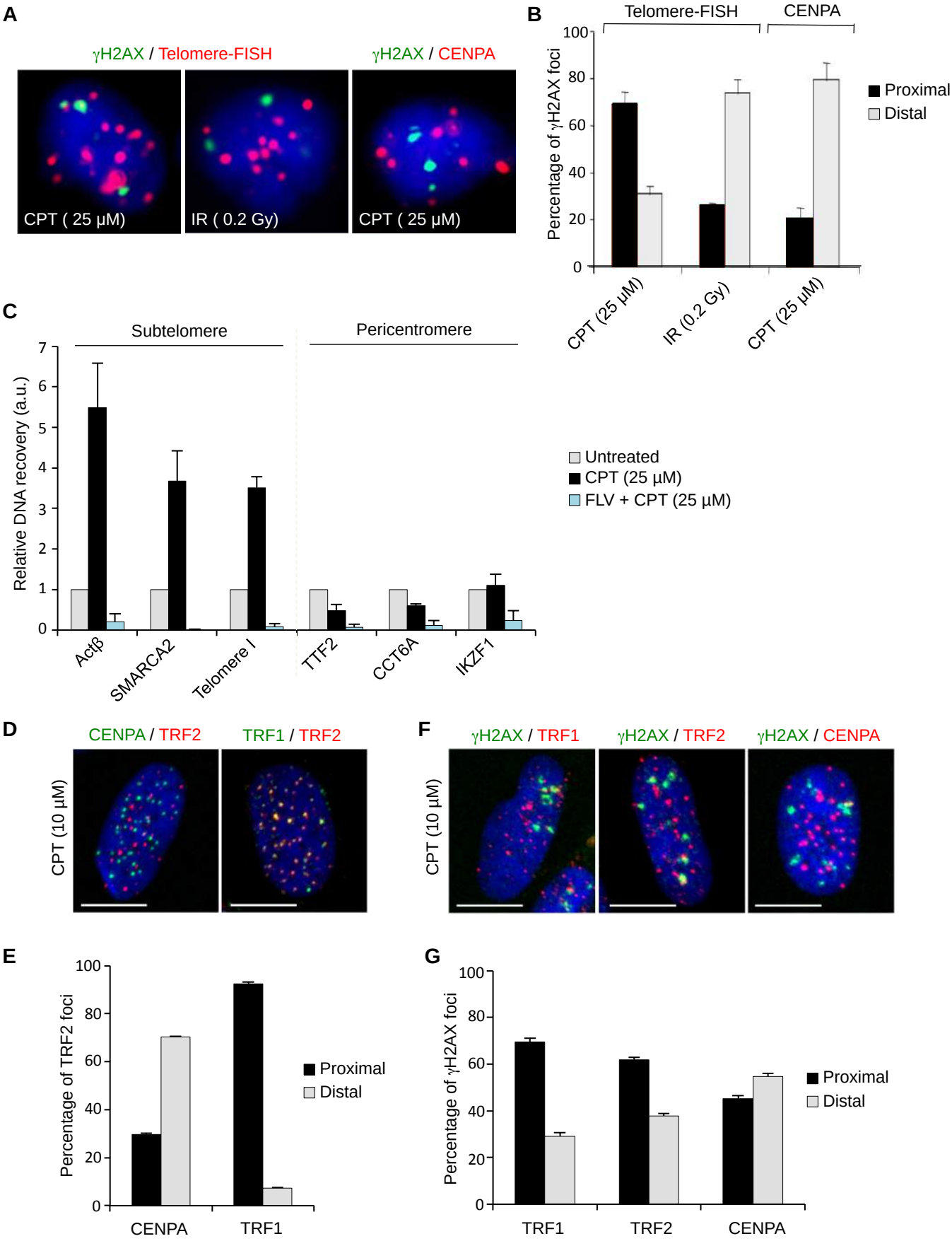
A
γH2AX / Telomere-FISH
γH2AX / CENPA
CPT (25 μM)
IR (0.2 Gy)
CPT (25 μM)
B
Telomere-FISH
CENPA
Percentage of γH2AX foci
Proximal
Distal
CPT (25 μM)
IR (0.2 Gy)
CPT (25 μM)
C
Subtelomere
Pericentromere
Relative DNA recovery (a.u.)
Untreated
CPT (25 μM)
FLV + CPT (25 μM)
Actβ
SMARCA2
Telomere I
TTF2
CCT6A
IKZF1
D
CENPA / TRF2
TRF1 / TRF2
CPT (10 μM)
F
γH2AX / TRF1
γH2AX / TRF2
γH2AX / CENPA
CPT (10 μM)
E
Percentage of TRF2 foci
Proximal
Distal
CENPA
TRF1
G
Percentage of γH2AX foci
Proximal
Distal
TRF1
TRF2
CENPA

Figure III

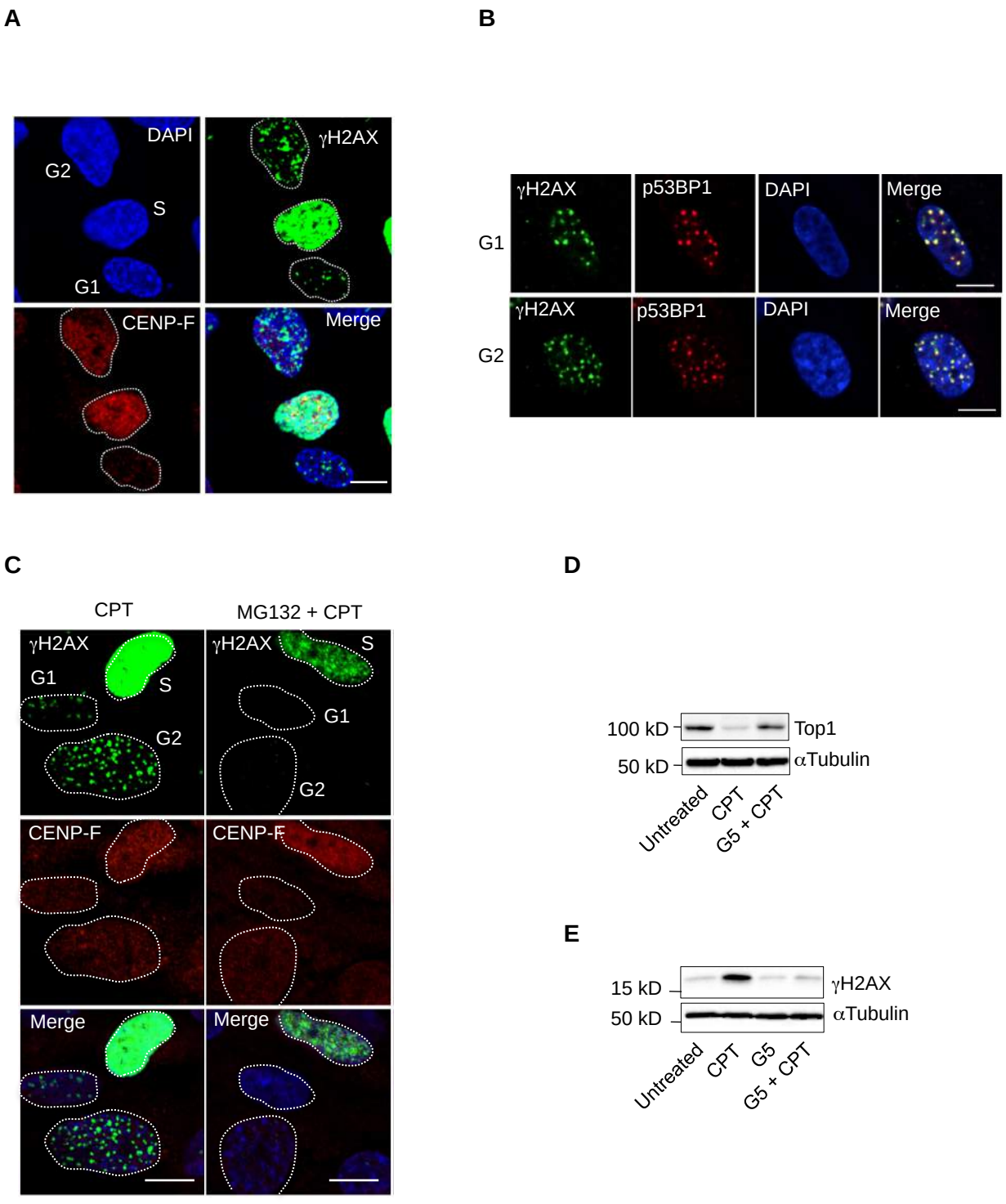
A
DAPI
γH2AX
G2
S
G1
CENP-F
Merge
B
γH2AX
p53BP1
DAPI
Merge
G1
G2
C
CPT
MG132 + CPT
γH2AX
S
G1
G2
CENP-F
Merge
D
100 kD
Top1
50 kD
αTubulin
Untreated
CPT
G5 + CPT
E
15 kD
γH2AX
50 kD
αTubulin
Untreated
CPT
G5
G5 + CPT

Figure IV

DISCUSSION AND PERSPECTIVES

My PhD's work has been focused on the study of DSBs produced by CPT-induced transcription-blocking Top1cc in the aim of uncovering their mechanisms of production and signalling. These DSBs are particular because:

- They are generated by Top1 covalently linked to DNA
- They are accompanied by an inhibition of the enzymatic activity of Top1, which results from Top1 trapping
- They are transcriptional DSBs: their production is dependent on transcription and they likely occur in actively transcribed regions.

The interest in characterizing these co-transcriptional DSBs is linked to the fact that they can be produced (i) endogenously as a result of Top1cc trapping by common DNA alterations or (ii) during chemotherapy as a result of selective Top1cc trapping by CPT derivatives. Our work reveals a new mechanism and a preferential genomic location of DSB production in response to stabilized Top1cc as well as a new function of DNA-PK in promoting ubiquitin signalling.

In the following section, we will discuss the main findings of this work in the context of literature, the open questions, the perspectives arising from this work and the possible relevance of transcriptional DSBs produced endogenously or during chemotherapy from transcription-blocking Top1cc.

1. The choice of quiescent cells as cellular model

To overcome the replication-related consequences of CPT treatment, we have chosen to use human primary WI38 fibroblasts immortalized with hTERT induced in quiescence by serum deprivation (**Figure 1A and B, paper**). Firstly, we have chosen primary cells because they have low genomic instability (Lobrich et al., 2010). Second, working in G1- and G2-phase cells requires the use of synchronization protocols that can potentially induce DNA damage or the use of cell cycle markers in asynchronously growing cells (**Figure IVA**) that are compatible with microscopy analyses (albeit not with multiple co-staining) but not with western blot experiments. Finally, post-mitotic cells also constitute a good model to study transcriptional DSBs (Sordet et al., 2009) but the available material is limited since they cannot be grown in culture. Another good model in complement to serum-starved quiescent cells for further experiments could be the SH-SY5Y neuroblastoma cell line. Different protocols can be used to differentiate SH-SY5Y in neuron-like cells that arrest to proliferate, form long neurites, express neuronal markers (Dwane et al., 2013) and behave like neurons in response to CPT (Tian et al., 2009).

2. Correlations between γH2AX foci and DSBs

γH2AX foci are the most common and used marker to detect DSBs, however the use of γH2AX has been debated as γH2AX can also reveal damage other than DSBs (Bonner et al., 2008; Lobrich et al., 2010). In our study we clearly demonstrated that CPT induces DSBs in non-cycling cells as (i) γH2AX foci colocalize with the other DDR proteins 53BP1 and MDC1 foci, (ii) neutral comet tail moment is increased, and (iii) ATM, DNA-PK and the downstream DDR pathway are activated.
In agreement with the literature (Sakai et al., 2012; Sakasai et al., 2010a; Sordet et al., 2009; Tian et al., 2009), TC-DSBs associate with large γH2AX and 53BP1 foci (**Figure 1F, paper**) compared with RC-DSBs or *AsiSi*-induced DSBs (**Figure 3F, paper**). A number of studies have shown a nearly one-to-one correlation between γH2AX foci and DSBs (Kinner et al., 2008; Lobrich et al., 2010). However, in our model few DSBs (≈3-5 foci/cells with 5-7.5 µM CPT, respectively) are able to increase the tail moment in neutral comet assay (**Figure 1I, paper**). This was unexpected as the limit of sensitivity of the neutral comet assay has been estimated to approximately 12.5-50 DSBs/cell depending on the cellular type (Olive and Banath, 2006; Redon et al., 2009; Wang et al., 2013). A tempting hypothesis might be that one large transcription-dependent γH2AX focus contains more than one DSB. For instance, multiple DSBs might occur simultaneously in a transcription factory as in the case of etoposide-induced DSBs (Cowell et al., 2012). To test whether one γH2AX focus corresponds to more than one DSB, it would be interesting to analyse the CPT-induced Ku and/or XRCC4 foci in serum-starved quiescent cells and determine how many Ku or XRCC4 foci are present in a single γH2AX focus as described (Britton et al., 2013). Detection of Ku foci would also be of interest in the context of DDR inhibition to directly visualize DSBs in the absence of γH2AX foci. Indeed, neutral comet assay shows an increase in DSBs in response to CPT upon ATM or DNA-PK inhibition (**Figure 5C, paper**) that cannot be studied by analysing DDR foci.

3. How are CPT-induced transcriptional DSBs produced?

Our results show that CPT-induced transcriptional DSBs produced in serum-starved quiescent cells arise from SSB intermediates generated during Top1cc repair by the Tdp1 excision pathway, independently of the nature of the SSBs (**Figure 2 and 4, paper and Figure IE and F**). Our model is consistent with previous works showing that: (i) CPT-induced Top1 downregulation is transcription and proteasome-dependent (Desai et al., 2001; Desai et al., 2003), (ii) Tdp1 primarily repairs transcription-blocking Top1cc (El-Khamisy et al., 2005; Miao et al., 2006) and requires

prior Top1 proteolysis (Debethune et al., 2002), (iii) proteasome inhibition prevents the activation of ATM in CPT-treated quiescent cells (Lin et al., 2008), and (iv) PARP inhibition or Tdp1 depletion increases the number of γH2AX and 53BP1 foci in response to CPT in post-mitotic and cycling cells (Katyal et al., 2014; Sakai et al., 2012; Zhang et al., 2011).

We have shown that similar to quiescent cells, CPT induces proteasome-dependent γH2AX foci in both G1- and G2-phase cells (**Figure IVA and B**). These observations strongly suggest that in replicating cells, transcriptional DSBs are produced during Top1cc repair by the same mechanism identified for quiescent cells. The results of *Zhang et al.* also support this possibility as PARP inhibition increases the number of γH2AX foci in response to CPT in the EdU negative population of replicating cells (Zhang et al., 2011). It would be interesting to further confirm the role of Top1cc repair in DSB production by analysing CPT-induced γH2AX foci in G1- and G2-phases in presence or not of transcription or proteasome inhibitors in genetically modified cell lines deficient for component of the Tdp1-excision pathway such as Tdp1 KO, PARP1 KO and Tdp1/PARP1 KO DT40 cells (Das et al., 2014; Murai et al., 2012) and PNKP shRNA human cells (Rasouli-Nia et al., 2004).

How to pass from a SSB to a DSB in the absence of replication?

How a SSB can give rise to a DSB in the absence of replication is still an unresolved question. Many scenarios are possible but our data clearly indicate that a required step for DSB production is the generation of a SSB during the repair of Top1cc and after Top1 proteolysis. Different hypothesis could be envisaged for DSB production:

- *A Top1-linked SSB opposite to a nicked DNA*

It has been shown that a DSB can arise by a CPT-induced Top1cc opposite to nicks or short gaps at positions -1/+1 or between the position +2/+6 from the Top1cc on the nonscissile strand (Pourquier et al., 1997a). Given the high rate of DNA damage per cell per day (Lindahl and Barnes, 2000), one possibility is that a DSB is generated by a nick or a gap in proximity of a Top1cc located in the opposite strand (**Figure 37A**).

- *Two nearby Top1cc*

A DSB may result from two nearby Top1cc-dependent SSBs within 10 bp (Pommier et al., 2014; Pourquier et al., 1997a; Wu and Liu, 1997) on opposing DNA strands. At least three possible configurations can be envisaged (**Figure 37B-D**): (i) two opposite SSBs generated after Top1 proteolysis (**Figure 37B**), (ii) one SSB generated after Top1 proteolysis and one SSB generated by an endonuclease (either to excise a Top1cc or not) (**Figure 37D**) (iii) one SSB generated after Top1

proteolysis and one unprocessed Top1cc (non-degraded Top1-linked SSB) (**Figure 37C**). The hypothesis that two Top1cc could be close to each other on opposing DNA strands is plausible because Top1 nicking-closing activity is increased in transcribed regions. It is also possible that two Top1cc on opposing DNA strands result from convergent transcription. To get insights into these hypotheses, it would be very helpful to determine where CPT-induced transcriptional DSBs are produced across the genome.

- *R-loop-dependent mechanism*

The second SSB may be caused by R-loop processing. A number of evidences support a participation of R-loops in the production of CPT-induced transcriptional DSBs: (i) Reduced Top1 activity causes R-loop formation (Drolet et al., 1994; Drolet et al., 1995; Tuduri et al., 2009) and CPT treatment increases R-loops *in vivo* (Groh et al., 2014; Marinello et al., 2013; Powell et al., 2013), (ii) RNaseH1 overexpression significantly reduces CPT-induced γH2AX signal in post-mitotic cells (Sordet et al., 2009) and (iii) R-loops formed in response to CPT are cleaved by the endonuclease XPG in replicating cells (Sollier et al., 2014).

To test if R-loops are implicated in DSB production in CPT-treated quiescent cells, we tried to overexpress RNaseH1 and analyse γH2AX. Unfortunately, we failed to overexpress RNaseH1 probably because of low transfection rate and/or low transcriptional rate of quiescent cells. Experiments are ongoing in the laboratory to deplete RNaseH1 by using siRNA as described (Groh et al., 2014; Tresini et al., 2015) and analyse the impact of RNAseH1 depletion in CPT-induced γH2AX foci in quiescent cells. In addition, it should be interesting to determine whether R-loops are in the same pathway of Top1cc's repair in the production of DSBs.

As the mechanism of DSB production seems to be the same in replicating cells outside of S-phase, we are planning to analyse the role of R-loops in cycling cells by using an ArrayScan Operetta. This could enable to avoid the employ of a cell-phase marker by using DAPI intensity to discriminate cell cycle phases. We could overexpress RNAseH1 in replicating cells and/or use cell lines inducible for WT or mutated RNAseH1 (Britton et al., 2014).

If R-loops are responsible for the production of the second SSB, the arising question is: how this second SSB is produced in the R-loop?

The ssDNA that is exposed during R-loop formation is particularly vulnerable to nucleases and other enzymes. The TCR flap endonucleases, XPF and XPG, have been recently identified as factors able to cleave R-loops (Sollier et al., 2014) (**Figure 37E and F**). Preliminary experiments in CPT-treated quiescent cells show that depletion of XPF significantly reduces the number of γH2AX foci (**Figure IIB and C**). Tdp1-excision pathway and XPF processing seem to contribute to DSB production by a common pathway, as XPF depletion decreases CPT-induced γH2AX foci in

quiescent cells depleted for Tdp1 or treated with PARP inhibitors (**Figure IIB-E**). Currently, we did not find consistent results for XPG depletion (data not shown). It will be interesting to confirm these observations by using other siRNA targeting XPF or XPG, by depleting ERCC1, the non-catalytic partner of XPF, and by using XPG- and XPF-deficient fibroblasts complemented with the wild type or the nuclease-dead proteins (as described (Sollier et al., 2014)) after serum-starvation.

However, in addition to the TCR pathway to process R-loop structures (Sollier et al., 2014), XPF can also work in the nuclease excision pathway to repair Top1cc (Vance and Wilson, 2002). It would be interesting to investigate the role of these cellular pathways in DSB production as both could account for the contribution of XPF to transcriptional DSBs that we observed (**Figure 37D and E**). To test the potential participation of TCR in CPT-induced transcriptional DSB, we could analyse the impact of CSB depletion in CPT-induced γH2AX foci, as CSB is also required for R-loop processing (Sollier et al., 2014). The work of *Sakai et al.* shows that CSB depletion partially decreases the number of transcriptional 53BP1 foci in response to CPT (Sakai et al., 2012) supporting this possibility. To investigate whether the role of XPF in CPT-induced transcriptional DSB depends on its role in Top1cc repair, we could analyse the impact of XPF depletion on Top1cc repair directly by measuring Top1cc levels or indirectly by measuring transcription resumption.

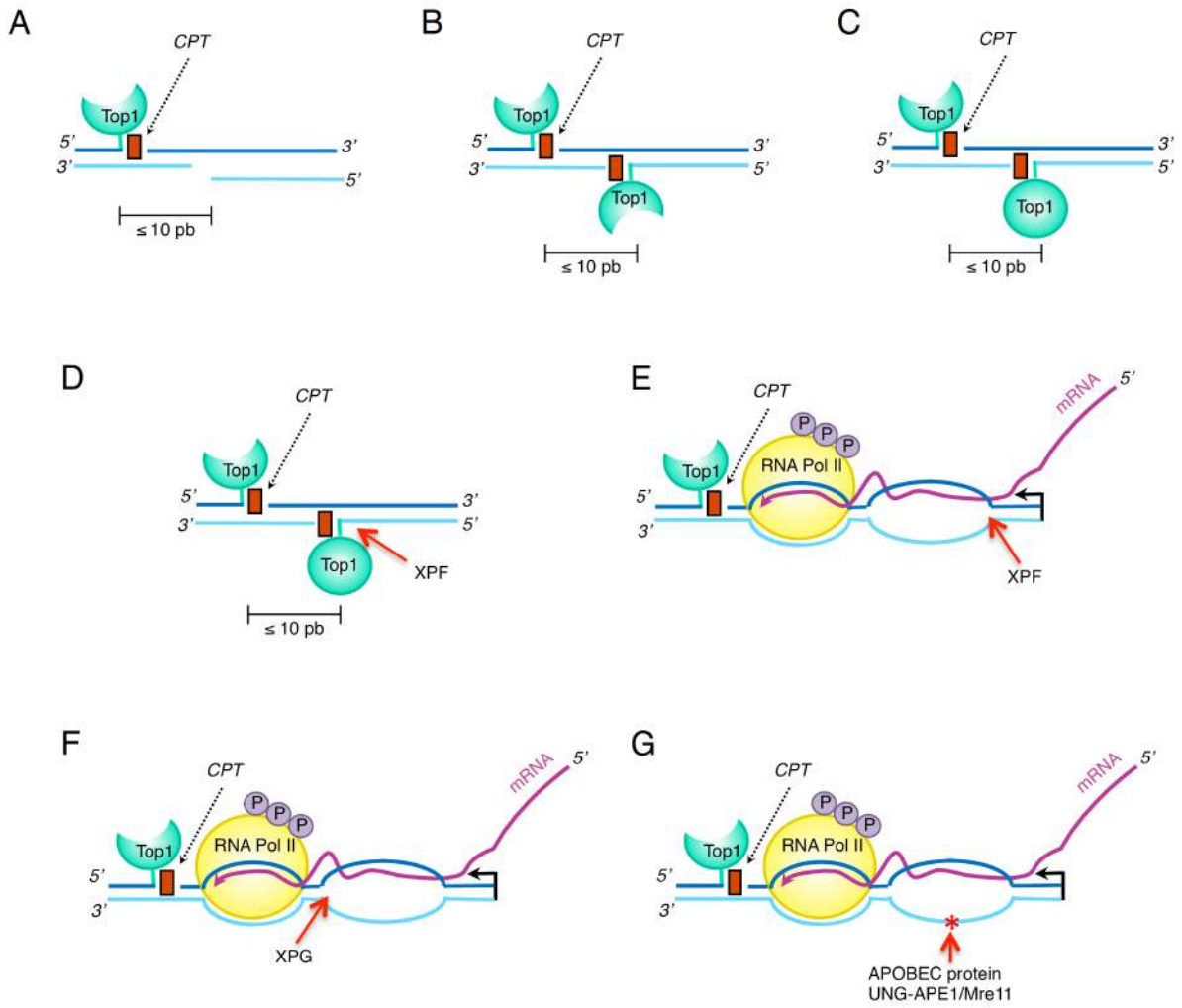

Figure 37: Possible mechanisms for generation of CPT-induced transcriptional-DSBs from a Top1cc. Formation of a DSB by a Top1cc-associated SSB and a second SSB created by (**A**) a pre-existing nick in the opposite strand, (**B-D**) another Top1cc in the opposite strand (see text for details), (**E**) the processing of the ssDNA exposed in a R-loop by the endonuclease XPF or (**F**) XPG or (**G**) by the deamination of a cytidine by an APOBEC protein followed by the generation of an AP site by UNG and the cleavage by the endonuclease APE1 or Mre11. Top1 is shown not proteolysed (full circle) or partially proteolysed (crescent-shaped). Red arrows indicate the cleavage of endonucleases and asterisk indicates the processing of a cytidine residue by the AID-UNG-APE1/Mre11 pathway.

In addition to TCR endonucleases, the ssDNA on the R-loop might be “attacked” by a cytidine deaminase member of the APOBEC (apolipoprotein B mRNA editing enzyme, catalytic polypeptide) family, of which AID (activation-induced cytidine deaminase) is a member. During CSR, AID promotes the conversion of cytidine to uracil specifically on ssDNA in co-transcriptional R-loops formed over the S (switch) regions at the Ig locus (Yu et al., 2003). Deamynated cytidine is deglycosylated by uracil-DNA glycosylase UNG with the subsequent creation of an abasic site, which can be converted in SSB by APE1 (apurinic-apirimidic endonuclease) or Mre11 endonucleases. In B-lymphocytes, AID can initiate DSBs in a small subset of non-Ig genes (Chiarle et al., 2011). It has been proposed that other APOBEC members might act in a similar manner in

cells that do not express AID (Burns et al., 2013; Sollier and Cimprich, 2015). Hence, we may consider also a possible participation of this mechanism to transcriptional DSBs (**Figure 37G**).

- *Other factors*

We can't exclude the participation of other factors, in particular nucleases that might cleave the opposite strand to Top1cc. Indeed, in post mitotic cells RNaseH1 overexpression only partially prevents γH2AX signal (about ≈50%) (Sordet et al., 2009) suggesting that other mechanisms in addition to R-loops should contribute to DSB formation. Similarly, XPF depletion does not completely prevent CPT-induced γH2AX foci in serum-starved quiescent cells. Therefore, it would be interesting to perform a siRNA screening to identify potential other factors implicated in DSB production.

4. Genomic localization of CPT-induced transcriptional DSBs

Our results show that transcriptional DSBs induced by CPT tend to form at subtelomeric regions in post-mitotic lymphocytes and quiescent WI38 fibroblasts (**Figure III**). Why CPT-induced transcriptional DSBs should be produced preferentially at subtelomeres?

Subtelomeric regions can be defined as the terminal 500 Kb of each euchromatic chromosome arm and they are highly enriched in transcripts (Riethman et al., 2005). Thus, one possibility is that CPT-induced transcriptional DSBs could be preferentially localized at those regions simply because of the high transcriptional rate that increases the probability of collisions of stabilized Top1cc with ongoing RNAPII.

Another possibility is that the sequence's characteristics of these regions may promote CPT-induced transcriptional DSBs. For instance, telomeric repeats may constitute a high concentration of nested Top1 cleavage sites, as each telomeric repeat represents a potential Top1 cleavage site *in vivo* (Kang et al., 2004). Indeed, Top1 can cleaves efficiently 5'-TT*AGGG-3' (cleavage site marked by *) telomeric repeats in the presence of CPT *in vitro* and Top1cc have also been detected at telomeric repeats *in vivo* in CPT-treated cells (Kang et al., 2004). Subtelomeric regions are enriched about 25-fold in $(TTAGGG)_n$ repeats compared to elsewhere in the genome (Riethman et al., 2005). Subtelomeres are also G-rich regions (Riethman et al., 2005) and G clusters and G density are two factors that promote the formation and the stabilization of R-loops (Roy et al., 2010). As R-loops are involved in DSBs production (Sordet et al., 2009), regions prone to R-loops formation may be enriched in DSBs.

A third possibility is that transcription-associated DSBs induced by Top1cc tend to form not generically at subtelomeric regions but at some specific genes localized at subtelomeric regions.

Consistently with this hypothesis, γH2AX foci have been found enriched at IgH locus, which is known to form R-loops during CSR, in unstimulated splenocytes treated with CPT (Sordet et al., 2010). The IgH genes constitute one of the subtelomeric gene families (Riethman et al., 2005).
The precise identification of some genes or regions where transcriptional-DSBs are produced across the genome should be extremely useful to understand the mechanism of DSB production and signalling:

- The analysis of the loci where DSBs are preferentially formed should give precious mechanistic information such as, for example, if DSBs are produced at convergent transcription units.
- DSB localization will allow the use of ChIP or ICC/DNA-FISH at specific sites. For instance, it should allow the mapping of the position of RNAPII and Top1cc relatively to the DSB. According to the "collision model", TC-DSBs have been predicted to occur in the 5' region of actively transcribed gene not far from the promoter (Wu and Liu, 1997) as Top1cc arrests RNAPII early in transcription (Khobta et al., 2006). Interestingly, nucleases XPF and XPG are enriched at promoter of particular genes, where they induce DNA breaks, DNA demethylation and the establishment of active chromatin marks required for gene expression (Le May et al., 2012). Thus, it should be interesting to analyse directly by ChIP at a single site, factors that mechanistically may promote DSB production from a transcription-blocking Top1cc.
- DNA sequence's characteristics should give insights about the correlation between DSB formation and the presence of R-loops or alternative DNA structures (such as G-quadruplex). The availability of antibodies against anti DNA-RNA hybrids (S9.6) (Boguslawski et al., 1986) or anti G-quadruplex (Biffi et al., 2013; Henderson et al., 2014), should then allow the direct detection of those structures at sites where γH2AX is enriched after CPT-treatment by ChIP/DNA or immunofluorescence experiments.

Experiments are ongoing in the laboratory to map transcriptional DSBs based on γH2AX genomic distribution in CPT-treated quiescent cells by using ChIP-sequencing approach.

5. What are the components of the ubiquitin-proteasome system that degrade Top1?

As already described in literature (Desai et al., 2003), we confirmed that CPT induces proteasomal degradation of Top1 in a transcription-dependent manner (**Figure S2A-C, paper**). Deciphering the ubiquitination cascade and the component of the UPS (ubiquitin-proteasome system) involved in Top1 downregulation is important in understanding the response of cancer cells to CPTs as deficient Top1 downregulation is a feature of many cancers and hypersensitizes cells to CPT (Desai

et al., 2001). We found that CPT treatment triggers accumulation of the E1-activating enzyme UBA1 (**Figure 7C, paper**) at chromatin supporting a role of UBA1 in catalysing Top1 ubiquitylation as previously suggested by defects in Top1 degradation in ts85 cells (Ban et al., 2013; Desai et al., 1997). While E2-ubiquitin conjugating enzymes for Top1 are not known, several E3 ligases have been implicated such as Cul3 (Lin et al., 2009; Zhang et al., 2004), Cul4A and Cul4B (Kerzendorfer et al., 2010). Our data confirmed that depletion of Cul3 and Cul4B prevents Top1 downregulation, but the effect is only partial (**Figure 3A and B, paper**) suggesting that other E3s may regulate Top1 ubiquitylation in addition to cullins. To evaluate the implication of cullins versus non-cullins E3-ligases, a new approach could be the use of the neddylation inhibitor MLN4924, which inhibits cullins' activity (Soucy et al., 2009). siRNA or shRNA-based approaches do not inhibit cullins' activity to a level comparable with MLN4924 (Brown et al., 2015). This could also explain the moderate effect in the prevention of Top1 degradation and γH2AX induction that we found with siRNA against Cul3 and Cul4B (**Figure 3A-C, paper**). If MLN4924 does not completely prevent Top1 degradation, it should mean that non-cullin E3 ligases might also directly ubiquitylate Top1. Accordingly with this possibility, BRCA1 depletion impairs Top1 downregulation (Sordet et al., 2008b) and BARD1 can interact with Top1 (Trzcinska et al., 2002). Similarly, we observe that siRNA against RNF2 prevent Top1 degradation of the same extent than that one found upon cullin's depletion (data not shown). Moreover, RNF2 can interact with Top1 (Cao et al., 2014). BMI-RNF1, that work in the same complex of RNF2 (PCR1) (Ismail et al., 2010), have also been described to ubiquitylate and to induce the degradation of Top2α in response to teniposide (Alchanati et al., 2009). Further studies should directly analyse whether BRCA1/BARD1 or RNF2/BMI1/RNF1 ubiquitinate Top1 in response to CPT *in vivo*. As alternative to siRNA approaches, PRT4165, an inhibitor of RNF1 and RNF2 recently described (Alchanati et al., 2009), could be used.

We also report for the first time the enrichment in the chromatin fraction of the 20S proteasomal subunit PSMA6 and of the proteasomal activity in response to CPT (**Figure 7C and 7E, paper**). It has already been described in literature that proteasome is recruited to chromatin in response to DSBs (Blickwedehl et al., 2007; Butler et al., 2012; Galanty et al., 2012; Levy-Barda et al., 2011). Proteasome subunits also accumulate at chromatin in response to etoposide and it has been proposed that this recruitment is dependent on Top2cc (Ban et al., 2013). Hence, the recruitment of proteasome at chromatin in response to CPT may be triggered by DSB production or it may depend on trapped Top1cc. We tried to analyse by immunofluorescence microscopy after detergent extraction the co-staining of PSMA6 and γH2AX. Although PSMA6 and γH2AX colocalize into laser "strip" (Levy-Barda et al., 2011), we were not able to detect a signal for PSMA6 in response

to CPT. Then, given the low level of DSBs in our system compared to laser microirradiation and given the massive Top1 degradation triggered by CPT, it can be speculated that the observed enrichment of proteasome at chromatin may be driven by Top1 trapping rather than by DSBs.

Proteasome accumulation at chromatin together with the requirement of Top1 proteolysis for Tdp1 to cleave the covalent bond between the Top1 catalytic tyrosine and the 3' end of the DNA support a model in which Top1 is degraded, at least in part, directly at chromatin. However, it should be interesting to evaluate whether the p97/VCP segregase also participates to Top1 downregulation by extracting Top1cc from chromatin and delivering them to the proteasome. Indeed, recently p97/VCP has been reported to extract Cul3/Cul4B K48-polyubiquitylated substrates from chromatin at UV lesion sites (Puumalainen et al., 2014). Thereby, Top1cc could be a potential p97/VCP substrate and the interaction between Top1 and p97/VCP has been already described (Yu et al., 2013). Interestingly, p97/VCP can also interact with BRCA1 (Zhang et al., 2000) and WRN (Indig et al., 2004) and can be phosphorylated by DNA-PK in response to DNA damage (Livingstone et al., 2005), all factors that control Top1 degradation (Christmann et al., 2008; Sordet et al., 2008b) (**Figure 7A and B, paper**).

6. DDR signalling of CPT-induced transcriptional DSBs

To study the DDR signalling activated by CPT-induced transcriptional DSBs, we analysed the three main kinases involved in H2AX phosphorylation, ATM, ATR and DNA-PK (Bonner et al., 2008). We found that ATR is not implicated in the formation of γH2AX foci in response to CPT in quiescent cells (**Figure 5A, paper**). This is consistent with ATR being expressed at low levels in non-cycling cells (Sordet et al., 2009) (**Figure S3D, paper**). In addition, although it has been reported that ATR can be activated by a transcriptional stress (Derheimer et al., 2007)**,** the main role of ATR is in the response to replication stress (Cimprich and Cortez, 2008; Zeman and Cimprich, 2014).

By contrast, CPT activates both ATM and DNA-PK and their inhibition impairs γH2AX foci formation without preventing DSB induction as measured by neutral comet assay (**Figure 5A-E, paper**). In agreement with previous findings in post-mitotic cells, ATM is the main transducer of TC-DSBs (Katyal et al., 2014; Sordet et al., 2009). Although ATM and DNA-PK function redundantly to phosphorylate H2AX (Stiff et al., 2004), in post-mitotic cells, DNA-PK is activated but it does not impact γH2AX foci in response to CPT (Katyal et al., 2014; Sordet et al., 2009) suggesting that its role may be different in serum-starved quiescent cells versus post-mitotic cells. However, after CPT removal, the maintaining of γH2AX foci is dependent on DNA-PK activity in

quiescent astrocytes (Katyal et al., 2014) indicating that DNA-PK may be implicated in DDR also in post-mitotic cells.

The functional relationship between ATM and DNA-PK in the DSB response is complex.

ATM can phosphorylate DNA-PK in T2609 (ABCDE cluster) in response to IR (Chen et al., 2007) and during apoptosis (Solier et al., 2009). In post-mitotic cells (Sordet et al., 2009) and in serum-starved quiescent cells (**Figure 5D and E, paper**) the activation of DNA-PK is dependent on ATM. We found that, in serum-starved quiescent cells, ATMi also blocks S2056 phosphorylation (**Figure 5E, paper**). By contrast, we found that CPT induces DNA-PK phosphorylation on S2056 in cycling WI38 hTERT cells in the presence of ATMi (data not shown), as already described in HeLa cells (Sakasai et al., 2010b).

The crosstalk between ATM and DNA-PK is mutual. Indeed, it has been described that depletion of DNA-PKcs triggers downregulation of ATM protein level (Chan et al., 1998; Gately et al., 1998; Peng et al., 2005). DNA-PK can also phosphorylate ATM on S1981 in apoptotic cells (Solier et al., 2009). Moreover, we describe a new role of DNA-PK in promoting ATM localization at chromatin in response to CPT (**Figure 5F-G, paper**). DNA-PK activity is not required for ATM activation in response to CPT (**Figure 5E, paper**), but it is required for the assembly of activated ATM into nuclear foci and for the phosphorylation of ATM substrates (**Figure 5F-G and S3F, paper**). This role of DNA-PK is independent of its function in NHEJ (**Figure S4, paper**) and it is likely related to the function of DNA-PK in promoting H2AX and H2A ubiquitylation (**Figure 6, paper**), which is required for ATM foci formation (Facchino et al., 2010; Pan et al., 2011).

Furthers studies are needed to clarify the complex interplay between ATM and DNA-PK and the differences in their reciprocal regulation in quiescent cells versus replicating cells.

7. A new function of DNA-PK in promoting ubiquitylation

To our knowledge, our work describes for the first time a function of DNA-PK in promoting ubiquitylation. We found that in response to CPT, DNA-PK activity stimulates ubiquitylation of histones H2A, H2AX (**Figure 6A-C, paper**) and Top1 proteolysis (**Figure 7A and B, paper**) and in addition, it favours the accumulation of ubiquitin-proteasome components and proteasome activity at chromatin (**Figure 7C and E, paper**). Previous studies have already suggested a possible connection between DNA-PK and proteasome. DNA-PK arrests transcription when the RNAPII machinery comes across a single DSB by a mechanism dependent on proteasome activity (Pankotai et al., 2012). DNA-PK activity is also required to recruit the coactivator PA200 and the 20S subunit of proteasome in response to high doses of IR (Blickwedehl et al., 2008). Furthermore, the

inhibition of proteasome by bortezomib has been reported to inhibit the formation of ATM foci in response to IR without blocking ATM activation (Jacquemont and Taniguchi, 2007), the same phenotype that we observe upon DNA-PK inhibition (**Figure 5E-G, paper**). This could be explained by a depletion of nuclear free ubiquitin pool driven by proteasome inhibition (Dantuma et al., 2006) that consequently leads to the loss of H2A and H2AX monoubiquitination on K119/K120 necessary for the assembly of activated ATM into foci (Facchino et al., 2010; Pan et al., 2011). Some works show that the absence of H2A(X) monoubiquitination impairs foci formation of early DDR proteins such as γH2AX and MDC1 (Facchino et al., 2010; Pan et al., 2011) while others show the detection of these early markers (Ismail et al., 2010). *Pan et al.* explain this apparent discrepancy by showing that in the absence of H2A(X) monoubiquitination, the kinetic of γH2AX foci is just delayed after IR since at later time points (also 1 hour) H2AX is phosphorylated in a DNA-PK-dependent manner (Pan et al., 2011). This is consistent with our experiments: in presence of DNA-PKi, H2A and H2AX are not ubiquitylated, activated ATM fails to accumulate to chromatin and to phosphorylate H2AX and inhibited DNA-PK cannot compensate for H2AX phosphorylation resulting in a defect in γH2AX foci (**Figure 5A-C, paper**). By contrary, although proteasome inhibition leads to a defect in H2A(X) monoubiquitination (Dantuma et al., 2006), it does not impact γH2AX foci formation in response to IR and to *AsiSI* (**Figure 3D-G, paper**) as DNA-PK may compensate for the defect of ATM activity.

How DNA-PK promotes ubiquitylation in response to CPT?

It would be interesting to determine how DNA-PK regulates protein ubiquitylation. Phosphorylation is known to regulate protein ubiquitylation mainly in two ways (Hunter, 2007):

- *Regulation of E3 ubiquitin-ligase activity*

Phosphorylation of E3 ligases positively or negatively regulates their ubiquitin transfer activity. Several E3 ubiquitin ligases have been implicated in the ubiquitylation of H2AX and H2A (RNF2, RNF8, RNF168, BRCA1) (Doil et al., 2009; Huen et al., 2007; Pan et al., 2011; Zhu et al., 2011) and of Top1 (Cul3, Cul4A, Cul4B, BRCA1) (Kerzendorfer et al., 2010; Sordet et al., 2008b; Zhang et al., 2004). Our preliminary results show also a possible implication of RNF2 in Top1 degradation (data not shown). To our knowledge, it is not known whether these ligases can be phosphorylated by DNA-PK *in vivo*. One attractive hypothesis is that DNA-PK by phosphorylating RNF2 and/or BRCA1 may positively regulate their activity and then, these E3 ligases may ubiquitinate H2A and/or Top1. Some evidences in literature could support this scenario:

(i) RNF2 and BRCA1 can form an E3-ligase complex (RNF2-BMI1 and BARD1-BRCA1) (Ismail et al., 2010; Nishikawa et al., 2004), participate to DSB response and are recruited to chromatin (Ismail et al., 2010; Wang et al., 2007).

(ii) RNF2 and BRCA1 can catalyse monoubiquitylation of H2A(X) (Pan et al., 2011; Zhu et al., 2011) and promote Top1 downregulation (data not shown) (Sordet et al., 2008b)

(iii) RNF2 (Cao et al., 2014) and BARD1 (Trzcinska et al., 2002) can interact with Top1 (analysed by using BioGRID v3.4 database, http://thebiogrid.org/)

(iv) BMI1 co-purify with DNA-PK (Facchino et al., 2010). In addition, RNF2 contains three putative phosphorylation sites for DNA-PK in its N-terminal region (S2, T10, S20) (predicted by using NetPhosK v1.0, http://www.cbs.dtu.dk/services/NetPhosK/). BRCA1 interacts with DNA-PK via its tBRCT domains (Davis et al., 2014) and it can be phosphorylated by DNA-PK *in vitro* on S1387 and S1466 (Kim et al., 1999).

Hence, it should be interesting to investigate whether DNA-PK can phosphorylate BRCA1 and RNF2 *in vitro* and *in vivo* and then, the eventual role of these phosphorylations in H2A and Top1 ubiquitination in response to CPT.

- *Regulation of E3 ubiquitin-ligase substrate selection: creation of a phosphodegron*

Phosphorylation itself can create a recognition signal for binding of an E3 ligase thereby it is possible that DNA-PK phosphorylates H2A(X) and Top1 targeting them for ubiquitylation. Effectively, DNA-PK can phosphorylate H2AX (Stiff et al., 2004) but it is unlikely that this is what primes H2AX for ubiquitination because H2A lacks S139 but is also ubiquitinated in response to DSBs (Mosammaparast et al., 2013). By contrast this scenario is plausible for Top1. Firstly, Top1 phosphorylation has been reported *in vitro* and *in vivo* and it seems to interest the first N-terminal amino acids of Top1 (Durban et al., 1985; Pommier et al., 1990). Secondly, DNA-PK interacts with the N-terminal domain of Top1 (Czubaty et al., 2005), which presents a potential phosphorylation site for DNA-PK (SQ motif on S10) (predicted by using NetPhosK v1.0). Top1 overexpressing cells are characterized by a lack of additional sensitivity compared to control cells and by the elimination of the hyperphosphorylated form of Top1 (St-Amant et al., 2006). As Top1 degradation is a potential mechanism of CPT resistance (Desai et al., 2001), one hypothesis is that phosphorylated Top1 might be targeted to degradation leading to CPT resistance. Further studies should be done to elucidate the role and the potential relevance of Top1 phosphorylation. Indeed, Top1 immunoprecipitation in presence or not of DNA-PKi and immunoblotting with an antibody recognizing phosphorylated serine should give a first information about the implication of DNA-PK in Top1 phosphorylation. If DNA-PK inhibition decreases the phosphorylation of Top1, it could be

interesting to generate a Top1 mutant non-phosphorylatable on S10 and analyse its ubiquitylation and its degradation in response to CPT.

These two mechanisms of regulation are both plausible and they are not mutually exclusive. Furthermore, other scenarios cannot be excluded:

- Phosphorylation can also regulates ubiquitination by regulating substrate/ligase interaction at the level of subcellular localization. For example, phosphorylation of p27Kip1 on S10 triggers nuclear export, allowing p27Kip1 to be degraded by cytoplasmic E3 ligases (Besson et al., 2006).
- E1 and/or E2 enzyme may also be regulated by DNA-PK phosphorylation or recruited by phosphorylation of the substrates, as we found that DNA-PK favours the recruitment of UBA1 at chromatin in response to CPT (**Figure 7C, paper**). As the specificity of ubiquitylation reaction is given by E3 ligases while few E1 and E2 enzymes regulate more substrates, the DNA-PK dependent regulation of an E1 or an E2 should mean that DNA-PK regulates ubiquitination of many cellular substrates by a general mechanism.
- Finally, phosphorylation may regulate the activity of DUBs (Villamil et al., 2012). Indeed, large-scale phosphoproteomic analyses of human DUBs have revealed that 37 of 55 USPs are phosphorylated (Olsen et al., 2006).

Does DNA-PK regulate the fate of stalled RNAPII at transcriptional DSBs produced by CPT?

DNA-PK might also regulate RNAPII turnover in the presence of transcription-blocking DSBs. One possible hypothesis is that DNA-PK phosphorylates RNAPII blocked by a CPT-induced TC-DSB targeting it for degradation. This possibility is compatible with data of *Pankotai et al.* showing that DNA-PK controls transcription inhibition in the presence of a single endonuclease-generated transcriptional DSB by a proteasome-dependent mechanism (Pankotai et al., 2012). Furthermore, DNA-PK is able to phosphorylate RNAPII *in vitro* (Dvir et al., 1992). RNAPII is also rapidly hyperphosphorylated in response to CPT on S5 (Sordet et al., 2008b) and S2 (Dutertre et al., 2010) and modestly degraded at later time point (6 h) (Desai et al., 2003). As expected, our preliminary observations confirm that 1 h of CPT treatment induces an increase of the hyperphosphorylated form of RNAPII and of the S5 phosphorylation. Hyperphosphorylation of both total RNAPII and S5 are decreased in presence of the DNA-PK inhibitor (data not shown). However, in response to UV, S5 phosphorylation of the CTD blocks RNAPII ubiquitination, whereas S2 phosphorylation promotes its ubiquitination (Somesh et al., 2005). Hence, it should be interesting to analyse the effect of DNA-PK inhibition on S2 phosphorylation in response to CPT. Further studies should

elucidate the fate of RNAPII stalling at CPT-induced transcriptional DSBs and the mechanism of RNAPII degradation induced at later time points. In particular, the identification of a site where a CPT-induced DSB is preferentially produced may be helpful in determining where and when RNAPII is degraded in response to CPT and whether degradation is controlled by DNA-PK dependent phosphorylation.

8. Caveats in studying the role of DNA-PK in the signalling of transcriptional-DSBs

To study the role of DNA-PK in DDR signalling of CPT-induced transcriptional DSBs in our system we used NU7441, a specific inhibitor of the DNA-PK kinase activity (Leahy et al., 2004). DNA-PKcs autophosphorylation is required for releasing DNA-PKcs from chromatin (Uematsu et al., 2007). Consistently, DNA-PKi leads to strong persistence of IR-induced Ku foci (Britton et al., 2013). During our work, we wondered whether the function of DNA-PK in CPT-induced DDR was related to the physical persistence of DNA-PK at DSBs as result of DNA-PK inhibition. However, it is not easy to answer to this point. We tried to deplete DNA-PKcs (**Figure S5B, paper**) or Ku70 (data not shown) by siRNAs. In both case, given the extremely abundance of these two proteins in cells, siRNAs downregulate protein level only at a little extent (approximately of 40-50%). Furthermore, consistently with literature (Peng et al., 2005), siRNAs against DNA-PK strongly decrease ATM protein level making difficult to decouple ATM- and DNA-PK-dependent DDR signalling (data not shown). The same problem is given by the use of DNA-PK deficient cells, like MO59J cells (Gately et al., 1998). A good possibility will be to use DNA-PK kinase dead (KD) cells to confirm the results obtained by using DNA-PKi. CHO and MEFs DNA-PK-KD are available (Jiang et al., 2015; Shrivastav et al., 2009). Furthermore, MEFs can be induced in quiescence by serum-starvation (Lin et al., 2008; Lin et al., 2013).

9. The cytotoxicity of CPT-induced transcriptional-DSBs

Our results show that CPT-induced DSBs can kill quiescent cells by apoptosis (**Figure 8, paper**). Our findings are consistent with published studies showing that CPT induces apoptosis in a transcription-dependent manner in neurons (Morris and Geller, 1996; Morris et al., 2001; Stefanis et al., 1999). We showed for the first time that this cytotoxicity is due to transcriptional DSBs. Indeed, by modulating the amount of DSBs it was possible to modulate the induction of apoptosis: blocking DSB production by inhibiting transcription or proteasome completely prevented apoptosis (**Figure**

7A-C, paper), while increasing the number of DSBs by inhibiting PARP enhanced apoptosis (**Figure 7D, paper**).

We also found that the main function of CPT-induced transcriptional DSB signalling is likely to promote cells survival as ATM or DNA-PK inhibition increases apoptosis (**Figure 7E and F, paper**). Interestingly, ATM-dependent signalling in quiescent cells has the same function in promoting cell survival than in G1-phase cycling cells (Sakasai et al., 2010a) while in neurons ATM promotes cell-cycle re-entry and apoptosis (Tian et al., 2009).

Speculations about the possible implication of our findings in neurodegenerative syndromes

Transcriptional DSBs might occur spontaneously in cells as Top1cc are stabilized by common DNA alterations such as DNA nicks, gaps, mismatches, abasic sites or misincorporated ribonucleotides (Kim et al., 2011; Pourquier and Pommier, 2001). Therefore, stabilized Top1cc may have a marked impact on non-replicating cell fate. Hence, it could be speculated that defective repair of Top1cc could lead to the accumulation of transcriptional DSBs that may be involved in neuronal death in AT (ATM deficiency) and SCAN1 (Tdp1 deficiency) patients. Indeed, these syndromes are both characterized by neurodegeneration and apparition of neurological defects relatively late, in childhood for AT and in the teenage years for SCAN1 patients (Rass et al., 2007). Neurons may be more relying on Top1cc-repair by the Tdp1 excision pathway compared to replicating cells and they may have particular tissue-specific features that increase the probability of Top1 trapping, such as (i) the high oxygen consumption that results in the high level of oxidative stress that can stabilize Top1, (ii) the high transcriptional rate which may increase the conversion of reversible Top1cc into suicide complex and (iii) the lack of replication that may impede to repair Top1cc by other repair pathways during replication such as helicase pathway, HR or NHEJ (Rass et al., 2007). We can speculate that AT and SCAN1 patients might accumulate unrepaired Top1cc trapped by endogenous DNA alterations that may be converted at very low frequencies into cytotoxic transcriptional-DSBs that accumulate over years.

This hypothesis is consistent with our data showing that Tdp1 depletion increases the induction of transcriptional DSBs produced by stabilized Top1cc (**Figure 4A and B, paper**) and that few DSBs are able to kill quiescent cells (**Figure 8, paper**). Evidences in literature could also be consistent with this possibility, (i) both Tdp1 and ATM participate to Top1cc repair (Alagoz et al., 2013; El-Khamisy et al., 2005) (ii) Tdp1 or ATM deficient neural tissues accumulate endogenous Top1cc compared to control tissues (Katyal et al., 2014), (iii) AT cells have higher endogenous level of Top1cc that are dependent on both transcription and ROS (Alagoz et al., 2013), (iv) ATM regulates

the level of ROS (Guo et al., 2010; Ito et al., 2004) and (v) DSBs in neurons can physiologically be produced as result of brain activity (Suberbielle et al., 2013).
Hence, it will be interesting to test the possible involvement of transcriptional DSBs in AT and SCAN1 pathologies by using neurons, neurons-like cells or astrocytes as cellular model.

Speculations about the possible implication of our findings in cancer therapy

In highly proliferative cancer cells, replication-induced DSBs are the primary cytotoxic mechanism of Top1 inhibitors (Holm et al., 1989; Horwitz and Horwitz, 1973). Hence, at clinical concentrations it is unlikely that transcriptional DSBs *per se* contribute to CPTs cytotoxicity in cancer cells (Borovitskaya and D'Arpa, 1998). Furthermore, the RC-DSBs-dependent cytotoxicity of CPT allows a S-phase-selective targeting of highly replicating tumour cells limiting side effects on slow-cycling nontransformed cells. Nevertheless, transcriptional implications associated with CPT-induced Top1 trapping may be relevant in cancer therapy:

- *Top1 proteolysis*: As already discussed, CPT-induced Top1 degradation is a mechanism of CPT resistance (Desai et al., 2001). Cancer cells are often deficient in Top1 degradation and more sensible to Top1 inhibitors (Desai et al., 2001). Deficiencies in Top1 degradation pathway should trigger a hypersensitivity to CPTs. For instance, CPT treatment may likely be beneficial in tumour with deficiencies in ATM or DNA-PK activity, not only because of the role of ATM and DNA-PK in DSB signalling and repair but also for their possible role in Top1 downregulation. Thus, it should be interesting to test whether ATM or DNA-PK depletion prevents Top1 downregulation in replicating cells such as in quiescent cells (**Figure 7A and B, S5D and F, paper**) (Alagoz et al., 2013; Katyal et al., 2014).

- *Transcriptional-DSBs*: The proteasome inhibitor bortezomib (Velcade) is approved in therapy for the treatment of multiple myeloma and lymphoma. Proteasome inhibition by bortezomib potentiates specifically CPT- (or irinotecan-) induced S-phase cytotoxicity (Zhang et al., 2004). By contrast, we show that proteasome inhibition blocks CPT-induced apoptosis in quiescent fibroblasts (**Figure 8C, paper**). It should be speculated that combining bortezomib with CPT derivatives might kill more tumours cells increasing CPT selectivity. A number of clinical trials have been done or are ongoing for this combination in different types of tumours (clinicaltrials.gov). It would be also interesting to test the combination of bortezomib, CPTs and olaparib, a PARP inhibitor recently approved in cancer therapy. PARP inhibitors (PARPi) potentiate the cytotoxicity of CPT in cancer cells (Zhang et al., 2011). We show that PARP inhibition also enhances CPT-dependent apoptosis in quiescent cells (**Figure 8D, paper**) by increasing the amount of transcriptional-DSBs (**Figure 4C**

and D, paper) and our preliminary experiments suggest that DSBs could be produced by the same mechanism in G1- and G2-phase cells (**Figure IVC-E**). Inhibiting proteasome may prevent CPT and PARPi cytotoxicity in non-S-phase cells thereby leading to enhanced cell killing specifically in S-phase.

- *CPT-induced transcriptional-SSBs during replication*: It could be also possible that some replication-coupled DSBs produced in response to CPT are dependent on transcription. Transcriptional-SSBs generated during Tdp1-excision pathway could be converted in DSBs during replication. This scenario is consistent with evidences in literature: (i) Tdp1 deficiency or PARP inhibition results in CPT hypersensitivity in replicating cells (Interthal et al., 2005b; Miao et al., 2006; Zhang et al., 2011), (ii) deficient Top1 proteolysis decreases the induction of RC-DSBs and γH2AX signal in response to CPT in replicating cells (Lin et al., 2009) (**Figure IVC-E**) and (iii) transcription-dependent activation of ATM activates the G1/S checkpoint in response to CPT likely to avoid the conversion of transcriptional-SSBs carried over from G1 to S-phase in DSBs during replication (Sakasai et al., 2010a). Furthermore, cells depleted for Top1 accumulate DSBs in particular in actively transcribed genes as a result of the frequent interference between replication and transcription (Tuduri et al., 2009).

BIBLIOGRAPHY

Adam, S., and S.E. Polo. 2014. Blurring the line between the DNA damage response and transcription: The importance of chromatin dynamics. *Exp Cell Res*.

Adam, S., S.E. Polo, and G. Almouzni. 2013. Transcription recovery after DNA damage requires chromatin priming by the H3.3 histone chaperone HIRA. *Cell*. 155:94-106.

Aguilar-Quesada, R., J.A. Muñoz-Gámez, D. Martín-Oliva, A. Peralta, M.T. Valenzuela, R. Matínez-Romero, R. Quiles-Pérez, J. Menissier-de Murcia, G. de Murcia, M. Ruiz de Almodóvar, and F.J. Oliver. 2007. Interaction between ATM and PARP-1 in response to DNA damage and sensitization of ATM deficient cells through PARP inhibition. *BMC Mol Biol*. 8:29.

Aguilera, A., and T. Garcia-Muse. 2012. R loops: from transcription byproducts to threats to genome stability. *Mol Cell*. 46:115-124.

Alagoz, M., S.C. Chiang, A. Sharma, and S.F. El-Khamisy. 2013. ATM deficiency results in accumulation of DNA-topoisomerase I covalent intermediates in neural cells. *PLoS One*. 8:e58239.

Alagoz, M., O.S. Wells, and S.F. El-Khamisy. 2014. TDP1 deficiency sensitizes human cells to base damage via distinct topoisomerase I and PARP mechanisms with potential applications for cancer therapy. *Nucleic Acids Res*. 42:3089-3103.

Albor, A., S. Kaku, and M. Kulesz-Martin. 1998. Wild-type and mutant forms of p53 activate human topoisomerase I: a possible mechanism for gain of function in mutants. *Cancer Res*. 58:2091-2094.

Alchanati, I., C. Teicher, G. Cohen, V. Shemesh, H.M. Barr, P. Nakache, D. Ben-Avraham, A. Idelevich, I. Angel, N. Livnah, S. Tuvia, Y. Reiss, D. Taglicht, and O. Erez. 2009. The E3 ubiquitin-ligase Bmi1/Ring1A controls the proteasomal degradation of Top2alpha cleavage complex - a potentially new drug target. *PLoS One*. 4:e8104.

Aleo, E., C.J. Henderson, A. Fontanini, B. Solazzo, and C. Brancolini. 2006. Identification of new compounds that trigger apoptosome-independent caspase activation and apoptosis. *Cancer Res*. 66:9235-9244.

Ali, A., J. Zhang, S. Bao, I. Liu, D. Otterness, N.M. Dean, R.T. Abraham, and X.F. Wang. 2004. Requirement of protein phosphatase 5 in DNA-damage-induced ATM activation. *Genes Dev*. 18:249-254.

Ali, A.A., G. Timinszky, R. Arribas-Bosacoma, M. Kozlowski, P.O. Hassa, M. Hassler, A.G. Ladurner, L.H. Pearl, and A.W. Oliver. 2012. The zinc-finger domains of PARP1 cooperate to recognize DNA strand breaks. *Nat Struct Mol Biol*. 19:685-692.

Altmeyer, M., K.J. Neelsen, F. Teloni, I. Pozdnyakova, S. Pellegrino, M. Grofte, M.B. Rask, W. Streicher, S. Jungmichel, M.L. Nielsen, and J. Lukas. 2015. Liquid demixing of intrinsically disordered proteins is seeded by poly(ADP-ribose). *Nat Commun*. 6:8088.

Amente, S., B. Gargano, G. Napolitano, L. Lania, and B. Majello. 2009. Camptothecin releases P-TEFb from the inactive 7SK snRNP complex. *Cell Cycle*. 8:1249-1255.

Andegeko, Y., L. Moyal, L. Mittelman, I. Tsarfaty, Y. Shiloh, and G. Rotman. 2001. Nuclear retention of ATM at sites of DNA double strand breaks. *The Journal of biological chemistry*. 276:38224-38230.

Andersen, F.F., T.O. Tange, T. Sinnathamby, J.R. Olesen, K.E. Andersen, O. Westergaard, J. Kjems, and B.R. Knudsen. 2002. The RNA splicing factor ASF/SF2 inhibits human topoisomerase I mediated DNA relaxation. *J Mol Biol*. 322:677-686.

Anderson, L., C. Henderson, and Y. Adachi. 2001. Phosphorylation and rapid relocalization of 53BP1 to nuclear foci upon DNA damage. *Mol Cell Biol*. 21:1719-1729.

Antony, S., K.K. Agama, Z.H. Miao, K. Takagi, M.H. Wright, A.I. Robles, L. Varticovski, M. Nagarajan, A. Morrell, M. Cushman, and Y. Pommier. 2007a. Novel indenoisoquinolines NSC 725776 and NSC 724998 produce persistent topoisomerase I cleavage complexes and overcome multidrug resistance. *Cancer Res*. 67:10397-10405.

Antony, S., P.B. Arimondo, J.S. Sun, and Y. Pommier. 2004a. Position- and orientation-specific enhancement of topoisomerase I cleavage complexes by triplex DNA structures. *Nucleic Acids Res*. 32:5163-5173.

Antony, S., M. Jayaraman, G. Laco, G. Kohlhagen, K.W. Kohn, M. Cushman, and Y. Pommier. 2003. Differential induction of topoisomerase I-DNA cleavage complexes by the indenoisoquinoline MJ-III-65 (NSC 706744) and camptothecin: base sequence analysis and activity against camptothecin-resistant topoisomerases I. *Cancer Res*. 63:7428-7435.

Antony, S., G. Kohlhagen, K. Agama, M. Jayaraman, S. Cao, F.A. Durrani, Y.M. Rustum, M. Cushman, and Y. Pommier. 2005. Cellular topoisomerase I inhibition and antiproliferative activity by MJ-III-65 (NSC 706744), an indenoisoquinoline topoisomerase I poison. *Mol Pharmacol*. 67:523-530.

Antony, S., C. Marchand, A.G. Stephen, L. Thibaut, K.K. Agama, R.J. Fisher, and Y. Pommier. 2007b. Novel high-throughput electrochemiluminescent assay for identification of human tyrosyl-DNA phosphodiesterase (Tdp1) inhibitors and characterization of furamidine (NSC 305831) as an inhibitor of Tdp1. *Nucleic Acids Res*. 35:4474-4484.

Antony, S., J.A. Theruvathu, P.J. Brooks, D.T. Lesher, M. Redinbo, and Y. Pommier. 2004b. Enhancement of camptothecin-induced topoisomerase I cleavage complexes by the acetaldehyde adduct N2-ethyl-2'-deoxyguanosine. *Nucleic Acids Res*. 32:5685-5692.

Ashour, M.E., R. Atteya, and S.F. El-Khamisy. 2015. Topoisomerase-mediated chromosomal break repair: an emerging player in many games. *Nat Rev Cancer*. 15:137-151.

Aune, G.J., K. Takagi, O. Sordet, J. Guirouilh-Barbat, S. Antony, V.A. Bohr, and Y. Pommier. 2008. Von Hippel-Lindau-coupled and transcription-coupled nucleotide excision repair-dependent degradation of RNA polymerase II in response to trabectedin. *Clin Cancer Res*. 14:6449-6455.

Aymard, F., B. Bugler, C.K. Schmidt, E. Guillou, P. Caron, S. Briois, J.S. Iacovoni, V. Daburon, K.M. Miller, S.P. Jackson, and G. Legube. 2014. Transcriptionally active chromatin recruits homologous recombination at DNA double-strand breaks. *Nat Struct Mol Biol*. 21:366-374.

Ayrapetov, M.K., O. Gursoy-Yuzugullu, C. Xu, Y. Xu, and B.D. Price. 2014. DNA double-strand breaks promote methylation of histone H3 on lysine 9 and transient formation of repressive chromatin. *Proc Natl Acad Sci U S A*. 111:9169-9174.

Bailly, C. 2000. Topoisomerase I poisons and suppressors as anticancer drugs. *Curr Med Chem*. 7:39-58.

Baker, S.D., R.M. Wadkins, C.F. Stewart, W.T. Beck, and M.K. Danks. 1995. Cell cycle analysis of amount and distribution of nuclear DNA topoisomerase I as determined by fluorescence digital imaging microscopy. *Cytometry*. 19:134-145.

Bakkenist, C.J., and M.B. Kastan. 2003. DNA damage activates ATM through intermolecular autophosphorylation and dimer dissociation. *Nature*. 421:499-506.

Ban, Y., C.W. Ho, R.K. Lin, Y.L. Lyu, and L.F. Liu. 2013. Activation of a novel ubiquitin-independent proteasome pathway when RNA polymerase II encounters a protein roadblock. *Mol Cell Biol*. 33:4008-4016.

Banin, S., L. Moyal, S. Shieh, Y. Taya, C.W. Anderson, L. Chessa, N.I. Smorodinsky, C. Prives, Y. Reiss, Y. Shiloh, and Y. Ziv. 1998. Enhanced phosphorylation of p53 by ATM in response to DNA damage. *Science (New York, N.Y.* 281:1674-1677.

Baranello, L., D. Bertozzi, M.V. Fogli, Y. Pommier, and G. Capranico. 2010. DNA topoisomerase I inhibition by camptothecin induces escape of RNA polymerase II from promoter-proximal pause site, antisense transcription and histone acetylation at the human HIF-1alpha gene locus. *Nucleic Acids Res*. 38:159-171.

Barthelme, D., and R.T. Sauer. 2012. Identification of the Cdc48*20S proteasome as an ancient AAA+ proteolytic machine. *Science (New York, N.Y.* 337:843-846.

Barthelme, D., and R.T. Sauer. 2013. Bipartite determinants mediate an evolutionarily conserved interaction between Cdc48 and the 20S peptidase. *Proc Natl Acad Sci U S A*. 110:3327-3332.

Barthelmes, H.U., M. Habermeyer, M.O. Christensen, C. Mielke, H. Interthal, J.J. Pouliot, F. Boege, and D. Marko. 2004. TDP1 overexpression in human cells counteracts DNA damage mediated by topoisomerases I and II. *The Journal of biological chemistry*. 279:55618-55625.

Bassing, C.H., and F.W. Alt. 2004. The cellular response to general and programmed DNA double strand breaks. *DNA repair*. 3:781-796.

Bassing, C.H., K.F. Chua, J. Sekiguchi, H. Suh, S.R. Whitlow, J.C. Fleming, B.C. Monroe, D.N. Ciccone, C. Yan, K. Vlasakova, D.M. Livingston, D.O. Ferguson, R. Scully, and F.W. Alt. 2002. Increased ionizing radiation sensitivity and genomic instability in the absence of histone H2AX. *Proc Natl Acad Sci U S A*. 99:8173-8178.

Basu, B., T.A. Yap, L.R. Molife, and J.S. de Bono. 2012. Targeting the DNA damage response in oncology: past, present and future perspectives. *Current opinion in oncology*. 24:316-324.

Baugh, J.M., E.G. Viktorova, and E.V. Pilipenko. 2009. Proteasomes can degrade a significant proportion of cellular proteins independent of ubiquitination. *J Mol Biol*. 386:814-827.

Beck, C., I. Robert, B. Reina-San-Martin, V. Schreiber, and F. Dantzer. 2014. Poly(ADP-ribose) polymerases in double-strand break repair: Focus on PARP1, PARP2 and PARP3. *Exp Cell Res*.

Been, M.D., R.R. Burgess, and J.J. Champoux. 1984. Nucleotide sequence preference at rat liver and wheat germ type 1 DNA topoisomerase breakage sites in duplex SV40 DNA. *Nucleic Acids Res*. 12:3097-3114.

Been, M.D., and J.J. Champoux. 1984. Breakage of single-stranded DNA by eukaryotic type 1 topoisomerase occurs only at regions with the potential for base-pairing. *J Mol Biol*. 180:515-531.

Beidler, D.R., and Y.C. Cheng. 1995. Camptothecin induction of a time- and concentration-dependent decrease of topoisomerase I and its implication in camptothecin activity. *Mol Pharmacol*. 47:907-914.

Bekker-Jensen, S., C. Lukas, R. Kitagawa, F. Melander, M.B. Kastan, J. Bartek, and J. Lukas. 2006. Spatial organization of the mammalian genome surveillance machinery in response to DNA strand breaks. *J Cell Biol*. 173:195-206.

Bekker-Jensen, S., and N. Mailand. 2010. Assembly and function of DNA double-strand break repair foci in mammalian cells. *DNA repair*. 9:1219-1228.

Bekker-Jensen, S., J. Rendtlew Danielsen, K. Fugger, I. Gromova, A. Nerstedt, C. Lukas, J. Bartek, J. Lukas, and N. Mailand. 2010. HERC2 coordinates ubiquitin-dependent assembly of DNA repair factors on damaged chromosomes. *Nat Cell Biol*. 12:80-86; sup pp 81-12.

Bendixen, C., B. Thomsen, J. Alsner, and O. Westergaard. 1990. Camptothecin-stabilized topoisomerase I-DNA adducts cause premature termination of transcription. *Biochemistry*. 29:5613-5619.

Bennetzen, M.V., D.H. Larsen, J. Bunkenborg, J. Bartek, J. Lukas, and J.S. Andersen. 2010. Site-specific phosphorylation dynamics of the nuclear proteome during the DNA damage response. *Molecular & cellular proteomics : MCP*. 9:1314-1323.

Bergerat, A., B. de Massy, D. Gadelle, P.C. Varoutas, A. Nicolas, and P. Forterre. 1997. An atypical topoisomerase II from Archaea with implications for meiotic recombination. *Nature*. 386:414-417.

Berkovich, E., R.J. Monnat, Jr., and M.B. Kastan. 2007. Roles of ATM and NBS1 in chromatin structure modulation and DNA double-strand break repair. *Nat Cell Biol*. 9:683-690.

Berndsen, C.E., and C. Wolberger. 2014. New insights into ubiquitin E3 ligase mechanism. *Nat Struct Mol Biol*. 21:301-307.

Berti, M., A. Ray Chaudhuri, S. Thangavel, S. Gomathinayagam, S. Kenig, M. Vujanovic, F. Odreman, T. Glatter, S. Graziano, R. Mendoza-Maldonado, F. Marino, B. Lucic, V. Biasin, M. Gstaiger, R. Aebersold, J.M. Sidorova, R.J. Monnat, Jr., M. Lopes, and A. Vindigni. 2013. Human RECQ1 promotes restart of replication forks reversed by DNA topoisomerase I inhibition. *Nat Struct Mol Biol*. 20:347-354.

Bertozzi, D., R. Iurlaro, O. Sordet, J. Marinello, N. Zaffaroni, and G. Capranico. 2011. Characterization of novel antisense HIF-1alpha transcripts in human cancers. *Cell Cycle*. 10.

Besson, A., M. Gurian-West, X. Chen, K.S. Kelly-Spratt, C.J. Kemp, and J.M. Roberts. 2006. A pathway in quiescent cells that controls p27Kip1 stability, subcellular localization, and tumor suppression. *Genes Dev*. 20:47-64.

Bester, A.C., M. Roniger, Y.S. Oren, M.M. Im, D. Sarni, M. Chaoat, A. Bensimon, G. Zamir, D.S. Shewach, and B. Kerem. 2011. Nucleotide deficiency promotes genomic instability in early stages of cancer development. *Cell*. 145:435-446.

Beucher, A., J. Birraux, L. Tchouandong, O. Barton, A. Shibata, S. Conrad, A.A. Goodarzi, A. Krempler, P.A. Jeggo, and M. Lobrich. 2009. ATM and Artemis promote homologous recombination of radiation-induced DNA double-strand breaks in G2. *EMBO J*. 28:3413-3427.

Bharti, A.K., M.O. Olson, D.W. Kufe, and E.H. Rubin. 1996. Identification of a nucleolin binding site in human topoisomerase I. *The Journal of biological chemistry*. 271:1993-1997.

Bhattacharyya, S., H. Yu, C. Mim, and A. Matouschek. 2014. Regulated protein turnover: snapshots of the proteasome in action. *Nat Rev Mol Cell Biol*. 15:122-133.

Biffi, G., D. Tannahill, J. McCafferty, and S. Balasubramanian. 2013. Quantitative visualization of DNA G-quadruplex structures in human cells. *Nat Chem*. 5:182-186.

Bird, A.W., D.Y. Yu, M.G. Pray-Grant, Q. Qiu, K.E. Harmon, P.C. Megee, P.A. Grant, M.M. Smith, and M.F. Christman. 2002. Acetylation of histone H4 by Esa1 is required for DNA double-strand break repair. *Nature*. 419:411-415.

Biss, M., and W. Xiao. 2012. Selective tumor killing based on specific DNA-damage response deficiencies. *Cancer Biol Ther*. 13:239-246.

Blickwedehl, J., M. Agarwal, C. Seong, R.K. Pandita, T. Melendy, P. Sung, T.K. Pandita, and N. Bangia. 2008. Role for proteasome activator PA200 and postglutamyl proteasome activity in genomic stability. *Proc Natl Acad Sci U S A*. 105:16165-16170.

Blickwedehl, J., S. McEvoy, I. Wong, P. Kousis, J. Clements, R. Elliott, P. Cresswell, P. Liang, and N. Bangia. 2007. Proteasomes and proteasome activator 200 kDa (PA200) accumulate on chromatin in response to ionizing radiation. *Radiat Res*. 167:663-674.

Blier, P.R., A.J. Griffith, J. Craft, and J.A. Hardin. 1993. Binding of Ku protein to DNA. Measurement of affinity for ends and demonstration of binding to nicks. *The Journal of biological chemistry*. 268:7594-7601.

Blot, N., R. Mavathur, M. Geertz, A. Travers, and G. Muskhelishvili. 2006. Homeostatic regulation of supercoiling sensitivity coordinates transcription of the bacterial genome. *EMBO Rep*. 7:710-715.

Boersma, V., N. Moatti, S. Segura-Bayona, M.H. Peuscher, J. van der Torre, B.A. Wevers, A. Orthwein, D. Durocher, and J.J. Jacobs. 2015. MAD2L2 controls DNA repair at telomeres and DNA breaks by inhibiting 5' end resection. *Nature*. 521:537-540.

Boguslawski, S.J., D.E. Smith, M.A. Michalak, K.E. Mickelson, C.O. Yehle, W.L. Patterson, and R.J. Carrico. 1986. Characterization of monoclonal antibody to DNA.RNA and its application to immunodetection of hybrids. *J Immunol Methods*. 89:123-130.

Bonner, W.M., C.E. Redon, J.S. Dickey, A.J. Nakamura, O.A. Sedelnikova, S. Solier, and Y. Pommier. 2008. gammaH2AX and cancer. *Nat Rev Cancer*. 8:957-967.

Bonven, B.J., E. Gocke, and O. Westergaard. 1985. A high affinity topoisomerase I binding sequence is clustered at DNAase I hypersensitive sites in Tetrahymena R-chromatin. *Cell*. 41:541-551.

Borovitskaya, A.E., and P. D'Arpa. 1998. Replication-dependent and -independent camptothecin cytotoxicity of seven human colon tumor cell lines. *Oncol Res*. 10:271-276.

Bothmer, A., D.F. Robbiani, N. Feldhahn, A. Gazumyan, A. Nussenzweig, and M.C. Nussenzweig. 2010. 53BP1 regulates DNA resection and the choice between classical and alternative end joining during class switch recombination. *J Exp Med*. 207:855-865.

Boubnov, N.V., K.T. Hall, Z. Wills, S.E. Lee, D.M. He, D.M. Benjamin, C.R. Pulaski, H. Band, W. Reeves, and E.A. Hendrickson. 1995. Complementation of the ionizing radiation sensitivity, DNA end binding, and V(D)J recombination defects of double-strand break repair mutants by the p86 Ku autoantigen. *Proc Natl Acad Sci U S A*. 92:890-894.

Boulton, S., S. Kyle, and B.W. Durkacz. 1999. Interactive effects of inhibitors of poly(ADP-ribose) polymerase and DNA-dependent protein kinase on cellular responses to DNA damage. *Carcinogenesis*. 20:199-203.

Bouwman, P., A. Aly, J.M. Escandell, M. Pieterse, J. Bartkova, H. van der Gulden, S. Hiddingh, M. Thanasoula, A. Kulkarni, Q. Yang, B.G. Haffty, J. Tommiska, C. Blomqvist, R. Drapkin, D.J. Adams, H. Nevanlinna, J. Bartek, M. Tarsounas, S. Ganesan, and J. Jonkers. 2010. 53BP1 loss rescues BRCA1 deficiency and is associated with triple-negative and BRCA-mutated breast cancers. *Nat Struct Mol Biol*. 17:688-695.

Bowman, K.J., D.R. Newell, A.H. Calvert, and N.J. Curtin. 2001. Differential effects of the poly (ADP-ribose) polymerase (PARP) inhibitor NU1025 on topoisomerase I and II inhibitor cytotoxicity in L1210 cells in vitro. *Br J Cancer*. 84:106-112.

Bregman, D.B., R. Halaban, A.J. van Gool, K.A. Henning, E.C. Friedberg, and S.L. Warren. 1996. UV-induced ubiquitination of RNA polymerase II: a novel modification deficient in Cockayne syndrome cells. *Proc Natl Acad Sci U S A*. 93:11586-11590.

Brill, S.J., S. DiNardo, K. Voelkel-Meiman, and R. Sternglanz. 1987. Need for DNA topoisomerase activity as a swivel for DNA replication for transcription of ribosomal RNA. *Nature*. 326:414-416.

Britton, S., J. Coates, and S.P. Jackson. 2013. A new method for high-resolution imaging of Ku foci to decipher mechanisms of DNA double-strand break repair. *J Cell Biol*. 202:579-595.

Britton, S., E. Dernoncourt, C. Delteil, C. Froment, O. Schiltz, B. Salles, P. Frit, and P. Calsou. 2014. DNA damage triggers SAF-A and RNA biogenesis factors exclusion from chromatin coupled to R-loops removal. *Nucleic Acids Res*. 42:9047-9062.

Brown, E.J., and D. Baltimore. 2000. ATR disruption leads to chromosomal fragmentation and early embryonic lethality. *Genes Dev*. 14:397-402.

Brown, J.S., and S.P. Jackson. 2015. Ubiquitylation, neddylation and the DNA damage response. *Open Biol*. 5:150018.

Brown, J.S., N. Lukashchuk, M. Sczaniecka-Clift, S. Britton, C. le Sage, P. Calsou, P. Beli, Y. Galanty, and S.P. Jackson. 2015. Neddylation promotes ubiquitylation and release of Ku from DNA-damage sites. *Cell reports*. 11:704-714.

Bryant, H.E., E. Petermann, N. Schultz, A.S. Jemth, O. Loseva, N. Issaeva, F. Johansson, S. Fernandez, P. McGlynn, and T. Helleday. 2009. PARP is activated at stalled forks to mediate Mre11-dependent replication restart and recombination. *EMBO J*. 28:2601-2615.

Bunting, S.F., E. Callén, N. Wong, H.T. Chen, F. Polato, A. Gunn, A. Bothmer, N. Feldhahn, O. Fernandez-Capetillo, L. Cao, X. Xu, C.X. Deng, T. Finkel, M. Nussenzweig, J.M. Stark, and A. Nussenzweig. 2010. 53BP1 inhibits homologous recombination in Brca1-deficient cells by blocking resection of DNA breaks. *Cell*. 141:243-254.

Burns, M.B., L. Lackey, M.A. Carpenter, A. Rathore, A.M. Land, B. Leonard, E.W. Refsland, D. Kotandeniya, N. Tretyakova, J.B. Nikas, D. Yee, N.A. Temiz, D.E. Donohue, R.M. McDougle, W.L. Brown, E.K. Law, and R.S. Harris. 2013. APOBEC3B is an enzymatic source of mutation in breast cancer. *Nature*. 494:366-370.

Butler, L.R., R.M. Densham, J. Jia, A.J. Garvin, H.R. Stone, V. Shah, D. Weekes, F. Festy, J. Beesley, and J.R. Morris. 2012. The proteasomal de-ubiquitinating enzyme POH1 promotes the double-strand DNA break response. *EMBO J*. 31:3918-3934.

Caldecott, K.W. 2008. Single-strand break repair and genetic disease. *Nat Rev Genet*. 9:619-631.

Callen, E., M. Di Virgilio, M.J. Kruhlak, M. Nieto-Soler, N. Wong, H.T. Chen, R.B. Faryabi, F. Polato, M. Santos, L.M. Starnes, D.R. Wesemann, J.E. Lee, A. Tubbs, B.P. Sleckman, J.A. Daniel, K. Ge, F.W. Alt, O. Fernandez-Capetillo, M.C. Nussenzweig, and A. Nussenzweig. 2013. 53BP1 mediates productive and mutagenic DNA repair through distinct phosphoprotein interactions. *Cell*. 153:1266-1280.

Camilloni, G., E. Di Martino, M. Caserta, and E. di Mauro. 1988. Eukaryotic DNA topoisomerase I reaction is topology dependent. *Nucleic Acids Res*. 16:7071-7085.

Canman, C.E., D.S. Lim, K.A. Cimprich, Y. Taya, K. Tamai, K. Sakaguchi, E. Appella, M.B. Kastan, and J.D. Siliciano. 1998. Activation of the ATM kinase by ionizing radiation and phosphorylation of p53. *Science (New York, N.Y.* 281:1677-1679.

Cao, Q., X. Wang, M. Zhao, R. Yang, R. Malik, Y. Qiao, A. Poliakov, A.K. Yocum, Y. Li, W. Chen, X. Cao, X. Jiang, A. Dahiya, C. Harris, F.Y. Feng, S. Kalantry, Z.S. Qin, S.M. Dhanasekaran, and A.M. Chinnaiyan. 2014. The central role of EED in the orchestration of polycomb group complexes. *Nat Commun*. 5:3127.

Capranico, G., and M. Binaschi. 1998. DNA sequence selectivity of topoisomerases and topoisomerase poisons. *Biochim Biophys Acta*. 1400:185-194.

Capranico, G., F. Ferri, M.V. Fogli, A. Russo, L. Lotito, and L. Baranello. 2007. The effects of camptothecin on RNA polymerase II transcription: roles of DNA topoisomerase I. *Biochimie*. 89:482-489.

Capranico, G., K.W. Kohn, and Y. Pommier. 1990. Local sequence requirements for DNA cleavage by mammalian topoisomerase II in the presence of doxorubicin. *Nucleic Acids Res*. 18:6611-6619.

Capranico, G., J. Marinello, and L. Baranello. 2010. Dissecting the transcriptional functions of human DNA topoisomerase I by selective inhibitors: implications for physiological and therapeutic modulation of enzyme activity. *Biochim Biophys Acta*. 1806:240-250.

Carlucci, A., and V. D'Angiolella. 2015. It is not all about BRCA: Cullin-Ring ubiquitin Ligases in ovarian cancer. *Br J Cancer*. 112:9-13.

Caron, P., F. Aymard, J.S. Iacovoni, S. Briois, Y. Canitrot, B. Bugler, L. Massip, A. Losada, and G. Legube. 2012. Cohesin protects genes against γH2AX Induced by DNA double-strand breaks. *PLoS Genet*. 8:e1002460.

Carty, S.M., and A.L. Greenleaf. 2002. Hyperphosphorylated C-terminal repeat domain-associating proteins in the nuclear proteome link transcription to DNA/chromatin modification and RNA processing. *Molecular & cellular proteomics : MCP*. 1:598-610.

Cedervall, B., R. Wong, N. Albright, J. Dynlacht, P. Lambin, and W.C. Dewey. 1995. Methods for the quantification of DNA double-strand breaks determined from the distribution of DNA fragment sizes measured by pulsed-field gel electrophoresis. *Radiat Res*. 143:8-16.

Celeste, A., O. Fernandez-Capetillo, M.J. Kruhlak, D.R. Pilch, D.W. Staudt, A. Lee, R.F. Bonner, W.M. Bonner, and A. Nussenzweig. 2003. Histone H2AX phosphorylation is dispensable for the initial recognition of DNA breaks. *Nat Cell Biol*. 5:675-679.

Celeste, A., S. Petersen, P.J. Romanienko, O. Fernandez-Capetillo, H.T. Chen, O.A. Sedelnikova, B. Reina-San-Martin, V. Coppola, E. Meffre, M.J. Difilippantonio, C. Redon, D.R. Pilch, A. Olaru, M. Eckhaus, R.D. Camerini-Otero, L. Tessarollo, F. Livak, K. Manova, W.M. Bonner, M.C. Nussenzweig, and A. Nussenzweig. 2002. Genomic instability in mice lacking histone H2AX. *Science (New York, N.Y.* 296:922-927.

Champoux, J.J. 1981. DNA is linked to the rat liver DNA nicking-closing enzyme by a phosphodiester bond to tyrosine. *The Journal of biological chemistry*. 256:4805-4809.

Champoux, J.J. 1998. Domains of human topoisomerase I and associated functions. *Prog Nucleic Acid Res Mol Biol*. 60:111-132.

Champoux, J.J. 2001. DNA TOPOISOMERASES: Structure, Function, and Mechanism. *Annu Rev Biochem*. 70:369-413.

Chan, D.W., D.P. Gately, S. Urban, A.M. Galloway, S.P. Lees-Miller, T. Yen, and J. Allalunis-Turner. 1998. Lack of correlation between ATM protein expression and tumour cell radiosensitivity. *Int J Radiat Biol*. 74:217-224.

Chan, D.W., and S.P. Lees-Miller. 1996. The DNA-dependent protein kinase is inactivated by autophosphorylation of the catalytic subunit. *The Journal of biological chemistry*. 271:8936-8941.

Chang, J.Y., L.A. Dethlefsen, L.R. Barley, B.S. Zhou, and Y.C. Cheng. 1992. Characterization of camptothecin-resistant Chinese hamster lung cells. *Biochem Pharmacol*. 43:2443-2452.

Chapman, J.R., P. Barral, J.B. Vannier, V. Borel, M. Steger, A. Tomas-Loba, A.A. Sartori, I.R. Adams, F.D. Batista, and S.J. Boulton. 2013. RIF1 is essential for 53BP1-dependent nonhomologous end joining and suppression of DNA double-strand break resection. *Mol Cell*. 49:858-871.

Chapman, J.R., and S.P. Jackson. 2008. Phospho-dependent interactions between NBS1 and MDC1 mediate chromatin retention of the MRN complex at sites of DNA damage. *EMBO Rep*. 9:795-801.

Chapman, J.R., A.J. Sossick, S.J. Boulton, and S.P. Jackson. 2012a. BRCA1-associated exclusion of 53BP1 from DNA damage sites underlies temporal control of DNA repair. *Journal of cell science*. 125:3529-3534.

Chapman, J.R., M.R. Taylor, and S.J. Boulton. 2012b. Playing the end game: DNA double-strand break repair pathway choice. *Mol Cell*. 47:497-510.

Chatterjee, S., M.F. Cheng, D. Trivedi, S.J. Petzold, and N.A. Berger. 1989. Camptothecin hypersensitivity in poly(adenosine diphosphate-ribose) polymerase-deficient cell lines. *Cancer Commun*. 1:389-394.

Chaudhuri, J., and F.W. Alt. 2004. Class-switch recombination: interplay of transcription, DNA deamination and DNA repair. *Nat Rev Immunol*. 4:541-552.

Chen, B.P., N. Uematsu, J. Kobayashi, Y. Lerenthal, A. Krempler, H. Yajima, M. Lobrich, Y. Shiloh, and D.J. Chen. 2007. Ataxia telangiectasia mutated (ATM) is essential for DNA-PKcs phosphorylations at the Thr-2609 cluster upon DNA double strand break. *The Journal of biological chemistry*. 282:6582-6587.

Chen, J., W. Feng, J. Jiang, Y. Deng, and M.S. Huen. 2012. Ring finger protein RNF169 antagonizes the ubiquitin-dependent signaling cascade at sites of DNA damage. *The Journal of biological chemistry*. 287:27715-27722.

Chen, X., H. Niu, W.H. Chung, Z. Zhu, A. Papusha, E.Y. Shim, S.E. Lee, P. Sung, and G. Ira. 2011. Cell cycle regulation of DNA double-strand break end resection by Cdk1-dependent Dna2 phosphorylation. *Nat Struct Mol Biol*. 18:1015-1019.

Chen, Y., A.A. Farmer, C.F. Chen, D.C. Jones, P.L. Chen, and W.H. Lee. 1996. BRCA1 is a 220-kDa nuclear phosphoprotein that is expressed and phosphorylated in a cell cycle-dependent manner. *Cancer Res*. 56:3168-3172.

Cheng, T.J., P.G. Rey, T. Poon, and C.C. Kan. 2002. Kinetic studies of human tyrosyl-DNA phosphodiesterase, an enzyme in the topoisomerase I DNA repair pathway. *European journal of biochemistry / FEBS*. 269:3697-3704.

Chernikova, S.B., J.A. Dorth, O.V. Razorenova, J.C. Game, and J.M. Brown. 2010. Deficiency in Bre1 impairs homologous recombination repair and cell cycle checkpoint response to radiation damage in mammalian cells. *Radiat Res*. 174:558-565.

Chiang, S.C., J. Carroll, and S.F. El-Khamisy. 2010. TDP1 serine 81 promotes interaction with DNA ligase IIIalpha and facilitates cell survival following DNA damage. *Cell Cycle*. 9:588-595.
Chiarle, R., Y. Zhang, R.L. Frock, S.M. Lewis, B. Molinie, Y.J. Ho, D.R. Myers, V.W. Choi, M. Compagno, D.J. Malkin, D. Neuberg, S. Monti, C.C. Giallourakis, M. Gostissa, and F.W. Alt. 2011. Genome-wide translocation sequencing reveals mechanisms of chromosome breaks and rearrangements in B cells. *Cell*. 147:107-119.
Chibazakura, T., F. Watanabe, S. Kitajima, K. Tsukada, Y. Yasukochi, and H. Teraoka. 1997. Phosphorylation of human general transcription factors TATA-binding protein and transcription factor IIB by DNA-dependent protein kinase--synergistic stimulation of RNA polymerase II basal transcription in vitro. *European journal of biochemistry / FEBS*. 247:1166-1173.
Chou, D.M., B. Adamson, N.E. Dephoure, X. Tan, A.C. Nottke, K.E. Hurov, S.P. Gygi, M.P. Colaiácovo, and S.J. Elledge. 2010. A chromatin localization screen reveals poly (ADP ribose)-regulated recruitment of the repressive polycomb and NuRD complexes to sites of DNA damage. *Proc Natl Acad Sci U S A*. 107:18475-18480.
Choudhury, A.D., H. Xu, and R. Baer. 2004. Ubiquitination and proteasomal degradation of the BRCA1 tumor suppressor is regulated during cell cycle progression. *The Journal of biological chemistry*. 279:33909-33918.
Chowdhury, D., M.C. Keogh, H. Ishii, C.L. Peterson, S. Buratowski, and J. Lieberman. 2005. gamma-H2AX dephosphorylation by protein phosphatase 2A facilitates DNA double-strand break repair. *Mol Cell*. 20:801-809.
Chowdhury, D., X. Xu, X. Zhong, F. Ahmed, J. Zhong, J. Liao, D.M. Dykxhoorn, D.M. Weinstock, G.P. Pfeifer, and J. Lieberman. 2008. A PP4-phosphatase complex dephosphorylates gamma-H2AX generated during DNA replication. *Mol Cell*. 31:33-46.
Christiansen, K., A.B. Svejstrup, A.H. Andersen, and O. Westergaard. 1993. Eukaryotic topoisomerase I-mediated cleavage requires bipartite DNA interaction. Cleavage of DNA substrates containing strand interruptions implicates a role for topoisomerase I in illegitimate recombination. *The Journal of biological chemistry*. 268:9690-9701.
Christiansen, K., and O. Westergaard. 1994. Characterization of intra- and intermolecular DNA ligation mediated by eukaryotic topoisomerase I. Role of bipartite DNA interaction in the ligation process. *The Journal of biological chemistry*. 269:721-729.
Christmann, M., M.T. Tomicic, C. Gestrich, W.P. Roos, V.A. Bohr, and B. Kaina. 2008. WRN protects against topo I but not topo II inhibitors by preventing DNA break formation. *DNA repair*. 7:1999-2009.
Ciccia, A., and S.J. Elledge. 2010. The DNA damage response: making it safe to play with knives. *Mol Cell*. 40:179-204.
Ciccia, A., N. McDonald, and S.C. West. 2008. Structural and functional relationships of the XPF/MUS81 family of proteins. *Annu Rev Biochem*. 77:259-287.
Cimprich, K.A., and D. Cortez. 2008. ATR: an essential regulator of genome integrity. *Nat Rev Mol Cell Biol*. 9:616-627.
Cimprich, K.A., T.B. Shin, C.T. Keith, and S.L. Schreiber. 1996. cDNA cloning and gene mapping of a candidate human cell cycle checkpoint protein. *Proc Natl Acad Sci U S A*. 93:2850-2855.
Claesson, A.K., B. Stenerlöw, L. Jacobsson, and K. Elmroth. 2007. Relative biological effectiveness of the alpha-particle emitter (211)At for double-strand break induction in human fibroblasts. *Radiat Res*. 167:312-318.
Coleman, K.A., and R.A. Greenberg. 2011. The BRCA1-RAP80 complex regulates DNA repair mechanism utilization by restricting end resection. *The Journal of biological chemistry*. 286:13669-13680.
Collins, I., A. Weber, and D. Levens. 2001. Transcriptional consequences of topoisomerase inhibition. *Mol Cell Biol*. 21:8437-8451.
Cook, D.N., D. Ma, N.G. Pon, and J.E. Hearst. 1992. Dynamics of DNA supercoiling by transcription in Escherichia coli. *Proc Natl Acad Sci U S A*. 89:10603-10607.
Cook, P.J., B.G. Ju, F. Telese, X. Wang, C.K. Glass, and M.G. Rosenfeld. 2009. Tyrosine dephosphorylation of H2AX modulates apoptosis and survival decisions. *Nature*. 458:591-596.
Coster, G., and M. Goldberg. 2010. The cellular response to DNA damage: a focus on MDC1 and its interacting proteins. *Nucleus*. 1:166-178.
Courilleau, C., C. Chailleux, A. Jauneau, F. Grimal, S. Briois, E. Boutet-Robinet, F. Boudsocq, D. Trouche, and Y. Canitrot. 2012. The chromatin remodeler p400 ATPase facilitates Rad51-mediated repair of DNA double-strand breaks. *J Cell Biol*. 199:1067-1081.
Covey, J.M., C. Jaxel, K.W. Kohn, and Y. Pommier. 1989. Protein-linked DNA strand breaks induced in mammalian cells by camptothecin, an inhibitor of topoisomerase I. *Cancer Res*. 49:5016-5022.
Cowell, I.G., Z. Sondka, K. Smith, K.C. Lee, C.M. Manville, M. Sidorczuk-Lesthuruge, H.A. Rance, K. Padget, G.H. Jackson, N. Adachi, and C.A. Austin. 2012. Model for MLL translocations in therapy-related leukemia involving topoisomerase IIbeta-mediated DNA strand breaks and gene proximity. *Proc Natl Acad Sci U S A*. 109:8989-8994.
Cremona, C.A., and A. Behrens. 2014. ATM signalling and cancer. *Oncogene*. 33:3351-3360.
Cron, K.R., K. Zhu, D.S. Kushwaha, G. Hsieh, D. Merzon, J. Rameseder, C.C. Chen, A.D. D'Andrea, and D. Kozono. 2013. Proteasome inhibitors block DNA repair and radiosensitize non-small cell lung cancer. *PLoS One*. 8:e73710.
Cui, X., Y. Yu, S. Gupta, Y.M. Cho, S.P. Lees-Miller, and K. Meek. 2005. Autophosphorylation of DNA-dependent protein kinase regulates DNA end processing and may also alter double-strand break repair pathway choice. *Mol Cell Biol*. 25:10842-10852.
Czubaty, A., A. Girstun, B. Kowalska-Loth, A.M. Trzcinska, E. Purta, A. Winczura, W. Grajkowski, and K. Staron. 2005. Proteomic analysis of complexes formed by human topoisomerase I. *Biochim Biophys Acta*. 1749:133-141.
D'Amours, D., and S.P. Jackson. 2002. The Mre11 complex: at the crossroads of dna repair and checkpoint signalling. *Nat Rev Mol Cell Biol*. 3:317-327.
Daley, J.M., and P. Sung. 2014. 53BP1, BRCA1, and the choice between recombination and end joining at DNA double-strand breaks. *Mol Cell Biol*. 34:1380-1388.
Dalgaard, J.Z. 2012. Causes and consequences of ribonucleotide incorporation into nuclear DNA. *Trends Genet*. 28:592-597.
Danielsen, J.R., L.K. Povlsen, B.H. Villumsen, W. Streicher, J. Nilsson, M. Wikstrom, S. Bekker-Jensen, and N. Mailand. 2012. DNA damage-inducible SUMOylation of HERC2 promotes RNF8 binding via a novel SUMO-binding Zinc finger. *J Cell Biol*. 197:179-187.

Dantuma, N.P., T.A. Groothuis, F.A. Salomons, and J. Neefjes. 2006. A dynamic ubiquitin equilibrium couples proteasomal activity to chromatin remodeling. *J Cell Biol*. 173:19-26.

Daroui, P., S.D. Desai, T.K. Li, A.A. Liu, and L.F. Liu. 2004. Hydrogen peroxide induces topoisomerase I-mediated DNA damage and cell death. *The Journal of biological chemistry*. 279:14587-14594.

Darzacq, X., Y. Shav-Tal, V. de Turris, Y. Brody, S.M. Shenoy, R.D. Phair, and R.H. Singer. 2007. In vivo dynamics of RNA polymerase II transcription. *Nat Struct Mol Biol*. 14:796-806.

Das, B.B., S. Antony, S. Gupta, T.S. Dexheimer, C.E. Redon, S. Garfield, Y. Shiloh, and Y. Pommier. 2009. Optimal function of the DNA repair enzyme TDP1 requires its phosphorylation by ATM and/or DNA-PK. *EMBO J*. 28:3667-3680.

Das, B.B., S.Y. Huang, J. Murai, I. Rehman, J.C. Ame, S. Sengupta, S.K. Das, P. Majumdar, H. Zhang, D. Biard, H.K. Majumder, V. Schreiber, and Y. Pommier. 2014. PARP1-TDP1 coupling for the repair of topoisomerase I-induced DNA damage. *Nucleic Acids Res*. 42:4435-4449.

Daub, H., J.V. Olsen, M. Bairlein, F. Gnad, F.S. Oppermann, R. Körner, Z. Greff, G. Kéri, O. Stemmann, and M. Mann. 2008. Kinase-selective enrichment enables quantitative phosphoproteomics of the kinome across the cell cycle. *Mol Cell*. 31:438-448.

Davies, D.R., H. Interthal, J.J. Champoux, and W.G. Hol. 2002a. The crystal structure of human tyrosyl-DNA phosphodiesterase, Tdp1. *Structure*. 10:237-248.

Davies, D.R., H. Interthal, J.J. Champoux, and W.G. Hol. 2002b. Insights into substrate binding and catalytic mechanism of human tyrosyl-DNA phosphodiesterase (Tdp1) from vanadate and tungstate-inhibited structures. *J Mol Biol*. 324:917-932.

Davies, D.R., H. Interthal, J.J. Champoux, and W.G. Hol. 2003. Crystal structure of a transition state mimic for Tdp1 assembled from vanadate, DNA, and a topoisomerase I-derived peptide. *Chem Biol*. 10:139-147.

Davis, A.J., L. Chi, S. So, K.J. Lee, E. Mori, K. Fattah, J. Yang, and D.J. Chen. 2014. BRCA1 modulates the autophosphorylation status of DNA-PKcs in S phase of the cell cycle. *Nucleic Acids Res*. 42:11487-11501.

Davis, A.J., S. So, and D.J. Chen. 2010. Dynamics of the PI3K-like protein kinase members ATM and DNA-PKcs at DNA double strand breaks. *Cell Cycle*. 9:2529-2536.

De Bont, R., and N. van Larebeke. 2004. Endogenous DNA damage in humans: a review of quantitative data. *Mutagenesis*. 19:169-185.

de Lange, T. 2005. Shelterin: the protein complex that shapes and safeguards human telomeres. *Genes Dev*. 19:2100-2110.

De Santa, F., I. Barozzi, F. Mietton, S. Ghisletti, S. Polletti, B.K. Tusi, H. Muller, J. Ragoussis, C.L. Wei, and G. Natoli. 2010. A large fraction of extragenic RNA pol II transcription sites overlap enhancers. *PLoS Biol*. 8:e1000384.

Debatisse, M., B. Le Tallec, A. Letessier, B. Dutrillaux, and O. Brison. 2012. Common fragile sites: mechanisms of instability revisited. *Trends Genet*. 28:22-32.

Debethune, L., G. Kohlhagen, A. Grandas, and Y. Pommier. 2002. Processing of nucleopeptides mimicking the topoisomerase I-DNA covalent complex by tyrosyl-DNA phosphodiesterase. *Nucleic Acids Res*. 30:1198-1204.

Deng, C., J.A. Brown, D. You, and J.M. Brown. 2005. Multiple endonucleases function to repair covalent topoisomerase I complexes in Saccharomyces cerevisiae. *Genetics*. 170:591-600.

Dephoure, N., C. Zhou, J. Villén, S.A. Beausoleil, C.E. Bakalarski, S.J. Elledge, and S.P. Gygi. 2008. A quantitative atlas of mitotic phosphorylation. *Proc Natl Acad Sci U S A*. 105:10762-10767.

Derheimer, F.A., H.M. O'Hagan, H.M. Krueger, S. Hanasoge, M.T. Paulsen, and M. Ljungman. 2007. RPA and ATR link transcriptional stress to p53. *Proc Natl Acad Sci U S A*. 104:12778-12783.

Desai, S.D., A.L. Haas, L.M. Wood, Y.C. Tsai, S. Pestka, E.H. Rubin, A. Saleem, E.K.A. Nur, and L.F. Liu. 2006. Elevated expression of ISG15 in tumor cells interferes with the ubiquitin/26S proteasome pathway. *Cancer Res*. 66:921-928.

Desai, S.D., T.K. Li, A. Rodriguez-Bauman, E.H. Rubin, and L.F. Liu. 2001. Ubiquitin/26S proteasome-mediated degradation of topoisomerase I as a resistance mechanism to camptothecin in tumor cells. *Cancer Res*. 61:5926-5932.

Desai, S.D., L.F. Liu, D. Vazquez-Abad, and P. D'Arpa. 1997. Ubiquitin-dependent destruction of topoisomerase I is stimulated by the antitumor drug camptothecin. *The Journal of biological chemistry*. 272:24159-24164.

Desai, S.D., L.M. Wood, Y.C. Tsai, T.S. Hsieh, J.R. Marks, G.L. Scott, B.C. Giovanella, and L.F. Liu. 2008. ISG15 as a novel tumor biomarker for drug sensitivity. *Mol Cancer Ther*. 7:1430-1439.

Desai, S.D., H. Zhang, A. Rodriguez-Bauman, J.M. Yang, X. Wu, M.K. Gounder, E.H. Rubin, and L.F. Liu. 2003. Transcription-dependent degradation of topoisomerase I-DNA covalent complexes. *Mol Cell Biol*. 23:2341-2350.

Desai-Mehta, A., K.M. Cerosaletti, and P. Concannon. 2001. Distinct functional domains of nibrin mediate Mre11 binding, focus formation, and nuclear localization. *Mol Cell Biol*. 21:2184-2191.

Desterro, J.M., M.S. Rodriguez, G.D. Kemp, and R.T. Hay. 1999. Identification of the enzyme required for activation of the small ubiquitin-like protein SUMO-1. *The Journal of biological chemistry*. 274:10618-10624.

Devgan, S.S., O. Sanal, C. Doil, K. Nakamura, S.A. Nahas, K. Pettijohn, J. Bartek, C. Lukas, J. Lukas, and R.A. Gatti. 2011. Homozygous deficiency of ubiquitin-ligase ring-finger protein RNF168 mimics the radiosensitivity syndrome of ataxia-telangiectasia. *Cell Death Differ*. 18:1500-1506.

Dexheimer, T.S., A. Kozekova, C.J. Rizzo, M.P. Stone, and Y. Pommier. 2008. The modulation of topoisomerase I-mediated DNA cleavage and the induction of DNA-topoisomerase I crosslinks by crotonaldehyde-derived DNA adducts. *Nucleic Acids Res*. 36:4128-4136.

Dexheimer, T.S., A.G. Stephen, M.J. Fivash, R.J. Fisher, and Y. Pommier. 2010. The DNA binding and 3'-end preferential activity of human tyrosyl-DNA phosphodiesterase. *Nucleic Acids Res*. 38:2444-2452.

Dinant, C., G. Ampatziadis-Michailidis, H. Lans, M. Tresini, A. Lagarou, M. Grosbart, A.F. Theil, W.A. van Cappellen, H. Kimura, J. Bartek, M. Fousteri, A.B. Houtsmuller, W. Vermeulen, and J.A. Marteijn. 2013. Enhanced chromatin dynamics by FACT promotes transcriptional restart after UV-induced DNA damage. *Mol Cell*. 51:469-479.

Dinant, C., M.S. Luijsterburg, T. Hofer, G. von Bornstaedt, W. Vermeulen, A.B. Houtsmuller, and R. van Driel. 2009. Assembly of multiprotein complexes that control genome function. *J Cell Biol*. 185:21-26.

Ding, Q., Y.V. Reddy, W. Wang, T. Woods, P. Douglas, D.A. Ramsden, S.P. Lees-Miller, and K. Meek. 2003. Autophosphorylation of the catalytic subunit of the DNA-dependent protein kinase is required for efficient end processing during DNA double-strand break repair. *Mol Cell Biol*. 23:5836-5848.

DiTullio, R.A., T.A. Mochan, M. Venere, J. Bartkova, M. Sehested, J. Bartek, and T.D. Halazonetis. 2002. 53BP1 functions in an ATM-dependent checkpoint pathway that is constitutively activated in human cancer. *Nat Cell Biol*. 4:998-1002.

Dobbs, T.A., J.A. Tainer, and S.P. Lees-Miller. 2010. A structural model for regulation of NHEJ by DNA-PKcs autophosphorylation. *DNA repair*. 9:1307-1314.

Doil, C., N. Mailand, S. Bekker-Jensen, P. Menard, D.H. Larsen, R. Pepperkok, J. Ellenberg, S. Panier, D. Durocher, J. Bartek, J. Lukas, and C. Lukas. 2009. RNF168 binds and amplifies ubiquitin conjugates on damaged chromosomes to allow accumulation of repair proteins. *Cell*. 136:435-446.

Douglas, P., X. Cui, W.D. Block, Y. Yu, S. Gupta, Q. Ding, R. Ye, N. Morrice, S.P. Lees-Miller, and K. Meek. 2007. The DNA-dependent protein kinase catalytic subunit is phosphorylated in vivo on threonine 3950, a highly conserved amino acid in the protein kinase domain. *Mol Cell Biol*. 27:1581-1591.

Douglas, P., J. Zhong, R. Ye, G.B. Moorhead, X. Xu, and S.P. Lees-Miller. 2010. Protein phosphatase 6 interacts with the DNA-dependent protein kinase catalytic subunit and dephosphorylates gamma-H2AX. *Mol Cell Biol*. 30:1368-1381.

Downs, J.A., S. Allard, O. Jobin-Robitaille, A. Javaheri, A. Auger, N. Bouchard, S.J. Kron, S.P. Jackson, and J. Cote. 2004. Binding of chromatin-modifying activities to phosphorylated histone H2A at DNA damage sites. *Mol Cell*. 16:979-990.

Drew, Y., and R. Plummer. 2009. PARP inhibitors in cancer therapy: two modes of attack on the cancer cell widening the clinical applications. *Drug Resist Updat*. 12:153-156.

Drolet, M. 2006. Growth inhibition mediated by excess negative supercoiling: the interplay between transcription elongation, R-loop formation and DNA topology. *Mol Microbiol*. 59:723-730.

Drolet, M., X. Bi, and L.F. Liu. 1994. Hypernegative supercoiling of the DNA template during transcription elongation in vitro. *The Journal of biological chemistry*. 269:2068-2074.

Drolet, M., S. Broccoli, F. Rallu, C. Hraiky, C. Fortin, E. Masse, and I. Baaklini. 2003. The problem of hypernegative supercoiling and R-loop formation in transcription. *Front Biosci*. 8:d210-221.

Drolet, M., P. Phoenix, R. Menzel, E. Masse, L.F. Liu, and R.J. Crouch. 1995. Overexpression of RNase H partially complements the growth defect of an Escherichia coli delta topA mutant: R-loop formation is a major problem in the absence of DNA topoisomerase I. *Proc Natl Acad Sci U S A*. 92:3526-3530.

Duann, P., M. Sun, C.T. Lin, H. Zhang, and L.F. Liu. 1999. Plasmid linking number change induced by topoisomerase I-mediated DNA damage. *Nucleic Acids Res*. 27:2905-2911.

Dubiel, W., G. Pratt, K. Ferrell, and M. Rechsteiner. 1992. Purification of an 11 S regulator of the multicatalytic protease. *The Journal of biological chemistry*. 267:22369-22377.

Dujardin, G., C. Lafaille, M. de la Mata, L.E. Marasco, M.J. Munoz, C. Le Jossic-Corcos, L. Corcos, and A.R. Kornblihtt. 2014. How slow RNA polymerase II elongation favors alternative exon skipping. *Mol Cell*. 54:683-690.

Dupré, A., L. Boyer-Chatenet, and J. Gautier. 2006. Two-step activation of ATM by DNA and the Mre11-Rad50-Nbs1 complex. *Nat Struct Mol Biol*. 13:451-457.

Duquette, M.L., P. Handa, J.A. Vincent, A.F. Taylor, and N. Maizels. 2004. Intracellular transcription of G-rich DNAs induces formation of G-loops, novel structures containing G4 DNA. *Genes Dev*. 18:1618-1629.

Durand-Dubief, M., J. Persson, U. Norman, E. Hartsuiker, and K. Ekwall. 2010. Topoisomerase I regulates open chromatin and controls gene expression in vivo. *EMBO J*. 29:2126-2134.

Durand-Dubief, M., J.P. Svensson, J. Persson, and K. Ekwall. 2011. Topoisomerases, chromatin and transcription termination. *Transcription*. 2:66-70.

Durban, E., M. Goodenough, J. Mills, and H. Busch. 1985. Topoisomerase I phosphorylation in vitro and in rapidly growing Novikoff hepatoma cells. *EMBO J*. 4:2921-2926.

Dutertre, M., G. Sanchez, M.C. De Cian, J. Barbier, E. Dardenne, L. Gratadou, G. Dujardin, C. Le Jossic-Corcos, L. Corcos, and D. Auboeuf. 2010. Cotranscriptional exon skipping in the genotoxic stress response. *Nat Struct Mol Biol*. 17:1358-1366.

Dvir, A., S.R. Peterson, M.W. Knuth, H. Lu, and W.S. Dynan. 1992. Ku autoantigen is the regulatory component of a template-associated protein kinase that phosphorylates RNA polymerase II. *Proc Natl Acad Sci U S A*. 89:11920-11924.

Dwane, S., E. Durack, and P.A. Kiely. 2013. Optimising parameters for the differentiation of SH-SY5Y cells to study cell adhesion and cell migration. *BMC Res Notes*. 6:366.

Eisenreich, A., V.Y. Bogdanov, A. Zakrzewicz, A. Pries, S. Antoniak, W. Poller, H.P. Schultheiss, and U. Rauch. 2009. Cdc2-like kinases and DNA topoisomerase I regulate alternative splicing of tissue factor in human endothelial cells. *Circ Res*. 104:589-599.

El Hage, A., S.L. French, A.L. Beyer, and D. Tollervey. 2010. Loss of Topoisomerase I leads to R-loop-mediated transcriptional blocks during ribosomal RNA synthesis. *Genes Dev*. 24:1546-1558.

El-Khamisy, S.F., E. Hartsuiker, and K.W. Caldecott. 2007. TDP1 facilitates repair of ionizing radiation-induced DNA single-strand breaks. *DNA repair*. 6:1485-1495.

El-Khamisy, S.F., G.M. Saifi, M. Weinfeld, F. Johansson, T. Helleday, J.R. Lupski, and K.W. Caldecott. 2005. Defective DNA single-strand break repair in spinocerebellar ataxia with axonal neuropathy-1. *Nature*. 434:108-113.

Eliezer, Y., L. Argaman, A. Rhie, A.J. Doherty, and M. Goldberg. 2009. The direct interaction between 53BP1 and MDC1 is required for the recruitment of 53BP1 to sites of damage. *The Journal of biological chemistry*. 284:426-435.

Elmroth, K., J. Nygren, S. Mårtensson, I.H. Ismail, and O. Hammarsten. 2003a. Cleavage of cellular DNA by calicheamicin gamma1. *DNA repair*. 2:363-374.

Elmroth, K., J. Nygren, B. Stenerlöw, and R. Hultborn. 2003b. Chromatin- and temperature-dependent modulation of radiation-induced double-strand breaks. *Int J Radiat Biol*. 79:809-816.

Enchev, R.I., B.A. Schulman, and M. Peter. 2015. Protein neddylation: beyond cullin-RING ligases. *Nat Rev Mol Cell Biol*. 16:30-44.

Enchev, R.I., D.C. Scott, P.C. da Fonseca, A. Schreiber, J.K. Monda, B.A. Schulman, M. Peter, and E.P. Morris. 2012. Structural basis for a reciprocal regulation between SCF and CSN. *Cell reports*. 2:616-627.

Eng, W.K., L. Faucette, R.K. Johnson, and R. Sternglanz. 1988. Evidence that DNA topoisomerase I is necessary for the cytotoxic effects of camptothecin. *Mol Pharmacol*. 34:755-760.

Eng, W.K., F.L. McCabe, K.B. Tan, M.R. Mattern, G.A. Hofmann, R.D. Woessner, R.P. Hertzberg, and R.K. Johnson. 1990. Development of a stable camptothecin-resistant subline of P388 leukemia with reduced topoisomerase I content. *Mol Pharmacol*. 38:471-480.

Erba, E., D. Bergamaschi, L. Bassano, G. Damia, S. Ronzoni, G.T. Faircloth, and M. D'Incalci. 2001. Ecteinascidin-743 (ET-743), a natural marine compound, with a unique mechanism of action. *Eur J Cancer*. 37:97-105.

Escribano-Diaz, C., A. Orthwein, A. Fradet-Turcotte, M. Xing, J.T. Young, J. Tkac, M.A. Cook, A.P. Rosebrock, M. Munro, M.D. Canny, D. Xu, and D. Durocher. 2013. A cell cycle-dependent regulatory circuit composed of 53BP1-RIF1 and BRCA1-CtIP controls DNA repair pathway choice. *Mol Cell*. 49:872-883.

Facchino, S., M. Abdouh, W. Chatoo, and G. Bernier. 2010. BMI1 confers radioresistance to normal and cancerous neural stem cells through recruitment of the DNA damage response machinery. *The Journal of neuroscience : the official journal of the Society for Neuroscience*. 30:10096-10111.

Falck, J., J. Coates, and S.P. Jackson. 2005. Conserved modes of recruitment of ATM, ATR and DNA-PKcs to sites of DNA damage. *Nature*. 434:605-611.

Farmer, H., N. McCabe, C.J. Lord, A.N. Tutt, D.A. Johnson, T.B. Richardson, M. Santarosa, K.J. Dillon, I. Hickson, C. Knights, N.M. Martin, S.P. Jackson, G.C. Smith, and A. Ashworth. 2005. Targeting the DNA repair defect in BRCA mutant cells as a therapeutic strategy. *Nature*. 434:917-921.

Fedier, A., R.A. Steiner, V.A. Schwarz, L. Lenherr, U. Haller, and D. Fink. 2003. The effect of loss of Brca1 on the sensitivity to anticancer agents in p53-deficient cells. *International journal of oncology*. 22:1169-1173.

Feng, L., and J. Chen. 2012. The E3 ligase RNF8 regulates KU80 removal and NHEJ repair. *Nat Struct Mol Biol*. 19:201-206.

Feng, L., J. Huang, and J. Chen. 2009. MERIT40 facilitates BRCA1 localization and DNA damage repair. *Genes Dev*. 23:719-728.

Ferdous, A., F. Gonzalez, L. Sun, T. Kodadek, and S.A. Johnston. 2001. The 19S regulatory particle of the proteasome is required for efficient transcription elongation by RNA polymerase II. *Mol Cell*. 7:981-991.

Ferdous, A., T. Kodadek, and S.A. Johnston. 2002. A nonproteolytic function of the 19S regulatory subunit of the 26S proteasome is required for efficient activated transcription by human RNA polymerase II. *Biochemistry*. 41:12798-12805.

Fernandez-Capetillo, O., A. Lee, M. Nussenzweig, and A. Nussenzweig. 2004. H2AX: the histone guardian of the genome. *DNA repair*. 3:959-967.

Finley, D., A. Ciechanover, and A. Varshavsky. 1984. Thermolability of ubiquitin-activating enzyme from the mammalian cell cycle mutant ts85. *Cell*. 37:43-55.

Fnu, S., E.A. Williamson, L.P. De Haro, M. Brenneman, J. Wray, M. Shaheen, K. Radhakrishnan, S.H. Lee, J.A. Nickoloff, and R. Hromas. 2011. Methylation of histone H3 lysine 36 enhances DNA repair by nonhomologous end-joining. *Proc Natl Acad Sci U S A*. 108:540-545.

Foray, N., D. Marot, A. Gabriel, V. Randrianarison, A.M. Carr, M. Perricaudet, A. Ashworth, and P. Jeggo. 2003. A subset of ATM- and ATR-dependent phosphorylation events requires the BRCA1 protein. *EMBO J*. 22:2860-2871.

Fradet-Turcotte, A., M.D. Canny, C. Escribano-Diaz, A. Orthwein, C.C. Leung, H. Huang, M.C. Landry, J. Kitevski-LeBlanc, S.M. Noordermeer, F. Sicheri, and D. Durocher. 2013. 53BP1 is a reader of the DNA-damage-induced H2A Lys 15 ubiquitin mark. *Nature*. 499:50-54.

Francia, S., F. Michelini, A. Saxena, D. Tang, M. de Hoon, V. Anelli, M. Mione, P. Carninci, and F.D. di Fagagna. 2012. Site-specific DICER and DROSHA RNA products control the DNA-damage response. *Nature*.

Fricke, B., S. Heink, J. Steffen, P.M. Kloetzel, and E. Kruger. 2007. The proteasome maturation protein POMP facilitates major steps of 20S proteasome formation at the endoplasmic reticulum. *EMBO Rep*. 8:1170-1175.

Fricke, W.M., and S.J. Brill. 2003. Slx1-Slx4 is a second structure-specific endonuclease functionally redundant with Sgs1-Top3. *Genes Dev*. 17:1768-1778.

Frit, P., R.Y. Li, D. Arzel, B. Salles, and P. Calsou. 2000. Ku entry into DNA inhibits inward DNA transactions in vitro. *The Journal of biological chemistry*. 275:35684-35691.

Fujimori, A., W.G. Harker, G. Kohlhagen, Y. Hoki, and Y. Pommier. 1995. Mutation at the catalytic site of topoisomerase I in CEM/C2, a human leukemia cell line resistant to camptothecin. *Cancer Res*. 55:1339-1346.

Furuta, T., H. Takemura, Z.Y. Liao, G.J. Aune, C. Redon, O.A. Sedelnikova, D.R. Pilch, E.P. Rogakou, A. Celeste, H.T. Chen, A. Nussenzweig, M.I. Aladjem, W.M. Bonner, and Y. Pommier. 2003. Phosphorylation of histone H2AX and activation of Mre11, Rad50, and Nbs1 in response to replication-dependent DNA double-strand breaks induced by mammalian DNA topoisomerase I cleavage complexes. *The Journal of biological chemistry*. 278:20303-20312.

Galanty, Y., R. Belotserkovskaya, J. Coates, and S.P. Jackson. 2012. RNF4, a SUMO-targeted ubiquitin E3 ligase, promotes DNA double-strand break repair. *Genes Dev*. 26:1179-1195.

Galanty, Y., R. Belotserkovskaya, J. Coates, S. Polo, K.M. Miller, and S.P. Jackson. 2009. Mammalian SUMO E3-ligases PIAS1 and PIAS4 promote responses to DNA double-strand breaks. *Nature*. 462:935-939.

Gandhi, M., V.N. Evdokimova, K.T. Cuenco, C.J. Bakkenist, and Y.E. Nikiforov. 2013. Homologous chromosomes move and rapidly initiate contact at the sites of double-strand breaks in genes in G_0-phase human cells. *Cell Cycle*. 12:547-552.

Gandhi, M., V.N. Evdokimova, K. T Cuenco, M.N. Nikiforova, L.M. Kelly, J.R. Stringer, C.J. Bakkenist, and Y.E. Nikiforov. 2012. Homologous chromosomes make contact at the sites of double-strand breaks in genes in somatic G0/G1-phase human cells. *Proc Natl Acad Sci U S A*. 109:9454-9459.

Ganguly, A., B. Das, A. Roy, N. Sen, S.B. Dasgupta, S. Mukhopadhayay, and H.K. Majumder. 2007. Betulinic acid, a catalytic inhibitor of topoisomerase I, inhibits reactive oxygen species-mediated apoptotic topoisomerase I-DNA cleavable complex formation in prostate cancer cells but does not affect the process of cell death. *Cancer Res*. 67:11848-11858.

Garg, L.C., S. DiAngelo, and S.T. Jacob. 1987. Role of DNA topoisomerase I in the transcription of supercoiled rRNA gene. *Proc Natl Acad Sci U S A*. 84:3185-3188.

Gartenberg, M.R., and J.C. Wang. 1992. Positive supercoiling of DNA greatly diminishes mRNA synthesis in yeast. *Proc Natl Acad Sci U S A*. 89:11461-11465.

Gately, D.P., J.C. Hittle, G.K. Chan, and T.J. Yen. 1998. Characterization of ATM expression, localization, and associated DNA-dependent protein kinase activity. *Molecular biology of the cell*. 9:2361-2374.

Gatti, M., S. Pinato, E. Maspero, P. Soffientini, S. Polo, and L. Penengo. 2012. A novel ubiquitin mark at the N-terminal tail of histone H2As targeted by RNF168 ubiquitin ligase. *Cell Cycle*. 11:2538-2544.

Germani, A., A. Prabel, S. Mourah, M.P. Podgorniak, A. Di Carlo, R. Ehrlich, S. Gisselbrecht, N. Varin-Blank, F. Calvo, and H. Bruzzoni-Giovanelli. 2003. SIAH-1 interacts with CtIP and promotes its degradation by the proteasome pathway. *Oncogene*. 22:8845-8851.

Gillette, T.G., F. Gonzalez, A. Delahodde, S.A. Johnston, and T. Kodadek. 2004. Physical and functional association of RNA polymerase II and the proteasome. *Proc Natl Acad Sci U S A*. 101:5904-5909.

Gilmour, D.S., G. Pflugfelder, J.C. Wang, and J.T. Lis. 1986. Topoisomerase I interacts with transcribed regions in Drosophila cells. *Cell*. 44:401-407.

Ginjala, V., K. Nacerddine, A. Kulkarni, J. Oza, S.J. Hill, M. Yao, E. Citterio, M. van Lohuizen, and S. Ganesan. 2011. BMI1 is recruited to DNA breaks and contributes to DNA damage-induced H2A ubiquitination and repair. *Mol Cell Biol*. 31:1972-1982.

Ginno, P.A., P.L. Lott, H.C. Christensen, I. Korf, and F. Chedin. 2012. R-loop formation is a distinctive characteristic of unmethylated human CpG island promoters. *Mol Cell*. 45:814-825.

Girard, P.M., E. Riballo, A.C. Begg, A. Waugh, and P.A. Jeggo. 2002. Nbs1 promotes ATM dependent phosphorylation events including those required for G1/S arrest. *Oncogene*. 21:4191-4199.

Gonzalez, F., A. Delahodde, T. Kodadek, and S.A. Johnston. 2002. Recruitment of a 19S proteasome subcomplex to an activated promoter. *Science (New York, N.Y.* 296:548-550.

Goodarzi, A.A., and P.A. Jeggo. 2012. The heterochromatic barrier to DNA double strand break repair: how to get the entry visa. *Int J Mol Sci*. 13:11844-11860.

Goodarzi, A.A., J.C. Jonnalagadda, P. Douglas, D. Young, R. Ye, G.B. Moorhead, S.P. Lees-Miller, and K.K. Khanna. 2004. Autophosphorylation of ataxia-telangiectasia mutated is regulated by protein phosphatase 2A. *EMBO J*. 23:4451-4461.

Goodarzi, A.A., T. Kurka, and P.A. Jeggo. 2011. KAP-1 phosphorylation regulates CHD3 nucleosome remodeling during the DNA double-strand break response. *Nat Struct Mol Biol*. 18:831-839.

Goodarzi, A.A., A.T. Noon, D. Deckbar, Y. Ziv, Y. Shiloh, M. Lobrich, and P.A. Jeggo. 2008. ATM signaling facilitates repair of DNA double-strand breaks associated with heterochromatin. *Mol Cell*. 31:167-177.

Goodwin, J.F., and K.E. Knudsen. 2014. Beyond DNA repair: DNA-PK function in cancer. *Cancer discovery*. 4:1126-1139.

Goto, T., and J.C. Wang. 1985. Cloning of yeast TOP1, the gene encoding DNA topoisomerase I, and construction of mutants defective in both DNA topoisomerase I and DNA topoisomerase II. *Proc Natl Acad Sci U S A*. 82:7178-7182.

Gottlieb, J.A., A.M. Guarino, J.B. Call, V.T. Oliverio, and J.B. Block. 1970. Preliminary pharmacologic and clinical evaluation of camptothecin sodium (NSC-100880). *Cancer Chemother Rep*. 54:461-470.

Grabarz, A., A. Barascu, J. Guirouilh-Barbat, and B.S. Lopez. 2012. Initiation of DNA double strand break repair: signaling and single-stranded resection dictate the choice between homologous recombination, non-homologous end-joining and alternative end-joining. *Am J Cancer Res*. 2:249-268.

Grewal, S.I., and D. Moazed. 2003. Heterochromatin and epigenetic control of gene expression. *Science (New York, N.Y.* 301:798-802.

Groh, M., and N. Gromak. 2014. Out of balance: R-loops in human disease. *PLoS Genet*. 10:e1004630.

Groh, M., M.M. Lufino, R. Wade-Martins, and N. Gromak. 2014. R-loops associated with triplet repeat expansions promote gene silencing in Friedreich ataxia and fragile X syndrome. *PLoS Genet*. 10:e1004318.

Groll, M., M. Bajorek, A. Kohler, L. Moroder, D.M. Rubin, R. Huber, M.H. Glickman, and D. Finley. 2000. A gated channel into the proteasome core particle. *Nature structural biology*. 7:1062-1067.

Gu, Y., S. Jin, Y. Gao, D.T. Weaver, and F.W. Alt. 1997. Ku70-deficient embryonic stem cells have increased ionizing radiosensitivity, defective DNA end-binding activity, and inability to support V(D)J recombination. *Proc Natl Acad Sci U S A*. 94:8076-8081.

Gudmundsdottir, K., C.J. Lord, and A. Ashworth. 2007. The proteasome is involved in determining differential utilization of double-strand break repair pathways. *Oncogene*. 26:7601-7606.

Guirouilh-Barbat, J., C. Redon, and Y. Pommier. 2008. Transcription-coupled DNA double-strand breaks are mediated via the nucleotide excision repair and the Mre11-Rad50-Nbs1 complex. *Molecular biology of the cell*. 19:3969-3981.

Gunn, A., N. Bennardo, A. Cheng, and J.M. Stark. 2011. Correct end use during end joining of multiple chromosomal double strand breaks is influenced by repair protein RAD50, DNA-dependent protein kinase DNA-PKcs, and transcription context. *The Journal of biological chemistry*. 286:42470-42482.

Guo, Z., S. Kozlov, M.F. Lavin, M.D. Person, and T.T. Paull. 2010. ATM activation by oxidative stress. *Science (New York, N.Y.* 330:517-521.

Gupta, A., G.G. Sharma, C.S. Young, M. Agarwal, E.R. Smith, T.T. Paull, J.C. Lucchesi, K.K. Khanna, T. Ludwig, and T.K. Pandita. 2005. Involvement of human MOF in ATM function. *Mol Cell Biol*. 25:5292-5305.

Guzzo, C.M., C.E. Berndsen, J. Zhu, V. Gupta, A. Datta, R.A. Greenberg, C. Wolberger, and M.J. Matunis. 2012. RNF4-dependent hybrid SUMO-ubiquitin chains are signals for RAP80 and thereby mediate the recruitment of BRCA1 to sites of DNA damage. *Science signaling*. 5:ra88.

Haber, J.E. 1999. DNA recombination: the replication connection. *Trends Biochem Sci*. 24:271-275.

Haince, J.F., S. Kozlov, V.L. Dawson, T.M. Dawson, M.J. Hendzel, M.F. Lavin, and G.G. Poirier. 2007. Ataxia telangiectasia mutated (ATM) signaling network is modulated by a novel poly(ADP-ribose)-dependent pathway in the early response to DNA-damaging agents. *The Journal of biological chemistry*. 282:16441-16453.

Haluska, P., Jr., A. Saleem, Z. Rasheed, F. Ahmed, E.W. Su, L.F. Liu, and E.H. Rubin. 1999. Interaction between human topoisomerase I and a novel RING finger/arginine-serine protein. *Nucleic Acids Res*. 27:2538-2544.

Hamilton, N.K., and N. Maizels. 2010. MRE11 function in response to topoisomerase poisons is independent of its function in double-strand break repair in Saccharomyces cerevisiae. *PLoS One*. 5:e15387.

Hamperl, S., and K.A. Cimprich. 2014. The contribution of co-transcriptional RNA:DNA hybrid structures to DNA damage and genome instability. *DNA repair*. 19:84-94.
Hanawalt, P.C., and G. Spivak. 2008. Transcription-coupled DNA repair: two decades of progress and surprises. *Nat Rev Mol Cell Biol*. 9:958-970.
Harding, S.M., J.A. Boiarsky, and R.A. Greenberg. 2015. ATM Dependent Silencing Links Nucleolar Chromatin Reorganization to DNA Damage Recognition. *Cell reports*. 13:251-259.
Harper, J.W., and S.J. Elledge. 2007. The DNA damage response: ten years after. *Mol Cell*. 28:739-745.
Harrigan, J.A., R. Belotserkovskaya, J. Coates, D.S. Dimitrova, S.E. Polo, C.R. Bradshaw, P. Fraser, and S.P. Jackson. 2011. Replication stress induces 53BP1-containing OPT domains in G1 cells. *J Cell Biol*. 193:97-108.
Hartlerode, A.J., and R. Scully. 2009. Mechanisms of double-strand break repair in somatic mammalian cells. *Biochem J*. 423:157-168.
Hartley, K.O., D. Gell, G.C. Smith, H. Zhang, N. Divecha, M.A. Connelly, A. Admon, S.P. Lees-Miller, C.W. Anderson, and S.P. Jackson. 1995. DNA-dependent protein kinase catalytic subunit: a relative of phosphatidylinositol 3-kinase and the ataxia telangiectasia gene product. *Cell*. 82:849-856.
Hartsuiker, E., M.J. Neale, and A.M. Carr. 2009. Distinct requirements for the Rad32(Mre11) nuclease and Ctp1(CtIP) in the removal of covalently bound topoisomerase I and II from DNA. *Mol Cell*. 33:117-123.
Hatfield, G.W., and C.J. Benham. 2002. DNA topology-mediated control of global gene expression in Escherichia coli. *Annu Rev Genet*. 36:175-203.
Haupt, Y., R. Maya, A. Kazaz, and M. Oren. 1997. Mdm2 promotes the rapid degradation of p53. *Nature*. 387:296-299.
Helleday, T. 2011. The underlying mechanism for the PARP and BRCA synthetic lethality: clearing up the misunderstandings. *Mol Oncol*. 5:387-393.
Helleday, T., E. Petermann, C. Lundin, B. Hodgson, and R.A. Sharma. 2008. DNA repair pathways as targets for cancer therapy. *Nat Rev Cancer*. 8:193-204.
Henderson, A., Y. Wu, Y.C. Huang, E.A. Chavez, J. Platt, F.B. Johnson, R.M. Brosh, Jr., D. Sen, and P.M. Lansdorp. 2014. Detection of G-quadruplex DNA in mammalian cells. *Nucleic Acids Res*. 42:860-869.
Heo, K., H. Kim, S.H. Choi, J. Choi, K. Kim, J. Gu, M.R. Lieber, A.S. Yang, and W. An. 2008. FACT-mediated exchange of histone variant H2AX regulated by phosphorylation of H2AX and ADP-ribosylation of Spt16. *Mol Cell*. 30:86-97.
Herrera-Moyano, E., X. Mergui, M.L. García-Rubio, S. Barroso, and A. Aguilera. 2014. The yeast and human FACT chromatin-reorganizing complexes solve R-loop-mediated transcription-replication conflicts. *Genes Dev*. 28:735-748.
Higgins, N.P., and A.V. Vologodskii. 2015. Topological Behavior of Plasmid DNA. *Microbiol Spectr*. 3.
Hirano, R., H. Interthal, C. Huang, T. Nakamura, K. Deguchi, K. Choi, M.B. Bhattacharjee, K. Arimura, F. Umehara, S. Izumo, J.L. Northrop, M.A. Salih, K. Inoue, D.L. Armstrong, J.J. Champoux, H. Takashima, and C.F. Boerkoel. 2007. Spinocerebellar ataxia with axonal neuropathy: consequence of a Tdp1 recessive neomorphic mutation? *EMBO J*. 26:4732-4743.
Hiraoka, L.R., J.J. Harrington, D.S. Gerhard, M.R. Lieber, and C.L. Hsieh. 1995. Sequence of human FEN-1, a structure-specific endonuclease, and chromosomal localization of the gene (FEN1) in mouse and human. *Genomics*. 25:220-225.
Hochster, H., L. Liebes, J. Speyer, J. Sorich, B. Taubes, R. Oratz, J. Wernz, A. Chachoua, R.H. Blum, and A. Zeleniuch-Jacquotte. 1997. Effect of prolonged topotecan infusion on topoisomerase 1 levels: a phase I and pharmacodynamic study. *Clin Cancer Res*. 3:1245-1252.
Hoeijmakers, J.H. 2009. DNA damage, aging, and cancer. *N Engl J Med*. 361:1475-1485.
Holm, C., J.M. Covey, D. Kerrigan, and Y. Pommier. 1989. Differential requirement of DNA replication for the cytotoxicity of DNA topoisomerase I and II inhibitors in Chinese hamster DC3F cells. *Cancer Res*. 49:6365-6368.
Hopfner, K.P., L. Craig, G. Moncalian, R.A. Zinkel, T. Usui, B.A. Owen, A. Karcher, B. Henderson, J.L. Bodmer, C.T. McMurray, J.P. Carney, J.H. Petrini, and J.A. Tainer. 2002. The Rad50 zinc-hook is a structure joining Mre11 complexes in DNA recombination and repair. *Nature*. 418:562-566.
Horie, K., A. Tomida, Y. Sugimoto, T. Yasugi, H. Yoshikawa, Y. Taketani, and T. Tsuruo. 2002. SUMO-1 conjugation to intact DNA topoisomerase I amplifies cleavable complex formation induced by camptothecin. *Oncogene*. 21:7913-7922.
Horwitz, S.B., C.K. Chang, and A.P. Grollman. 1971. Studies on camptothecin. I. Effects of nucleic acid and protein synthesis. *Mol Pharmacol*. 7:632-644.
Horwitz, S.B., and M.S. Horwitz. 1973. Effects of camptothecin on the breakage and repair of DNA during the cell cycle. *Cancer Res*. 33:2834-2836.
Hsiang, Y.H., R. Hertzberg, S. Hecht, and L.F. Liu. 1985. Camptothecin induces protein-linked DNA breaks via mammalian DNA topoisomerase I. *The Journal of biological chemistry*. 260:14873-14878.
Hsiang, Y.H., M.G. Lihou, and L.F. Liu. 1989a. Arrest of replication forks by drug-stabilized topoisomerase I-DNA cleavable complexes as a mechanism of cell killing by camptothecin. *Cancer Res*. 49:5077-5082.
Hsiang, Y.H., L.F. Liu, M.E. Wall, M.C. Wani, A.W. Nicholas, G. Manikumar, S. Kirschenbaum, R. Silber, and M. Potmesil. 1989b. DNA topoisomerase I-mediated DNA cleavage and cytotoxicity of camptothecin analogues. *Cancer Res*. 49:4385-4389.
Hsiao, K.Y., and C.A. Mizzen. 2013. Histone H4 deacetylation facilitates 53BP1 DNA damage signaling and double-strand break repair. *Journal of molecular cell biology*. 5:157-165.
Huang, H.S., J.A. Allen, A.M. Mabb, I.F. King, J. Miriyala, B. Taylor-Blake, N. Sciaky, J.W. Dutton, Jr., H.M. Lee, X. Chen, J. Jin, A.S. Bridges, M.J. Zylka, B.L. Roth, and B.D. Philpot. 2012. Topoisomerase inhibitors unsilence the dormant allele of Ube3a in neurons. *Nature*. 481:185-189.
Huang, S.N., Y. Pommier, and C. Marchand. 2011. Tyrosyl-DNA Phosphodiesterase 1 (Tdp1) inhibitors. *Expert Opin Ther Pat*. 21:1285-1292.
Huang, S.Y., J. Murai, I. Dalla Rosa, T.S. Dexheimer, A. Naumova, W.H. Gmeiner, and Y. Pommier. 2013. TDP1 repairs nuclear and mitochondrial DNA damage induced by chain-terminating anticancer and antiviral nucleoside analogs. *Nucleic Acids Res*. 41:7793-7803.
Huang, T.H., H.C. Chen, S.M. Chou, Y.C. Yang, J.R. Fan, and T.K. Li. 2010. Cellular processing determinants for the activation of damage signals in response to topoisomerase I-linked DNA breakage. *Cell Res*. 20:1060-1075.

Hudson, J.J., S.C. Chiang, O.S. Wells, C. Rookyard, and S.F. El-Khamisy. 2012. SUMO modification of the neuroprotective protein TDP1 facilitates chromosomal single-strand break repair. *Nat Commun*. 3:733.
Huen, M.S., and J. Chen. 2010. ATM Creates a veil of transcriptional silence. *Cell*. 141:924-926.
Huen, M.S., R. Grant, I. Manke, K. Minn, X. Yu, M.B. Yaffe, and J. Chen. 2007. RNF8 transduces the DNA-damage signal via histone ubiquitylation and checkpoint protein assembly. *Cell*. 131:901-914.
Hunter, T. 2007. The age of crosstalk: phosphorylation, ubiquitination, and beyond. *Mol Cell*. 28:730-738.
Huyen, Y., O. Zgheib, R.A. Ditullio, Jr., V.G. Gorgoulis, P. Zacharatos, T.J. Petty, E.A. Sheston, H.S. Mellert, E.S. Stavridi, and T.D. Halazonetis. 2004. Methylated lysine 79 of histone H3 targets 53BP1 to DNA double-strand breaks. *Nature*. 432:406-411.
Hyman, A.A., C.A. Weber, and F. Julicher. 2014. Liquid-liquid phase separation in biology. *Annu Rev Cell Dev Biol*. 30:39-58.
Iacovoni, J.S., P. Caron, I. Lassadi, E. Nicolas, L. Massip, D. Trouche, and G. Legube. 2010. High-resolution profiling of gammaH2AX around DNA double strand breaks in the mammalian genome. *EMBO J*. 29:1446-1457.
Inamdar, K.V., J.J. Pouliot, T. Zhou, S.P. Lees-Miller, A. Rasouli-Nia, and L.F. Povirk. 2002. Conversion of phosphoglycolate to phosphate termini on 3' overhangs of DNA double strand breaks by the human tyrosyl-DNA phosphodiesterase hTdp1. *The Journal of biological chemistry*. 277:27162-27168.
Indig, F.E., J.J. Partridge, C. von Kobbe, M.I. Aladjem, M. Latterich, and V.A. Bohr. 2004. Werner syndrome protein directly binds to the AAA ATPase p97/VCP in an ATP-dependent fashion. *J Struct Biol*. 146:251-259.
Interthal, H., and J.J. Champoux. 2011. Effects of DNA and protein size on substrate cleavage by human tyrosyl-DNA phosphodiesterase 1. *Biochem J*. 436:559-566.
Interthal, H., H.J. Chen, and J.J. Champoux. 2005a. Human Tdp1 cleaves a broad spectrum of substrates, including phosphoamide linkages. *The Journal of biological chemistry*. 280:36518-36528.
Interthal, H., H.J. Chen, T.E. Kehl-Fie, J. Zotzmann, J.B. Leppard, and J.J. Champoux. 2005b. SCAN1 mutant Tdp1 accumulates the enzyme--DNA intermediate and causes camptothecin hypersensitivity. *Embo J*. 24:2224-2233.
Interthal, H., J.J. Pouliot, and J.J. Champoux. 2001. The tyrosyl-DNA phosphodiesterase Tdp1 is a member of the phospholipase D superfamily. *Proc Natl Acad Sci U S A*. 98:12009-12014.
Inukai, N., Y. Yamaguchi, I. Kuraoka, T. Yamada, S. Kamijo, J. Kato, K. Tanaka, and H. Handa. 2004. A novel hydrogen peroxide-induced phosphorylation and ubiquitination pathway leading to RNA polymerase II proteolysis. *The Journal of biological chemistry*. 279:8190-8195.
Ioanoviciu, A., S. Antony, Y. Pommier, B.L. Staker, L. Stewart, and M. Cushman. 2005. Synthesis and mechanism of action studies of a series of norindenoisoquinoline topoisomerase I poisons reveal an inhibitor with a flipped orientation in the ternary DNA-enzyme-inhibitor complex as determined by X-ray crystallographic analysis. *J Med Chem*. 48:4803-4814.
Iossifov, I., M. Ronemus, D. Levy, Z. Wang, I. Hakker, J. Rosenbaum, B. Yamrom, Y.H. Lee, G. Narzisi, A. Leotta, J. Kendall, E. Grabowska, B. Ma, S. Marks, L. Rodgers, A. Stepansky, J. Troge, P. Andrews, M. Bekritsky, K. Pradhan, E. Ghiban, M. Kramer, J. Parla, R. Demeter, L.L. Fulton, R.S. Fulton, V.J. Magrini, K. Ye, J.C. Darnell, R.B. Darnell, E.R. Mardis, R.K. Wilson, M.C. Schatz, W.R. McCombie, and M. Wigler. 2012. De novo gene disruptions in children on the autistic spectrum. *Neuron*. 74:285-299.
Ismail, I.H., C. Andrin, D. McDonald, and M.J. Hendzel. 2010. BMI1-mediated histone ubiquitylation promotes DNA double-strand break repair. *J Cell Biol*. 191:45-60.
Ito, K., A. Hirao, F. Arai, S. Matsuoka, K. Takubo, I. Hamaguchi, K. Nomiyama, K. Hosokawa, K. Sakurada, N. Nakagata, Y. Ikeda, T.W. Mak, and T. Suda. 2004. Regulation of oxidative stress by ATM is required for self-renewal of haematopoietic stem cells. *Nature*. 431:997-1002.
Ivanov, A.V., H. Peng, V. Yurchenko, K.L. Yap, D.G. Negorev, D.C. Schultz, E. Psulkowski, W.J. Fredericks, D.E. White, G.G. Maul, M.J. Sadofsky, M.M. Zhou, and F.J. Rauscher. 2007. PHD domain-mediated E3 ligase activity directs intramolecular sumoylation of an adjacent bromodomain required for gene silencing. *Mol Cell*. 28:823-837.
Jackson, S.P., and J. Bartek. 2009. The DNA-damage response in human biology and disease. *Nature*. 461:1071-1078.
Jackson, S.P., J.J. MacDonald, S. Lees-Miller, and R. Tjian. 1990. GC box binding induces phosphorylation of Sp1 by a DNA-dependent protein kinase. *Cell*. 63:155-165.
Jacq, X., M. Kemp, N.M. Martin, and S.P. Jackson. 2013. Deubiquitylating enzymes and DNA damage response pathways. *Cell Biochem Biophys*. 67:25-43.
Jacquemont, C., and T. Taniguchi. 2007. Proteasome function is required for DNA damage response and fanconi anemia pathway activation. *Cancer Res*. 67:7395-7405.
Jasin, M. 1996. Genetic manipulation of genomes with rare-cutting endonucleases. *Trends Genet*. 12:224-228.
Jaxel, C., G. Capranico, D. Kerrigan, K.W. Kohn, and Y. Pommier. 1991. Effect of local DNA sequence on topoisomerase I cleavage in the presence or absence of camptothecin. *The Journal of biological chemistry*. 266:20418-20423.
Jaxel, C., K.W. Kohn, M.C. Wani, M.E. Wall, and Y. Pommier. 1989. Structure-activity study of the actions of camptothecin derivatives on mammalian topoisomerase I: evidence for a specific receptor site and a relation to antitumor activity. *Cancer Res*. 49:1465-1469.
Jazayeri, A., J. Falck, C. Lukas, J. Bartek, G.C. Smith, J. Lukas, and S.P. Jackson. 2006. ATM- and cell cycle-dependent regulation of ATR in response to DNA double-strand breaks. *Nat Cell Biol*. 8:37-45.
Jette, N., and S.P. Lees-Miller. 2015. The DNA-dependent protein kinase: A multifunctional protein kinase with roles in DNA double strand break repair and mitosis. *Prog Biophys Mol Biol*. 117:194-205.
Jha, D.K., and B.D. Strahl. 2014. An RNA polymerase II-coupled function for histone H3K36 methylation in checkpoint activation and DSB repair. *Nat Commun*. 5:3965.
Jiang, G., and A. Sancar. 2006. Recruitment of DNA damage checkpoint proteins to damage in transcribed and nontranscribed sequences. *Mol Cell Biol*. 26:39-49.
Jiang, W., J.L. Crowe, X. Liu, S. Nakajima, Y. Wang, C. Li, B.J. Lee, R.L. Dubois, C. Liu, X. Yu, L. Lan, and S. Zha. 2015. Differential phosphorylation of DNA-PKcs regulates the interplay between end-processing and end-ligation during nonhomologous end-joining. *Mol Cell*. 58:172-185.

Jones, G.G., P.M. Reaper, A.R. Pettitt, and P.D. Sherrington. 2004. The ATR-p53 pathway is suppressed in noncycling normal and malignant lymphocytes. *Oncogene*. 23:1911-1921.
Jowsey, P., N.A. Morrice, C.J. Hastie, H. McLauchlan, R. Toth, and J. Rouse. 2007. Characterisation of the sites of DNA damage-induced 53BP1 phosphorylation catalysed by ATM and ATR. *DNA repair*. 6:1536-1544.
Juge, F., C. Fernando, W. Fic, and J. Tazi. 2010. The SR protein B52/SRp55 is required for DNA topoisomerase I recruitment to chromatin, mRNA release and transcription shutdown. *PLoS Genet*. 6:e1001124.
Jung, Y., and S.J. Lippard. 2006. RNA polymerase II blockage by cisplatin-damaged DNA. Stability and polyubiquitylation of stalled polymerase. *The Journal of biological chemistry*. 281:1361-1370.
Kagey, M.H., J.J. Newman, S. Bilodeau, Y. Zhan, D.A. Orlando, N.L. van Berkum, C.C. Ebmeier, J. Goossens, P.B. Rahl, S.S. Levine, D.J. Taatjes, J. Dekker, and R.A. Young. 2010. Mediator and cohesin connect gene expression and chromatin architecture. *Nature*. 467:430-435.
Kaidi, A., B.T. Weinert, C. Choudhary, and S.P. Jackson. 2010. Human SIRT6 promotes DNA end resection through CtIP deacetylation. *Science (New York, N.Y.* 329:1348-1353.
Kakarougkas, A., A. Ismail, A.L. Chambers, E. Riballo, A.D. Herbert, J. Künzel, M. Löbrich, P.A. Jeggo, and J.A. Downs. 2014. Requirement for PBAF in Transcriptional Repression and Repair at DNA Breaks in Actively Transcribed Regions of Chromatin. *Mol Cell*. 55:723-732.
Kanagasabai, R., S. Liu, S. Salama, E.F. Yamasaki, L. Zhang, K.B. Greenchurch, and R.M. Snapka. 2009. Ubiquitin-family modifications of topoisomerase I in camptothecin-treated human breast cancer cells. *Biochemistry*. 48:3176-3185.
Kang, M.R., M.T. Muller, and I.K. Chung. 2004. Telomeric DNA damage by topoisomerase I. A possible mechanism for cell killing by camptothecin. *The Journal of biological chemistry*. 279:12535-12541.
Kann, H.E., Jr., and K.W. Kohn. 1972. Effects of deoxyribonucleic acid-reactive drugs on ribonucleic acid synthesis in leukemia L1210 cells. *Mol Pharmacol*. 8:551-560.
Kanu, N., and A. Behrens. 2007. ATMIN defines an NBS1-independent pathway of ATM signalling. *EMBO J*. 26:2933-2941.
Kapusta, A., and C. Feschotte. 2014. Volatile evolution of long noncoding RNA repertoires: mechanisms and biological implications. *Trends Genet*. 30:439-452.
Katyal, S., S.F. el-Khamisy, H.R. Russell, Y. Li, L. Ju, K.W. Caldecott, and P.J. McKinnon. 2007. TDP1 facilitates chromosomal single-strand break repair in neurons and is neuroprotective in vivo. *Embo J*. 26:4720-4731.
Katyal, S., Y. Lee, K.C. Nitiss, S.M. Downing, Y. Li, M. Shimada, J. Zhao, H.R. Russell, J.H. Petrini, J.L. Nitiss, and P.J. McKinnon. 2014. Aberrant topoisomerase-1 DNA lesions are pathogenic in neurodegenerative genome instability syndromes. *Nat Neurosci*. 17:813-821.
Kennedy, R.D., C.C. Chen, P. Stuckert, E.M. Archila, M.A. De la Vega, L.A. Moreau, A. Shimamura, and A.D. D'Andrea. 2007. Fanconi anemia pathway-deficient tumor cells are hypersensitive to inhibition of ataxia telangiectasia mutated. *J Clin Invest*. 117:1440-1449.
Kerzendorfer, C., A. Whibley, G. Carpenter, E. Outwin, S.C. Chiang, G. Turner, C. Schwartz, S. El-Khamisy, F.L. Raymond, and M. O'Driscoll. 2010. Mutations in Cullin 4B result in a human syndrome associated with increased camptothecin-induced topoisomerase I-dependent DNA breaks. *Hum Mol Genet*. 19:1324-1334.
Keskin, H., Y. Shen, F. Huang, M. Patel, T. Yang, K. Ashley, A.V. Mazin, and F. Storici. 2014. Transcript-RNA-templated DNA recombination and repair. *Nature*.
Kessel, D. 1971. Effects of camptothecin on RNA synthesis in leukemia L1210 cells. *Biochim Biophys Acta*. 246:225-232.
Kessel, D., H.B. Bosmann, and K. Lohr. 1972. Camptothecin effects on DNA synthesis in murine leukemia cells. *Biochim Biophys Acta*. 269:210-216.
Khobta, A., F. Ferri, L. Lotito, A. Montecucco, R. Rossi, and G. Capranico. 2006. Early effects of topoisomerase I inhibition on RNA polymerase II along transcribed genes in human cells. *J Mol Biol*. 357:127-138.
Kim, H., J. Huang, and J. Chen. 2007. CCDC98 is a BRCA1-BRCT domain-binding protein involved in the DNA damage response. *Nat Struct Mol Biol*. 14:710-715.
Kim, M.Y., T. Zhang, and W.L. Kraus. 2005. Poly(ADP-ribosyl)ation by PARP-1: 'PAR-laying' NAD+ into a nuclear signal. *Genes Dev*. 19:1951-1967.
Kim, N., S.Y. Huang, J.S. Williams, Y.C. Li, A.B. Clark, J.E. Cho, T.A. Kunkel, Y. Pommier, and S. Jinks-Robertson. 2011. Mutagenic processing of ribonucleotides in DNA by yeast topoisomerase I. *Science (New York, N.Y.* 332:1561-1564.
Kim, S.T., D.S. Lim, C.E. Canman, and M.B. Kastan. 1999. Substrate specificities and identification of putative substrates of ATM kinase family members. *The Journal of biological chemistry*. 274:37538-37543.
Kim, Y., G.S. Spitz, U. Veturi, F.P. Lach, A.D. Auerbach, and A. Smogorzewska. 2013. Regulation of multiple DNA repair pathways by the Fanconi anemia protein SLX4. *Blood*. 121:54-63.
Kim, Y.C., G. Gerlitz, T. Furusawa, F. Catez, A. Nussenzweig, K.S. Oh, K.H. Kraemer, Y. Shiloh, and M. Bustin. 2009. Activation of ATM depends on chromatin interactions occurring before induction of DNA damage. *Nat Cell Biol*. 11:92-96.
King, I.F., C.N. Yandava, A.M. Mabb, J.S. Hsiao, H.S. Huang, B.L. Pearson, J.M. Calabrese, J. Starmer, J.S. Parker, T. Magnuson, S.J. Chamberlain, B.D. Philpot, and M.J. Zylka. 2013. Topoisomerases facilitate transcription of long genes linked to autism. *Nature*. 501:58-62.
Kinner, A., W. Wu, C. Staudt, and G. Iliakis. 2008. Gamma-H2AX in recognition and signaling of DNA double-strand breaks in the context of chromatin. *Nucleic Acids Res*. 36:5678-5694.
Kitagawa, R., C.J. Bakkenist, P.J. McKinnon, and M.B. Kastan. 2004. Phosphorylation of SMC1 is a critical downstream event in the ATM-NBS1-BRCA1 pathway. *Genes Dev*. 18:1423-1438.
Kleiman, F.E., F. Wu-Baer, D. Fonseca, S. Kaneko, R. Baer, and J.L. Manley. 2005. BRCA1/BARD1 inhibition of mRNA 3' processing involves targeted degradation of RNA polymerase II. *Genes Dev*. 19:1227-1237.
Kolas, N.K., J.R. Chapman, S. Nakada, J. Ylanko, R. Chahwan, F.D. Sweeney, S. Panier, M. Mendez, J. Wildenhain, T.M. Thomson, L. Pelletier, S.P. Jackson, and D. Durocher. 2007. Orchestration of the DNA-damage response by the RNF8 ubiquitin ligase. *Science (New York, N.Y.* 318:1637-1640.

Koster, D.A., V. Croquette, C. Dekker, S. Shuman, and N.H. Dekker. 2005. Friction and torque govern the relaxation of DNA supercoils by eukaryotic topoisomerase IB. *Nature*. 434:671-674.
Koster, D.A., K. Palle, E.S. Bot, M.A. Bjornsti, and N.H. Dekker. 2007. Antitumour drugs impede DNA uncoiling by topoisomerase I. *Nature*. 448:213-217.
Kouzine, F., A. Gupta, L. Baranello, D. Wojtowicz, K. Ben-Aissa, J. Liu, T.M. Przytycka, and D. Levens. 2013. Transcription-dependent dynamic supercoiling is a short-range genomic force. *Nat Struct Mol Biol*. 20:396-403.
Kozlov, S.V., M.E. Graham, C. Peng, P. Chen, P.J. Robinson, and M.F. Lavin. 2006. Involvement of novel autophosphorylation sites in ATM activation. *EMBO J*. 25:3504-3514.
Kretzschmar, M., M. Meisterernst, and R.G. Roeder. 1993. Identification of human DNA topoisomerase I as a cofactor for activator-dependent transcription by RNA polymerase II. *Proc Natl Acad Sci U S A*. 90:11508-11512.
Kristensen, C.N., K.M. Bystol, B. Li, L. Serrano, and M.A. Brenneman. 2010. Depletion of DSS1 protein disables homologous recombinational repair in human cells. *Mutation research*. 694:60-64.
Kroeger, P.E., and T.C. Rowe. 1992. Analysis of topoisomerase I and II cleavage sites on the Drosophila actin and Hsp70 heat shock genes. *Biochemistry*. 31:2492-2501.
Kruhlak, M., E.E. Crouch, M. Orlov, C. Montano, S.A. Gorski, A. Nussenzweig, T. Misteli, R.D. Phair, and R. Casellas. 2007. The ATM repair pathway inhibits RNA polymerase I transcription in response to chromosome breaks. *Nature*. 447:730-734.
Kruhlak, M.J., A. Celeste, G. Dellaire, O. Fernandez-Capetillo, W.G. Müller, J.G. McNally, D.P. Bazett-Jones, and A. Nussenzweig. 2006. Changes in chromatin structure and mobility in living cells at sites of DNA double-strand breaks. *J Cell Biol*. 172:823-834.
Laine, J.P., P.L. Opresko, F.E. Indig, J.A. Harrigan, C. von Kobbe, and V.A. Bohr. 2003. Werner protein stimulates topoisomerase I DNA relaxation activity. *Cancer Res*. 63:7136-7146.
Lam, M.T., W. Li, M.G. Rosenfeld, and C.K. Glass. 2014. Enhancer RNAs and regulated transcriptional programs. *Trends Biochem Sci*. 39:170-182.
Lamarche, B.J., N.I. Orazio, and M.D. Weitzman. 2010. The MRN complex in double-strand break repair and telomere maintenance. *FEBS Lett*. 584:3682-3695.
Lambert, S., and A.M. Carr. 2013. Impediments to replication fork movement: stabilisation, reactivation and genome instability. *Chromosoma*. 122:33-45.
Landais, I., S. Hiddingh, M. McCarroll, C. Yang, A. Sun, M.S. Turker, J.P. Snyder, and M.E. Hoatlin. 2009. Monoketone analogs of curcumin, a new class of Fanconi anemia pathway inhibitors. *Molecular cancer*. 8:133.
Lanza, A., S. Tornaletti, C. Rodolfo, M.C. Scanavini, and A.M. Pedrini. 1996. Human DNA topoisomerase I-mediated cleavages stimulated by ultraviolet light-induced DNA damage. *The Journal of biological chemistry*. 271:6978-6986.
Lavergne, O., L. Lesueur-Ginot, F. Pla Rodas, P.G. Kasprzyk, J. Pommier, D. Demarquay, G. Prevost, G. Ulibarri, A. Rolland, A.M. Schiano-Liberatore, J. Harnett, D. Pons, J. Camara, and D.C. Bigg. 1998. Homocamptothecins: synthesis and antitumor activity of novel E-ring-modified camptothecin analogues. *J Med Chem*. 41:5410-5419.
Lavin, M.F. 2008. Ataxia-telangiectasia: from a rare disorder to a paradigm for cell signalling and cancer. *Nat Rev Mol Cell Biol*. 9:759-769.
Le May, N., D. Fradin, I. Iltis, P. Bougneres, and J.M. Egly. 2012. XPG and XPF endonucleases trigger chromatin looping and DNA demethylation for accurate expression of activated genes. *Mol Cell*. 47:622-632.
Leahy, J.J., B.T. Golding, R.J. Griffin, I.R. Hardcastle, C. Richardson, L. Rigoreau, and G.C. Smith. 2004. Identification of a highly potent and selective DNA-dependent protein kinase (DNA-PK) inhibitor (NU7441) by screening of chromenone libraries. *Bioorganic & medicinal chemistry letters*. 14:6083-6087.
Lebedeva, N.A., N.I. Rechkunova, and O.I. Lavrik. 2011. AP-site cleavage activity of tyrosyl-DNA phosphodiesterase 1. *FEBS Lett*. 585:683-686.
Lee, J., J.R. Thompson, M.V. Botuyan, and G. Mer. 2008. Distinct binding modes specify the recognition of methylated histones H3K4 and H4K20 by JMJD2A-tudor. *Nat Struct Mol Biol*. 15:109-111.
Lee, J.H., and T.T. Paull. 2005. ATM activation by DNA double-strand breaks through the Mre11-Rad50-Nbs1 complex. *Science (New York, N.Y.* 308:551-554.
Lee, J.H., and T.T. Paull. 2007. Activation and regulation of ATM kinase activity in response to DNA double-strand breaks. *Oncogene*. 26:7741-7748.
Lee, M.P., S.D. Brown, A. Chen, and T.S. Hsieh. 1993. DNA topoisomerase I is essential in Drosophila melanogaster. *Proc Natl Acad Sci U S A*. 90:6656-6660.
Lehmann, A.R., and R.P. Fuchs. 2006. Gaps and forks in DNA replication: Rediscovering old models. *DNA repair*. 5:1495-1498.
Lempiäinen, H., and T.D. Halazonetis. 2009. Emerging common themes in regulation of PIKKs and PI3Ks. *EMBO J*. 28:3067-3073.
Leng, F., and R. McMacken. 2002. Potent stimulation of transcription-coupled DNA supercoiling by sequence-specific DNA-binding proteins. *Proc Natl Acad Sci U S A*. 99:9139-9144.
Leppard, J.B., and J.J. Champoux. 2005. Human DNA topoisomerase I: relaxation, roles, and damage control. *Chromosoma*. 114:75-85.
Lesher, D.T., Y. Pommier, L. Stewart, and M.R. Redinbo. 2002. 8-Oxoguanine rearranges the active site of human topoisomerase I. *Proc Natl Acad Sci U S A*. 99:12102-12107.
Leteurtre, F., G. Kohlhagen, M.R. Fesen, A. Tanizawa, K.W. Kohn, and Y. Pommier. 1994. Effects of DNA methylation on topoisomerase I and II cleavage activities. *The Journal of biological chemistry*. 269:7893-7900.
Levy-Barda, A., Y. Lerenthal, A.J. Davis, Y.M. Chung, J. Essers, Z. Shao, N. van Vliet, D.J. Chen, M.C. Hu, R. Kanaar, Y. Ziv, and Y. Shiloh. 2011. Involvement of the nuclear proteasome activator PA28gamma in the cellular response to DNA double-strand breaks. *Cell Cycle*. 10:4300-4310.
Li, A., J.M. Eirin-Lopez, and J. Ausio. 2005. H2AX: tailoring histone H2A for chromatin-dependent genomic integrity. *Biochemistry and cell biology = Biochimie et biologie cellulaire*. 83:505-515.
Li, T., J. Guan, Z. Huang, X. Hu, and X. Zheng. 2014. RNF168-mediated H2A neddylation antagonizes ubiquitylation of H2A and regulates DNA damage repair. *Journal of cell science*. 127:2238-2248.

Li, X., and J.L. Manley. 2005. Inactivation of the SR protein splicing factor ASF/SF2 results in genomic instability. *Cell*. 122:365-378.
Lin, C.P., Y. Ban, Y.L. Lyu, S.D. Desai, and L.F. Liu. 2008. A ubiquitin-proteasome pathway for the repair of topoisomerase I-DNA covalent complexes. *The Journal of biological chemistry*. 283:21074-21083.
Lin, C.P., Y. Ban, Y.L. Lyu, and L.F. Liu. 2009. Proteasome-dependent processing of topoisomerase I-DNA adducts into DNA double strand breaks at arrested replication forks. *The Journal of biological chemistry*. 284:28084-28092.
Lin, R.K., C.W. Ho, L.F. Liu, and Y.L. Lyu. 2013. Topoisomerase IIbeta deficiency enhances camptothecin-induced apoptosis. *The Journal of biological chemistry*. 288:7182-7192.
Lin, Y.L., and P. Pasero. 2012. Interference between DNA replication and transcription as a cause of genomic instability. *Curr Genomics*. 13:65-73.
Lindahl, T., and D.E. Barnes. 2000. Repair of endogenous DNA damage. *Cold Spring Harb Symp Quant Biol*. 65:127-133.
Lindahl, T., and B. Nyberg. 1972. Rate of depurination of native deoxyribonucleic acid. *Biochemistry*. 11:3610-3618.
Listerman, I., A.K. Sapra, and K.M. Neugebauer. 2006. Cotranscriptional coupling of splicing factor recruitment and precursor messenger RNA splicing in mammalian cells. *Nat Struct Mol Biol*. 13:815-822.
Liu, C., J.J. Pouliot, and H.A. Nash. 2002. Repair of topoisomerase I covalent complexes in the absence of the tyrosyl-DNA phosphodiesterase Tdp1. *Proc Natl Acad Sci U S A*. 99:14970-14975.
Liu, F., and W.H. Lee. 2006. CtIP activates its own and cyclin D1 promoters via the E2F/RB pathway during G1/S progression. *Mol Cell Biol*. 26:3124-3134.
Liu, L.F., T.C. Rowe, L. Yang, K.M. Tewey, and G.L. Chen. 1983. Cleavage of DNA by mammalian DNA topoisomerase II. *The Journal of biological chemistry*. 258:15365-15370.
Liu, L.F., and J.C. Wang. 1987. Supercoiling of the DNA template during transcription. *Proc Natl Acad Sci U S A*. 84:7024-7027.
Liu, S., B. Shiotani, M. Lahiri, A. Maréchal, A. Tse, C.C. Leung, J.N. Glover, X.H. Yang, and L. Zou. 2011. ATR autophosphorylation as a molecular switch for checkpoint activation. *Mol Cell*. 43:192-202.
Livingstone, M., H. Ruan, J. Weiner, K.R. Clauser, P. Strack, S. Jin, A. Williams, H. Greulich, J. Gardner, M. Venere, T.A. Mochan, R.A. DiTullio, Jr., K. Moravcevic, V.G. Gorgoulis, A. Burkhardt, and T.D. Halazonetis. 2005. Valosin-containing protein phosphorylation at Ser784 in response to DNA damage. *Cancer Res*. 65:7533-7540.
Ljungman, M., and P.C. Hanawalt. 1996. The anti-cancer drug camptothecin inhibits elongation but stimulates initiation of RNA polymerase II transcription. *Carcinogenesis*. 17:31-35.
Ljungman, M., and D.P. Lane. 2004. Transcription - guarding the genome by sensing DNA damage. *Nat Rev Cancer*. 4:727-737.
Ljungman, M., H.M. O'Hagan, and M.T. Paulsen. 2001. Induction of ser15 and lys382 modifications of p53 by blockage of transcription elongation. *Oncogene*. 20:5964-5971.
Llorca, O., A. Rivera-Calzada, J. Grantham, and K.R. Willison. 2003. Electron microscopy and 3D reconstructions reveal that human ATM kinase uses an arm-like domain to clamp around double-stranded DNA. *Oncogene*. 22:3867-3874.
Löbrich, M., P.K. Cooper, and B. Rydberg. 1996. Non-random distribution of DNA double-strand breaks induced by particle irradiation. *Int J Radiat Biol*. 70:493-503.
Lobrich, M., A. Shibata, A. Beucher, A. Fisher, M. Ensminger, A.A. Goodarzi, O. Barton, and P.A. Jeggo. 2010. gammaH2AX foci analysis for monitoring DNA double-strand break repair: strengths, limitations and optimization. *Cell Cycle*. 9:662-669.
Lodge, J.K., T. Kazic, and D.E. Berg. 1989. Formation of supercoiling domains in plasmid pBR322. *J Bacteriol*. 171:2181-2187.
Lotito, L., A. Russo, S. Bueno, G. Chillemi, M.V. Fogli, and G. Capranico. 2009. A specific transcriptional response of yeast cells to camptothecin dependent on the Swi4 and Mbp1 factors. *Eur J Pharmacol*. 603:29-36.
Lotito, L., A. Russo, G. Chillemi, S. Bueno, D. Cavalieri, and G. Capranico. 2008. Global transcription regulation by DNA topoisomerase I in exponentially growing Saccharomyces cerevisiae cells: activation of telomere-proximal genes by TOP1 deletion. *J Mol Biol*. 377:311-322.
Lou, Z., B.P. Chen, A. Asaithamby, K. Minter-Dykhouse, D.J. Chen, and J. Chen. 2004. MDC1 regulates DNA-PK autophosphorylation in response to DNA damage. *The Journal of biological chemistry*. 279:46359-46362.
Lou, Z., K. Minter-Dykhouse, S. Franco, M. Gostissa, M.A. Rivera, A. Celeste, J.P. Manis, J. van Deursen, A. Nussenzweig, T.T. Paull, F.W. Alt, and J. Chen. 2006. MDC1 maintains genomic stability by participating in the amplification of ATM-dependent DNA damage signals. *Mol Cell*. 21:187-200.
Lou, Z., K. Minter-Dykhouse, X. Wu, and J. Chen. 2003. MDC1 is coupled to activated CHK2 in mammalian DNA damage response pathways. *Nature*. 421:957-961.
Lovejoy, C.A., and D. Cortez. 2009. Common mechanisms of PIKK regulation. *DNA repair*. 8:1004-1008.
Lu, C.S., L.N. Truong, A. Aslanian, L.Z. Shi, Y. Li, P.Y. Hwang, K.H. Koh, T. Hunter, J.R. Yates, 3rd, M.W. Berns, and X. Wu. 2012. The RING finger protein RNF8 ubiquitinates Nbs1 to promote DNA double-strand break repair by homologous recombination. *The Journal of biological chemistry*. 287:43984-43994.
Lu, J., and M.J. Matunis. 2013. A mediator methylation mystery: JMJD1C demethylates MDC1 to regulate DNA repair. *Nat Struct Mol Biol*. 20:1346-1348.
Lukas, C., J. Falck, J. Bartkova, J. Bartek, and J. Lukas. 2003. Distinct spatiotemporal dynamics of mammalian checkpoint regulators induced by DNA damage. *Nat Cell Biol*. 5:255-260.
Lukas, C., V. Savic, S. Bekker-Jensen, C. Doil, B. Neumann, R.S. Pedersen, M. Grofte, K.L. Chan, I.D. Hickson, J. Bartek, and J. Lukas. 2011a. 53BP1 nuclear bodies form around DNA lesions generated by mitotic transmission of chromosomes under replication stress. *Nat Cell Biol*. 13:243-253.
Lukas, J., C. Lukas, and J. Bartek. 2011b. More than just a focus: The chromatin response to DNA damage and its role in genome integrity maintenance. *Nat Cell Biol*. 13:1161-1169.
Luo, K., H. Zhang, L. Wang, J. Yuan, and Z. Lou. 2012. Sumoylation of MDC1 is important for proper DNA damage response. *EMBO J*. 31:3008-3019.
Lynch, A.S., and J.C. Wang. 1993. Anchoring of DNA to the bacterial cytoplasmic membrane through cotranscriptional synthesis of polypeptides encoding membrane proteins or proteins for export: a mechanism of plasmid hypernegative supercoiling in mutants deficient in DNA topoisomerase I. *J Bacteriol*. 175:1645-1655.

Ma, J., and M.D. Wang. 2014. RNA polymerase is a powerful torsional motor. *Cell Cycle*. 13:337-338.
Ma, T., Y. Chen, F. Zhang, C.Y. Yang, S. Wang, and X. Yu. 2013. RNF111-dependent neddylation activates DNA damage-induced ubiquitination. *Mol Cell*. 49:897-907.
Mabb, A.M., P.H. Kullmann, M.A. Twomey, J. Miriyala, B.D. Philpot, and M.J. Zylka. 2014. Topoisomerase 1 inhibition reversibly impairs synaptic function. *Proc Natl Acad Sci U S A*. 111:17290-17295.
Madden, K.R., L. Stewart, and J.J. Champoux. 1995. Preferential binding of human topoisomerase I to superhelical DNA. *EMBO J*. 14:5399-5409.
Magdalou, I., B.S. Lopez, P. Pasero, and S.A. Lambert. 2014. The causes of replication stress and their consequences on genome stability and cell fate. *Semin Cell Dev Biol*. 30:154-164.
Mailand, N., S. Bekker-Jensen, H. Faustrup, F. Melander, J. Bartek, C. Lukas, and J. Lukas. 2007. RNF8 ubiquitylates histones at DNA double-strand breaks and promotes assembly of repair proteins. *Cell*. 131:887-900.
Makharashvili, N., A.T. Tubbs, S.H. Yang, H. Wang, O. Barton, Y. Zhou, R.A. Deshpande, J.H. Lee, M. Lobrich, B.P. Sleckman, X. Wu, and T.T. Paull. 2014. Catalytic and noncatalytic roles of the CtIP endonuclease in double-strand break end resection. *Mol Cell*. 54:1022-1033.
Maldonado, E., R. Shiekhattar, M. Sheldon, H. Cho, R. Drapkin, P. Rickert, E. Lees, C.W. Anderson, S. Linn, and D. Reinberg. 1996. A human RNA polymerase II complex associated with SRB and DNA-repair proteins. *Nature*. 381:86-89.
Mallette, F.A., F. Mattiroli, G. Cui, L.C. Young, M.J. Hendzel, G. Mer, T.K. Sixma, and S. Richard. 2012. RNF8- and RNF168-dependent degradation of KDM4A/JMJD2A triggers 53BP1 recruitment to DNA damage sites. *EMBO J*. 31:1865-1878.
Manis, J.P., Y. Gu, R. Lansford, E. Sonoda, R. Ferrini, L. Davidson, K. Rajewsky, and F.W. Alt. 1998. Ku70 is required for late B cell development and immunoglobulin heavy chain class switching. *J Exp Med*. 187:2081-2089.
Mao, Y., S. Okada, L.S. Chang, and M.T. Muller. 2000a. p53 dependence of topoisomerase I recruitment in vivo. *Cancer Res*. 60:4538-4543.
Mao, Y., M. Sun, S.D. Desai, and L.F. Liu. 2000b. SUMO-1 conjugation to topoisomerase I: A possible repair response to topoisomerase-mediated DNA damage. *Proc Natl Acad Sci U S A*. 97:4046-4051.
Marchand, C., S. Antony, K.W. Kohn, M. Cushman, A. Ioanoviciu, B.L. Staker, A.B. Burgin, L. Stewart, and Y. Pommier. 2006. A novel norindenoisoquinoline structure reveals a common interfacial inhibitor paradigm for ternary trapping of the topoisomerase I-DNA covalent complex. *Mol Cancer Ther*. 5:287-295.
Marinello, J., G. Chillemi, S. Bueno, S.G. Manzo, and G. Capranico. 2013. Antisense transcripts enhanced by camptothecin at divergent CpG-island promoters associated with bursts of topoisomerase I-DNA cleavage complex and R-loop formation. *Nucleic Acids Res*.
Marston, N.J., W.J. Richards, D. Hughes, D. Bertwistle, C.J. Marshall, and A. Ashworth. 1999. Interaction between the product of the breast cancer susceptibility gene BRCA2 and DSS1, a protein functionally conserved from yeast to mammals. *Mol Cell Biol*. 19:4633-4642.
Marti, T.M., E. Hefner, L. Feeney, V. Natale, and J.E. Cleaver. 2006. H2AX phosphorylation within the G1 phase after UV irradiation depends on nucleotide excision repair and not DNA double-strand breaks. *Proc Natl Acad Sci U S A*. 103:9891-9896.
Masse, E., and M. Drolet. 1999a. Escherichia coli DNA topoisomerase I inhibits R-loop formation by relaxing transcription-induced negative supercoiling. *The Journal of biological chemistry*. 274:16659-16664.
Masse, E., and M. Drolet. 1999b. Relaxation of transcription-induced negative supercoiling is an essential function of Escherichia coli DNA topoisomerase I. *The Journal of biological chemistry*. 274:16654-16658.
Mathas, S., and T. Misteli. 2009. The dangers of transcription. *Cell*. 139:1047-1049.
Matsuoka, S., B.A. Ballif, A. Smogorzewska, E.R. McDonald, 3rd, K.E. Hurov, J. Luo, C.E. Bakalarski, Z. Zhao, N. Solimini, Y. Lerenthal, Y. Shiloh, S.P. Gygi, and S.J. Elledge. 2007. ATM and ATR substrate analysis reveals extensive protein networks responsive to DNA damage. *Science (New York, N.Y.* 316:1160-1166.
Mattiroli, F., J.H. Vissers, W.J. van Dijk, P. Ikpa, E. Citterio, W. Vermeulen, J.A. Marteijn, and T.K. Sixma. 2012. RNF168 ubiquitinates K13-15 on H2A/H2AX to drive DNA damage signaling. *Cell*. 150:1182-1195.
McClendon, A.K., and N. Osheroff. 2006. The geometry of DNA supercoils modulates topoisomerase-mediated DNA cleavage and enzyme response to anticancer drugs. *Biochemistry*. 45:3040-3050.
McConnell, J.L., R.J. Gomez, L.R. McCorvey, B.K. Law, and B.E. Wadzinski. 2007. Identification of a PP2A-interacting protein that functions as a negative regulator of phosphatase activity in the ATM/ATR signaling pathway. *Oncogene*. 26:6021-6030.
Meek, K., V. Dang, and S.P. Lees-Miller. 2008. DNA-PK: the means to justify the ends? *Adv Immunol*. 99:33-58.
Meek, K., P. Douglas, X. Cui, Q. Ding, and S.P. Lees-Miller. 2007. trans Autophosphorylation at DNA-dependent protein kinase's two major autophosphorylation site clusters facilitates end processing but not end joining. *Mol Cell Biol*. 27:3881-3890.
Meerang, M., D. Ritz, S. Paliwal, Z. Garajova, M. Bosshard, N. Mailand, P. Janscak, U. Hubscher, H. Meyer, and K. Ramadan. 2011. The ubiquitin-selective segregase VCP/p97 orchestrates the response to DNA double-strand breaks. *Nat Cell Biol*. 13:1376-1382.
Meng, L.H., Z.Y. Liao, and Y. Pommier. 2003. Non-camptothecin DNA topoisomerase I inhibitors in cancer therapy. *Curr Top Med Chem*. 3:305-320.
Merino, A., K.R. Madden, W.S. Lane, J.J. Champoux, and D. Reinberg. 1993. DNA topoisomerase I is involved in both repression and activation of transcription. *Nature*. 365:227-232.
Miao, Z.H., K. Agama, O. Sordet, L. Povirk, K.W. Kohn, and Y. Pommier. 2006. Hereditary ataxia SCAN1 cells are defective for the repair of transcription-dependent topoisomerase I cleavage complexes. *DNA repair*.
Miao, Z.H., A. Player, U. Shankavaram, Y.H. Wang, D.B. Zimonjic, P.L. Lorenzi, Z.Y. Liao, H. Liu, T. Shimura, H.L. Zhang, L.H. Meng, Y.W. Zhang, E.S. Kawasaki, N.C. Popescu, M.I. Aladjem, D.J. Goldstein, J.N. Weinstein, and Y. Pommier. 2007. Nonclassic functions of human topoisomerase I: genome-wide and pharmacologic analyses. *Cancer Res*. 67:8752-8761.
Miller, K.M., J.V. Tjeertes, J. Coates, G. Legube, S.E. Polo, S. Britton, and S.P. Jackson. 2010. Human HDAC1 and HDAC2 function in the DNA-damage response to promote DNA nonhomologous end-joining. *Nat Struct Mol Biol*. 17:1144-1151.

Mimori, T., J.A. Hardin, and J.A. Steitz. 1986. Characterization of the DNA-binding protein antigen Ku recognized by autoantibodies from patients with rheumatic disorders. *The Journal of biological chemistry*. 261:2274-2278.
Min, J., A. Allali-Hassani, N. Nady, C. Qi, H. Ouyang, Y. Liu, F. MacKenzie, M. Vedadi, and C.H. Arrowsmith. 2007. L3MBTL1 recognition of mono- and dimethylated histones. *Nat Struct Mol Biol*. 14:1229-1230.
Mizutani, M., T. Ohta, H. Watanabe, H. Handa, and S. Hirose. 1991a. Negative supercoiling of DNA facilitates an interaction between transcription factor IID and the fibroin gene promoter. *Proc Natl Acad Sci U S A*. 88:718-722.
Mizutani, M., K. Ura, and S. Hirose. 1991b. DNA superhelicity affects the formation of transcription preinitiation complex on eukaryotic genes differently. *Nucleic Acids Res*. 19:2907-2911.
Mo, X., and W.S. Dynan. 2002. Subnuclear localization of Ku protein: functional association with RNA polymerase II elongation sites. *Mol Cell Biol*. 22:8088-8099.
Mo, Y.Y., C. Wang, and W.T. Beck. 2000. A novel nuclear localization signal in human DNA topoisomerase I. *The Journal of biological chemistry*. 275:41107-41113.
Mochan, T.A., M. Venere, R.A. DiTullio, and T.D. Halazonetis. 2003. 53BP1 and NFBD1/MDC1-Nbs1 function in parallel interacting pathways activating ataxia-telangiectasia mutated (ATM) in response to DNA damage. *Cancer Res*. 63:8586-8591.
Mondal, N., and J.D. Parvin. 2001. DNA topoisomerase IIalpha is required for RNA polymerase II transcription on chromatin templates. *Nature*. 413:435-438.
Mondal, N., Y. Zhang, Z. Jonsson, S.K. Dhar, M. Kannapiran, and J.D. Parvin. 2003. Elongation by RNA polymerase II on chromatin templates requires topoisomerase activity. *Nucleic Acids Res*. 31:5016-5024.
Moon, S.H., L. Lin, X. Zhang, T.A. Nguyen, Y. Darlington, A.S. Waldman, X. Lu, and L.A. Donehower. 2010. Wild-type p53-induced phosphatase 1 dephosphorylates histone variant gamma-H2AX and suppresses DNA double strand break repair. *The Journal of biological chemistry*. 285:12935-12947.
Mordes, D.A., and D. Cortez. 2008. Activation of ATR and related PIKKs. *Cell Cycle*. 7:2809-2812.
Morham, S.G., K.D. Kluckman, N. Voulomanos, and O. Smithies. 1996. Targeted disruption of the mouse topoisomerase I gene by camptothecin selection. *Mol Cell Biol*. 16:6804-6809.
Morris, E.J., and H.M. Geller. 1996. Induction of neuronal apoptosis by camptothecin, an inhibitor of DNA topoisomerase-I: evidence for cell cycle-independent toxicity. *J Cell Biol*. 134:757-770.
Morris, E.J., E. Keramaris, H.J. Rideout, R.S. Slack, N.J. Dyson, L. Stefanis, and D.S. Park. 2001. Cyclin-dependent kinases and P53 pathways are activated independently and mediate Bax activation in neurons after DNA damage. *The Journal of neuroscience : the official journal of the Society for Neuroscience*. 21:5017-5026.
Morris, J.R., C. Boutell, M. Keppler, R. Densham, D. Weekes, A. Alamshah, L. Butler, Y. Galanty, L. Pangon, T. Kiuchi, T. Ng, and E. Solomon. 2009. The SUMO modification pathway is involved in the BRCA1 response to genotoxic stress. *Nature*. 462:886-890.
Mosammaparast, N., H. Kim, B. Laurent, Y. Zhao, H.J. Lim, M.C. Majid, S. Dango, Y. Luo, K. Hempel, M.E. Sowa, S.P. Gygi, H. Steen, J.W. Harper, B. Yankner, and Y. Shi. 2013. The histone demethylase LSD1/KDM1A promotes the DNA damage response. *J Cell Biol*. 203:457-470.
Mosammaparast, N., and Y. Shi. 2010. Reversal of histone methylation: biochemical and molecular mechanisms of histone demethylases. *Annu Rev Biochem*. 79:155-179.
Moudry, P., C. Lukas, L. Macurek, H. Hanzlikova, Z. Hodny, J. Lukas, and J. Bartek. 2012. Ubiquitin-activating enzyme UBA1 is required for cellular response to DNA damage. *Cell Cycle*. 11:1573-1582.
Moyal, L., Y. Lerenthal, M. Gana-Weisz, G. Mass, S. So, S.Y. Wang, B. Eppink, Y.M. Chung, G. Shalev, E. Shema, D. Shkedy, N.I. Smorodinsky, N. van Vliet, B. Kuster, M. Mann, A. Ciechanover, J. Dahm-Daphi, R. Kanaar, M.C. Hu, D.J. Chen, M. Oren, and Y. Shiloh. 2011. Requirement of ATM-dependent monoubiquitylation of histone H2B for timely repair of DNA double-strand breaks. *Mol Cell*. 41:529-542.
Muggia, F.M., P.J. Creaven, H.H. Hansen, M.H. Cohen, and O.S. Selawry. 1972. Phase I clinical trial of weekly and daily treatment with camptothecin (NSC-100880): correlation with preclinical studies. *Cancer Chemother Rep*. 56:515-521.
Muller, M.T. 1985. Quantitation of eukaryotic topoisomerase I reactivity with DNA. Preferential cleavage of supercoiled DNA. *Biochim Biophys Acta*. 824:263-267.
Muller, M.T., W.P. Pfund, V.B. Mehta, and D.K. Trask. 1985. Eukaryotic type I topoisomerase is enriched in the nucleolus and catalytically active on ribosomal DNA. *EMBO J*. 4:1237-1243.
Muller, S., C. Hoege, G. Pyrowolakis, and S. Jentsch. 2001. SUMO, ubiquitin's mysterious cousin. *Nat Rev Mol Cell Biol*. 2:202-210.
Murai, J., S.Y. Huang, B.B. Das, T.S. Dexheimer, S. Takeda, and Y. Pommier. 2012. Tyrosyl-DNA phosphodiesterase 1 (TDP1) repairs DNA damage induced by topoisomerases I and II and base alkylation in vertebrate cells. *The Journal of biological chemistry*. 287:12848-12857.
Murakawa, Y., E. Sonoda, L.J. Barber, W. Zeng, K. Yokomori, H. Kimura, A. Niimi, A. Lehmann, G.Y. Zhao, H. Hochegger, S.J. Boulton, and S. Takeda. 2007. Inhibitors of the proteasome suppress homologous DNA recombination in mammalian cells. *Cancer Res*. 67:8536-8543.
Muratani, M., and W.P. Tansey. 2003. How the ubiquitin-proteasome system controls transcription. *Nat Rev Mol Cell Biol*. 4:192-201.
Murr, R., J.I. Loizou, Y.G. Yang, C. Cuenin, H. Li, Z.Q. Wang, and Z. Herceg. 2006. Histone acetylation by Trrap-Tip60 modulates loading of repair proteins and repair of DNA double-strand breaks. *Nat Cell Biol*. 8:91-99.
Muslimović, A., S. Nyström, Y. Gao, and O. Hammarsten. 2009. Numerical analysis of etoposide induced DNA breaks. *PLoS One*. 4:e5859.
Myers, J.S., and D. Cortez. 2006. Rapid activation of ATR by ionizing radiation requires ATM and Mre11. *The Journal of biological chemistry*. 281:9346-9350.
Nagy, Z., and E. Soutoglou. 2009. DNA repair: easy to visualize, difficult to elucidate. *Trends Cell Biol*. 19:617-629.

Nakada, S., I. Tai, S. Panier, A. Al-Hakim, S. Iemura, Y.C. Juang, L. O'Donnell, A. Kumakubo, M. Munro, F. Sicheri, A.C. Gingras, T. Natsume, T. Suda, and D. Durocher. 2010. Non-canonical inhibition of DNA damage-dependent ubiquitination by OTUB1. *Nature*. 466:941-946.

Nakamura, K., A. Kato, J. Kobayashi, H. Yanagihara, S. Sakamoto, D.V. Oliveira, M. Shimada, H. Tauchi, H. Suzuki, S. Tashiro, L. Zou, and K. Komatsu. 2011. Regulation of homologous recombination by RNF20-dependent H2B ubiquitination. *Mol Cell*. 41:515-528.

Nakamura, K., T. Kogame, H. Oshiumi, A. Shinohara, Y. Sumitomo, K. Agama, Y. Pommier, K.M. Tsutsui, K. Tsutsui, E. Hartsuiker, T. Ogi, S. Takeda, and Y. Taniguchi. 2010. Collaborative action of Brca1 and CtIP in elimination of covalent modifications from double-strand breaks to facilitate subsequent break repair. *PLoS Genet*. 6:e1000828.

Nam, E.A., and D. Cortez. 2011. ATR signalling: more than meeting at the fork. *Biochem J*. 436:527-536.

Nam, E.A., R. Zhao, G.G. Glick, C.E. Bansbach, D.B. Friedman, and D. Cortez. 2011. Thr-1989 phosphorylation is a marker of active ataxia telangiectasia-mutated and Rad3-related (ATR) kinase. *The Journal of biological chemistry*. 286:28707-28714.

Nazarov, I.B., A.N. Smirnova, R.I. Krutilina, M.P. Svetlova, L.V. Solovjeva, A.A. Nikiforov, S.L. Oei, I.A. Zalenskaya, P.M. Yau, E.M. Bradbury, and N.V. Tomilin. 2003. Dephosphorylation of histone gamma-H2AX during repair of DNA double-strand breaks in mammalian cells and its inhibition by calyculin A. *Radiat Res*. 160:309-317.

Neale, B.M., Y. Kou, L. Liu, A. Ma'ayan, K.E. Samocha, A. Sabo, C.F. Lin, C. Stevens, L.S. Wang, V. Makarov, P. Polak, S. Yoon, J. Maguire, E.L. Crawford, N.G. Campbell, E.T. Geller, O. Valladares, C. Schafer, H. Liu, T. Zhao, G. Cai, J. Lihm, R. Dannenfelser, O. Jabado, Z. Peralta, U. Nagaswamy, D. Muzny, J.G. Reid, I. Newsham, Y. Wu, L. Lewis, Y. Han, B.F. Voight, E. Lim, E. Rossin, A. Kirby, J. Flannick, M. Fromer, K. Shakir, T. Fennell, K. Garimella, E. Banks, R. Poplin, S. Gabriel, M. DePristo, J.R. Wimbish, B.E. Boone, S.E. Levy, C. Betancur, S. Sunyaev, E. Boerwinkle, J.D. Buxbaum, E.H. Cook, Jr., B. Devlin, R.A. Gibbs, K. Roeder, G.D. Schellenberg, J.S. Sutcliffe, and M.J. Daly. 2012. Patterns and rates of exonic de novo mutations in autism spectrum disorders. *Nature*. 485:242-245.

Neale, M.J., and S. Keeney. 2006. Clarifying the mechanics of DNA strand exchange in meiotic recombination. *Nature*. 442:153-158.

Nicassio, F., N. Corrado, J.H. Vissers, L.B. Areces, S. Bergink, J.A. Marteijn, B. Geverts, A.B. Houtsmuller, W. Vermeulen, P.P. Di Fiore, and E. Citterio. 2007. Human USP3 is a chromatin modifier required for S phase progression and genome stability. *Curr Biol*. 17:1972-1977.

Niida, H., and M. Nakanishi. 2006. DNA damage checkpoints in mammals. *Mutagenesis*. 21:3-9.

Nikiforova, M.N., J.R. Stringer, R. Blough, M. Medvedovic, J.A. Fagin, and Y.E. Nikiforov. 2000. Proximity of chromosomal loci that participate in radiation-induced rearrangements in human cells. *Science (New York, N.Y.* 290:138-141.

Nishikawa, H., S. Ooka, K. Sato, K. Arima, J. Okamoto, R.E. Klevit, M. Fukuda, and T. Ohta. 2004. Mass spectrometric and mutational analyses reveal Lys-6-linked polyubiquitin chains catalyzed by BRCA1-BARD1 ubiquitin ligase. *The Journal of biological chemistry*. 279:3916-3924.

Nitiss, J., and J.C. Wang. 1988. DNA topoisomerase-targeting antitumor drugs can be studied in yeast. *Proc Natl Acad Sci U S A*. 85:7501-7505.

Nitiss, J.L. 2009. Targeting DNA topoisomerase II in cancer chemotherapy. *Nat Rev Cancer*. 9:338-350.

Nitiss, K.C., M. Malik, X. He, S.W. White, and J.L. Nitiss. 2006. Tyrosyl-DNA phosphodiesterase (Tdp1) participates in the repair of Top2-mediated DNA damage. *Proc Natl Acad Sci U S A*. 103:8953-8958.

Noon, A.T., A. Shibata, N. Rief, M. Löbrich, G.S. Stewart, P.A. Jeggo, and A.A. Goodarzi. 2010. 53BP1-dependent robust localized KAP-1 phosphorylation is essential for heterochromatic DNA double-strand break repair. *Nat Cell Biol*. 12:177-184.

Nordheim, A., E.M. Lafer, L.J. Peck, J.C. Wang, B.D. Stollar, and A. Rich. 1982. Negatively supercoiled plasmids contain left-handed Z-DNA segments as detected by specific antibody binding. *Cell*. 31:309-318.

Nussenzweig, A., K. Sokol, P. Burgman, L. Li, and G.C. Li. 1997. Hypersensitivity of Ku80-deficient cell lines and mice to DNA damage: the effects of ionizing radiation on growth, survival, and development. *Proc Natl Acad Sci U S A*. 94:13588-13593.

O'Connor, P.M., W. Nieves-Neira, D. Kerrigan, R. Bertrand, J. Goldman, K.W. Kohn, and Y. Pommier. 1991. S-phase population analysis does not correlate with the cytotoxicity of camptothecin and 10,11-methylenedioxycamptothecin in human colon carcinoma HT-29 cells. *Cancer Commun*. 3:233-240.

Oberdoerffer, P., S. Michan, M. McVay, R. Mostoslavsky, J. Vann, S.K. Park, A. Hartlerode, J. Stegmuller, A. Hafner, P. Loerch, S.M. Wright, K.D. Mills, A. Bonni, B.A. Yankner, R. Scully, T.A. Prolla, F.W. Alt, and D.A. Sinclair. 2008. SIRT1 redistribution on chromatin promotes genomic stability but alters gene expression during aging. *Cell*. 135:907-918.

Ochi, T., A.N. Blackford, J. Coates, S. Jhujh, S. Mehmood, N. Tamura, J. Travers, Q. Wu, V.M. Draviam, C.V. Robinson, T.L. Blundell, and S.P. Jackson. 2015. DNA repair. PAXX, a paralog of XRCC4 and XLF, interacts with Ku to promote DNA double-strand break repair. *Science (New York, N.Y.* 347:185-188.

Okuno, Y., A. Nakamura-Ishizu, K. Otsu, T. Suda, and Y. Kubota. 2012. Pathological neoangiogenesis depends on oxidative stress regulation by ATM. *Nat Med*. 18:1208-1216.

Oliner, J.D., J.A. Pietenpol, S. Thiagalingam, J. Gyuris, K.W. Kinzler, and B. Vogelstein. 1993. Oncoprotein MDM2 conceals the activation domain of tumour suppressor p53. *Nature*. 362:857-860.

Olive, P.L., and J.P. Banath. 2006. The comet assay: a method to measure DNA damage in individual cells. *Nat Protoc*. 1:23-29.

Oliveira, D.V., A. Kato, K. Nakamura, T. Ikura, M. Okada, J. Kobayashi, H. Yanagihara, Y. Saito, H. Tauchi, and K. Komatsu. 2014. Histone chaperone FACT regulates homologous recombination by chromatin remodeling through interaction with RNF20. *Journal of cell science*. 127:763-772.

Olsen, J.V., B. Blagoev, F. Gnad, B. Macek, C. Kumar, P. Mortensen, and M. Mann. 2006. Global, in vivo, and site-specific phosphorylation dynamics in signaling networks. *Cell*. 127:635-648.

Pai, C.C., R.S. Deegan, L. Subramanian, C. Gal, S. Sarkar, E.J. Blaikley, C. Walker, L. Hulme, E. Bernhard, S. Codlin, J. Bähler, R. Allshire, S. Whitehall, and T.C. Humphrey. 2014. A histone H3K36 chromatin switch coordinates DNA double-strand break repair pathway choice. *Nat Commun*. 5:4091.

Pan, M.R., G. Peng, W.C. Hung, and S.Y. Lin. 2011. Monoubiquitination of H2AX protein regulates DNA damage response signaling. *The Journal of biological chemistry*. 286:28599-28607.

Panier, S., Y. Ichijima, A. Fradet-Turcotte, C.C. Leung, L. Kaustov, C.H. Arrowsmith, and D. Durocher. 2012. Tandem protein interaction modules organize the ubiquitin-dependent response to DNA double-strand breaks. *Mol Cell*. 47:383-395.

Pankotai, T., C. Bonhomme, D. Chen, and E. Soutoglou. 2012. DNAPKcs-dependent arrest of RNA polymerase II transcription in the presence of DNA breaks. *Nat Struct Mol Biol*.

Pankotai, T., and E. Soutoglou. 2013. Double strand breaks: hurdles for RNA polymerase II transcription? *Transcription*. 4:34-38.

Patel, A., H.O. Lee, L. Jawerth, S. Maharana, M. Jahnel, M.Y. Hein, S. Stoynov, J. Mahamid, S. Saha, T.M. Franzmann, A. Pozniakovski, I. Poser, N. Maghelli, L.A. Royer, M. Weigert, E.W. Myers, S. Grill, D. Drechsel, A.A. Hyman, and S. Alberti. 2015. A Liquid-to-Solid Phase Transition of the ALS Protein FUS Accelerated by Disease Mutation. *Cell*. 162:1066-1077.

Patel, A.G., K.S. Flatten, P.A. Schneider, N.T. Dai, J.S. McDonald, G.G. Poirier, and S.H. Kaufmann. 2012. Enhanced killing of cancer cells by poly(ADP-ribose) polymerase inhibitors and topoisomerase I inhibitors reflects poisoning of both enzymes. *The Journal of biological chemistry*. 287:4198-4210.

Paull, T.T., and M. Gellert. 1999. Nbs1 potentiates ATP-driven DNA unwinding and endonuclease cleavage by the Mre11/Rad50 complex. *Genes Dev*. 13:1276-1288.

Peak, J.G., and M.J. Peak. 1990. Ultraviolet light induces double-strand breaks in DNA of cultured human P3 cells as measured by neutral filter elution. *Photochem Photobiol*. 52:387-393.

Pei, H., L. Zhang, K. Luo, Y. Qin, M. Chesi, F. Fei, P.L. Bergsagel, L. Wang, Z. You, and Z. Lou. 2011. MMSET regulates histone H4K20 methylation and 53BP1 accumulation at DNA damage sites. *Nature*. 470:124-128.

Pellegrini, M., A. Celeste, S. Difilippantonio, R. Guo, W. Wang, L. Feigenbaum, and A. Nussenzweig. 2006. Autophosphorylation at serine 1987 is dispensable for murine Atm activation in vivo. *Nature*. 443:222-225.

Peng, Y., R.G. Woods, H. Beamish, R. Ye, S.P. Lees-Miller, M.F. Lavin, and J.S. Bedford. 2005. Deficiency in the catalytic subunit of DNA-dependent protein kinase causes down-regulation of ATM. *Cancer Res*. 65:1670-1677.

Peter, B.J., J. Arsuaga, A.M. Breier, A.B. Khodursky, P.O. Brown, and N.R. Cozzarelli. 2004. Genomic transcriptional response to loss of chromosomal supercoiling in Escherichia coli. *Genome Biol*. 5:R87.

Petersen, S., R. Casellas, B. Reina-San-Martin, H.T. Chen, M.J. Difilippantonio, P.C. Wilson, L. Hanitsch, A. Celeste, M. Muramatsu, D.R. Pilch, C. Redon, T. Ried, W.M. Bonner, T. Honjo, M.C. Nussenzweig, and A. Nussenzweig. 2001. AID is required to initiate Nbs1/gamma-H2AX focus formation and mutations at sites of class switching. *Nature*. 414:660-665.

Pfister, S.X., S. Ahrabi, L.P. Zalmas, S. Sarkar, F. Aymard, C.Z. Bachrati, T. Helleday, G. Legube, N.B. La Thangue, A.C. Porter, and T.C. Humphrey. 2014. SETD2-dependent histone H3K36 trimethylation is required for homologous recombination repair and genome stability. *Cell reports*. 7:2006-2018.

Pinder, J.B., K.M. Attwood, and G. Dellaire. 2013. Reading, writing, and repair: the role of ubiquitin and the ubiquitin-like proteins in DNA damage signaling and repair. *Front Genet*. 4:45.

Plo, I., Z.Y. Liao, J.M. Barcelo, G. Kohlhagen, K.W. Caldecott, M. Weinfeld, and Y. Pommier. 2003. Association of XRCC1 and tyrosyl DNA phosphodiesterase (Tdp1) for the repair of topoisomerase I-mediated DNA lesions. *DNA repair*. 2:1087-1100.

Polo, S.E., and S.P. Jackson. 2011. Dynamics of DNA damage response proteins at DNA breaks: a focus on protein modifications. *Genes Dev*. 25:409-433.

Pommier, Y. 2006. Topoisomerase I inhibitors: camptothecins and beyond. *Nat Rev Cancer*. 6:789-802.

Pommier, Y. 2013. Drugging topoisomerases: lessons and challenges. *ACS Chem Biol*. 8:82-95.

Pommier, Y., J.M. Barcelo, V.A. Rao, O. Sordet, A.G. Jobson, L. Thibaut, Z.H. Miao, J.A. Seiler, H. Zhang, C. Marchand, K. Agama, J.L. Nitiss, and C. Redon. 2006. Repair of topoisomerase I-mediated DNA damage. *Prog Nucleic Acid Res Mol Biol*. 81:179-229.

Pommier, Y., G. Capranico, A. Orr, and K.W. Kohn. 1991. Local base sequence preferences for DNA cleavage by mammalian topoisomerase II in the presence of amsacrine or teniposide. *Nucleic Acids Res*. 19:5973-5980.

Pommier, Y., S.Y. Huang, R. Gao, B.B. Das, J. Murai, and C. Marchand. 2014. Tyrosyl-DNA-phosphodiesterases (TDP1 and TDP2). *DNA repair*. 19:114-129.

Pommier, Y., J. Jenkins, G. Kohlhagen, and F. Leteurtre. 1995. DNA recombinase activity of eukaryotic DNA topoisomerase I; effects of camptothecin and other inhibitors. *Mutation research*. 337:135-145.

Pommier, Y., D. Kerrigan, K.D. Hartman, and R.I. Glazer. 1990. Phosphorylation of mammalian DNA topoisomerase I and activation by protein kinase C. *The Journal of biological chemistry*. 265:9418-9422.

Pommier, Y., G. Kohlhagen, G.S. Laco, H. Kroth, J.M. Sayer, and D.M. Jerina. 2002. Different effects on human topoisomerase I by minor groove and intercalated deoxyguanosine adducts derived from two polycyclic aromatic hydrocarbon diol epoxides at or near a normal cleavage site. *The Journal of biological chemistry*. 277:13666-13672.

Pommier, Y., G. Kohlhagen, P. Pourquier, J.M. Sayer, H. Kroth, and D.M. Jerina. 2000a. Benzo[a]pyrene diol epoxide adducts in DNA are potent suppressors of a normal topoisomerase I cleavage site and powerful inducers of other topoisomerase I cleavages. *Proc Natl Acad Sci U S A*. 97:2040-2045.

Pommier, Y., G.S. Laco, G. Kohlhagen, J.M. Sayer, H. Kroth, and D.M. Jerina. 2000b. Position-specific trapping of topoisomerase I-DNA cleavage complexes by intercalated benzo[a]- pyrene diol epoxide adducts at the 6-amino group of adenine. *Proc Natl Acad Sci U S A*. 97:10739-10744.

Pommier, Y., E. Leo, H. Zhang, and C. Marchand. 2010. DNA topoisomerases and their poisoning by anticancer and antibacterial drugs. *Chem Biol*. 17:421-433.

Pommier, Y., P. Pourquier, Y. Fan, and D. Strumberg. 1998. Mechanism of action of eukaryotic DNA topoisomerase I and drugs targeted to the enzyme. *Biochim Biophys Acta*. 1400:83-105.

Pommier, Y., P. Pourquier, Y. Urasaki, J. Wu, and G.S. Laco. 1999. Topoisomerase I inhibitors: selectivity and cellular resistance. *Drug Resist Updat*. 2:307-318.

Pommier, Y., C. Redon, V.A. Rao, J.A. Seiler, O. Sordet, H. Takemura, S. Antony, L. Meng, Z. Liao, G. Kohlhagen, H. Zhang, and K.W. Kohn. 2003. Repair of and checkpoint response to topoisomerase I-mediated DNA damage. *Mutation research*. 532:173-203.

Pouliot, J.J., K.C. Yao, C.A. Robertson, and H.A. Nash. 1999. Yeast gene for a Tyr-DNA phosphodiesterase that repairs topoisomerase I complexes. *Science (New York, N.Y.* 286:552-555.

Poulsen, M., C. Lukas, J. Lukas, S. Bekker-Jensen, and N. Mailand. 2012. Human RNF169 is a negative regulator of the ubiquitin-dependent response to DNA double-strand breaks. *J Cell Biol*. 197:189-199.

Pourquier, P., M.A. Bjornsti, and Y. Pommier. 1998. Induction of topoisomerase I cleavage complexes by the vinyl chloride adduct 1,N6-ethenoadenine. *The Journal of biological chemistry*. 273:27245-27249.

Pourquier, P., and A. Lansiaux. 2011. [Molecular determinants of response to topoisomerase I inhibitors]. *Bull Cancer*. 98:1287-1298.

Pourquier, P., A.A. Pilon, G. Kohlhagen, A. Mazumder, A. Sharma, and Y. Pommier. 1997a. Trapping of mammalian topoisomerase I and recombinations induced by damaged DNA containing nicks or gaps. Importance of DNA end phosphorylation and camptothecin effects. *The Journal of biological chemistry*. 272:26441-26447.

Pourquier, P., and Y. Pommier. 2001. Topoisomerase I-mediated DNA damage. *Adv Cancer Res*. 80:189-216.

Pourquier, P., L.M. Ueng, G. Kohlhagen, A. Mazumder, M. Gupta, K.W. Kohn, and Y. Pommier. 1997b. Effects of uracil incorporation, DNA mismatches, and abasic sites on cleavage and religation activities of mammalian topoisomerase I. *The Journal of biological chemistry*. 272:7792-7796.

Pourquier, P., J.L. Waltman, Y. Urasaki, N.A. Loktionova, A.E. Pegg, J.L. Nitiss, and Y. Pommier. 2001. Topoisomerase I-mediated cytotoxicity of N-methyl-N'-nitro-N-nitrosoguanidine: trapping of topoisomerase I by the O6-methylguanine. *Cancer Res*. 61:53-58.

Povirk, L.F. 1996. DNA damage and mutagenesis by radiomimetic DNA-cleaving agents: bleomycin, neocarzinostatin and other enediynes. *Mutation research*. 355:71-89.

Powell, W.T., R.L. Coulson, M.L. Gonzales, F.K. Crary, S.S. Wong, S. Adams, R.A. Ach, P. Tsang, N.A. Yamada, D.H. Yasui, F. Chedin, and J.M. LaSalle. 2013. R-loop formation at Snord116 mediates topotecan inhibition of Ube3a-antisense and allele-specific chromatin decondensation. *Proc Natl Acad Sci U S A*. 110:13938-13943.

Puc, J., P. Kozbial, W. Li, Y. Tan, Z. Liu, T. Suter, K.A. Ohgi, J. Zhang, A.K. Aggarwal, and M.G. Rosenfeld. 2015. Ligand-dependent enhancer activation regulated by topoisomerase-I activity. *Cell*. 160:367-380.

Puumalainen, M.R., D. Lessel, P. Ruthemann, N. Kaczmarek, K. Bachmann, K. Ramadan, and H. Naegeli. 2014. Chromatin retention of DNA damage sensors DDB2 and XPC through loss of p97 segregase causes genotoxicity. *Nat Commun*. 5:3695.

Radulescu, I., K. Elmroth, and B. Stenerlöw. 2004. Chromatin organization contributes to non-randomly distributed double-strand breaks after exposure to high-LET radiation. *Radiat Res*. 161:1-8.

Ramadan, K. 2012. p97/VCP- and Lys48-linked polyubiquitination form a new signaling pathway in DNA damage response. *Cell Cycle*. 11:1062-1069.

Ramanathan, Y., S.M. Rajpara, S.M. Reza, E. Lees, S. Shuman, M.B. Mathews, and T. Pe'ery. 2001. Three RNA polymerase II carboxyl-terminal domain kinases display distinct substrate preferences. *The Journal of biological chemistry*. 276:10913-10920.

Rasouli-Nia, A., F. Karimi-Busheri, and M. Weinfeld. 2004. Stable down-regulation of human polynucleotide kinase enhances spontaneous mutation frequency and sensitizes cells to genotoxic agents. *Proc Natl Acad Sci U S A*. 101:6905-6910.

Rass, U., I. Ahel, and S.C. West. 2007. Defective DNA repair and neurodegenerative disease. *Cell*. 130:991-1004.

Ray Chaudhuri, A., Y. Hashimoto, R. Herrador, K.J. Neelsen, D. Fachinetti, R. Bermejo, A. Cocito, V. Costanzo, and M. Lopes. 2012. Topoisomerase I poisoning results in PARP-mediated replication fork reversal. *Nat Struct Mol Biol*. 19:417-423.

Raymond, A.C., M.C. Rideout, B. Staker, K. Hjerrild, and A.B. Burgin, Jr. 2004. Analysis of human tyrosyl-DNA phosphodiesterase I catalytic residues. *J Mol Biol*. 338:895-906.

Redinbo, M.R., J.J. Champoux, and W.G. Hol. 2000. Novel insights into catalytic mechanism from a crystal structure of human topoisomerase I in complex with DNA. *Biochemistry*. 39:6832-6840.

Redinbo, M.R., L. Stewart, P. Kuhn, J.J. Champoux, and W.G. Hol. 1998. Crystal structures of human topoisomerase I in covalent and noncovalent complexes with DNA. *Science (New York, N.Y.* 279:1504-1513.

Redon, C.E., J.S. Dickey, W.M. Bonner, and O.A. Sedelnikova. 2009. gamma-H2AX as a biomarker of DNA damage induced by ionizing radiation in human peripheral blood lymphocytes and artificial skin. *Adv Space Res*. 43:1171-1178.

Regairaz, M., Y.W. Zhang, H. Fu, K.K. Agama, N. Tata, S. Agrawal, M.I. Aladjem, and Y. Pommier. 2011. Mus81-mediated DNA cleavage resolves replication forks stalled by topoisomerase I-DNA complexes. *J Cell Biol*. 195:739-749.

Reid, L.J., R. Shakya, A.P. Modi, M. Lokshin, J.T. Cheng, M. Jasin, R. Baer, and T. Ludwig. 2008. E3 ligase activity of BRCA1 is not essential for mammalian cell viability or homology-directed repair of double-strand DNA breaks. *Proc Natl Acad Sci U S A*. 105:20876-20881.

Reynolds, J.J., A.K. Walker, E.C. Gilmore, C.A. Walsh, and K.W. Caldecott. 2012. Impact of PNKP mutations associated with microcephaly, seizures and developmental delay on enzyme activity and DNA strand break repair. *Nucleic Acids Res*. 40:6608-6619.

Richardson, C., and M. Jasin. 2000. Frequent chromosomal translocations induced by DNA double-strand breaks. *Nature*. 405:697-700.

Riches, L.C., A.M. Lynch, and N.J. Gooderham. 2008. Early events in the mammalian response to DNA double-strand breaks. *Mutagenesis*. 23:331-339.

Rideout, M.C., A.C. Raymond, and A.B. Burgin, Jr. 2004. Design and synthesis of fluorescent substrates for human tyrosyl-DNA phosphodiesterase I. *Nucleic Acids Res*. 32:4657-4664.

Riethman, H., A. Ambrosini, and S. Paul. 2005. Human subtelomere structure and variation. *Chromosome Res*. 13:505-515.

Roberts, R.W., and D.M. Crothers. 1992. Stability and properties of double and triple helices: dramatic effects of RNA or DNA backbone composition. *Science (New York, N.Y.* 258:1463-1466.

Roberts, S.A., N. Strande, M.D. Burkhalter, C. Strom, J.M. Havener, P. Hasty, and D.A. Ramsden. 2010. Ku is a 5'-dRP/AP lyase that excises nucleotide damage near broken ends. *Nature*. 464:1214-1217.

Rockstroh, A., A. Kleinert, M. Kramer, F. Grosse, and K. Soe. 2007. Cellular stress triggers the human topoisomerase I damage response independently of DNA damage in a p53 controlled manner. *Oncogene*. 26:123-131.
Rodriguez, R., K.M. Miller, J.V. Forment, C.R. Bradshaw, M. Nikan, S. Britton, T. Oelschlaegel, B. Xhemalce, S. Balasubramanian, and S.P. Jackson. 2012. Small-molecule-induced DNA damage identifies alternative DNA structures in human genes. *Nat Chem Biol*. 8:301-310.
Rogakou, E.P., C. Boon, C. Redon, and W.M. Bonner. 1999. Megabase chromatin domains involved in DNA double-strand breaks in vivo. *J Cell Biol*. 146:905-916.
Rogakou, E.P., D.R. Pilch, A.H. Orr, V.S. Ivanova, and W.M. Bonner. 1998. DNA double-stranded breaks induce histone H2AX phosphorylation on serine 139. *The Journal of biological chemistry*. 273:5858-5868.
Rose, K.M., J. Szopa, F.S. Han, Y.C. Cheng, A. Richter, and U. Scheer. 1988. Association of DNA topoisomerase I and RNA polymerase I: a possible role for topoisomerase I in ribosomal gene transcription. *Chromosoma*. 96:411-416.
Rosenberg, M., A.X. Fan, I.J. Lin, S.Y. Liang, and J. Bungert. 2013. Cell-cycle specific association of transcription factors and RNA polymerase ii with the human beta-globin gene locus. *J Cell Biochem*. 114:1997-2006.
Rossi, F., E. Labourier, T. Forne, G. Divita, J. Derancourt, J.F. Riou, E. Antoine, G. Cathala, C. Brunel, and J. Tazi. 1996. Specific phosphorylation of SR proteins by mammalian DNA topoisomerase I. *Nature*. 381:80-82.
Rostagno, P., J. Gioanni, E. Garino, P. Vallino, M. Namer, and M. Frenay. 2003. A mutation analysis of the BRCA1 gene in 140 families from southeast France with a history of breast and/or ovarian cancer. *Journal of human genetics*. 48:362-366.
Roy, D., K. Yu, and M.R. Lieber. 2008. Mechanism of R-loop formation at immunoglobulin class switch sequences. *Mol Cell Biol*. 28:50-60.
Roy, D., Z. Zhang, Z. Lu, C.L. Hsieh, and M.R. Lieber. 2010. Competition between the RNA transcript and the nontemplate DNA strand during R-loop formation in vitro: a nick can serve as a strong R-loop initiation site. *Mol Cell Biol*. 30:146-159.
Rubin, E., V. Wood, A. Bharti, D. Trites, C. Lynch, S. Hurwitz, S. Bartel, S. Levy, A. Rosowsky, D. Toppmeyer, and et al. 1995. A phase I and pharmacokinetic study of a new camptothecin derivative, 9-aminocamptothecin. *Clin Cancer Res*. 1:269-276.
Rudin, N., and J.E. Haber. 1988. Efficient repair of HO-induced chromosomal breaks in Saccharomyces cerevisiae by recombination between flanking homologous sequences. *Mol Cell Biol*. 8:3918-3928.
Ruiz de Almodóvar, J.M., C. Bush, J.H. Peacock, G.G. Steel, S.J. Whitaker, and T.J. McMillan. 1994. Dose-rate effect for DNA damage induced by ionizing radiation in human tumor cells. *Radiat Res*. 138:S93-96.
Saintigny, Y., F. Delacote, G. Vares, F. Petitot, S. Lambert, D. Averbeck, and B.S. Lopez. 2001. Characterization of homologous recombination induced by replication inhibition in mammalian cells. *EMBO J*. 20:3861-3870.
Sakai, A., R. Sakasai, Y. Kakeji, H. Kitao, and Y. Maehara. 2012. PARP and CSB modulate the processing of transcription-mediated DNA strand breaks. *Genes Genet Syst*. 87:265-272.
Sakasai, R., H. Teraoka, M. Takagi, and R.S. Tibbetts. 2010a. Transcription-dependent activation of ataxia telangiectasia mutated prevents DNA-dependent protein kinase-mediated cell death in response to topoisomerase I poison. *The Journal of biological chemistry*. 285:15201-15208.
Sakasai, R., H. Teraoka, and R.S. Tibbetts. 2010b. Proteasome inhibition suppresses DNA-dependent protein kinase activation caused by camptothecin. *DNA repair*. 9:76-82.
Samejima, K., P.A. Svingen, G.S. Basi, T. Kottke, P.W. Mesner, Jr., L. Stewart, F. Durrieu, G.G. Poirier, E.S. Alnemri, J.J. Champoux, S.H. Kaufmann, and W.C. Earnshaw. 1999. Caspase-mediated cleavage of DNA topoisomerase I at unconventional sites during apoptosis. *The Journal of biological chemistry*. 274:4335-4340.
Sartori, A.A., C. Lukas, J. Coates, M. Mistrik, S. Fu, J. Bartek, R. Baer, J. Lukas, and S.P. Jackson. 2007. Human CtIP promotes DNA end resection. *Nature*. 450:509-514.
Savic, V., B. Yin, N.L. Maas, A.L. Bredemeyer, A.C. Carpenter, B.A. Helmink, K.S. Yang-Iott, B.P. Sleckman, and C.H. Bassing. 2009. Formation of dynamic gamma-H2AX domains along broken DNA strands is distinctly regulated by ATM and MDC1 and dependent upon H2AX densities in chromatin. *Mol Cell*. 34:298-310.
Savitsky, K., A. Bar-Shira, S. Gilad, G. Rotman, Y. Ziv, L. Vanagaite, D.A. Tagle, S. Smith, T. Uziel, S. Sfez, M. Ashkenazi, I. Pecker, M. Frydman, R. Harnik, S.R. Patanjali, A. Simmons, G.A. Clines, A. Sartiel, R.A. Gatti, L. Chessa, O. Sanal, M.F. Lavin, N.G. Jaspers, A.M. Taylor, C.F. Arlett, T. Miki, S.M. Weissman, M. Lovett, F.S. Collins, and Y. Shiloh. 1995. A single ataxia telangiectasia gene with a product similar to PI-3 kinase. *Science (New York, N.Y.* 268:1749-1753.
Schoeffler, A.J., and J.M. Berger. 2008. DNA topoisomerases: harnessing and constraining energy to govern chromosome topology. *Q Rev Biophys*. 41:41-101.
Schreiber, V., F. Dantzer, J.C. Ame, and G. de Murcia. 2006. Poly(ADP-ribose): novel functions for an old molecule. *Nat Rev Mol Cell Biol*. 7:517-528.
Schulman, B.A., and J.W. Harper. 2009. Ubiquitin-like protein activation by E1 enzymes: the apex for downstream signalling pathways. *Nat Rev Mol Cell Biol*. 10:319-331.
Seiler, J.A., C. Conti, A. Syed, M.I. Aladjem, and Y. Pommier. 2007. The intra-S-phase checkpoint affects both DNA replication initiation and elongation: single-cell and -DNA fiber analyses. *Mol Cell Biol*. 27:5806-5818.
Sekiguchi, J., and S. Shuman. 1997. Site-specific ribonuclease activity of eukaryotic DNA topoisomerase I. *Mol Cell*. 1:89-97.
Sen, N., B. Banerjee, B.B. Das, A. Ganguly, T. Sen, S. Pramanik, S. Mukhopadhyay, and H.K. Majumder. 2007. Apoptosis is induced in leishmanial cells by a novel protein kinase inhibitor withaferin A and is facilitated by apoptotic topoisomerase I-DNA complex. *Cell Death Differ*. 14:358-367.
Seol, Y., H. Zhang, Y. Pommier, and K.C. Neuman. 2013. A kinetic clutch governs religation by type IB topoisomerases and determines camptothecin sensitivity. *Proc Natl Acad Sci U S A*. 109:16125-16130.
Shanbhag, N.M., I.U. Rafalska-Metcalf, C. Balane-Bolivar, S.M. Janicki, and R.A. Greenberg. 2010. ATM-dependent chromatin changes silence transcription in cis to DNA double-strand breaks. *Cell*. 141:970-981.
Shao, G., D.R. Lilli, J. Patterson-Fortin, K.A. Coleman, D.E. Morrissey, and R.A. Greenberg. 2009. The Rap80-BRCC36 de-ubiquitinating enzyme complex antagonizes RNF8-Ubc13-dependent ubiquitination events at DNA double strand breaks. *Proc Natl Acad Sci U S A*. 106:3166-3171.

Shao, R.G., C.X. Cao, H. Zhang, K.W. Kohn, M.S. Wold, and Y. Pommier. 1999. Replication-mediated DNA damage by camptothecin induces phosphorylation of RPA by DNA-dependent protein kinase and dissociates RPA:DNA-PK complexes. *Embo J*. 18:1397-1406.

Shao, Z., A.J. Davis, K.R. Fattah, S. So, J. Sun, K.J. Lee, L. Harrison, J. Yang, and D.J. Chen. 2012. Persistently bound Ku at DNA ends attenuates DNA end resection and homologous recombination. *DNA repair*. 11:310-316.

Shen, J., E.C. Gilmore, C.A. Marshall, M. Haddadin, J.J. Reynolds, W. Eyaid, A. Bodell, B. Barry, D. Gleason, K. Allen, V.S. Ganesh, B.S. Chang, A. Grix, R.S. Hill, M. Topcu, K.W. Caldecott, A.J. Barkovich, and C.A. Walsh. 2010. Mutations in PNKP cause microcephaly, seizures and defects in DNA repair. *Nat Genet*. 42:245-249.

Shiloh, Y. 2006. The ATM-mediated DNA-damage response: taking shape. *Trends Biochem Sci*. 31:402-410.

Shiloh, Y. 2014. ATM: expanding roles as a chief guardian of genome stability. *Exp Cell Res*. 329:154-161.

Shiloh, Y., E. Shema, L. Moyal, and M. Oren. 2011. RNF20-RNF40: A ubiquitin-driven link between gene expression and the DNA damage response. *FEBS Lett*. 585:2795-2802.

Shiloh, Y., and Y. Ziv. 2013. The ATM protein kinase: regulating the cellular response to genotoxic stress, and more. *Nat Rev Mol Cell Biol*. 14:197-210.

Shkreta, L., U. Froehlich, E.R. Paquet, J. Toutant, S.A. Elela, and B. Chabot. 2008. Anticancer drugs affect the alternative splicing of Bcl-x and other human apoptotic genes. *Mol Cancer Ther*. 7:1398-1409.

Shreeram, S., O.N. Demidov, W.K. Hee, H. Yamaguchi, N. Onishi, C. Kek, O.N. Timofeev, C. Dudgeon, A.J. Fornace, C.W. Anderson, Y. Minami, E. Appella, and D.V. Bulavin. 2006. Wip1 phosphatase modulates ATM-dependent signaling pathways. *Mol Cell*. 23:757-764.

Shrivastav, M., C.A. Miller, L.P. De Haro, S.T. Durant, B.P. Chen, D.J. Chen, and J.A. Nickoloff. 2009. DNA-PKcs and ATM co-regulate DNA double-strand break repair. *DNA repair*. 8:920-929.

Shykind, B.M., J. Kim, L. Stewart, J.J. Champoux, and P.A. Sharp. 1997. Topoisomerase I enhances TFIID-TFIIA complex assembly during activation of transcription. *Genes Dev*. 11:397-407.

Sibanda, B.L., D.Y. Chirgadze, and T.L. Blundell. 2010. Crystal structure of DNA-PKcs reveals a large open-ring cradle comprised of HEAT repeats. *Nature*. 463:118-121.

Silver, D.P., and D.M. Livingston. 2012. Mechanisms of BRCA1 tumor suppression. *Cancer discovery*. 2:679-684.

Sims, R.J., 3rd, R. Belotserkovskaya, and D. Reinberg. 2004. Elongation by RNA polymerase II: the short and long of it. *Genes Dev*. 18:2437-2468.

Sirikantaramas, S., M. Yamazaki, and K. Saito. 2008. Mutations in topoisomerase I as a self-resistance mechanism coevolved with the production of the anticancer alkaloid camptothecin in plants. *Proc Natl Acad Sci U S A*. 105:6782-6786.

Skourti-Stathaki, K., and N.J. Proudfoot. 2014. A double-edged sword: R loops as threats to genome integrity and powerful regulators of gene expression. *Genes Dev*. 28:1384-1396.

Skourti-Stathaki, K., N.J. Proudfoot, and N. Gromak. 2011. Human senataxin resolves RNA/DNA hybrids formed at transcriptional pause sites to promote Xrn2-dependent termination. *Mol Cell*. 42:794-805.

Smith, H.M., and A.J. Grosovsky. 1999. PolyADP-ribose-mediated regulation of p53 complexed with topoisomerase I following ionizing radiation. *Carcinogenesis*. 20:1439-1443.

Smith, L.M., E. Willmore, C.A. Austin, and N.J. Curtin. 2005. The novel poly(ADP-Ribose) polymerase inhibitor, AG14361, sensitizes cells to topoisomerase I poisons by increasing the persistence of DNA strand breaks. *Clin Cancer Res*. 11:8449-8457.

Smits, V.A., P.M. Reaper, and S.P. Jackson. 2006. Rapid PIKK-dependent release of Chk1 from chromatin promotes the DNA-damage checkpoint response. *Curr Biol*. 16:150-159.

Snapka, R.M. 1986. Topoisomerase inhibitors can selectively interfere with different stages of simian virus 40 DNA replication. *Mol Cell Biol*. 6:4221-4227.

So, S., A.J. Davis, and D.J. Chen. 2009. Autophosphorylation at serine 1981 stabilizes ATM at DNA damage sites. *J Cell Biol*. 187:977-990.

Sobhian, B., G. Shao, D.R. Lilli, A.C. Culhane, L.A. Moreau, B. Xia, D.M. Livingston, and R.A. Greenberg. 2007. RAP80 targets BRCA1 to specific ubiquitin structures at DNA damage sites. *Science (New York, N.Y.* 316:1198-1202.

Soe, K., A. Rockstroh, P. Schache, and F. Grosse. 2004. The human topoisomerase I damage response plays a role in apoptosis. *DNA repair*. 3:387-393.

Solier, S., J. Barb, B.R. Zeeberg, S. Varma, M. Ryan, K.W. Kohn, J.N. Weinstein, P.J. Munson, and Y.G. Pommier. 2010. Genome-wide analysis of novel splice variants induced by topoisomerase I poisoning shows preferential occurrence in genes encoding splicing factors. *Cancer Res*.

Solier, S., M.C. De Cian, A. Bettaieb, L. Desoche, E. Solary, and L. Corcos. 2008. PKC zeta controls DNA topoisomerase-dependent human caspase-2 pre-mRNA splicing. *FEBS Lett*. 582:372-378.

Solier, S., A. Lansiaux, E. Logette, J. Wu, J. Soret, J. Tazi, C. Bailly, L. Desoche, E. Solary, and L. Corcos. 2004. Topoisomerase I and II inhibitors control caspase-2 pre-messenger RNA splicing in human cells. *Mol Cancer Res*. 2:53-61.

Solier, S., M.C. Ryan, S.E. Martin, S. Varma, K.W. Kohn, H. Liu, B.R. Zeeberg, and Y. Pommier. 2013. Transcription poisoning by Topoisomerase I is controlled by gene length, splice sites, and miR-142-3p. *Cancer Res*. 73:4830-4839.

Solier, S., O. Sordet, K.W. Kohn, and Y. Pommier. 2009. Death receptor-induced activation of the Chk2- and histone H2AX-associated DNA damage response pathways. *Mol Cell Biol*. 29:68-82.

Sollier, J., and K.A. Cimprich. 2015. Breaking bad: R-loops and genome integrity. *Trends Cell Biol*.

Sollier, J., C.T. Stork, M.L. Garcia-Rubio, R.D. Paulsen, A. Aguilera, and K.A. Cimprich. 2014. Transcription-coupled nucleotide excision repair factors promote R-loop-induced genome instability. *Mol Cell*. 56:777-785.

Solovjeva, L.V., M.P. Svetlova, V.O. Chagin, and N.V. Tomilin. 2007. Inhibition of transcription at radiation-induced nuclear foci of phosphorylated histone H2AX in mammalian cells. *Chromosome Res*. 15:787-797.

Somesh, B.P., J. Reid, W.F. Liu, T.M. Sogaard, H. Erdjument-Bromage, P. Tempst, and J.Q. Svejstrup. 2005. Multiple mechanisms confining RNA polymerase II ubiquitylation to polymerases undergoing transcriptional arrest. *Cell*. 121:913-923.

Sordet, O., A. Goldman, and Y. Pommier. 2006. Topoisomerase II and tubulin inhibitors both induce the formation of apoptotic topoisomerase I cleavage complexes. *Mol Cancer Ther*. 5:3139-3144.

Sordet, O., A. Goldman, C. Redon, S. Solier, V.A. Rao, and Y. Pommier. 2008a. Topoisomerase I requirement for death receptor-induced apoptotic nuclear fission. *The Journal of biological chemistry*. 283:23200-23208.

Sordet, O., Q.A. Khan, K.W. Kohn, and Y. Pommier. 2003. Apoptosis induced by topoisomerase inhibitors. *Curr Med Chem Anticancer Agents*. 3:271-290.

Sordet, O., Q.A. Khan, I. Plo, P. Pourquier, Y. Urasaki, A. Yoshida, S. Antony, G. Kohlhagen, E. Solary, M. Saparbaev, J. Laval, and Y. Pommier. 2004a. Apoptotic topoisomerase I-DNA complexes induced by staurosporine-mediated oxygen radicals. *The Journal of biological chemistry*. 279:50499-50504.

Sordet, O., Q.A. Khan, and Y. Pommier. 2004b. Apoptotic topoisomerase I-DNA complexes induced by oxygen radicals and mitochondrial dysfunction. *Cell Cycle*. 3:1095-1097.

Sordet, O., S. Larochelle, E. Nicolas, E.V. Stevens, C. Zhang, K.M. Shokat, R.P. Fisher, and Y. Pommier. 2008b. Hyperphosphorylation of RNA polymerase II in response to topoisomerase I cleavage complexes and its association with transcription- and BRCA1-dependent degradation of topoisomerase I. *J Mol Biol*. 381:540-549.

Sordet, O., Z. Liao, H. Liu, S. Antony, E.V. Stevens, G. Kohlhagen, H. Fu, and Y. Pommier. 2004c. Topoisomerase I-DNA complexes contribute to arsenic trioxide-induced apoptosis. *The Journal of biological chemistry*. 279:33968-33975.

Sordet, O., A.J. Nakamura, C.E. Redon, and Y. Pommier. 2010. DNA double-strand breaks and ATM activation by transcription-blocking DNA lesions. *Cell Cycle*. 9:274-278.

Sordet, O., C.E. Redon, J. Guirouilh-Barbat, S. Smith, S. Solier, C. Douarre, C. Conti, A.J. Nakamura, B.B. Das, E. Nicolas, K.W. Kohn, W.M. Bonner, and Y. Pommier. 2009. Ataxia telangiectasia mutated activation by transcription- and topoisomerase I-induced DNA double-strand breaks. *EMBO Rep*. 10:887-893.

Sordet, O., and S. Solier. 2012. Topoisomerases and Apoptosis. In Pommier Y (ed) DNA Topoisomerases and Cancer, Humana Press Inc., Totowa, NJ.

Soret, J., M. Gabut, C. Dupon, G. Kohlhagen, J. Stevenin, Y. Pommier, and J. Tazi. 2003. Altered serine/arginine-rich protein phosphorylation and exonic enhancer-dependent splicing in Mammalian cells lacking topoisomerase I. *Cancer Res*. 63:8203-8211.

Soubeyrand, S., L. Pope, and R.J. Haché. 2010. Topoisomerase IIalpha-dependent induction of a persistent DNA damage response in response to transient etoposide exposure. *Mol Oncol*. 4:38-51.

Soucy, T.A., P.G. Smith, M.A. Milhollen, A.J. Berger, J.M. Gavin, S. Adhikari, J.E. Brownell, K.E. Burke, D.P. Cardin, S. Critchley, C.A. Cullis, A. Doucette, J.J. Garnsey, J.L. Gaulin, R.E. Gershman, A.R. Lublinsky, A. McDonald, H. Mizutani, U. Narayanan, E.J. Olhava, S. Peluso, M. Rezaei, M.D. Sintchak, T. Talreja, M.P. Thomas, T. Traore, S. Vyskocil, G.S. Weatherhead, J. Yu, J. Zhang, L.R. Dick, C.F. Claiborne, M. Rolfe, J.B. Bolen, and S.P. Langston. 2009. An inhibitor of NEDD8-activating enzyme as a new approach to treat cancer. *Nature*. 458:732-736.

Soutoglou, E., and T. Misteli. 2008. Activation of the cellular DNA damage response in the absence of DNA lesions. *Science (New York, N.Y.*. 320:1507-1510.

Sparks, J.L., and P.M. Burgers. 2015. Error-free and mutagenic processing of topoisomerase 1-provoked damage at genomic ribonucleotides. *EMBO J*. 34:1259-1269.

Spataro, A., and D. Kessel. 1972. Studies on camptothecin-induced degradation and apparent reaggregation of DNA from L1210 cells. *Biochem Biophys Res Commun*. 48:643-648.

Squires, S., A.J. Ryan, H.L. Strutt, and R.T. Johnson. 1993. Hypersensitivity of Cockayne's syndrome cells to camptothecin is associated with the generation of abnormally high levels of double strand breaks in nascent DNA. *Cancer Res*. 53:2012-2019.

St-Amant, C., S. Lussier, J. Lehoux, R.M. Laberge, and G. Boissonneault. 2006. Altered phosphorylation of topoisomerase I following overexpression in an ovarian cancer cell line. *Biochemistry and cell biology = Biochimie et biologie cellulaire*. 84:55-66.

Staker, B.L., M.D. Feese, M. Cushman, Y. Pommier, D. Zembower, L. Stewart, and A.B. Burgin. 2005. Structures of three classes of anticancer agents bound to the human topoisomerase I-DNA covalent complex. *J Med Chem*. 48:2336-2345.

Staker, B.L., K. Hjerrild, M.D. Feese, C.A. Behnke, A.B. Burgin, Jr., and L. Stewart. 2002. The mechanism of topoisomerase I poisoning by a camptothecin analog. *Proc Natl Acad Sci U S A*. 99:15387-15392.

Stamm, S., S. Ben-Ari, I. Rafalska, Y. Tang, Z. Zhang, D. Toiber, T.A. Thanaraj, and H. Soreq. 2005. Function of alternative splicing. *Gene*. 344:1-20.

Starita, L.M., A.A. Horwitz, M.C. Keogh, C. Ishioka, J.D. Parvin, and N. Chiba. 2005. BRCA1/BARD1 ubiquitinate phosphorylated RNA polymerase II. *The Journal of biological chemistry*. 280:24498-24505.

Stefanis, L., D.S. Park, W.J. Friedman, and L.A. Greene. 1999. Caspase-dependent and -independent death of camptothecin-treated embryonic cortical neurons. *The Journal of neuroscience : the official journal of the Society for Neuroscience*. 19:6235-6247.

Stevnsner, T., U.H. Mortensen, O. Westergaard, and B.J. Bonven. 1989. Interactions between eukaryotic DNA topoisomerase I and a specific binding sequence. *The Journal of biological chemistry*. 264:10110-10113.

Stewart, A.F., R.E. Herrera, and A. Nordheim. 1990. Rapid induction of c-fos transcription reveals quantitative linkage of RNA polymerase II and DNA topoisomerase I enzyme activities. *Cell*. 60:141-149.

Stewart, G.S., S. Panier, K. Townsend, A.K. Al-Hakim, N.K. Kolas, E.S. Miller, S. Nakada, J. Ylanko, S. Olivarius, M. Mendez, C. Oldreive, J. Wildenhain, A. Tagliaferro, L. Pelletier, N. Taubenheim, A. Durandy, P.J. Byrd, T. Stankovic, A.M. Taylor, and D. Durocher. 2009. The RIDDLE syndrome protein mediates a ubiquitin-dependent signaling cascade at sites of DNA damage. *Cell*. 136:420-434.

Stewart, G.S., T. Stankovic, P.J. Byrd, T. Wechsler, E.S. Miller, A. Huissoon, M.T. Drayson, S.C. West, S.J. Elledge, and A.M. Taylor. 2007. RIDDLE immunodeficiency syndrome is linked to defects in 53BP1-mediated DNA damage signaling. *Proc Natl Acad Sci U S A*. 104:16910-16915.

Stewart, L., G.C. Ireton, and J.J. Champoux. 1996. The domain organization of human topoisomerase I. *The Journal of biological chemistry*. 271:7602-7608.

Stewart, L., M.R. Redinbo, X. Qiu, W.G. Hol, and J.J. Champoux. 1998. A model for the mechanism of human topoisomerase I. *Science (New York, N.Y.*. 279:1534-1541.

Stiff, T., M. O'Driscoll, N. Rief, K. Iwabuchi, M. Lobrich, and P.A. Jeggo. 2004. ATM and DNA-PK function redundantly to phosphorylate H2AX after exposure to ionizing radiation. *Cancer Res*. 64:2390-2396.

Stone, H.R., and J.R. Morris. 2014. DNA damage emergency: cellular garbage disposal to the rescue? *Oncogene*. 33:805-813.

Stracker, T.H., I. Roig, P.A. Knobel, and M. Marjanovic. 2013. The ATM signaling network in development and disease. *Front Genet*. 4:37.

Strande, N., S.A. Roberts, S. Oh, E.A. Hendrickson, and D.A. Ramsden. 2012. Specificity of the dRP/AP lyase of Ku promotes nonhomologous end joining (NHEJ) fidelity at damaged ends. *The Journal of biological chemistry*. 287:13686-13693.

Straub, T., P. Grue, A. Uhse, M. Lisby, B.R. Knudsen, T.O. Tange, O. Westergaard, and F. Boege. 1998. The RNA-splicing factor PSF/p54 controls DNA-topoisomerase I activity by a direct interaction. *The Journal of biological chemistry*. 273:26261-26264.

Streich, F.C., Jr., and C.D. Lima. 2014. Structural and functional insights to ubiquitin-like protein conjugation. *Annu Rev Biophys*. 43:357-379.

Strumberg, D., A.A. Pilon, M. Smith, R. Hickey, L. Malkas, and Y. Pommier. 2000. Conversion of topoisomerase I cleavage complexes on the leading strand of ribosomal DNA into 5'-phosphorylated DNA double-strand breaks by replication runoff. *Mol Cell Biol*. 20:3977-3987.

Stuckey, R., N. Garcia-Rodriguez, A. Aguilera, and R.E. Wellinger. 2015. Role for RNA:DNA hybrids in origin-independent replication priming in a eukaryotic system. *Proc Natl Acad Sci U S A*. 112:5779-5784.

Stucki, M., J.A. Clapperton, D. Mohammad, M.B. Yaffe, S.J. Smerdon, and S.P. Jackson. 2005. MDC1 directly binds phosphorylated histone H2AX to regulate cellular responses to DNA double-strand breaks. *Cell*. 123:1213-1226.

Suberbielle, E., P.E. Sanchez, A.V. Kravitz, X. Wang, K. Ho, K. Eilertson, N. Devidze, A.C. Kreitzer, and L. Mucke. 2013. Physiologic brain activity causes DNA double-strand breaks in neurons, with exacerbation by amyloid-beta. *Nat Neurosci*. 16:613-621.

Subramanian, D., B.S. Rosenstein, and M.T. Muller. 1998. Ultraviolet-induced DNA damage stimulates topoisomerase I-DNA complex formation in vivo: possible relationship with DNA repair. *Cancer Res*. 58:976-984.

Sun, Y., X. Jiang, S. Chen, N. Fernandes, and B.D. Price. 2005. A role for the Tip60 histone acetyltransferase in the acetylation and activation of ATM. *Proc Natl Acad Sci U S A*. 102:13182-13187.

Sun, Y., X. Jiang, Y. Xu, M.K. Ayrapetov, L.A. Moreau, J.R. Whetstine, and B.D. Price. 2009. Histone H3 methylation links DNA damage detection to activation of the tumour suppressor Tip60. *Nat Cell Biol*. 11:1376-1382.

Sun, Y., Y. Xu, K. Roy, and B.D. Price. 2007. DNA damage-induced acetylation of lysine 3016 of ATM activates ATM kinase activity. *Mol Cell Biol*. 27:8502-8509.

Svejstrup, J.Q. 2010. The interface between transcription and mechanisms maintaining genome integrity. *Trends Biochem Sci*. 35:333-338.

Takagi, K., T.S. Dexheimer, C. Redon, O. Sordet, K. Agama, G. Lavielle, A. Pierre, S.E. Bates, and Y. Pommier. 2007. Novel E-ring camptothecin keto analogues (S38809 and S39625) are stable, potent, and selective topoisomerase I inhibitors without being substrates of drug efflux transporters. *Mol Cancer Ther*. 6:3229-3238.

Takashima, H., C.F. Boerkoel, J. John, G.M. Saifi, M.A. Salih, D. Armstrong, Y. Mao, F.A. Quiocho, B.B. Roa, M. Nakagawa, D.W. Stockton, and J.R. Lupski. 2002. Mutation of TDP1, encoding a topoisomerase I-dependent DNA damage repair enzyme, in spinocerebellar ataxia with axonal neuropathy. *Nat Genet*. 32:267-272.

Takeshita, T., W. Wu, A. Koike, M. Fukuda, and T. Ohta. 2009. Perturbation of DNA repair pathways by proteasome inhibitors corresponds to enhanced chemosensitivity of cells to DNA damage-inducing agents. *Cancer Chemother Pharmacol*. 64:1039-1046.

Tammaro, M., P. Barr, B. Ricci, and H. Yan. 2013

. Replication-dependent and transcription-dependent mechanisms of DNA double-strand break induction by the topoisomerase 2-targeting drug etoposide. *PLoS One*. 8:e79202.

Tanaka, T., H.D. Halicka, X. Huang, F. Traganos, and Z. Darzynkiewicz. 2006. Constitutive histone H2AX phosphorylation and ATM activation, the reporters of DNA damage by endogenous oxidants. *Cell Cycle*. 5:1940-1945.

Tang, J., N.W. Cho, G. Cui, E.M. Manion, N.M. Shanbhag, M.V. Botuyan, G. Mer, and R.A. Greenberg. 2013. Acetylation limits 53BP1 association with damaged chromatin to promote homologous recombination. *Nat Struct Mol Biol*. 20:317-325.

Tanizawa, A., A. Fujimori, Y. Fujimori, and Y. Pommier. 1994. Comparison of topoisomerase I inhibition, DNA damage, and cytotoxicity of camptothecin derivatives presently in clinical trials. *J. Natl. Cancer Inst.* 86:836-842.

Tanizawa, A., K.W. Kohn, and Y. Pommier. 1993. Induction of cleavage in topoisomerase I c-DNA by topoisomerase I enzymes from calf thymus and wheat germ in the presence and absence of camptothecin. *Nucleic Acids Res*. 21:5157-5166.

Tarpey, P.S., F.L. Raymond, S. O'Meara, S. Edkins, J. Teague, A. Butler, E. Dicks, C. Stevens, C. Tofts, T. Avis, S. Barthorpe, G. Buck, J. Cole, K. Gray, K. Halliday, R. Harrison, K. Hills, A. Jenkinson, D. Jones, A. Menzies, T. Mironenko, J. Perry, K. Raine, D. Richardson, R. Shepherd, A. Small, J. Varian, S. West, S. Widaa, U. Mallya, J. Moon, Y. Luo, S. Holder, S.F. Smithson, J.A. Hurst, J. Clayton-Smith, B. Kerr, J. Boyle, M. Shaw, L. Vandeleur, J. Rodriguez, R. Slaugh, D.F. Easton, R. Wooster, M. Bobrow, A.K. Srivastava, R.E. Stevenson, C.E. Schwartz, G. Turner, J. Gecz, P.A. Futreal, M.R. Stratton, and M. Partington. 2007. Mutations in CUL4B, which encodes a ubiquitin E3 ligase subunit, cause an X-linked mental retardation syndrome associated with aggressive outbursts, seizures, relative macrocephaly, central obesity, hypogonadism, pes cavus, and tremor. *Am J Hum Genet*. 80:345-352.

Teicher, B.A. 2008. Next generation topoisomerase I inhibitors: Rationale and biomarker strategies. *Biochem Pharmacol*. 75:1262-1271.

Thomas, M., R.L. White, and R.W. Davis. 1976. Hybridization of RNA to double-stranded DNA: formation of R-loops. *Proc Natl Acad Sci U S A*. 73:2294-2298.

Tian, B., Q. Yang, and Z. Mao. 2009. Phosphorylation of ATM by Cdk5 mediates DNA damage signalling and regulates neuronal death. *Nat Cell Biol*. 11:211-218.

Tomicic, M.T., M. Christmann, and B. Kaina. 2005. Topotecan-triggered degradation of topoisomerase I is p53-dependent and impacts cell survival. *Cancer Res*. 65:8920-8926.

Tomicic, M.T., and B. Kaina. 2013

. Topoisomerase degradation, DSB repair, p53 and IAPs in cancer cell resistance to camptothecin-like topoisomerase I inhibitors. *Biochim Biophys Acta*. 1835:11-27.

Tous, C., and A. Aguilera. 2007. Impairment of transcription elongation by R-loops in vitro. *Biochem Biophys Res Commun*. 360:428-432.

Tresini, M., D.O. Warmerdam, P. Kolovos, L. Snijder, M.G. Vrouwe, J.A. Demmers, I.W.F. van, F.G. Grosveld, R.H. Medema, J.H. Hoeijmakers, L.H. Mullenders, W. Vermeulen, and J.A. Marteijn. 2015. The core spliceosome as target and effector of non-canonical ATM signalling. *Nature*. 523:53-58.

Trzcinska, A.M., A. Girstun, A. Piekielko, B. Kowalska-Loth, and K. Staron. 2002. Potential protein partners for the N-terminal domain of human topoisomerase I revealed by phage display. *Mol Biol Rep*. 29:347-352.

Tsao, Y.P., A. Russo, G. Nyamuswa, R. Silber, and L.F. Liu. 1993. Interaction between replication forks and topoisomerase I-DNA cleavable complexes: studies in a cell-free SV40 DNA replication system. *Cancer Res*. 53:5908-5914.

Tuduri, S., L. Crabbe, C. Conti, H. Tourriere, H. Holtgreve-Grez, A. Jauch, V. Pantesco, J. De Vos, A. Thomas, C. Theillet, Y. Pommier, J. Tazi, A. Coquelle, and P. Pasero. 2009. Topoisomerase I suppresses genomic instability by preventing interference between replication and transcription. *Nat Cell Biol*. 11:1315-1324.

Tuzon, C.T., T. Spektor, X. Kong, L.M. Congdon, S. Wu, G. Schotta, K. Yokomori, and J.C. Rice. 2014. Concerted activities of distinct H4K20 methyltransferases at DNA double-strand breaks regulate 53BP1 nucleation and NHEJ-directed repair. *Cell reports*. 8:430-438.

Uematsu, N., E. Weterings, K. Yano, K. Morotomi-Yano, B. Jakob, G. Taucher-Scholz, P.O. Mari, D.C. van Gent, B.P. Chen, and D.J. Chen. 2007. Autophosphorylation of DNA-PKCS regulates its dynamics at DNA double-strand breaks. *J Cell Biol*. 177:219-229.

Uemura, T., and M. Yanagida. 1984. Isolation of type I and II DNA topoisomerase mutants from fission yeast: single and double mutants show different phenotypes in cell growth and chromatin organization. *EMBO J*. 3:1737-1744.

Ui, A., Y. Nagaura, and A. Yasui. 2015. Transcriptional elongation factor ENL phosphorylated by ATM recruits polycomb and switches off transcription for DSB repair. *Mol Cell*. 58:468-482.

Unsal-Kaçmaz, K., A.M. Makhov, J.D. Griffith, and A. Sancar. 2002. Preferential binding of ATR protein to UV-damaged DNA. *Proc Natl Acad Sci U S A*. 99:6673-6678.

Urasaki, Y., G. Laco, Y. Takebayashi, C. Bailly, G. Kohlhagen, and Y. Pommier. 2001. Use of camptothecin-resistant mammalian cell lines to evaluate the role of topoisomerase I in the antiproliferative activity of the indolocarbazole, NB-506, and its topoisomerase I binding site. *Cancer Res*. 61:504-508.

Ustrell, V., L. Hoffman, G. Pratt, and M. Rechsteiner. 2002. PA200, a nuclear proteasome activator involved in DNA repair. *EMBO J*. 21:3516-3525.

Uziel, T., Y. Lerenthal, L. Moyal, Y. Andegeko, L. Mittelman, and Y. Shiloh. 2003. Requirement of the MRN complex for ATM activation by DNA damage. *Embo J*. 22:5612-5621.

van der Burg, M., H. Ijspeert, N.S. Verkaik, T. Turul, W.W. Wiegant, K. Morotomi-Yano, P.O. Mari, I. Tezcan, D.J. Chen, M.Z. Zdzienicka, J.J. van Dongen, and D.C. van Gent. 2009. A DNA-PKcs mutation in a radiosensitive T-B- SCID patient inhibits Artemis activation and nonhomologous end-joining. *J Clin Invest*. 119:91-98.

van Hoffen, A., J. Venema, R. Meschini, A.A. van Zeeland, and L.H. Mullenders. 1995. Transcription-coupled repair removes both cyclobutane pyrimidine dimers and 6-4 photoproducts with equal efficiency and in a sequential way from transcribed DNA in xeroderma pigmentosum group C fibroblasts. *EMBO J*. 14:360-367.

van Wijk, S.J., and H.T. Timmers. 2010. The family of ubiquitin-conjugating enzymes (E2s): deciding between life and death of proteins. *FASEB J*. 24:981-993.

Vance, J.R., and T.E. Wilson. 2002. Yeast Tdp1 and Rad1-Rad10 function as redundant pathways for repairing Top1 replicative damage. *Proc Natl Acad Sci U S A*. 99:13669-13674.

Vaz, B., S. Halder, and K. Ramadan. 2013. Role of p97/VCP (Cdc48) in genome stability. *Front Genet*. 4:60.

Veloso, A., B. Biewen, M.T. Paulsen, N. Berg, L. Carmo de Andrade Lima, J. Prasad, K. Bedi, B. Magnuson, T.E. Wilson, and M. Ljungman. 2013. Genome-wide transcriptional effects of the anti-cancer agent camptothecin. *PLoS One*. 8:e78190.

Viard, T., and C.B. de la Tour. 2007. Type IA topoisomerases: a simple puzzle? *Biochimie*. 89:456-467.

Vidal-Eychenie, S., C. Decaillet, J. Basbous, and A. Constantinou. 2013. DNA structure-specific priming of ATR activation by DNA-PKcs. *J Cell Biol*. 202:421-429.

Villamil, M.A., Q. Liang, J. Chen, Y.S. Choi, S. Hou, K.H. Lee, and Z. Zhuang. 2012. Serine phosphorylation is critical for the activation of ubiquitin-specific protease 1 and its interaction with WD40-repeat protein UAF1. *Biochemistry*. 51:9112-9123.

Voeller, D.M., J.L. Grem, Y. Pommier, K. Paull, and C.J. Allegra. 2000. Identification and proposed mechanism of action of thymidine kinase inhibition associated with cellular exposure to camptothecin analogs. *Cancer Chemother Pharmacol*. 45:409-416.

Vyas, R., R. Kumar, F. Clermont, A. Helfricht, P. Kalev, P. Sotiropoulou, I.A. Hendriks, E. Radaelli, T. Hochepied, C. Blanpain, A. Sablina, H. van Attikum, J.V. Olsen, A.G. Jochemsen, A.C. Vertegaal, and J.C. Marine. 2013. RNF4 is required for DNA double-strand break repair in vivo. *Cell Death Differ*. 20:490-502.

Wahba, L., S.K. Gore, and D. Koshland. 2013. The homologous recombination machinery modulates the formation of RNA-DNA hybrids and associated chromosome instability. *Elife*. 2:e00505.

Walker, A.I., T. Hunt, R.J. Jackson, and C.W. Anderson. 1985. Double-stranded DNA induces the phosphorylation of several proteins including the 90 000 mol. wt. heat-shock protein in animal cell extracts. *EMBO J*. 4:139-145.

Walker, J.R., R.A. Corpina, and J. Goldberg. 2001. Structure of the Ku heterodimer bound to DNA and its implications for double-strand break repair. *Nature*. 412:607-614.
Wall, W., Cook, Palmer, McPhail, Sim. 1966. Plant Antitumor Agents. I. The Isolation and Structure of Camptothecin, a Novel Alkaloidal Leukemia and Tumor Inhibitor from Camptotheca acuminata. *J. Am. Chem. Soc*:3888–3890.
Waltes, R., R. Kalb, M. Gatei, A.W. Kijas, M. Stumm, A. Sobeck, B. Wieland, R. Varon, Y. Lerenthal, M.F. Lavin, D. Schindler, and T. Dörk. 2009. Human RAD50 deficiency in a Nijmegen breakage syndrome-like disorder. *Am J Hum Genet*. 84:605-616.
Walton, C., H. Interthal, R. Hirano, M.A. Salih, H. Takashima, and C.F. Boerkoel. 2010. Spinocerebellar ataxia with axonal neuropathy. *Adv Exp Med Biol*. 685:75-83.
Wang, B., S. Matsuoka, B.A. Ballif, D. Zhang, A. Smogorzewska, S.P. Gygi, and S.J. Elledge. 2007. Abraxas and RAP80 form a BRCA1 protein complex required for the DNA damage response. *Science (New York, N.Y.* 316:1194-1198.
Wang, B., S. Matsuoka, P.B. Carpenter, and S.J. Elledge. 2002. 53BP1, a mediator of the DNA damage checkpoint. *Science (New York, N.Y.* 298:1435-1438.
Wang, C., and S.P. Lees-Miller. 2013. Detection and repair of ionizing radiation-induced DNA double strand breaks: new developments in nonhomologous end joining. *Int J Radiat Oncol Biol Phys*. 86:440-449.
Wang, H., L. Wang, H. Erdjument-Bromage, M. Vidal, P. Tempst, R.S. Jones, and Y. Zhang. 2004. Role of histone H2A ubiquitination in Polycomb silencing. *Nature*. 431:873-878.
Wang, J., Z. Gong, and J. Chen. 2011. MDC1 collaborates with TopBP1 in DNA replication checkpoint control. *J Cell Biol*. 193:267-273.
Wang, J.C. 2002. Cellular roles of DNA topoisomerases: a molecular perspective. *Nat Rev Mol Cell Biol*. 3:430-440.
Wang, M., W. Wu, B. Rosidi, L. Zhang, H. Wang, and G. Iliakis. 2006. PARP-1 and Ku compete for repair of DNA double strand breaks by distinct NHEJ pathways. *Nucleic Acids Res*. 34:6170-6182.
Wang, X., K.A. Henningfeld, and S.M. Hecht. 1998. DNA topoisomerase I-mediated formation of structurally modified DNA duplexes. Effects of metal ions and topoisomerase I inhibitors. *Biochemistry*. 37:2691-2700.
Wang, Y., C. Xu, L.Q. Du, J. Cao, J.X. Liu, X. Su, H. Zhao, F.Y. Fan, B. Wang, T. Katsube, S.J. Fan, and Q. Liu. 2013. Evaluation of the comet assay for assessing the dose-response relationship of DNA damage induced by ionizing radiation. *Int J Mol Sci*. 14:22449-22461.
Ward, I.M., and J. Chen. 2001. Histone H2AX is phosphorylated in an ATR-dependent manner in response to replicational stress. *The Journal of biological chemistry*. 276:47759-47762.
Ward, I.M., K. Minn, J. van Deursen, and J. Chen. 2003. p53 Binding protein 53BP1 is required for DNA damage responses and tumor suppression in mice. *Mol Cell Biol*. 23:2556-2563.
Watanabe, S., K. Watanabe, V. Akimov, J. Bartkova, B. Blagoev, J. Lukas, and J. Bartek. 2013. JMJD1C demethylates MDC1 to regulate the RNF8 and BRCA1-mediated chromatin response to DNA breaks. *Nat Struct Mol Biol*. 20:1425-1433.
Wei, S.J., J.G. Williams, H. Dang, T.A. Darden, B.L. Betz, M.M. Humble, F.M. Chang, C.S. Trempus, K. Johnson, R.E. Cannon, and R.W. Tennant. 2008. Identification of a specific motif of the DSS1 protein required for proteasome interaction and p53 protein degradation. *J Mol Biol*. 383:693-712.
Wei, W., Z. Ba, M. Gao, Y. Wu, Y. Ma, S. Amiard, C.I. White, J.M. Rendtlew Danielsen, Y.G. Yang, and Y. Qi. 2012. A role for small RNAs in DNA double-strand break repair. *Cell*. 149:101-112.
Weinstock, D.M., E. Brunet, and M. Jasin. 2007. Formation of NHEJ-derived reciprocal chromosomal translocations does not require Ku70. *Nat Cell Biol*. 9:978-981.
Weisshaar, S.R., K. Keusekotten, A. Krause, C. Horst, H.M. Springer, K. Gottsche, R.J. Dohmen, and G.J. Praefcke. 2008. Arsenic trioxide stimulates SUMO-2/3 modification leading to RNF4-dependent proteolytic targeting of PML. *FEBS Lett*. 582:3174-3178.
Westover, K.D., D.A. Bushnell, and R.D. Kornberg. 2004. Structural basis of transcription: separation of RNA from DNA by RNA polymerase II. *Science (New York, N.Y.* 303:1014-1016.
Whitehouse, C.J., R.M. Taylor, A. Thistlethwaite, H. Zhang, F. Karimi-Busheri, D.D. Lasko, M. Weinfeld, and K.W. Caldecott. 2001. XRCC1 stimulates human polynucleotide kinase activity at damaged DNA termini and accelerates DNA single-strand break repair. *Cell*. 104:107-117.
Williams, G.J., S.P. Lees-Miller, and J.A. Tainer. 2010. Mre11-Rad50-Nbs1 conformations and the control of sensing, signaling, and effector responses at DNA double-strand breaks. *DNA repair*. 9:1299-1306.
Williams, J.S., D.J. Smith, L. Marjavaara, S.A. Lujan, A. Chabes, and T.A. Kunkel. 2013. Topoisomerase 1-mediated removal of ribonucleotides from nascent leading-strand DNA. *Mol Cell*. 49:1010-1015.
Wood, L.M., S. Sankar, R.E. Reed, A.L. Haas, L.F. Liu, P. McKinnon, and S.D. Desai. 2011. A novel role for ATM in regulating proteasome-mediated protein degradation through suppression of the ISG15 conjugation pathway. *PLoS One*. 6:e16422.
Woodgett, J.R. 1993. A kinase with Ku-dos. *Curr Biol*. 3:449-450.
Woods, D., and J.J. Turchi. 2013. Chemotherapy induced DNA damage response: convergence of drugs and pathways. *Cancer Biol Ther*. 14:379-389.
Wu, J., Y. Chen, L.Y. Lu, Y. Wu, M.T. Paulsen, M. Ljungman, D.O. Ferguson, and X. Yu. 2011. Chfr and RNF8 synergistically regulate ATM activation. *Nat Struct Mol Biol*. 18:761-768.
Wu, J., and L.F. Liu. 1997. Processing of topoisomerase I cleavable complexes into DNA damage by transcription. *Nucleic Acids Res*. 25:4181-4186.
Wu, L., and I.D. Hickson. 2003. The Bloom's syndrome helicase suppresses crossing over during homologous recombination. *Nature*. 426:870-874.
Wu-Baer, F., K. Lagrazon, W. Yuan, and R. Baer. 2003. The BRCA1/BARD1 heterodimer assembles polyubiquitin chains through an unconventional linkage involving lysine residue K6 of ubiquitin. *The Journal of biological chemistry*. 278:34743-34746.
Wyman, C., and R. Kanaar. 2006. DNA double-strand break repair: all's well that ends well. *Annu Rev Genet.* 40:363-383.
Xia, Y., G.M. Pao, H.W. Chen, I.M. Verma, and T. Hunter. 2003. Enhancement of BRCA1 E3 ubiquitin ligase activity through direct interaction with the BARD1 protein. *The Journal of biological chemistry*. 278:5255-5263.

Xiao, A., H. Li, D. Shechter, S.H. Ahn, L.A. Fabrizio, H. Erdjument-Bromage, S. Ishibe-Murakami, B. Wang, P. Tempst, K. Hofmann, D.J. Patel, S.J. Elledge, and C.D. Allis. 2009. WSTF regulates the H2A.X DNA damage response via a novel tyrosine kinase activity. *Nature*. 457:57-62.

Xiao, Z., Z. Chen, A.H. Gunasekera, T.J. Sowin, S.H. Rosenberg, S. Fesik, and H. Zhang. 2003. Chk1 mediates S and G2 arrests through Cdc25A degradation in response to DNA-damaging agents. *The Journal of biological chemistry*. 278:21767-21773.

Xirodimas, D.P., M.K. Saville, J.C. Bourdon, R.T. Hay, and D.P. Lane. 2004. Mdm2-mediated NEDD8 conjugation of p53 inhibits its transcriptional activity. *Cell*. 118:83-97.

Xu, G., J.R. Chapman, I. Brandsma, J. Yuan, M. Mistrik, P. Bouwman, J. Bartkova, E. Gogola, D. Warmerdam, M. Barazas, J.E. Jaspers, K. Watanabe, M. Pieterse, A. Kersbergen, W. Sol, P.H. Celie, P.C. Schouten, B. van den Broek, A. Salman, M. Nieuwland, I. de Rink, J. de Ronde, K. Jalink, S.J. Boulton, J. Chen, D.C. van Gent, J. Bartek, J. Jonkers, P. Borst, and S. Rottenberg. 2015. REV7 counteracts DNA double-strand break resection and affects PARP inhibition. *Nature*. 521:541-544.

Xu, Y., and B.D. Price. 2011. Chromatin dynamics and the repair of DNA double strand breaks. *Cell Cycle*. 10:261-267.

Xu, Y., Y. Sun, X. Jiang, M.K. Ayrapetov, P. Moskwa, S. Yang, D.M. Weinstock, and B.D. Price. 2010. The p400 ATPase regulates nucleosome stability and chromatin ubiquitination during DNA repair. *J Cell Biol*. 191:31-43.

Xu, Y.a.H.C. 2015. Inhibition of Topoisomerase (DNA) I (TOP1): DNA Damage Repair and Anticancer Therapy. *Biomolecules*. 5:1652-1670.

Yajima, H., K.J. Lee, and B.P. Chen. 2006. ATR-dependent phosphorylation of DNA-dependent protein kinase catalytic subunit in response to UV-induced replication stress. *Mol Cell Biol*. 26:7520-7528.

Yang, S.W., A.B. Burgin, Jr., B.N. Huizenga, C.A. Robertson, K.C. Yao, and H.A. Nash. 1996. A eukaryotic enzyme that can disjoin dead-end covalent complexes between DNA and type I topoisomerases. *Proc Natl Acad Sci U S A*. 93:11534-11539.

Yang, X., L. Li, J. Liang, L. Shi, J. Yang, X. Yi, D. Zhang, X. Han, N. Yu, and Y. Shang. 2013. Histone acetyltransferase 1 promotes homologous recombination in DNA repair by facilitating histone turnover. *The Journal of biological chemistry*. 288:18271-18282.

Yoo, H.Y., A. Kumagai, A. Shevchenko, A. Shevchenko, and W.G. Dunphy. 2009. The Mre11-Rad50-Nbs1 complex mediates activation of TopBP1 by ATM. *Molecular biology of the cell*. 20:2351-2360.

Yoshioka, K., Y. Yoshioka, and P. Hsieh. 2006. ATR kinase activation mediated by MutSalpha and MutLalpha in response to cytotoxic O6-methylguanine adducts. *Mol Cell*. 22:501-510.

Yu, C.C., J.C. Yang, Y.C. Chang, J.G. Chuang, C.W. Lin, M.S. Wu, and L.P. Chow. 2013. VCP phosphorylation-dependent interaction partners prevent apoptosis in Helicobacter pylori-infected gastric epithelial cells. *PLoS One*. 8:e55724.

Yu, K., F. Chedin, C.L. Hsieh, T.E. Wilson, and M.R. Lieber. 2003. R-loops at immunoglobulin class switch regions in the chromosomes of stimulated B cells. *Nat Immunol*. 4:442-451.

Zechiedrich, E.L., and N. Osheroff. 1990. Eukaryotic topoisomerases recognize nucleic acid topology by preferentially interacting with DNA crossovers. *EMBO J*. 9:4555-4562.

Zeman, M.K., and K.A. Cimprich. 2014. Causes and consequences of replication stress. *Nat Cell Biol*. 16:2-9.

Zhang, A., Y.L. Lyu, C.P. Lin, N. Zhou, A.M. Azarova, L.M. Wood, and L.F. Liu. 2006. A protease pathway for the repair of topoisomerase II-DNA covalent complexes. *The Journal of biological chemistry*. 281:35997-36003.

Zhang, H., J.C. Wang, and L.F. Liu. 1988. Involvement of DNA topoisomerase I in transcription of human ribosomal RNA genes. *Proc Natl Acad Sci U S A*. 85:1060-1064.

Zhang, H., Q. Wang, K. Kajino, and M.I. Greene. 2000. VCP, a weak ATPase involved in multiple cellular events, interacts physically with BRCA1 in the nucleus of living cells. *DNA Cell Biol*. 19:253-263.

Zhang, H.F., A. Tomida, R. Koshimizu, Y. Ogiso, S. Lei, and T. Tsuruo. 2004. Cullin 3 promotes proteasomal degradation of the topoisomerase I-DNA covalent complex. *Cancer Res*. 64:1114-1121.

Zhang, Y.W., M. Regairaz, J.A. Seiler, K.K. Agama, J.H. Doroshow, and Y. Pommier. 2011. Poly(ADP-ribose) polymerase and XPF-ERCC1 participate in distinct pathways for the repair of topoisomerase I-induced DNA damage in mammalian cells. *Nucleic Acids Res*. 39:3607-3620.

Zhao, H., M. Zhu, G. Dou, H. Zhao, B. Zhu, J. Li, J. Liao, and X. Xu. 2014. BCL10 regulates RNF8/RNF168-mediated ubiquitination in the DNA damage response. *Cell Cycle*. 13:1777-1787.

Zheng, J., X. Yang, J.M. Harrell, S. Ryzhikov, E.H. Shim, K. Lykke-Andersen, N. Wei, H. Sun, R. Kobayashi, and H. Zhang. 2002. CAND1 binds to unneddylated CUL1 and regulates the formation of SCF ubiquitin E3 ligase complex. *Mol Cell*. 10:1519-1526.

Zheng, L., M. Zhou, Q. Chai, J. Parrish, D. Xue, S.M. Patrick, J.J. Turchi, S.M. Yannone, D. Chen, and B. Shen. 2005. Novel function of the flap endonuclease 1 complex in processing stalled DNA replication forks. *EMBO Rep*. 6:83-89.

Zhou, Y., P. Caron, G. Legube, and T.T. Paull. 2014. Quantitation of DNA double-strand break resection intermediates in human cells. *Nucleic Acids Res*. 42:e19.

Zhou, Y., F.G. Gwadry, W.C. Reinhold, L.D. Miller, L.H. Smith, U. Scherf, E.T. Liu, K.W. Kohn, Y. Pommier, and J.N. Weinstein. 2002. Transcriptional regulation of mitotic genes by camptothecin-induced DNA damage: microarray analysis of dose- and time-dependent effects. *Cancer Res*. 62:1688-1695.

Zhu, Q., G.M. Pao, A.M. Huynh, H. Suh, N. Tonnu, P.M. Nederlof, F.H. Gage, and I.M. Verma. 2011. BRCA1 tumour suppression occurs via heterochromatin-mediated silencing. *Nature*. 477:179-184.

Zimmermann, M., F. Lottersberger, S.B. Buonomo, A. Sfeir, and T. de Lange. 2013. 53BP1 regulates DSB repair using Rif1 to control 5' end resection. *Science (New York, N.Y.* 339:700-704.

APPENDIX

1. TITLE PAGE

R-loop formation and accumulation of antisense and sense transcripts by camptothecin at active promoters.

Marinello Jessica, Bertoncini Stefania, Cristini Agnese, Malagoli Tagliazucchi Guidantonio, Forcato Mattia, Sordet Olivier and Capranico Giovanni

Affiliations:

JM, SB, GC: Department of Pharmacy and Biotechnology, University of Bologna, via Irnerio 48, 40126 Bologna, Italy.

AC, OS: Cancer Research Center of Toulouse, INSERM UMR1037, 31037, Toulouse, France.

GMT, MF: Center for Genome Research, Department of Life Sciences, University of Modena and Reggio Emilia, Modena, Italy.

GMT: Current Affiliation: INGM Istituto Nazionale Genetica Molecolare, IRCCS Ospedale Maggiore Polilclinico, Milano, Italy

2. RUNNING TITLE PAGE

Camptothecin effects on transcripts and R-loops at active promoters

Corresponding author: G. Capranico, Department of Pharmacy and Biotechnology, University of Bologna, via Irnerio 48, 40126 Bologna, Italy. Email: giovanni.capranico@unibo.it. Phone number: 00390512091209.

Text Pages: 24

Total number of figures: 5

Total number of references: 43

Number of words in Abstract: 236

Number of words in Introduction: 723

Number of words in Discussion: 872

List of abbreviations:

CPT: Camptothecin

Top1cc: Topoisomerase I-DNA-cleavage complexes

aRNA: antisense transcript

CGI: CpG-island promoter

R-loop: DNA/RNA hybrids

3. ABSTRACT

Topoisomerase I-DNA-cleavage complexes (Top1cc) stabilized by camptothecin (CPT) have specific effects at transcriptional levels. We recently reported that Top1cc increase antisense transcript levels (aRNAs) at bidirectional CpG-island promoters (CGI) and, transiently, DNA/RNA hybrids (R-loop) in nuclear and mitochondrial genomes of colon cancer HCT116 cells. However, the relationship between R-loops and aRNAs was not established. Here, we show that aRNAs can form R-loops under physiological conditions in HCT116 cells, and that Top1cc stabilize promoter-associated R-loops immediately upon cell exposure to CPT. In contrast, persistent Top1cc reduce the majority of R-loops suggesting that CPT-accumulated aRNAs are not commonly involved in R-loops. The enhancement of aRNAs by Top1ccs is present both in human colon cancer HCT116 cells and WI38 fibroblasts suggesting a common response of cancer and normal cells. Although Top1ccs lead to DSB and DDR activation, we do not reveal a correlation between aRNA accumulation and ATM or DNAPK activity. Moreover, the cell response to persistent Top1cc can involve an impairment of aRNA turnover rather than a higher synthesis rate. Finally, a genome-wide analysis shows that persistent Top1cc also determine an accumulation of sense transcripts at 5'-end gene regions suggesting an increased occurrence of truncated transcripts. Taken together, these results indicate that Top1 may regulate transcription initiation by modulating RNA polymerase-generated negative supercoils, which can in turn favor R-loop formation at promoters, and that transcript accumulation at TSS is a response to persistent transcriptional stress by Top1 poisoning.

4. NO VISUAL ABSTRACT

5. INTRODUCTION

Topoisomerase I (Top1) is a fundamental enzyme regulating DNA superhelicity, and its activity is required for a proper progression of transcription and replication machineries in mammalian cells. Enzyme activity can essentially be divided in four steps: substrate binding, DNA cleavage, controlled rotation of the cut strand around the other one, and DNA resealing. Top1 poisons, such as camptothecin (CPT), inhibit Top1 by binding at the interface of a Top1-DNA complex forming a ternary structure (Top1cc) in which the drug molecule prevents DNA resealing and leaves Top1 covalently bound to a DNA strand (Pommier, 2006). Top1cc can lead to irreversible DNA damage when a collision occurs with replication forks or elongating RNA polymerases (RNA Pol) (Capranico et al., 2010; Pommier et al., 2006). The replication-dependent irreversible DNA damage is commonly considered the molecular mechanisms of CPT cytotoxicity and hence antitumor activity, as it can act as a potent inducer of apoptosis of cancer cells (Li and Liu, 2001).

In addition to the cell killing activity, Top1 poisons have specific effects at transcriptional levels that may impact gene expression profiles of normal and/or cancer cells contributing to drug therapeutic outcomes (Baranello et al., 2009; Capranico et al., 2010; Marinello et al., 2013; Solier et al., 2013; Sordet et al., 2008; Veloso et al., 2013). Recently, treatments with Top1 poisons have been shown to de-repress the paternal Ube3A allele in an Angelman disease murine model (Huang et al., 2011) providing an interesting case in which CPT derivatives can permanently change the expression of a specific gene in mammalian cells. Thus, understanding the mechanisms of Top1 regulation of gene expression and the interference of Top1 inhibitors with them can provide significant insights to discover new anticancer therapeutics.

Top1 is a very active enzyme at transcribed regions (Champoux, 2001; Khobta et al., 2006; Wang, 2002). Recently, it has been reported that Top1 mainly regulates DNA superhelicity at intermediately-active genes as its inhibition by CPT increased local negative supercoils at their promoters (Kouzine et al., 2013). Interestingly, we have demonstrated that CPT impacts transcription regulation with characteristic and specific effects on RNA Pol II recruitment and pausing, nucleosome density and promoter-associated antisense RNA levels (Baranello et al., 2009; Bertozzi et al., 2011; Capranico et al., 2010). In particular, a genome-wide analysis revealed that CPT increases antisense transcripts levels at active divergent CpG-island promoters (CGI) in a manner dependent on Top1cc formation at the promoter (Marinello et al., 2013). Whether the increase in negative DNA supercoils at promoters is mechanistically linked to the specific effects on RNA PolII and antisense transcripts was left to be defined.

Top1 silencing is known to increase non-B DNA structures, such as R loops, that are prone to DNA damage and genome instability (Costantino and Koshland, 2015; El Hage et al., 2010; Groh and Gromak, 2014). R loops are three-strand structures constituted by a DNA-RNA hybrid duplex and a displaced DNA strand. Stable R-loops exist in living prokaryotic and eukaryotic cells at origin of replication where they have a role in the regulation of replication initiation (Lombrana et al., 2015; Sollier and Cimprich, 2015; Stuckey et al., 2015). R loops also constitute a necessary step of the immunoglobulin recombination mechanism as they form at IgG class switch regions where they can extend over a kilobase (Roy et al., 2008; Yu et al., 2003). Moreover, differential stabilization of R-loops could influence gene expression in many organisms. For instance, R-loop structures allow the presence of the substrate for a single-strand DNA binding protein that represses the expression of COOLAIR ncRNA in Arabidopsis (Sun et al., 2013). In addition, R-loops can be enriched over human CGI and involved in maintaining their hypomethylated state (Ginno et al., 2012). Gene mutations affecting nucleic acid degradation have recently been shown to cause global DNA hypomethylation and R-loop accumulation in fibroblasts of patients with autoimmune disorders (Lim et al., 2015). Interestingly, Top1 poisoning by CPT can induce specific double-stranded DNA cleavage in post-mitotic cells that can be suppressed by the overexpression of RNaseH1, suggesting the involvement of transcriptionally-linked R loops in CPT induction of DNA damage (Sordet et al., 2009). Increased R-loop levels by CPT have been shown at specific loci such as Angelman imprinting locus and Fragile X syndrome site (Groh et al., 2014; Powell et al., 2013). With a time course analysis in human colon cancer cells by confocal cell microscopy, we showed that CPT effects on R-loops are highly dynamic as it triggers a transient increase of global R-loops in the nuclear and mitochondrial genomes (Marinello et al., 2013). However, the genomic location of such dynamic R-loop structures and their relationships with aRNA have not been established yet.

Therefore, we have here asked whether CPT-increased antisense transcripts can form R loops with DNA template at promoters. Our findings show that Top1 inhibition by CPT specifically impacts on RNA Pol II activity at promoters by affecting R-loop formation and that antisense and sense transcripts are likely accumulated by persistent Top1ccs due to the inhibition of their degradation.

6. MATERIALS AND METHODS

Cell Lines. The cancer cell lines HCT116 and N-Tera-2 cl.D1 were purchased from ATCC (LGC Standards S.r.l., Milan, Italy) and were grown in DMEM medium with 10% fetal bovine serum (Carlo Erba, Milan, Italy). Cells were maintained at 37° C in a humidified incubator containing 20% O_2 and 5% CO_2. Cell line identity was certified with Cell ID System (Promega) by BMR Genomics Srl (Padova, Italy). Immortalized WI-38 human embryonic fibroblasts (WI-38hTERT) were obtained from Carl Mann (CEA, Gif-sur-Yvette, France) and Estelle Nicolas (Université de Toulouse, Toulouse, France) (Jeanblanc et al., 2012). WI-38hTERT cells were cultured in modified Eagle's medium (MEM) supplemented with 10% fetal bovine serum, 1 mM sodium pyruvate, 2 mM L-glutamine and 0.1 mM MEM non-essential amino acids (Life Technologies). For quiescence induction, cells were washed twice with serum-free medium and grown in MEM with 0.2% serum for 72 h.

Drugs and cell treatments. CPT and flavopiridol were purchased from Sigma-Aldrich. ATM inhibitor (KU55933) and DNA-PK inhibitor (NU7441) were obtained from Calbiochem and Tocris respectively. Serum-starved or exponentially growing cells were exposed to 10 μM CPT for the indicated time at 37° C, unless specified otherwise. In case of co-treatments, cells were previously incubated with various inhibitors for 1 h before the addition of CPT to the medium for further 4 hours.

RNA extraction and cDNA preparation. Total cellular RNA was purified with the acid phenol method (Bertozzi et al., 2011; Bertozzi et al., 2013) and quantified by UV absorbance. After verifying its quality on a 1% agarose gel, 1 μg of total RNA was used to prepare cDNA using SuperScript III (Invitrogen) following the manufacturer's instruction. Random (N6) and poly(T) primers were used for total RNA retrotranscription. Reactions included a 25°C pre-annealing step for 5 min, and then retrotranscription was performed at 50°C for 50 min.

Quantitative Real-Time PCR. Real-time PCR were performed using Applied Biosystems StepOne and SYBR Select Master Mix for CFX (Applied Biosystems). Quantification and melting curve analyses were performed using StepOne Software v2.2.3 as indicated by the supplier. Specificity of PCR products was routinely controlled by melting curve analysis and agarose gel electrophoresis.

Expression and purification of MBP-RNAse H1 (D145N). Protocol was obtained from Ginno et al 2012 (Ginno et al., 2012) and the plasmid expressing a mutated and inactive RNAseH1 was kindly provided by F. Chedin (University of California, DAVIS). In particular, transformed Rosetta 2(DE3) cells of E. coli were inoculated in LB medium supplemented with 2 g/L of glucose, 100 µg/mL of ampicillin, and 30 µg/mL of chloramphenicol. After induction for 4 hours with IPTG, cells were pelletted and lysed using for 80 ml of cell culture, 1.2 ml of lysis buffer [200 mM NaCl; 20 mM Tris-HCl (pH 7.5); 1 mM EDTA; 10 mM DTT; Aprotinin 2 µg/ml; Leupeptin 1 µg/ml; Pepstatin 1 µg/ml; PMSF 1 mM and Lysozym 200 µg/ml]. Lysate was sonicated for 10 min with 30 sec on/off cycles and finally centrifuged at 4°C, 14000g for 20'. The isolation of MBP-fusion protein was performed with Amylose Magnetic Beads (New England Biolabs). In particular 100 µl of beads suspension were equilibrated twice with 500 µl of MBP column buffer [200 mM NaCl; 20 mM Tris-HCl (pH 7.4); 1 mM EDTA and 1 mM DTT] thus incubated with 500 µl of cell culture supernatant at 4° C with agitation for 1 hour. Supernatant was discarded and beads washed three times with 500 µl of MBP column buffer. The purified MBP-RNAse H1 (D145N) was eluted from the beads twice with 50 µl of MBP column buffer containing 10 mM maltose for 10 minutes at 4° C with agitation. Alternatively MBP-RNAse H1 (D145N) was purified using Amylose Resin (New England Biolabs). In particular, 1 ml resin was poured in a column and washed with 5 column volumes of MBP column buffer. Crude extract was loaded after 1:1 dilution with MBP column buffer and the resin was washed with 12 column volumes of MBP column buffer. Elution of the fusion protein was performed with 5 volumes MBP column buffer containing 10 mM maltose. Purified protein was concentrated with a centrifugal filter unit (Millipore).

DRIVE (DNA:RNA In Vitro Enrichment). The procedure was performed as in Ginno et al (Ginno et al., 2012). In particular, lysis of ~4x106 NTera-2 cl.D1 cells was performed with 1.6 ml TE-SDS Lysis Buffer [10 mM Tris-HCl (pH 8.0); 1mM EDTA and 0.5% SDS] at 37° C for 5 min. Proteinase K was then added (125 ng/µl) and samples incubated for 5 h at 37° C. An equal volume of phenol (pH 8.0) was added and the samples were mixed gently, thus centrifuged at 3000g for 2 min. The upper phase was collected and an equal volume of chloroform/isoamylic alcohol (24:1) was added to it, then mixed gently and centrifuged again at 3000g for 2 min. Genomic DNA was precipitated with 2.5 volumes of ethanol 100% and 1/10 volume of NaOAc 3M (pH 5.2), in presence of glycogen. Using a hooked glass rod, DNA were spooled out and washed several times with 70% EtOH. Genomic DNA was resuspended in 500µl of TE buffer [10 mM Tris-HCl (pH 8.0); 1 mM EDTA] avoiding vortexing to preserve RNA/DNA hybrids. Genomic DNA was then digested O/N at 37° C in TANGO BUFFER 2X with 2 mM Spermidine and a cocktail of restriction

enzymes: 20 U EcoRI; 20 U Xbal; 20 U Hind III; 20 U SspI and 20 U BsrG1 (ThermoFisher Scientific). Each sample was thus splitted in three: 1,5 µg were used as input, 1,5 µg were incubated for 2 hours at 37° C with 10U of RNAse H and 1,5 µg were incubated for 2 hours at 37° C without RNAse H (Life Technologies). Samples incubated with or without RNAseH were added of 50 µl of Binding Buffer 10x [100 mM Na_2PO_4 (pH 7.0); 1.4 M NaCl; 0.5% Triton X-100], MBP-RNAse H D145N (w/w ratio according titration) and TE buffer (pH 7.4) to final volume of 500 µl. RNAse H D145N was allowed to bind specifically for 2 hours at 4° C on agitation. 50 µl/sample Amylose Magnetic Beads (New England Biolabs) were equilibrated twice with 500 µl of MBP column buffer [200 mM NaCl; 20 mM Tris-HCl (pH 7.4); 1 mM EDTA and 1 mM DTT], then incubated with 500 µl of reaction mix at 4° C with agitation for 75 min. Supernatant was discarded and beads washed three times with 500 µl of MBP column buffer. The purified MBP-RNAse H1 (D145N) bound to RNA/DNA hybrid was eluted from the beads twice with 100 µl of MBP column buffer containing 10 mM maltose for 10 minutes at 4° C with agitation. TE (pH 7.4) and SDS (final concentration 0.5%) were added to a final volume of 250 µl. 140 µg of Proteinase K were added and samples incubated at 55° C for 45 min. Samples, included inputs, were thus brought to 300 µl final volume with BDW and phenol/chloroform extraction was performed. To allow precipitation 2,5 volumes of ethanol 100%, 1/10 volume of NaOAc 3M (pH 5.2) and glycogen were added and samples were incubated O/N at -20° C. For data analysis, RNA/DNA hybrid enrichment of each sample is calculated as "% of Input" after subtracting the background signal, as determined by the same sample treated with RNAseH1 before DRIVE precipitation. Then the enrichment value is normalized against the 2-min CPT sample of the RPL13A amplicon of the same experiment.

Bioinformatics analysis. Due to update versions of specific softwares for RNA-Seq analysis, we re-align raw data of previous published experiments (Marinello et al., 2013) to improve revious results. Then, we checked the quality of each sequenced sample using FastQC (http://www.bioinformatics.babraham.ac.uk/projects/fastqc/). Low-quality sequenced bases were filtered out using Trimmomatic v0.33 (Bolger et al., 2014). The bisulfite-treated paired reads were then mapped twice to the hg19 human genome assembly in which all the cytosines were mutated in thymines (CT-hg19) or all the guanine in adenine (GA-hg19) to identify the strand originating the sequence fragment. Sequences coming from positive strand transcripts align to the CT-hg19, whereas negative strand transcripts align to the GA-hg19. The read alignment was carried out with Bowtie2 v2.2.0 (Langmead and Salzberg, 2012) and TopHat v2.0.10 (Kim et al., 2013; Trapnell et al., 2009) to identify known transcripts. For each of the four experiments, reads that aligned to both CT-hg19 and GA-hg19 were discarded. Cufflinks package v2.2.0 (Trapnell et al., 2010) was used to

assemble and identify novel transcripts, using modified reference genomes (CT-hg19 and GA-hg19). Gene expression levels were estimated in FPKM units (expected number of Fragments Per Kilobase of transcript sequence per Millions of sequenced nucleotides) using Cufflinks. Sense tags distribution, along non-overlapping Refseq genes, were analyzed in a region from 2000 bases upstream the TSS (Transcription Start Site) to 2000 bases downstream the TES using NGSplot software v2.41 (Shen et al., 2014).

7. RESULTS

Increased antisense transcripts form R-loops in untreated cells. Both immunofluorescence imaging and RNAseH1 overexpression experiments have previously demonstrated that CPT-trapped Top1ccs induce a significant increase of R-loop structures that likely mediate drug-induced genome instability (Marinello et al., 2013; Sordet et al., 2009). However, the genomic sites of such R-loops are not known. Here, we used the DRIVE technique (Ginno et al., 2013; Ginno et al., 2012) to determine whether or not R-loops form under physiological conditions at divergent promoters in human NTERA-2 cells. First of all, we analyzed previously-published R-loop positive and negative loci (Ginno et al., 2012) to check the DRIVE method. Figure 1A (white bars) shows we could clearly discriminate between regions known to form (RPL13A, BTBD19 and MYADM) and those depleted of (SNRPN and a-Sat) R-loops as a significant recovery is shown at the former rather than the latter loci. Moreover, we determined R-loop levels at the D-loop region of mitochondrial genome (mtDNA), where a well-known and stable R-loop is implicated in replication priming of mtDNA (Xu and Clayton, 1996). Of the three selected regions, the RB31-R3 amplicon corresponds exactly to the R-loop-forming site while 1A-1B and 4A-4B amplicons correspond to the D-loop and a more distant region, respectively (Figure1B, map). The two non R-loop-forming regions show a recovery significantly lower as compared with RB31-R3 (Figure 1B). Overall, the data showed that we can accurately detect R-loops with the DRIVE technique in mitochondrial and nuclear genomes.

Next, we asked whether divergent promoters might form R-loops under physiological conditions in untreated NTERA-2 cells. To that purpose, promoters were selected on the basis of their ability to show increase of antisense transcripts after Top1 inhibition by CPT, as reported in Fig. 1C. Therefore, we investigated 8 promoters (TAF4, POLR2K, SP2, GPC1, MDM2, PCIF1, ATF1, SMARCA4) showing an increase of aRNA and one negative promoter (TNIK) with no aRNA increase (Fig. 1C)(Marinello et al., 2013). The results show that we can detect R-loops in untreated cells at all positive promoters, though at different levels, whereas no signal was present at the TNIK promoter (Fig. 1A). Even though DNA enrichment values for the 8 promoter regions are lower than mtDNA sites and other positive controls (RPL13A, BTBD19 and MYADM), they are consistently higher than negative controls (SNRPN, a-Sat and TNIK). We may notice that the studied sites correspond to promoter regions upstream to the TSS (Transcription Start Site) where we detected antisense transcripts in control untreated cells, the levels of which are marked lower than mRNAs (Marinello et al., 2013). In contrast, the RPL13A, BTBD19 and MYADM control regions correspond to the first intron of transcribed genes, hence, in the latter case R-loops are at regions of higher transcription rates. As these R-loops are likely associated with the transcription

process (Ginno et al., 2012), the results may suggest that R-loop formation rate correlates with transcription levels in the studied regions.

Taken together, the results show that antisense transcripts of the studied divergent promoters are able to form R-loops in untreated cells that are likely in the opposite orientation as compared with mRNAs transcription.

Promoter-associated antisense R loops can be transiently increased by CPT and then markedly reduced with longer treatment times. Next, we have investigated whether Top1 inhibition by CPT increases R-loop levels at the studied promoters and control regions. We found that the R-loop signal increases after 2-10 minutes from drug addition, and R-loops are maintained up to 4 hours of CPT treatment at the mitochondrial replication origin (Fig. 2A). Mitochondrial non-R-loop-forming regions show recoveries unchanged by CPT and significantly lower than the R-loop-forming region. Therefore, the R loop at the mitochondrial replication origin is substantially stable in the presence of a Top1 poison, which can even increase its level at short treatment times.

A different pattern was observed for R-loops at the transcribed RPL13A, BTBD19 and MYADM nuclear loci. Here, R-loops are maintained, or slightly increased, after short times (2 and 10 minutes), whereas they are markedly reduced after longer time of treatment (4 hours) (Figure 2A). Similarly, antisense R-loops at the studied divergent promoters show an increase of their levels after short treatment time whereas they are completely lost after 4 hours of treatment, with the exception of TAF4 promoter (Fig. 2A). Thus, Top1 inhibition by CPT can stabilize antisense and sense R-loops at active divergent promoters but only for a short time.

We next wondered whether CPT treatment could affect the length of the DNA-RNA hybrid. Thus, we investigated close regions at two of the studied promoters: TAF4 and PCIF1 (Figure 2B). These two gene promoters were chosen as they also present GC skew segments that can be prone to R-loop formation (Ginno et al., 2013). Interestingly, at short times of treatment, CPT determines an extension of R loops or formation of new R-loops, as after 2 minutes the R-loop signal was also detected in $TAF4_{(4)}$ and $PCIF1_{(2)}$ amplicons (Figure 2B). Therefore, CPT can likely modulate R-loops length at these two promoters. Taken together, our findings show that following a short time of treatments, CPT can modify R-loops present in untreated cells while longer CPT treatments almost fully abolish R-loops at the studied transcribed genes. The results thus suggest that Top1 may modulate R-loop levels by controlling the levels of negative supercoils at promoter regions (Kouzine et al., 2013).

Therefore, all the above results show that Top1ccs likely stabilize and extend antisense R-loops for a very short time at the studied divergent promoters. With persistent Top1ccs, the majority

of R-loops are mostly reduced at these loci suggesting that the accumulated antisense transcripts are not generally involved in R-loop structures. As CPT inhibits transcription elongation with high efficacy and R loops are formed by newly synthesized RNAs, the marked reduction of R loops at active regions is likely due to persistent inhibition of transcription by CPT. Interestingly, our data show exceptions to that as R-loops can persist for long times of CPT treatment at certain genomic loci (TAF4 and mtDNA).

Antisense transcripts are increased by CPT in human resting normal WI38 cells and are dependent on ongoing transcription. Next, we further characterized aRNAs. In particular we asked if their induction was dependent or not on transcription and specific of cancer vs normal cells, and finally if their increase was dependent on Top1cc DSBs formation. To understand whether ongoing transcription is critical for increased levels of promoter-associated antisense RNAs, we have investigated CPT effects in resting cells and in the presence of flavopiridol (FLV), a specific inhibitor of cdk9 and RNA PolII transcription. As Top1ccs specifically increase antisense transcripts upstream to the TSS of divergent CGI promoters in human colon cancer HTC116 cells (Marinello et al., 2013), here we extended the study to human fibroblast-like embryonic cells (WI38) at genomic loci selected on previous findings (Marinello et al., 2013). Treatments with 10 μM CPT in replicating WI38 cells stimulates antisense accumulation in four out of seven of the selected loci (Fig 3), showing that CPT stimulates antisense transcription in non-cancer cells as well. However, the promoter pattern of antisense accumulation is different between the two cell lines, and the CPT effects are lower in WI38 than HCT116 cells at the selected loci.

To evaluate the role of replication on drug effects, we studied the CPT response in serum-starved quiescent WI38 cells (Figure 3, quiescent WI38). Among the studied loci, ATF1 gene promoter accumulates antisense transcripts at the highest levels in both proliferating and resting cells. As in resting cells the enhancement of antisense transcript levels was partially reduced and this reduction could be due to a lower transcription rate in quiescent as compared with replicating cells, we suggest that the CPT effect may be independent from DNA replication. In serum-starved quiescent WI38 cells, we performed a drug dose-response after 1 and 4 hours of treatment (Supplementary Figure 1) showing some increase over time. To determine the role of transcription on CPT effects, we pretreated for 1 hour quiescent WI38 cells with FLV. Under these conditions, no increase of antisense transcript could be detected at the selected loci (Supplementary Figure 2), showing that the drug effect is highly dependent on active transcription in resting human cells.

As transcription-blocking Top1ccs produce DSBs and activate ATM in post-mitotic neurons and lymphocytes (Sordet et al., 2010; Sordet et al., 2009), we next investigated if accumulation of

antisense RNAs could potentially be due to activation of selected kinases (DNA-PK and ATM) of the DNA damage response (DDR) after Top1cc interference with transcription. Cells were first exposed to ATM inhibitor or DNAPK inhibitor for 1 hour, and then CPT was added to the medium for additional 4 hours, in both HCT116 and WI38 cell lines. In all tested conditions, inhibition of the studied DDR kinases did not significantly alter CPT effects on antisense accumulation (Supplementary Figure 3). Therefore, the data suggest that ATM or DNA-PK activation is not apparently required for CPT effects. The data did not allow us to establish a direct connection between increased antisense RNAs and DDR pathways, however, we cannot exclude that other DDR proteins are involved or that the studied kinases act redundantly in the mechanisms of antisense accumulation.

To determine if CPT actively modify the turnover of antisense RNAs, we treated HCT116 cell with CPT for 4 hours, and then determine the levels of the studied transcripts at different times to evaluate their degradation rates. The experiments were performed adding FLV at the end of the 4 hour period of CPT treatment to block transcription. Under these conditions, the degradation rates of TDG and TAF4 antisense transcripts (Fig. 4) and others (see Supplementary figure 5) are lower in the presence of CPT and the transcripts are lost faster in drug-free medium (Supplementary figure 4). Thus, the data clearly show that CPT seems to stabilize antisense RNAs, likely preventing their fast removal and degradation.

CPT determines the accumulation of truncated sense transcripts at 5'-end regions of intermediately active genes. The above findings show that persistent Top1 inhibition by CPT promotes the stabilization of antisense transcripts upstream to the TSS and a general reduction of antisense R-loops at those loci after long treatment time. As R-loops have been shown to form also downstream the TSS (Ginno et al., 2013; Ginno et al., 2012) (see also Fig 1A), we have then investigated whether CPT induced the accumulation of sense transcripts at the 5'-end of genes as well. We have then mapped paired sequence tags obtained from total cellular RNA depleted of ribosomal RNAs and treated with bisulfite to maintain the information of strand direction (Marinello et al., 2013). Non overlapping genes were grouped depending on their FPKM in four categories from low to high expression levels, and we focused on gene regions from -2000 bases upstream the TSS to +2000 bases downstream the TES (transcription end site) in both CPT-treated and control HCT116 cells. Then we plotted the distribution of the sense reads along these genes.

Sense tag levels of all non-overlapping genes were clearly dependent on gene expression levels, however they were similar among expressed gene sets (Supplementary Figs. 6 and 7). Tag distribution of control cells almost overlapped with that of CPT-treated cells with the exception of

the region immediately downstream to the TSS in HCT116 cells (Supplementary Fig. 6). In particular, sense tags were increased at the 5'-end of genes of the two intermediate expression categories following CPT treatment (Supplementary Fig. 6). The increased was lower in HCT116-shRNATop1 cells indicating that it was dependent on the cellular level of Top1 in response to CPT (Supplementary Fig. 7).

Thus, as the intermediately active genes show such a drug effect, we selected genes showing an increase of sense reads within the first 1000 bases downstream the TSS as well as reduced or equal levels of sense reads 1000 bases upstream the TES (Figure 5). For these genes we observed a marked and specific increase of sense tags (Figure 5) in the two gene sets that was clearly dependent on Top1 as in HCT116-shRNATop1 CPT had a lower effect (Fig. 5). The specific accumulation of sense tags at 5'-end regions was then confirmed at specific loci by rtqPCR (Supplementary Figures 8 and 9). Gene ontology analyses of the two gene sets did not reveal any significant gene attribute enriched in the studied groups (splice variants were enriched but with a low p-value), suggesting the lack of a simple common functional or structural characteristic among them.

8. DISCUSSION

A fine regulation of Top1 activity at active genes is essential to maintain a proper transcription process as Top1 deficient cells show impaired transcriptional processes and accumulate abortive transcripts by RNA PolI (El Hage et al., 2010). We have previously demonstrated that Top1 inhibition by CPT leads to unbalanced sense/antisense transcript levels at bidirectional CpG-island promoters (Marinello et al., 2013). The newly-identified antisense transcripts, with a median size of about 800 bases, are accumulated during drug treatment in a Top1-dependent manner mainly at promoters of intermediate activity. In the present work, we aimed to better characterize these aRNA and to establish a relationship between them and R-loop formation at divergent promoters. Our data show that aRNAs can form antisense R-loops at promoters in unperturbed NTERA-2 cells and that, immediately after Top1 inhibition by CPT, the physiological R-loops can be extended in size or new R-loops can be formed at active TSS. In contrast, persistent CPT inhibition of Top1 markedly reduces R-loop structures and accumulates truncated sense transcripts at 5' ends of intermediately active genes. Thus, the findings indicate that Top1 may regulate transcription initiation by regulating RNA Pol II-generated negative supercoils, which in turn can favor R loop formation at promoters, and that transcript accumulation at TSS is a transcriptional response to persistent Top1 poisoning. The proposed role of Top1 at promoters is in agreement with previous findings on the effects of Top1 deletion (El Hage et al., 2010; Kouzine et al., 2013).

As R-loops can either trigger genome instability or mediate transcription regulation (Ginno et al., 2012; Sollier and Cimprich, 2015), we have defined whether or not transcriptional stress induced by Top1 inhibition could be mediated by formation of R-loops at active regions. The results show that R-loop can likely form in the antisense orientation at the studied divergent CGI promoters in untreated cells. Interestingly, CPT perturbs R-loops immediately upon addition to the growth medium as short CPT treatments (2-10 minutes) extend or generate new R-loops at the studied promoters whereas the Top1 poison completely abolishes R-loops at most of the studied promoters following longer treatment times. Therefore, it is likely that Top1 inhibition has a direct and rapid effect on R loop formation favored by excess negative supercoils behind elongating RNA Pol II, which has not be relieved by Top1. This increase is indeed transient as other homeostatic control of DNA superhelicity (for instance, by other DNA topoisomerases) can likely restore default levels of template supercoils. This is in agreement with a recent paper (Kouzine et al., 2013) showing that Top1 is most efficiently recruited at promoters of intermediate activity and that a short CPT treatment determines increased negative supercoils upstream and immediately adjacent to the TSS. Such an increase of negative supercoiling of the DNA template would likely favor both stabilization and extention of R-loop structures at active promoters.

Our findings also show that when Top1 is persistently inhibited by CPT then R-loop formation is also reduced at promoters of active genes. As R-loop levels are dependent on active transcription, then persistent CPT treatments, which are known to strongly inhibit transcription elongation (Capranico et al., 2007), may preclude the formation of R loops. Nevertheless, CPT may have more dynamic effects on R loops in relation to their genomic location, as we observed that R loops persistent even after 4 hour of CPT treatment at mitochondrial replication origin and at TAF4 promoter. In postmitotic neurons, persistent CPT treatments have been shown to affect cell viability (Morris and Geller, 1996) and induce transcriptional DSBs in an R-loop-dependent manner (Sordet et al., 2009). Thus, it can be speculated that R-loops formed at specific genomic location may be stabilized by CPT leading to irreversible double-strand breakage and apoptosis. Here, we have attempted to evaluate if the increase of antisense RNAs at promoters is downstream to DDR pathway activated by CPT, and our findings show that antisense transcript increase is not simply related to either ATM or DNAPK activation in HCT116 and WI38 human cells. However, it remains to be established whether DSBs themselves or other DDR proteins or a combination of both may be implicated in aRNA induction in response to CPT.

The increase of antisense and sense transcripts may in principle be originated by an enhanced synthesis and/or a reduced degradation of them. We previously reported that CPT still determines a similar increase rate of promoter-associated transcripts when transcription was inhibited by DRB as compared with the absence of DRB (Marinello et al., 2013), suggesting that an enhanced synthesis of antisense RNA is unlikely even if we cannot rule out completely this possibility. In agreement with these data, the present findings show that CPT impairs degradation of antisense transcripts. As exosome silencing has been shown to increase the levels of cryptic antisense RNA at promoters (Preker et al., 2011), our findings suggest that exosome activity may be somewhat reduced in cells treated with CPT.

The present findings have established that antisense transcripts can form antisense R-loops at the studied divergent promoters, and that Top1 inhibition by CPT have dynamic and site-specific effects on them. In particular, immediately upon addition, CPT can favor R-loop formation whereas, at longer time of treatment, CPT markedly reduces R-loop levels. Interestingly, R-loops persist at certain active promoters and other genomic loci along with a more general induction of truncated sense and antisense RNAs at active TSS. The findings define new aspects of the specific CPT effects at transcriptional levels in human cancer and normal cells.

9. ACKNOWLEDGMENTS

This work was supported by grant from the “Associazione Italiana per la Ricerca sul Cancro” (AIRC), Milan, Italy [IG15886 grant to G. Capranico]. A.C. is supported by grant from the Ministère de l’Enseignement Supérieur et de la Recherche and from the Fondation pour la Recherche Médicale [FDT20140931166].

10. AUTHORSHIP CONTRIBUTIONS

Participated in research design: Marinello, Capranico.

Conducted experiments: Marinello, Bertoncini, Cristini.

Contributed new reagents or analytic tools: Malagoli Tagliazucchi, Forcato.

Performed data analysis: Marinello, Bertoncini, Cristini, Sordet, Capranico.

Wrote or contributed to the writing of the manuscript: Marinello, Capranico.

11. REFERENCES

Baranello L, Bertozzi D, Fogli MV, Pommier Y and Capranico G (2009) DNA topoisomerase I inhibition by camptothecin induces escape of RNA polymerase II from promoter-proximal pause site, antisense transcription and histone acetylation at the human HIF-1alpha gene locus. *Nucleic Acids Res* **38**(1):159-171.

Bertozzi D, Iurlaro R, Sordet O, Marinello J, Zaffaroni N and Capranico G (2011) Characterization of novel antisense HIF-1alpha transcripts in human cancers. *Cell Cycle* **10**(18):3189-3197.

Bertozzi D, Marinello J, Manzo SG, Fornari F, Gramantieri L and Capranico G (2013) The natural inhibitor of DNA topoisomerase I, camptothecin, modulates HIF-1alpha activity by changing miR expression patterns in human cancer cells. *Mol Cancer Ther* **13**(1):239-248.

Bolger AM, Lohse M and Usadel B (2014) Trimmomatic: a flexible trimmer for Illumina sequence data. *Bioinformatics* **30**(15):2114-2120.

Capranico G, Ferri F, Fogli MV, Russo A, Lotito L and Baranello L (2007) The effects of camptothecin on RNA polymerase II transcription: roles of DNA topoisomerase I. *Biochimie* **89**(4):482-489.

Capranico G, Marinello J and Baranello L (2010) Dissecting the transcriptional functions of human DNA topoisomerase I by selective inhibitors: implications for physiological and therapeutic modulation of enzyme activity. *Biochim Biophys Acta* **1806**(2):240-250.

Champoux JJ (2001) DNA topoisomerases: structure, function, and mechanism. *Annu Rev Biochem* **70**:369-413.

Costantino L and Koshland D (2015) The Yin and Yang of R-loop biology. *Curr Opin Cell Biol* **34**:39-45.

El Hage A, French SL, Beyer AL and Tollervey D (2010) Loss of Topoisomerase I leads to R-loop-mediated transcriptional blocks during ribosomal RNA synthesis. *Genes Dev* **24**(14):1546-1558.

Ginno PA, Lim YW, Lott PL, Korf I and Chedin F (2013) GC skew at the 5' and 3' ends of human genes links R-loop formation to epigenetic regulation and transcription termination. *Genome Res* **23**(10):1590-1600.

Ginno PA, Lott PL, Christensen HC, Korf I and Chedin F (2012) R-loop formation is a distinctive characteristic of unmethylated human CpG island promoters. *Mol Cell* **45**(6):814-825.

Groh M and Gromak N (2014) Out of balance: R-loops in human disease. *PLoS Genet* **10**(9):e1004630.

Groh M, Lufino MM, Wade-Martins R and Gromak N (2014) R-loops associated with triplet repeat expansions promote gene silencing in Friedreich ataxia and fragile X syndrome. *PLoS Genet* **10**(5):e1004318.

Huang HS, Allen JA, Mabb AM, King IF, Miriyala J, Taylor-Blake B, Sciaky N, Dutton JW, Jr., Lee HM, Chen X, Jin J, Bridges AS, Zylka MJ, Roth BL and Philpot BD (2011) Topoisomerase inhibitors unsilence the dormant allele of Ube3a in neurons. *Nature* **481**(7380):185-189.

Jeanblanc M, Ragu S, Gey C, Contrepois K, Courbeyrette R, Thuret JY and Mann C (2012) Parallel pathways in RAF-induced senescence and conditions for its reversion. *Oncogene* **31**(25):3072-3085.

Khobta A, Ferri F, Lotito L, Montecucco A, Rossi R and Capranico G (2006) Early effects of topoisomerase I inhibition on RNA polymerase II along transcribed genes in human cells. *J Mol Biol* **357**(1):127-138.

Kim D, Pertea G, Trapnell C, Pimentel H, Kelley R and Salzberg SL (2013) TopHat2: accurate alignment of transcriptomes in the presence of insertions, deletions and gene fusions. *Genome Biol* **14**(4):R36.

Kouzine F, Gupta A, Baranello L, Wojtowicz D, Ben-Aissa K, Liu J, Przytycka TM and Levens D (2013) Transcription-dependent dynamic supercoiling is a short-range genomic force. *Nat Struct Mol Biol* **20**(3):396-403.

Langmead B and Salzberg SL (2012) Fast gapped-read alignment with Bowtie 2. *Nat Methods* **9**(4):357-359.

Li TK and Liu LF (2001) Tumor cell death induced by topoisomerase-targeting drugs. *Annu Rev Pharmacol Toxicol* **41**:53-77.

Lim YW, Sanz LA, Xu X, Hartono SR and Chedin F (2015) Genome-wide DNA hypomethylation and RNA:DNA hybrid accumulation in Aicardi-Goutieres syndrome. *Elife* **4**.

Lombrana R, Almeida R, Alvarez A and Gomez M (2015) R-loops and initiation of DNA replication in human cells: a missing link? *Front Genet* **6**:158.

Marinello J, Chillemi G, Bueno S, Manzo SG and Capranico G (2013) Antisense transcripts enhanced by camptothecin at divergent CpG-island promoters associated with bursts of topoisomerase I-DNA cleavage complex and R-loop formation. *Nucleic Acids Res* **41**(22):10110-10123.

Morris EJ and Geller HM (1996) Induction of neuronal apoptosis by camptothecin, an inhibitor of DNA topoisomerase-I: evidence for cell cycle-independent toxicity. *J Cell Biol* **134**(3):757-770.

Pommier Y (2006) Topoisomerase I inhibitors: camptothecins and beyond. *Nat Rev Cancer* **6**(10):789-802.

Pommier Y, Barcelo JM, Rao VA, Sordet O, Jobson AG, Thibaut L, Miao ZH, Seiler JA, Zhang H, Marchand C, Agama K, Nitiss JL and Redon C (2006) Repair of topoisomerase I-mediated DNA damage. *Prog Nucleic Acid Res Mol Biol* **81**:179-229.

Powell WT, Coulson RL, Gonzales ML, Crary FK, Wong SS, Adams S, Ach RA, Tsang P, Yamada NA, Yasui DH, Chedin F and LaSalle JM (2013) R-loop formation at Snord116 mediates topotecan inhibition of Ube3a-antisense and allele-specific chromatin decondensation. *Proc Natl Acad Sci U S A* **110**(34):13938-13943.

Preker P, Almvig K, Christensen MS, Valen E, Mapendano CK, Sandelin A and Jensen TH (2011) PROMoter uPstream Transcripts share characteristics with mRNAs and are produced upstream of all three major types of mammalian promoters. *Nucleic Acids Res* **39**(16):7179-7193.

Roy D, Yu K and Lieber MR (2008) Mechanism of R-loop formation at immunoglobulin class switch sequences. *Mol Cell Biol* **28**(1):50-60.

Shen L, Shao N, Liu X and Nestler E (2014) ngs.plot: Quick mining and visualization of next-generation sequencing data by integrating genomic databases. *BMC Genomics* **15**:284.

Solier S, Ryan MC, Martin SE, Varma S, Kohn KW, Liu H, Zeeberg BR and Pommier Y (2013) Transcription poisoning by Topoisomerase I is controlled by gene length, splice sites, and miR-142-3p. *Cancer Res* **73**(15):4830-4839.

Sollier J and Cimprich KA (2015) Breaking bad: R-loops and genome integrity. *Trends Cell Biol*.

Sordet O, Larochelle S, Nicolas E, Stevens EV, Zhang C, Shokat KM, Fisher RP and Pommier Y (2008) Hyperphosphorylation of RNA polymerase II in response to topoisomerase I cleavage complexes and its association with transcription- and BRCA1-dependent degradation of topoisomerase I. *J Mol Biol* **381**(3):540-549.

Sordet O, Nakamura AJ, Redon CE and Pommier Y (2010) DNA double-strand breaks and ATM activation by transcription-blocking DNA lesions. *Cell Cycle* **9**(2):274-278.

Sordet O, Redon CE, Guirouilh-Barbat J, Smith S, Solier S, Douarre C, Conti C, Nakamura AJ, Das BB, Nicolas E, Kohn KW, Bonner WM and Pommier Y (2009) Ataxia telangiectasia mutated activation by transcription- and topoisomerase I-induced DNA double-strand breaks. *EMBO Rep* **10**(8):887-893.

Stuckey R, Garcia-Rodriguez N, Aguilera A and Wellinger RE (2015) Role for RNA:DNA hybrids in origin-independent replication priming in a eukaryotic system. *Proc Natl Acad Sci U S A* **112**(18):5779-5784.

Sun Q, Csorba T, Skourti-Stathaki K, Proudfoot NJ and Dean C (2013) R-loop stabilization represses antisense transcription at the Arabidopsis FLC locus. *Science* **340**(6132):619-621.

Trapnell C, Pachter L and Salzberg SL (2009) TopHat: discovering splice junctions with RNA-Seq. *Bioinformatics* **25**(9):1105-1111.

Trapnell C, Williams BA, Pertea G, Mortazavi A, Kwan G, van Baren MJ, Salzberg SL, Wold BJ and Pachter L (2010) Transcript assembly and quantification by RNA-Seq reveals unannotated transcripts and isoform switching during cell differentiation. *Nat Biotechnol* **28**(5):511-515.

Veloso A, Biewen B, Paulsen MT, Berg N, Carmo de Andrade Lima L, Prasad J, Bedi K, Magnuson B, Wilson TE and Ljungman M (2013) Genome-wide transcriptional effects of the anti-cancer agent camptothecin. *PLoS One* **8**(10):e78190.

Wang JC (2002) Cellular roles of DNA topoisomerases: a molecular perspective. *Nat Rev Mol Cell Biol* **3**(6):430-440.

Xu B and Clayton DA (1996) RNA-DNA hybrid formation at the human mitochondrial heavy-strand origin ceases at replication start sites: an implication for RNA-DNA hybrids serving as primers. *EMBO J* **15**(12):3135-3143.

Yu K, Chedin F, Hsieh CL, Wilson TE and Lieber MR (2003) R-loops at immunoglobulin class switch regions in the chromosomes of stimulated B cells. *Nat Immunol* **4**(5):442-451.

12. FOOTNOTES

This work was supported by grant from the “Associazione Italiana per la Ricerca sul Cancro” (AIRC), Milan, Italy [IG15886 grant to G. Capranico].

13. FIGURE LEGENDS

Figure 1. R-loop formation at the studied genomic and mitochondrial regions in untreated control NTERA-2 cl.D1 cells. DNA enrichment of each sample is subtracted of the enrichment value of the same sample treated with RNAseH1 before DRIVE precipitation. Then the enrichment value is normalized against the 2-min CPT sample (see figure 2) of the RPL13A amplicon of the same experiment. Values are means ±SEM of two to four independent experiments. The data show a higher SEM than commonly published as we report median values of several experiments and not a single representative one. (A) DRIVE assay was performed to determine R-loop levels downstream TSS (white bars) and upstream TSS (black bars). Three negative loci for R-loop formation are also reported (SNRPN, a-SAT, TNIK). (B) Mitochondrial DNA was analyzed with DRIVE assay. Three regions of interest were selected: red for the r-loop forming region (RB31-R3), green for the D-loop region (1A-1B) and blue for the non-D-loop region (4A-4B). Map on the right of the panel shows the heavy (H) and the light (L) strands of mitochondrial DNA, with the three Conserved Sequence Blocks (CSB) and the studied regions (in red, green and blue respectively). (C) Antisense transcription after CPT treatment in NTERA-2 cl.D1 cells. Promoter-associated antisense transcripts were evaluated by rtqPCR after 4 hours CPT treatment at 10 μM. PCR determinations were normalized to cytochrome b mRNA and to untreated cells (dotted line). Values are means +/− SEM of two determinations from at least two independent experiments.

Figure 2. R-loops are transiently stabilized and extended by Top1 inhibition by CPT. DNA enrichment of each sample is subtracted of the enrichment value of the same sample treated with RNAseH1 before DRIVE precipitation. Then the enrichment value is normalized against the 2-min CPT sample of the RPL13A amplicon of the same experiment. Values are means ±SEM of two to four independent experiments. (A) DRIVE assay was performed to determine R-loop levels at genomic regions (on the left) and at mitochondrial regions (on the right) respectively after 2 min, 10 min and 4 hours with 10 μM CPT. Control cells are reported from Figs. 1A and 1B to better appreciate any variation after drug treatment. (B) Scan by DRIVE assay of R-loop formation around transcription start site of TAF4 and PCIF1 genes after a time course treatment with CPT. Genome browser view show the genomic localization of the analyzed regions (right panel). The pattern of enzyme digestion used for DRIVE experiment guarantee the regions are properly separated during r-loop recovery and are therefore reported for clearness on the maps. One representative experiment for each locus is here reported.

Figure 3. Antisense transcript levels induced by CPT in replicating HCT116 and WI38, and in quiescent WI38 cells. Promoter-associated antisense transcripts were evaluated by rtqPCR after 4 hours CPT treatment at 10 μM. PCR determinations were normalized to cytochrome b mRNA and to untreated cells (dotted line). Values are means +/− SEM of two determinations from at least two independent experiments.

Figure 4. Turnover of aRNAs is influenced by CPT. Cells where firstly stimulated for antisense accumulation by a 4 hours treatment with CPT. Then FLV was added to block transcription in absence (solid lines) and in presence (dotted lines) of CPT, and antisense transcript levels determined by rtqPCR after additional 20, 40 and 60 minutes. PCR determinations were normalized to cytochrome b mRNA and to aRNAs levels before FLV addition (time 0). A representative experiment is here reported.

Figure 5. Sense tags distribution, along non-overlapping Refseq genes of HCT116 cells and HCT116-shRNATop1 cells, were analyzed in a region from 2000 bases upstream the TSS to 2000 bases downstream the TES using NGSplot software. Here, genes have been divided in two groups based on their FPKM. These genes have been selected for an accumulation of sense reads in the 5' region (CPT-reads minus Control-reads: 10 ≥ 100) and a reduction of sense reads at the 3' region (CPT-reads minus Control-reads: ≤ 5). Furthermore, genes selected have a fold change above 2 and a minimum number of sense reads above 5 in the 5' region of CPT treated sample. Reads were normalized to the length of each region (1000 bp). Control reads are reported in gray dotted line and CPT reads in black line. Black arrows indicate an accumulation of reads at 5' level after CPT treatment (10 μM for 4 hours).

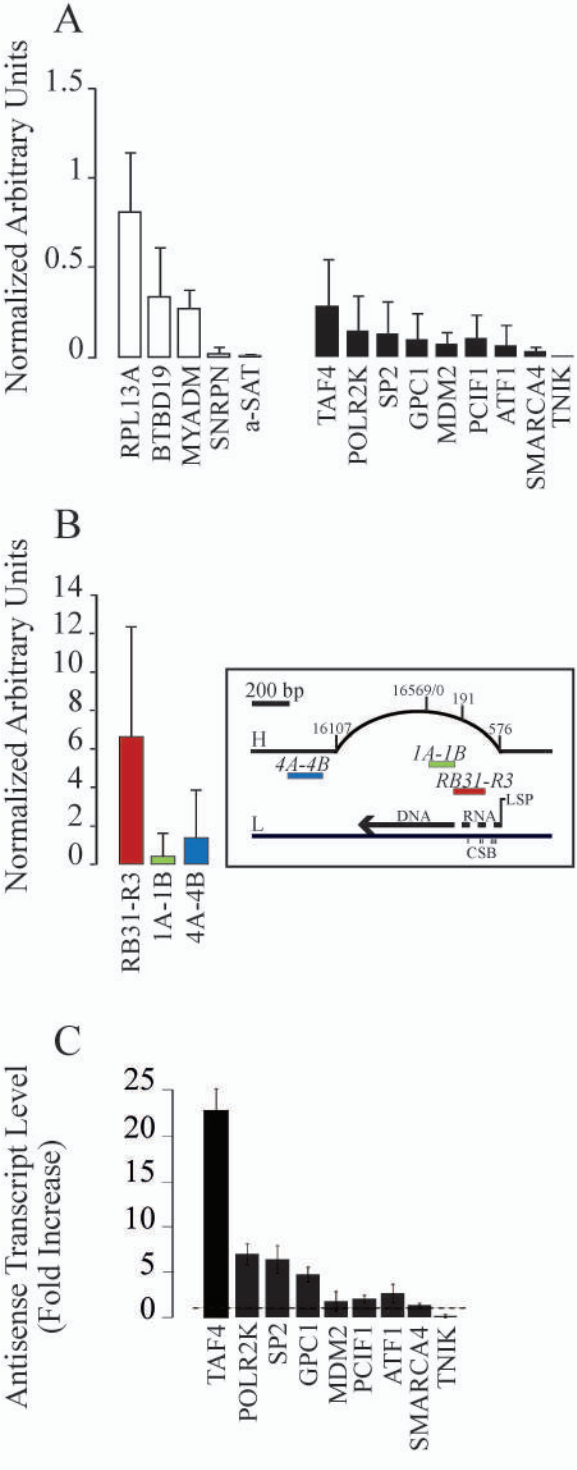
A
Normalized Arbitrary Units
1.5
1
0.5
0
RPL13A
BTBD19
MYADM
SNRPN
a-SAT
TAF4
POLR2K
SP2
GPC1
MDM2
PCIF1
ATF1
SMARCA4
TNIK
B
Normalized Arbitrary Units
14
12
10
8
6
4
2
0
RB31-R3
1A-1B
4A-4B
200 bp
16569/0
191
16107
576
H
4A-4B
1A-1B
RB31-R3
LSP
DNA
RNA
L
CSB
C
Antisense Transcript Level
(Fold Increase)
25
20
15
10
5
0
TAF4
POLR2K
SP2
GPC1
MDM2
PCIF1
ATF1
SMARCA4
TNIK

Figure 1

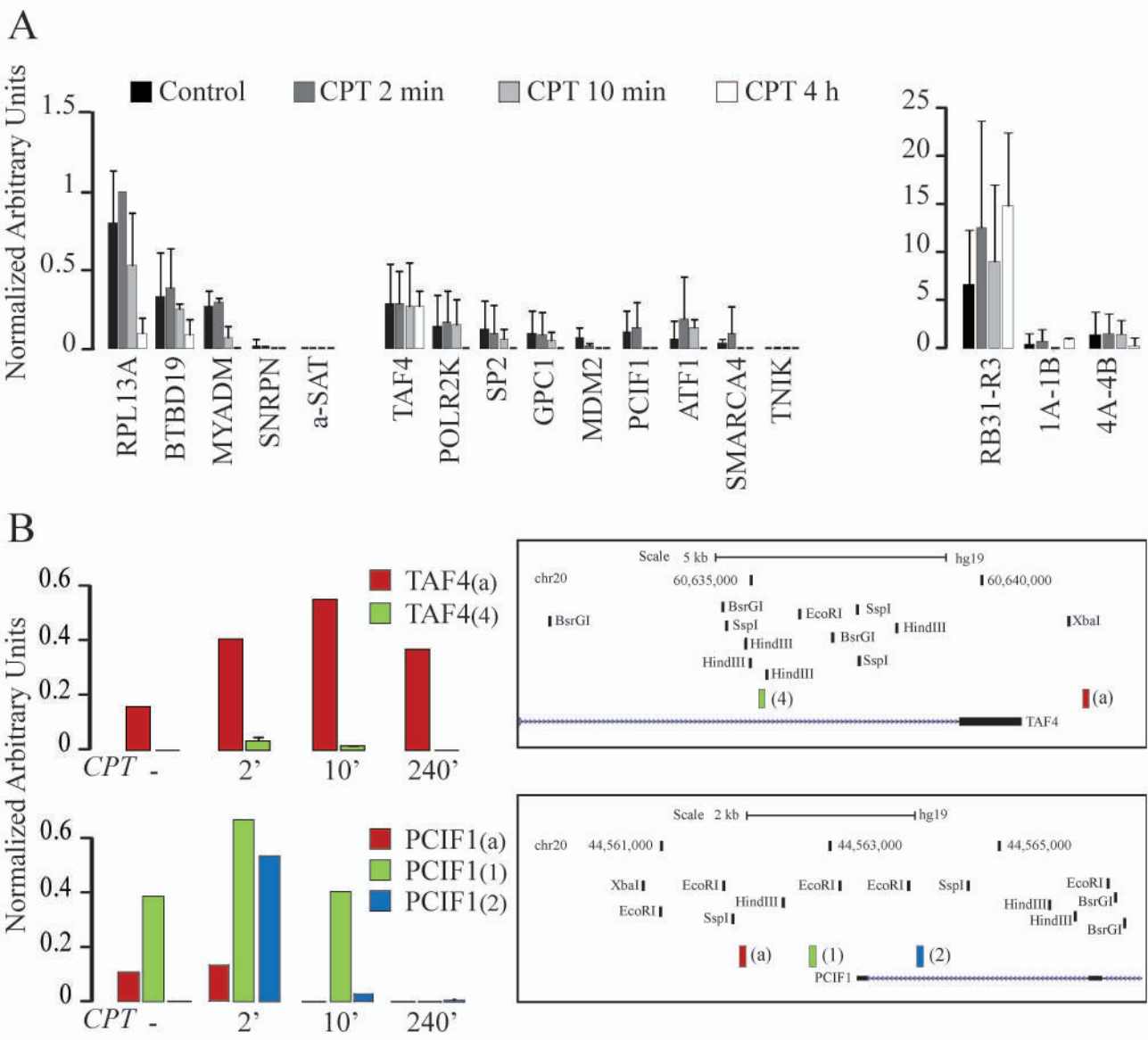
A
Normalized Arbitrary Units
Control
CPT 2 min
CPT 10 min
CPT 4 h
RPL13A
BTBD19
MYADM
SNRPN
a-SAT
TAF4
POLR2K
SP2
GPC1
MDM2
PCIF1
ATF1
SMARCA4
TNIK
RB31-R3
1A-1B
4A-4B
B
TAF4(a)
TAF4(4)
CPT -
2'
10'
240'
Scale 5 kb
hg19
chr20
60,635,000
60,640,000
BsrGI
SspI
EcoRI
HindIII
XbaI
(4)
(a)
TAF4
PCIF1(a)
PCIF1(1)
PCIF1(2)
Scale 2 kb
44,561,000
44,563,000
44,565,000
XbaI
EcoRI
HindIII
SspI
BsrGI
(a)
(1)
(2)
PCIF1

Figure 2

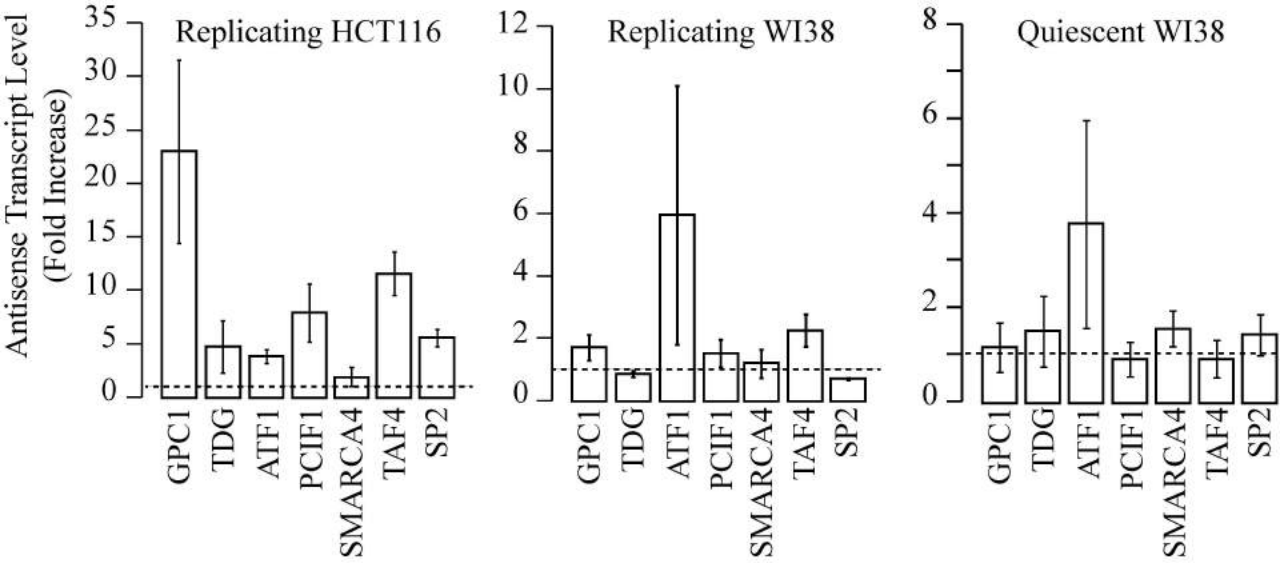
Antisense Transcript Level
(Fold Increase)
Replicating HCT116
Replicating WI38
Quiescent WI38
GPC1
TDG
ATF1
PCIF1
SMARCA4
TAF4
SP2

Figure 3

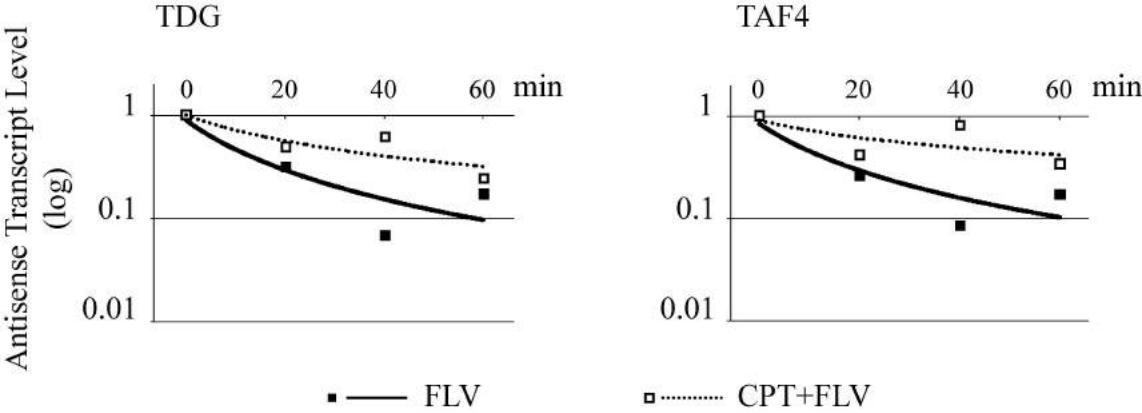
TDG
TAF4
Antisense Transcript Level (log)
0
20
40
60
min
1
0.1
0.01
FLV
CPT+FLV

Figure 4

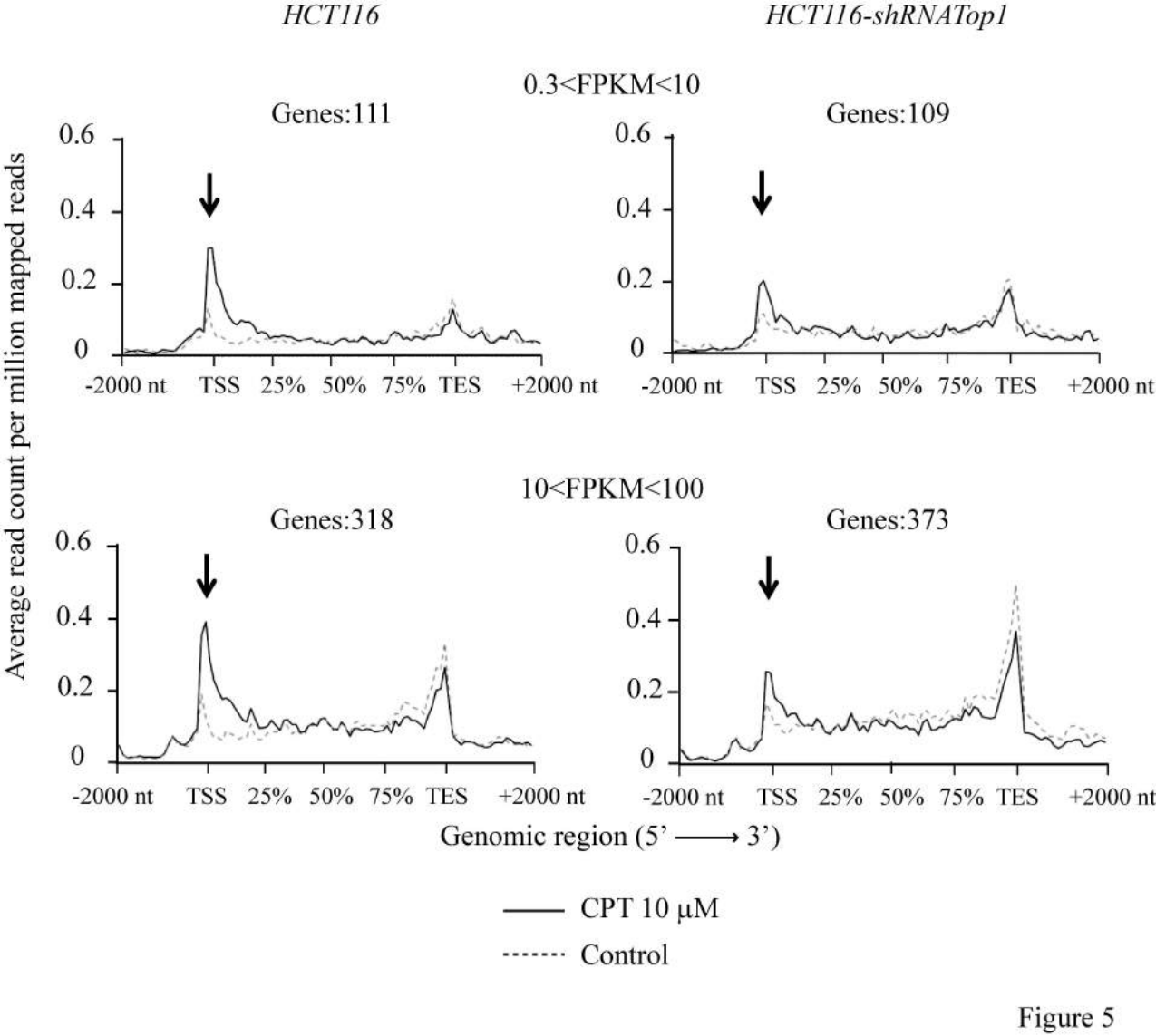
HCT116
HCT116-shRNATop1
0.3<FPKM<10
Genes:111
Genes:109
10<FPKM<100
Genes:318
Genes:373
Average read count per million mapped reads
0.6
0.4
0.2
0
-2000 nt
TSS
25%
50%
75%
TES
+2000 nt
Genomic region (5' ⟶ 3')
CPT 10 μM
Control

Figure 5

SUPPLEMENTARY INFORMATIONS

R-loop formation and accumulation of antisense and sense transcripts by camptothecin at active promoters.

Marinello Jessica, Bertoncini Stefania, Cristini Agnese, Malagoli Tagliazucchi Guidantonio, Forcato Mattia, Sordet Olivier and Capranico Giovanni

SUPPLEMENTARY FIGURES.

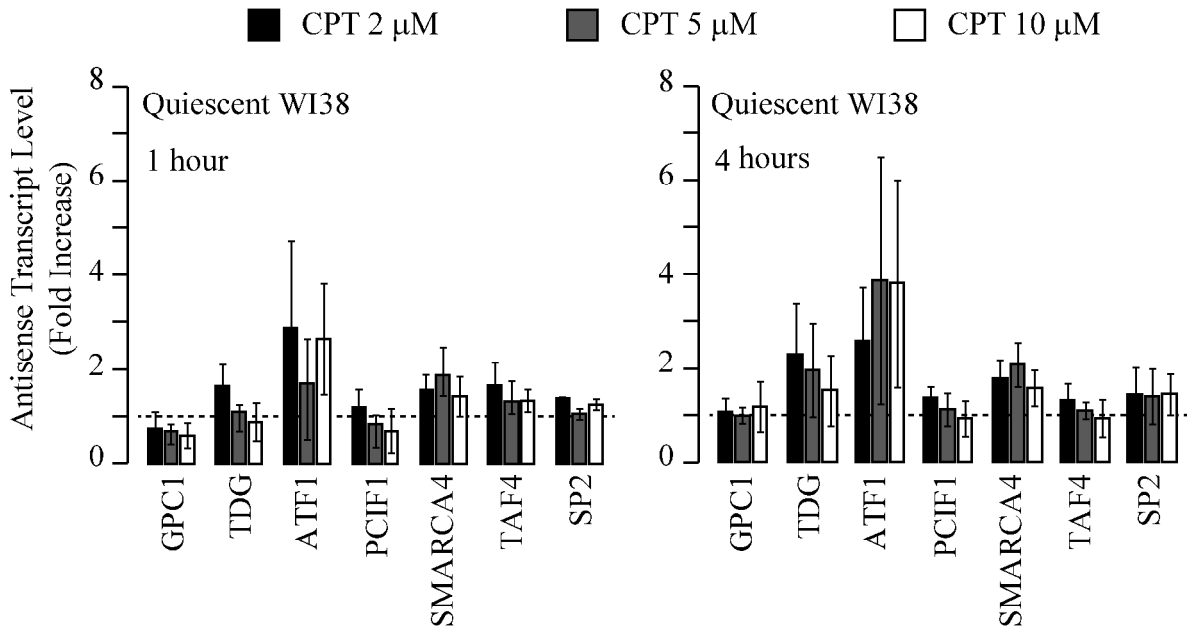

Supplementary Figure 1: Time course and dose response in quiescent WI38 cells. Promoter-associated antisense transcripts were evaluated by rtqPCR after 1 and 4 hours of CPT treatment at different doses (2, 5 and 10 μM). PCR determinations were normalized to cytochrome b mRNA and to untreated cells (dotted line). Values are means +/− SEM of at two determinations of at least two independent experiments.

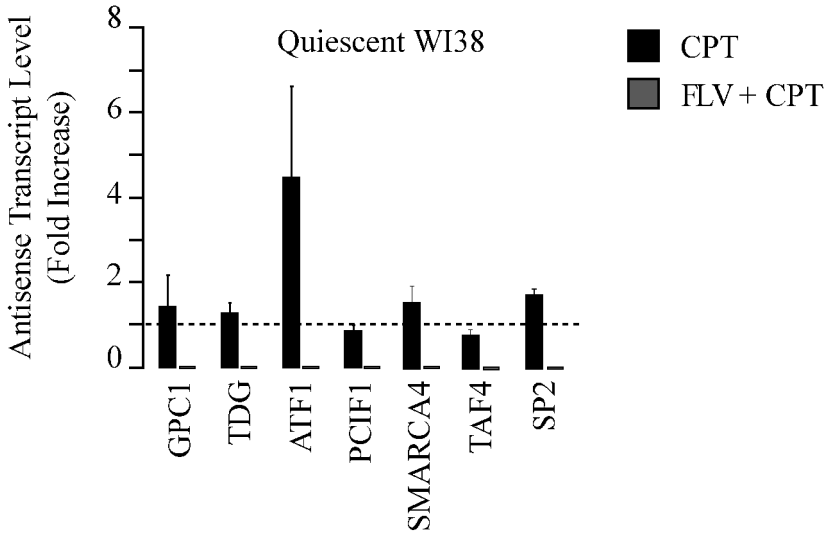

Supplementary Figure 2: Effect of FLV treatment on antisense transcription. Promoter-associated antisense transcripts were evaluated by rtqPCR after 4 hours of CPT treatment (10 μM) in presence of FLV (gray bars). PCR determinations were normalized to cytochrome b mRNA and to untreated cells (dotted line). Values are means +/− SEM of at two determinations of at least two independent experiments.

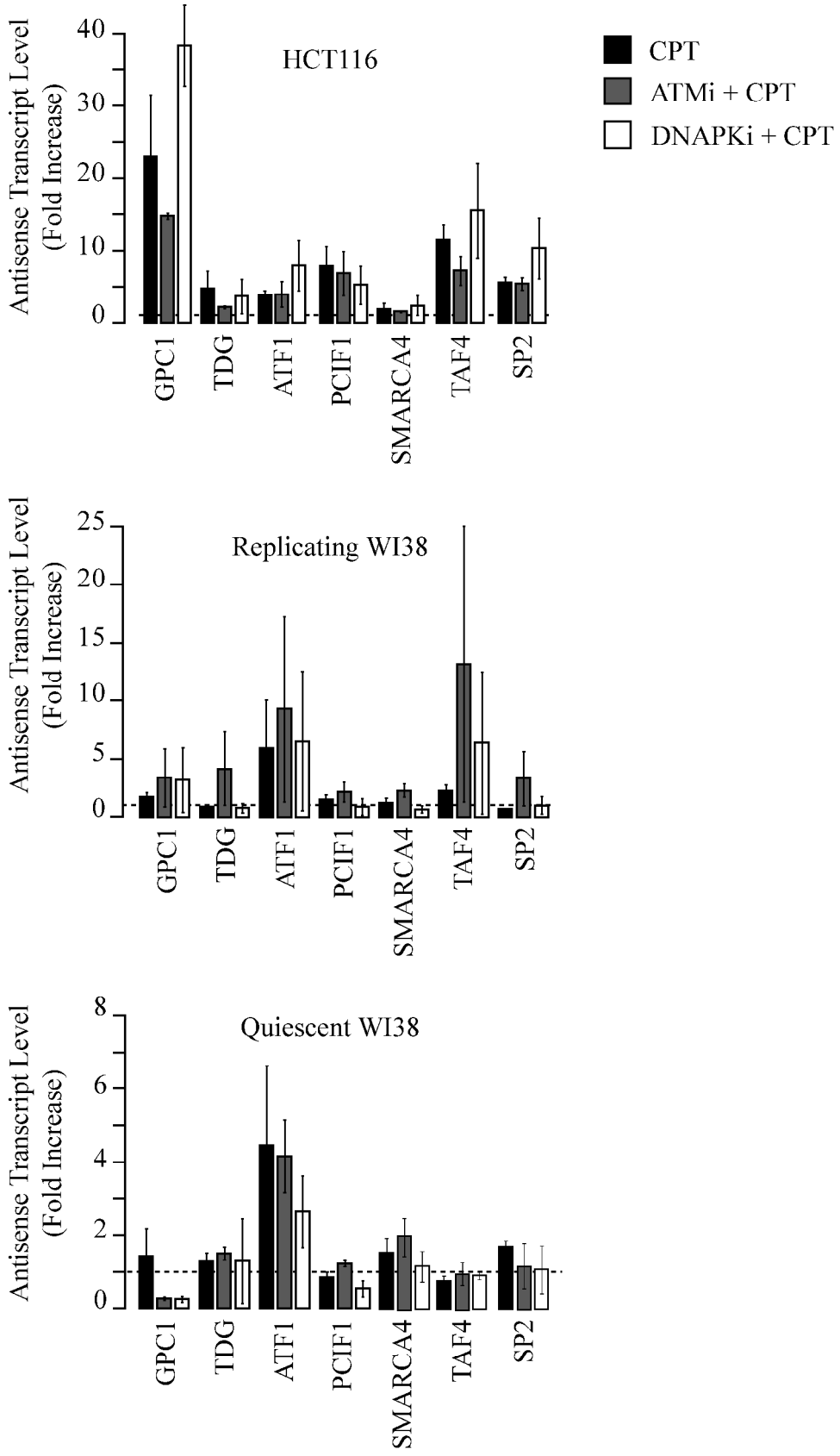

Supplementary Figure 3: DDR activation effect on antisense transcription. Promoter-associated antisense transcripts were evaluated by rtqPCR after 4 hours of CPT treatment (10 μM) in presence of ATM (gray bars) and DNAPK (white bars) inhibitors. PCR determinations were normalized to cytochrome b mRNA and to untreated cells (dotted line). Values are means +/− SEM of at two determinations of at least two independent experiments.

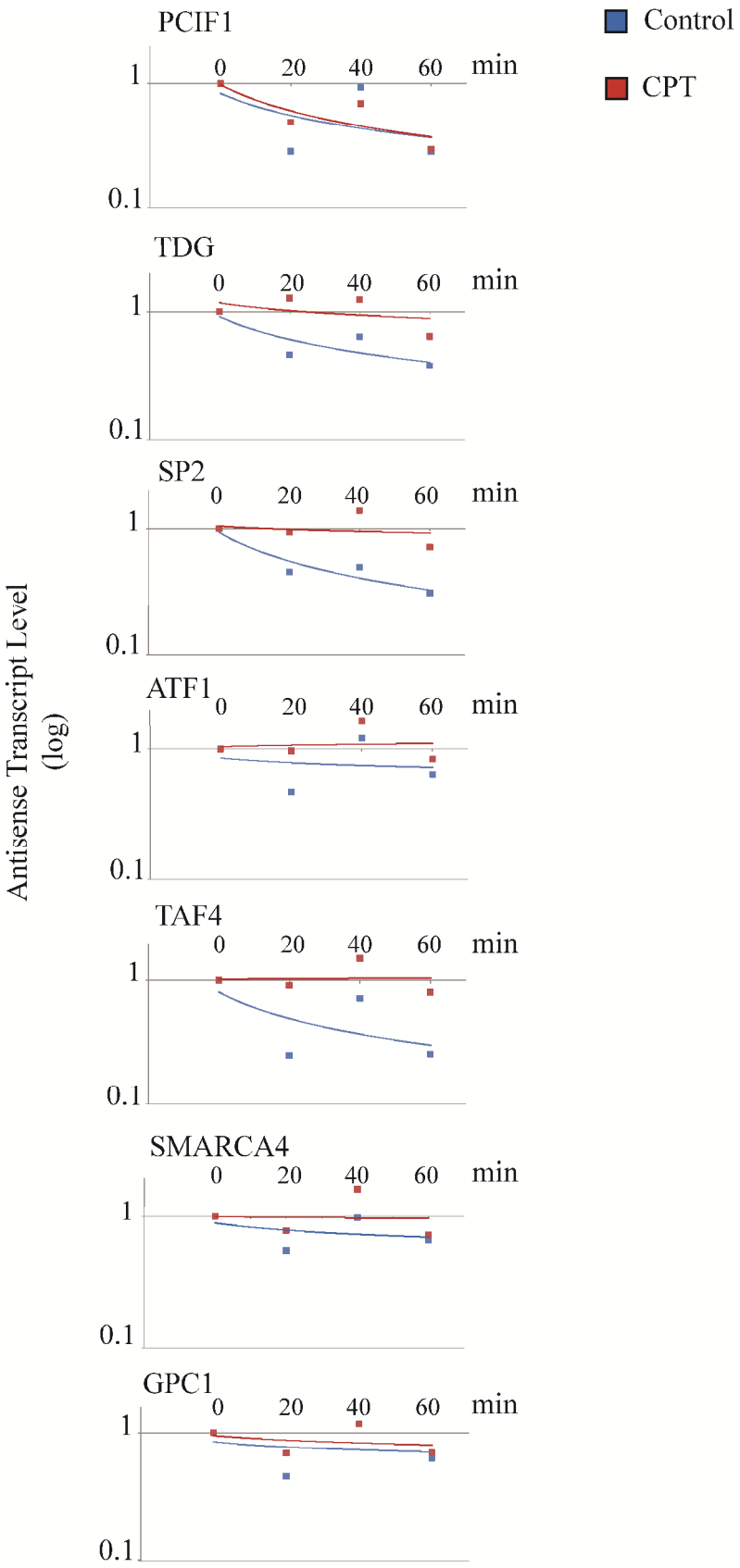

Supplementary Figure 4: Degradation rates of aRNAs. Cells where firstly stimulated for antisense accumulation by a 4 hours treatment with CPT. Then the drug was removed (blu lines) or maintained (red lines) for additional 60 minutes, and antisense transcript levels determined by rtqPCR. PCR determinations were normalized to cytochrome b mRNA and to aRNAs levels at time 0. A representative experiment is here reported.

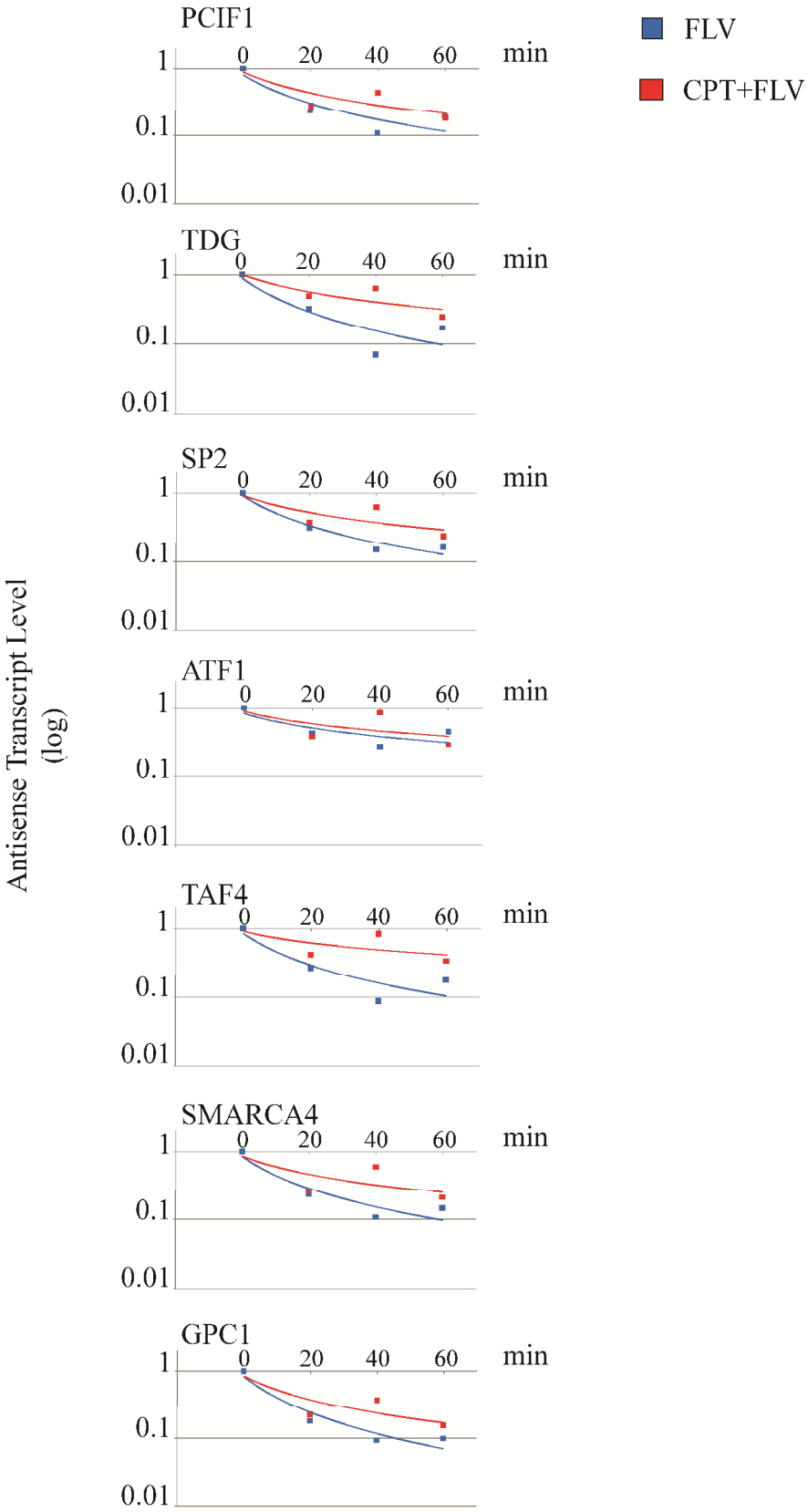

Supplementary Figure 5: Degradation rates of aRNAs. Cells where firstly stimulated for antisense accumulation by a 4 hours treatment with CPT. Then FLV was added to block transcription in absence (blu lines) and in presence (red lines) of CPT, and antisense transcript levels determined by rtqPCR after additional 20, 40 and 60 minutes. PCR determinations were normalized to cytochrome b mRNA and to aRNAs levels before FLV addition (time 0). A representative experiment is here reported.

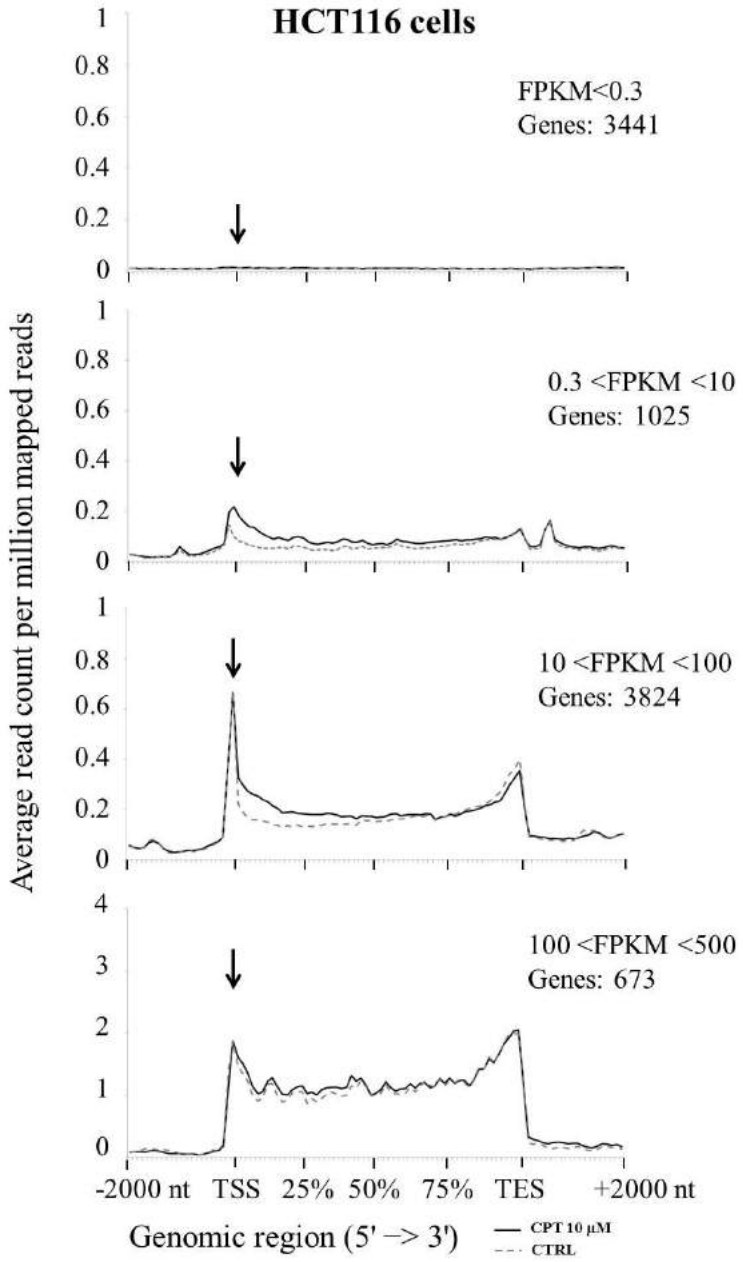

Supplementary Figure 6: Sense tags distribution, along non-overlapping Refseq genes of HCT116 cells, were analyzed in a region from 2000 bases upstream the TSS to 2000 bases downstream the TES using NGSplot software. Here are reported genes whose FPKM value is below 0,3 up to 500 divided in four groups. Control reads are reported in gray dotted line and CPT reads in black line. Black arrows indicate an accumulation or not of reads in the 5' region after CPT treatment (10 µM for 4h).

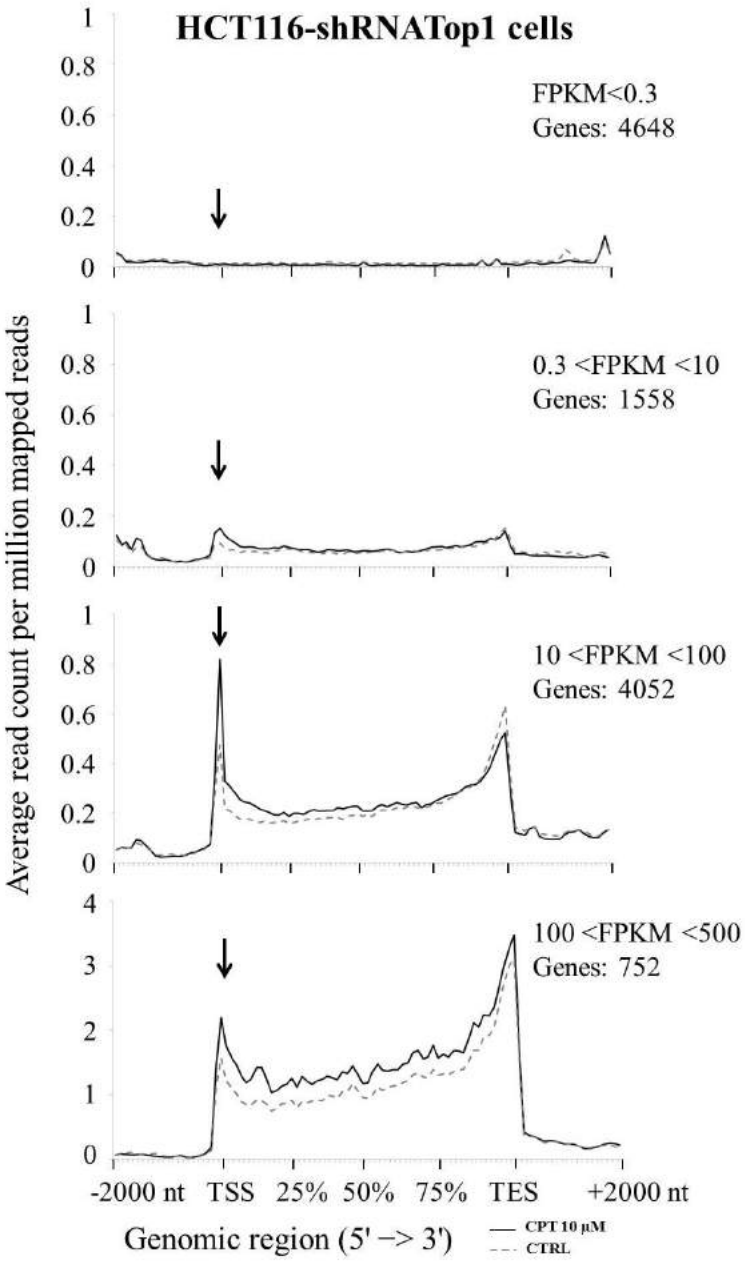

Supplementary Figure 7: Sense tags distribution, along non-overlapping Refseq genes of HCT116-shRNATop1 cells, were analyzed in a region from 2000 bases upstream the TSS to 2000 bases downstream the TES using NGSplot software. Here are reported genes whose FPKM value is below 0,3 up to 500 divided in four groups. Control reads are reported in gray dotted line and CPT reads in black line. Black arrows indicate an accumulation or not of reads in the 5' region after CPT treatment (10 µM for 4h).

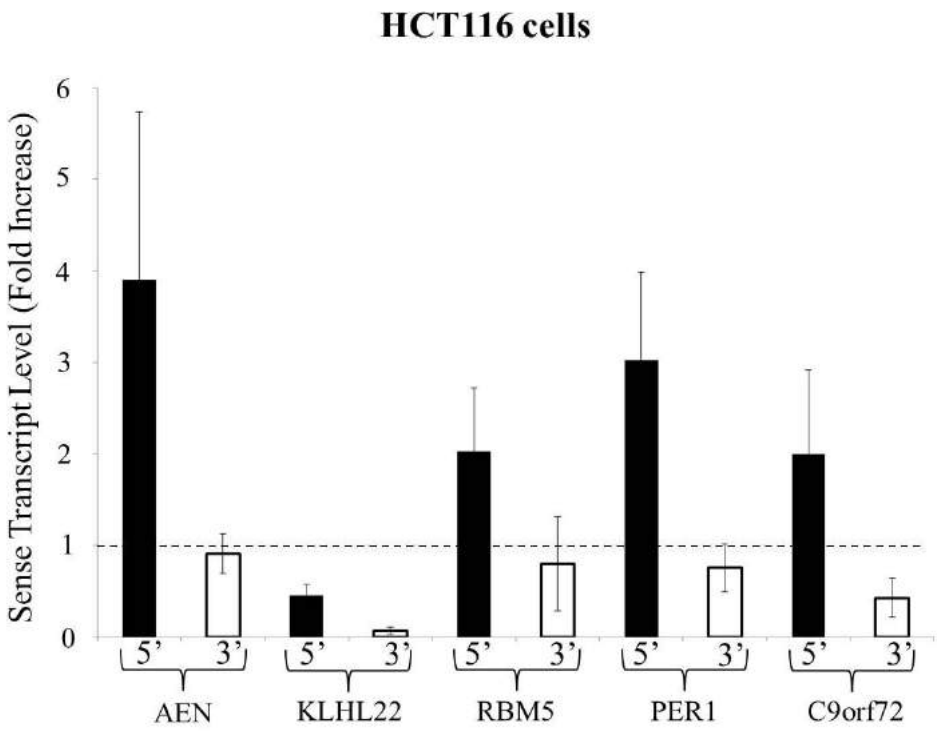

Supplementary Figure 8: The accumulation of sense transcripts in the 5' region and the reduction of sense transcripts in 3' region of selected genes were determined by rtPCR in the HCT116 cells and were evaluated after treatment of the indicated cell lines with CPT 10 µM for 4h. The selected genes showed a CPT-increased in the 5' region and a reduction in the 3' region tag clusters as determined with RNA-seq data, with the exception of KLHL22 gene that had a sense transcript reduced by CPT. PCR determinations were normalized to cytochrome b mRNA and to untreated cells (dotted line). Values are means ± SEM of at least four determinations of six independent experiments for each panel.

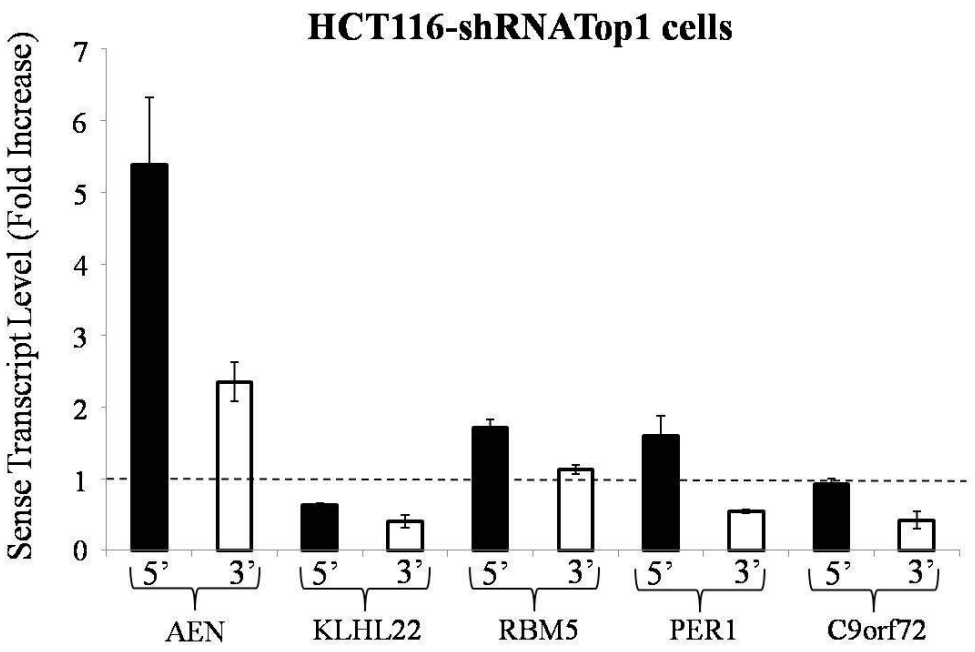

Supplementary Figure 9: The accumulation of sense transcripts in the 5' region and the reduction of sense transcripts in 3' region of selected genes were determined by rtPCR in the HCT116-shRNATop1 cells and were evaluated after treatment of the indicated cell line with CPT 10 µM for 4h. The selected genes showed a lower CPT-increased in the 5' region and a lower reduction in the 3' region tag clusters as determined with RNA-seq data, with the exception of AEN gene that had a higher sense transcript increased by CPT, taking into account the HCT116 cells line. PCR determinations were normalized to cytochrome b mRNA and to untreated cells (dotted line).Values are means ± SEM of at least four determinations of two independent experiments.

MCB Journals.ASM.org

RhoB Promotes γH2AX Dephosphorylation and DNA Double-Strand Break Repair

Kenza Mamouni,[a,b] Agnese Cristini,[a,b] Josée Guirouilh-Barbat,[c] Sylvie Monferran,[a,b] Anthony Lemarié,[a,b] Jean-Charles Faye,[a] Bernard S. Lopez,[c] Gilles Favre,[a,b] Olivier Sordet[a]

Cancer Research Center of Toulouse, INSERM UMR1037, Institut Claudius Regaud, Toulouse, France[a]; Université de Toulouse, Toulouse, France[b]; CNRS UMR8200, Institut de Cancérologie Gustave Roussy, Université Paris XI, Villejuif, France[c]

Unlike other Rho GTPases, RhoB is rapidly induced by DNA damage, and its expression level decreases during cancer progression. Because inefficient repair of DNA double-strand breaks (DSBs) can lead to cancer, we investigated whether camptothecin, an anticancer drug that produces DSBs, induces RhoB expression and examined its role in the camptothecin-induced DNA damage response. We show that in camptothecin-treated cells, DSBs induce RhoB expression by a mechanism that depends notably on Chk2 and its substrate HuR, which binds to RhoB mRNA and protects it against degradation. RhoB-deficient cells fail to dephosphorylate γH2AX following camptothecin removal and show reduced efficiency of DSB repair by homologous recombination. These cells also show decreased activity of protein phosphatase 2A (PP2A), a phosphatase for γH2AX and other DNA damage and repair proteins. Thus, we propose that DSBs activate a Chk2-HuR-RhoB pathway that promotes PP2A-mediated dephosphorylation of γH2AX and DSB repair. Finally, we show that RhoB-deficient cells accumulate endogenous γH2AX and chromosomal abnormalities, suggesting that RhoB loss increases DSB-mediated genomic instability and tumor progression.

RhoB is a small GTPase from the Rho family of proteins implicated in various intracellular functions, including actin cytoskeletal organization (1). Besides its well-established roles, RhoB emerged as an early DNA damage-inducible gene. RhoB is readily induced in response to various genotoxic agents, including UV and cisplatin (2, 3), although the molecular mechanisms of induction and functional relevance remain unclear. RhoB also differs from other Rho proteins, as it possesses tumor suppressor functions. The RhoB expression level decreases during the progression of various tumors, and loss of RhoB promotes cell proliferation, invasion, and metastasis (4–8).

DNA double-strand breaks (DSBs) are among the most severe lesions, and their inefficient repair can initiate genomic instability, ultimately leading to cancer (9–11). DSB repair requires the recruitment of DNA damage response (DDR) proteins in the vicinity of damaged chromatin (12). The serine/threonine kinases ATM, ATR, and DNA-dependent protein kinase (DNA-PK) are readily activated by DSBs and phosphorylate various DDR proteins, including histone H2AX and checkpoint kinase 2 (Chk2). Phosphorylation of these proteins is critical for efficient DDR and repair (10, 13). These phosphorylations are reversible and removed by specific serine/threonine phosphatases, including protein phosphatase 2A (PP2A), PP4, PP1, PP6, and Wip1 (14). Accumulating studies indicate that the timely dephosphorylation of DDR proteins is required for DSB repair (15–17).

Topoisomerase I (Top1) removes DNA torsional stress generated during replication and transcription. It relaxes DNA by producing transient Top1-DNA cleavage complexes (Top1cc), which are Top1-linked DNA single-strand breaks (18). The rapid resealing of Top1cc is inhibited by camptothecin (CPT) and its derivatives, which are used to treat cancers and which bind selectively at the Top1-DNA interface (18). Stabilized Top1cc interfere with the progression of replication and transcription complexes, which results in the production of DSBs (19–21). CPT is a sharp tool to dissect the cellular response to DSBs, as it has no other target besides Top1. CPT also has the advantage of trapping Top1cc reversibly. Indeed, Top1cc reverse fully within minutes after washing out CPT (18). Here we used CPT to determine whether DSBs induce RhoB and examined both the mechanisms of induction and its functional relevance.

MATERIALS AND METHODS

Drugs, chemical reagents, and cell culture. CPT, okadaic acid, fostriecin, and the DNA-PK inhibitor NU7026 were obtained from Sigma-Aldrich. Human osteosarcoma (U2OS) and colon carcinoma (HCT116 and HCT15) cells were obtained from the American Type Culture Collection (ATCC). HCT15 cells stably expressing wild-type Chk2 (Chk2-WT) or a kinase-dead Chk2 D347A mutant (Chk2-KD) were obtained from Yves Pommier (NIH, Bethesda, MD) (22, 23). WT and RhoB$^{-/-}$ E6-immortalized mouse embryonic fibroblast (MEF) cells were established in the laboratory from SV129 mice obtained from G. C. Prendergast (Lankenau Institute for Medical Research) by using a protocol described previously (24). WT and RhoB$^{-/-}$ primary mouse dermal fibroblast (MDF) cells were isolated from SKH1 mice (established in the laboratory from SV129 mice), as described previously (25), and cultured for a maximum of 9 passages. The subline RG37, containing the homologous recombination substrate (pDR-GFP), was made as described previously (26). The subline GC92, containing the nonhomologous end joining (NHEJ) substrate (pCOH-CD4), was made as described previously (27). All of the above-described cells were cultured in Dulbecco's modified Eagle's medium supplemented with 10% fetal bovine serum.

Western blotting. Whole-cell extracts were obtained by lysing cells in buffer (1% SDS, 10 mM Tris-HCl [pH 7.4]) supplemented with protease

Received 19 November 2013 Returned for modification 5 December 2013
Accepted 28 May 2014
Published ahead of print 9 June 2014
Address correspondence to Gilles Favre, favre.gilles@claudiusregaud.fr, or Olivier Sordet, olivier.sordet@inserm.fr.
G.F. and O.S. contributed equally to this work.

doi:10.1128/MCB.01525-13

(Complete; Roche Diagnostics) and phosphatase (Cocktail 3; Sigma-Aldrich) inhibitors. Viscosity of the samples was reduced by brief sonication, and proteins were separated by SDS-PAGE and immunoblotted with the following antibodies: anti-Chk2 (catalog number 2662; Cell Signaling), anti-Chk2-pS516 (catalog number 2669; Cell Signaling), anti-Chk2-pT68 (catalog number 2661; Cell Signaling), anti-H2AX (catalog number ab11175; Abcam), anti-γH2AX (catalog number 05-636; Millipore), anti-HuR (catalog number sc-5261; Santa Cruz), anti-PP2A(C) (catalog number 1512-1; Epitomics), anti-Rad51 (catalog number PC-130; Millipore), anti-RhoA (catalog number sc-418; Santa Cruz), anti-RhoB (catalog number sc-180; Santa Cruz), and anti-α-tubulin (catalog number T5168; Sigma-Aldrich). Immunoblotting was revealed by chemiluminescence using autoradiography or a ChemiDoc MP system (Bio-Rad). Quantification of protein levels was done by using ImageJ (version 1.40g) in Fig. 1E and 3F and with Image Lab software (version 4.1) in Fig. 3L and 5D.

RNA immunoprecipitation (RIP). Immunoprecipitation of HuR-associated RNAs was done as described previously (28), with minor modifications. Forty million cells were lysed for 30 min at 4°C in 750 μl buffer containing 25 mM Tris-HCl (pH 7.4), 150 mM KCl, 0.5% NP-40, 2 mM EDTA, 1 mM NaF, and 0.5 mM dithiothreitol (DTT), supplemented with 0.2 U RNasin (Promega) and protease inhibitors (Complete; Roche Diagnostics). After centrifugation at 10,000 × *g* for 10 min, supernatants were precleared for 30 min at 4°C with 20 μl of protein A/G-agarose beads (Sigma-Aldrich) previously blocked for 5 h at 4°C in washing buffer (300 mM KCl, 50 mM Tris-HCl [pH 7.4], 1 mM $MgCl_2$, 0.1% NP-40) containing 5 μg/μl yeast tRNA (Invitrogen), 1 μg/μl acetylated bovine serum albumin (BSA; Sigma-Aldrich), and protease inhibitors (Complete; Roche Diagnostics). Beads (20 μl) were coupled with 15 μg of mouse anti-HuR antibody (catalog number sc-5261; Santa Cruz) or 15 μg of mouse nonimmune antibody (control IgG) (catalog number 02-6502; Invitrogen) for 4 h at 4°C and incubated with 2 mg precleared cell lysate overnight at 4°C. After several washes in washing buffer and proteinase K (Roche Diagnostics) treatment, immunoprecipitated RNAs were extracted by using TRIzol LS reagent (Invitrogen) and treated with Turbo DNase (Ambion) before quantitative reverse transcription-PCR (RT-qPCR) experiments.

Quantitative reverse transcription-PCR. Total RNAs (MasterPure RNA purification kit; Epicentre) were subjected to RT by using the iScript cDNA synthesis kit (Bio-Rad). qPCR analyses were performed on a CFX96 real-time system device (Bio-Rad) by using IQ SYBR green Supermix (Bio-Rad) according to the manufacturer's instructions. All samples were analyzed in triplicate, and β-actin mRNA was used as an endogenous control in the $\Delta\Delta C_T$ analysis. The primer pairs used were *RhoA*-FW (5′-TGG AAG ATG GCA TAA CCT GTC-3′) and *RhoA*-RV (5′-AAC TGG TGG CTC CTC TGG-3′), *RhoB*-FW (5′-TTG TGC CTG TCC TAG AAG TG-3′) and *RhoB*-RV (5′-CAA GTG TGG TCA GAA TGC TAC-3′), *RhoC*-FW (5′-TGT CAT CCT CAT GTG CTT CTC-3′) and *RhoC*-RV (5′-GTG CTC GTC TTG CCT CAG-3′), *RhoE*-FW (5′-CCT GCT CCT CTC GCT CTC-3′) and *RhoE*-RV (5′-TCT GGC TGG CTC TTC TCT C-3′), and β-*actin*-FW (5′-TCC CTG GAG AGG AGC TAC GA-3′) and β-*actin*-RV (5′-AGG AAG GAA GGC TGG AAG AG-3′).

Cell transfection (siRNAs and plasmids). For cell transfection with small interfering RNAs (siRNAs), cells were transfected with HuR-, Rad51-, or RhoB-targeting siRNAs or nontargeting siRNAs (Eurogentec) by using Oligofectamine transfection reagent (Invitrogen) according to the manufacturer's protocol. Target DNA sequences were 5′-GAG GCA ATT ACC AGT TTC A-3′ for HuR, 5′-GAA GCT ATG TTC GCC ATT A-3′ for Rad51, 5′-GGC ATT CTC TAA AGC TAT G-3′ for siRNA RhoB#1, 5′-GTC CAA GAA ACT GAT GTT A-3′ for siRNA RhoB#2, 5′-GCT AAG ATG GTG TTA TTT A-3′ for siRNA RhoB#3, and 5′-GAC GTG GGA CTG AAG GGG T-3′ for nontargeting siRNA. Experiments were performed 48 h after transfection. siRNA RhoB#1 was used in Fig. 4B and G, siRNA RhoB#2 was used in Fig. 4B to E and G and 5D, and siRNA RhoB#3 was used in Fig. 3G and H. For cell transfection with plasmids, cells were transfected with a plasmid encoding hemagglutinin (HA)-RhoB (29) by using jetPEI DNA transfection reagent (Polyplus transfection) according to the manufacturer's protocol. Experiments were performed 24 h after transfection.

Neutral Comet assays. Neutral Comet assays were performed according to the manufacturer's instructions (Trevigen), except that electrophoresis was performed at 4°C. Comet tail moments were measured by using ImageJ (version 1.47v) using a macro provided by Robert Bagnell (https://www.med.unc.edu/microscopy/resources/imagej-plugins-and-macros/comet-assay).

DSB repair assays. RG37 and GC92 cells, for homologous recombination and end joining assays, respectively, were plated at 5×10^5 cells per well into six-well plates and transfected after 24 h with nontargeting or RhoB-targeting siRNAs. Forty-eight hours after siRNA transfection, cells were transfected with 1 μg of an I-SceI-encoding plasmid (pBASCe-ISceI) by using JetPEI reagent. Cells were collected 72 h later with phosphate-buffered saline (PBS)–50 mM EDTA and fixed in PBS–2% paraformaldehyde for 15 min at room temperature. Green fluorescent protein (GFP)-positive RG37 cells were detected by flow cytometry using a FACSCalibur instrument. For NHEJ assays, GC92 cells were incubated with PBS and 2% (wt/vol) BSA and then stained for 15 min with 1 μl of anti-CD4-phycoerythrin (PE) (Miltenyi Biotech) in PBS–1% (wt/vol) BSA. The cells were washed in PBS before fluorescence-activated cell sorter (FACS) analysis.

WST-1 cell viability assays. WT and $RhoB^{-/-}$ MEF cells were seeded in triplicate into 96-well microplates at a density of 1,000 cells per well. Twenty-four hours after plating, cells were treated with various concentrations of CPT (from 1.6 nM to 50 μM) and cultured for 72 h. The WST-1 reagent (Roche Diagnostics) was then applied for 1 h at 37°C. The formazan dye was quantified at 450 nm by using a plate reader (LabSystems Multiskan). Data are expressed as the percentage of cell survival (mean ± standard deviation [SD] of treated cells normalized to the mean ± SD of untreated cells, which was set to 100%).

Protein phosphatase 2A activity assays. Protein phosphatase 2A (PP2A) activity was assayed by using a PP2A immunoprecipitation phosphatase assay kit (Upstate) according to the manufacturer's protocol. Briefly, cells were lysed on ice in phosphatase extraction buffer (20 mM imidazole-HCl [pH 7.0], 2 mM EDTA, 2 mM EGTA) supplemented with a protease inhibitor cocktail (Sigma-Aldrich). The cell lysate (500 μg) was incubated for 2 h at 4°C with protein A-agarose beads coupled with 4 μg of mouse anti-PP2A(C) antibody (clone 1D6; Upstate) or mouse nonimmune antibody (control IgG) (catalog number 02-6502; Invitrogen). Phosphatase activity was assayed by incubating the immunoprecipitated proteins with the synthetic threonine phosphopeptide K-R-pT-I-R-R at 30°C for 10 min prior to detection with malachite green phosphate detection solution. After 15 min, free phosphate was quantified by measuring the absorbance at 620 nm in a microplate reader. Phosphatase activity was calculated by using a phosphate standard curve. All samples were analyzed in triplicate.

Detection of Top1-DNA cleavage complexes. Cellular Top1-DNA cleavage complexes (Top1cc) were detected as previously described (30), except that immunoblotting was revealed with a rabbit monoclonal anti-Top1 antibody from Abcam (ab109374) and by chemiluminescence using autoradiography or a ChemiDoc MP system (Bio-Rad). Quantification for Fig. 3L was performed by using Image Lab software (version 4.1).

Immunofluorescence microscopy. Immunofluorescence microscopy of γH2AX was performed, as described previously (20), with an anti-γH2AX antibody from Millipore (catalog number 05-636). Immunofluorescence microscopy of Rad51 was performed as described previously (31) by using an anti-Rad51 antibody from Millipore (catalog number PC-130), except that cells were fixed/permeabilized with ice-cold methanol for 15 min at 4°C and further permeabilized with 0.5% Triton X-100 for 5 min at room temperature. Slides were visualized by using a fluorescence microscope (Eclipse 90i; Nikon), and pictures were analyzed with Photoshop CS3 (Adobe).

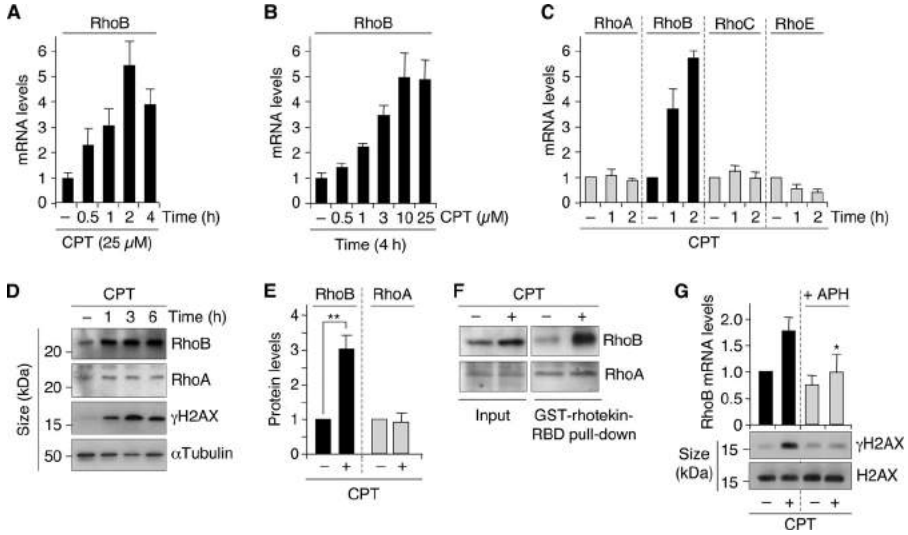

FIG 1 Rapid and selective increase of RhoB by CPT-induced DSBs. (A and B) RhoB mRNA was analyzed by RT-qPCR in cells treated for the indicated times with 25 μM CPT (U2OS cells) (A) and with the indicated CPT concentrations for 4 h (HCT15/Chk2-WT cells) (B). Data shown are means ± SD for triplicate samples. (C) The indicated transcripts were analyzed by RT-qPCR in U2OS cells treated with 25 μM CPT (means ± SD for three independent experiments). (D) Western blotting of RhoB, RhoA, and γH2AX in U2OS cells treated with 25 μM CPT. α-Tubulin was the loading control. (E) Quantification of RhoB and RhoA protein levels by Western blotting in U2OS cells treated with CPT (25 μM for 4.5 h). Data shown are the means ± SD for three independent experiments. **, $P < 0.01$ by *t* test. (F) Active (GTP-bound) Rho proteins were pulled down with GST-rhotekin-RBD (Rho binding domain) beads in extracts from U2OS cells treated with 25 μM CPT for 4 h. The active forms of RhoB and RhoA were detected by Western blotting with antibodies against RhoB and RhoA, respectively. Total RhoB and RhoA protein levels were examined in the extracts before pulldown (input). (G) HCT15/Chk2-WT cells were treated with the replication inhibitor aphidicolin (APH) (1 μM for 15 min) before the addition of CPT (1 μM for 2 h). (Top) RT-qPCR analysis of RhoB mRNA. Data shown are means ± SD for three independent experiments. The asterisk denotes a significant difference from CPT-treated cells without APH ($P < 0.05$ by *t* test). (Bottom) Western blotting of γH2AX and H2AX.

DNA extraction and comparative genomic hybridization (CGH) arrays. Genomic DNA was extracted from WT and RhoB$^{-/-}$ primary MDF cells by using the QIAamp DNA kit (Qiagen). DNA from WT and RhoB$^{-/-}$ cells was labeled with Cy3 and Cy5 (Dual color labeling kit; Roche-Nimblegen), respectively, before hybridization on 720K whole-genome tiling arrays (Roche-Nimblegen). Slides were scanned by using the MS200 scanner (Tecan), and images were analyzed by using DEVA 2.1 software (Roche-Nimblegen) with segmentation and background correction. Amplification and deletion were considered significant events when at least 5 consecutive probes had a $\log_2$ value of ≥0.3 (amplification) or a $\log_2$ value of ≤−0.4 (deletion). We determined the genomic instability index with the formula (number of deletions + number of amplifications)^2/number of altered chromosomes, as previously described (32). Sexual chromosomes were excluded from the analysis.

RhoB and RhoA activity assays. The Rho binding domain (RBD) of rhotekin, an effector of Rho proteins that selectively binds to the GTP-loaded form, was expressed as a recombinant fusion with glutathione *S*-transferase (GST) in *Escherichia coli* and purified through binding to glutathione (GSH)-Sepharose beads. Cells (8×10^6) were lysed on ice in 800 μl lysis buffer (50 mM Tris-HCl [pH 7.5], 500 mM NaCl, 10 mM $MgCl_2$, 1% Triton X-100, 10 mM DTT) supplemented with a protease inhibitor cocktail (Sigma-Aldrich) and phosphatase inhibitors (Halt phosphatase inhibitor cocktail; Thermo Scientific). GST-RBD beads (30 μl) were incubated with the cell lysate for 30 min at 4°C. An aliquot from each lysate was removed as a control for equivalent input for the assay. After three washes in ice-cold washing buffer (50 mM Tris-HCl [pH 7.5], 500 mM NaCl, 10 mM $MgCl_2$, 1% Triton X-100), bound Rho proteins were eluted from the beads with SDS-PAGE sample buffer at 95°C and analyzed by Western blotting with anti-RhoB (catalog number sc-180; Santa Cruz) or anti-RhoA (catalog number sc-418; Santa Cruz) antibodies.

RhoB promoter activity. U2OS cells were cotransfected with a plasmid encoding the RhoB promoter linked to the firefly luciferase reporter gene and a plasmid encoding the cytomegalovirus (CMV) promoter linked to the *Renilla* luciferase reporter gene (internal control), as described previously (2). Luciferase activities were measured 48 h after transfection by using the Dual Luciferase assay system (Promega), and results were expressed as the ratio of the activity of the firefly luciferase to the activity of the *Renilla* luciferase.

BrdU incorporation assays. Cells were incubated with 30 μM bromodeoxyuridine (BrdU; Sigma-Aldrich) for 30 min and labeled with anti-BrdU antibody according to the manufacturer's protocol (clone B44; BD Biosciences). Cells were analyzed on a Becton, Dickinson FACScan flow cytometer (BD Biosciences).

RESULTS

RhoB is rapidly and selectively induced in response to DSBs. Exposure of human cancer cells to 25 μM CPT revealed a 2-fold increase of the RhoB mRNA level within 30 min (Fig. 1A). At this CPT concentration, the levels of RhoB mRNA reached a maximum 5-fold increase after 2 h (Fig. 1A). To investigate whether the induction of RhoB mRNA was dose dependent, cells were treated for 4 h with increasing CPT concentrations. RhoB induction was clearly detected at 1 μM and increased with increasing CPT concentrations (Fig. 1B). In contrast, the two RhoB homologs RhoA and RhoC were not induced after short exposures to CPT (Fig. 1C). RhoE, another member of the Rho family, has been identified as a p53-inducible gene in response to genotoxic agents (33). The authors of that study focused on upregulation of RhoE mRNA after long exposures to genotoxic agents, typically 12 h or longer. Figure 1C shows no increase in the RhoE mRNA level after short exposures to CPT in p53 wild-type U2OS cells under conditions where RhoB mRNA levels reached a maximum increase.

The increase in the RhoB mRNA level was associated with an increase in the RhoB protein level that was detectable 1 h after CPT

treatment (Fig. 1D and E). Pulldown of active (GTP-bound) Rho proteins followed by immunoblotting with an anti-RhoB antibody indicated that CPT induced both total and active RhoB proteins (Fig. 1F), although it is still unclear whether these two events are connected. Under these conditions, the levels of total and active RhoA remained unchanged (Fig. 1D to F), which is consistent with the lack of induction of RhoA mRNA after CPT treatment (Fig. 1C).

Because DSBs are readily produced in CPT-treated cells (18), we tested whether they could be the initiating events for RhoB induction. Figure 1D shows that the increase in the level of RhoB protein coincided with the phosphorylation of H2AX at Ser139 (referred to as γH2AX), a marker for DSBs (9). To assess more directly the role of DSBs, we prevented their production in CPT-treated cells. DSBs are primarily produced during DNA replication at low concentrations (≤1 μM) of CPT (18). As expected (19), inhibition of replication with aphidicolin prevented the induction of γH2AX in response to CPT (Fig. 1G, bottom). Under these conditions, aphidicolin also prevented the induction of RhoB mRNA (Fig. 1G, top). These results suggest that DSBs promote RhoB upregulation.

Although RhoB can be induced in cells undergoing apoptosis (34), it is unlikely that the early increase in the level of RhoB induced by CPT resulted from the activation of apoptotic pathways. The increase of the RhoB level preceded the caspase-dependent cleavage of poly(ADP-ribose) polymerase (PARP) by several hours and was not prevented by the pancaspase inhibitor benzyloxycarbonyl-Val-Ala-DL-Asp(OMe)-fluoromethyl ketone (zVAD-fmk) (data not shown). Together, these results indicate that RhoB is induced rapidly and selectively in response to CPT-induced DSBs prior to and independently of apoptosis.

HuR-dependent stabilization of RhoB mRNA in CPT-treated cells. Increases of both transcription and transcript stability have been involved in the upregulation of RhoB mRNA in UV-exposed cells (2, 35). To examine RhoB transcription, we linked its promoter to a luciferase reporter gene. Figure 2A shows that CPT did not increase luciferase activity in cells transfected with this construct, indicating that transcription is unlikely to account for the upregulation of RhoB mRNA. Next, we compared the stability of RhoB mRNA between untreated and CPT-treated cells. Experiments performed in the presence of the transcription inhibitor flavopiridol revealed that the half-life of RhoB mRNA was greatly prolonged in CPT-treated cells (Fig. 2B).

The RNA binding protein HuR is known to bind to and stabilize target mRNAs (36). RhoB mRNA contains a HuR binding site in its 3′ untranslated region (UTR) (28), and a constitutive HuR-RhoB mRNA interaction has been found by RNA immunoprecipitation coupled with microarray analyses (RIP-chip) (37, 38). To test the potential role of HuR in the enhanced stability of RhoB mRNA, we tested whether HuR inhibition affected CPT-induced RhoB mRNA. Figure 2C shows that siRNA-mediated depletion of HuR decreased the induction of RhoB mRNA. To further implicate HuR, we examined its binding to RhoB mRNA by RIP experiments. Endogenous HuR was immunoprecipitated, and the levels of coimmunoprecipitated RhoB mRNA were analyzed by RT-qPCR. In untreated cells, RhoB transcripts were enriched in HuR immunoprecipitates compared with those in control IgG immunoprecipitates (Fig. 2D), indicating that HuR binds to RhoB mRNA under normal conditions, as expected (37, 38). Cellular exposure to CPT resulted in a further enrichment of RhoB mRNA in HuR immunoprecipitates, which was detected within 30 min and increased with the time of CPT exposure (Fig. 2D). A similar increase in HuR-RhoB mRNA interactions has been observed after short exposures to UV (35), suggesting that HuR-dependent stabilization of RhoB mRNA is a common mechanism for the early induction of RhoB by genotoxic agents.

Chk2-dependent HuR-RhoB mRNA interaction in response to DSBs. Chk2 is a serine/threonine kinase readily activated by DSBs (39). Active Chk2 phosphorylates HuR with RNA recognition motifs and modulates HuR binding to target mRNAs (37, 40–42). As expected (43), CPT induced rapid phosphorylation of Chk2 at Thr68 (Fig. 2E), which reflects its activation (44). Chk2 Thr68 phosphorylation was detected 30 min after CPT treatment (Fig. 2E) and coincided with the increased association of HuR with RhoB mRNA (Fig. 2D).

To assess directly the involvement of Chk2, we used HCT15 cells (Chk2 deficient) stably expressing wild-type Chk2 (Chk2-WT) or kinase-dead Chk2 (Chk2-KD). The levels of HuR protein were comparable in Chk2-WT and Chk2-KD cells and were unaffected by CPT treatment (Fig. 2H). Figure 2F shows that HuR binding to RhoB mRNA was reduced in Chk2-KD cells compared to Chk2-WT cells in response to CPT. These results led us to test whether the level of CPT-induced RhoB was also reduced in Chk2-KD cells. The induction of RhoB mRNA (Fig. 2G) and protein (Fig. 2H) was defective in Chk2-KD cells treated with CPT. As a control, parental HCT15 cells (Chk2 deficient) exhibited a similar induction defect in RhoB mRNA (data not shown) as that of Chk2-KD cells (Fig. 2G). Both WT and Chk2-KD cells showed identical induction of γH2AX in response to CPT (Fig. 2H), indicating that the defective response of Chk2-KD cells is not caused by a decreased amount of DSBs.

RhoB facilitates γH2AX dephosphorylation in CPT-treated cells. To assess the potential role of RhoB in the cellular response to CPT, we compared survival of WT and RhoB-deficient ($RhoB^{-/-}$) E6-immortalized MEF cells after CPT treatment. Cells were treated with increasing concentrations of CPT, and CPT sensitivity was assessed by WST-1 survival assays. Figure 3A shows that $RhoB^{-/-}$ cells are more sensitive to CPT than are WT cells, indicating that RhoB participates in the cellular response to CPT.

Because the cytotoxicity of CPT depends on Top1-linked DNA single-strand break (Top1cc)-induced DSBs (18), we analyzed the influence of RhoB on both the formation of Top1cc and the production of DSBs. Primary cells (WT and $RhoB^{-/-}$) were used, as they normally have low background levels of γH2AX (45). Our results indicated that CPT-induced Top1cc (Fig. 3B) and γH2AX (Fig. 3C) levels were similar in WT and $RhoB^{-/-}$ cells.

We therefore hypothesized that the hypersensitivity of $RhoB^{-/-}$ cells could instead result from a defect in the repair of these DSBs. To determine the kinetics of DSB repair, we analyzed the kinetics of γH2AX dephosphorylation (45). WT and $RhoB^{-/-}$ cells were exposed to CPT for 1 h and washed, and γH2AX dephosphorylation was monitored post-CPT treatment (release) (Fig. 3D). Unlike continuous exposure to CPT, this protocol allows the study of DSB repair, as Top1cc reverse fully within minutes after washing out CPT (18), and DSBs are then no longer produced. After termination of the CPT treatment, γH2AX levels decreased by approximately 70% within 7 h in WT cells (Fig. 3E and F), which is consistent with the kinetics and magnitude of γH2AX focus loss after exposure to ionizing radiation (46). Under these conditions, γH2AX levels were not significantly reduced in

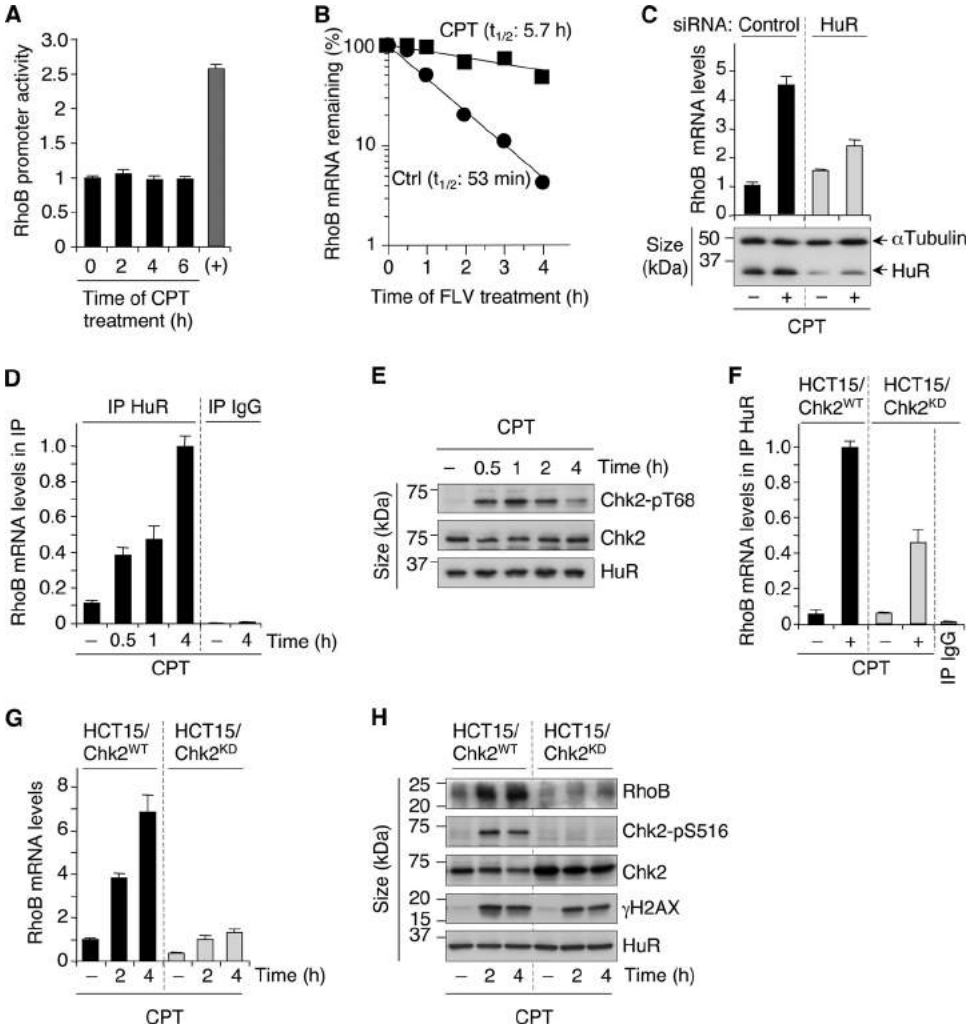

FIG 2 Chk2- and HuR-dependent stabilization of RhoB mRNA in response to CPT. (A) RhoB promoter activity was determined after transfection of U2OS cells with a RhoB promoter-luciferase reporter gene construct before treatment with 25 μM CPT. Data shown are means ± SD for three independent experiments. The positive control (+) was cells treated with trichostatin A (1 μM for 15 h). (B) U2OS cells were left untreated (Ctrl) or were treated with CPT (25 μM for 2 h) before the addition of the transcription inhibitor flavopiridol (FLV) (1 μM). RhoB mRNA was analyzed by RT-qPCR and normalized to the level at the time of flavopiridol addition, which was set to 100% (averages of data from two independent experiments). The half-life ($t_{1/2}$) of RhoB mRNA is indicated. (C) HCT116 cells were transfected with HuR-targeting or nontargeting (control) siRNAs before treatment with CPT (25 μM for 6 h). (Top) RT-qPCR analysis of RhoB mRNA (means ± SD for triplicate samples). (Bottom) Western blotting showing the efficiency of HuR silencing. α-Tubulin was the loading control. (D) Increased HuR-RhoB mRNA interaction upon CPT treatment. HuR was immunoprecipitated (IP) from HCT15/Chk2-WT cells treated with 25 μM CPT. The control was immunoprecipitation with nonimmune IgG. Coimmunoprecipitated RhoB mRNA was analyzed by RT-qPCR relative to β-actin mRNA levels in the input samples (means ± SD for triplicate samples). (E) Phosphorylation of Chk2 on Thr68 was examined by Western blotting in HCT15/Chk2-WT cells treated with 25 μM CPT. Chk2 and HuR were examined in parallel. (F) Chk2-dependent binding of HuR to RhoB mRNA. HCT15/Chk2-WT and HCT15/Chk2-KD cells were treated with 25 μM CPT for 4 h, and RhoB mRNA was analyzed in HuR immunoprecipitations, as described above for panel D. (G and H) HCT15/Chk2-WT and HCT15/Chk2-KD cells were treated with 25 μM CPT. (G) RhoB mRNA was analyzed by RT-qPCR (means ± SD for triplicate samples). (H) Western blotting of the indicated proteins. Phosphorylation of Chk2 on Ser516, which is an autophosphorylation site in response to DNA damage (64), was used to control Chk2 kinase activity in cells expressing WT or kinase-dead Chk2.

RhoB$^{-/-}$ cells (Fig. 3E and F). Immunofluorescence microscopy confirmed the pronounced defect of γH2AX dephosphorylation in RhoB$^{-/-}$ cells after removal of CPT (data not shown). In addition, siRNA-mediated depletion of RhoB in human HCT116 cells (Fig. 3G) also resulted in a marked reduction of γH2AX dephosphorylation after removal of CPT (Fig. 3H). Neutral Comet assays confirmed that the persistence of γH2AX in RhoB-deficient cells post-CPT treatment corresponded to unrepaired DSBs (Fig. 3I and J). Analysis of endogenous Top1cc showed that they reversed efficiently in both WT and RhoB$^{-/-}$ cells after removal of CPT (Fig. 3K and L). Thus, it is unlikely that the persistent γH2AX signal in RhoB$^{-/-}$ cells resulted simply from the further production of DSBs after termination of the CPT treatment. These results indicate that RhoB promotes γH2AX dephosphorylation and DSB repair.

RhoB promotes DSB repair by homologous recombination. Homologous recombination and nonhomologous end joining (NHEJ) are the prevalent pathways for the repair of DSBs (47). To assess directly the involvement of RhoB in DSB repair, we used human RG37 fibroblast cells that contain a single chromosomally

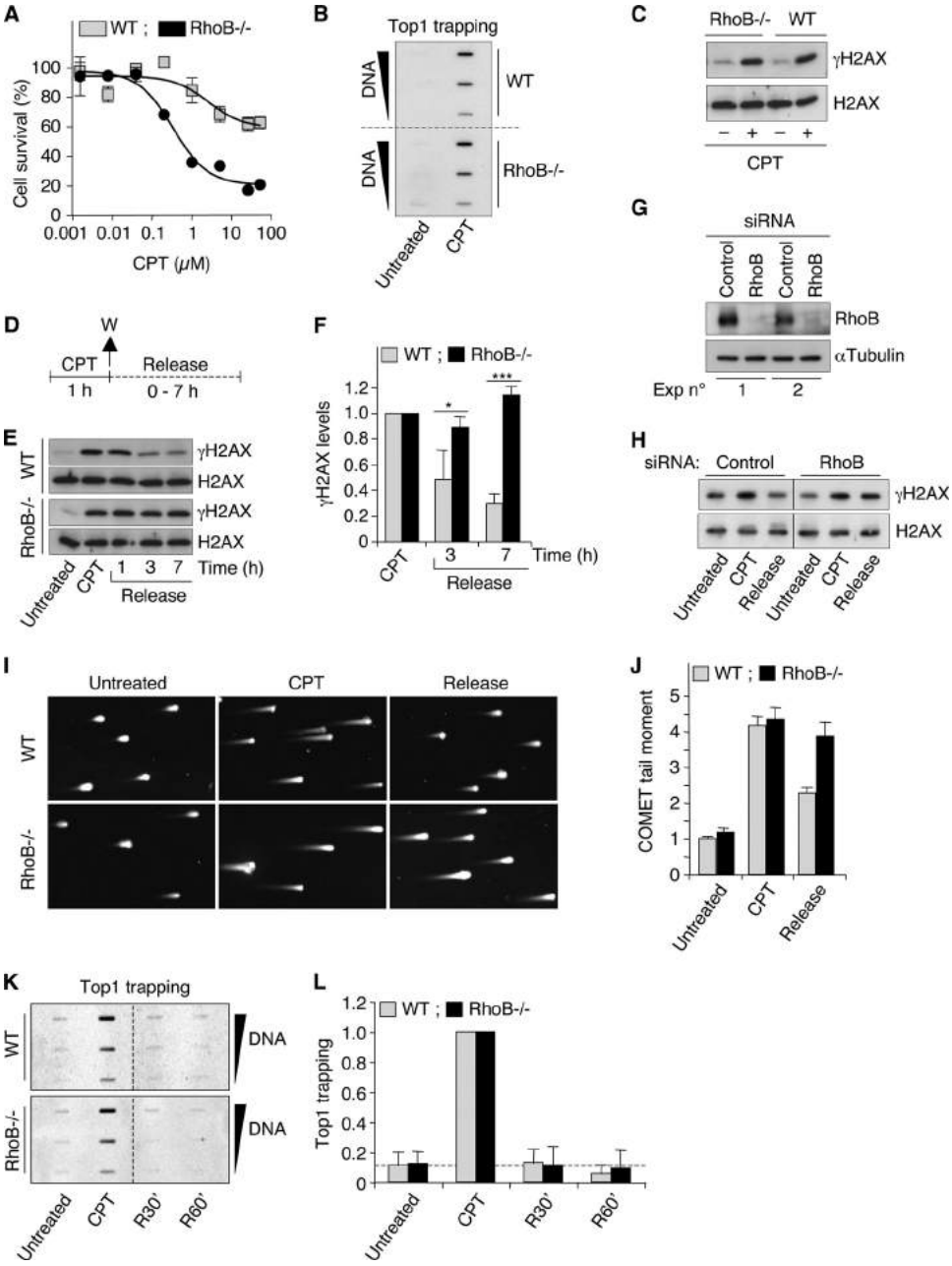

FIG 3 RhoB-deficient cells are defective for γH2AX dephosphorylation after CPT removal. (A) WT and RhoB$^{-/-}$ MEF cells were treated with the indicated concentrations of CPT for 72 h, and cell survival was analyzed by a WST-1 assay (means ± SD for triplicate samples). (B) Detection of Top1-DNA cleavage complexes (Top1cc) in WT and RhoB$^{-/-}$ primary mouse dermal fibroblast (MDF) cells treated with CPT (25 μM for 1 h). Different amounts of genomic DNA (5, 2.5, and 1.25 μg) were probed with an anti-Top1 antibody. (C) Western blotting of γH2AX and H2AX in WT and RhoB$^{-/-}$ primary MDF cells treated with CPT (25 μM for 1 h). (D) Cell treatment protocol for the study of γH2AX dephosphorylation (E to H), DSB repair (I and J), and Top1cc reversal (K and L) in response to CPT. Cells were treated with CPT for 1 h and washed (W) and cultured in CPT-free medium (release) for the indicated times. (E and F) Western blotting of γH2AX and H2AX in WT and RhoB$^{-/-}$ primary MDF cells (CPT, 25 μM). (E) Representative experiment. (F) Quantification of γH2AX protein levels (means ± SD for three independent experiments). *, $P < 0.05$; ***, $P < 0.001$ (by t test). (G and H) HCT116 cells were transfected with RhoB-targeting or nontargeting (control) siRNAs. (G) Western blotting showing the efficiency of RhoB silencing in two independent experiments. α-Tubulin was the loading control. (H) Western blotting of γH2AX and H2AX (CPT, 1 μM; release, 6 h). Lines indicate that intervening wells have been spliced out. (I and J) Detection of DSBs by a neutral Comet assay in WT and RhoB$^{-/-}$ primary MDF cells (CPT, 25 μM; release, 1 h). (I) Representative pictures of nuclei. (J) Quantification of Comet tail moment (averages ± standard errors of the means). Sixty cells were examined per group. (K and L) Detection of Top1cc in MEF cells treated with 25 μM CPT for 1 h. R30′ and R60′ indicate cells harvested 30 and 60 min after CPT removal, respectively. Different amounts of genomic DNA (5, 2.5, and 1.25 μg) were probed with an anti-Top1 antibody. (K) Representative experiment. Dashed lines indicate where panels have been reorganized to facilitate reading. (L) Quantification of Top1cc normalized to values for CPT-treated cells (means ± SD for three independent experiments). The dashed line indicates Top1cc levels in WT untreated cells.

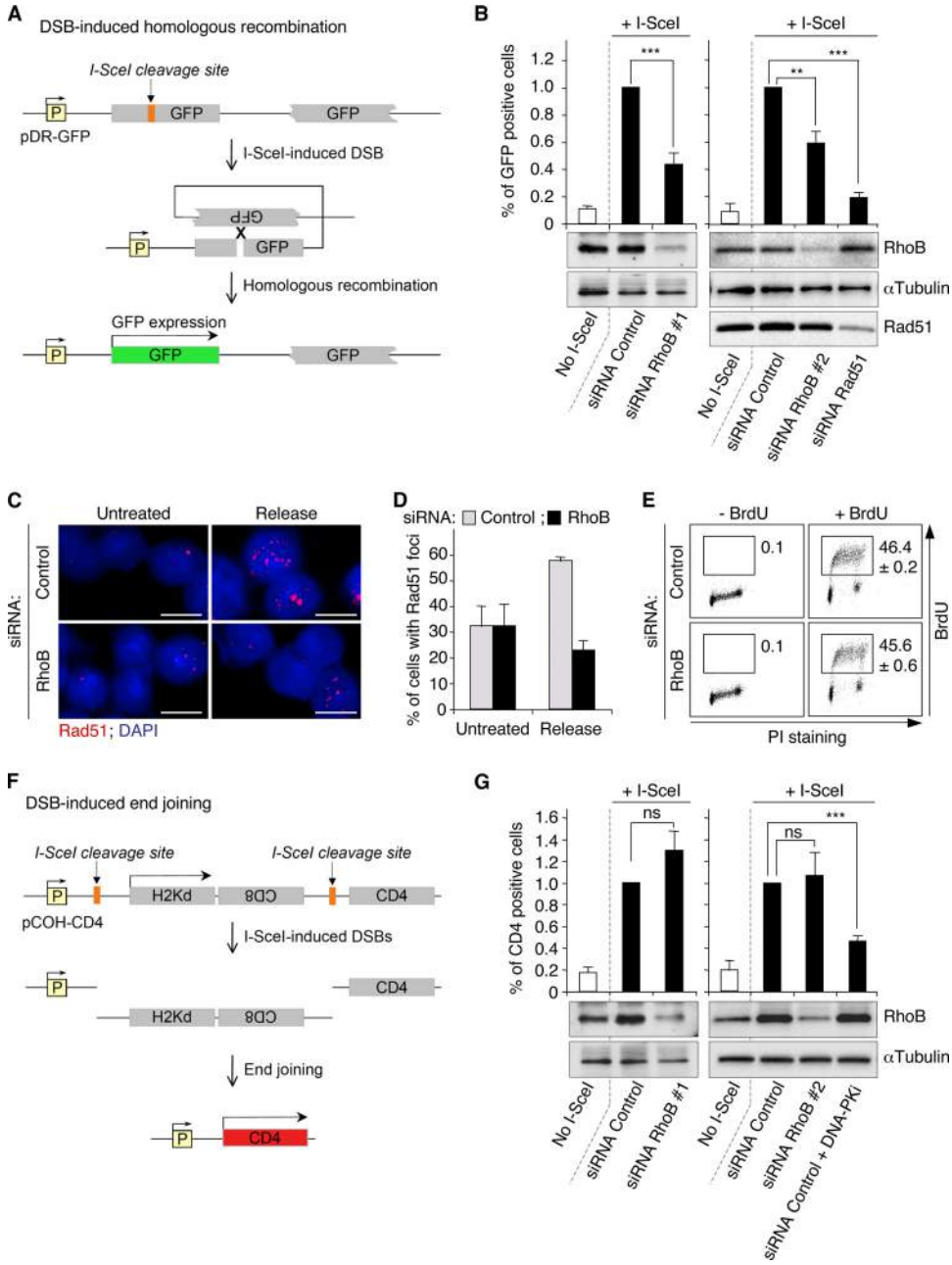

FIG 4 RhoB-deficient cells are defective for DSB repair by homologous recombination. (A) Substrate and strategy used to measure DSB-induced homologous recombination (26, 48). The pDR-GFP substrate contains two inactive genes coding for GFP under the control of a promoter (P). The 5′ gene is inactive because of the insertion of a cleavage site for I-SceI. The 3′ gene is inactive because it is deleted in both the 5′ and 3′ directions. When a DSB is produced by I-SceI, recombination between these two inactive genes (specifically gene conversion) restores a functional GFP coding sequence by either intrachromatid homologous recombination (represented) or unequal sister chromatid exchange (not represented). (B) RG37 cells stably expressing the pDR-GFP substrate were transfected with RhoB-targeting or nontargeting (control) siRNAs for 2 days and then transfected with an I-SceI plasmid for an additional 3 days. Cells transfected with Rad51-targeting siRNAs were used as a control for the pDR-GFP substrate. "No I-SceI" corresponds to cells transfected with an empty plasmid for 3 days. (Top) Percentages of GFP-positive recombinant cells determined by flow cytometry and normalized to the level of cells cotransfected with control siRNAs and I-SceI, which was set to a value of 1. Data shown are means ± standard errors of the means for five (with RhoB#1 siRNA) or three (with RhoB#2 and Rad51 siRNAs) independent experiments. ***, $P < 0.001$; **, $P < 0.01$ (by t test). (Bottom) Western blotting of RhoB and Rad51. α-Tubulin was the loading control. (C and D) HCT15/Chk2-WT cells were transfected with RhoB-targeting or nontargeting (control) siRNAs and left untreated or were treated with 1 μM CPT for 1 h. Rad51 foci were analyzed by immunofluorescence microscopy at 6 h post-CPT treatment (Release) (see protocol described in the legend to Fig. 3D). (C) Representative images. DAPI, 4′,6-diamidino-2-phenylindole. Bar, 10 μm. (D) Percentages of cells with at least five Rad51 foci. At least 200 cells were analyzed in each group (means ± standard errors of the means). (E) HCT15/Chk2-WT cells were transfected with RhoB-targeting or nontargeting (control) siRNAs, labeled with 30 μM BrdU for 30 min, and analyzed by flow cytometry. Numbers indicate percentages of BrdU-positive cells (means ± SD for three experiments). Unlabeled cells were used as negative controls for anti-BrdU staining. PI, propidium iodide. (F) Substrate and strategy used to measure DSB-induced end joining (49). The pCOH-CD4 substrate contains genes coding for the membrane antigens H2Kd, CD8, and CD4. The only expressed gene is H2Kd. CD8 is not expressed because it is in an inverted orientation, and CD4 is not expressed because it is too far from the promoter (P). Two cleavage sites for I-SceI are present in noncoding sequences, which are in direct orientation generating cohesive ends between the two sites. When two DSBs are produced by I-SceI, the internal fragment

integrated copy of the pDR-GFP substrate (26) (Fig. 4A). This substrate allows the monitoring of homologous recombination, specifically gene conversion, induced by a DSB produced by the nuclease I-SceI (48). Plasmid pDR-GFP consists of a tandem repeat of two inactive GFP genes, one of them containing a cleavage site for I-SceI. Transient expression of I-SceI produces a DSB in the chromosomal recombination substrate, which can induce homologous recombination and recreates a functional GFP (Fig. 4A). The recombinant cells become fluorescent and can be detected by flow cytometry. In RG37 cells, siRNA-mediated depletion of RhoB decreased the induction of GFP-positive recombinant cells in response to I-SceI expression (Fig. 4B). In agreement with these results, siRNA-mediated depletion of RhoB also prevented the formation of Rad51 foci post-CPT treatment (Fig. 4C and D), a key protein in homologous recombination that is recruited at DSB sites (47). Flow cytometry analysis of BrdU incorporation versus DNA content showed that the percentages of S-phase cells were similar in cells transfected with control and RhoB-targeting siRNAs (Fig. 4E) as well as in WT and RhoB$^{-/-}$ MEF cells (WT cells, 46.3% ± 2%; RhoB$^{-/-}$ cells 45.0% ± 0.7%) (data not shown). Thus, RhoB deficiency did not result in a lower proportion of S-phase cells, which excludes the possibility that fewer cells in S phase account for the reduced DSB repair by homologous recombination.

To assess the potential involvement of RhoB in NHEJ repair, we used human GC92 fibroblast cells stably expressing the pCOH-CD4 substrate (27, 49, 50) (Fig. 4F). This substrate contains genes encoding the membrane antigens H2Kd, CD8, and CD4. Before expression of I-SceI, neither CD8 nor CD4 is expressed. I-SceI expression produces the excision of the H2Kd/CD8 fragment, and rejoining of the DNA ends leads to the expression of the CD4 gene (Fig. 4F). Cells expressing CD4 at the plasma membrane can be detected by flow cytometry using an anti-CD4 antibody. Figure 4G shows that siRNA-mediated depletion of RhoB did not significantly affect the induction of CD4-positive cells in response to I-SceI expression. Together, these results indicate that RhoB is involved in DSB repair primarily by homologous recombination.

RhoB-deficient cells are defective for PP2A activity. Inhibition of PP2A is known to impair DSB repair by homologous recombination (16). In addition, although several serine/threonine phosphatases (PP2A, PP4, PP1, PP6, and Wip1) can dephosphorylate γH2AX (14), PP2A seems to be the main phosphatase for γH2AX in response to CPT (15). PP2A inhibition induces persistent γH2AX and DSBs in CPT-treated cells and increases cellular sensitivity to CPT (15), effects similar to those observed in RhoB-deficient cells (Fig. 3). We therefore examined whether RhoB inhibition could affect PP2A activity.

Consistent with the prevalent role of PP2A in removing γH2AX in CPT-treated cells (15), inhibition of PP2A with fostriecin or okadaic acid completely prevented γH2AX dephosphorylation following removal of CPT (Fig. 5A). Next, we measured PP2A activity in WT, RhoB$^{-/-}$, and RhoB$^{-/-}$ cells complemented with HA-RhoB. The levels of PP2A(C) protein were similar in all cell populations (Fig. 5B). Figure 5C shows that PP2A activity was reduced in RhoB$^{-/-}$ cells compared to WT and RhoB$^{-/-}$ cells complemented with HA-RhoB. To determine whether RhoB and PP2A are in the same pathway to dephosphorylate γH2AX, we compared the levels of γH2AX post-CPT treatment when RhoB is expressed or not under conditions where PP2A activity is inhibited. Figure 5D shows that RhoB suppression with siRNA did not further increase the level of γH2AX in cells exposed to okadaic acid post-CPT treatment. From these results, we propose that RhoB promotes PP2A activity and DSB repair.

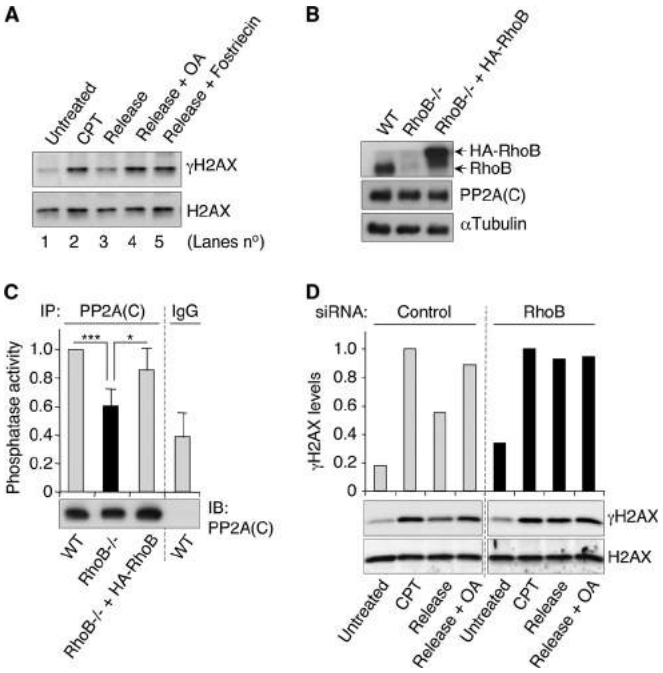

FIG 5 RhoB-deficient cells are defective for PP2A activity. (A) Western blotting of γH2AX and H2AX in HCT15/Chk2-WT cells treated with 1 μM CPT for 1 h and washed and cultured in CPT-free medium for 5 h (release). Okadaic acid (OA) (100 nM) (lane 4) and fostriecin (100 nM) (lane 5) were added immediately after CPT removal (washes). See also the treatment protocol described in the legend of Fig. 3D. (B and C) Primary MDF cells of each genotype were analyzed for RhoB and PP2A(C) expression by Western blotting (B) and for PP2A activity after PP2A(C) immunoprecipitation (IP) using the Thr phosphopeptide K-R-pT-I-R-R as a substrate (C). Data shown are means ± SD for three independent experiments. *, $P < 0.05$; ***, $P < 0.001$ (by *t* test). IB, immunoblotting. (D) HCT15/Chk2-WT cells were transfected with RhoB-targeting or nontargeting (control) siRNAs before treatment, as described above for panel A. Western blotting of γH2AX and H2AX. The top panel shows quantification of γH2AX expression normalized to the expression level of H2AX, shown at the bottom.

RhoB-deficient cells reveal endogenous γH2AX foci and genomic instability. Because we found that RhoB promotes DSB repair, we examined whether RhoB-deficient cells would accumu-

H2Kd/CD8 is excised, and rejoining of the DNA ends leads to the expression of the CD4 gene. (G) GC92 cells stably expressing the pCOH-CD4 substrate were transfected as described above for panel B, and percentages of CD4-positive cells were determined by flow cytometry using an anti-CD4 antibody. Nontargeting-siRNA-transfected cells treated with the DNA-PK inhibitor NU7026 (DNA-PKi) (10 μM) at the time of transfection with the I-SceI plasmid were used as a control for the pCOH-CD4 substrate. Data shown are means ± standard errors of the means for seven (with siRNA RhoB#1) or three (with siRNA RhoB#2 and the siRNA control plus the DNA-PK inhibitor) independent experiments. ns, nonsignificant ($P = 0.15$ [with siRNA RhoB#1] and $P = 0.14$ [with siRNA RhoB#2]); ***, $P < 0.001$ (by *t* test).

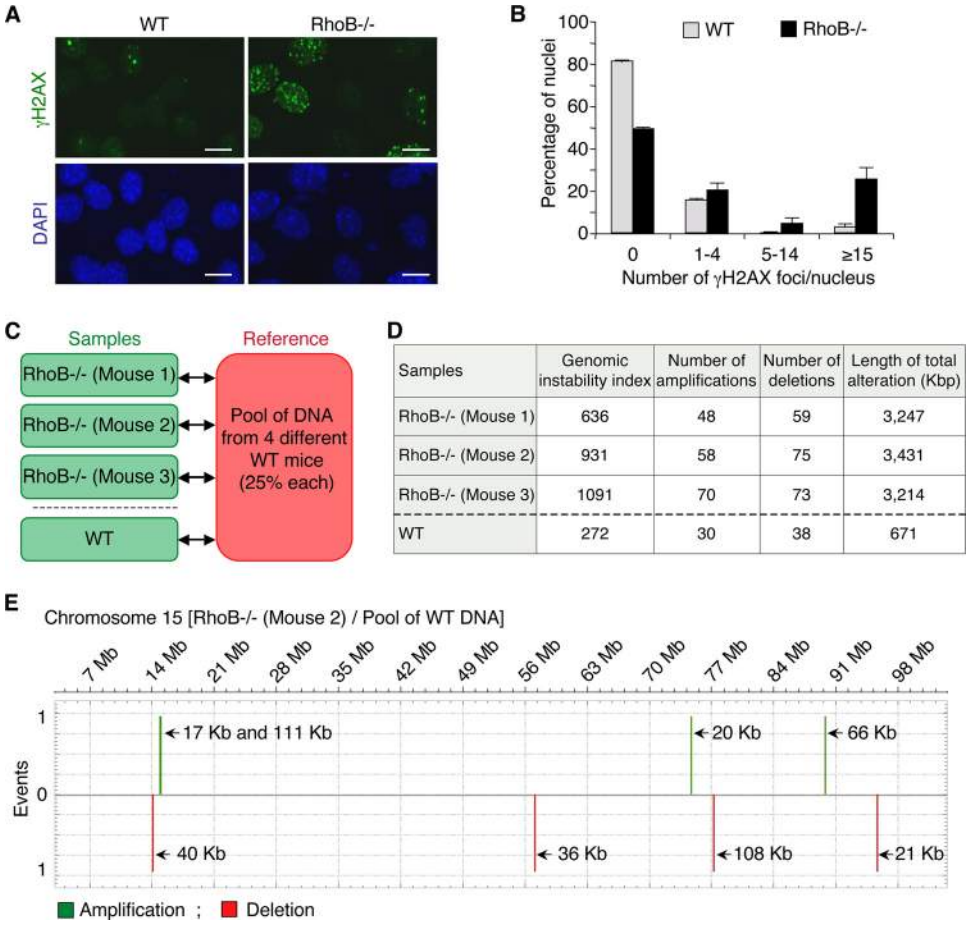

Samples	Genomic instability index	Number of amplifications	Number of deletions	Length of total alteration (Kbp)
RhoB-/- (Mouse 1)	636	48	59	3,247
RhoB-/- (Mouse 2)	931	58	75	3,431
RhoB-/- (Mouse 3)	1091	70	73	3,214
WT	272	30	38	671

FIG 6 RhoB loss is accompanied by increased γH2AX levels and chromosomal abnormalities. (A) Representative images of WT and RhoB$^{-/-}$ primary MDF cells after staining for γH2AX. DNA was counterstained with DAPI (blue). Bar, 10 μm. (B) Quantification of the number of γH2AX foci per nucleus. A minimum of 500 nuclei was analyzed per cell type (means ± SD for three independent experiments). (C) Design of the CGH array analysis. Genomic DNA of RhoB$^{-/-}$ MDF cells was compared to a pool of genomic DNA of MDF cells from four different WT syngeneic mice. As a control, to determine the number of genomic alterations due to interindividual variability, genomic DNA of WT MDF cells was compared to the pool of genomic DNA from WT mice. (D) Table showing whole-genome chromosomal amplification and deletion events as well as the total length (in kbp) of chromosomal alterations in RhoB$^{-/-}$ MDF cells compared to WT MDF cells analyzed by CGH arrays. The genomic instability index was calculated with the formula (number of deletions + number of amplifications)^2/number of altered chromosomes, as previously described (32). (E) Chromosome plots for chromosome 15 of RhoB$^{-/-}$ MDF cells from mouse 2 compared to the pool of WT MDF cells, as determined by a CGH array. This chromosome is representative of the mean numbers of amplification and deletion events in RhoB$^{-/-}$ MDF cells.

late endogenous DSBs. We analyzed γH2AX nuclear foci by immunofluorescence microcopy in WT and RhoB$^{-/-}$ cells in the absence of treatment. This technique is much more sensitive than Western blotting, as it can detect a single DSB focus per cell (9). Figure 6A reveals increased numbers of γH2AX foci in RhoB$^{-/-}$ cells compared to WT cells. Quantitative analyses of the microscopy images showed that approximately 25% of RhoB$^{-/-}$ nuclei formed >15 γH2AX foci, compared to 3% in WT cells (Fig. 6B).

Inefficient repair of DSBs can initiate genomic instability (9, 10). To evaluate genomic instability in RhoB$^{-/-}$ cells, we performed comparative genomic hybridization (CGH) whole-genome tiling arrays. Genomic DNA of primary mouse dermal fibroblast (MDF) cells from RhoB$^{-/-}$ mice was compared to a pool of genomic DNA of MDF cells from four WT syngeneic mice. As a control for genomic alterations due to interindividual variability, genomic DNA of MDF cells from a WT mouse was compared to the pool of WT genomic DNA (Fig. 6C). The three RhoB$^{-/-}$ mice analyzed revealed an increased number of chromosomal amplification and deletion events compared to the WT mouse (Fig. 6D). A representative chromosome is shown in Fig. 6E. In accordance with these results, the total length of chromosomal alterations and the genomic instability index, which reflects the number of alterations per chromosome (32), were also higher in RhoB$^{-/-}$ mice (Fig. 6D). Together, these experiments suggest that RhoB loss increases the number of endogenous DSBs and genomic instability.

DISCUSSION

Here we identify RhoB as the first GTPase involved in the signaling and repair of DSBs. Our data support a model in which DSBs activate a Chk2-HuR-RhoB pathway that promotes PP2A-mediated dephosphorylation of γH2AX and repair (Fig. 7). DSBs are likely the initiating events for RhoB upregulation, as inhibition of CPT-induced DSBs by blocking of replication suppressed the induction of RhoB mRNA (Fig. 1G). Also, the induction of RhoB depends on Chk2 (Fig. 2), a checkpoint kinase readily activated by DSBs (39). Other parallel pathways besides Chk2 probably also

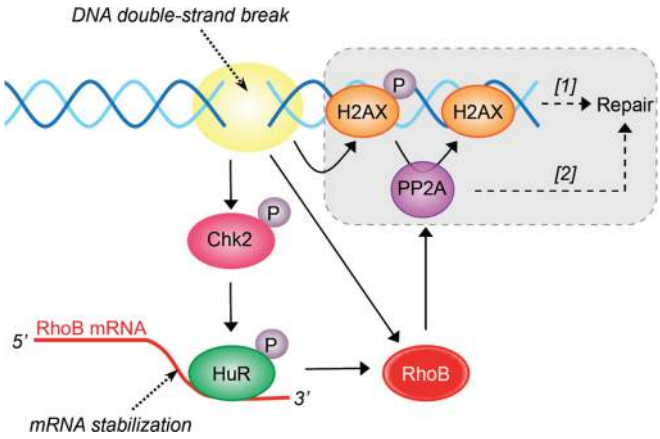

FIG 7 Proposed molecular pathways for the role of RhoB in the DDR and repair. The gray box indicates that PP2A promotes DSB repair by dephosphorylating γH2AX ([1]) and/or non-DDR proteins ([2]) (see Discussion).

contribute to RhoB induction, as Chk2-KD cells are not completely defective for HuR-RhoB mRNA interaction (Fig. 2F) and RhoB induction in response to CPT (Fig. 2G and H). The Chk2-independent induction of RhoB (Fig. 7) may be sufficient to promote γH2AX dephosphorylation, as Chk2-KD cells dephosphorylate γH2AX with an efficiency similar to that of Chk2-WT cells 5 h after CPT removal (data not shown). Moreover, because Chk2 is a major player in DSB repair (it phosphorylates/activates Brca1, p53, and PP2A) (39), these results also raise the possibility that Chk2-KD cells have evolved and compensate by increasing Chk2-independent pathways to repair DSBs. Such pathways may implicate Chk1. Indeed, CPT is known to activate the ATR-Chk1 pathway (18, 19), and Chk1 can promote HuR-dependent stabilization of mRNAs by inhibiting Cdk1-mediated phosphorylation of HuR (51, 52). Moreover, Chk1 can also promote DSB repair by phosphorylating the repair factor Rad51 (53). In addition, the effect of Chk2 loss seems to be less pronounced on HuR-RhoB mRNA interactions than on RhoB mRNA levels after CPT treatment, which raises the possibility that other pathways besides HuR also participate in the induction of RhoB mRNA by Chk2. Further support for the role of DSBs is provided by independent studies showing that RhoB is also upregulated early in response to UV and cisplatin (2, 3), which can produce DSBs in replicating cells (54–56).

RhoB appears to be implicated in the repair of DSBs from different origins. Indeed, RhoB-deficient cells maintain elevated γH2AX levels in response to CPT (Fig. 3), which produces DSBs indirectly during replication (19) and transcription (20) as well as in response to endogenous DSBs (Fig. 6). RhoB-deficient cells are also defective in the repair of DSBs that are produced directly by the endonuclease I-SceI (Fig. 4). DSBs are potentially lethal DNA lesions if not repaired (9). In agreement with the involvement of RhoB in DSB repair, RhoB-deficient cells are hypersensitive to CPT (Fig. 3A) and other genotoxic agents that can also induce DSBs, such as ionizing radiation (57) and UV (2).

It is now well documented that inhibition of PP2A activity impairs DSB repair (15–17). Hence, our finding that RhoB-deficient cells are defective for PP2A activity (Fig. 5) links RhoB expression to DSB repair. Although RhoB can bind PP2A(C) (58), it is not known whether this interaction is important for PP2A activity. PP2A may stimulate DSB repair by the timely dephosphorylation of γH2AX (15). Our analysis showing that RhoB-deficient cells are defective for DSB repair by homologous recombination but not for DSB repair by end joining (Fig. 4) further suggests that γH2AX dephosphorylation might be specifically required for homologous recombination. In line with this possibility, it has been reported that γH2AX dephosphorylation (removal) is required for efficient DNA end resection, which is a prerequisite for homology-mediated DSB repair (59). Besides RhoB promoting DSB repair by PP2A-mediated γH2AX dephosphorylation (Fig. 7), it is possible that RhoB also promotes DSB repair by PP2A-independent pathways, which may in turn further increase PP2A-mediated γH2AX dephosphorylation. PP2A may also stimulate DSB repair by homologous recombination by dephosphorylating non-DDR proteins such as Akt1 (60). Indeed, phosphorylated/active Akt1 has been reported to inhibit homologous recombination by inducing cytoplasmic retention of Brca1 and Rad51 (61). It is therefore possible that RhoB inhibition prevents DSB repair by inhibiting the PP2A-dependent dephosphorylation of Akt1. This hypothesis is concordant with our previous and current findings that the loss of RhoB expression promotes the activation of Akt1 (7) and prevents DSB repair by homologous recombination (Fig. 4). Besides γH2AX (and Akt), it is likely that RhoB loss affected other PP2A substrates, as RhoB loss decreased the global activity of PP2A, which was measured by using a nonspecific threonine phosphopeptide (Fig. 5C). Although PP2A can also promote DSB repair by NHEJ by dephosphorylating Ku70, Ku80, and DNA-PKcs (17), RhoB downregulation did not significantly affect end-joining-repair events (Fig. 4). Hence, the predominant role of RhoB-dependent PP2A activity is likely to promote DSB repair by homologous recombination. Besides PP2A, it is possible that RhoB loss also decrease a PP4 activity. Indeed, PP4 loss is primarily involved in the basal increase in the level of γH2AX (62), and we found that RhoB-deficient cells have elevated endogenous γH2AX levels (Fig. 6).

RhoB expression commonly decreases during tumor progression (4–8), and RhoB knockout (KO) mice are more susceptible to tumor formation and/or progression in response to UVB (63) and 7,12-dimethylbenz[a]anthracene (DMBA), whose metabolites induce DNA damage (24). However, very little is known about the molecular mechanisms by which the loss of RhoB promotes tumor progression. We show here that RhoB-deficient cells are defective for DSB repair (Fig. 3 and 4) and that, consistent with this, they have elevated endogenous γH2AX levels and chromosomal abnormalities (Fig. 6). We recently reported that RhoB-deficient human skin tumors also have elevated γH2AX levels compared to RhoB-proficient tumors (63). Hence, our findings suggest that loss of RhoB could promote oncogenesis by increasing DSB-mediated genomic instability.

ACKNOWLEDGMENTS

We thank Y. Pommier for Chk2-WT and Chk2-KD HCT15 cells and for stimulating discussions; G. C. Prendergast for WT and RhoB$^{-/-}$ mice; A. Peyret-Lacombe, J. Cherier, R. Gence, and I. Lajoie-Mazenc for preparing primary mouse dermal fibroblast cells from these mice; and L. Trouilh from the GenoToul Biochips platform for her kind help in the analyses of CGH arrays. We also thank S. Cabantous, E. Nicolas, and C. E. Redon for critically reading the manuscript.

This research was supported by grants from the Ligue Nationale Contre le Cancer and the Region Midi-Pyrénées.

We declare that we have no conflicts of interest.

REFERENCES

1. **Etienne-Manneville S, Hall A.** 2002. Rho GTPases in cell biology. Nature **420:**629–635. http://dx.doi.org/10.1038/nature01148.
2. **Canguilhem B, Pradines A, Baudouin C, Boby C, Lajoie-Mazenc I, Charveron M, Favre G.** 2005. RhoB protects human keratinocytes from UVB-induced apoptosis through epidermal growth factor receptor signaling. J. Biol. Chem. **280:**43257–43263. http://dx.doi.org/10.1074/jbc.M508650200.
3. **Fritz G, Kaina B, Aktories K.** 1995. The ras-related small GTP-binding protein RhoB is immediate-early inducible by DNA damaging treatments. J. Biol. Chem. **270:**25172–25177. http://dx.doi.org/10.1074/jbc.270.42.25172.
4. **Adnane J, Muro-Cacho C, Mathews L, Sebti SM, Munoz-Antonia T.** 2002. Suppression of rho B expression in invasive carcinoma from head and neck cancer patients. Clin. Cancer Res. **8:**2225–2232.
5. **Mazieres J, Tovar D, He B, Nieto-Acosta J, Marty-Detraves C, Clanet C, Pradines A, Jablons D, Favre G.** 2007. Epigenetic regulation of RhoB loss of expression in lung cancer. BMC Cancer **7:**220. http://dx.doi.org/10.1186/1471-2407-7-220.
6. **Zhou J, Zhu Y, Zhang G, Liu N, Sun L, Liu M, Qiu M, Luo D, Tang Q, Liao Z, Zheng Y, Bi F.** 2011. A distinct role of RhoB in gastric cancer suppression. Int. J. Cancer **128:**1057–1068. http://dx.doi.org/10.1002/ijc.25445.
7. **Bousquet E, Mazieres J, Privat M, Rizzati V, Casanova A, Ledoux A, Mery E, Couderc B, Favre G, Pradines A.** 2009. Loss of RhoB expression promotes migration and invasion of human bronchial cells via activation of AKT1. Cancer Res. **69:**6092–6099. http://dx.doi.org/10.1158/0008-5472.CAN-08-4147.
8. **Huang M, Prendergast GC.** 2006. RhoB in cancer suppression. Histol. Histopathol. **21:**213–218.
9. **Bonner WM, Redon CE, Dickey JS, Nakamura AJ, Sedelnikova OA, Solier S, Pommier Y.** 2008. GammaH2AX and cancer. Nat. Rev. Cancer **8:**957–967. http://dx.doi.org/10.1038/nrc2523.
10. **Harper JW, Elledge SJ.** 2007. The DNA damage response: ten years after. Mol. Cell **28:**739–745. http://dx.doi.org/10.1016/j.molcel.2007.11.015.
11. **Jeggo PA, Lobrich M.** 2007. DNA double-strand breaks: their cellular and clinical impact? Oncogene **26:**7717–7719. http://dx.doi.org/10.1038/sj.onc.1210868.
12. **Lukas J, Lukas C, Bartek J.** 2011. More than just a focus: the chromatin response to DNA damage and its role in genome integrity maintenance. Nat. Cell Biol. **13:**1161–1169. http://dx.doi.org/10.1038/ncb2344.
13. **Shiloh Y.** 2006. The ATM-mediated DNA-damage response: taking shape. Trends Biochem. Sci. **31:**402–410. http://dx.doi.org/10.1016/j.tibs.2006.05.004.
14. **Freeman AK, Monteiro AN.** 2010. Phosphatases in the cellular response to DNA damage. Cell Commun. Signal. **8:**27. http://dx.doi.org/10.1186/1478-811X-8-27.
15. **Chowdhury D, Keogh MC, Ishii H, Peterson CL, Buratowski S, Lieberman J.** 2005. Gamma-H2AX dephosphorylation by protein phosphatase 2A facilitates DNA double-strand break repair. Mol. Cell **20:**801–809. http://dx.doi.org/10.1016/j.molcel.2005.10.003.
16. **Kalev P, Simicek M, Vazquez I, Munck S, Chen L, Soin T, Danda N, Chen W, Sablina A.** 2012. Loss of PPP2R2A inhibits homologous recombination DNA repair and predicts tumor sensitivity to PARP inhibition. Cancer Res. **72:**6414–6424. http://dx.doi.org/10.1158/0008-5472.CAN-12-1667.
17. **Wang Q, Gao F, Wang T, Flagg T, Deng X.** 2009. A nonhomologous end-joining pathway is required for protein phosphatase 2A promotion of DNA double-strand break repair. Neoplasia **11:**1012–1021.
18. **Pommier Y.** 2006. Topoisomerase I inhibitors: camptothecins and beyond. Nat. Rev. Cancer **6:**789–802. http://dx.doi.org/10.1038/nrc1977.
19. **Furuta T, Takemura H, Liao ZY, Aune GJ, Redon C, Sedelnikova OA, Pilch DR, Rogakou EP, Celeste A, Chen HT, Nussenzweig A, Aladjem MI, Bonner WM, Pommier Y.** 2003. Phosphorylation of histone H2AX and activation of Mre11, Rad50, and Nbs1 in response to replication-dependent DNA double-strand breaks induced by mammalian DNA topoisomerase I cleavage complexes. J. Biol. Chem. **278:**20303–20312. http://dx.doi.org/10.1074/jbc.M300198200.
20. **Sordet O, Redon CE, Guirouilh-Barbat J, Smith S, Solier S, Douarre C, Conti C, Nakamura AJ, Das BB, Nicolas E, Kohn KW, Bonner WM, Pommier Y.** 2009. Ataxia telangiectasia mutated activation by transcription- and topoisomerase I-induced DNA double-strand breaks. EMBO Rep. **10:**887–893. http://dx.doi.org/10.1038/embor.2009.97.
21. **Zhang YW, Regairaz M, Seiler JA, Agama KK, Doroshow JH, Pommier Y.** 2011. Poly(ADP-ribose) polymerase and XPF-ERCC1 participate in distinct pathways for the repair of topoisomerase I-induced DNA damage in mammalian cells. Nucleic Acids Res. **39:**3607–3620. http://dx.doi.org/10.1093/nar/gkq1304.
22. **Aris SM, Pommier Y.** 2012. Potentiation of the novel topoisomerase I inhibitor indenoisoquinoline LMP-400 by the cell checkpoint and Chk1-Chk2 inhibitor AZD7762. Cancer Res. **72:**979–989. http://dx.doi.org/10.1158/0008-5472.CAN-11-2579.
23. **Kass EM, Ahn J, Tanaka T, Freed-Pastor WA, Keezer S, Prives C.** 2007. Stability of checkpoint kinase 2 is regulated via phosphorylation at serine 456. J. Biol. Chem. **282:**30311–30321. http://dx.doi.org/10.1074/jbc.M704642200.
24. **Liu AX, Rane N, Liu JP, Prendergast GC.** 2001. RhoB is dispensable for mouse development, but it modifies susceptibility to tumor formation as well as cell adhesion and growth factor signaling in transformed cells. Mol. Cell. Biol. **21:**6906–6912. http://dx.doi.org/10.1128/MCB.21.20.6906-6912.2001.
25. **Aasen T, Izpisua Belmonte JC.** 2010. Isolation and cultivation of human keratinocytes from skin or plucked hair for the generation of induced pluripotent stem cells. Nat. Protoc. **5:**371–382. http://dx.doi.org/10.1038/nprot.2009.241.
26. **Dumay A, Laulier C, Bertrand P, Saintigny Y, Lebrun F, Vayssiere JL, Lopez BS.** 2006. Bax and Bid, two proapoptotic Bcl-2 family members, inhibit homologous recombination, independently of apoptosis regulation. Oncogene **25:**3196–3205. http://dx.doi.org/10.1038/sj.onc.1209344.
27. **Rass E, Grabarz A, Plo I, Gautier J, Bertrand P, Lopez BS.** 2009. Role of Mre11 in chromosomal nonhomologous end joining in mammalian cells. Nat. Struct. Mol. Biol. **16:**819–824. http://dx.doi.org/10.1038/nsmb.1641.
28. **Glorian V, Maillot G, Poles S, Iacovoni JS, Favre G, Vagner S.** 2011. HuR-dependent loading of miRNA RISC to the mRNA encoding the Ras-related small GTPase RhoB controls its translation during UV-induced apoptosis. Cell Death Differ. **18:**1692–1701. http://dx.doi.org/10.1038/cdd.2011.35.
29. **Lajoie-Mazenc I, Tovar D, Penary M, Lortal B, Allart S, Favard C, Brihoum M, Pradines A, Favre G.** 2008. MAP1A light chain-2 interacts with GTP-RhoB to control epidermal growth factor (EGF)-dependent EGF receptor signaling. J. Biol. Chem. **283:**4155–4164. http://dx.doi.org/10.1074/jbc.M709639200.
30. **Regairaz M, Zhang YW, Fu H, Agama KK, Tata N, Agrawal S, Aladjem MI, Pommier Y.** 2011. Mus81-mediated DNA cleavage resolves replication forks stalled by topoisomerase I-DNA complexes. J. Cell Biol. **195:**739–749. http://dx.doi.org/10.1083/jcb.201104003.
31. **Cron KR, Zhu K, Kushwaha DS, Hsieh G, Merzon D, Rameseder J, Chen CC, D'Andrea AD, Kozono D.** 2013. Proteasome inhibitors block DNA repair and radiosensitize non-small cell lung cancer. PLoS One **8:**e73710. http://dx.doi.org/10.1371/journal.pone.0073710.
32. **Lagarde P, Perot G, Kauffmann A, Brulard C, Dapremont V, Hostein I, Neuville A, Wozniak A, Sciot R, Schoffski P, Aurias A, Coindre JM, Debiec-Rychter M, Chibon F.** 2012. Mitotic checkpoints and chromosome instability are strong predictors of clinical outcome in gastrointestinal stromal tumors. Clin. Cancer Res. **18:**826–838. http://dx.doi.org/10.1158/1078-0432.CCR-11-1610.
33. **Ongusaha PP, Kim HG, Boswell SA, Ridley AJ, Der CJ, Dotto GP, Kim YB, Aaronson SA, Lee SW.** 2006. RhoE is a pro-survival p53 target gene that inhibits ROCK I-mediated apoptosis in response to genotoxic stress. Curr. Biol. **16:**2466–2472. http://dx.doi.org/10.1016/j.cub.2006.10.056.
34. **Kim CH, Won M, Choi CH, Ahn J, Kim BK, Song KB, Kang CM, Chung KS.** 2010. Increase of RhoB in gamma-radiation-induced apoptosis is regulated by c-Jun N-terminal kinase in Jurkat T cells. Biochem. Biophys. Res. Commun. **391:**1182–1186. http://dx.doi.org/10.1016/j.bbrc.2009.12.012.
35. **Westmark CJ, Bartleson VB, Malter JS.** 2005. RhoB mRNA is stabilized by HuR after UV light. Oncogene **24:**502–511. http://dx.doi.org/10.1038/sj.onc.1208224.
36. **Brennan CM, Steitz JA.** 2001. HuR and mRNA stability. Cell. Mol. Life Sci. **58:**266–277. http://dx.doi.org/10.1007/PL00000854.
37. **Masuda K, Abdelmohsen K, Kim MM, Srikantan S, Lee EK, Tominaga K, Selimyan R, Martindale JL, Yang X, Lehrmann E, Zhang Y, Becker KG, Wang JY, Kim HH, Gorospe M.** 2011. Global dissociation of HuR-mRNA complexes promotes cell survival after ionizing radiation. EMBO J. **30:**1040–1053. http://dx.doi.org/10.1038/emboj.2011.24.
38. **Calaluce R, Gubin MM, Davis JW, Magee JD, Chen J, Kuwano Y,**

Gorospe M, Atasoy U. 2010. The RNA binding protein HuR differentially regulates unique subsets of mRNAs in estrogen receptor negative and estrogen receptor positive breast cancer. BMC Cancer **10:**126. http://dx.doi.org/10.1186/1471-2407-10-126.
39. **Pommier Y, Sordet O, Rao VA, Zhang H, Kohn KW.** 2005. Targeting chk2 kinase: molecular interaction maps and therapeutic rationale. Curr. Pharm. Des. **11:**2855–2872. http://dx.doi.org/10.2174/1381612054546716.
40. **Abdelmohsen K, Pullmann R, Jr, Lal A, Kim HH, Galban S, Yang X, Blethrow JD, Walker M, Shubert J, Gillespie DA, Furneaux H, Gorospe M.** 2007. Phosphorylation of HuR by Chk2 regulates SIRT1 expression. Mol. Cell **25:**543–557. http://dx.doi.org/10.1016/j.molcel.2007.01.011.
41. **Liu L, Rao JN, Zou T, Xiao L, Wang PY, Turner DJ, Gorospe M, Wang JY.** 2009. Polyamines regulate c-Myc translation through Chk2-dependent HuR phosphorylation. Mol. Biol. Cell **20:**4885–4898. http://dx.doi.org/10.1091/mbc.E09-07-0550.
42. **Yu TX, Wang PY, Rao JN, Zou T, Liu L, Xiao L, Gorospe M, Wang JY.** 2011. Chk2-dependent HuR phosphorylation regulates occludin mRNA translation and epithelial barrier function. Nucleic Acids Res. **39:**8472–8487. http://dx.doi.org/10.1093/nar/gkr567.
43. **Takemura H, Rao VA, Sordet O, Furuta T, Miao ZH, Meng L, Zhang H, Pommier Y.** 2006. Defective Mre11-dependent activation of Chk2 by ataxia telangiectasia mutated in colorectal carcinoma cells in response to replication-dependent DNA double strand breaks. J. Biol. Chem. **281:**30814–30823. http://dx.doi.org/10.1074/jbc.M603747200.
44. **Melchionna R, Chen XB, Blasina A, McGowan CH.** 2000. Threonine 68 is required for radiation-induced phosphorylation and activation of Cds1. Nat. Cell Biol. **2:**762–765. http://dx.doi.org/10.1038/35036406.
45. **Lobrich M, Shibata A, Beucher A, Fisher A, Ensminger M, Goodarzi AA, Barton O, Jeggo PA.** 2010. GammaH2AX foci analysis for monitoring DNA double-strand break repair: strengths, limitations and optimization. Cell Cycle **9:**662–669. http://dx.doi.org/10.4161/cc.9.4.10764.
46. **Goodarzi AA, Noon AT, Deckbar D, Ziv Y, Shiloh Y, Lobrich M, Jeggo PA.** 2008. ATM signaling facilitates repair of DNA double-strand breaks associated with heterochromatin. Mol. Cell **31:**167–177. http://dx.doi.org/10.1016/j.molcel.2008.05.017.
47. **Khanna KK, Jackson SP.** 2001. DNA double-strand breaks: signaling, repair and the cancer connection. Nat. Genet. **27:**247–254. http://dx.doi.org/10.1038/85798.
48. **Pierce AJ, Johnson RD, Thompson LH, Jasin M.** 1999. XRCC3 promotes homology-directed repair of DNA damage in mammalian cells. Genes Dev. **13:**2633–2638. http://dx.doi.org/10.1101/gad.13.20.2633.
49. **Guirouilh-Barbat J, Huck S, Bertrand P, Pirzio L, Desmaze C, Sabatier L, Lopez BS.** 2004. Impact of the KU80 pathway on NHEJ-induced genome rearrangements in mammalian cells. Mol. Cell **14:**611–623. http://dx.doi.org/10.1016/j.molcel.2004.05.008.
50. **Guirouilh-Barbat J, Rass E, Plo I, Bertrand P, Lopez BS.** 2007. Defects in XRCC4 and KU80 differentially affect the joining of distal nonhomologous ends. Proc. Natl. Acad. Sci. U. S. A. **104:**20902–20907. http://dx.doi.org/10.1073/pnas.0708541104.
51. **Al-Khalaf HH, Aboussekhra A.** ATR controls the UV-related upregulation of the CDKN1A mRNA in a Cdk1/HuR-dependent manner. Mol. Carcinog., in press.
52. **Kim HH, Abdelmohsen K, Gorospe M.** 2010. Regulation of HuR by DNA damage response kinases. J. Nucleic Acids **2010:**981487. http://dx.doi.org/10.4061/2010/981487.
53. **Sorensen CS, Hansen LT, Dziegielewski J, Syljuasen RG, Lundin C, Bartek J, Helleday T.** 2005. The cell-cycle checkpoint kinase Chk1 is required for mammalian homologous recombination repair. Nat. Cell Biol. **7:**195–201. http://dx.doi.org/10.1038/ncb1212.
54. **Ward IM, Chen J.** 2001. Histone H2AX is phosphorylated in an ATR-dependent manner in response to replicational stress. J. Biol. Chem. **276:**47759–47762.
55. **Limoli CL, Giedzinski E, Bonner WM, Cleaver JE.** 2002. UV-induced replication arrest in the xeroderma pigmentosum variant leads to DNA double-strand breaks, gamma-H2AX formation, and Mre11 relocalization. Proc. Natl. Acad. Sci. U. S. A. **99:**233–238. http://dx.doi.org/10.1073/pnas.231611798.
56. **Frankenberg-Schwager M, Kirchermeier D, Greif G, Baer K, Becker M, Frankenberg D.** 2005. Cisplatin-mediated DNA double-strand breaks in replicating but not in quiescent cells of the yeast Saccharomyces cerevisiae. Toxicology **212:**175–184. http://dx.doi.org/10.1016/j.tox.2005.04.015.
57. **Ader I, Delmas C, Bonnet J, Rochaix P, Favre G, Toulas C, Cohen-Jonathan-Moyal E.** 2003. Inhibition of Rho pathways induces radiosensitization and oxygenation in human glioblastoma xenografts. Oncogene **22:**8861–8869. http://dx.doi.org/10.1038/sj.onc.1207095.
58. **Lee WJ, Kim DU, Lee MY, Choi KY.** 2007. Identification of proteins interacting with the catalytic subunit of PP2A by proteomics. Proteomics **7:**206–214. http://dx.doi.org/10.1002/pmic.200600480.
59. **Helmink BA, Tubbs AT, Dorsett Y, Bednarski JJ, Walker LM, Feng Z, Sharma GG, McKinnon PJ, Zhang J, Bassing CH, Sleckman BP.** 2011. H2AX prevents CtIP-mediated DNA end resection and aberrant repair in G1-phase lymphocytes. Nature **469:**245–249. http://dx.doi.org/10.1038/nature09585.
60. **Kuo YC, Huang KY, Yang CH, Yang YS, Lee WY, Chiang CW.** 2008. Regulation of phosphorylation of Thr-308 of Akt, cell proliferation, and survival by the B55alpha regulatory subunit targeting of the protein phosphatase 2A holoenzyme to Akt. J. Biol. Chem. **283:**1882–1892. http://dx.doi.org/10.1074/jbc.M709585200.
61. **Plo I, Laulier C, Gauthier L, Lebrun F, Calvo F, Lopez BS.** 2008. AKT1 inhibits homologous recombination by inducing cytoplasmic retention of BRCA1 and RAD51. Cancer Res. **68:**9404–9412. http://dx.doi.org/10.1158/0008-5472.CAN-08-0861.
62. **Chowdhury D, Xu X, Zhong X, Ahmed F, Zhong J, Liao J, Dykxhoorn DM, Weinstock DM, Pfeifer GP, Lieberman J.** 2008. A PP4-phosphatase complex dephosphorylates gamma-H2AX generated during DNA replication. Mol. Cell **31:**33–46. http://dx.doi.org/10.1016/j.molcel.2008.05.016.
63. **Meyer N, Peyret-Lacombe A, Canguilhem B, Medale-Giamarchi C, Mamouni K, Cristini A, Monferran S, Lamant L, Filleron T, Pradines A, Sordet O, Favre G.** 2014. RhoB promotes cancer initiation by protecting keratinocytes from UVB-induced apoptosis but limits tumor aggressiveness. J. Investig. Dermatol. **134:**203–212. http://dx.doi.org/10.1038/jid.2013.278.
64. **Wu X, Chen J.** 2003. Autophosphorylation of checkpoint kinase 2 at serine 516 is required for radiation-induced apoptosis. J. Biol. Chem. **278:**36163–36168. http://dx.doi.org/10.1074/jbc.M303795200.

RhoB Promotes Cancer Initiation by Protecting Keratinocytes from UVB-Induced Apoptosis but Limits Tumor Aggressiveness

Nicolas Meyer[1,2,3,7], Alexis Peyret-Lacombe[1,2,7], Bruno Canguilhem[1,2], Claire Médale-Giamarchi[1,2], Kenza Mamouni[1,2], Agnese Cristini[1,2], Sylvie Monferran[1,2], Laurence Lamant[1,2,4], Thomas Filleron[5], Anne Pradines[1,2,6], Olivier Sordet[1,2] and Gilles Favre[1,2,6]

The role of UVB-induced apoptosis in the formation of squamous cell carcinoma (SCC) is recognized. We previously identified the small RhoB (Ras homolog gene family, member B) GTPase, an early response gene to cellular stress, as a critical protein controlling apoptosis of human keratinocytes after UVB exposure. Here we generated SKH1 (hairless immunocompetent mouse) mice invalidated for RhoB to evaluate its role in UVB-induced skin carcinogenesis *in vivo*. We show that *rhob* −/− mice have a lower risk of developing UVB-induced keratotic tumors and actinic keratosis that is associated with a higher sensitivity of UVB-exposed keratinocytes to apoptosis. We extend this observation to primary cultures of normal human keratinocytes in which RhoB was downregulated with small interfering RNA (siRNA) and further show that the hypersensitivity to apoptosis depends on B-cell lymphoma 2 (Bcl-2) downregulation. In *rhob* −/− mice, the UVB-induced tumors were preferentially undifferentiated and highly proliferative. Finally, we show in humans an almost constant loss of RhoB expression in undifferentiated SCCs. These undifferentiated and RhoB-deficient tumors have elevated phosphorylated histone H2AX (γH2AX) and 53BP1, two markers of DNA double-strand breaks. Together, our results indicate that UVB-induced RhoB expression participates in *in vivo* SCC initiation by increasing keratinocyte survival. Conversely, RhoB may limit tumor aggressiveness as loss of RhoB expression in tumor cells is associated with tumor progression.

Journal of Investigative Dermatology (2014) **134,** 203–212; doi:10.1038/jid.2013.278; published online 18 July 2013

INTRODUCTION

Cutaneous squamous cell carcinomas (SCCs) represent one of the most common human cancer type (Madan *et al.*, 2010). Approximately 85% of SCCs are cured by surgery, whereas the remaining 15% display poor prognosis. Currently, there are no specific markers to predict tumor aggressiveness and risk of recurrence in patients.

It is largely admitted that UVB plays a crucial role in the development of SCC (Goodwin *et al.*, 2004). The response of keratinocytes to UVB is complex and depends upon a balance between cell death and survival pathways. Deregulation of genes controlling this balance is considered as a key factor in the early phases of photocarcinogenesis (De Gruijl and Voskamp, 2009). We previously identified the GTPase RhoB (Ras homolog gene family, member B) as a key regulator of the apoptotic response of human HaCaT keratinocytes to UVB. We demonstrated that RhoB is critical for EGFR-induced cell survival after UVB exposure through regulation of Ak thymoma (AKT) phosphorylation (Canguilhem *et al.*, 2005).

RhoB belongs to the Rho GTPase family, a group of proteins controlling many cellular functions such as cell survival and migration, the deregulation of which are implicated in cancer initiation and progression (Karlsson *et al.*, 2009). *rhob* is an early inducible gene activated by cellular stress including hypoxia (Skuli *et al.*, 2006), ionizing radiation (Milia *et al.*, 2005; Monferran *et al.*, 2008), cytotoxic agents (Liu *et al.*, 2001), and UV irradiation (Fritz and Kaina, 2001; Canguilhem *et al.*, 2005). When activated, RhoB triggers a signaling cascade promoting the activation of AKT and NF-κB survival pathways (Mazières *et al.*, 2005). Moreover, RhoB displays tumor-suppressor gene functions in many cell types as well as in mouse models (Chen *et al.*, 2000; Liu *et al.*, 2001; Prendergast, 2001; Jiang *et al.*, 2004). RhoB expression

[1]*Inserm, UMR 1037-CRCT, Toulouse, France;* [2]*Université Paul Sabatier, Toulouse, France;* [3]*Department of Dermatology, Hôpital Larrey, Toulouse, France;* [4]*Department of Pathology, Hôpital Purpan, Toulouse, France;* [5]*Department of Biostatistics, Institut Claudius Regaud, Toulouse, France and* [6]*Department of Biopathology, Institut Claudius Regaud, Toulouse, France*

[7]*These authors contributed equally to this work.*

Correspondence: Gilles Favre, INSERM UMR 1037, Département de Biologie Clinique, Institut Claudius Regaud, 20-24 Rue du Pont Saint Pierre, 31052 Toulouse Cedex, France. E-mail: favre.gilles@claudiusregaud.fr

Abbreviations: AK, actinic keratosis; AKT, Ak thymoma; Bcl-2, B-cell lymphoma 2; DSB, double-strand break; FFPE, formalin-fixed, paraffin-embedded; γH2AX, phosphorylated histone H2AX; NHK, normal human keratinocyte; RAS, rat sarcoma; RhoB, Ras homolog gene family, member B; SCC, squamous cell carcinoma; siRNA, small interfering RNA; SKH1, hairless immunocompetent mouse

Received 21 December 2012; revised 30 April 2013; accepted 20 May 2013; accepted article preview online 21 June 2013; published online 18 July 2013

decreases during the progression of various tumors. Loss of RhoB expression was shown to promote cell proliferation, invasion, and metastasis.

Here, we develop hairless immunocompetent mice (SKH1) invalidated for *rhob* to study its *in vivo* role in UVB-induced photocarcinogenesis in mice. We also evaluated the relevance of RhoB in humans using primary cultures of human keratinocytes and human SCC tumor samples. Altogether, our work emphasizes the critical role of RhoB in both the initiation and the progression of skin SCC.

RESULTS

rhob−/− mice experience a lower incidence of SCC precursor tumors following chronic exposure to UVB

To evaluate *in vivo* the influence of RhoB on UVB-induced skin carcinogenesis, we crossed the SKH1 mouse that mimics UVB-induced photocarcinogenesis in humans (De Gruijl and Forbes, 1995; Benavides *et al.*, 2009; Sharma *et al.*, 2011) with *rhob* knockout (*rhob*−/−) mice (Liu *et al.*, 2001). The SKH1 mice *rhob*−/−, *rhob*+/−, and *rhob*+/+ were exposed daily to 0.1 J cm^{-2} UVB, corresponding to one minimal erythemal dose. Animals started to develop actinic keratosis (AK)–like lesions after 12 weeks of chronic UVB exposure and all mice exhibited at least one AK at 24 weeks. AKs are precursors of SCC (Salasche, 2000). Mice also developed small keratotic and large ulcerated tumors that have a similar appearance to human SCC (De Gruijl and Forbes, 1995). Notably, the relative distribution of AKs and tumors varied, with mice developing primarily numerous AKs together with a prevalence of small keratotic tumors, whereas others only few AKs with primarily large ulcerated tumors (Supplementary Figure S1 online).

The primary assessment of the extent of AKs in mice was performed after 17 weeks of daily UVB exposure. Animals were categorized as highly sensitive to UVB-induced photocarcinogenesis if they had AKs covering >50% of the dorsal skin (group A). Animals experiencing <50% of their dorsal skin covered by AKs were included in the low sensitivity (group B; Figure 1a and Supplementary Figure S1 online; also see Materials and Methods). Figure 1b shows that the mice with high sensitivity to UVB-induced photocarcinogenesis were almost exclusively the +/+ and +/− *rhob* mice, whereas mice presenting lower sensitivity were mainly *rhob*−/−. In *rhob*−/− mice, the lower occurrence of AKs was associated with a reduced total number of skin tumors (Figure 1c and Supplementary Figure S2 online). These results were confirmed in a second set of experiments (Supplementary Figure S3a and b online). Analysis of the tumor type revealed that small keratotic tumors were less prevalent in *rhob*−/− mice (Figure 1d and Supplementary Figure S4a online), whereas the prevalence of large ulcerated tumors was not significantly different in *rhob*+/+ and *rhob*−/− mice (Figure 1e). We concluded that the absence of RhoB is associated with a reduction in the occurrence of AKs and small keratotic tumors upon chronic exposure to UVB without significantly affecting the induction of large ulcerated tumors (Supplementary Figure S4b online).

UVB irradiation induces RhoB expression in normal human skin tissues

Because SCCs develop from the *stratum spinosum* in response to UVB (Ratushny *et al.*, 2012), we analyzed RhoB expression in the human epidermis. After surgical excision, human skin tissues from two healthy donors were left untreated or exposed to 0.4 J cm^{-2} UVB. At 8 hours after irradiation, expression of RhoB was analyzed by immunohistochemistry (Figure 2a and b and Supplementary Figure S5 online). In the absence of treatment, RhoB was expressed at very low levels at the suprabasal layers of the epidermis and was mostly detected at the basal layer (Figure 2a and b). Keratinocytes from the basal layer are the replicating cells ensuring renewal of suprabasal layers. Following UVB exposure, RhoB expression was markedly increased at the suprabasal layers of the epidermis (Figure 2b). Altogether, these results suggest that the induction of RhoB at the suprabasal layers of the epidermis in response to UVB may be involved in the development of AKs and small keratotic tumors.

Keratinocytes of *rhob*−/− mice are hypersensitive to UVB-induced apoptosis

To gain insight into the mechanism of RhoB-induced skin carcinogenesis, we analyzed the role of RhoB in the apoptotic response to UVB. Apoptosis is a major anticancer barrier (Lowe and Lin, 2000; Wong, 2011). We have previously shown that knocking down RhoB in human HaCaT cells confers hypersensitivity to UVB-induced apoptosis (Canguilhem *et al.*, 2005). It is also clearly demonstrated that RhoB is involved in the apoptotic response to genotoxics, including ionizing radiation (Fritz and Kaina, 2001; Liu *et al.*, 2001; Jiang *et al.*, 2004; Milia *et al.*, 2005). To test whether the reduced number of AKs and small keratotic tumors in *rhob*−/− mice could be related to an excess of apoptosis, we compared UVB-induced apoptosis of *rhob*+/+ and *rhob*−/− mice keratinocytes. Mice were exposed to 0.2 J cm^{-2} UVB and apoptotic DNA fragmentation was assessed 24 hours later by TUNEL assay (Samejima and Earnshaw, 2005) on formalin-fixed, paraffin-embedded (FFPE) skin samples by microscopy. Figure 3a shows that the percentage of TUNEL-positive keratinocytes was significantly higher in *rhob*−/− mice than in *rhob*+/+ mice.

We also tested whether tumoral keratinocytes of *rhob*−/− mice were more sensitive to UVB-induced apoptosis. All FFPE tumor samples collected after chronic UVB exposure of *rhob*+/+ ($n=17$) and *rhob*−/− ($n=23$) mice were assessed for apoptosis by cleaved caspase-3 immunostaining (Supplementary Figure S6 online). A significantly higher proportion of cleaved caspase-3-positive keratinocytes was found in *rhob*−/− mice tumors compared with *rhob*+/+ mice tumors (Figure 3b). Together, these results indicate that RhoB deficiency confers hypersensitivity of both normal and tumoral keratinocytes to UVB-induced apoptosis, which could protect *rhob*−/− mice against UVB-induced tumor initiation.

RhoB protects human keratinocytes from UVB-induced apoptosis through Bax/Bcl-2 ratio modulation

To determine whether these results could be extended to humans, we isolated normal human keratinocytes (NHKs)

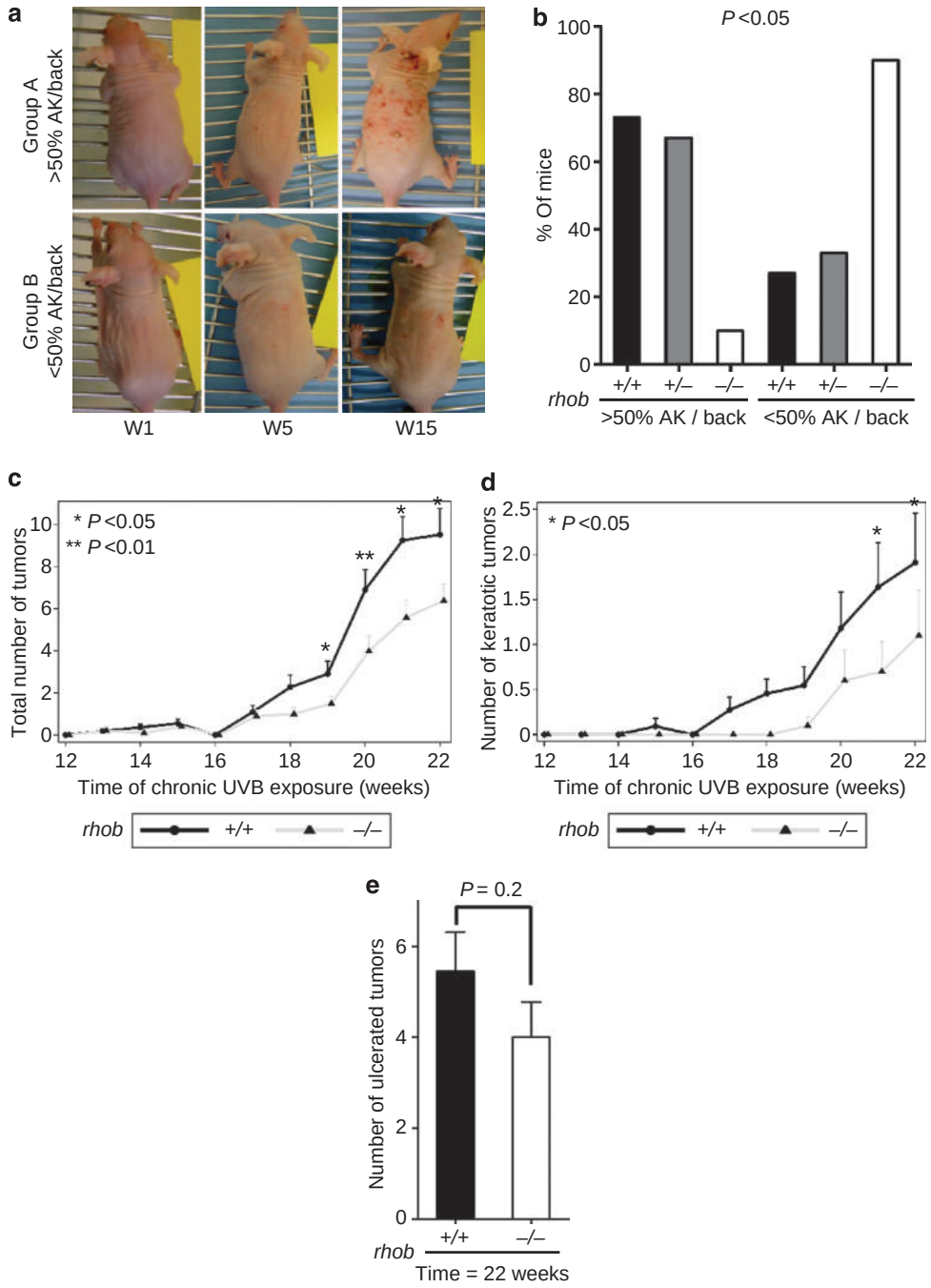

Figure 1. The rhob −/− mice develop fewer skin tumors after chronic exposure to UVB. The *rhob*+/+, *rhob*+/− and *rhob*−/− mice were chronically exposed to UVB (0.1 J cm^{-2}). (**a**) Mice were separated into two groups according to the percentage of actinic keratoses (AKs) on the skin of their back at week 17: group A (>50%) and group B (<50%). (**b**) Percentage of mice of the two groups according to their genotype. (**c**) Number of tumors (keratotic, ulcerated) per mouse at the indicated times (mean + SD). AK lesions were excluded. (**d**) Number of keratotic tumors at the indicated times (mean + SD). (**e**) Number of ulcerated tumors per mouse after 22 weeks (mean + SD). Examples of AK and tumors (keratotic, ulcerated) are presented in Supplementary Figure S1 online. *P*-values are calculated as described in the Statistical Analysis section of the Materials and Methods.

from healthy donors. RhoB expression was downregulated by transient transfection with small interfering RNA (siRNA) duplexes. Then, cells were exposed to 0.4 J cm^{-2} UVB and apoptosis was assessed after 24 hours. The siRNA-mediated depletion of RhoB in human NHK (Supplementary Figure S7 online) resulted in marked increase of cleaved caspase-3 (Figure 3c), caspase-3-dependent cleavage of poly (ADP-ribose) polymerase (Figure 3d), and apoptotic DNA fragmentation (Figure 3e).

It has been demonstrated that the Bax/B-cell lymphoma 2 (Bcl-2) ratio, a critical element determining cell death or cell survival, increases after UVB exposure in HaCaT

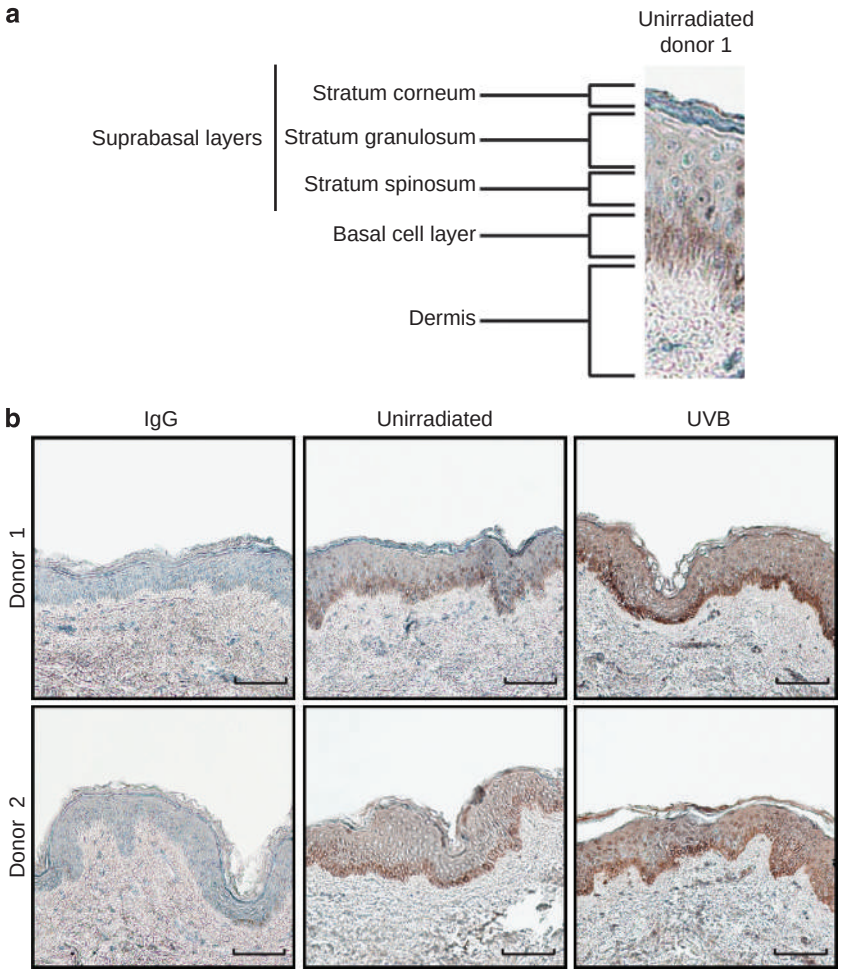

Figure 2. RhoB (Ras homolog gene family, member B) is induced in human healthy skin explants after UVB exposure. (**a**) RhoB immunostaining on human healthy skin explant. The expression of RhoB is weak and mainly localized in basal layer keratinocytes. (**b**) RhoB immunostaining on human skin explants from two healthy donors (scale = 20 μm), unirradiated or 8 hours after 0.4 J cm^{-2} UVB irradiation. The expression of RhoB is markedly increased and detectable in the entire epidermis.

(Reagan-Shaw *et al.*, 2006) and NHK cells (Afaq *et al.*, 2007). UVB irradiation (0.4 J cm^{-2}) of NHKs increased Bax expression and decreased Bcl-2 expression, causing a 3-fold increase in the Bax/Bcl-2 ratio after 24 hours (Figure 4a and b). Under these conditions, RhoB downregulation with siRNA further decreased Bcl-2 expression without changing Bax expression (Figure 4a and b), leading to a 15-fold increase in the Bax/Bcl-2 ratio.

Because Bcl-2 expression can be regulated by many survival proteins including AKT (Maddika *et al.*, 2007), we investigated the role of RhoB on AKT phosphorylation/activation in NHKs exposed to UVB. Figure 4c shows that RhoB downregulation with siRNA prevented UVB-induced AKT phosphorylation on serine 473 after 4 and 8 hours. This was associated with a reduction of Bcl-2 expression (Figure 4c). These data suggest that RhoB favors NHK survival after UVB through upregulation of the AKT/Bcl-2 pathway, leading to a decrease in the Bax/Bcl-2 ratio. It is unlikely that the protective effect of RhoB on apoptosis could be related to p53 because its expression was not affected in both RhoB-deficient cells (Supplementary Figure S8a online) and RhoB- deficient mouse tumors (Supplementary Figure S8b online). Moreover, p53 and RhoB expressions were not correlated in human tumors (Supplementary Table S1 online).

RhoB loss is associated with the preferential induction of undifferentiated tumors

Tumor differentiation is inversely related to tumor progression and metastatic potential. Undifferentiated tumors frequently display a higher proliferative and invasive potential (Spector *et al.*, 2011). To evaluate the levels of differentiation of individual tumors from *rhob*+/+ and *rhob*−/− mice, all FFPE tumor samples collected after chronic exposure were divided into two categories as exemplified in Figure 5a: mild-to-well-differentiated tumors were defined as tumors with organoid differentiation without significant cytokeratin-8 expression, whereas low-differentiated to undifferentiated tumors were tumors without organoid differentiation and without significant cytokeratin-1 expression. Figure 5b shows that the proportion of low-to-undifferentiated tumors was higher in *rhob*−/− than in *rhob*+/+ mice. Tumors from *rhob*−/− mice showed a higher proportion of

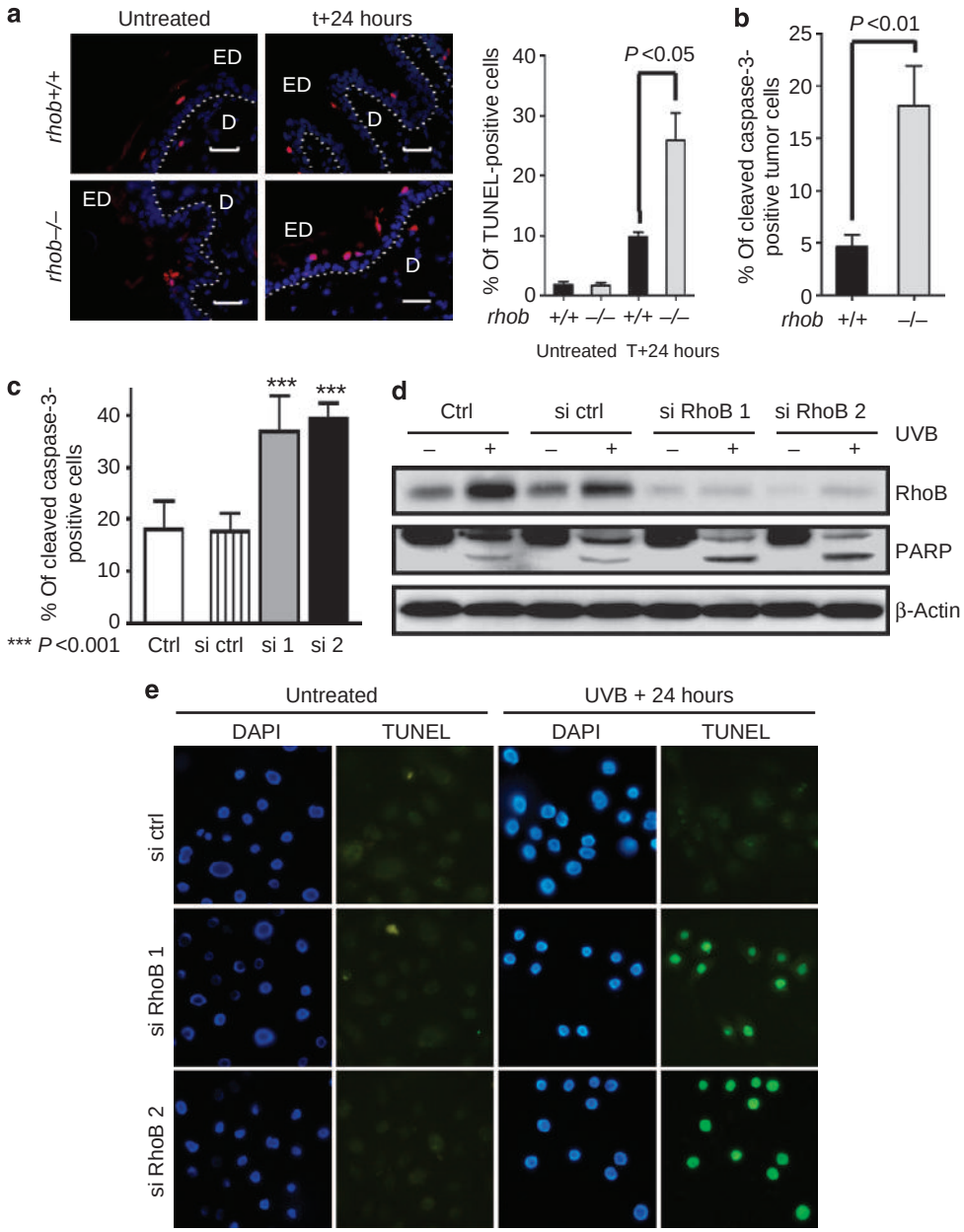

Figure 3. Keratinocytes deficient for RhoB (Ras homolog gene family, member B) are hypersensitive to UVB-induced apoptosis. (**a**) Mice of the indicated genotype were exposed to a single UVB dose (0.2 J cm^{-2}). TUNEL staining. Epidermis (ED) and dermis (D) are separated by the dotted white line (scale = 5 μm). Graph represents the percentage of TUNEL-positive cells in the epidermis (mean + SD; two fields per slide; from 71 to 244 cells per field). (**b**) Percentage of cleaved caspase-3 in UVB-induced mice tumors (mean + SD; two fields per slide; from 199 to 584 cells per field). (**c**, **d**) Normal human keratinocytes (NHKs) were exposed to UVB (0.4 J cm^{-2}) and analyzed 24 hours later. (**c**) Percentage of cleaved caspase-3-positive NHKs (mean + SD). (**d**) PARP (poly (ADP-ribose) polymerase) cleavage. (**e**) NHKs plated on coverslip were exposed to UVB (0.4 J cm^{-2}) and then stained for 4′,6-diamidino-2-phenylindole (DAPI) and TUNEL 16 hours after exposure. Ctrl, control; si, small interfering RNA.

cells positive for the proliferation marker Ki67 (Figure 5c) (Batinac *et al.*, 2006). These results are in agreement with *rhob*−/− mice developing less small keratotic tumors (Figure 1d), which are normally more differentiated than ulcerated tumors, and suggest that RhoB deficiency increases tumor aggressiveness.

We then analyzed RhoB expression in individual tumors from *rhob*+/+ mice, depending on their differentiation grade. Reverse transcriptase–quantitative PCR analyses revealed that levels of RhoB transcripts were markedly reduced in mildly differentiated tumors as compared with well-differentiated tumors (Figure 5d), suggesting that RhoB expression decreases during progression of skin tumors upon chronic UVB exposure. Although we demonstrated that oncogenic ras mutants downregulated RhoB expression in lung tumors (Bousquet *et al.*, 2009), we did not find any mutations in H-ras, N-ras, and K-ras genes in *rhob*+/+ and *rhob*−/− mice SCCs.

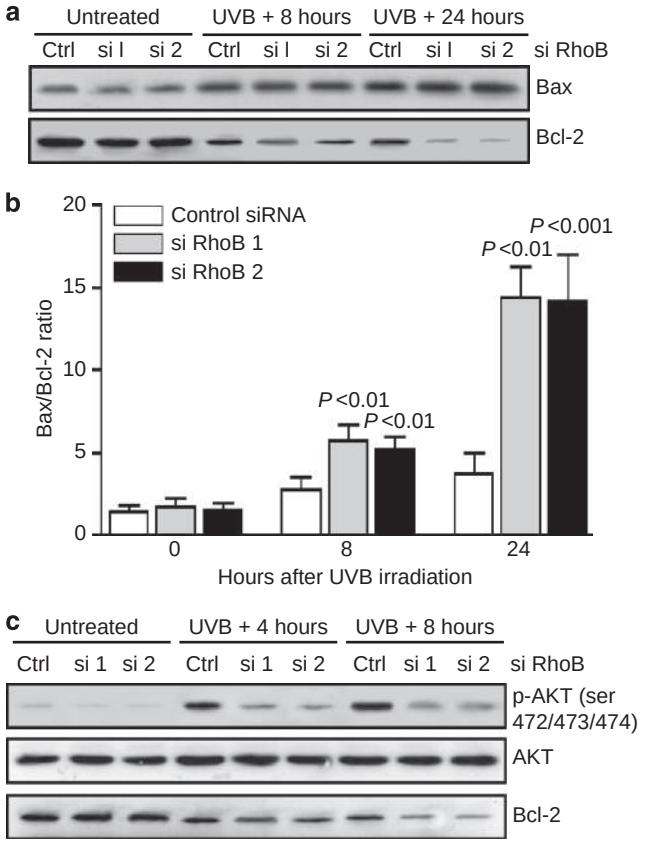

Figure 4. RhoB (Ras homolog gene family, member B) protects keratinocytes from UVB-induced apoptosis through Bax/B-cell lymphoma 2 (Bcl-2) ratio modulation. (**a**) Normal human keratinocytes (NHKs) were treated with small interfering RNA (siRNA) RhoB 1 (si 1) or 2 (si 2) or control siRNA (Ctrl) for 24 hours. Western blotting analyses of Bax and Bcl-2 at 8 and 24 hours after UVB exposure (0.4 J cm^{-2}). (**b**) Bax/Bcl-2 band density ratio (mean + SEM). (**c**) NHKs were treated with siRNA RhoB 1 (si 1) or 2 (si 2) or Ctrl for 24 hours. Western blotting analyses of phospho-AKT (ser472/473/474), AKT, and Bcl-2 at 4 and 8 hours after UVB exposure (0.4 J cm^{-2}). The presented blots are representative of two independent experiments on NHK primary cultures from two different donors.

RhoB loss is associated with increased levels of DNA double-strand breaks

To determine whether these results could be extended to humans, we analyzed RhoB expression on human invasive SCC by immunohistochemistry and microscopy. A total of 80 tumor samples were selected according to their level of differentiation (as described above for mice tumors) in the tumor bank of Toulouse-Purpan Hospital. Two groups were constituted: the first group with 40 well-differentiated SCCs, and the second one with 40 undifferentiated SCCs. We observed that almost all undifferentiated human SCCs did not express RhoB (Figure 6a and Supplementary Figure S9 online).

On these human tumor samples, we also analyzed the expression of phosphorylated histone H2AX (referred to as γH2AX), a marker for DNA double-strand breaks (DSBs) (Bonner *et al.*, 2008). DSBs are severe lesions and their inefficient/inaccurate repair can contribute to genomic instability and cancer progression (Bonner *et al.*, 2008). Figure 6b shows that the undifferentiated and RhoB-deficient human skin tumors have elevated γH2AX expression; RhoB and γH2AX expression were inversely correlated (Spearman's $r = -0.50$; 95% confidence interval: -0.77 to -0.06). Besides γH2AX, we analyzed p53 binding protein 1 (53BP1), another DNA damage response protein that accumulates at sites of DSBs (Lukas *et al.*, 2011). Figure 6c shows that undifferentiated human skin tumors have elevated expression of 53BP1. Consistent with these results, tumors from *rhob*−/− mice show elevated γH2AX- and 53BP1-positive cells compared with tumors from *rhob*+/+ mice (Figure 6d and 6e and Supplementary Figure S10a, b online). These results suggest that loss of RhoB expression increases the levels of endogenous DSBs. To test more directly this hypothesis, we compared γH2AX expression of *rhob*+/+ and *rhob*−/− basal layer keratinocytes from normal skin tissues. We observed a significant increase of γH2AX labeling in keratinocytes from *rhob*−/− mice (Figure 6f and Supplementary Figure S10c online). Immunofluorescence microscopy experiments further show that γH2AX-positive cells from *rhob*−/− skin tissues were also positive for 53BP1 (Figure 6g). Because *rhob*+/+ and *rhob*−/− cells have similar proliferation rate (Supplementary Figure S11 online), it is unlikely that the increase of γH2AX in *rhob*−/− skin tissues simply resulted from increased DNA replication. Together, these results indicate that RhoB deficiency is accompanied with increased levels of DSBs, suggesting that loss of RhoB expression might contribute to genomic instability and skin tumor progression.

DISCUSSION

This study provides insights, which to our knowledge are previously unreported, in the understanding of UVB-induced keratinocyte carcinogenesis *in vivo*, emphasizing the role of RhoB. We demonstrate that UVB-induced RhoB expression participates in maintaining cell survival, thus favoring the development of SCCs. Our data clearly show that keratinocytes from RhoB-deficient mice are more sensitive to UVB-induced apoptosis and that these mice develop fewer AKs and keratotic tumors than the wild-type counterparts. These results are consistent with our previous work showing that RhoB downregulation sensitized HaCaT immortalized keratinocytes to UVB-induced apoptosis (Canguilhem *et al.*, 2005). We further extended these observations to human keratinocytes isolated from the skin of healthy donors. In addition, we show that basal expression of RhoB in human skin is almost only detectable in keratinocytes from the basal layer, and that UVB exposure induces a strong holoepidermic expression of RhoB. Together, these observations support the possibility that UVB-induced RhoB expression protects UVB-exposed keratinocytes from apoptosis, thereby promoting the initiation of carcinogenesis. RhoB may protect keratinocytes from UVB-induced apoptosis by activating cell survival pathways. Indeed, we have previously demonstrated that UVB-induced EGFR survival pathway depends on RhoB in HaCaT cells through regulation of AKT phosphorylation (Canguilhem *et al.*, 2005). Increased Bcl-2 expression has been reported to favor photocarcinogenesis by preventing apoptosis (Nakagawa *et al.*, 1994; Delehedde *et al.*, 1999). We demonstrate here that RhoB is a critical determinant for Bcl-2 expression after

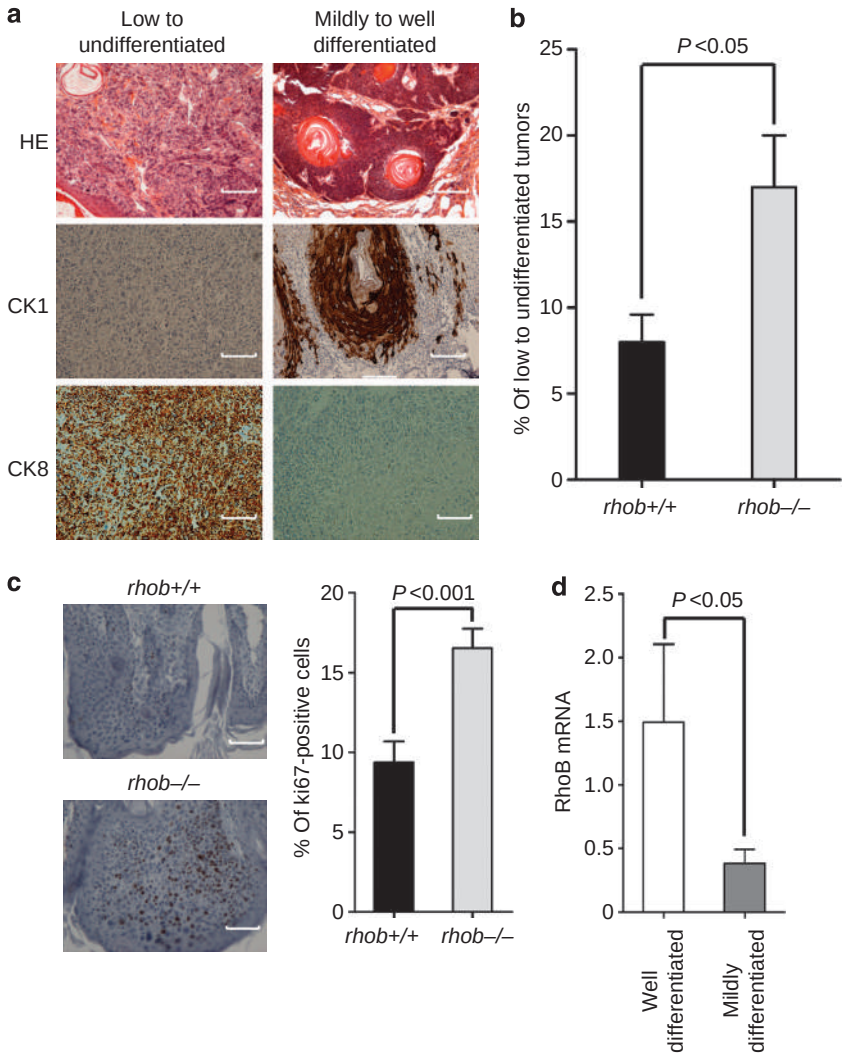

Figure 5. RhoB (Ras homolog gene family, member B) loss is associated with the preferential induction of undifferentiated skin tumors. Histopathological analysis and CK1, CK8, and Ki67 immunostaining were performed on formalin-fixed, paraffin-embedded (FFPE) samples of all tumors resulting from chronic exposure of the mice (*rhob* −/−: $n=23$; *rhob*+/+: $n=17$). (**a**) Example representative of pathological examination, and CK1 and CK8 immunostaining of tumors (scale = 10 μm). (**b**) Percentage of low-to-undifferentiated squamous cell carcinomas (SCCs) among all mouse tumor samples. (**c**) Ki67 immunostaining (scale = 10 μm). The graph represents the percentage of Ki67-positive cells in the tumors (mean + SD; from 189 to 607 cells per field). (**d**) Quantification of RhoB mRNA in cells from tumors resulting from chronic exposure of wild-type (WT) mice (normalized as $2e^{-(CqRhoB-CqActin)}$; mean + SD).

UVB exposure (Figure 4) and therefore suggest that the RhoB/Bcl-2 axis is involved in early phase of UVB-induced carcinogenesis.

RhoB also participates in the control of skin tumor progression. This is supported by three lines of evidence: (1) *rhob*−/− mice are prone to the development of UVB-induced aggressive SCCs, (2) in *rhob*+/+ mice exposed to UVB, RhoB expression is downregulated in poorly differentiated and thereby aggressive SCCs (Figure 5d), and (3) RhoB expression is also selectively lost in undifferentiated human skin tumors (Figure 6a). Moreover, because the number of ulcerated tumors is similar in the *rhob*+/+ and *rhob*−/− genotypes (Figure 1e), it is likely that RhoB does not prevent the occurrence of undifferentiated tumors. This is in agreement with our hypothesis that tumor progression requires loss of RhoB expression. These results are in agreement with our previous work on lung cancer showing that loss of RhoB occurs in the most aggressive tumors (Mazieres *et al.*, 2004) and promotes invasion of human bronchial cancer cells (Bousquet *et al.*, 2009). Consistently, Adnane *et al* (2002). reported loss of RhoB expression in invasive human SCCs of the head and neck. Although the tumor-suppressor role of RhoB is now well documented, its mechanism remains to be elucidated. Our experiments indicate that RhoB-deficient cells have elevated endogenous DSBs (Figure 6), and therefore suggest that loss of RhoB expression during progression of skin tumors (this study) and potentially the above-mentioned tumors (Adnane *et al.*, 2002; Mazieres *et al.*, 2004; Bousquet *et al.*, 2009) could promote oncogenesis by increasing DSB-mediated genomic instability. Further studies will be required to determine the molecular mechanisms by which loss of RhoB enhances endogenous DSBs.

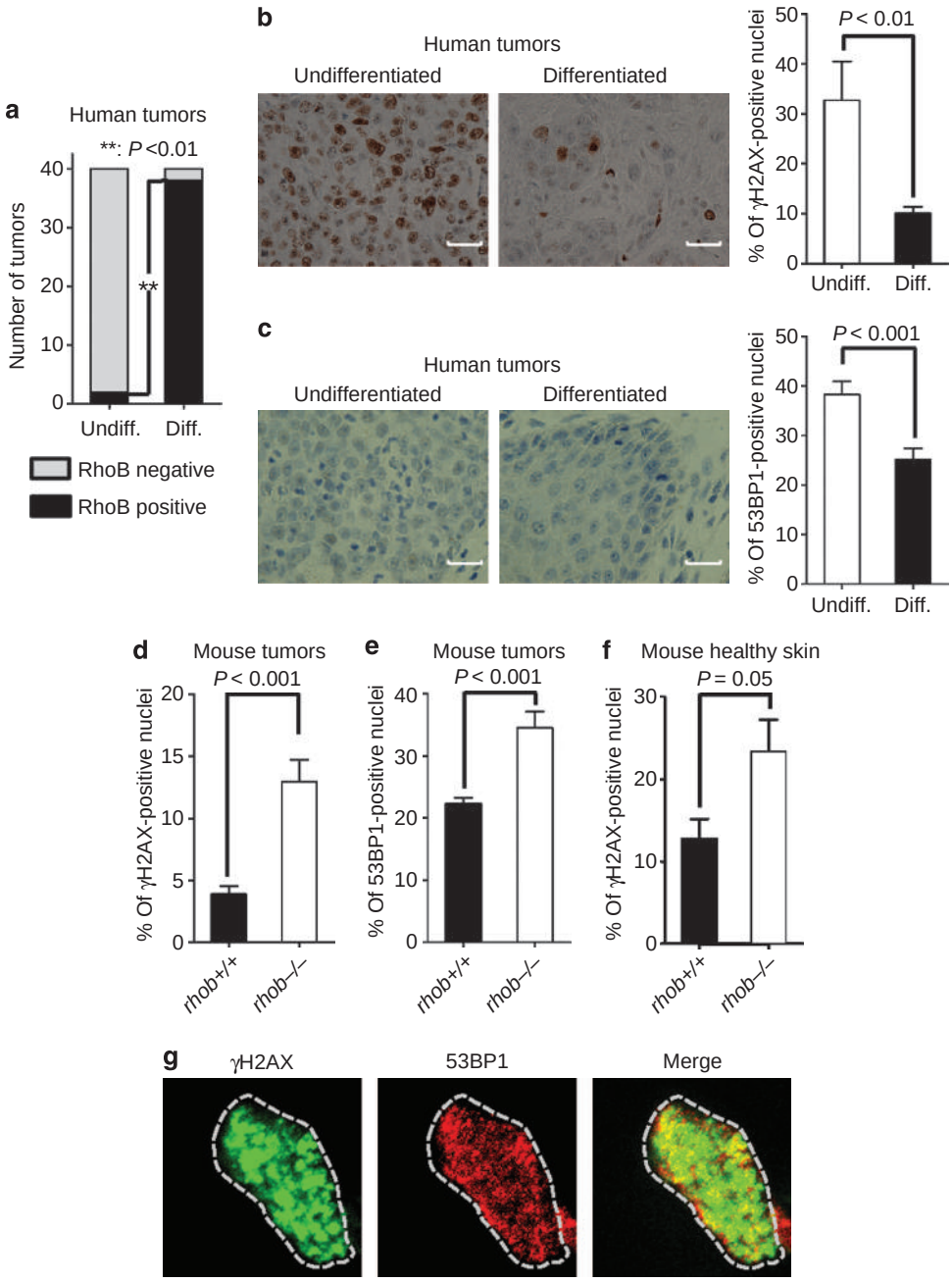

Figure 6. RhoB (Ras homolog gene family, member B) loss is associated with increased levels of DNA double-strand breaks. (**a**) RhoB immunostaining on human squamous cell carcinomas (SCCs). Graph shows the proportion of tumors expressing RhoB depending on the level of differentiation. Diff., differentiated; Undiff., undifferentiated. (**b**) Phosphorylated histone H2AX (γH2AX) immunostaining on human SCCs (scale = 5 μm). Graph shows the percentage of γH2AX-positive cells depending on the level of differentiation (mean + SD). (**c**) The 53BP1 immunostaining on human SCCs (scale = 5 μm). Graph shows the percentage of positive cells depending on the level of differentiation (mean + SD). Percentages of (**d**) γH2AX-positive cells and (**e**) 53BP1-positive cells in mouse tumors depending on *rhob* genotype (mean + SD). (**f**) Proportion of γH2AX-positive keratinocytes in the epidermal basal layer (mean + SD). (**g**) γH2AX and 53BP1 dual staining on *rhob* −/− mouse healthy skin, confocal imaging.

Our results support the hypothesis that RhoB plays a double-edged role in oncogenesis. Beside its role as a negative regulator of tumor progression, we report here a new aspect of the role of RhoB in skin oncogenesis in promoting tumor initiation through survival of UVB-exposed cells. RhoB could favor early stages of oncogenesis but at the same time could limit tumor aggressiveness. In this model, alteration of gene expression leading to RhoB down-regulation would then become necessary for tumor progression. These results are in agreement with our previous report on lung cancer (Mazieres *et al.*, 2004), in which we observed the expression of RhoB in *in situ* carcinoma of the lung and subsequent loss of RhoB expression in invasive cancers.

Understanding the role of RhoB in photocarcinogenesis could help to find novel strategies into routine clinical practice for the 15% of human SCCs displaying poor prognosis. Indeed, our results suggest that loss of RhoB may be considered a negative prognostic marker of human SCCs of the skin. Further studies are needed to assess the prognostic value of RhoB expression on large cohorts of patients with SCCs. Deciphering the RhoB pathway involved in the control of skin photocarcinogenesis may help the development of new therapeutic strategies against SCCs.

In conclusion, our results show that RhoB is a critical determinant for SCC initiation and that loss of RhoB expression in SCCs may predict tumor aggressiveness.

MATERIALS AND METHODS

Mice

SKH1 mice (Charles River, L'Arbresle, France) were crossed with Sv129/*rhob*−/− mice (Supplementary Figure S1 online) (Liu *et al.*, 2001). The Claudius Regaud Institute animal ethic committee approval (no. ICR-2009-016) was obtained for the use of the animal model and the study protocols.

UV exposure

Protocols of mice and cells UVB exposure are described in Supplementary Materials and Methods online.

Definition of the UV-induced phenotypes

A clinical evaluation of the mice at week 17 was performed on standardized photographs. Mice were separated in two groups according to the extent (> or <50%) of UV-induced AK on the dorsal skin defined as the skin between the base of the neck and the base of the tail (Figure 1a and Supplementary Figure S1 online). The 17-week UVB exposure end point for assessment of the effect of UVB on the occurrence of SCC precursors was chosen as the latest time at which all mice were alive. No consensus definition exists on the severity categorization of AK in humans or mice. The threshold of 50% for AK coverage of the dorsal skin of mice was chosen as an indicator of high UVB-induced skin damage.

NHK culture and siRNA transfection

NHK primary cultures were prepared from skin explants from patients undergoing mammary plastic surgery (see Supplementary Materials and Methods online). Transfection of NHKs by siRNAs (10 nM) (described in Canguilhem *et al.*, 2005) was performed using Oligofectamine (Life Technologies SAS, Saint Aubin, France) in keratinocyte serum-free medium according to the manufacturer's instructions on cells at 30–50% confluence in 60-mm cell culture dishes and seeded 24 hours before experiments.

Immunoblot analysis

Immunoblot analysis of RhoB was performed as previously described (Canguilhem *et al.*, 2005), see Supplementary Materials and Methods online.

Pathological examination of the tumors

FFPE mouse tumor samples were cut in 4-μm-thick sections. Sections were incubated at 100 °C for 15 minutes and then deparaffinized with xylene and rehydrated. Sections were stained with hematoxylin and eosin, and read by a trained dermatopathologist.

Human SCCs of the skin

A total of 80 FFPE human SCCs were obtained from the tumor bank of the department of pathology (Toulouse-Purpan Hospital, France) after written informed consent. The specimens consisted of 40 mild-to-well-differentiated and 40 low-to-undifferentiated invasive SCCs of the skin.

Immunostaining of tissues

Immunostainings were performed as described in Supplementary Materials and Methods online.

Immunofluorescent staining of tissues

Sections of cryoconserved tumor samples were fixed in 3% paraformaldehyde and permeabilized with 0.1% Triton X-100. After a saturation step in 3% BSA/phosphate-buffered saline, cells were incubated with mAb against γH2AX (9718, Cell Signaling, Danvers, MA) and then with Alexa Fluor 488 antibody (Life Technologies SAS). Coverslips were mounted on slides with Mowiol solution containing 4′,6-diamidino-2-phenylindole. Staining was detected by fluorescence microscopy.

Flow cytometry analyses of cleaved caspase-3 in NHKs

The phycoerythrin-conjugated Polyclonal Active Caspase-3 Antibody Apoptosis Kit (BD Pharmingen, Franklin Lakes, NJ) was used according to the manufacturer's instructions. Fluorescence was analyzed by flow cytometry on a BD-FACS Calibur (Le Pont de Claix, France).

Quantitative reverse transcribed–PCR

Flash-frozen tissue (50 mg) was homogenized in a TissueLyser system (Qiagen, Courtaboeuf, France). RNA was isolated using miRNeasy kit following the manufacturer's instructions (Qiagen) and reverse transcribed using iScript cDNA Synthesis kit (Bio-Rad, Hercules, CA). Quantitative PCR was performed with a CFx-96 real-time system (Bio-Rad). The specific murine primer pairs are described in Supplementary Materials and Methods online.

Statistical analysis

Comparisons of percentages were made using the χ^2 test. For mean comparisons between groups the two-sample *t*-test and the Mann–Whitney test were used as appropriate. The Kaplan–Meier method was used to estimate the distribution time taken to reach 10 tumors or 5 keratotic tumors, and differences among the groups were tested by the log-rank test. All tests were two sided with an α risk of 5%.

CONFLICT OF INTEREST

The authors state no conflict of interest.

ACKNOWLEDGMENTS

This study was supported by Institut National de la Recherche Médicale (INSERM), Institut Claudius Regaud Comprehensive Cancer Center, Centre Hospitalier et Universitaire (CHU) de Toulouse, Université Paul-Sabatier, the Ligue Nationale de Lutte Contre le Cancer, Comité Haute-Garonne, and The Research and Therapeutic Innovation in Cancer (RTIC) Foundation. We thank GC Prendergast (The Lankenau Institute for Medical Research, Wynnewood, PA) for kindly providing the *rhob*−/− mice, Philippe Rochaix for his technical contribution and fruitful discussions, S Cabantous for reading the manuscript, and D Berg for technical assistance.

SUPPLEMENTARY MATERIAL

Supplementary material is linked to the online version of the paper at http://www.nature.com/jid

REFERENCES

Adnane J, Muro-Cacho C, Mathews L *et al.* (2002) Suppression of rho B expression in invasive carcinoma from head and neck cancer patients. *Clin Cancer Res* 8:2225–32

Afaq F, Syed DN, Malik A *et al.* (2007) Delphinidin, an anthocyanidin in pigmented fruits and vegetables, protects human HaCaT keratinocytes and mouse skin against UVB-mediated oxidative stress and apoptosis. *J Invest Dermatol* 127:222–32

Batinac T, Zamolo G, Coklo M *et al.* (2006) Expression of cell cycle and apoptosis regulatory proteins in keratoacanthoma and squamous cell carcinoma. *Pathol Res Pract* 202:599–607

Benavides F, Oberyszyn TM, VanBuskirk AM *et al.* (2009) The hairless mouse in skin research. *J Dermatol Sci* 53:10–8

Bonner WM, Redon CE, Dickey JS *et al.* (2008) GammaH2AX and cancer. *Nat Rev Cancer* 8:957–67

Bousquet E, Mazières J, Privat M *et al.* (2009) Loss of RhoB expression promotes migration and invasion of human bronchial cells via activation of AKT1. *Cancer Res* 69:6092–9

Canguilhem B, Pradines A, Baudouin C *et al.* (2005) RhoB protects human keratinocytes from UVB-induced apoptosis through epidermal growth factor receptor signaling. *J Biol Chem* 280:43257–63

Chen Z, Sun J, Pradines A *et al.* (2000) Both farnesylated and geranylgeranylated RhoB inhibit malignant transformation and suppress human tumor growth in nude mice. *J Biol Chem* 275:17974–8

Delehedde M, Cho SH, Sarkiss M *et al.* (1999) Altered expression of bcl-2 family member proteins in nonmelanoma skin cancer. *Cancer* 85:1514–22

Fritz G, Kaina B (2001) Transcriptional activation of the small GTPase gene *rhoB* by genetoxic stress is regulated via CCAAT element. *Nucleic Acids Res* 29:792–8

Goodwin RG, Holme SA, Roberts DL (2004) Variations in registration of skin cancer in the United Kingdom. *Clin Exp Dermatol* 29:328–30

De Gruijl FR, Forbes PD (1995) UV-induced skin cancer in a hairless mouse model. *Bioessays* 17:651–60

De Gruijl FR, Voskamp P (2009) Photocarcinogenesis–DNA damage and gene mutations. *Cancer Treat Res* 146:101–8

Jiang K, Sun J, Cheng J *et al.* (2004) Akt mediates Ras downregulation of RhoB, a suppressor of transformation, invasion, and metastasis. *Mol Cell Biol* 24:5565–76

Karlsson R, Pedersen ED, Wang Z *et al.* (2009) Rho GTPase function in tumorigenesis. *Biochim Biophys Acta* 1796:91–8

Liu Ax, Cerniglia GJ, Bernhard EJ *et al.* (2001) RhoB is required to mediate apoptosis in neoplastically transformed cells after DNA damage. *Proc Natl Acad Sci USA* 98:6192–7

Lowe SW, Lin AW (2000) Apoptosis in cancer. *Carcinogenesis* 21: 485–95

Lukas J, Lukas C, Bartek J (2011) More than just a focus: the chromatin response to DNA damage and its role in genome integrity maintenance. *Nat Cell Biol* 13:1161–9

Madan V, Lear JT, Szeimies R-M (2010) Non-melanoma skin cancer. *Lancet* 375:673–85

Maddika S, Ande SR, Panigrahi S *et al.* (2007) Cell survival, cell death and cell cycle pathways are interconnected: implications for cancer therapy. *Drug Resist Updat* 10:13–29

Mazieres J, Antonia T, Daste G *et al.* (2004) Loss of RhoB expression in human lung cancer progression. *Clin Cancer Res* 10:2742–50

Mazières J, Tillement V, Allal C *et al.* (2005) Geranylgeranylated, but not farnesylated, RhoB suppresses Ras transformation of NIH-3T3 cells. *Exp Cell Res* 304:354–64

Milia J, Teyssier F, Dalenc F *et al.* (2005) Farnesylated RhoB inhibits radiation-induced mitotic cell death and controls radiation-induced centrosome overduplication. *Cell Death Differ* 12:492–501

Monferran S, Skuli N, Delmas C *et al.* (2008) Alphavbeta3 and alphavbeta5 integrins control glioma cell response to ionising radiation through iLK and RhoB. *Int J Cancer* 123:357–64

Nakagawa K, Yamamura K, Maeda S *et al.* (1994) bcl-2 expression in epidermal keratinocytic diseases. *Cancer* 74:1720–4

Prendergast GC (2001) Actin' up: RhoB in cancer and apoptosis. *Nat Rev Cancer* 1:162–8

Ratushny V, Gober MD, Hick R *et al.* (2012) From keratinocyte to cancer: the pathogenesis and modeling of cutaneous squamous cell carcinoma. *J Clin Invest* 122:464–72

Reagan-Shaw S, Breur J, Ahmad N (2006) Enhancement of UVB radiation-mediated apoptosis by sanguinarine in HaCaT human immortalized keratinocytes. *Mol Cancer Ther* 5:418–29

Salasche SJ (2000) Epidemiology of actinic keratoses and squamous cell carcinoma. *J Am Acad Dermatol* 42:4–7

Samejima K, Earnshaw WC (2005) Trashing the genome: the role of nucleases during apoptosis. *Nat Rev Mol Cell Biol* 6:677–88

Sharma MR, Werth B, Werth VP (2011) Animal models of acute photodamage: comparisons of anatomic, cellular and molecular responses in C57BL/6J, SKH1 and Balb/c mice. *Photochem Photobiol* 87:690–8

Skuli N, Monferran S, Delmas C *et al.* (2006) Activation of RhoB by hypoxia controls hypoxia-inducible factor-1alpha stabilization through glycogen synthase kinase-3 in U87 glioblastoma cells. *Cancer Res* 66:482–9

Spector ME, Wilson KF, Light E *et al.* (2011) Clinical and pathologic predictors of recurrence and survival in spindle cell squamous cell carcinoma. *Otolaryngol Head Neck Surg* 145:242–7

Wong RSY (2011) Apoptosis in cancer: from pathogenesis to treatment. *J Exp Clin Cancer Res* 30:87

Author: Agnese CRISTINI

PhD Director: Dr. Olivier SORDET

TITLE: DNA double-strand break formation and signalling in response to transcription-blocking topoisomerase I complexes

Summary

Topoisomerase I (Top1) removes DNA supercoiling generated during transcription by producing Top1-DNA cleavage complexes (Top1cc). These transient Top1cc can be stabilized by camptothecins, from which anticancer drugs are derived, and by common DNA alterations. Although stabilized Top1cc are potent transcription-blocking lesions, our understanding regarding the molecular processes resulting from the stalling of transcription complexes by Top1cc is currently limited. Previous work showed that stabilized Top1cc produce transcription-dependent DNA double-strand breaks (DSBs) that activate ATM signalling. In this project, we used camptothecin-treated quiescent cells to induce transcription-blocking Top1cc and study the mechanisms of DSB production and signalling. We show that DSBs form preferentially at subtelomeric regions during the repair of transcription-blocking Top1cc from DNA single-strand breaks generated after Top1 proteolysis and before Tdp1 action. Analysis of DSB signalling reveals a novel function of DNA-PK in promoting protein ubiquitination leading (i) to full ATM activity at DSB sites by promoting H2AX and H2A ubiquitination, and (ii) to enhancement of Top1cc repair by promoting Top1 proteolysis. Finally, we show that co-transcriptional DSBs kill quiescent cells. Together, these findings provide new insights into the cellular responses to camptothecins and further suggest that DSBs arising from transcription-blocking Top1cc may contribute to the pathogenesis of the neurodegenerative SCAN1 syndrome, which is caused by Tdp1 deficiency.

TITRE: Formation et signalisation des cassures double-brin de l'ADN lors d'un blocage de la transcription par les complexes topoisomerase I-ADN

Résumé

La topoisomérase I (Top1) élimine les surenroulements de l'ADN générés lors de la transcription en produisant transitoirement des complexes de clivage Top1-ADN (Top1cc). Ces Top1cc transitoires peuvent être stabilisés par les camptothécines, dont sont dérivés des agents anticancéreux, et par les fréquentes altérations de l'ADN. Bien que les Top1cc stabilisés soient des lésions qui bloquent efficacement la transcription, la compréhension des processus moléculaires qui résultent du blocage des complexes transcriptionnels par les Top1cc est encore limitée. Des travaux précédents ont montré que les Top1cc stabilisés produisent des cassures double-brin (DSBs) de l'ADN dépendantes de la transcription qui activent ATM. Dans ce projet, nous avons utilisé des cellules quiescentes traitées avec la camptothécine pour induire des Top1cc bloquant la transcription et nous avons étudié les mécanismes de la production et de la signalisation des DSBs. Nous montrons que les DSBs sont produites préférentiellement dans les régions sub-télomériques lors de la réparation des Top1cc bloquant la transcription par les cassures simple-brin de l'ADN générées après la protéolyse de la Top1 et avant l'action de Tdp1. L'analyse de la signalisation de ces DSBs révèle une nouvelle fonction de DNA-PK dans la promotion de l'ubiquitinylation conduisant (i) à l'activité complète d'ATM aux sites des DSBs en favorisant l'ubiquitination d'H2AX et H2A, et (ii) à l'augmentation de la réparation des Top1cc en favorisant la protéolyse de la Top1. Enfin, nous montrons que les DSBs co-transcriptionnelles induisent la mort des cellules quiescentes. L'ensemble de ces résultats apportent un nouvel aperçu des réponses cellulaires aux camptothécines, et suggèrent que les DSBs qui résultent des Top1cc bloquant la transcription puissent contribuer à la pathogénèse du syndrome neurodégénératif SCAN1, qui est causé par une déficience en Tdp1.

Keywords: Topoisomerase, double-strand breaks, DNA-PK, ubiquitin, camptothecin, transcription, Tdp1, DNA damage